PROGRESS
IN
COSMIC RAY PHYSICS

EDITED BY

J. G. WILSON, M.A., Ph.D., F. Inst. P.

UNIVERSITY OF MANCHESTER

CONTRIBUTORS:

U. CAMERINI
W. O. LOCK
D. H. PERKINS
C. C. BUTLER
L. MICHEL
B. PETERS
H. V. NEHER
G. PUPPI
N. DALLAPORTA
E. P. GEORGE
H. ELLIOT

1952

NORTH-HOLLAND PUBLISHING COMPANY, AMSTERDAM
INTERSCIENCE PUBLISHERS, INC. NEW YORK

IIA Lib.,

Sole Distributors for U.S.A.
Interscience Publishers, Inc. New York

PRINTED IN THE NETHERLANDS
DRUKKERIJ HOLLAND N.V., AMSTERDAM

PREFACE

"Progress in Cosmic Ray Physics" is intended to provide a series of reviews covering, in particular, those aspects of the physics of cosmic radiation in which advances of broad significance are now being made.

It is a characteristic of cosmic ray physics that in spite of the extensive specialized research of the last five years, the separation of the subject into more or less independent topics has not gone very far. The main geophysical investigations remain among the most fruitful sources in which hitherto unknown interactions are identified, while the interpretation of these large scale phenomena must essentially depend on a detailed understanding of the single nucleon-nucleon encounter. Interrelations between the various geophysical features are still closer, while neither the relevance of the broad conclusions of fundamental particle theory to the experimental pursuit of these particles, nor the importance to the theorist of a balanced assessment of the changing experimental position, need be stressed. Up to date surveys of the state of knowledge in the various branches of the subject are accordingly likely to be of particular value to active workers on specialized problems, and the reviews of this volume, which in general give the standpoint of the early months of 1951, have this requirement in view. They aim also to cover the much wider need of workers in related subjects, particularly in nuclear physics and in astrophysics, for information about current trends in cosmic ray work.

It is not possible, in a single volume of moderate size, to survey all the main lines of cosmic ray investigations, and rather drastic selection has been necessary. It is hoped, however, to cover other subjects in later volumes, where further reports on topics in rapid development would also appear.

I am grateful to the various authors and to the publishers, for the very active co-operation which has made quick publication possible.

J. G. WILSON

Manchester, September 1951

CONTENTS

CHAPTER I

THE ANALYSIS OF ENERGETIC NUCLEAR ENCOUNTERS OCCURRING IN PHOTOGRAPHIC EMULSIONS

INTRODUCTION 3

PART I

RADIATIVE COLLISIONS

1. MESON PRODUCTION IN NUCLEON-NUCLEON COLLISIONS 5
  1. 1 Theories 5
  1. 2 Experimental methods; nomenclature and technique . . . 6
  1. 3 Yield curve for mesons 7
  1. 4 The production of neutral mesons 12
  1. 5 Comparison of multiplicity — primary energy relationship with theory 13
  1. 6 Variation of N_h and N_g with primary energy and multiplicity 16
2. MESON-NUCLEON INTERACTION 18
  2. 1 The collision mean free path 18
  2. 2 Stars produced by identified π-mesons 20
  2. 3 The interactions of π-mesons of energy greater than 1 BeV 21
  2. 4 Conclusions 21
3. PROPERTIES OF THE SHOWER PARTICLES 22
  3. 1 Lorentz transformation to centre of mass system (multiple theory) 22
  3. 2 Energy and angular distributions of the shower particles . . 23
  3. 3 Interaction of the shower particles with the nucleus . . . 29
4. INDIVIDUAL HIGH ENERGY EVENTS 30
  4. 1 Stars produced by neutrons and singly charged primary particles 30
  4. 2 Stars produced by fast α-particles 32
5. CONCLUSIONS 32

PART II

ELASTIC COLLISIONS

6. INTRODUCTION 34

7. FREQUENCY, ENERGY AND ANGULAR DISTRIBUTION OF FAST NUCLEONS (GREY TRACKS) 34
  7.1 Frequency of grey tracks 34
  7.2 Energy distribution of protons producing grey tracks . . . 35
  7.3 Angular distribution of grey tracks 36
  7.4 Proportion of grey and black tracks 37

8. FREQUENCY, ENERGY AND ANGULAR DISTRIBUTION OF SLOW PARTICLES (BLACK TRACKS); THE EVAPORATION PROCESS 38
  8.1 Introduction 38
  8.2 Energy distribution of low energy protons 40
  8.3 Energy distribution of low energy α-particles 44
  8.4 Angular distribution of low energy protons 46
  8.5 Angular distribution of low energy α-particles 47
  8.6 Emission probabilities for various types of particles . . . 48
  8.7 Relation between prong number and thermal excitation energy 49

9. EMISSION OF HEAVY FRAGMENTS IN STARS 51
  9.1 Frequency of fragment emission 51
  9.2 Angular distribution of fragments 53
  9.3 Emission of low energy fragments (less than 4 MeV per nucleon) 54
  9.4 Emission of high energy fragments (more than 4 MeV per nucleon) 55

10. CONCLUSIONS 56

11. OUTSTANDING PROBLEMS 57

ACKNOWLEDGEMENTS 58

REFERENCES 59

CHAPTER II

UNSTABLE HEAVY COSMIC RAY PARTICLES

INTRODUCTION 65

PART I

THE DECAY OF NEUTRAL V-PARTICLES

1. THE FIRST NEUTRAL V-SHAPED TRACK 67

2. INVESTIGATIONS OF V-SHAPED TRACKS 68
2. 1 Experimental arrangements used for the detection of neutral V-shaped tracks 68
2. 2 Statistical data 70
2. 3 The source of the neutral V-shaped tracks 73

3. THE NATURE OF THE SECONDARY PARTICLES 73
3. 1 Heavily-ionizing secondary particles 73
3. 2 The penetrating properties of the secondary particles . . . 78
3. 3 The differential momentum spectrum of the secondary particles 79

4. POSSIBLE EXPLANATIONS OF THE NEUTRAL V-SHAPED TRACKS 82
4. 1 Interactions in the gas of the cloud chamber 82
4. 2 Large-angle single scattering of particles in the gas of the cloud chamber 85

5. SUGGESTED DECAY PROCESSES 85
5. 1 The number of secondary particles 85
5. 2 Possible two-particle decay schemes 86

6. MASS DETERMINATIONS 89
6. 1 The decay of V_1^0-particles into protons and π-mesons 89
6. 2 The decay of V_2^0-particles into two π-mesons 91

7. THE DYNAMICS OF DECAY SCHEMES WITH TWO SECONDARY PARTICLES 93
7. 1 The dynamics of the decay scheme: $V_1^0 \rightarrow p^+ + \pi^-$ . . . 93
7. 2 The dynamics of the decay scheme: $V_2^0 \rightarrow \pi^+ + \pi^-$ . . . 98

8. THE MEAN REST LIFETIME OF NEUTRAL V-PARTICLES 101

9. CONCLUSIONS 101

PART II

THE DECAY OF HEAVY CHARGED PARTICLES

10. THE DECAY OF τ-MESONS 105

11. THE DECAY OF CHARGED V-PARTICLES 109
11. 1 The first charged V-shaped track 109
11. 2 The statistical data on charged V-shaped tracks 109
11. 3 The explanation of the charged V-shaped tracks 110
11. 4 The nature of the secondary particles of charged V-particles 114

11. 5 The mass of the charged V-particles 116
11. 6 The mean rest life-time of charged V-particles 120

12. CONCLUSIONS 121

ACKNOWLEDGEMENTS 122

REFERENCES 123

CHAPTER III

COUPLING PROPERTIES OF NUCLEONS, MESONS AND LEPTONS

INTRODUCTION 127

1. THE PHYSICS OF PARTICLES 127
1. 1 Experimental data 128
1. 2 Theoretical methods 129
1. 3 The conservation laws 131
1. 4 Coupling between fields 133
1. 5 Couplings commonly used 136
1. 6 Couplings not commonly used 139
1. 7 Units 141
1. 8 Isotopic variable 141
1. 9 Furry's theorem 142
1. 10 Equivalence theorem, radiative corrections, renormalization and regularization 144

2. π-MESONS AND HEAVIER MESONS 145
2. 1 Nuclear forces 145
2. 2 The nature of the π^0-meson 147
2. 3 The nature of the $\pi^{\pm}$-meson 149
2. 4 Are π^0 and $\pi^{\pm}$ mesons symmetrical pseudoscalar mesons? 151
2. 5 Neutral V-mesons 153
2. 6 Heavier charged mesons, V and τ 155

3. INTERACTION BETWEEN FOUR FERMIONS 159
3. 1 The neutrino 159
3. 2 μ-meson decay 161
3. 3 The radioactivity of the neutron 163
3. 4 Nature of the coupling of β-radioactivity 166
3. 5 The capture of μ-mesons by nuclei 172
3. 6 Universal direct coupling between four fermions 174

4. POSSIBLE COUPLING SCHEMES 176
    4. 1 Coupling scheme (1) 176
    4. 2 Coupling scheme (2): an alternative to scheme (1) . . . 179
    4. 3 Is direct coupling necessary for β-radioactivity? 179
    4. 4 Summary 181
5. CONCLUSION 182
ACKNOWLEDGEMENTS 184
REFERENCES 185

CHAPTER IV

THE NATURE OF PRIMARY COSMIC RADIATION

INTRODUCTION 193
1. THE STUDY OF HEAVY PRIMARY PARTICLES IN NUCLEAR EMULSIONS 195
    1. 1 Tracks produced by heavy nuclei 195
    1. 2 Charge determination of heavy primary nuclei 197
2. NUCLEAR INTERACTIONS AND ENERGY MEASUREMENTS 202
    2. 1 Different types of nuclear interaction 202
    2. 2 Mean free path for nuclear collisions 209
    2. 3 Energy determination for non-relativistic nuclei 210
    2. 4 Energy determination for relativistic nuclei 212
3. THE FLUX AND ENERGY SPECTRUM OF PRIMARY COSMIC RAY NUCLEI 216
    3. 1 The flux of primary α-particles 218
    3. 2 The flux of primary nuclei of charge $Z > 2$ 221
    3. 3 The low energy cut-off for heavy primary nuclei 224
    3. 4 Time fluctuations in the flux of heavy nuclei 225
    3. 5 The energy spectrum of primary cosmic rays 225
4. THE CHEMICAL COMPOSITION OF PRIMARY COSMIC RADIATION 228
    4. 1 The charge spectrum between latitudes $\lambda = 55°$ and $\lambda = 30°$ 228
    4. 2 Comparison of the cosmic abundance of elements with their abundance in primary cosmic rays 231
5. THE COMPOSITION OF PRIMARY COSMIC RADIATION AND THE PROBLEM OF ITS ORIGIN 233
REFERENCES 241

CHAPTER V

RECENT DATA ON GEOMAGNETIC EFFECTS

INTRODUCTION 245

1. AN OUTLINE OF THE THEORY OF GEOMAGNETIC EFFECTS 246
   1. 1 The earth's magnetic field 246
   1. 2 Application of Liouville's theorem 247
   1. 3 Units of energy and momentum 247
   1. 4 Application of Störmer's theory 248
   1. 5 Modifications to Störmer's theory 249
   1. 6 Corrections for eccentricity of dipole 251
   1. 7 Definition of geomagnetic effects 253

2. COSMIC RAYS IN THE ATMOSPHERE 254
   2. 1 Units of cosmic ray intensity 254
   2. 2 Relation of intensity in the atmosphere to that above the atmosphere 255
   2. 3 Are there any primary electrons in cosmic rays? 256
   2. 4 Correlation between measurements taken with ionization chambers and counter telescopes 256

3. DATA ON GEOMAGNETIC EFFECTS 262
   3. 1 Introduction 262
   3. 2 Description of the apparatus 263
   3. 3 Experiments performed 266
   3. 4 Internal calibrations 267
   3. 5 Corrections to the telescope readings 268
   3. 6 Reduction to absolute values 271
   3. 7 Experimental results 272

4. CORRELATION OF GEOMAGNETIC EFFECTS 288
   4. 1 Introduction 288
   4. 2 Correlation of latitude effect and zenith angle effect with the calculations of VALLARTA *et al.* 289
   4. 3 Correlation of azimuthal effect with zenith angle effect at the equator 294
   4. 4 Correlation of latitude, zenith angle and longitude effects 295
   4. 5 Summary of correlation of geomagnetic effects 296

5. ENERGY DISTRIBUTION OF THE PRIMARY RADIATION 297
   5. 1 Introduction 297
   5. 2 Normalization of counter telescope curves 297
   5. 3 Empirical relations 301
   5. 4 Consequences of the above distribution of cosmic ray energy 303

6. SOME CONCLUSIONS ON THE GROSS BEHAVIOUR OF COSMIC RAYS IN THE ATMOSPHERE 304
  6. 1 Introduction 304
  6. 2 Absorption in lead as a function of minimum momentum of the primaries 304
  6. 3 Multiplicity of charged particles 306
  6. 4 Consequences of dependence of multiplicity on energy of the primaries 311

7. SUMMARY 311

REFERENCES 313

CHAPTER VI

THE EQUILIBRUM OF THE COSMIC RAY BEAM IN THE ATMOSPHERE

INTRODUCTION 317

1. THE PRIMARY COMPONENT AT THE TOP OF THE ATMOSPHERE 317
  1. 1 Vertical data 318
  1. 2 Secondary processes and asymmetries 320
  1. 3 The primary spectrum 322
  1. 4 Discussion on the hypothesis of primary electrons 324
  1. 5 Discussion on the hypothesis of negative primaries . . . 326
  1. 6 Heavy nuclei in the primary radiation 327

2. COSMIC RADIATION UNDERGROUND 330

3. COSMIC RAYS IN THE ATMOSPHERE 332
  3. 1 Experimental data at sea-level 333

4. THE μ-COMPONENT 336
  4. 1 Intensity-height distribution 336
  4. 2 The spectrum at sea-level 339
  4. 3 The positive excess 342
  4. 4 Asymmetries of the positive excess 347

5. THE ELECTRON-PHOTON COMPONENT 348
  5. 1 The total intensity-height distribution 349
  5. 2 The latitude effect 351
  5. 3 The energy spectrum; the ratio of electrons to photons 351

6. THE N-COMPONENT 352
  6. 1 Absorption and latitude effect 354

6. 2 Absolute intensity of the nucleonic component 357
6. 3 The spectrum of the nucleonic component 359
6. 4 The ratio of neutrons to protons 361

7. THE GENETIC RELATION 363

8. HIGH ENERGY EVENTS IN THE N-COMPONENT 364
8. 1 Multiple and plural processes 365
8. 2 Diffusion of the high energy N-component 366

9. THE π-MESONS 367
9. 1 The generation spectrum of charged π-mesons 368
9. 2 Relation between the spectra of π-mesons and μ-particles 370
9. 3 Diffusion equation for π-mesons 370
9. 4 Neutral π°-mesons 372
9. 5 τ and V-particles 373

10. LOW ENERGY EVENTS IN THE N-COMPONENT 373
10. 1 Equilibrium between stars and neutrons 375

11. EXTENSIVE AIR SHOWERS 380

12. ENERGY BALANCE OF THE COSMIC RAY BEAM 380
12. 1 Flux measurements 381
12. 2 Ratio between neutral and charged π-mesons 384
12. 3 Variation with energy of the absorption length of the N-component 386

ACKNOWLEDGEMENTS. 387

REFERENCES 388

CHAPTER VII

OBSERVATIONS OF COSMIC RAYS UNDERGROUND AND THEIR INTERPRETATION

INTRODUCTION 395

1. THE DEPTH-INTENSITY RELATION: ABSORPTION MEASUREMENTS 395
1. 1 Depth-intensity relation, experimental 395
1. 2 Absorption measurements 398
1. 3 Angular distribution of the penetrating radiation 401
1. 4 Depth-intensity relation, corrected values 402

2. CLOUD CHAMBER EVIDENCE CONCERNING THE NATURE OF THE RADIATION 403

2. 1 Observations at moderate depths, 20—60 m. 403
2. 2 Observations at great depths 407

3. THE DEPTH-INTENSITY RELATION: THEORETICAL . . 408
3. 1 Energy losses of μ-mesons 408
3. 2 The range-energy relation for energetic μ-mesons 412
3. 3 The energy spectrum at sea-level 414
3. 4 The influence of π-meson interactions 416

4. TIME VARIATIONS; TEMPERATURE COEFFICIENTS . . . 418
4. 1 The observations of Rau 418
4. 2 The observations of MacAnuff 420
4. 3 Comparison of observations of Rau and MacAnuff 424

5. STARS AND SLOW MESONS IN EMULSIONS 424
5. 1 Observations of nuclear disintegrations 424
5. 2 Observations of slow mesons 432
5. 3 Summary of emulsion work 435

6. SLOW NEUTRONS 436

7. UNDERGROUND SHOWERS 438
7. 1 Soft showers 438
7. 2 Penetrating showers 441
7. 3 Extensive showers 443

8. IONIZATION BURSTS 444

9. PENETRATING PAIRS OF PARTICLES 448

ACKNOWLEDGEMENTS 449

REFERENCES 450

CHAPTER VIII

TIME VARIATIONS OF COSMIC RAY INTENSITY

INTRODUCTION 455

1. VARIATIONS OF ATMOSPHERIC ORIGIN 456
1. 1 Atmospheric temperature and μ-meson decay 456
1. 2 The positive temperature effect 458
1. 3 The seasonal variation 461

2. THE SOLAR DAILY VARIATION 466
2. 1 Omni-directional measurements 466
2. 2 Measurements using directional counter arrays 472

2. 3 The relation between the daily variation and geomagnetic activity 477
2. 4 The daily variation at great altitudes 480
2. 5 The semi-diurnal variation 481

3. THE SIDEREAL DAILY VARIATION 484
3. 1 Galactic rotation and the cosmic ray intensity 484
3. 2 The separation of solar and sidereal daily variations . . . 485
3. 3 Recent experimental results 488

4. VARIATIONS ASSOCIATED WITH GEOMAGNETIC AND SOLAR ACTIVITY 492
4. 1 Magnetic storms and the cosmic ray intensity 492
4. 2 The 27-day recurrence tendency 497
4. 3 Increases of intensity associated with solar flares 502

APPENDIX. Geographic and geomagnetic coordinates of cosmic ray intensity recording stations 511

REFERENCES 512

AUTHOR INDEX 515

SUBJECT INDEX 549

CHAPTER I

THE ANALYSIS OF ENERGETIC NUCLEAR ENCOUNTERS OCCURRING IN PHOTOGRAPHIC EMULSIONS

BY

U. CAMERINI, W. O. LOCK and D. H. PERKINS
The H. H. Wills Physical Laboratory, University of Bristol

INTRODUCTION 3

PART I

RADIATIVE COLLISIONS

1. MESON PRODUCTION IN NUCLEON-NUCLEON COLLISIONS 5
2. MESON-NUCLEON INTERACTION 18
3. PROPERTIES OF THE SHOWER PARTICLES 22
4. INDIVIDUAL HIGH ENERGY EVENTS 30
5. CONCLUSIONS 32

PART II

ELASTIC COLLISIONS

6. INTRODUCTION 34
7. FREQUENCY, ENERGY AND ANGULAR DISTRIBUTION OF FAST NUCLEONS (GREY TRACKS). 34
8. FREQUENCY, ENERGY AND ANGULAR DISTRIBUTION OF SLOW PARTICLES (BLACK TRACKS); THE EVAPORATION PROCESS. 38
9. EMISSION OF HEAVY FRAGMENTS IN STARS. 51
10. CONCLUSIONS 56
11. OUTSTANDING PROBLEMS 57
ACKNOWLEDGEMENTS 58
REFERENCES 59

INTRODUCTION

With the development of electron-sensitive emulsions, the field of research open to the emulsion technique has been greatly extended, and it has become possible to apply this method, with advantage, to the study of problems which had hitherto been the province of the geiger counter and the cloud chamber.

In particular, the method permits detailed observations on the penetrating showers of particles created in energetic nuclear encounters, and it is the purpose of this article to describe observations made in this field.

Before entering into a detailed discussion of the experimental results relating to penetrating showers, we shall outline the types of interaction which are believed to occur in the nucleon-nucleon encounters. This will be done in the order in which the processes are assumed to occur in the nucleus.

The incident high energy nucleon, which we shall call the primary, makes, within a time of the order of 10^{-23} sec. (the time of traversal of the nucleus) a series of collisions with the individual nucleons of the nucleus; collisions which may either be elastic or radiative. In the latter case various types of quanta may be radiated. It is generally believed that these are π-mesons, and possibly heavier mesons or nucleon pairs, but that direct creation of photons or μ-mesons does not occur. At present very little is known about the production of mesons heavier than π-mesons, and we shall therefore limit ourselves to interactions leading to creation of π-mesons only. The radiative processes will be discussed in Part I.

In both elastic and inelastic collisions recoil nucleons will be produced which, together with the primary and any mesons created, can interact further with the nucleus. In this process lower energy nucleons are generated and by further successive encounters these distribute part of their energy through the nucleus, although they will in general escape from it before losing all their kinetic energy. In this way a statistical distribution of energy will be attained in a time large compared with the interval between successive nucleon-nucleon encounters. The ensuing evaporation process will be described in Part II.

It will be noted that in this sketch we have assumed, in accordance with contemporary theories, that all the collisions are nucleon-nucleon. We assume, in other words, that a nucleon cannot interact with an assemblage of nucleons as a whole. This hypothesis appears reasonable in view both of the low binding energy of the nucleons, and of the fact that the wavelength of the incident nucleon is small compared with the internuclear distance and the range of nuclear forces. However, the experimental results of PERKINS [1950], CRUSSARD [1950] and of SÖRENSEN [1949, 1951], showing that energetic nuclei of helium, lithium, beryllium and boron can be ejected from an excited nucleus, are inconsistent with this simplifying hypothesis. These phenomena will also be dealt with in Part II.

It is an important feature of the processes under consideration that very little information can be obtained relating directly to the individual collisions. The experimental data on which discussion must be based are the descriptions of the final result of the mixed meson-nucleon cascade throughout the nucleus. From these observations one must work backwards in an attempt to determine at least some of the properties of the original collisions.

A large part of the work to be described in the first part of this article has been carried out in this laboratory, and the results have been published as a series of papers under the general title of "*Nuclear Transmutations produced by Cosmic Ray Particles of Great Energy*". These papers will be referred to in the text by the number of the part in question.

PART I

RADIATIVE COLLISIONS

1. MESON PRODUCTION IN NUCLEON-NUCLEON COLLISIONS

1.1 Theories

Any description of the process of meson production in nucleon-nucleon collisions involves a number of parameters which are common to any theory. Some of these are:

(a) the collision cross-section per nucleon, which is made up of both radiative and elastic scattering cross section;

(b) the degree of inelasticity, K, of the collision, i.e. the fraction of available energy radiated as mesons;

(c) the energy and angular distributions of the mesons in the centre of mass (C) system.

All these quantities can presumably vary with the energy of the incident nucleon and with the impact parameter for the collision.

The theories relating to the primary collision process may be divided into two classes, "plural", and "multiple". The "plural" theory has been advanced by HEITLER and JANOSSY, [1949, 1950] and the multiple theory is exemplified by the work of WATAGHIN [1938, 1946], LEWIS, OPPENHEIMER, WOUTHUYSEN [1948], HEISENBERG [1949] and FERMI [1950, 1951]. The two theories, in their extreme forms at least, differ fundamentally in principle.

Thus in the plural theory, the radiation damping effect is assumed to be so strong that in the overwhelming majority of cases only a single meson can be produced in a single nucleon-nucleon collision. The primary loses only a small fraction of its energy in the first collision, and provided that the cross-section for collision is sufficiently high, a single primary makes several collisions, thus producing a shower of mesons in traversing a large nucleus.

On the other hand, in the multiple theory it is assumed that several mesons can be created in a single collision which is so highly inelastic that the primary has often insufficient energy to generate further mesons. Thus in a large nucleus, the final results, as seen in the form of a shower of mesons, may not be very different according to the two theories. They would, in fact, only predict radically different types of shower in hydrogen.

The total cross-section for nucleon-nucleon collisions at high energies is at present unknown, but it is generally assumed to be of the order of the geometrical value $(\hbar/m_\pi c)^2$. It could be found from the observed intensity of showers attributable to pure proton-proton collisions in photographic emulsions. However, the technical difficulties associated with the observation of this type of collision make the result uncertain.

1. 2 Experimental methods; nomenclature and technique

The only detailed experimental information at present available relating to the properties of high energy collisions is contained in the results obtained in photographic emulsions and in cloud chambers. The disintegrations produced are called "stars" and we classify them according to the following nomenclature, (Brown, Camerini, Fowler, Heitler, King and Powell [1949] (I)). The tracks emanating from the disintegration are divided into three classes, according to their grain density g, as compared with g_{min}, the grain density of a relativistic particle of charge (e):

(i) "Thin" tracks, $g_{\text{min}} \leqslant g < 1.4\ g_{\text{min}}$ (shower particles).
(ii) "Grey" tracks, $1.4\ g_{\text{min}} < g < 6.8\ g_{\text{min}}$.
(iii) "Black" tracks, $g > 6.8\ g_{\text{min}}$.

The limit of $6.8\ g_{\text{min}}$ corresponds to a proton of 25 MeV; most of the evaporation protons have kinetic energies below this value, (Part II). The sum of the "grey" and "black" tracks from a star is called the number of heavily ionising branches N_h, and the number of shower particles is designated by n_s. A star is therefore described by $N_h + n_s$ followed by a suffix to denote the nature of the primary particle, i.e. n, p, or π. Stars with $n_s \geqslant 2$ are sometimes called "showers".

It should be noted that the "shower particles" as defined above correspond both to protons of kinetic energy greater than 500 MeV and to π-mesons of kinetic energy greater than 80 MeV; there is no evidence of an appreciable admixture of energetic electrons amongst these particles. This definition of a shower particle is different from that usually employed by cloud chamber workers; care must be taken, therefore, in comparing results obtained by the two techniques.

Work on stars in electron-sensitive emulsions has usually been referred to the star parameters defined above. In the case of less sensitive emulsions, such as Ilford C2, the total number of tracks observed is only slightly greater than the number of black tracks as defined above.

There are at the moment three methods whereby the energy of a fast charged particle may be determined. When the length of the track in the emulsion is sufficiently great, an estimate of energy may be made by measurement of its multiple Coulomb scattering (GOLDSCHMIDT–CLERMONT [1950]; FOWLER [1950]). Alternatively, a comparison may be made between the stars observed in emulsions exposed at different geomagnetic latitudes. At 31° N, for example, the protons in the primary radiation which are incident vertically all have a kinetic energy greater than 8 BeV, whereas at 57° N the minimum allowed energy in the vertical direction is 1 BeV. The difference between the characteristics of the two sets of stars is then attributed to the primary particles of energy intermediate between the two cut-off values (SALANT, HORNBOSTEL, FISK and SMITH [1950]). Measurement of the deflection of the particles in a strong magnetic field can also be usefully employed (DILWORTH, GOLDSACK, GOLDSCHMIDT–CLERMONT and LEVY [1950]).

1. 3 Yield curve for mesons

The work of PICCIONI [1950] and of FOWLER [1950] (III) has shown that the majority of the shower particles are π-mesons. It has further been shown by CAMERINI, FOWLER, LOCK and MUIRHEAD [1950] (IV) that the small admixture of protons amongst these particles is approximately compensated by the number of π-mesons of energy less than 150 MeV. The number of shower particles observed is, therefore, to a first approximation, equal to the total number of charged mesons produced. CAMERINI, DAVIES, FOWLER, FRANZINETTI, LOCK, PERKINS and YEKUTIELI [1951] (VI) have recently carried out an analysis of meson "showers" produced in photographic emulsions exposed at an atmospheric depth of 52 gm.cm^{-2}. The distribution in the number of shower particles emitted from a nuclear disintegration is plotted in Fig. 1 for various ranges of the energy of the primary particle.

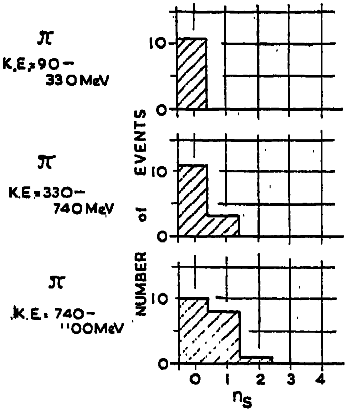

a

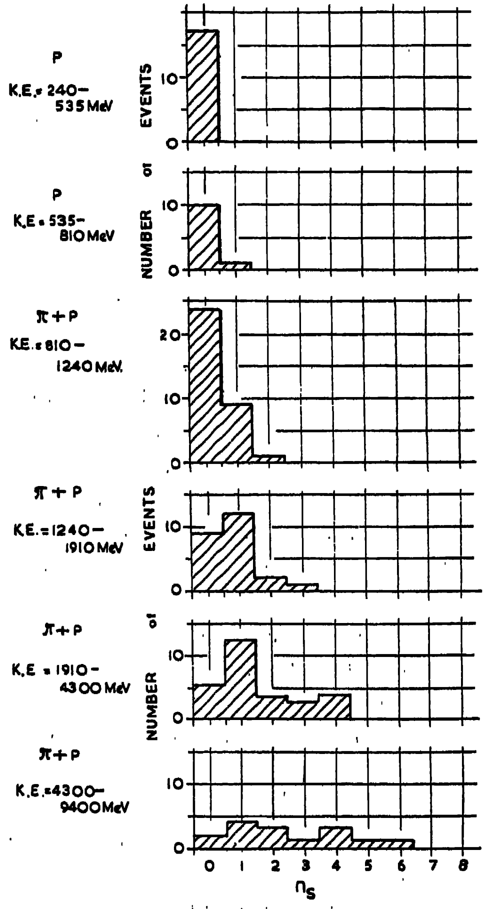

b

Fig. 1 – Distribution of multiplicity, n_s, in stars produced by (a) π-mesons, (b) protons and "π-p" particles, as a function of energy.

It can be seen that for any given primary energy there is a wide spread in the number of charged mesons created. This is due in part to the fluctuation in the proportion of neutral mesons produced in an individual encounter [1]. The remaining fluctuation may be attributed to variations of the average energy with which the mesons are created. For a given primary energy and inelasticity K (i.e. a fixed amount of energy radiated) the number of mesons created is inversely proportional to their mean energy. Furthermore, one can expect fluctuations in K. These two types of fluctuation are implicit in Fermi's theory, and the resulting spread in multiplicity is in good agreement with the experimental results.

---

[1] In what follows we shall assume that the ratio of charged mesons to the total number of mesons $\frac{n_s}{N_s} = {}^2/_3$.

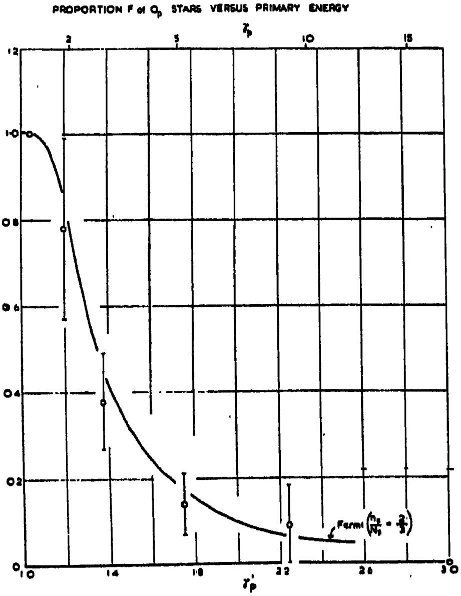

Fig. 2 – Proportion of "0_p stars" plotted as a function of γ_p, the total energy of the primary proton in terms of its rest energy. The curve represents the values predicted by Fermi's theory.

These data may be represented in alternative forms. The percentage of stars not containing shower particles (π-mesons of energy > 80 MeV and protons of energy > 500 MeV) is plotted as a function of primary energy in Fig. 2. The curve falls sharply above the threshold for meson production in a nucleon-nucleon encounter, reaches a value of 50 per cent at a primary energy of 2.6 BeV, and begins to flatten out above ~ 6 BeV.

At very low energies any elastic collisions which the incident nucleon may suffer will reduce its energy to such an extent as to make the probability of its second collision being radiative negligibly small. The steep part of the curve therefore gives an indication of how the elastic scattering cross-section falls off with primary energy. The curve drawn shows the values predicted from Fermi's statistical theory which, however, refers to mesons of all energies whilst the experimental points refer to mesons of energies > 80 MeV.

The stars in which the number of heavily ionising particles (N_h) is greater than 8 are certainly due to the disintegration of the heavy nuclei of the emulsion (silver and bromine). On the other hand, stars with N_h less than 8 can be due to the disintegration of both light and heavy nuclei and the exact proportion of the contribution from heavy nuclei is not accurately known. In Fig. 3 is plotted, as a function of primary energy, the average multi-

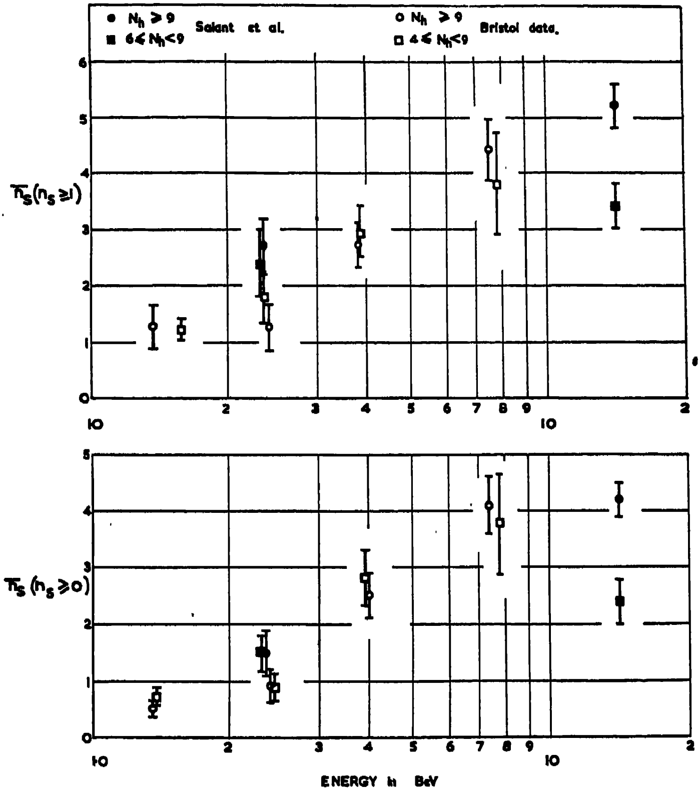

Fig. 3 – Observed variation of average multiplicity $\bar{n}_s$, with kinetic energy of primary in BeV, for stars of different prong number N_h.

plicity for these two classes of stars, while Fig. 4 shows the multiplicity curve irrespective of N_h. The results of SALANT *et al.* [1950] are also shown in Figure 3. These workers have determined the average multiplicity of stars of different N_h for primary energies

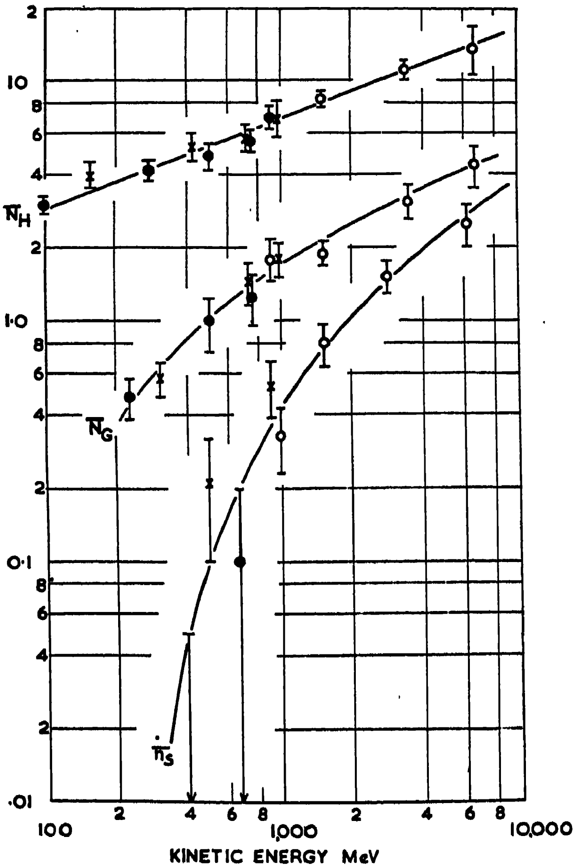

Fig. 4 – Variation of $\overline{N}_h$, $\overline{N}_g$ and $\overline{n}_s$ with the kinetic energy of the primary particle, × ; stars produced by π-mesons; ● proton initiated stars; o; stars initiated by "π-μ" particles.

greater than 1 BeV and greater than 8 BeV. The average multiplicity for a star produced by a primary particle having an energy between 1 and 8 BeV may therefore be calculated.

At high primary energies there is a significant difference between the average multiplicity of stars with $N_h < 9$ and $N_h \geqslant 9$. A similar result has been obtained from a cloud chamber study of nuclear disintegrations caused by high energy nucleons in light and heavy elements (LOVATI, MURA, SALVINI, and TAGLIAFERRI [1950]; GREGORY and TINLOT [1951]).

1.4 The production of neutral mesons

It has been known for some years that energetic electronic showers are frequently associated with showers of penetrating particles observed in cloud chamber and counter systems. Careful work with cloud chambers (FRETTER [1949], CHAO [1949], COCCONI [1949], GREGORY, ROSSI and TINLOT [1950], GREGORY and TINLOT [1951]) established that these showers were in general initiated by photons; it was not possible to decide whether the gamma rays were emitted directly from the disintegrating nucleus or were the decay products of neutral mesons emitted together with the charged mesons. However, recent work at Berkeley (BJORKLUND, CRANDALL, MOYER and YORK [1950], STEINBERGER, PANOFSKY and STELLER [1950]) seems to provide decisive evidence for the production of neutral mesons. Their mass has been shown to be $264 \pm 14\, m_e$ (PANOFSKY, AAMODT and YORK [1950], PANOFSKY, AAMODT, HADLEY and PHILLIPS [1950]), and their lifetime is probably less than 5×10^{-14} sec. (CARLSON, HOOPER and KING [1950] (V)).

An estimate of their frequency of occurrence in penetrating showers compared with the number of charged π-mesons has been made by CARLSON *et al.* [1950] (V), from a consideration of the number of related electron pairs found near penetrating showers in photographic emulsions. A value of 0.45 ± 0.1 was obtained. From a similar study using a cloud chamber TINLOT and GREGORY [1951] obtained a figure of ~ 0.37. Both these results refer to showers of $n_s \geqslant 3$, corresponding to a mean multiplicity of ~ 4.5. CAMERINI *et al.* [1951] (VI) made an analysis of the energy balance in the showers. For those with $n_s \leqslant 4$ (average multiplicity $= 1.1$) the ratio of the number of neutral to charged mesons was found to be 1.1 ± 0.4. The available evidence therefore indicates that at high primary energies the ratio of neutral to charged mesons is $\sim \frac{1}{2}$. The higher value of this ratio obtained for smaller multiplicities can be explained in terms of the following considerations:

(a) in collisions where only a single meson is produced the assumption of charge independence of nuclear forces leads to a ratio $\frac{3}{4}$;

(b) by selecting showers of small *charged* multiplicities one preferentially selects showers with higher neutral to charged ratio.

1. 5 Comparison of multiplicity — primary energy relationship with theory

It is now of interest to compare the results given in the previous section with the predictions of the existing theories of meson production in order to determine if it is possible to distinguish between them.

(a) *Comparison with the plural theory of Heitler and Janossy*

In the plural theory, the total multiplicity is given by the number of encounters, N_s, made by the primary particle in traversing the nucleus, since only one meson is assumed to be created at each collision. We have, if γ_p is the total energy of the primary nucleon in units of the rest energy,

$$N_s = \frac{\log(\gamma_p - 1) - \log(\gamma_c - 1)}{-\log(1 - \sigma)} + 1 \tag{1}$$

where γ_c is the cut-off energy below which the primary cannot generate further mesons, and where σ (a constant) is the fractional kinetic energy loss of the primary at each collision; Heitler takes $\sigma = 0.25$. The recoil nucleon and the meson created in the collision take, respectively, a fraction α and $(\sigma - \alpha)$ of the primary energy. γ_c is, of course, arbitrary. However, if only those mesons of total energy $\gamma_s > 1.7$ (shower particles) are considered, then the cut-off is given by

$$(\sigma - \alpha) R (\gamma_c - 1) = 1.7; \quad R = \frac{M_p}{M_\pi} = 6.7$$

so that the multiplicity curve is fixed by σ and α only. Heitler further assumes $\alpha = \sigma - \alpha = \frac{1}{8}$, from which $\gamma_c = 3.1$. The relation (1) is plotted in Fig. 5 and shows good agreement with the experimental data.

At high primary energies, the recoil nucleons themselves can produce mesons; the number in the second generation can be estimated and is also shown in Fig. 5. The observations however, do not extend to sufficiently high energies to enable one to differentiate between the two curves. Also included in this figure are the data from showers produced by α-particles of known energy

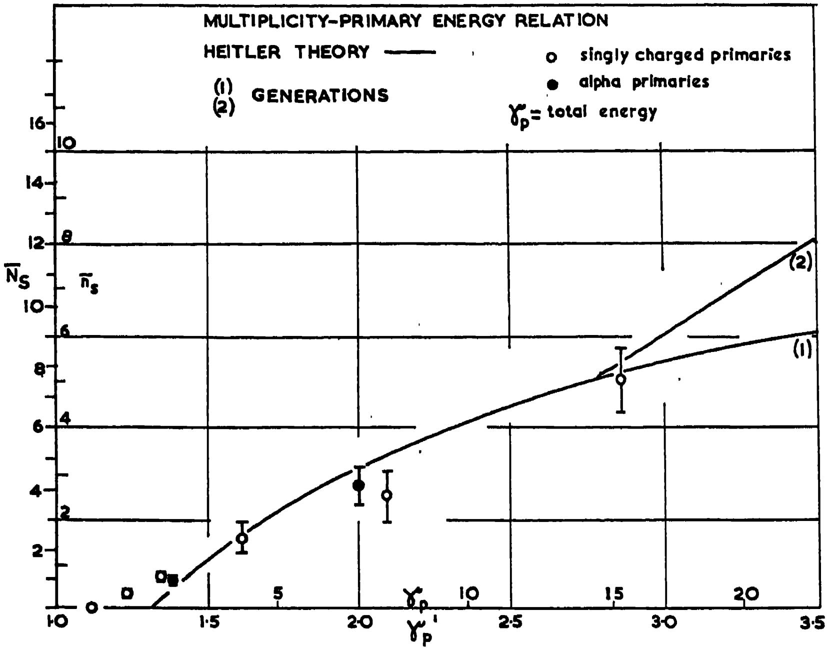

Fig. 5 – Variation of average multiplicity with primary energy; comparison of the experimental results with the predictions of the plural theory. γ_p = total energy of primary proton in terms of its rest energy. For the α-particles, the multiplicity per nucleon is plotted against energy per nucleon.

in which the multiplicity per nucleon is plotted against energy per nucleon. The agreement between these data and that for single charged primaries is good. This suggests that, as one would have expected, the four nucleons of the α-particle behave (as far as meson production is concerned) independently of each other.

(b) *Comparison with the multiple theory*

The variation of n_s with primary energy on the basis of Heisenberg's theory for different values of the inelasticity of the collision K has also been computed. Heisenberg defines the inelasticity as the ratio of the energy radiated in mesons in the centre of mass system of the two colliding nucleons, to the maximum amount of energy available in this system.

The results are shown in Fig. 6. At low energies, it is necessary to assume a small mean value of K in order to obtain agreement with the experimental data. A proportion of the collisions will clearly be completely elastic ($K = 0$) and the remainder will correspond to a finite value, which from energetic considerations must be near unity. At high primary energies, if one assumes only a single meson-producing collision in the nucleus, a higher mean value of K must be invoked. In fact, from considerations of equipartition of momentum, one expects a mean value of K near to unity at sufficiently high multiplicities.

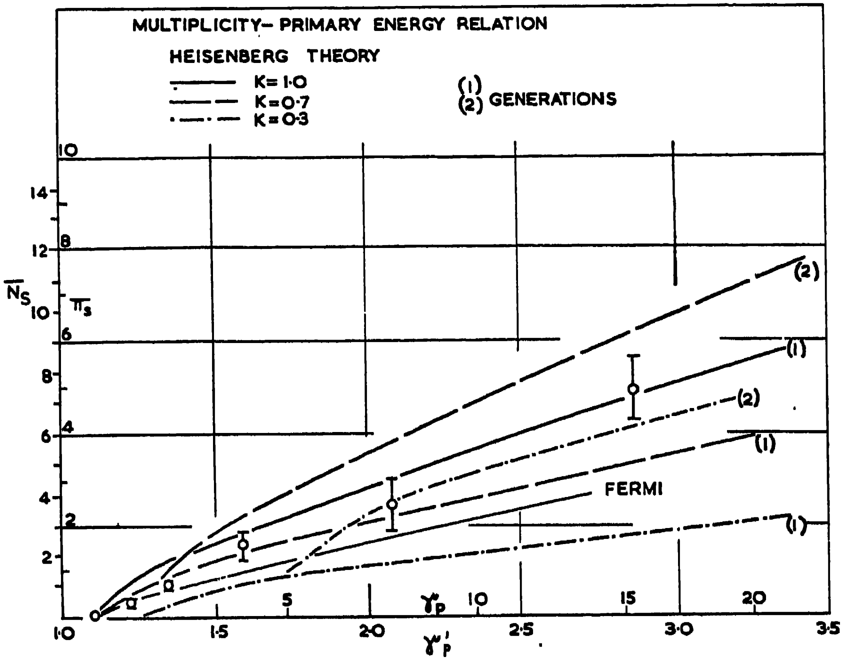

Fig. 6 – Variation of average multiplicity with primary energy; comparison of the experimental results with the predictions of the multiple theory.

$$\gamma'_p = \sqrt{\frac{\gamma_p + 1}{2}} = \text{energy of nucleon in C-system.}$$

The yield curve, according to Fermi's theory is also given in Fig. 6. The values of n_s at high energies appear somewhat low, though presumably the agreement could be improved by a suitable choice of his parameters.

Secondary collisions

Better agreement between the observations and the predictions of the Fermi or the Heisenberg theory for small K may be obtained by assuming more than one collision in the nucleus, i.e. secondary generation of mesons by nucleons (or mesons) recoiling from the first collisions.

The result of such a calculation is given in Fig. 6 for the above three values of K, where only further nucleon-nucleon collisions have been considered. In making the calculations an infinitely large nucleus (or a sufficiently high cross-section) was assumed. The results therefore, represent an upper limit to the average multiplicity, n_s. In the region below a primary energy of about 2 BeV there is only sufficient energy to produce on the average a single meson, and all theories must lead to the same result.

1. 6 Variation of N_h and N_g with primary energy and multiplicity

In the previous sections the variation of the number of shower particles, n_s, with primary energy has been considered. It is also possible to determine the variation of the number of heavily ionising particles, N_h and of the number of "grey" particles, N_g, with primary energy. The results obtained by CAMERINI *et al.* [1951] (VI) are shown in Fig. 4.

At present, reliable measurements of the primary energy extend only up to about 15 BeV. The only information available at higher primary energies is the variation of different star parameters with the multiplicity, n_s. The results obtained by Camerini *et al.* are shown in Fig. 7; they will be discussed in a later section (§ 3. 3).

From the data shown in Fig. 7 it is possible to estimate, taking neutrons into account, an upper limit for the total number of knock-on nucleons as a function of the number of shower particles, n_s. The increase in the number of "knock-ons" is thus found to be less than 1 per charged meson created; the mean rise is only 0.5 per meson. Bearing in mind the fact that this represents an upper limit, and that there is at least one neutral meson for every two charged, one arrives at a figure of less than 0.3 observed knock-ons per meson created.

Now nucleons of energy less than 1.5 BeV will, when crossing a nucleus, lose most of their energy in elastic collisions, giving rise to "black" and "grey" particles. The nucleons which recoil from the meson producing collisions would, on the hypothesis of Heitler and Janossy, frequently have energies below this value. One would thus expect the energy appearing in the star ("black" and "grey" particles) to increase linearly with the number of recoil nucleons. The original plural theory of Heitler and Janossy predicted about one recoil nucleon for each meson created, and is thus inconsistent with the experimental results.

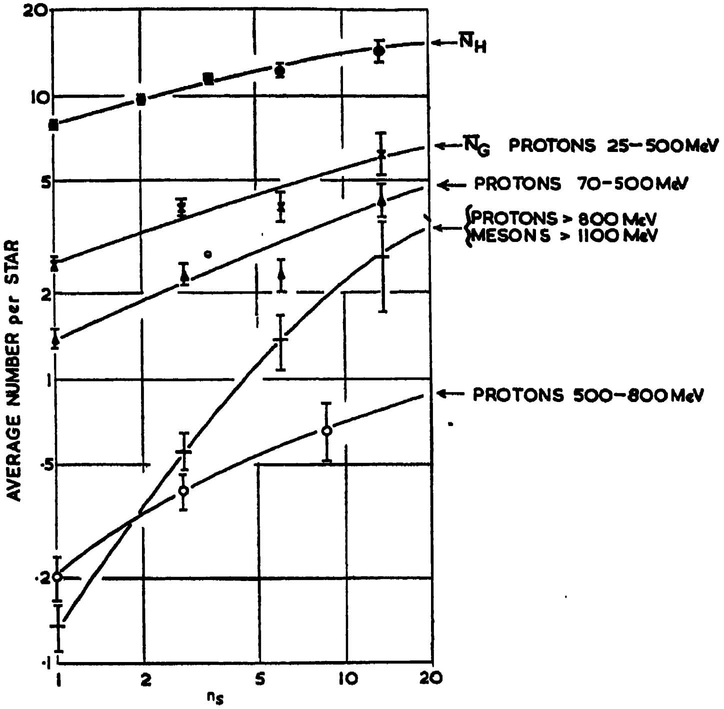

Fig. 7 – Variation with multiplicity of the number of protons and mesons of different energies, and of the number of heavily ionizing particles $\overline{N}_h$.

However, it has been pointed out by **Heitler** and **Therreaux** (**Heitler** [1950, 1951]) that if many-body collisions are taken into consideration, it is possible to reduce substantially the number of recoil nucleons. This would bring the predictions of the plural theory into agreement with the experimental results.

2. Meson-nucleon interaction

In the previous section we have considered the creation of mesons in nucleon-nucleon collisions. We shall now summarise the available experimental evidence about meson-nucleon interactions.

2. 1 The collision mean free path

The cross section for interaction of mesons with nuclear matter has been determined by many workers using a variety of techniques and the results obtained are summarised in Table 1. The earlier discrepancy between the results obtained by the use of cloud chambers and by the use of photographic emulsions now appears to have been removed, (Lovati, Mura, Succi and Tagliaferri [1951], Gregory and Tinlot [1951]). It seems reasonable to assume that the high results for the mean free path obtained by some cloud chamber workers were due partly to insufficient allowance being made for interactions fully contained within the absorbing material in the interior of the cloud chamber, and partly to the bias introduced by the counter selection system. An example of the bias towards the selection of high energy events introduced using cloud chamber techniques is shown in Fig. 8. This

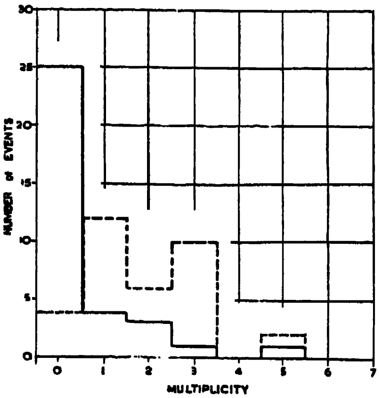

Fig. 8 – The multiplicity distribution of secondary stars produced by shower particles. ··· results obtained by Lovati *et al.* in a cloud chamber containing thin foils of absorbing materials; — the distribution observed by Lock and Yekutieli using photographic emulsions.

TABLE 1

Method	Authors	*Mean free path*		Energy range (MeV) (for mesons)
		Observed ($gm.cm.^{-2}$)	Ratio Obs./ Geom.	
Counter system at mountain altitudes	Piccioni	1200 (Fe)	14.0	> 400
Cloud Chamber at mountain altitudes	Fretter	750 (Pb) (uncorrected)	4.7	> 150 ($n_s \geqslant 2$)
	Brown & McKay	316 ± 70 (Pb)	2.0	> 150
	Hartzler	230 ± 60 (Au)	1.5	> 1000
	Lovati et al. [1950]	300 ± 100 (Pb) (corrected)	1.9	> 150 ($n_s \geqslant 2$)
	Lovati et al. [1951]	200 ± 50 (Pb) (corrected)	1.25	> 150 ($n_s \geqslant 2$)
	Gregory & Tinlot	172 ± 30 (Pb) 164 ± 50 (Al)	1.1 2.0	($n_s \geqslant 3$)
Cloud Chamber at sea level	Butler, Rosser & Barker	400 (Pb) (uncorrected)	2.5	> 1000
	Butler & Barker	200 (Pb) (corrected)	1.25	> 1000
Photographic emulsion	Harding & Perkins	120 (Ice)	2.0	> 100
	Camerini et al.	100 ± 30 (emulsion)	1.1	> 100
	Lock & Yekutieli	110 ± 25 (emulsion)	1.2	> 100
	Bernadini et al.	115 (emulsion)	1.3	30–50 70–90

shows the multiplicity distribution of the secondary stars as observed by Lovati *et al.* [1951] using a cloud chamber and by Lock and Yekutieli [1951] using photographic emulsions.

It thus seems well established that the value of the cross-section is between 60 and 100 % of the geometrical value for energies up to about 5 BeV.

2. 2 Stars produced by identified π-mesons

In this laboratory, Lock and Yekutieli [1951] have made a study of stars produced by π-mesons of kinetic energy between 0 and 1 BeV. The variation of N_h and N_g with primary energy for such stars is included in the data given in Fig. 4. A comparison with stars produced by identified protons of similar energy (see also Fig. 4) shows that protons and mesons lose approximately the same amount of energy in such collisions.

Preliminary results indicate that in approximately half the cases the incident π-meson emerges from the nucleus. In the majority of such cases its fractional energy loss appears to be very great; some typical examples observed are given in Table 2. This suggests that the incident meson must, in general, suffer more than one collision in its passage through the nucleus. Similar results have been obtained by Bernadini, Booth, Lederman and Tinlot [1950b] from a study of the nuclear scattering of π-mesons of between 70 and 90 MeV kinetic energy.

TABLE 2

Star Type	Kinetic Energy of Incident Meson. MeV.	Kinetic Energy of Outgoing Meson. MeV.	Percentage Energy Loss.
$2 + 0\,\pi$	80	67	16
$3 + 1\,\pi$	295	185	37
$1 + 1\,\pi$	490	305	38
$7 + 1\,\pi$	670	40	94
$6 + 0\,\pi$	740	70	90
$6 + 1\,\pi$	760	430	43
$5 + 0\,\pi$	840	20	98
$6 + 0\,\pi$	950	30	97
$3 + 1\,\pi$	1085	135	88
$3 + 2\,\pi$	1085	365	66
		375	65

When no meson is observed to be ejected from the disintegration, the incident meson has either been absorbed or lost its charge.

One case has been observed in which a π-meson of kinetic energy 1.1 BeV produced a disintegration in which two π-mesons are ejected (Plate I). From energy considerations the event may be explained on the hypothesis of direct creation of a meson in a meson-nucleon encounter (HEITLER and JANOSSY [1950]).

2. 3 The interactions of π-mesons of energy greater than 1 BeV

It is difficult to obtain direct evidence of the behaviour of π-mesons of energy greater than 1 BeV, since there is as yet no means whereby they may be distinguished from relativistic protons. However, since at least 50 per cent of the shower particles with energy greater than 1 BeV are probably π-mesons (BUTLER and BARKER [1951]) indirect evidence may be obtained from a study of the interactions of the energetic secondary particles of penetrating showers.

ROSSER and SWIFT [1951] have exposed photographic plates above and below 30 cm of lead at an altitude of 2860 m. These workers find that for showers with two or more penetrating particles ($n_s \geqslant 2$) the ratio of charged primaries to neutral primaries is 0.86 ± 0.21 above the lead and 1.76 ± 0.48 below the lead. They suggest that the increase in the number of showers with charged primaries may be due to fast π-mesons produced in the lead. The average energy of a primary nucleon which produces a penetrating shower of $n_s = 2$ is of the order of 4 BeV. If the showers observed are produced by nucleons "knocked-on" by the π-mesons, the incident π-mesons must have energies much greater than 4 BeV. The number of π-mesons of such great energy does not appear to be sufficient to explain the magnitude of the effect observed. The results may be explained if it is assumed that π-mesons of energy greater than 1 BeV can produce showers of π-mesons directly in meson-nucleon collisions. The cross-section of the nucleus for this process would have to be approximately geometrical.

2. 4 Conclusions

The evidence presented in the preceding sections establishes that, over a wide range of energy, π-mesons have a strong interaction with nuclear matter, with a cross-section of the order of the geometrical value. The π-mesons, when of sufficient energy, can themselves lead to the creation of further mesons.

3. PROPERTIES OF THE SHOWER PARTICLES

3.1 Lorentz transformation to centre of mass system (multiple theory)

In favourable cases it is possible to measure the energy of both the primary and one or more of the secondaries of a shower. It is then possible to determine the energy spectrum and the angular distribution of the mesons created in the centre of mass system on the basis of the following assumptions:

(a) All the mesons are produced in a single nucleon-nucleon collision

(b) The shape of their energy spectrum in the C-system does not depend on the energy of the primary particle, up to a cut-off energy which is equal to the maximum possible energy of ejection of a single meson.

(c) The loss of energy and change in direction of the mesons in their passage through the nucleus can be neglected.

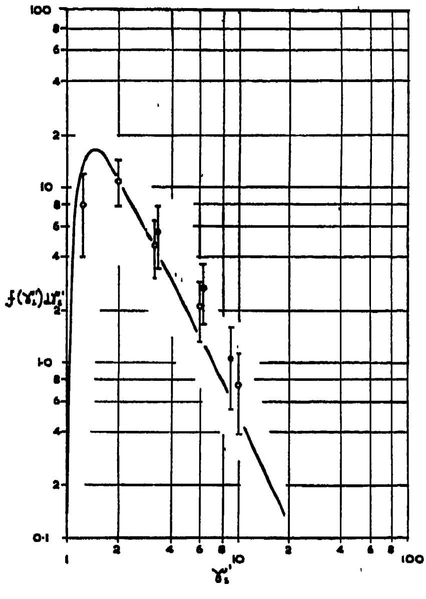

Fig. 9 – The energy spectrum of the mesons in the C-system derived on the assumption of a single nucleon-nucleon collision. γ_s' is the total energy of the meson in terms of the rest energy.

⧳ K = 0.5; ⧲ K = 1.0. The curve represents the spectrum $\sqrt{\gamma_s'^2 - 1}.\,/\gamma_s'^3 d\gamma_s'$.

The energy spectrum in the centre of mass system obtained by CAMERINI *et al.* [1951] (VI) under the above assumptions is shown in Fig. 9 for $K = 1$ and $K = 0.5$. It can be represented analytically by a differential distribution $f(\gamma_s')d\gamma_s'$ which falls off at high energies as $d\gamma_s'/\gamma_s'^2$. This is in reasonable agreement with the spectrum assumed by Heisenberg. The angular distribution of the mesons in the C-system is consistent with an isotropic distribution; the ratio of "backward" to "forward" mesons is 0.95 ± 0.44. In § 3. 3 it is shown that in fact the mesons must suffer some scattering in their passage through the nucleus, and that while no great significance can then be attached to the "angular distribution in the C-system" determined above, the form of the energy spectrum is not greatly affected.

3. 2 Energy and angular distributions of the shower particles

It has not been possible to determine the angular and energy distributions of the shower particles as a function of primary energy since the number of stars with measured primaries is small. Instead, the distributions have been referred to the star parameters N_h and n_s. It is an unfortunate feature of the analysis that n_s is a very poor index of the primary energy (see for example, Fig. 1).

Energy distribution

For energy considerations we may divide the shower particles into three groups, viz:

(i) Identified mesons, π_s of kinetic energy between 80 and 1100 MeV.

(ii) Identified protons, p_s, of kinetic energy between 500 and 800 MeV. Since they are few in number, they will not be discussed here.

(iii) Particles with a mean angle of scattering, $\bar{\alpha}$, less than 0.0226 degrees per 100 μ. For smaller values of the scattering the grain densities of mesons and protons become equal so that the two types of particle are indistinguishable. We therefore call these particles $\pi - p$.

The energy distribution of the shower particle mesons, π_s, has been determined by CAMERINI *et al.* [1950] (IV) and their results are shown in Fig. 10. Included in this figure are the differential energy distributions of protons from 30 to 800 MeV and of deuterons and tritons between 50 and 800 MeV.

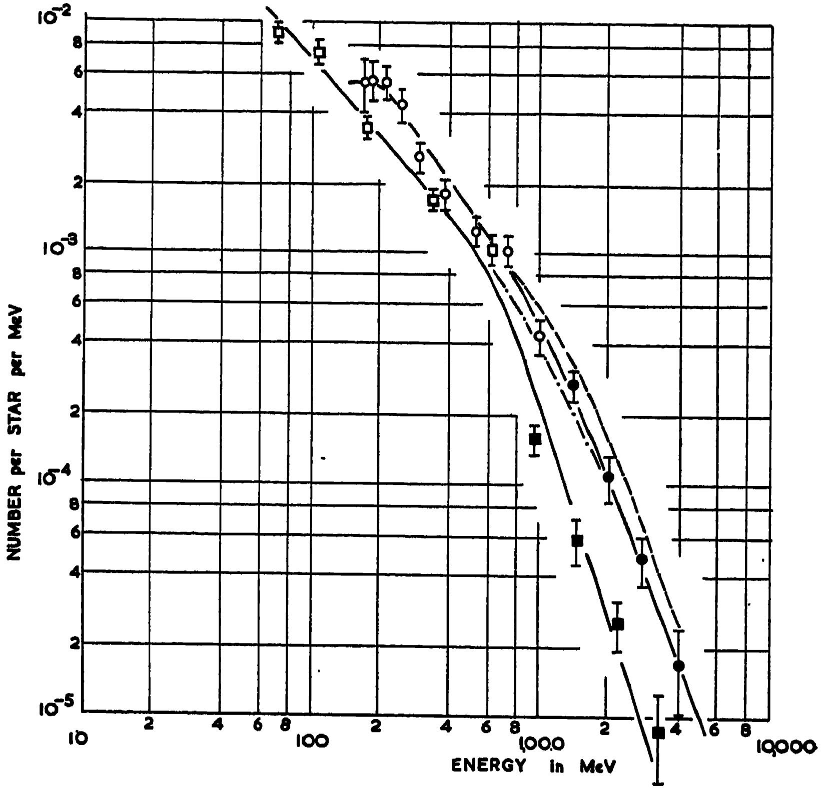

Fig. 10 – The full lines show the differential energy spectrum of mesons and protons ejected from stars of $n_s \geqslant 1$ (mesons plotted against total energy)

Mesons ○ Estimated mesons ●

Protons □ Estimated protons ■

– – – indicates spectrum of π-mesons if all π-p particles are mesons.

–·–· indicates spectrum of protons if all π-p particles are protons.

The spectrum of the identified mesons can be represented by the expression $N(E)dE = E^{-1.4}\,dE$ (E = total energy) in the energy region between 200 and 1100 MeV, and its shape seems not to depend strongly on N_h or n_s. This observation is, however, subject to large statistical uncertainty.

At higher energies it is not possible to determine the energy spectra of the mesons and protons separately. **Camerini** *et al.* [1950] (IV) estimate that about 66 % of the "$\pi - p$" particles are π-mesons, in good agreement with the results obtained by **Butler** and **Barker** [1951] using a cloud chamber.

TABLE 3

Average Total Energy of Shower Particles $(\pi_s + (\pi\text{-}p) + p_s)$ as a function of N_h & n_s.

n_s	1	2 – 4	> 4
$\bar{E}$	750 ± 40 MeV	850 ± 40 MeV	910 ± 45 MeV
N_h	3 – 8	9 – 14	14
$\bar{E}$	855 ± 40 MeV	755 ± 55 MeV	730 ± 45 MeV

The number of $\pi - p$ particles per shower particle is shown as a function of N_h and n_s in Table 3. There is a significant increase in their frequency of occurrence in large showers (n_s) and a decrease for increasing size of star (N_h). The latter result is an indication that secondary interactions must occur within the nucleus.

The average energy of the shower particles has been computed for the different star types, and the results are shown in Table 4. The variations throughout this table are entirely due to the different proportions of high energy particles as shown in Table 3.

TABLE 4

Number of π-p-particles per Shower Particle

	$3 \leqslant N_h \leqslant 8$	$N_h > 8$	$N_h > 2$
$n_s = 1$	0.15 ± 0.04	0.09 ± 0.05	0.13 ± 0.03
$2 \leqslant n_s \leqslant 4$ . .	0.22 ± 0.05	0.22 ± 0.05	0.22 ± 0.03
$n_s > 4$	0.41 ± 0.09	0.14 ± 0.04	0.23 ± 0.04
n_s (all)	0.23 ± 0.03	0.16 ± 0.02	0.20 ± 0.02

Angular distribution

The angular distribution of the shower particles with respect to the primary has been determined for more than one thousand stars (**Camerini** *et al.* [1951] (VI)). The resulting distribution, plotted as a function of n_s, is shown in Fig. 11, and as a function of N_h in Fig. 12.

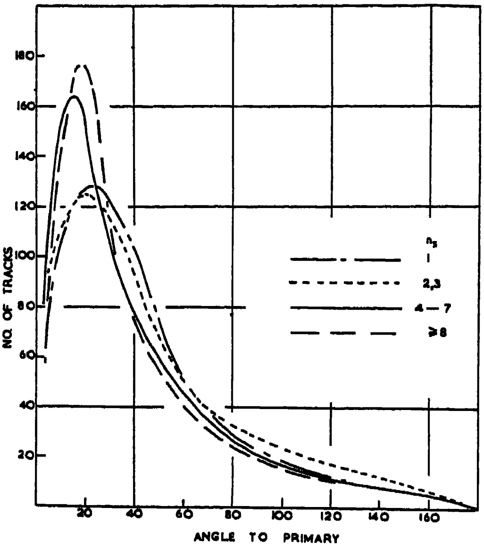

Fig. 11 – The angular distributions of shower particles in the laboratory system for different ranges of multiplicity. The ordinate gives the number of tracks per angular interval.

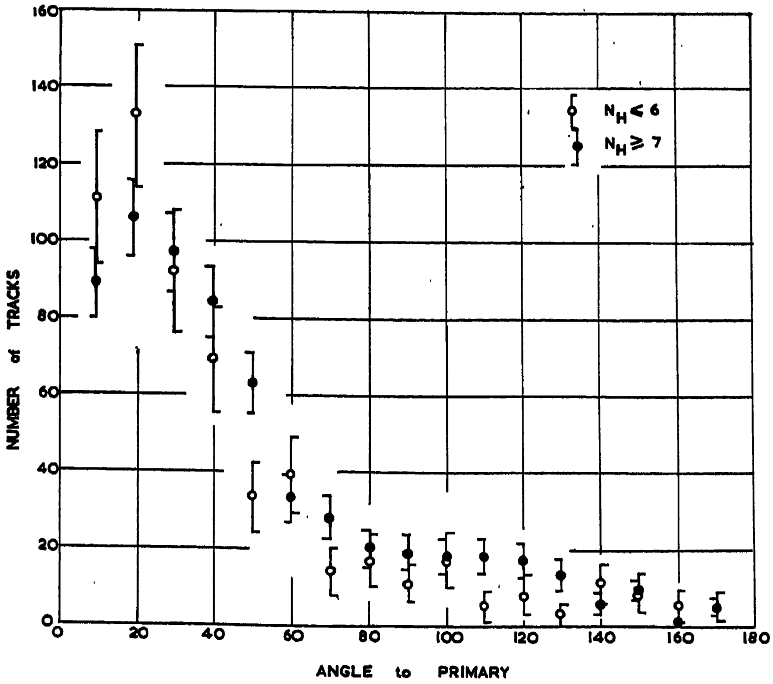

Fig. 12 – The angular distribution of shower particles for stars of $N_h \leqslant 6$ and $N_h \geqslant 7$.

The median angle η of the distribution decreases slowly with increasing n_s, (Fig. 11). A similar result has been obtained by Osborne [1951]. The curve indicates the variation expected from the assumption of multiple production (single collision). There is reasonable agreement with observations at low multiplicity. At high multiplicity the discrepancy is indicative of secondary effects.

The proportion, B, of mesons projected backwards in the laboratory system is much greater than can reasonably be expected on the basis of a single collision (Fig. 13). Furthermore, the angular distribution in the backward hemisphere is almost isotropic in the laboratory system.

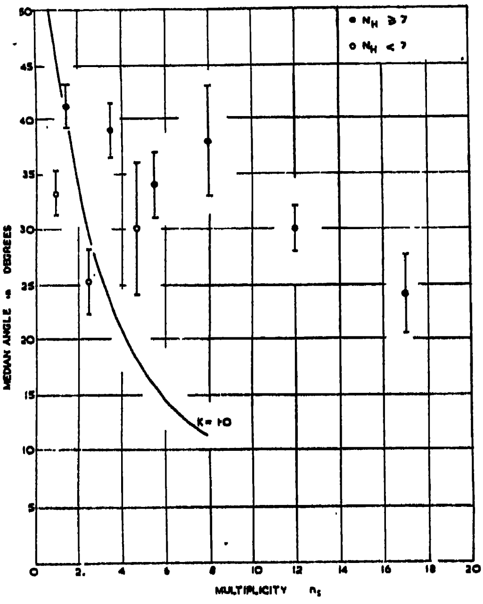

Fig. 13 – The variation of the median angle of the showers with the multiplicity, for stars of $N_h \leqslant 6$ and $N_h \geqslant 7$. The curve shows the variation expected on the assumption of multiple production in a single nucleon-nucleon collision ($K = 1.0$).

The value of B depends strongly on the value of N_h. For stars with $N_h \leqslant 7$ it is equal to $0.113 \pm .016$ while for stars of $N_h \geqslant 8$ it is $0.171 \pm .012$.

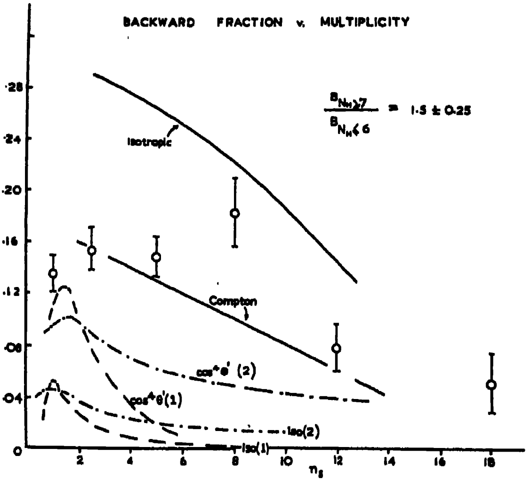

Fig. 14 – The variation of backward fraction with multiplicity. 'iso'.... calculated variation on the assumption of pure multiple production with isotropic angular distribution of the mesons in the C-system of the colliding nucleons for (1) and (2) generations. '$\cos^4\theta$''.... variation calculated on the assumption of an angular distribution in the C-system of form $\cos^4\theta'\sin\theta'd\theta'$. The full line curves indicate the fraction projected backward on the assumption that each meson is elastically scattered by a nucleon in its exit through the nucleus, either by Compton-type scattering, or by scattering isotropic in the C-system of meson and nucleon, with cross-section independent of energy.

Discussion

Camerini *et al.* [1951] (VI) have shown that multiple small angle scattering in the nucleus of mesons produced in a single nucleon-nucleon collision cannot explain the main features of the angular distribution of the shower particles, viz: —

(a) The backward mesons are almost isotropic in angular distribution and strongly depend in intensity on N_h; whereas,

(b) the angular distribution of the forward mesons is but little dependent on N_h; and

(c) both η and B vary slowly with n_s.

It thus seems that in order to obtain agreement between the observed angular distribution and the multiple theory one has to assume one or both of the following hypotheses:

(i) A small percentage of the mesons are elastically scattered in collisions with nucleons with an angular distribution which is isotropic in the centre of mass system. The cross-section per nucleon for this process must be of the order of 10 % of the geometrical value. In general, few mesons are lost or created.

(ii) Secondary generations occur, i.e. both nucleons and mesons, in collisions with nucleons, produce further mesons.

It is not possible at the present time to determine if the predictions of Therreaux will agree with the above features of the angular distribution of the shower particles.

3. 3 The interaction of the shower particles with the nucleus

The experimental results presented in § 1. 6 showed that both N_h and N_g vary only slowly with multiplicity. For a shower with two shower particles the average number of "grey particles" is ~ 3, while for a shower with twenty shower particles this figure has only risen to ~ 7. It thus seems that only a very small fraction of the mesons created can interact with the nucleus before they escape from it (for a meson of energy 800 MeV commonly makes a star with ~ 6 heavy branches when it interacts with nuclear matter), (LOCK and YEKUTIELI [1951]). This conclusion is in contradiction with the evidence for a strong interaction between mesons and nuclear matter presented in § 2.

It seems unlikely that this discrepancy can be due to a quantum interference of the mesons tending to decrease their field of force, nor does it seem likely that "soaking" of the nucleus occurs at any but the highest multiplicities. By "soaking" of the nucleus we mean the following effect: the volume of that part of the nucleus which is being crossed by the shower particles is, in general, small and thus will contain few nucleons. If the number of shower particles is of the same order of magnitude as, or greater than the number of nucleons in this volume, the fractional energy loss of the shower particles to the nucleons may become considerably smaller than the value to be expected from the results shown in § 2.

Alternatively, it may be postulated that only a few high energy mesons are produced in the original nucleon-nucleon collisions. These subsequently reproduce themselves in collisions with nucleons, giving rise to a greater number of lower energy mesons. It seems possible that these final collisions may take place sufficiently close to the surface of the nucleus for the mesons created to escape from it without losing an appreciable proportion of their energy. Thus both the main features of the angular distribution and the lack of interaction of the shower particles would be explained.

4. INDIVIDUAL HIGH ENERGY EVENTS

Several events have been found in photographic emulsions exposed to the cosmic radiation which have been characterized by the ejection of a large number of relativistic particles. These events have, in general, been interpreted as providing evidence for the multiple production of mesons. However, it has been shown by Heitler and Therreaux, (HEITLER [1950, 1951]) that such events can also be explained in terms of the modified plural theory mentioned in § 1. 6.

4. 1 Stars produced by neutrons and singly charged primary particles

A star of type $27 + 27\,n$ was observed by LEPRINCE-RINGUET, BOUSSER, HOANG-TCHANG-FONG, JAUNEAU and MORELLET [1949]. On the assumption that 17 of the relativistic particles were mesons, these authors concluded that pluro-multiple production of the mesons probably occurred.

LORD, FAINBERG and SCHEIN [1950] have published an analysis of a star of type $2 + 15\,p$ in which seven of the shower particles were emitted in a very narrow central cone (half width .003 rad.). The remaining eight shower particles were emitted in a much more diffuse cone. The energy of the primary particle, assumed to be a proton, was calculated from the half width of the central cone and found to be of the order of 3×10^4 BeV. Only one of the two heavily ionizing tracks could be attributed to a nucleon ejected by a process of evaporation, which indicated that the reaction took place in a nucleus of a light element present in the emulsion. The fact that 15 shower particles were observed was therefore considered as evidence for multiple production, while the low multiplicity for the high primary energy involved favoured the theory of Fermi.

A star with a minimum of 95 prongs has recently been observed by LORD and SCHEIN [1951] and is shown in Fig. 15. The energy of the primary particle was estimated to be 3 × 10^3 BeV, and from charge considerations at least 55 mesons were created.

In this laboratory Davies and Perkins (unpublished) have analysed in detail an event of type 8 + 41 *p* (Plate II) observed in a photographic emulsion exposed under 30 cm. of lead at the Jungfraujoch. Of the 41 shower particles, 27 possessed tracks of sufficient length in the emulsion for their energy to be determined by scattering measurements. In this way one of the particles was identified as a proton, 8 as mesons, and the remaining 18 as "$\pi - p$" particles. From their mean energy the total energy associated with

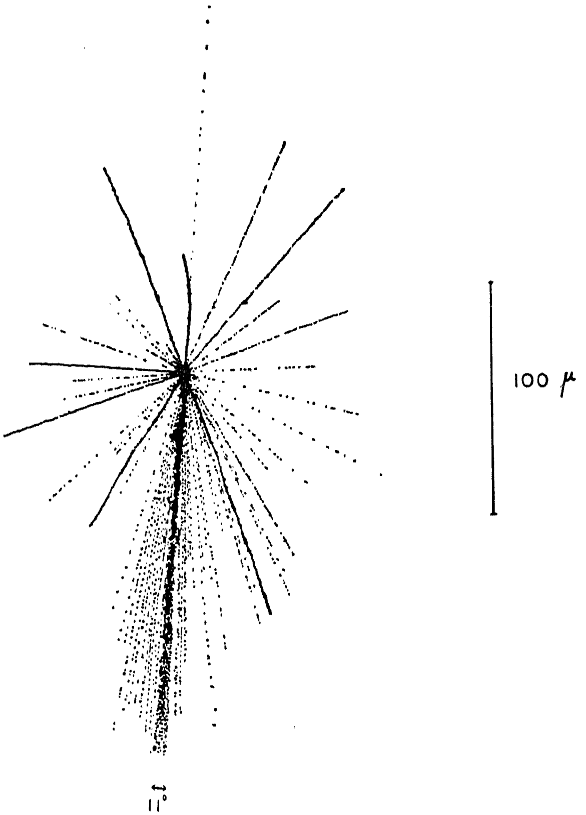

Fig. 15 – A star with at least 95 prongs observed by Lord and Schein in a photographie emulsion exposed at 95,000′.

the shower particles was estimated to be 90 BeV, which corresponds to approximately 140 BeV when allowance is made for the production of neutral mesons. This is therefore a lower limit for the energy of the primary particle.

On the hypothesis of pure multiple production, the half angle of the forward cone of the shower particles in the laboratory system would be less than 6°. The observed value was 12°, only 30 ± 10 % of the shower particles falling within a 6° cone. On the basis of a multiple theory this may be regarded as evidence for the existence of secondary processes. However, it seems likely that this observation also is not inconsistent with the predictions of the plural theory.

4. 2 Stars produced by fast α-particles

A shower containing some 56 singly charged relativistic particles (type $18 + 56a$) produced by a primary α-particle of energy between 10^3—10^4 BeV has been observed by BRADT, KAPLON and PETERS [1950]. Approximately half of the shower particles were concentrated in a narrow core of 1.5° half width, the remainder being spread out over an angular interval of ± 60°. It was shown that these features of the event could be explained by the assumption of multiple meson production in primary, secondary and tertiary encounters in the target nucleus. It is considered by Heitler that this particular event may also be explained in terms of the plural theory.

Many other examples of nuclear disintegrations caused by fast α-particles have been found by various workers. However, a detailed examination of the characteristics of such events, and of those produced by particles of greater charge, has not yet been carried out. Some examples of such events are given in the article by Dr B. Peters in this volume, (Peters' Fig. 10 is the shower referred to above).

5. CONCLUSIONS

From a consideration of the evidence of various workers which has been presented in the previous sections, we may formulate the following general conclusions: —

(1) At low primary energies (< 1 BeV) nucleon-nucleon col-

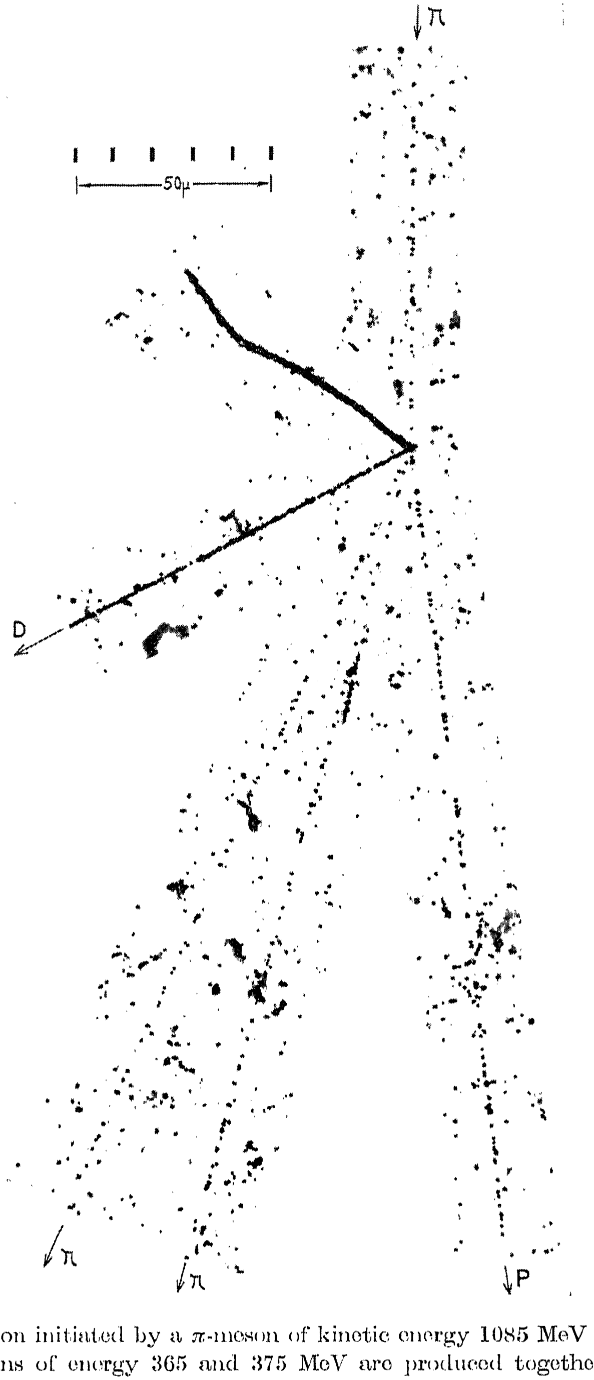

Disintegration initiated by a π-meson of kinetic energy 1085 MeV in which two π-mesons of energy 365 and 375 MeV are produced together with a proton of 270 MeV.

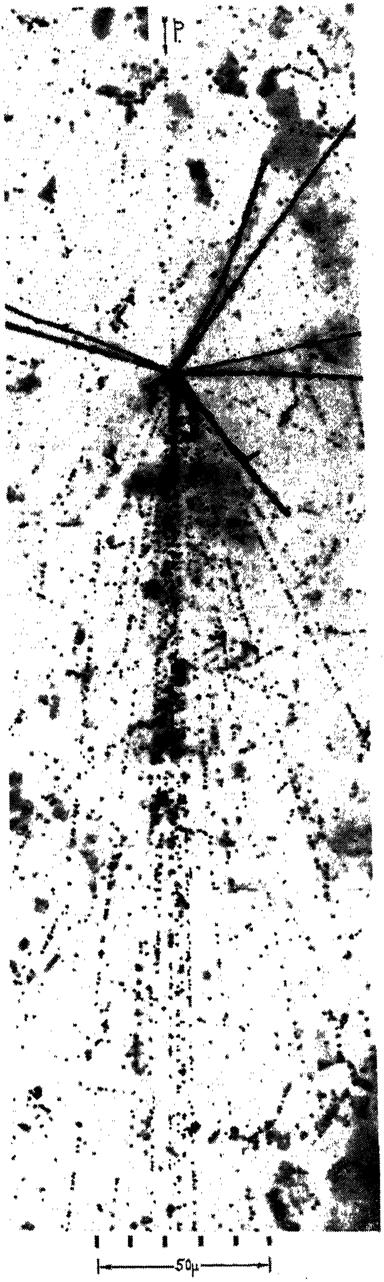

A star of type 8 + 41p. The energies of 27 of the secondaries have been determined.

lisions are, in general, completely elastic. The elastic and inelastic scattering cross-sections become comparable only at a primary energy of the order of 3 BeV.

(2) At a given primary energy there is a large spread in the number of charged mesons observed.

(3) The experimental results appear to be inconsistent with the predictions of the plural theory based on two-body nucleon-nucleon collisions. Agreement can, however, be obtained if many-body interactions are invoked (Heitler and Therreaux).

(4) Re-absorption of mesons in the same nucleus in which they were created is, in general, negligible, although this process may be responsible for the very large stars of small multiplicity. The cross-section for large angle elastic scattering of these mesons by nucleons is of the order of $\sim 10\%$ of the geometrical value, on the assumption that multiplication of the mesons in such collisions is not important. The energy transfer to the nucleus expected from this cross-section is in rough agreement with the data in Fig. 12 and Table IV.

(5) On the other hand, single fast π-mesons ($E < 1$ BeV) interact strongly with nuclear matter; in 50 % of the cases they emerge from the disintegrating nucleus having lost a large fraction of their energy. It is not possible to determine whether in the remaining cases the mesons are absorbed or suffer charge exchange.

(6) π-mesons of sufficiently high energy ($E > 2$ BeV) can, when in collision with a nucleus, lead to the creation of further mesons. This process probably occurs directly in a meson-nucleon collision.

(7) There appears to be a discrepancy between the small fractional energy loss suffered by a meson in emerging from the nucleus in which it has been created, and the large energy loss of an isolated meson in traversing nuclear matter. This may be explained by assuming that only a few high energy mesons are in general created in the primary collisions, and that these mesons undergo multiplication in subsequent meson-nucleon collisions.

(8) The data on the angular distribution of shower particles suggests that the hypothesis of multiple production of mesons in a single nucleon-nucleon interaction, with no further radiative collisions, is insufficient. More mesons must, in general, be produced in further nucleon-nucleon and meson-nucleon collisions.

PART II

ELASTIC COLLISIONS

6. INTRODUCTION

In the above discussion of the radiative collisions we have seen that a high energy primary nucleon can initiate, within the nucleus, a "cascade" of energetic mesons and nucleons. As this cascade develops through the nucleus the mean energy of the particles of which it is composed decreases. The radiation processes cease when the particles have energies below 1 BeV and thereafter only elastic collisions need be considered. Such particles are chiefly responsible for the repartition of energy among the remaining nucleons by means of successive collisions.

However, some of the nucleons will have succeeded in escaping after relatively few collisions, before a statistical distribution of energy throughout the nucleus has been attained. These particles will, in general, have energies between 25 and 1000 MeV (assuming them to be protons). Those of energy between 25 and 500 MeV, which constitute the great majority, correspond to the grey tracks; the remainder are shower particles. On account of the small number, and of the difficulty of identifying the particles of energy greater than 500 MeV, we shall limit ourselves exclusively to the study of the grey tracks.

7. FREQUENCY, ENERGY AND ANGULAR DISTRIBUTION OF FAST NUCLEONS (GREY TRACKS)

7.1 Frequency of grey tracks

A grey track has been defined as one produced by a particle of ionisation between 1.4 and 6.8 times minimum. These particles have been shown to be composed of 72 % protons, 22 % deuterons and tritons, 6 % mesons, and a negligible proportion of α-particles (CAMERINI *et al.* [1950]; IV). However, in this analysis we shall for simplicity assume all the grey tracks to be produced by protons.

We can express the relation between N_g and n_s as

$$N_g = K_1 + K_2 n_s; \; (K_1 = 2.5, \; K_2 = 0.4)$$

Some at least of the increase of N_g with increasing multiplicity ($K_2 n_s$) must be due to projection of nucleons by the mesons in their passage through the nucleus. The cross-section derived in § 3. 2 for this scattering is reasonably consistent with the above assumption. The remaining contribution to the number of greys must then be attributed to recoils knocked on in nucleon-nucleon collisions only.

Unfortunately, it does not seem possible to make reliable quantitative estimates about these nucleon-nucleon collisions nor to deduce the energy spectrum at production. Calculations of the number of particles emitted and of their energy spectrum have been made in the low energy region by Goldberger [1948], but the analysis is very lengthy and many of the assumptions made are necessarily arbitrary.

7. 2 Energy distribution of protons producing grey tracks

The energy distribution of the protons producing grey tracks is given in Fig. 10, and follows a power law of the form $dE/E^{2.5}$. The average energy also appears to be almost independent of primary energy (see Fig. 16) and of N_h (Camerini *et al.* [1951]; VI).

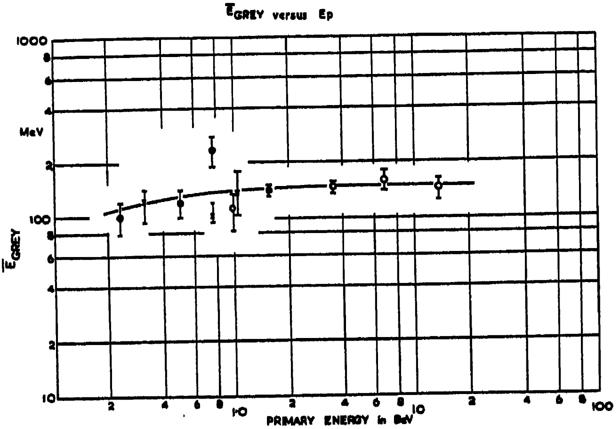

Fig. 16 – The average energy of a "grey" proton as a function of primary energy for stars initiated by mesons (×), by protons (●), and by "π-p" particles (○).

7. 3 Angular distribution of grey tracks

The angular distribution, with respect to the primary, of the "grey" particles is shown in Fig. 17 (Camerini *et al.* [1951]; VI). Most of the grey tracks originated in stars containing shower particles and the total of 1500 tracks has been divided into 3 regions of energy. The degree of collimation increases with increasing energy of the "grey" particles. A similar result has been obtained by Crussard [1950], Harding [1951] and Osborne [1951]. The Bristol results for the variation of the mean value of cos θ (θ = angle with primary) with energy of the particles, are given in Table 5. They are in good agreement with the results deduced by other authors.

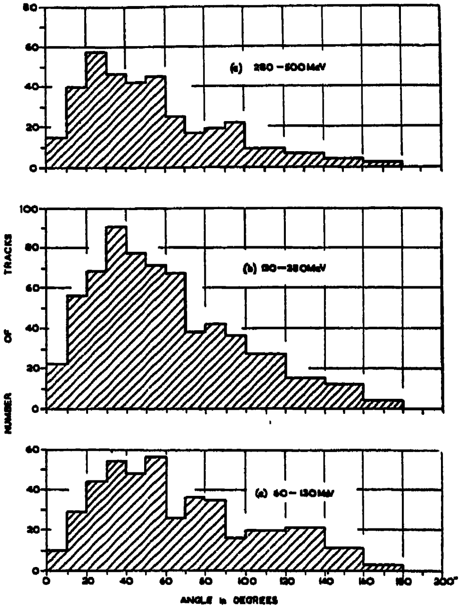

Fig. 17 - The angular distribution of the "grey" protons as a function of energy.

TABLE 5

Grain density. . . .	16—20	20—30	30—40	40—50
Proton energy (MeV)	500—280	280—130	130—80	80—60
cos θ	0.50 ± 0.05	0.41 ± 0.04	0.30 ± 0.05	0.35 ± 0.08

Table 6 indicates the variation of $\overline{\cos\theta}$ with the number of shower particles n_s:

The angular distribution of the "grey" particles therefore depends only slightly on n_s; this seems to support the assumption that most of the "greys" result from nucleon-nucleon rather than meson-nucleon collisions.

TABLE 6

n_s	0 – 1	2 – 3	> 3
$\overline{\cos\theta}$	0.37 ± 0.04	0.32 ± 0.04	0.35 ± 0.04

It is clear from Fig. 17 that most of the "grey" particles are not in fact "δ-rays" knocked-on directly by the primary of the star. In such a case, the primary energy E_p and the energy of the "grey" particle E_g would be related by the (non-relativistic) formula $E_g = E_p \cos^2\theta$. The most probable value of θ is $\sim 45°$, of $E_g \sim 200$ MeV, yielding $E_p \sim 400$ MeV. However, most of the primaries of the stars considered produced shower particles and therefore had energies above 2 BeV. This result indicates that the "grey" particles are not generally knocked-on directly by the primary, but by one or more intermediary nucleons.

7. 4 Proportion of grey and black tracks

The "grey" protons under consideration are those which manage

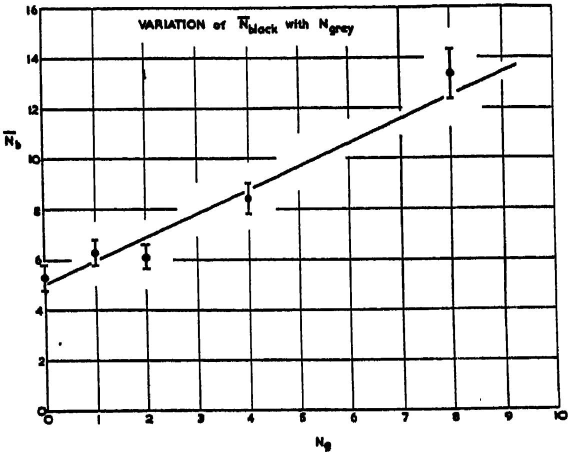

Fig. 18 – Variation of the average number of 'black' tracks, $\overline{N}_{\text{black}}$, with the number of 'grey' particles N_g.

to escape from the nucleus with energies above 30 MeV. Even if all the nucleons projected in the initial elastic collisions originally have energies above this value, some will undergo so many interactions in their passage through the nucleus that they cannot escape immediately but only during the much slower process of evaporation. Such nucleons, and others with which they collide, will be observed as "black" tracks. As can be seen from Fig. 18, the average number of black tracks increases almost linearly with the number of "greys" observed.

8. FREQUENCY, ENERGY AND ANGULAR DISTRIBUTION OF SLOW PARTICLES (BLACK TRACKS); THE EVAPORATION PROCESS

8.1 Introduction

Chronologically, the analysis of the tracks of the low energy particles from nuclear disintegrations preceded that of the showers. The early emulsions, (Agfa and Ilford Halftone dilute emulsions, and Ilford B1, B2 and C2 concentrated emulsions) in use before 1948, could not record protons of energies above about 50 MeV.

Before describing the observations on the low energy particles, we shall outline briefly the theoretical picture of the emission process, since this was in fact put forward before direct observations had been made.

We have seen, in § 7, that the primary, through the medium of the faster "recoil nucleons", can transfer energy to further particles in the nucleus. In this section, we shall consider only those particles finally emitted with energies below 30 MeV.

In analysing the process of energy transfer, one could of course trace the history of each recoil separately, choosing the energy loss per collision by some random method, as was done by Goldberger. We could thus obtain the distribution of the total energy transferred among all the nucleons. However, in a large nucleus at least, such a procedure is extremely lengthy.

Although the tracing through the nucleus of individual interactions between some hundred nucleons is so complex as to be almost unmanageable, it was first pointed out by Bohr that it is just this extreme facility of interaction which allows of a simple statistical treatment of the problem, considering the nucleus as a whole. We assume that at some stage in the process, a definite amount of energy U has been transferred to the nucleus and that the faster nucleons of energy above 30 MeV (i.e. the "grey" particles) have already left the nucleus. We now suppose that this dispersion of energy is, statistically speaking, completed before the expulsion of any further particles — that is, every nucleon has undergone a large number of collisions before it escapes.

The disintegration from this excited state may then be treated as quite independent of the process by which it is formed. The energy content of the nucleus may be compared with the heat energy of a liquid or solid droplet and, as pointed out by Frenkel, the disintegration which follows is analogous to a process of evaporation. In this evaporation process, the energy spectrum of emitted particles is of Maxwellian form, and their distribution in direction quite random.

The analogy is, however, not very exact, since the number of particles in the nucleus is small and the statistical fluctuations about the mean energy per particle correspondingly large. For this reason, we shall limit ourselves to the comparison of theory with the observations on stars produced in heavy nuclei only (Ag, Br). Further complications are that the so-called nuclear "temperature" falls rapidly during the course of the disintegration, and that the emission of charged particles is affected by the Coulomb barrier.

Weisskopf [1937] showed that in a large nucleus (e.g. silver) at excitation energies large compared with the binding energy per nucleon, the level density is so great that the levels may be treated as a continuum and a quantitative treatment of the disintegration along classical thermodynamical lines is possible. The probability of a neutron being emitted with energy between E and $(E + dE)$ was then found to be approximately

$$P(E)dE = \frac{E}{T^2} \exp(-E/T)\, dE \tag{1}$$

where the parameter T is the nuclear temperature measured in energy units (MeV) and is, strictly speaking, the temperature *after* emission of the neutron.

Assuming the Coulomb barrier to be impenetrable and of height V (MeV), the spectrum (1) is modified for charged particles, simply by shifting it to higher energies by an amount V

$$P(E)dE = \frac{(E-V)}{T^2} \exp \frac{(-(E-V))}{T} dE \tag{2}$$

The relation between T and the total excitation energy U depends on the particular nuclear model assumed.

8. 2 Energy distribution of low energy protons

The first extensive measurements on the energy and angular distribution of the low energy particles from stars were made by Blau and Wambacher [1937]. Using a grain count to determine the energy of the particle, they showed that the energy spectrum was well represented by an equation of type (2) for $E < 25$ MeV. However, the stars were taken from both light and heavy elements of the emulsion, and the discrimination between α-particles and protons was rather poor in the Ilford Halftone plates used. For this reason, an accurate test of the evaporation theory could not be made.

Bagge [1941] calculated the energy distribution of protons evaporated from stars, and compared his predictions with the results of Ortner and Blau and Wambacher. He made allowance for the "cooling down" of the nucleus during the evaporation process. By treating the nucleus as a degenerate gas of particles obeying Fermi statistics (analogous to the electron gas in a metal) and neglecting the interactions between the nucleons, one obtains

$$U = KAT^2 \tag{3}$$

where A = total number of nucleons, $K = \pi^2/4\mathcal{G}$, $\mathcal{G}$ being the kinetic energy of the highest occupied state in the unexcited nucleus (= 22 MeV). According to Bethe [1937] the effect of nuclear interaction will be to increase K by a factor of the order of 2. Thus $K \sim 0.1$. Following the treatment of Bagge, one obtains for the average energy loss dU of the nucleus when dA neutrons are evaporated,

$$\begin{aligned} \frac{dU}{dA} &= 2\,KA\,\frac{dT}{dA} + KT^2 \\ &= 2T + E_0 \end{aligned} \tag{4}$$

where, from (1), $2T$ is the average kinetic energy of a particle, E_0 is the binding energy per nucleon, assumed constant, T the instantaneous temperature. The process is treated as continuous and the emission of neutrons is assumed to be independent of that of protons. Integration of equation (4) gives the instantaneous temperature as a function of the initial temperature T_0 and the initial and instantaneous mass numbers of the nucleus, A_0 and A respectively. Integrating over the whole range of temperature, Bagge then obtained the true energy distributions of the evaporated particles for any initial nucleus A_0 (in this case silver or bromine). He found that this spectrum could be expressed approximately by

$$P(E)dE = \frac{E}{(E+E_0)} \exp \frac{(-E)}{T_0}\, dE \tag{5}$$

which may be compared with (1), which refers to an instantaneous temperature. Equation (5) gives the spectrum of neutrons, and Bagge obtained that for protons by multiplying (5) by a factor corresponding to the mean of the Gamow factors for the initial and final nucleus.

Bagge assumed that, at high energies, U, the formation of surface waves on the nuclear surface was possible, these resulting in a mean increase in nuclear radius and consequent decrease in the barrier. This decrease in barrier with increasing temperature is shown in Table 7.

TABLE 7

Mean excitation energy U (MeV)	0	170	500	830
Estimated barrier height observed (MeV)	—	11	5	3
Mean conventional barrier height (MeV)	13.0	11.8	10.7	9.5
Ratio $\frac{\text{observed}}{\text{calculated}}$	—	0.94	0.47	0.31
Ratio computed by Bagge . . .	—	0.70	0.57	0.52

Despite these refinements in the theory, Bagge was unable to obtain satisfactory agreement with the data of ORTNER [1940] from stars in silver and bromine, which showed a peak in the energy spectrum at only 2—3 MeV. Although both authors explained the discrepancy on a hypothesis of fission of the nucleus it appears, in the light of subsequent experiments, that the accuracy of the observations was open to question.

With the introduction of the Ilford B2 and C2 concentrated emulsions, more accurate observations of the energy spectra became possible. (HARDING, LATTIMORE and PERKINS [1949]; PAGE [1950]; PERKINS [1950a]; BERNARDINI, CORTINI and MANFREDINI [1950]).

HARDING *et al.* determined by the method of grain-counting, the energy distribution of low energy protons from stars in silver and bromine for four ranges of excitation energy U (Fig. 19). The values of U were estimated from the number of charged particles and their mean energy, allowance being made for emission of equal numbers of neutrons and protons. Their figures were amended by PERKINS [1950a] such that the number of neutrons emitted was that resulting in a stable residual nucleus. Account was taken of "cooling" by the Bagge method, and the proton distribution was calculated from the neutron spectrum, by multiplying by the quantum-mechanical barrier penetrability. Assuming the Fermi gas model, these authors computed the constant K in (2a), and found a value in very good agreement with the theoretical one ($K \sim 0.1$). The variation of initial temperatures with excitation energy U was determined and found to be in good agreement with the formula $U = KAT^2$. This may be regarded as confirmation of the Fermi gas model of the nucleus.

Harding *et al.* also carried out similar computations for the "liquid drop model" of the nucleus. When a liquid drop is thermally excited – at high temperatures this applies also to a nucleus – both surface and volume waves are possible. At high energies, only volume waves will be important. If, therefore, one assumes that all the energy U is concentrated in volume waves, one finds $U =$ const. T^4.

This model gives a much slower rate of increase of temperature with U than the Fermi gas model, and the above authors showed that it predicted too few high energy protons for large values of U.

In their treatment of the "cooling" both Bagge and Harding *et al.* assumed zero correlation between neutron and proton emission, so that the two processes were treated quite independently. Such correlations have been allowed for in an extension of the evaporation theory in two recent papers by LE COUTEUR [1950], who took into account both the neutron excess and the effect of thermal expansion of the nucleus.

In his analysis, Le Couteur, with more exact expressions for the energy loss per particle emitted, obtained the probabilities at any instantaneous temperature for the emission of six different types of particles — neutrons, protons, deuterons, tritons, alpha-

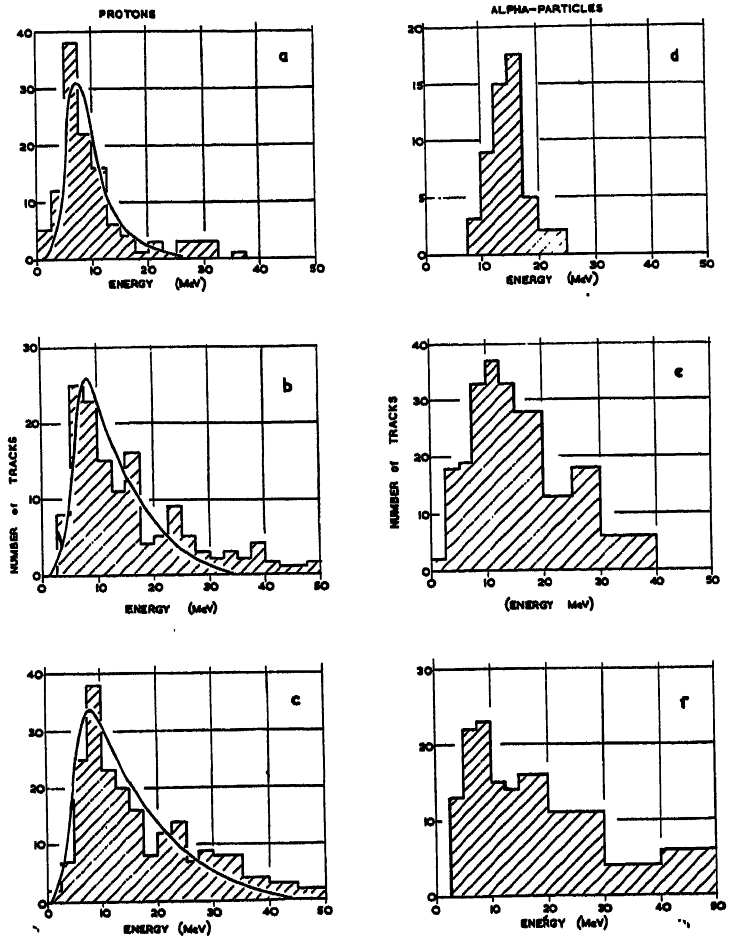

Fig. 19 – Energy distributions of protons (a, b, c) and α-particles (d, e, f) emitted from stars of different prong number, in silver and bromine nuclei, C2 emulsion.

(a) and (d) stars of 3—6 prongs (excitation energy $U \sim 170$ MeV).
(b) 10—14 prongs ($U \sim 550$ MeV)
(c) 15—22 prongs ($U \sim 700$ MeV)
(e) 7—16 prongs ($U \sim 500$ MeV)
(f) 17—31 prongs ($U \sim 830$ MeV).

particles and He^3 nuclei. These probabilities he integrated over the whole emission process, and in this sense allowed for "cooling down" of the nucleus.

Le Couteur found that the best fit with experimental data was obtained on the assumption of a decrease in potential barrier with increasing excitation energy as first suggested by Bagge. This point will be further discussed below.

Somewhat similar calculations have been made by FUJIMOTO and YAMAGUCHI [1949a, 1950a]. They neglect the thermal expansion of the nucleus, which is in any case small, and take into account correlations between neutrons, protons and α-particles only. They have also considered the fluctuations in the number of particles evaporated. (See § 8. 7).

Decay protons

Le Couteur calculated the excitation energy at which the probability of proton, neutron or α-particle emission is equal to that of γ or β-decay. The threshold energies he found are:

$$Q_n = 10 \text{ MeV}, \quad Q_p = 7 \text{ MeV}, \quad Q_\alpha = 9 \text{ MeV}.$$

Thus, if after emission of the penultimate nucleon, the excitation energy lies between 7 and 10 MeV, a proton is emitted (with kinetic energy between 0.5 and 3.5 MeV); if below 7 MeV, γ-rays are emitted. At 9 MeV, proton emission is, of course, much more likely than α-emission.

Le Couteur's estimate of the number of decay protons was ~ 0.2 per star. This number is almost constant, increasing slightly at low excitation energies.

This mechanism probably explains the slight discrepancy at low energies between the experimental and the theoretical results in Fig. 19a. The decay process was also proposed independently by FUJIMOTO and YAMAGUCHI [1949b].

8. 3 Energy distribution of low energy α-particles

The distribution in energy of slow α-particles ($E < 50$ MeV) from stars has been determined by HARDING *et al.* [1949], PAGE [1950], PERKINS [1950a] and BERNADINI, CORTINI, and MANFREDINI [1950]. Owing to the very high grain densities of such tracks, the energies were determined by range measurement. Fig. 19 shows measurements by Perkins at different excitation energies. The energy spectrum of α-particles from stars in Ag Br containing less than 7 prongs was obtained by subtracting from the distribution for stars in both light and heavy nuclei of the emulsion, the normalized distribution from the light nuclei only. The latter was deduced from observations on gelatine "sandwich" plates.

It will be seen that the most probable energy of the α-particles *decreases* with the increasing excitation energy.

The effective height of the barrier to α-particles deduced from these results is given below as a function of excitation energy, (Table 7). The third row of the table gives the barrier height in the ground state, of a nucleus having a charge equal to the mean of that of the nucleus before and after the evaporation process. At 800 MeV excitation energy, the observed barrier has dropped to one-third of the calculated value.

The figures given in the last row of the table were computed by BAGGE [1944] on the assumption that all the thermal energy was concentrated in surface waves. However, when the effects of Coulombian repulsion between protons inside the nucleus and the variation of surface tension with nuclear temperature are considered, a further substantial reduction in the barrier will be obtained (Bagge; private communication). It therefore appears that the observations may be satisfactorily explained on the hypothesis of surface oscillations of the nucleus.

It has been pointed out by Le Couteur that, despite the lowering of the barrier, the low energy end of the proton spectrum (below 5 MeV) will not change significantly with excitation energy, on account of the decay protons. Their absolute contribution is more or less constant, and their percentage contribution to the spectrum varies inversely as the prong number. The decay protons therefore mask the increased contribution of low energy protons due to decrease in barrier. Furthermore, the alpha/proton emission ratio increases as the barrier drops, and this factor also reduces the contribution of low energy protons at high excitation energies. These considerations can probably account for the small proportion of slow particles in the proton spectrum at high excitation energies, in contrast with that in the α-spectrum.

8. 4 Angular distribution of low energy protons

The angular distribution of low energy protons was measured by Blau and Wambacher [1937], Harding *et al.* [1949], Bernardini *et al.* [1950] and others. On the evaporation model, the particles should be emitted isotropically from the nucleus. In the case of a silver or bromine nucleus, the downward velocity $\beta = v/c$ transferred to it when excited to an energy U(MeV) will be of the order of $10^{-5}\ U$, and for thermal excitation energies below 1000 MeV is therefore $\leqslant .01$.

The fractional excess of evaporated protons of energy E(MeV) projected downward in the laboratory system will therefore be less than $0.2/\sqrt{E}$, which is therefore very small for the proton energies considered.

The measurements of Harding *et al.* and Bernardini *et al.* indicate that the protons below 30 MeV in stars of more than 7 prongs are ejected almost isotropically from the nucleus. A more precise check of the isotropy of ejection of the protons can be obtained by measuring the downward excess of these particles.

The following table shows the downward excess of protons of energy between 0 and 30 MeV, obtained at the Jungfraujoch. At this height the star-producing radiation is fairly well collimated and the forward excess relative to the vertical is not very different from that relative to the primary. The results were obtained by subtracting from the results for protons of $0 < E < 50$ MeV, (Perkins [1950a]), the contribution of those between 30 and 50 MeV as estimated from the observations of Brown *et al.* ([1949]; I) and Harding [1951].

The downward momentum of the nucleus (in MeV/c) can be taken as numerically equal to the excitation energy (in MeV) as calculated from the star prong number, (Harding [1949]). From the average energy of the ejected protons, one can then estimate the expected downward excess, assuming isotropic emission from the moving nucleus. There is good agreement with the observed downward excess (Table 8).

This conclusion is valid even for the largest stars observed (thermal excitation energy $U \sim 800$ MeV). Thus the evaporation hypothesis holds fairly accurately for low energy protons up to excitation energies comparable with, or exceeding, the total nuclear

TABLE 8

Average number of black prongs (protons up to 30 MeV)	18	13	8
Estimated value of excitation energy U (MeV)	830	610	390
Observed downward excess of protons (0—30 MeV).	$(38 \pm 24)/600$ $= 0.063 \pm 0.040$	$(18 \pm 23)/513$ $= 0.035 \pm 0.045$	$(14 \pm 16)/279$ $= 0.50 \pm 0.057$
Calculated downward excess of protons. . .	0.08	0.005	0.039

binding energy. From these measurements one can conclude that "knock-ons" in the 0—30 MeV region represent less than $5/p$ % of the evaporation protons, where p is the downward excess for such knock-ons.

8.5 Angular distribution of low energy α-particles

The zenith angle distribution of α-particles ($E < 50$ MeV) from stars was measured by Perkins for three ranges of excitation energy. The results are given in Table 9. Considering the two larger groups of stars, the downward excess of the α-particles calculated on the evaporation hypothesis is 0.09, that observed is .03 ± .04. The discrepancy is only just outside the standard deviation, and can hardly be considered significant.

TABLE 9

Number of black prongs	18	13	8
Estimated value of U (MeV)	830	610	390
Observed downward excess of α-particles	$(6 \pm 18)/322$ $= 0.019 \pm 0.057$	$(12 \pm 17)/296$ $= 0.041 \pm 0.042$	$(18 \pm 13)/168$ $= 0.107 \pm 0.078$
Calculated downward excess of α-particles .	0.10	0.079	0.054

Crussard [1950] has measured the average value of the cosine of the angle θ between the α-particle and the star-producing primary in G5 emulsion. He also finds that for α-particles of energy below 60 MeV in stars of more than 8 prongs, the angular distribution is consistent with isotropy.

8. 6 Emission probabilities for various types of particles

The probability of emission of various types of particles can be calculated from the formula of Weisskopf [1937], and this constitutes a further point of comparison of the evaporation theory with observations. (Le Couteur [1950]; Fujimoto and Yamaguchi [1950]).

(i) *alpha-proton emission ratio*

A quantity readily obtainable from observations on stars is the ratio, R, of doubly to singly-charged particles emitted. (Harding *et al.* [1949]; Page [1950]; Perkins [1950a]; Bernardini, Cortini and Manfredini [1950]). The doubly-charged particles consist of α-particles and He^3 nuclei; the singly-charged are protons, deuterons and tritons. R is, however, nearly equal to the ratio of α-particles to protons. Averaged over all stars, Bernardini *et al.* find a ratio of 0.35; Page an average value of 0.37 for stars of more than six prongs; Perkins obtained rather higher values (0.5 for stars of more than 6 prongs). The reason for this discrepancy is not clear.

All the measurements, however, give the same order of magnitude for the ratio, which is found to change only slowly with excitation energy. In Fig. 20 are shown the experimental results of Page and Perkins. Perkins' results were corrected at small prong numbers for the contribution due to light nuclei, and at high prong

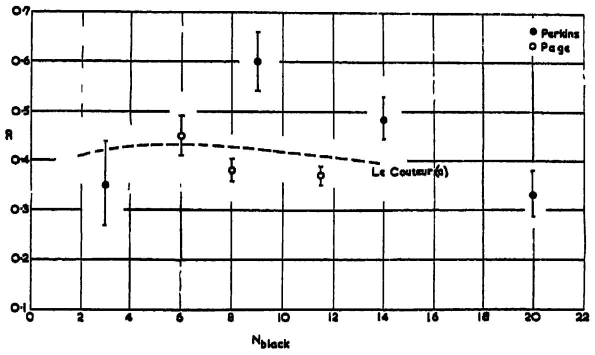

Fig. 20 – The variation of the ratio R of the numbers of doubly to singly charged particles emitted from stars, as a function of the number of black tracks. The dotted curve shows the result of the calculations of Le Couteur (1950a) using his parameter 'a'.

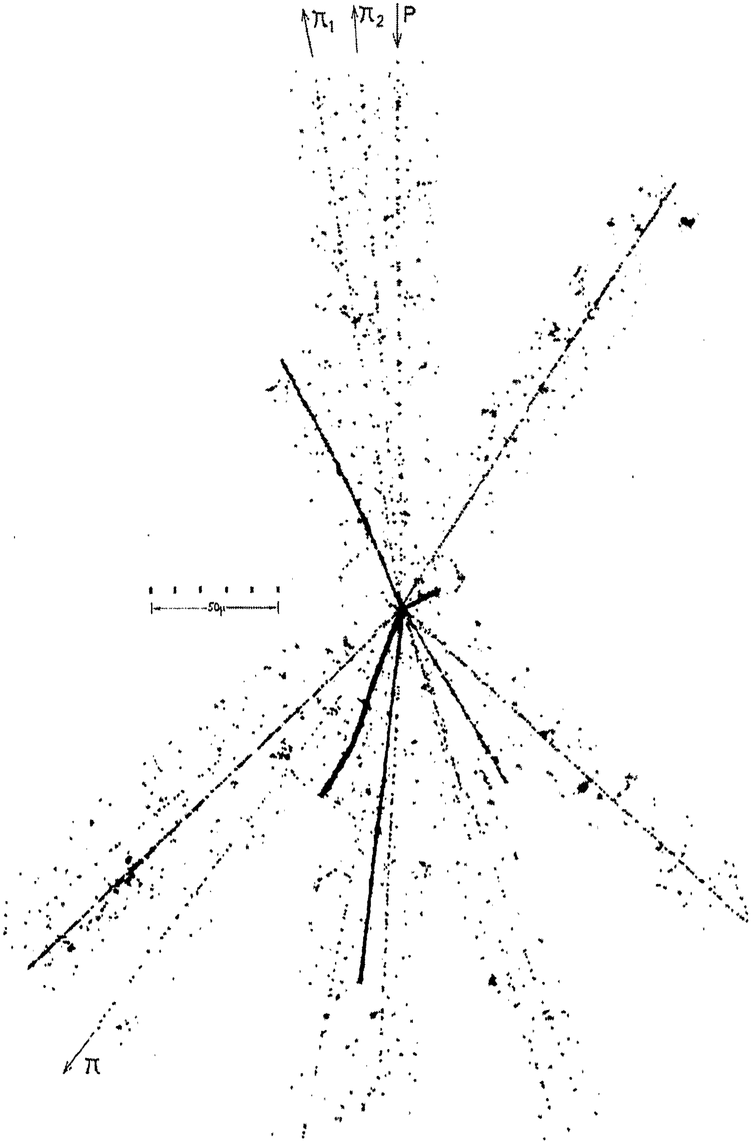

A star of type 11 + 8p in which two mesons of energy ~ 80 MeV are ejected backwards in the laboratory system. Three of the forward shower particles have been identified as π-mesons.

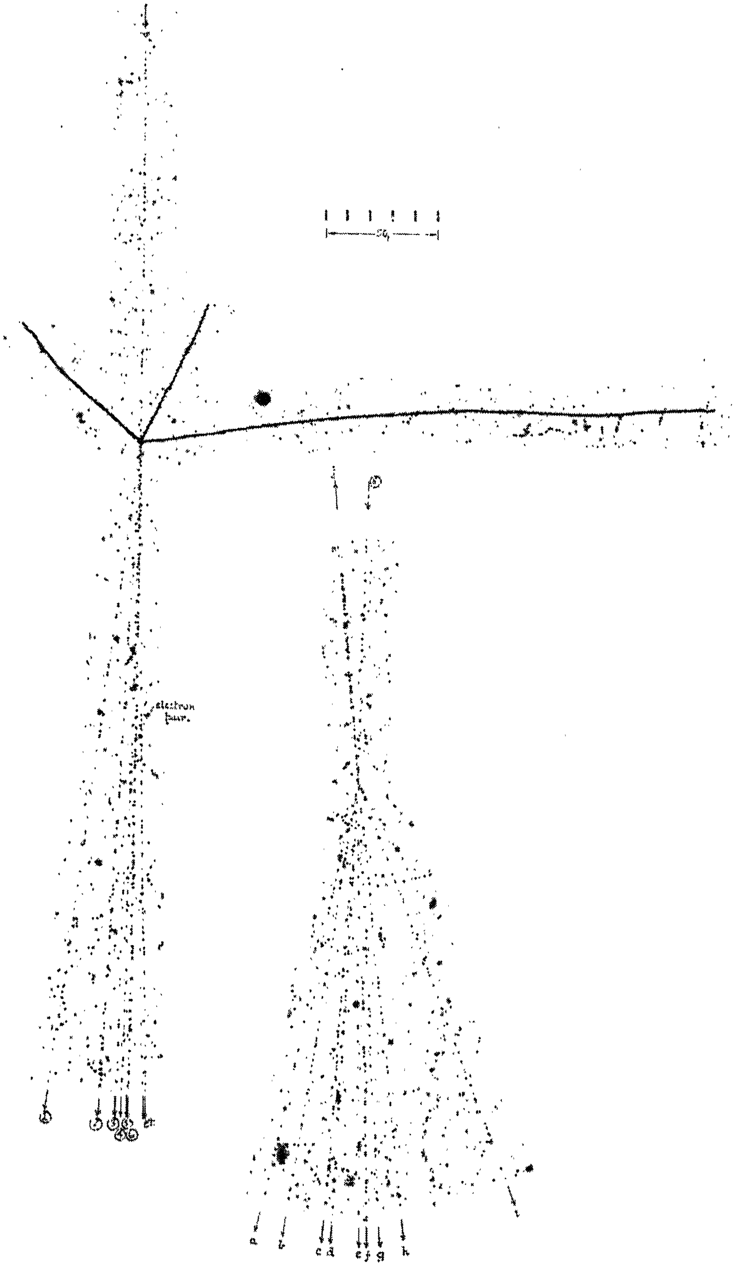

An event in which a star of type 1 + 9p is initiated by a shower particle from a star of type 3 + 6p.

numbers for heavier fragments which could have been recorded as α-particles. In the same graph is plotted a curve calculated by Le Couteur for Ag and Br nuclei.

It has been pointed out by Le Couteur that in Weisskopf's formula there are no explicit factors representing the "probability of existence" of. α-particles inside the nucleus, and that if such factors were introduced, one would no longer obtain agreement with the experimental data. These "existence factors" only enter the formula through the dependence of the level density of the residual nucleus on the mass, binding energy and charge of the emitted particle. This dependence is especially important at high energies, and accounts for the maximum in the theoretical α-proton ratio.

(ii) *The proportion of tritons and deuterons in the singly-charged particles*

For stars of about ten prongs, LE COUTEUR [1950] gives a ratio of about 0.3 for the proportion of deuterons and tritons in the singly-charged particles, (H^1, H^2, H^3). An experimental check on this ratio is rather difficult to obtain. Differentiation between protons and the heavier isotopes of hydrogen is possible by grain counting only if the tracks of the particles are of long range and if they come to rest in the emulsion. HARDING *et al.* report that on the assumption of identical energy spectra, only about 20 ± 5 % of the singly-charged particles emitted in stars of more than 7 prongs are H^2 and H^3.

A second and more accurate method for differentiating between deuterons, tritons and protons is the measurement of the multiple scattering as a function of residual range. MENON and ROCHAT [1951] identified these particles in the energy range 15—50 MeV. Again assuming identical energy spectra, they find an emission ratio of $(H^2 + H^3)$ to $(H^1 + H^2 + H^3)$ of $0.21 \pm .08$ for stars of less than 7 black tracks, and of $0.43 \pm .15$ for stars of more than 7 prongs. These figures are in rough agreement with the grain-counting results and the predictions of Le Couteur. (It should be pointed out that the scattering results will include some knock-on particles with energies above 30 MeV).

8. 7 Relation between prong number and thermal excitation energy

A relation which is very useful in the interpretation of nuclear disintegrations is that between the number of black prongs, N_b, and the mean thermal energy U (Fig. 21).

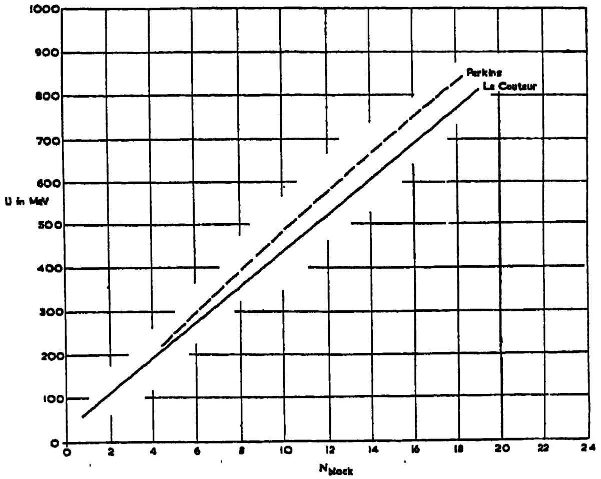

Fig. 21 – The relation between the excitation energy U in MeV and N_{black}. The full curve is that calculated theoretically by Le Couteur; the broken line shows the experimental results of Perkins.

The experimental data give the average value of U for a given range of prong number; the theoretical curve of Le Couteur gives the mean prong number for fixed U. There appears to be good agreement between experimental and theoretical curves, which are well approximated by the relation $U = (40 + 42\ N_b)$ MeV.

FUJIMOTO and YAMAGUCHI (1949a] have investigated the fluctuations to be expected for fixed U, in the total number of particles, ν, emitted (neutrons, protons and α-particles). They find a roughly Gaussian distribution, the standard deviation about the mean value being $\sim \sqrt{\bar{\nu}}$.

In the evaporation process, the relative probability of emission of protons or neutrons is rather strictly regulated at each instant by the temporary neutron excess or deficit; this strong correlation implies that the fluctuations in relative numbers of neutrons and protons emitted will be negligible, for large ν.

On the other hand, the emission of α-particles is only weakly correlated with that of the neutrons and protons, and the fluctuation about the mean number of α-particles will therefore be practically Poissonian. Thus the deviation about the mean number of charged particles (protons and α-particles) emitted will be only slightly smaller than $\sqrt{\overline{N}_b}$.

Since U is a linear function of N_b it follows that, for a fixed prong number, the fluctuations on U will also be Gaussian with deviation $\sim \sqrt{42\,\overline{U}}$.

9. EMISSION OF HEAVY FRAGMENTS IN STARS

In addition to the emission of individual nucleons or small nucleon aggregates, a characteristic process which is found especially in the bigger stars, is the ejection of larger nuclear fragments, heavier than α-particles (BONNETTI and DILWORTH [1949]; HODGSON and PERKINS [1949]; SÖRENSEN [1949, 1951]; LOVERA [1947]; SCHOPPER [1947]; PERKINS [1950b]; CRUSSARD [1950]; MARQUEZ and PERLMAN [1951]). In what follows we shall use the term fragment to denote any nucleus with mass greater than that of an α-particle.

The fragments have been identified in various ways. Perhaps the most reliable method for determining the charge Z is that of δ-ray counting. This method was used by Sörensen, Bonnetti and Dilworth, Perkins and Crussard. It suffers from the disadvantage that it can only be applied to fragments of long range. If the fragment has a fairly high charge, it may show a decrease of ionisation or "tapering" at the end of the range, which can be used to determine the charge (FREIER, LOFGREN, NEY and OPPENHEIMER [1948] and PERKINS [1950]). This method is, however, rather inaccurate.

In those cases where the ejected fragments are unstable they may disintegrate either in flight or after coming to rest. In the former case, the disintegration products will sometimes emanate from the star in the form of a narrow cone. In this way, Perkins identified the fragments of Be^8 ($\rightarrow 2He^4$), B^9 ($\rightarrow 2He^4 + H^1$) and 0^{16} ($\rightarrow 4He^4$); these results were confirmed by Crussard. Alternatively the fragment, if β-active, will disintegrate after coming to rest (e.g. $Li^8 \rightarrow 2He^4 + \varepsilon^-$). See Plate VI.

9.1 Frequency of fragment emission

We shall first investigate to what extent fragment emission may be viewed as an evaporation process.

A readily identifiable fragment is that of Li^8 which shows the characteristic "hammer" track. The frequency of emission from Ag and Br nuclei, as a function of excitation energy, has been measured by Hodgson [1951] and his results are shown in Table 10.

TABLE 10

Approximate excitation energy U (MeV) . . .	250	600	800
Number of tracks . . .	6	13	19
Number of observed hammer tracks/star .	0.003 ± 0.001	0.012 ± 0.007	0.03 ± 0.01
Number/star calculated for evaporation process (Le Couteur)	0.005	0.011	0.013

It is here assumed that all the hammer tracks are due to Li_3^8; on the evaporation theory, the emission of B_5^8, which would also give a hammer track, is only about one quarter as probable.

There appears to be reasonable agreement between the observed frequency and the predictions of the evaporation theory. The discrepancy for the largest stars is hardly statistically significant.

The emission of heavier fragments (charge $Z = 3 - 10$) has been described by Perkins [1950]. He finds that the emission probability per star for all fragments increases rapidly with excitation energy, and is about unity for U above 600 MeV. (Table 11). The relative frequencies with which fragments of various charges are found to be emitted is given in Table 12.

TABLE 11

Mean number of black prongs	8	13	17	23
Excitation energy U (MeV)	370	600	750	900
Fragment frequency per star	0.2 ± 0.1	0.75 ± 0.2	1.5 ± 0.4	1.4 ± 0.7

TABLE 12

Z	3	4	5	6	7	8	9	10
Number	14±5	78±19	17±6	14±6	4±4	8±5.5	4±4	4±4

The evaporation theory predicts an absolute frequency of fragment emission much smaller than that observed, and a more rapid decrease in intensity with increasing mass.

Quite frequently, stars are observed containing two or even three fragments (Bonnetti and Dilworth; Perkins). There is some evidence that the probability with which these events are observed is greater than would be expected if each individual fragment were emitted independently. This is strongly suggestive of a process akin to fission occurring in the nucleus.

Both Sörensen and Perkins established that there was no correlation between the emission of a fragment and the creation of a meson shower in the same nucleus.

9. 2 Angular distribution of fragments

The results described above for the protons and α-particles, namely that the higher the energy of the particles the more strongly are they collimated with the primary, is also true for the heavier fragments. Their angular distribution has been measured by Perkins, Sörensen and Crussard.

Denoting by E/A the kinetic energy in MeV per nucleon in the fragment, θ the angle with the primary, the results are shown in Table 13 and Fig. 22.

TABLE 13

Author	CRUSSARD		PERKINS		SÖRENSEN	
Charge Z of fragment .	3–9		3–10		3	
Total number of fragments	71		79		10	
	E/A	cos θ	E/A	cos θ	E/A	cos θ
	4–5	0.54	0–4	0.06		
	5–10	0.60	4–10	0.12		
	10–15	0.73	10–20	0.60	13	0.65
	15–35	0.96	20–30	0.87		

For E/A greater than 10 MeV there is reasonable agreement between the various measurements. Below 10 MeV there is a discrepancy between the results of Perkins and those of Crussard. However, the statistical errors associated with the observations are large, and on account of the difficulty in identifying and measuring the energy of the fragments with any precision, there may well be a systematic error in both sets of observations.

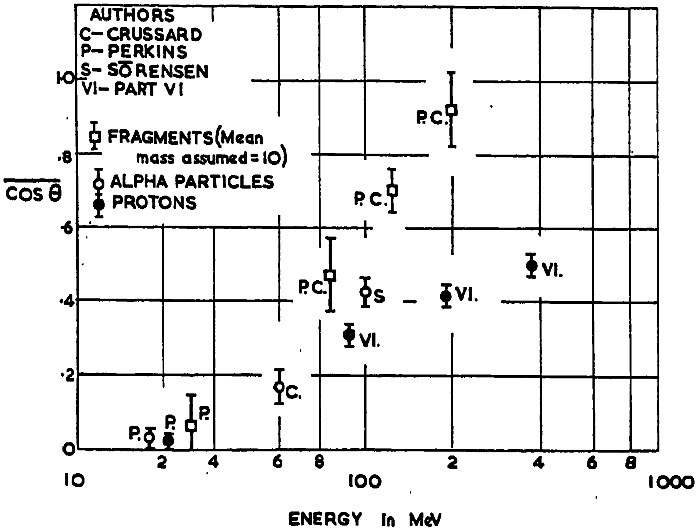

Fig. 22 – Variation with kinetic energy, of $\overline{\cos\theta}$, the average cosine of the angle with the primary, for protons, α-particles and heavier fragments emitted from stars. The results of Crussard and Perkins for energetic heavy fragments have been combined.

9. 3 Emission of low energy fragments (less than 4 MeV per nucleon)

In the large stars at least, it seems fairly certain that the fragments cannot usually result from the nuclear evaporation, and the observations are in fact somewhat suggestive of a process of fission.

When the nucleus is highly excited it is to be expected that, because of the reduced "viscosity" of the nuclear matter, energy may be concentrated in both volume and surface oscillations rather than in heating the nucleus as a whole. Evidence for such surface waves was found above from the energy spectra of the α-particles. At high temperatures, because of the rapid drop of surface tension with increasing nuclear temperature, fission as a result of surface oscillations should be very probable (Fujimoto and Yamaguchi [1950b]). According to these authors, the fission width will be comparable with the neutron width when the thermal excitation energy U exceeds the total nuclear binding energy (800 MeV). This point seems to be borne out by Table 11.

On this "fission" hypothesis, the mean downward velocity component of the fragments should be about equal to that of the parent nucleus, as is the case for the evaporating protons and α-particles. Considering only those fragments of energy below 4 MeV per nucleon, Perkins finds a value of 0.013 ± .006 for this downward velocity — a figure which is certainly consistent with the value estimated from the excitation energy (see Table 8). The average energy acquired by these fragments would appear to be explained quite satisfactorily in terms of electrostatic repulsion from the parent nucleus.

9. 4 Emission of high energy fragments (more than 4 MeV per nucleon)

However, the considerations above cannot explain the production of high energy fragments. The latter are strongly collimated in the direction of the primary particle and they must obviously be generated in a preliminary process. As has been shown by SÖRENSEN [1951], they do not in general result from a direct knocking on by the primary particle, and they are not correlated with the creation of meson showers.

The energetic fragments must therefore as a rule result from interactions intermediate between this extreme and that of statistical equilibrium. In this sense they are in the same category as the "grey" protons (§ 7).

A striking feature of the energetic protons, α-particles and heavier fragments is the strong correlation between energy and angle θ with primary, (Fig. 22).

From this graph one sees that for a given $\overline{\cos\theta}$ the energy of the particles decreases with increasing mass. Although the details of the actual emission process may be rather complicated, this result is what would be expected from the conservation laws if the particles resulted from a small number of elastic collisions.

In collisions between high energy nucleons and fragments it seems necessary not only to postulate the temporary existence of nucleon aggregates inside the nucleus, but also to invoke nuclear forces of long range which can act over an assembly of nucleons without breaking it up. Similar interactions are met with in the fragmentation processes occurring when heavy primary cosmic ray particles collide with nuclei.

10. CONCLUSIONS

As in § 6 we may summarise the observations described in the preceding sections in the following general conclusions:

(1) Particles with energies below about 1 BeV have a very low probability of generating further mesons and we have assumed that only elastic collisions are important.

(2) Energy from the primary interaction is transferred to further nucleons by the successive elastic collisions, until approximate statistical equilibrium throughout the nucleus is established. By this time the faster nucleons have already escaped. These nucleons have energies between about 30 and 1000 MeV; those of highest energy are most strongly collimated in the direction of the primary.

(3) The protons (and neutrons) emitted with kinetic energies less than 30 MeV, and the α-particles below 50 MeV, have energy distributions in good agreement with those expected from the evaporation theory. The observed isotropy in the coordinate system of the nucleus is, however, probably the strongest argument in favour of the statistical model. This conclusion holds up to the highest "thermal" excitation energies considered ($U \sim 800$ MeV).

(4) At low excitation energies ($<$ 300 MeV) fragments heavier than α-particles are emitted very rarely, probably in the normal process of evaporation.

(5) The observed proportions of protons and α-particles, and of deuterons, tritons and protons emitted, is in excellent agreement with the predictions of the evaporation theory.

(6) At high excitation energies, the reduction of "surface tension" and "viscosity" with increasing nuclear temperature makes possible concentration of energy in surface and volume oscillations of the nucleus. The surface deformations result in a large decrease in the height of the Coulomb barrier. When these are sufficiently great they result in an asymmetrical "fission" of the nucleons, and the ejection of heavily charged fragments becomes very probable.

(7) The above considerations apply to protons $E/A < 30$ MeV;

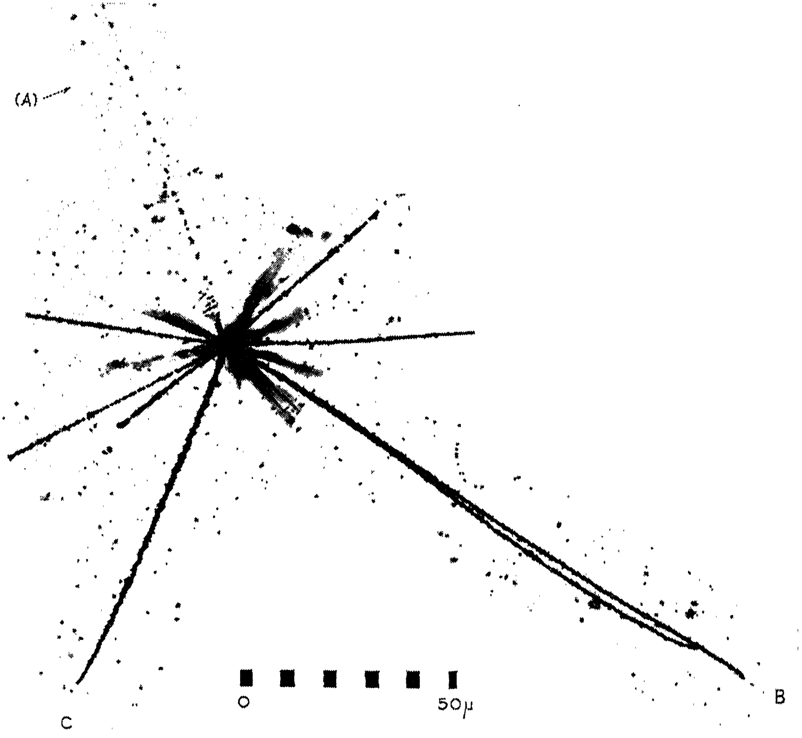

Disintegration of silver or bromine nucleus by a singly-charged primary (A) leading to the emission of two fragments (B) & (C). The charge of (C) is greater than 10 units and its track shows characteristic "taper". The pair of α-particles (B) result from a nucleus of Be^8 which disintegrates in flight.

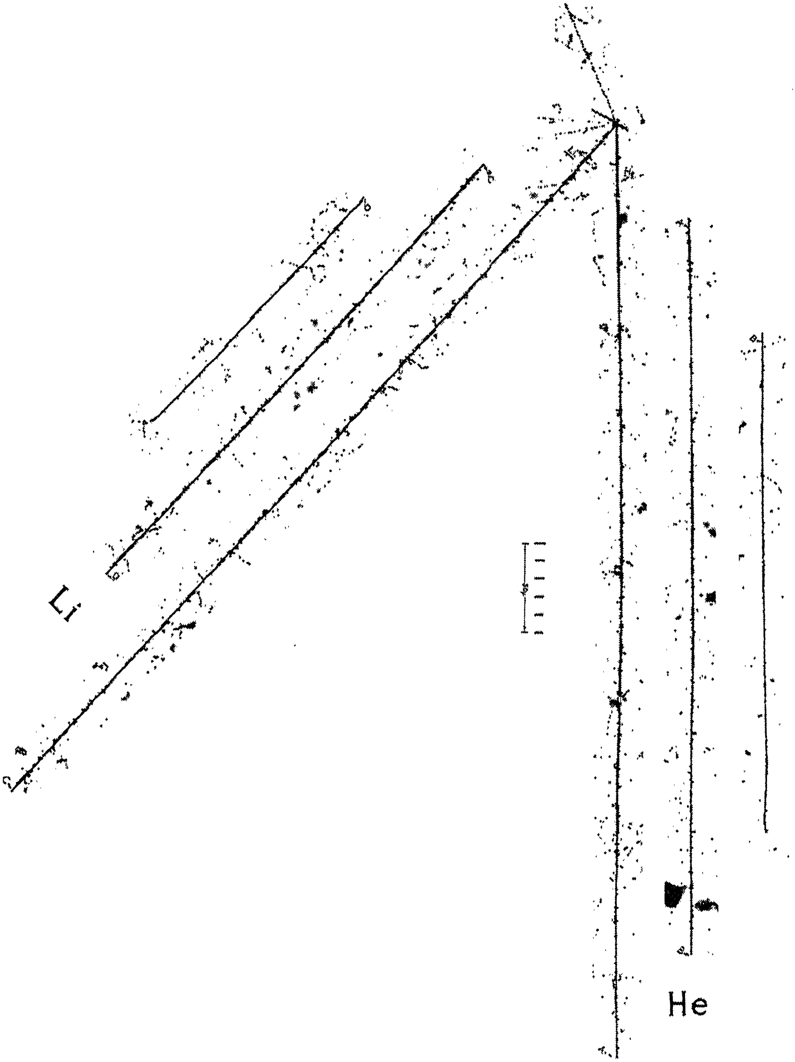

Simultaneous ejection of an energetic helium particle and a lithium fragment from a nuclear explosion.

α-particles $E/A < 15$ MeV; heavier nuclei $E/A < 4$ MeV (E/A = energy per nucleon).

(8) α-particles of energy above 50 MeV, and fragments of energy above 4 MeV per nucleon, are strongly collimated with the primary, in the same manner as the fast nucleons. The evidence suggests that these fragments are not correlated with the creation of mesons, nor can they be knocked on directly by the primary particle. It seems necessary to postulate long-range components to the nuclear forces, and many body collisions, to account for these phenomena.

11. OUTSTANDING PROBLEMS

In the present article we have attempted to give a description, largely qualitative, of the radiative and elastic interactions occurring as a result of the impact of energetic primary particles with the nuclei of the photographic emulsion.

The emission of the low energy particles follows a statistical distribution of energy throughout the nucleus and depends but little on the properties of the individual collisions. It is found that this process can in fact be treated very successfully along purely thermodynamical lines.

On the other hand the interpretation of the experimental observations relating to high energy collisions has been unsatisfactory because (a) of the absence of any comprehensive theoretical models for these high energy radioactive and elastic collisions, and (b) the cascade of mesons and nucleons which develops in medium sized nuclei, and which makes it very difficult to relate directly the quantities observable to the properties of the individual collisions.

It does not appear likely that further experimental work on these lines will furnish much precise quantitative information relating to these problems. To overcome this difficulty it appears essential to carry out experiments of a more detailed and penetrating nature, in particular those using hydrogen as the target nucleus.

Such an investigation is, of course, best carried out with beams of artificially accelerated particles. However, the production of meson showers of high multiplicity, and the creation of mesons other than π-mesons, and of nucleon pairs, is not likely to be attained by such means for some years to come. Meanwhile the study of such energetic collisions remains in the province of cosmic ray research. In this connection it may be noted that, although hydrogen is present in quantity in nuclear emulsions, a systematic survey of emulsions for proton-proton and meson-proton collisions has not yet been attempted.

In the immediate future, a detailed study of the interaction of low energy π-mesons with nuclei, at present being carried out with both artificially-accelerated and naturally-occurring beams of π-mesons, appears to be a very fruitful line of advance, and is probably of most immediate help to the theoreticians.

Whilst the study of the nucleon-nucleon and meson-nucleon collisions remains the most urgent problem in nuclear physics of the high-energy region, the evidence presented above for many-body interactions seems also to be of considerable interest, although so far it has received little theoretical consideration.

ACKNOWLEDGEMENTS

We should like to express our thanks to Professor W. Heitler for several informative discussions, and for permission to quote the unpublished calculations of M. Therreaux; Professor Marcel Schein for kindly sending us the photograph reproduced in Fig. 15; Dr S. F. Singer for reading the manuscript; Miss P. Dyer and Mr R. A. Gattiker for the photographs, and Miss J. Burnell and Dr H. Heitler for the figures.

REFERENCES

Bagge, E., 1941, Ann. Phys., Lpz., 39, 512.

Bagge, E., 1944, Physik. Zeit., 21, 461.

Bernardini, G., G. Cortini and A. Manfredini, 1950, Phys. Rev., 79, 952.

Bernardini, G., E. T. Booth, L. Lederman and J. H. Tinlot, 1950a, Phys. Rev., 80, 924.

Bernardini, G., E. T. Booth, L. Lederman and J. H. Tinlot, 1950b, Bombay Conference on Fundamental Particles.

Bethe, H. A., 1937, Rev. Mod. Phys., 9, 70.

Bjorklund, R., W. E. Crandall, B. J. Moyer and H. F. York, 1950, Phys. Rev., 77, 213.

Blau, M. and H. Wambacher, 1937, S. B. Akad. Wiss. Wien, 146, 623.

Bonnetti, A. and C. C. Dilworth, 1949, Phil. Mag., 40, 585.

Bradt, H. L., M. F. Kaplon and B. Peters, 1950, Helv. Phys. Acta, 23, 24.

Brown, R. H., U. Camerini, P. H. Fowler, H. Heitler, D. T. King and C. F. Powell, 1949, Phil Mag., 40, 862.

Brown, W. W. and A. S. McKay, 1950, Phys. Rev., 77, 342.

Butler, C. C., W. G. V. Rosser and K. H. Barker, 1950, Proc. Phys. Soc., A63, 145.

Butler, C. C. and K. H. Barker, 1951, Proc. Phys. Soc., A64, 4.

Camerini, U., T. Coor, J. H. Davies, P. H. Fowler, W. O. Lock, H. Muirhead and N. Tobin, 1949, Phil. Mag., 40, 1073 (II).

Camerini, U., P. H. Fowler, W. O. Lock and H. Muirhead, 1950, Phil. Mag., 41, 413.

Camerini, U., J. H. Davies, P. H. Fowler, C. Franzinetti, W. O. Lock, D. H. Perkins and G. Yekutieli, 1951, Phil. Mag. In course of publication (VI).

Carlson, A. G., J. E. Hooper and D. T. King, 1950, Phil. Mag., 41, 701 (V).

Chao, C. Y., 1949, Phys. Rev., 75, 581.

Cocconi, J., 1950, Bombay Conference on Fundamental Particles.

Crussard, J., 1950, Bombay Conference on Fundamental Particles.

Dilworth, C. C., S. J. Goldsack, Y. Goldschmidt–Clermont and F. Levy, 1950, Phil. Mag., 41, 1032.

Fermi, E., 1950, Progr. Theor. Phys., 5, 570.

Fermi, E., 1951, Phys. Rev., 81, 683.

Fowler, P. H., 1950, Phil. Mag., 41, 169 (III).

Freier, P., E. Lofgren, E. Ney and F. Oppenheimer, 1948, Phys. Rev., 74, 1818.

FRETTER, W. B., 1949, Phys. Rev., 76, 511.

FUJIMOTO, Y. and Y. YAMAGUCHI, 1949a, Progr. Theor. Phys., 4, 468.

FUJIMOTO, Y. and Y. YAMAGUCHI, 1949b, Phys. Rev., 75, 1276.

FUJIMOTO, Y. and Y. YAMAGUCHI, 1950a, Progr. Theor. Phys., 5, 787.

FUJIMOTO, Y. and Y. YAMAGUCHI, 1950b, Progr. Theor. Phys., 5, 76.

GOLDBERGER, M. L., 1948, Phys. Rev., 74, 1269.

GOLDSCHMIDT–CLERMONT, Y., 1950, Nuovo Cim., 7, 331.

GREGORY, B. P., B. ROSSI and J. H. TINLOT, 1950, Phys. Rev., 77, 299.

GREGORY, B. P. and J. H. TINLOT, 1951, Phys. Rev., 81, 667, 675.

HARDING, J. B., 1949, Phil. Mag., 40, 530.

HARDING, J. B., 1951, Phil. Mag., 42, 63.

HARDING, J. B. and D. H. PERKINS, 1949, Nature, Lond., 164, 285.

HARDING, J. B., S. LATTIMORE and D. H. PERKINS, 1949, Proc. Roy. Soc., A196, 325.

HARTZLER, A. J., 1951, Phys. Rev., 81, 323 (A).

HEISENBERG, W., 1949, Z. Phys., 126, 569.

HEITLER, W. and L. JANOSSY, 1949, Proc. Phys. Soc., A62, 364, 669.

HEITLER, W. and L. JANOSSY, 1950, Helv. Phys. Acta, 23, 417.

HEITLER, W., 1950, Bombay Conference on Fundamental Particles.

HEITLER, W., 1951, Private communication.

HODGSON, P., 1951, Phil. Mag., 42, 207.

HODGSON, P. and D. H. PERKINS, 1949, Nature, Lond., 163, 439.

LE COUTEUR, K. J., 1950, Proc. Phys. Soc., A63, 259, 498.

LEPRINCE–RINGUET, L., F. BOUSSER, HOANG–TCHANG–FONG, L. JAUNEAU and D. MORELLET, 1949, Phys. Rev., 76, 1273.

LEWIS, H. W., J. R. OPPENHEIMER and S. A. WOUTHUYSEN, 1948, Phys. Rev., 73, 127.

LOCK, W. O. and G. YEKUTIELI, 1951, Phil. Mag. In course of publication.

LORD, J. J., J. FAINBERG and M. SCHEIN, 1950, Phys. Rev., 80, 970.

LORD, J. J. and M. SCHEIN, 1951. Private communication.

LOVATI, A., A. MURA, G. SALVINI and G. TAGLIAFERRI, 1950, Phys. Rev., 77, 284.

LOVATI, A., A. MURA, C. SUCCI and G. TAGLIAFERRI, 1951, Nuovo Cim., 8, 271.

LOVERA, G., 1947, Ric. Sci. Ricostruz., 17, 2045.

MARQUEZ, L. and I. PERLMAN, 1951, Phys. Rev., 81, 953.

MENON, M. G. K. and O. ROCHAT, 1951. Private communication.

ORTNER, G., 1940, S. B. Akad. Wiss. Wien, 149, 259.

OSBORNE, L. S., 1951, Phys. Rev., 81, 239.

PAGE, N., 1950, Proc. Phys. Soc., A63, 250.

PANOFSKY, W. K. H., L. AAMODT and H. F. YORK, 1950, Phys. Rev., 78, 825.

PANOFSKY, W. K. H., L. AAMODT, J. HADLEY and R. PHILLIPS, 1950, Phys. Rev., 80, 94.

PERKINS, D. H., 1950a, Phil. Mag., 41, 138.

PERKINS, D. H., 1950b, Proc. Roy. Soc., A203, 399.

PICCIONI, O., 1950, Phys. Rev., 77, 1, 6.

ROSSER, W. G. V. and M. J. SWIFT, 1951. Private communication.

SALANT, E. O., J. HORNBOSTEL, C. B. FISK and J. E. SMITH, 1950, Phys. Rev., 79, 184.

SANDS, M., 1950, Phys. Rev., 77, 180.

SCHOPPER, E., 1947, Naturwiss., 34, 118.

STEINBERGER, J., W. K. H. PANOFSKY and J. STELLER, 1950, Phys. Rev., 78, 802.

SÖRENSEN, S. O. C., 1949, Phil. Mag., 40, 947.

SÖRENSEN, S. O. C., 1951, Phil. Mag., 42, 188.

WATAGHIN, G., 1938, Accad. Lincei, Atti, 27, 675.

WATAGHIN, G., 1946, Phys. Rev., 70, 787.

WEISSKOPF, V., 1937, Phys. Rev., 52, 295.

CHAPTER II

UNSTABLE HEAVY COSMIC RAY PARTICLES

BY

C. C. BUTLER

The Physical Laboratories, University of Manchester

INTRODUCTION 65

PART I

THE DECAY OF NEUTRAL V-PARTICLES

1. THE FIRST NEUTRAL V-SHAPED TRACK 67
2. INVESTIGATIONS OF V-SHAPED TRACKS 68
3. THE NATURE OF THE SECONDARY PARTICLES 73
4. POSSIBLE EXPLANATIONS OF THE NEUTRAL V-SHAPED TRACKS 82
5. SUGGESTED DECAY PROCESSES 85
6. MASS DETERMINATIONS 88
7. THE DYNAMICS OF DECAY SCHEMES WITH TWO SECONDARY PARTICLES 93
8. THE MEAN REST LIFETIME OF NEUTRAL V-PARTICLES 101
9. CONCLUSIONS 101

PART II

THE DECAY OF HEAVY CHARGED PARTICLES

10. THE DECAY OF τ-MESONS 105
11. THE DECAY OF CHARGED V-PARTICLES 109
12. CONCLUSIONS 121
ACKNOWLEDGEMENTS 122
REFERENCES 123

INTRODUCTION

During a detailed study of the properties of showers of penetrating cosmic-ray particles **Rochester** and **Butler** [1947] discovered two remarkable forks in the gas of their cloud chamber. These events, reproduced in Plates I and II, were attributed to the spontaneous decay of a neutral and of a charged particle, each of minimum mass about 1000 m_e. The discovery was first confirmed by Anderson and his colleagues (**Seriff** *et al.* [1950]) and subsequently by **Armenteros** *et al.* [1951], by **Fretter** [1951], by **Bridge** and **Annis** [1951], by **Astbury** *et al.* [1951], by **Thompson** *et al.* [1951] and by **Leighton** *et al.* [1951].

Professor P. M. S. Blackett has suggested that the term "V-shaped track" should be used to describe the phenomena shown in Plates I and II. If the claim that these tracks arise from the decay of hitherto-unknown unstable particles can be justified, then these particles are called V-particles. This nomenclature will be used until more information about the properties of the particles becomes available.

The new decay processes have been studied mainly in the Wilson cloud chamber, but the observation of one neutral V-shaped track in a photographic emulsion has been claimed by **Hopper** and **Biswas** [1950]. During the course of a detailed study of the μ-meson decay process in photographic emulsion, **O'Ceallaigh** [1951] has found an example of the decay at rest of a charged V-particle.

The photographic emulsion technique has been used extensively during the last few years for the investigation of nuclear interactions of all types. The decay of a slow particle, heavier than a π-meson, into three charged particles was found by **Brown** *et al.* [1949]; two examples of the same process were found by **Harding** [1950]. These unstable particles, called τ-mesons, appear to be very rare.

This article is concerned only with the decay process of heavy particles. The first evidence, however, for the existence of a particle with a mass between those of the π-meson and the proton is of a different kind. **Leprince–Ringuet** and **l'Héritier** [1946] observed the collision of a fast cosmic-ray particle with an electron in a cloud chamber operated in a magnetic field. From the dynamics of the collision, the mass of the fast particle appeared to be about 1000 m_e.

Extensive range-momentum measurements on particles in the cosmic-ray beam at an altitude of about 3,000 m. have been made by ALIKHANIYAN *et al.* [1948], who concluded that many types of charged mesons exist. They described these particles as "varitrons".

Finally, a few unusual stars in photographic emulsions have been observed by several workers, for example, by LEPRINCE-RINGUET *et al.* [1949], WAGNER and COOPER [1949] and FORSTER [1950]. These stars were produced by the nuclear capture of particles, whose mass was less than that of the proton but greater than that of the π-meson. Estimates of the minimum mass of the incident particle can be made; these measurements are not accurate or conclusive, but the minimum mass value appears to be about 700 m_e.

A detailed discussion of the properties and modes of decay of neutral V-particles is given in Part I. The results of a detailed examination of the available data on the decay of τ-mesons and charged V-particles are given in Part II.

PART I

THE DECAY OF NEUTRAL V-PARTICLES

1. THE FIRST NEUTRAL V-SHAPED TRACK

The V-shaped track observed by ROCHESTER and BUTLER [1947] is typical of many that have been found more recently. A description of this first event, reproduced in Plate I, serves as an introduction to the recent work. Tracks (1) and (2) constitute the V-shaped track, the opening angle of which is 67°. These tracks are both at minimum ionization and must have been due to singly-charged particles. Careful reprojection of the stereoscopic photographs shows that the tracks are copunctal; moreover, the tracks start at a point well inside the illuminated region of the cloud chamber where the presence of uniform background condensation indicates that the conditions for track condensation were excellent. The event is a two-pronged fork with the apex in the gas; there is no sign of a recoil track or evaporation tracks from the apex. In these sea-level experiments, very few events at all similar to this fork were observed in the 3.4 cm. lead plate which was across the centre of the chamber, but if the fork were due to any type of collision process, one would have expected several hundred times as many in the plate as in the gas. Rochester and Butler concluded that the fork could not have arisen at a collision, but must have been due to a spontaneous process for which the probability depended on the distance, and not on the amount of matter, traversed.

This V-shaped track was observed in a magnetic field of 3500 gauss. The momentum of the positive particle, track (1), was approximately (0.2—0.3) BeV/c and, since the ionization was indistinguishable from the minimum value, it was unlikely to have been a proton. As the track of the negative particle is very short, reliable momentum measurements cannot be made. However, if the neutral particle decayed into only two particles, both charged, and assuming that the path of the neutral V-particle followed the general direction of the main shower, a momentum range of

(0.7—1.0) BeV/c is estimated for the negative particle. If it is postulated that the secondary particles were π-mesons, an assumption which will be discussed in detail in §§ 5. 2 and 6. 2, then the mass of the neutral V-particle lies within the range (1000—1200) m_e.

The work of Rochester and Butler was continued at sea-level by BUTLER *et al.* [1950] and by BARKER and BUTLER [1951], but no further example of this decay process was found.

2. INVESTIGATIONS OF V-SHAPED TRACKS

Since the summer of 1949, several extensive investigations of the properties of V-shaped tracks have been started. In particular, Anderson and his colleagues (SERIFF *et al.* [1950]) have worked at sea-level and on White Mountain (3200 m.). The apparatus used by Rochester and Butler has been installed in the observatory on the Pic-du-Midi (2867 m.) near Bagnères de Bigorre in the French Pyrenees, and a preliminary report covering the first 6 months operation has been given by ARMENTEROS *et al.* [1951]. Later reference to these workers describes them as the Pic-du-Midi group. Cloud-chamber studies have been started by FRETTER [1951], by BRIDGE and ANNIS [1951], by ASTBURY *et al.* [1951], by THOMPSON *et al.* [1951] and by LEIGHTON *et al.* [1951].

2. 1 Experimental arrangements used for the detection of neutral V-shaped tracks

SERIFF *et al.* [1950] employed a small magnet to provide a field of 6500 gauss across a cloud chamber, 30 cm. in diameter, fitted with a 2 cm. lead plate. The air gap in the iron circuit was just large enough to take the chamber, which was triggered by a Geiger-counter arrangement. It then fell freely and was photographed when clear of the magnet coils. Unfortunately, distortions occurred in the chamber, presumably due to convection currents operating during the rather long time of free fall before the photograph was taken; consequently it proved almost impossible to make reliable momentum measurements above 0.2 BeV/c.

SERIFF *et al.* used a six-fold coincidence arrangement of Geiger counters to select showers of penetrating particles; two trays of counters were situated above the chamber and one below. To expand the chamber, three particles were needed in the top tray, two in the second tray, which was immediately above the chamber, and one in the bottom tray. The top counters were shielded by a transition layer of about 20 cm. of lead and the second tray was separated from the top tray by 5 cm. of lead.

The magnet and cloud chamber on the Pic-du-Midi are installed in a laboratory of permanent construction and the conditions of operation are as favourable as in the laboratory at sea-level. With a field of 7500 gauss, the maximum detectable momentum is 8 BeV/c for tracks of at least 6 cm. length. The six-fold counter arrangement is shown schematically in Fig. 1 and may be compared with that of SERIFF *et al.* already described.

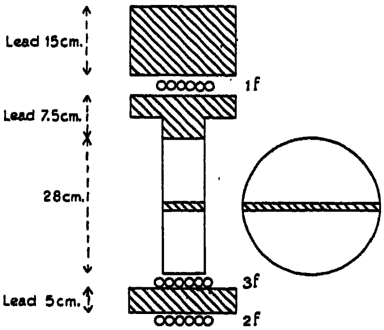

Fig. 1 – Side view of the cloud chamber operated on the Pic-du-Midi.

The counting rate of these two counter arrangements is approximately 7 c.p.h. at 3000 m. altitude. At least half the counts must arise from interactions of high-energy neutrons and protons which produce penetrating showers. The arrangement of SERIFF *et al.* is more compact and is probably sensitive to showers of lower energy than those photographed on the Pic-du-Midi, whose mean energy is estimated to be greater than 10 BeV. The arrangement used on the Pic-du-Midi appears to have several advantages over that of SERIFF *et al.* A greater yield of tracks in the chamber is achieved since at least three particles must traverse the counters below the chamber, whereas SERIFF *et al.* require only one particle. Fast protons and neutrons can interact in the top 15 cm. lead layer and protons can interact in the lead immediately above the chamber and in the lead plate inside the chamber. Hence showers of fast particles can be produced quite close to the top of the chamber. This is a great advantage if the neutral V-particles have a short lifetime. The arrangement of Seriff *et al.* requires multiplicity above the chamber, and most of the showers originated at least 20 cm. above the top of the chamber.

Astbury *et al.* [1951] have recently installed a 50 cm. cloud chamber in an electromagnet on the Jungfraujoch (3200 m.) and have found several V-shaped tracks during the preliminary experiments. Thompson *et al.* [1951] have started experiments at sea-level, using a 30 cm. chamber in a magnetic field. They have made momentum measurements on several V-shaped tracks.

Fretter used a large chamber at sea-level containing 7 plates each 6 mm. thick with 5 cm. gaps between them. He employed a non-selective 3-fold coincidence arrangement consisting of one counter above the chamber and two below, separated from one another by a thin block of lead. Bridge and Annis also used a large multiplate cloud chamber without a magnetic field but they worked at 3000 m. altitude. The triggering system was a penetrating shower set, of the type used by Tinlot [1948]. For part of the time this set was immediately on top of the chamber, but for the remaining time it was 150 cm. above the chamber. Most of the observed V-shaped tracks came from secondary nuclear interactions in the lead plates. This disposition of counters was employed in a study of penetrating showers and was not intended to be an efficient arrangement for the detection of V-shaped tracks.

2. 2 Statistical data

The results of the four groups of workers available to the author (up to April 1st, 1951) are outlined in Table 1.

Fretter and the Pic-du-Midi group both found one neutral V-shaped track per 25 high-energy interactions in the lead plates. In addition, the latter found approximately one neutral V-shaped track per 100 penetrating showers initiated above the chamber. A more detailed analysis of the Pic-du-Midi results is given in Table 2.

The counting rate, corrected for the chamber re-setting time was (7.2 ± 0.1) c.p.h. For series A and C, the number of penetrating showers has been found using the following definition. A shower is described as a penetrating shower if it contains two or more pene-

TABLE 1

Statistical data

Group	*Seriff et al*		*Fretter*	*Pic-du-Midi*	*Bridge and Annis*
Altitude	sea-level	3200 m.	sea-level	2867 m.	3200 m.
Approximate no. of photographs	3,000	8,000	17,000	10,000	10,000
Approximate no. of penetrating showers from above chamber	5,000		0	5,000	—
No. of interactions in lead plate	—		600	200	—
Total no. of neutral *V*-shaped tracks	6	24	24	53	4
No. of *V*-shaped tracks from above chamber .	25		0	44	—
No. of *V*-shaped tracks from lead plates . .	5		24	9	4

trating particles or one penetrating particle and one or more heavily-ionizing particles. The lead plate was 7 mm. thick in series C so that the penetrating power of the particles listed in the last column was not very great, and therefore a few electrons will have been counted as penetrating particles. Approximately 200 nuclear interactions of all types, nine of which had associated V-shaped tracks, were observed in the lead plate during series A and C.

TABLE 2

Analysis of Pic-du-Midi data 15th July, 1950 to 1st March, 1951

Series	Thickness of lead plate (cm.)	No. of photographs	Sensitive time [1]) (hrs.)	No. of pen. showers	No. of pen. particles
A	2.0	5,539	727	615	1,844
B	0	2,390	370	—	—
C	0.7	2,213	316	467	1,540
Total . .		10,142	1,413	1,082	3,384

[1]) excluding the chamber re-setting time.

PLATE I

THE DECAY OF A NEUTRAL V-PARTICLE PRODUCED ABOVE THE CHAMBER

(ROCHESTER and BUTLER [1947])

The momentum of the positive track (1) is (0.2 — 0.3) BeV/c. Track (2) cannot be measured. The angle of the fork is 67°. If the path of the neutral V-particle followed the general direction of the main shower and provided that there were only two secondary particles, then the momentum of track (2) must be within the range (0.7 — 1.0) BeV/c.

The positive particle was not a proton, and the fork may be interpreted by the decay scheme:

$$V_2^0 \rightarrow \pi^+ + \pi^-$$

where the mass of the neutral V-particle is about 1100 m_e.

PLATE II

THE DECAY OF A POSITIVE V-PARTICLE PRODUCED ABOVE THE CHAMBER

(ROCHESTER and BUTLER [1947])

The incident particle, track (1), was apparently deflected through 19° in the gas. The positive secondary particle subsequently penetrated the 3.4 cm. lead plate. Track (1) cannot be measured, track (2) has a measured momentum of 0.77 BeV/c below the plate.

The V-shaped track was due to the decay in flight of a positive V-particle into a charged particle, probably a π-meson, and one or more neutral particles. Because the momentum of the V-particle cannot be measured its mass cannot be calculated. If different decay schemes are assumed then the minimum mass for each can be calculated. The values for a number of possible schemes are given in Table 11 of § 11. 5.

PLATE I (see §§ 1 and 6.2)

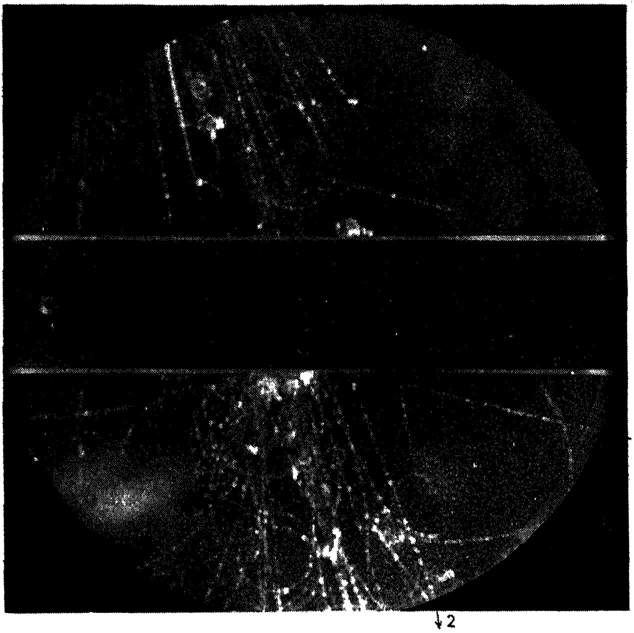

PLATE II (see § 11.1)

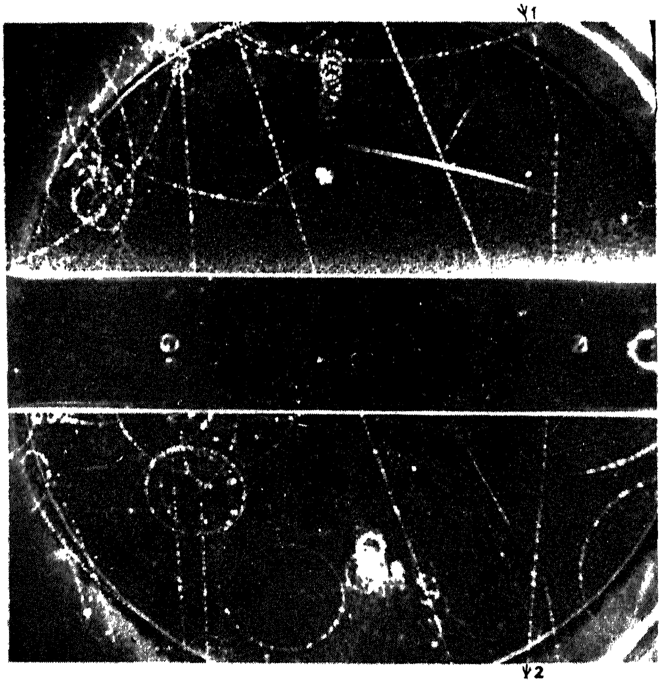

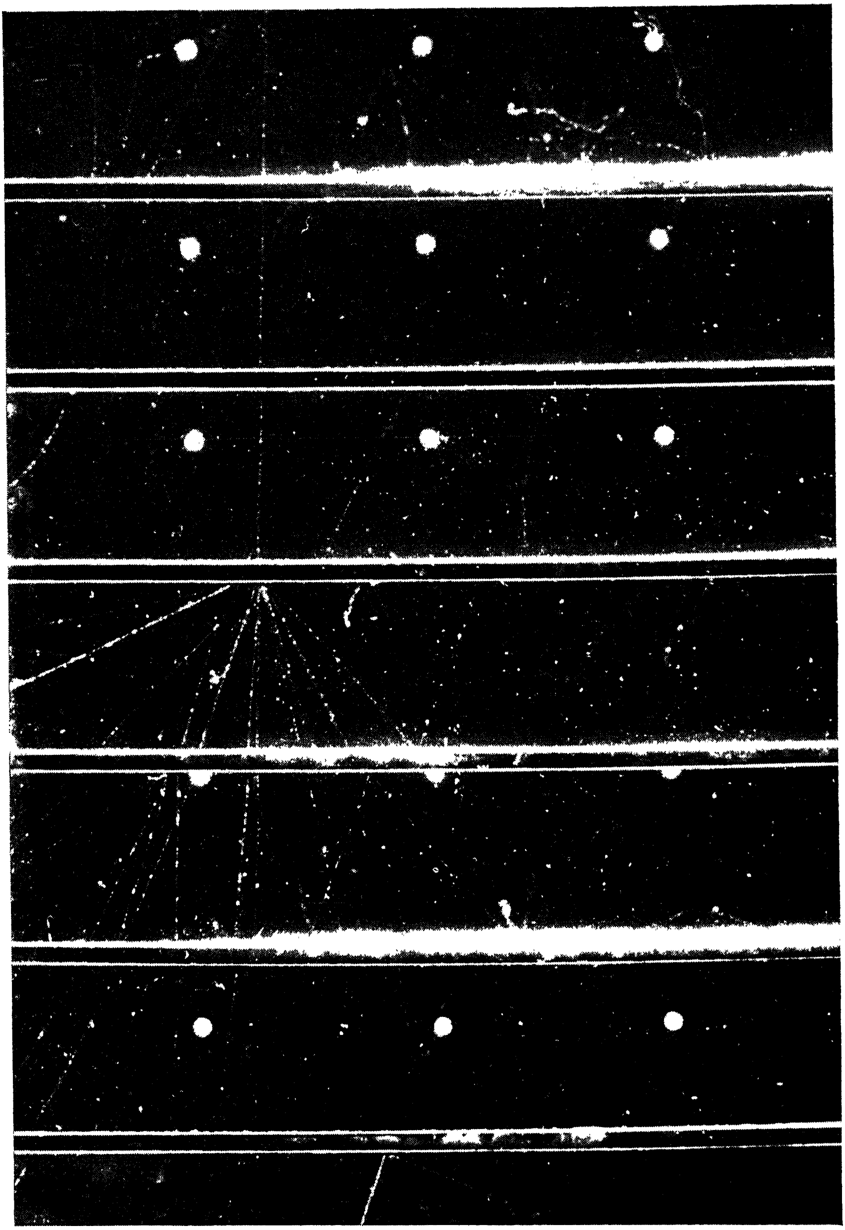

THE ORIGIN OF A NEUTRAL V-PARTICLE
(FRETTER [1951])

A high-energy nuclear interaction was produced in the 3rd lead plate by a charged particle. The V-shaped track can be seen between plates 3 and 4. The path length of the neutral V-particle was probably less than 2 cm. Both secondary particles appear to be at minimum ionization; the right-hand particle penetrated at least two plates and suffered a large scatter in the 4th plate.

2. 3 The source of the neutral V-shaped tracks

Almost all the V-shaped tracks obtained by Fretter pointed back towards high-energy nuclear interactions in the thin lead plates. These interactions are typical of those produced by protons and neutrons of energy greater than 5 BeV. Nine of the neutral V-shaped tracks obtained on the Pic-du-Midi are of a similar type. The production of neutral particles, responsible for V-shaped tracks, is shown in Plates III, IV and V.

3. THE NATURE OF THE SECONDARY PARTICLES

In most cases the two charged secondary particles cannot be identified unambiguously by the usual cloud-chamber techniques. They are always singly charged and occasionally are heavily ionizing or are seen to penetrate a lead plate without multiplication or interaction.

3. 1 Heavily-ionizing secondary particles

SERIFF *et al.*, FRETTER, BRIDGE and ANNIS, THOMPSON *et al.* and the Pic-du-Midi group all report the occurrence of heavily-ionizing particles among the secondaries. If momentum measurements can be made and, at the same time, estimates of the degree of ionization, then the particles may often be identified with considerable certainty, but in no case have both secondary particles been identified at the same time. SERIFF *et al.* found one slow particle with a mass between 150 m_e and 350 m_e. In five other cases, they found that the mass of one secondary particle must be less than that of the proton. One event appeared to consist of two heavily-ionizing tracks which could not be identified, presumably owing to distortions in the chamber. This event is illustrated in Plate VI. Fretter, and Bridge and Annis have found several examples of heavily-ionizing secondary particles, but no identifications could be made. THOMPSON *et al.* have identified two slow protons at sea-level.

The Pic-du-Midi group have found nine heavily-ionizing particles, which have been separated into protons and negative π- or μ-mesons. Five of these slow particles can be identified, with considerable certainty, as protons; an example is reproduced in Plate VII.

PLATE IV

THE ORIGIN OF A NEUTRAL V-PARTICLE

(FRETTER [1951])

A high-energy nuclear interaction was produced in the 4th lead plate. The neutral V-shaped track can be seen between the 4th and 5th plates and consists of a heavily-ionizing track and one at substantially minimum ionization. The slow particle was absorbed in the 5th plate; the thin secondary track can be traced almost to the 7th plate and was appreciably scattered in the 6th plate.

From the orientation of the V-shaped track with respect to the point of formation of the V-particle, it can be concluded that the momentum of the slow particle was higher than that of the penetrating secondary. It is most probable that the slow particle was a proton and that the other secondary particle was a meson.

Plate IV (see § 2. 3)

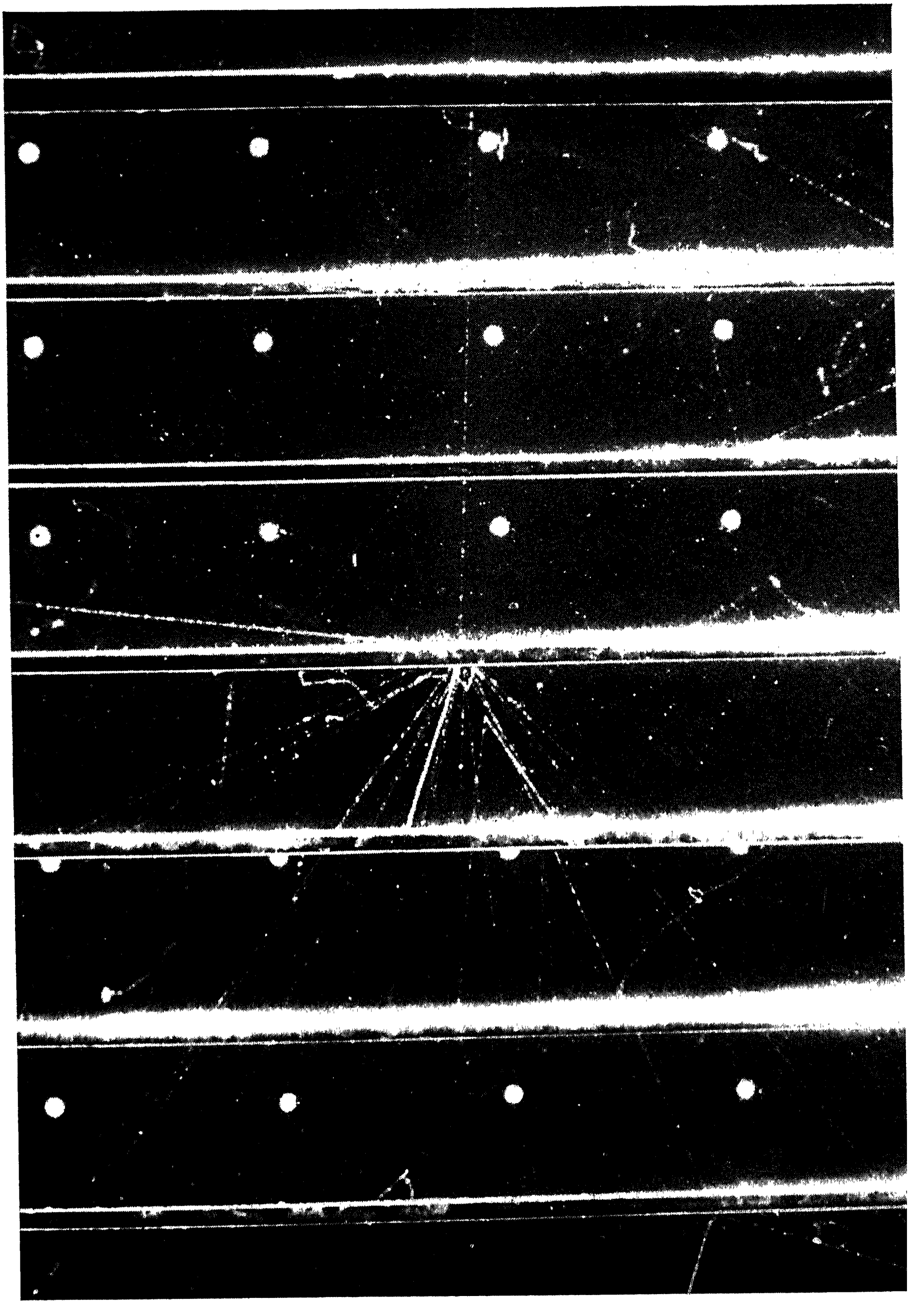

Plate V (see §§ 2. 3 and 6. 2)

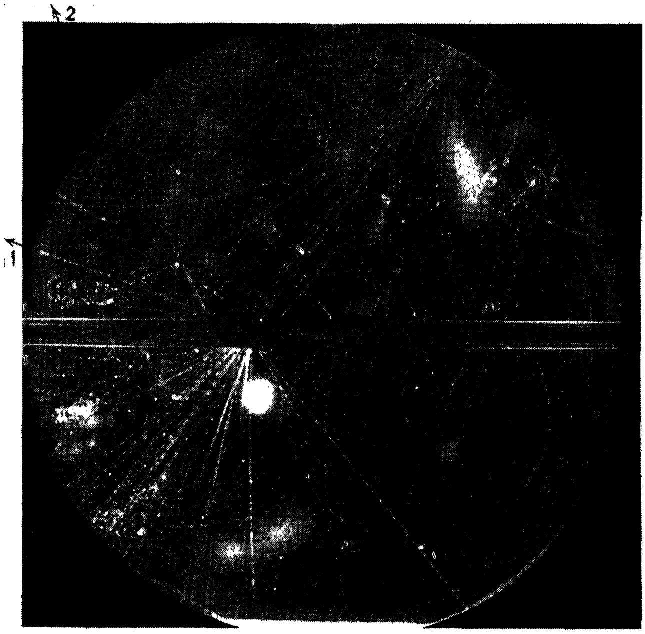

Plate VI (see § 3. 1)

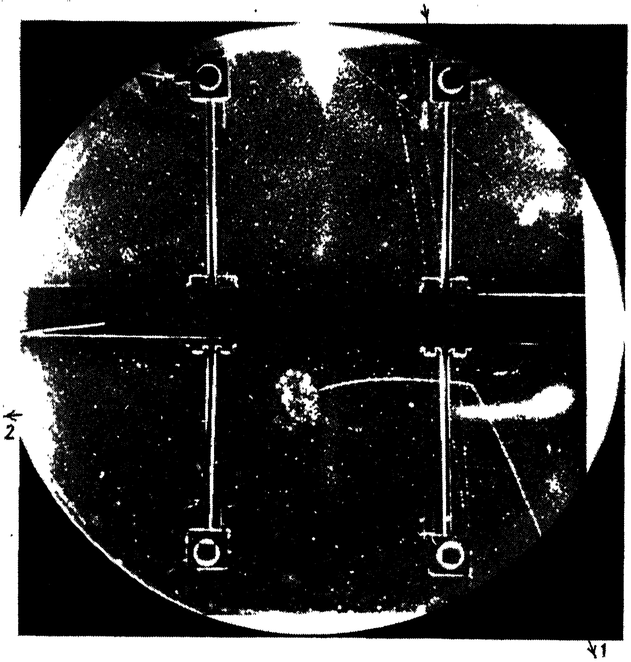

PLATE V

A BACK-SCATTERED NEUTRAL V-PARTICLE

(The Pic-du-Midi group)

A very high-energy nuclear interaction occurred in the 7 mm. lead plate; several slow particles can be seen below the plate in addition to many fast particles which were probably protons and mesons. The interaction was secondary to one of still higher energy which occurred above the chamber. Tracks (1) and (2) form the backscattered neutral V-shaped track; the angle between them is 77°.

The momentum of the positive track (1) is 0.27 BeV/c and that of the negative track (2) approximately 0.13 BeV/c. It was probably due to a negative π-meson. The positive particle cannot have been as heavy as a proton and it is concluded that the fork can be interpreted by the decay scheme:

$$V_2^0 \rightarrow \pi^+ + \pi^-,$$

where the mass of the neutral V-particle is about 700 m_e (cf. Table 9 of § 6. 2).

PLATE VI

A NEUTRAL V-SHAPED TRACK WITH TWO SLOW SECONDARIES

(SERIFF *et al.* [1950])

Tracks (1) and (2) form the neutral V-shaped track, the angle between them is about 120°. Because of distortions reliable momentum measurements could not be made; some general observations can, however, be made. If the line of flight of the neutral V-particle was parallel with the two fast particles, which crossed the top of the chamber, then the momentum of track (1) is several times that of track (2), provided that only two secondary particles were produced. Track (2) was probably due to a slow meson and track (1) to a slow proton but definite identifications cannot be made.

PLATE VII

THE DECAY OF A NEUTRAL V-PARTICLE INTO A PROTON AND A MESON

(The Pic-du-Midi group)

Tracks (1) and (2) form the neutral V-shaped track; the angle between them is 50.5°. The estimated ionization of track (1) is (3—4) minimum and the measured momentum 0.48 BeV/c. The particle can be identified with considerable certainty as a proton. The negative secondary had a momentum of 0.19 BeV/c and was probably a π-meson.

The neutral V-shaped track is interpreted by the scheme:

$$V_1^0 \rightarrow p^+ + \pi^-,$$

where the mass of the neutral V-particle is $2220m_e$ (cf. Table 7 of § 6. 1).

PLATE VIII

AN IDENTIFIED NEGATIVE MESON SECONDARY OF A NEUTRAL V-PARTICLE

(The Pic-du-Midi group)

The negative track (1) has a measured momentum of 82 MeV/c (± 5 %) and the estimated ionization is (2.5—3.5) times the minimum value. The ionization of a π-meson of this momentum would be 3.0 times minimum. The positive secondary particle dipped steeply into the piston; the projected angle of the fork is about 27°.

PLATE VII (see §§ 3. 1 and 6. 1)

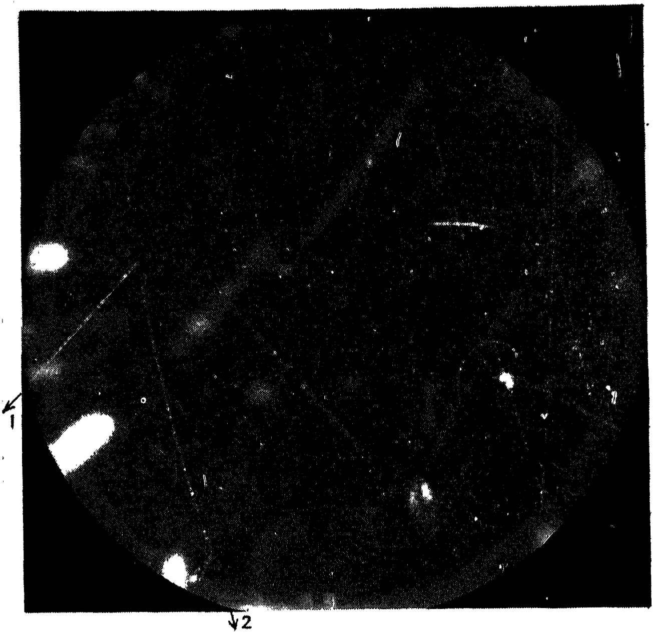

PLATE VIII (see § 3. 1)

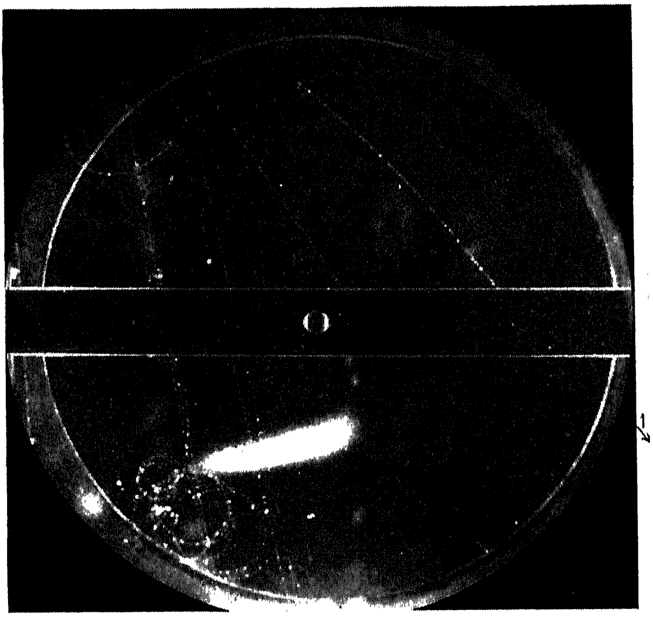

PLATE IX (see § 3. 2)

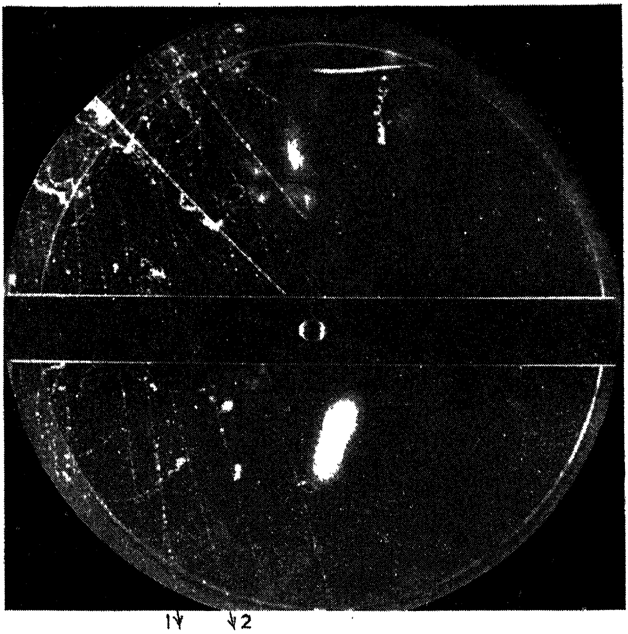

PLATE X (see § 3. 2)

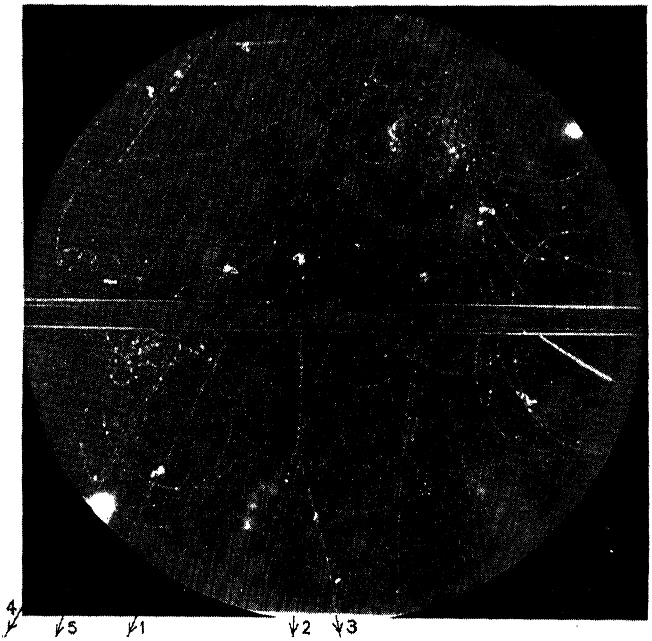

PLATE IX

A NEUTRAL V-PARTICLE WITH TWO PENETRATING SECONDARIES

(The Pic-du-Midi group)

Tracks (1) and (2) constitute a neutral V-shaped track, the angle of which is about 6°. The momenta can only be measured below the plate; the measured momentum of the positive track (1) is 2.6 BeV/c and that of the negative track (2) 3.0 BeV/c. The fact that both secondaries penetrated the 2 cm. lead plate without making interactions indicates that they were not electrons.

This V-shaped track can be interpreted most satisfactorily according to the scheme:

$$V_2^0 \rightarrow \pi^+ + \pi^-,$$

where the mass of the neutral V-particle is 796 m_e (cf. Table 8 of § 6. 1 and also §§ 7. 1 and 7. 2).

PLATE X

A NEUTRAL V-SHAPED TRACK WITH AN IDENTIFIED π-MESON SECONDARY

(The Pic-du-Midi group)

A neutral V-particle decayed just above the plate into particles (1) and (2). Track (1) is that of the positive particle and cannot be measured precisely but its momentum was probably greater than 1 BeV/c. Track (2), that of the negative secondary, is very short above the plate and the ionization is probably above the minimum value. Below the 7 mm. plate this secondary was heavily ionizing but was deflected through 23° in the gas. The measurements on this particle and its secondary (track 3) are given in Table 4 of § 3. 2. Track (2) was due to a π-meson which decayed in flight into a μ-meson, track (3). This photograph provides evidence for the existence of π-mesons among the negative secondaries of neutral V-particles. The positive secondary was probably a proton and the V-particle decayed according to the scheme:

$$V_1^0 \rightarrow p^+ + \pi^-.$$

There is a second V-shaped track on this photograph, formed by tracks (4) and (5), at an angle of about 10°. The positive track (4) has a measured momentum of 0.32 BeV/c and that of the negative track (5) is 0.66 BeV/c. Neither of the secondaries can have been as heavy as the proton; consequently the fork can be interpreted by the scheme:

$$V_2^0 \rightarrow \pi^+ + \pi^-,$$

where the calculated mass of the V_2^0-particle is about 610 m_e (cf. Table 9 of § 6. 2).

The momentum and ionization estimates for these particles are given in Table 3.

TABLE 3

Momentum and ionization measurements on five proton tracks

Event no.	33	43	47	56	13
Momenta (× BeV/c)					
positive track (1) . .	0.24	0.48	0.35	0.45	~0.5
negative track (2) . .	0.25	0.19	0.14	0.16	0.12
Estimated ionization of track (1) (× min.)	8–15	3–4	4–6	3–4	3–4
Calculated ionization for a proton, assuming measured momentum (× min.)	9	3.0	5.0	3.5	3

Four negative tracks with momenta less than 0.1 BeV/c are heavily ionizing and are probably due either to π- or μ-mesons; one example is shown in Plate VIII. No example of an identified positive meson has yet been found.

3. 2 The penetrating properties of the secondary particles

Seriff *et al.* and the Pic-du-Midi group have found fifteen secondary particles, which penetrated the 2 cm. lead plates without making interactions or radiative collisions; in five photographs both secondaries penetrated the plate. In addition, one secondary particle produced a disintegration in one of the lead plates, one particle appeared to suffer catastrophic absorption and two were scattered through large angles. Thus four interactions are associated with fifteen traversals of the 2 cm. plates, and the interaction length of the secondary particles is therefore about 7.5 cm. of lead. The geometrical cross section in lead corresponds to an interaction length of 15 cm. of lead; the experimental result for the secondary particles is probably not significantly different from this value. Thus both the positive and negative secondary particles appear to have strong nuclear interactions and so are unlikely to have been electrons or μ-mesons. A neutral V-shaped track with two penetrating secondaries is shown in Plate IX.

The Pic-du-Midi group used a 7 mm. plate across the chamber during series C. One neutral V-shaped track, with the negative secondary near minimum ionization, was produced above the plate; this secondary was heavily ionizing below the plate. The ionization and momentum measurements are consistent with the particle having been either a π- or a μ-meson. Another V-shaped track was produced above the thin lead plate; it is reproduced in Plate X. Track (2), that of the negative secondary, is very short above the plate and the ionization is probably above the minimum value. Below the plate this secondary was heavily ionizing but was deflected through an angle of 23° in the gas. The measurements on the negative particle are summarised in Table 4, from which it is concluded that the particle was probably a π-meson.

TABLE 4

Measurements on the decay of a π-meson in flight

	Track (2)	Track (3)
Momentum (× MeV/c)	78 (± 5%)	61 (± 5%)
Estimated ionization (× min.) . . .	3–4	3–4
Calculated ionization for π-meson . .	2.8	4.0
Calculated ionization for μ-meson . .	2.0	2.8

This event was almost certainly a $\pi \rightarrow \mu$ decay; a scattering of a π-meson by a nucleon would be very much less probable. The angle of the decay is close to the maximum value corresponding to the momentum of the π-meson (cf. § 11. 3).

3. 3 The differential momentum spectrum of the secondary particles

Accurate momentum measurements can be made on both the secondaries of twenty-six neutral V-events obtained by the Pic-du-Midi group. The results are given in Table 5, in the form of differential momentum spectra for the positive and negative secondary particles.

In general, the momenta of the negative secondaries were lower

TABLE 5

The differential momentum spectrum of the secondary particles

Momentum category .	1 .	2	3	4	5
Momentum range (BeV/c)	0–0.1	0.1–0.5	0.5–1.0	1.0–1.5	> 1.5
Positive particles . . .	0	10	7	2	7
Negative particles . . .	1	16	4	0	5

PLATE XI

A NUCLEAR INTERACTION IN THE GAS

(The Pic-du-Midi group)

The interaction was produced below the plate by particle (1); tracks (3) and (4) were produced, along with a heavy blob of ionization, which was probably due to a nuclear recoil. Track (1) cannot be measured because it is partially obscured by a low-energy δ-ray. The positive track (2) has a measured momentum of 0.35 BeV/c and an ionization of (4-5) times minimum; it was probably due to a proton. The positive track (3) has a measured momentum of 0.65 BeV/c and is inclined at an angle of about 7° to the plane defined by tracks (1) and (2). Momentum is apparently not conserved in a direction at right angles to the incident particle. Thus the event is not a simple elastic scattering. The simplest scheme appears to be:

$$p^+ + p^+ \rightarrow n^\circ + p^+ + \pi^+.$$

PLATE XII

A NARROW-ANGLE, HIGH-ENERGY, V-SHAPED TRACK

(The Pic-du-Midi group)

The fork consists of two high-energy tracks (1) and (2) at an angle of 12°. The measured momentum of the positive track (1) is 1.5 BeV/c and that of the negative track (2) is 1.6 BeV/c. A detailed consideration of the dynamics of the decay process leads to the conclusion that the V-particle probably decayed according to the scheme:

$$V_2^0 \rightarrow \pi^+ + \pi^-,$$

and the mass is 840 m_e (cf. Table 8, § 6. 1).

PLATE XI (see § 4. 1)

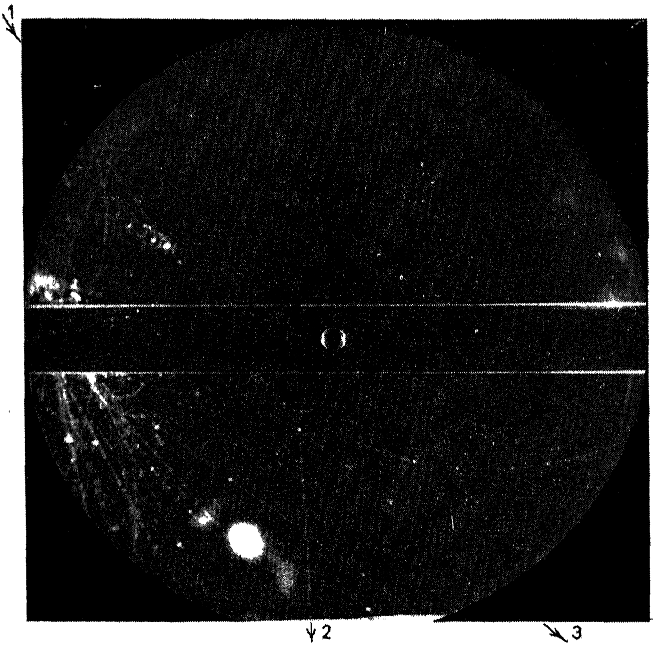

PLATE XII (see § 6. 1)

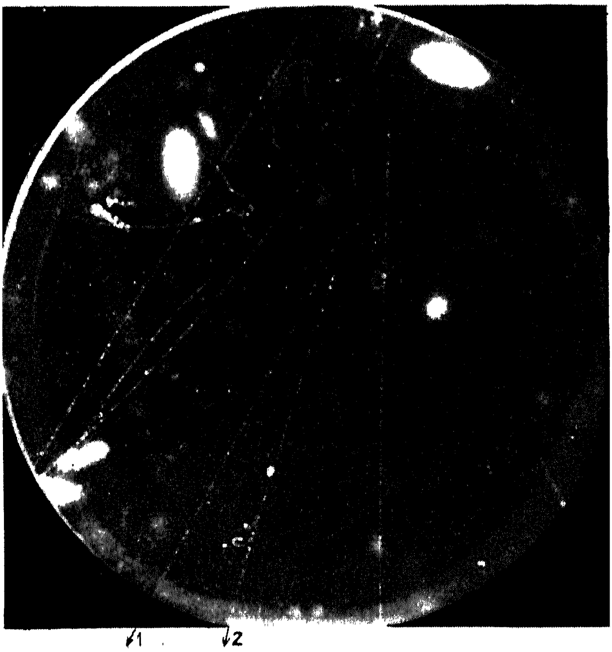

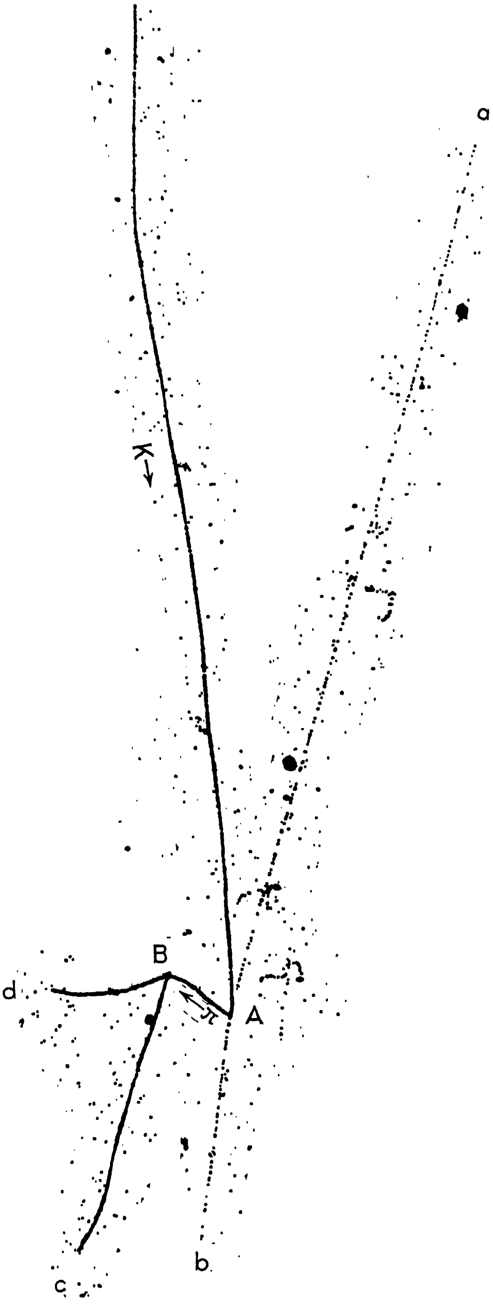
a
K
B
d
π
A
b
c

PLATE XIII

THE DECAY OF A SLOW τ-MESON

(BROWN *et al.* [1949])

Particle k came to rest at A and produced particles a, b and a slow π-meson; subsequently the π-meson was captured at B. From measurements of the grain density as a function of range, the mass of particle k was found to be (1080 ± 160) m_e. Detailed arguments have been given by Brown *et al.* which show that particle k was not captured at A by a nucleus, which then emitted particle a, b and π. Careful measurements show that the tracks of these secondary particles are coplanar and the event can only be interpreted by the spontaneous decay of particle k. It can be shown that tracks a and b were due to mesons, probably π-mesons and their energies can be measured from the observed grain densities and scatterings. Using these values and the known energy of the slow π-meson the mass of the unstable particle, known as a τ-meson, was found to be 985 m_e, in good agreement with the mass value obtained from a study of track k.

(This photograph is reproduced by the kind permission of the Editors of Nature.)

than those of the positive particles. The sixteen negative particles in momentum category 2 were all at minimum ionization and therefore could not have been as heavy as the proton. Likewise three of the positive particles in category 2 and one in category 3 (near 0.5 BeV/c) could not have been as heavy as protons. Two of these positive particles were directly associated with negative particles of mass smaller than the proton mass. Three other positive particles were found to be lighter than the proton; their corresponding negative particles could not be measured. Thus seven positive particles lighter than protons have been found, but none has actually been identified.

4. Possible explanations of the neutral V-shaped tracks

It is important to consider carefully whether the neutral V-shaped tracks can be explained in terms of well-known processes, such as the interactions of neutral particles or radiation in the gas of the chamber, or as examples of large-angle scattering. If the observed number of neutral V-events cannot be so explained, then they will be interpreted by the spontaneous decay in flight of neutral particles. The detailed information required for this analysis is only available, at present, from the work of the Pic-du-Midi group.

4. 1 Interactions in the gas of the cloud chamber

Electromagnetic and nuclear interactions can occur in the argon and oxygen filling of the chamber. Electron pair production in the gas is occasionally observed; at least 10 pairs with energies of a few MeV have been found, while most of the neutral V-shaped tracks have a total energy of about 1 BeV. A photon of this energy would produce an electron pair with an opening angle very much less than 1°, a far smaller angle than is ever observed. In view of the identification of many of the secondary particles as protons and mesons, electron pair production cannot explain the observed V-events.

Nuclear interactions in the gas can be produced by neutrons or by high-energy photons. The cross-section for the production of stars by energetic neutrons corresponds closely to the geometric value, but the cross-section for the production of similar events by photons is very much smaller and may be neglected. The Pic-du-

Midi group observed twenty-three neutral V-shaped tracks during the period when the 2 cm. lead plate was in use. If all these events were the result of interactions between incident neutrons and gas atoms then, assuming that the cross-section is the geometrical one, about 400 times as many forks, that is nearly 10,000, should have been formed in the lead plate. In practice, not all these forks would be observable owing to the absorption of some of the prongs in the lead. Half of the V-events, however, were of high energy and would be visible in the chamber even if produced near the top of the lead plate. In fact, very few energetic two-pronged stars came from the lead plate. About 200 nuclear interactions of all types occurred in the plate during the same period as the twenty-three neutral V-events. Using the data of Barker and Butler [1951], it is possible to estimate that about 200 additional interactions took place in the plate which were not visible in the chamber, and so only 400 nuclear interactions of all types occurred in the plate. Therefore it is not possible to interpret all the V-shaped tracks in the gas as nuclear interactions.

The number of stars in the gas, similar to the neutral V-shaped tracks, can be calculated using an estimate of the neutron flux. It is only necessary to consider the interactions of the energetic neutrons, since each of the stars must contain a meson and the cross-section for meson production by neutrons does not approach the geometrical value until their energy exceeds about 1 BeV. It may be assumed that the flux of neutrons, with momenta greater than 1 BeV/c, is equal to the number of protons with similar momenta. Barker and Butler [1951] found that, at sea level, the number of fast protons is between 25 and 50 % of the penetrating particles. Thus the number of fast neutrons can be determined from the flux of the penetrating particles, whose spectrum has also been measured by Barker and Butler. The number of fast neutrons traversing the cloud chamber in all of the penetrating showers (with 2 cm. lead plate) is between 300 and 500; these would produce about 0.2 stars in the gas.

Thus the twenty-three V-events cannot be explained as neutron-induced stars. Further detailed arguments can be given to support this conclusion. The absence of evaporation tracks and nuclear recoils is significant. The argon nucleus is relatively small and transparent to fast neutrons but, even so, only a small proportion of the stars produced would not have evaporation tracks or visible recoils.

If the neutral V-events were due to neutrons, then we should have found a comparable number of high-energy stars otherwise similar but produced by ionizing particles. In fact, the Pic-du-Midi group has observed two such stars produced by ionizing particles. The first of these is shown in Plate XI and described in the caption. The Y-shaped event cannot be explained as a simple elastic collision and must have been due to an interaction, possibly according to the scheme:

$$p^+ + p^+ \rightarrow p^+ + n^0 + \pi^+, \tag{1}$$

since both the charged secondary particles are positive and one is identified as a proton. A large blob of ionization at the point of the interaction is almost certainly the nuclear recoil. A negative meson was produced in the second Y-shaped event together with a long nuclear recoil; this interaction may have been produced by a fast π-meson. Thus, comparing the Y-shaped events with all the neutral V-shaped events, at most two or three of the latter could have been due to neutrons.

HOPPER and BISWAS [1950] have observed a neutral V-shaped track close to a very large star in a photographic emulsion. One secondary was identified as a proton, the other, a minimum ionization track of about the same momentum, could have been either a π-meson, a μ-meson or an electron. A large grain was observed at the apex of the fork, but Hopper and Biswas argued that this grain was not large enough for a nuclear recoil. They concluded that the event could only be explained as the decay of a neutral particle of mass (2370 ± 60) m_e into a proton and a π-meson. The plane of the fork did not pass through the origin of the large star and so, if the neutral V-particle decayed into only two particles, it was not produced in the star. It is hardly possible to substantiate the explanation offered by Hopper and Biswas, without carrying out a detailed analysis of all two-pronged stars which are found more frequently in emulsions than in the cloud-chamber experiments. For example, it may be possible to explain the event as a glancing collision of a neutron with a silver or bromine nucleus, according to the following scheme:

$$n^0 + n^0 \rightarrow p^+ + n^0 + \pi^- \tag{2}$$

4. 2 Large-angle single scattering of particles in the gas of the cloud chamber

Many more neutral than charged V-shaped tracks have been discovered. This result would be very surprising if they are all produced by large-angle scattering processes, since a preponderance of relatively small angle scattering, with the appearance of charged V-shaped events (e.g. Plate II), would be expected. The second objection to this explanation is again the absence of recoil tracks. An argon nucleus of momentum 50 MeV/c can produce a distinctive blob of ionization. The Pic-du-Midi group has found only one such blob at the apex of a neutral V-shaped track; this one event, therefore, could be explained as large-angle scattering. In all the other neutral V-shaped tracks, a visible recoil would be expected if the events are to be explained by scattering.

It is therefore concluded that the only explanation of the majority of the V-shaped tracks is that first suggested by ROCHESTER and BUTLER [1947] and adopted by SERIFF *et al.* [1950] and ARMENTEROS *et al.* [1951], namely, that they are due to spontaneous decay processes.

5. SUGGESTED DECAY PROCESSES

The nature of the two charged secondaries from a V-particle decay has already been discussed. If these are the only secondary particles then possible decay schemes can be considered.

5. 1 The number of secondary particles

Nineteen of the neutral V-particles observed by SERIFF *et al.* [1950] were associated with other contemporary tracks; in twelve cases, it was possible to use these tracks to find the points of origin of the main nuclear interactions. Most of these events must have been at least 15 cm. above the top of the chamber, and, owing to the multiple-Coulomb scattering and the secondary interactions of shower particles in the lead, the points of origin could not have been located very precisely. These workers found that the planes of all twelve forks contained the points of the primary interactions, within the limits of experimental error. It is difficult to assess the significance of this result, which, however, appears to favour two-particle decay processes.

The Pic-du-Midi group find that it is impossible to locate precisely the point of origin of neutral V-particles if they occur in the top transition material. Nine of their neutral V-shaped tracks came from interactions in the lead plate, and, of these, two have secondary tracks which are long enough for the planes to be determined fairly accurately. These planes contain the primary interactions within the errors of measurement, but the two decay points are close to the lead plate, so that the planes of the forks are bound to pass fairly close to the points of the primary interactions. In addition, the directions of the two neutral V-particles divide the angles of the forks in the ratios expected from the momenta of the secondaries, assuming that they are the only products of the decays.

Fretter observed two neutral V-shaped tracks which apparently did not point back to the nuclear interactions visible in the chamber. Unless these V-particles came from outside the chamber or from secondary interactions, without any recognisable prongs, one or more neutral particles must also have been produced at the decays.

It is difficult to assess the present significance of these measurements on the orientation of the forks with respect to the points of origin of the V-particles. The few decays examined in detail appear to involve only the two charged secondaries, but much more data will be required before a definite conclusion can be reached. Meanwhile the available V-events can be analysed profitably on the assumption that there are only two secondary particles.

5.2 Possible two-particle decay schemes

Protons and negative mesons, probably π-mesons, have been identified among the secondary particles, consequently the decay scheme:

$$V_1^0 \rightarrow p^+ + \pi^- \tag{3}$$

may apply to many of the observed decays. In § 4.3 several V-shaped tracks were shown to have secondaries lighter than the proton; the simplest two-particle process for these events appears to be:

$$V_2^0 \rightarrow \pi^+ + \pi^- \tag{4}$$

where the π-mesons might, as far as direct observations are concerned, be replaced by μ-mesons.

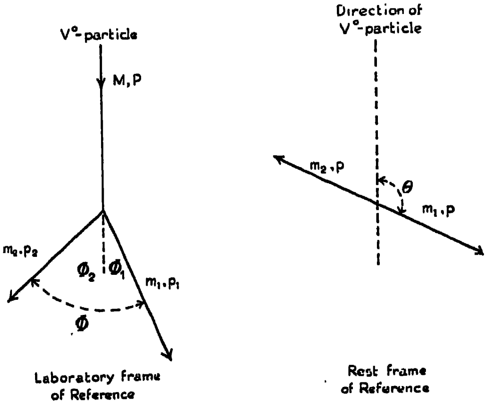

Fig. 2

If a decay scheme is assumed, then the masses of the V-particles can be calculated using only the laws of conservation of energy and momentum, provided that the momenta of the secondaries and the angles of the forks in the laboratory frame of reference are all known. Using the symbols shown in Fig. 2, and writing the masses in energy units, the necessary equations are: —

$$\sqrt{M^2 + P^2} = \sqrt{m_1^2 + p_1^2} + \sqrt{m_2^2 + p_2^2} \tag{5}$$

and

$$P^2 = p_1^2 + p_2^2 + 2p_1p_2 \cos\phi.$$

The equations (5) can be combined to give

$$M^2 = m_1^2 + m_2^2 + 2p_1p_2\left[\left\{1 + \left(\frac{m_1}{p_1}\right)^2\right\}^{\frac{1}{2}}\left\{1 + \left(\frac{m_2}{p_2}\right)^2\right\}^{\frac{1}{2}} - \cos\phi\right]. \tag{6}$$

A study of equation (6) leads to the following conclusions:

(a) If either m_1/p_1 or $m_2/p_2 \geqslant 1$, then the term $\cos\phi$ has little effect on the value of M.

(b) The term $\cos\phi$ is only important when m_1/p_1 or $m_2/p_2 \ll 1$, that is, for very high values of p_1 and p_2. The value of ϕ will then usually be less than 15°, but if it is measured to within about 1°, the principal errors are still in p_1 and p_2.

(c) In general, the most important error is contained in the term $2\,p_1 p_2$.

If the conclusions of § 5. 1 are incorrect and the decays each involve three secondary particles, then equations (5) may be extended in the following manner:

$$\begin{aligned} \sqrt{M^2+P^2} &= \sqrt{m_1^2+p_1^2}+\sqrt{m_2^2+p_2^2}+\sqrt{m_3^2+p_3^2} \\ \mathbf{P} &= \mathbf{p}_1+\mathbf{p}_2+\mathbf{p}_3 \end{aligned} \tag{7}$$

where the second equation is the vector equation for the conservation of momentum. If a decay is really of this form, but is interpreted as a two-particle decay, then a comparison of equations (6) and (7) shows that the calculated mass will be smaller than the true value.

Values of p_1, p_2 and ϕ can be found for twenty-five neutral V-particles obtained by the Pic-du-Midi group and for Rochester and Butler's sea-level event. The measurements are not all of comparable accuracy, since in many cases the tracks are rather short. The maximum detectable momentum, for tracks at least 6 cm. long, was found to be about 8 BeV/c; thirteen of the V-events have both secondaries at least 6 cm. long.

The differential momentum spectrum of the twenty-six neutral V-particles can be calculated using the second of equations (5) and is shown in Table 6. No unusual features have been noticed in this very limited data.

TABLE 6

The differential momentum spectrum of the neutral V-particles

Momentum range (× BeV/c)	0.1–0.5	0.5–1.0	1.0–1.5	1.5–2.0	> 2.0
No. of V^0-particles . . .	3	8	3	5	7

6. Mass determinations

It is necessary to divide the twenty-six V-shaped tracks, which have been measured completely, between the two possible decay schemes. A procedure for the partial division of the Pic-du-Midi data between the two schemes will now be described.

6.1 The decay of V_1^0-particles into protons and π-mesons

Four of the measured forks contain identified protons and can only be explained by decay scheme (3); the mass determinations for these are given in Table 7.

TABLE 7

The masses for four V_1^0-particles each with an identified proton secondary

(1) Event no.	(2) Approx. track length (cm.)	(3) Measured momenta (× BeV/c)	(4) Ratio (p_+/p_-)	(5) Angle of fork (deg.)	(6) Mass using scheme equation (3) (× m_e)
33	9	+ 0.242	0.95	27	2277 ± 40
	4	− 0.254			
43	6	+ 0.480	2.5	50.5	2218 ± 10
	10	− 0.192			
47	6	+ 0.350	2.5	87.5	2228 ± 10
	18	− 0.142			
56	18	+ 0.450	2.8	44	2181 ± 10
	14	− 0.162			

The standard deviations on the measured momenta values in column (3) are all approximately 10 % of the average values except for the negative particle of event 33, for which the standard deviation may be as high as 20 % of the quoted value. For these particular events the uncertainties in the magnetic field and in the curvature measurements are appreciable sources of error. Corrections have been made for the non-uniformity of the magnetic field and the angles of the forks have been determined accurately from reconstructions of the events. The momenta were all quite low and the errors arising from the chamber distortions are not large. The standard deviations of the mass values are given in column (6) and the average value is (2226 ± 10) m_e.

THOMPSON *et al.* have measured a V-shaped track which is similar to those described in Table 7. The positive particle was only just heavily ionizing and the mass of the V-particle was found to be $(2165 \pm 20)\, m_e$.

Eight of the remaining eighteen forks found by the Pic-du-Midi group each have both secondary tracks longer than 6 cm., which have been measured accurately; several are high-energy tracks for which gas distortions in the chamber are the principal source of error. The angles of the forks have been measured by reprojecting the stereoscopic photographs, those of less than about 10° have been measured to within 10 % and for most cases the larger angles to within 5 %. Each of the eight positive secondary tracks could have been due to a proton; in most of the events, the negative tracks are of lower momentum than the positive tracks.

The mass values obtained for these events are not all in good agreement with the results given in Table 7. An average mass of 2200 m_e is obtained from the data on four of the V-tracks, but the remaining four have significantly higher values of about 2700 m_e and were due to high-energy V-particles. The data for these forks are given in Table 8; two have long secondary tracks and the standard deviations on their mass values are about $\pm$ 50 m_e.

The evidence is not yet conclusive, but the mass values in column

TABLE 8

The masses of four V-particles which probably decayed into two π-mesons

(1) Event No.	(2) Approx. track length (cm.)	(3) Measured momenta ($\times$BeV/c)	(4) Ratio (p_+/p_-)	(5) Angle of fork (deg.)	(6) Mass (scheme of equation (3)) ($\times m_e$)	(7) Mass (scheme of equation (4)) ($\times m_e$)
5	6	+ 2.6	0.9	6	2800	796
(Plate IX)	7	− 3.0				
38	10	+ 1.4	2.0	20	2400	872
	15	− 0.7				
53	10	+ 1.5	0.9	12	2690	841
(Plate XII)	16	− 1.6				
69	9	+ 2.2	1.2	5.5	2560	673
	9	− 1.9				

(6) of Table 8 are so different from those in column (6) of Table 7 that, either several V-particles exist which have the same mode of decay, or the decays did not all follow the same scheme.

The fourteen remaining forks each have at least one secondary shorter than 6 cm.; these tracks cannot always be measured accurately. Five of these cases cannot be explained in terms of decay scheme (3), since the positive particles were not protons; six give masses within the range (2150—2350) m_e and three values around 2700 m_e using scheme (3).

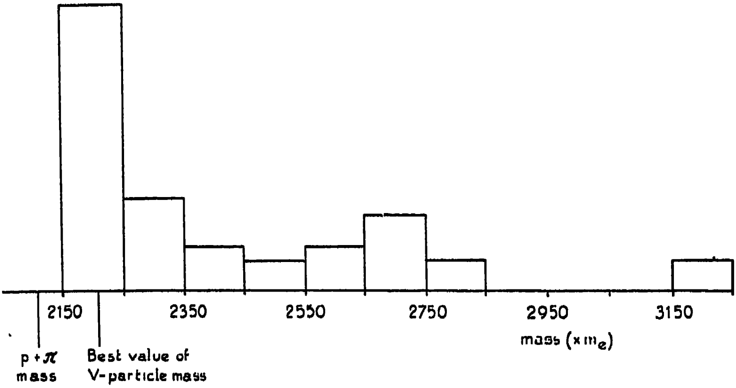

Fig. 3

Altogether twenty-one neutral V-shaped tracks can be interpreted in terms of scheme (3); fourteen of these give masses within the range (2180—2350) m_e and seven masses of around 2700 m_e. A mass histogram for the twenty-one events is shown in Fig. 3. As may be anticipated from the nature of the decay process, the mass distribution around 2200 m_e is asymmetrical. The best value of the mass, obtained by weighting the fifteen events according to the accuracy of the individual masses, is about 2210 m_e.

6. 2 The decay of V_2^0-particles into two π-mesons

Evidence has already been given for the decay of neutral V-particles into two π-mesons. Five of the measured V-tracks can be interpreted by this scheme, since their positive particles could not have been protons, while, in addition, the negative particles of two of the events (63 and 66) were not as massive as the proton.

TABLE 9

The masses of four V-particles which probably decayed into two π-mesons

(1) Event no.	(2) Approx. track length (cm.)	(3) Measured momenta (× BeV/c)	(4) Ratio (p_+/p_-)	(5) Angle of fork (deg.)	(6) Mass (scheme of equation (4)) (× m_e)
66 (Plate V)	6 3	+ 0.26 −∼ 0.13	2	77	700
63	4 7	+ 0.30 −∼ 0.5	0.6	46	820
65 (Plate X)	5 5	+ 0.32 − 0.66	0.5	∼10	∼ 610
1	5 5	+ 0.35 −∼ 0.5	0.7	14	∼ 600
R & B (1947) (Plate I)	5 4	+ 0.20 − 0.85	0.3	67	∼1120

Several track lengths, of the five forks listed in Table 9, are very short, consequently their momenta cannot be measured accurately. The result for photograph 66 is the best although the momentum of the negative particle is somewhat uncertain. The negative track on photograph 63 is near the edge of the chamber and its momentum is uncertain. The angle of the fork on photograph 65 is uncertain, as the V-shaped track cannot be reprojected accurately owing to the confusion produced by other particles in the shower. The negative particle of event R & B could not be measured accurately; the momentum quoted in the table has been determined from the geometry of the fork and the main shower. It may be considerably in error, which may explain the high mass value. A definite conclusion cannot be reached from these five events; they all have positive particles which have been measured accurately, but several of the values for the negative particles are uncertain. There is, however, evidence for the existence of a neutral V-particle of mass about 800 m_e.

If the V-particle decay processes involve only two secondary particles, it must be concluded that the events observed by the Pic-du-Midi group can best be explained by two neutral V-particles.

The mass of the first type is not yet certain, but the best value from the available data is 2210 m_e. The mass of the second type is probably within the range (700—800) m_e. Many of the neutral V-shaped tracks have both secondaries at minimum ionization and so could fit either scheme (3) or scheme (4). It is necessary, therefore, to invoke any possible additional arguments to assist in the separation of the data between the schemes. Valuable additional information can be obtained from a study of the dynamics of the two decay schemes.

7. THE DYNAMICS OF DECAY SCHEMES WITH TWO SECONDARY PARTICLES

Evidence has been presented showing that neutral V-particles decay according to two different schemes, provided that there are only two secondary particles. The dynamics of these schemes will now be discussed with special reference to the most probable appearance of the V-tracks in the laboratory frame of reference.

7.1 The dynamics of the decay scheme: $V_1^0 \to p^+ + \pi^-$

If a neutral V-particle decays into a proton (mass m_1) and a π-meson (mass m_2) then these secondaries will be emitted in opposite directions in their centre-of-mass frame of reference as shown in Fig. 2. In fact the pair of particles will be emitted at random in this frame of reference. It can easily be shown that the fraction of all the events with values of θ between θ_1 and θ_2 is given by $\frac{1}{2}(\cos\theta_1 - \cos\theta_2)$. For example, half the observed forks will have values of θ between 60° and 120°. The most likely value of θ is $\pi/2$, that is, the most probable direction of emission for the secondary particles in the rest system of the V-particle is at right angles to the line of flight of the V-particle.

The momentum of each of the secondaries in the rest frame of reference of the V-particle is given by

$$(8) \qquad p = \frac{1}{2M}\{[M^2 - (m_1 - m_2)^2]\,[M^2 - (m_1 + m_2)^2]\}^{\frac{1}{2}}$$

where M is the mass of the V-particle in energy units. The appearance of the fork in the laboratory frame of reference can be found by the application of Lorentz transformations to the velocities of the secondaries in the rest frame of reference of the V-particle. The components of p transverse to the line of flight of the V-particle are unaffected by the transformations, but the components of p along the line of flight are transformed. Alternatively, a geometrical procedure, based on the Lorentz transformation, devised by BLATON [1950] may be used.

The transformed momenta of the two secondaries are dependent on their energies in the rest frame of reference of the V-particle. If they have quite different masses, such as those of the proton and the π-meson, then the two transformed momenta will, in general, be very different. The proton will have a higher momentum than the π-meson in the laboratory frame of reference. This excess of positive over negative particle momentum for the secondaries is very marked, except for the very high- or low-energy events. If the momentum measurements on a number of forks are examined, the momentum distributions for each type of secondary, will be very different. The Pic-du-Midi group found the differential momentum spectrum of the positive secondaries to be quite different from that of the negative secondaries, the positive particles had significantly higher momenta values than the negative particles (cf. § 3. 3). A study of Table 7 (§ 6. 1), for example, reveals that three of the identified protons had much higher momenta than the corresponding negative particles. This is also true of all the events with masses in the range (2180—2350) m_e, but is not observed for three of the events with masses about 2700 m_e (according to scheme (3), cf. Table 8, § 6. 1). These three events have average values of the ratio p_+/p_- of about unity. This result is to be expected if the secondaries were of equal, or nearly equal, mass, and indicates that the three particles probably did not decay according to the scheme of equation (3). This conclusion will be supported by further evidence given later in this section. When more data is available, a study of the ratio p_+/p_- will be a very valuable procedure for dividing the data between the two decay schemes.

The two secondary particles have the same momenta in the rest frame of reference, consequently the velocity of the meson is much higher than that of the proton. If the velocity of the unstable V-particle is greater than that of one of the secondaries in the rest frame of reference then the direction of the secondary in the laboratory system always forms an acute angle with the direction of the V-particle, that is, the secondary is always thrown forwards.

For example, suppose that the velocity of the V-particle exceeds that of the meson in the centre-of-mass frame of the secondaries, then both secondaries are thrown forwards and produce an acute-angled fork. If the velocity of the V-particle exceeds that of the proton, but is less than that of the meson in the rest system, then the proton is always thrown forwards, but the meson can move backwards in the laboratory system. Both secondaries can move backwards in the laboratory system when the velocity of the V-particle is less than that of either of the secondaries in the rest system.

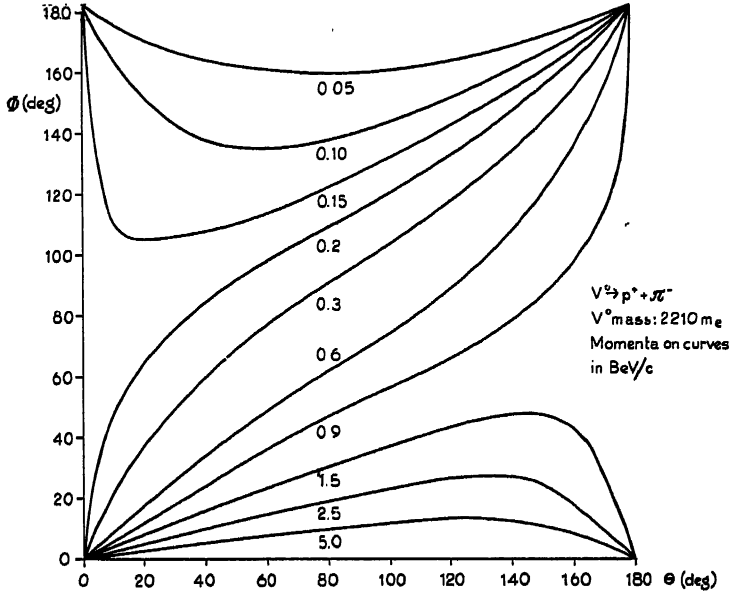

Fig. 4 – Angular relations for the scheme $V_1^0 \rightarrow p^+ + \pi^-$
V^0 mass = 2210 m_e
Momenta on curves in BeV/c.

These properties of the decay scheme can be examined further by calculating ϕ as a function of θ for given values of P and M. A set of curves for a mass of 2210 m_e is shown in Fig. 4 which shows that, when P is greater than 1.0 BeV/c, ϕ is limited. The values of ϕ are always greater than a minimum value when P is less than 0.16 BeV/c. Between these two critical values of the V-particle momentum, all values of ϕ between 0° and 180° are possible. In this region the proton is always thrown forwards in the laboratory system, but the meson can be emitted backwards.

The probability distribution of the value of ϕ for a particular momentum of the V-particle can be calculated from the curves of Fig. 4. Three typical differential probability distributions of the values of ϕ are shown in Fig. 5; they have been calculated for 10° intervals. If ϕ is restricted in value, then the forks are most likely to have angles close to $\phi_{\max}$. For example, it can be seen that, if M is 2210 m_e and P is 1.5 BeV/c then $\phi_{\max}$ is 46° and 58 % of the forks will have values of ϕ between 30° and 46°. When P is 0.9 BeV/c, all values of ϕ are possible but 95 % of the forks will have ϕ less than 90°.

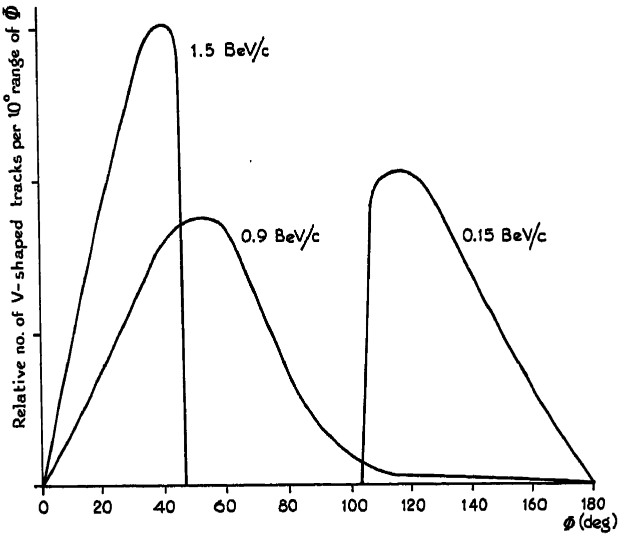

Fig. 5

It is useful to develop a procedure to decide if the angles of all the forks, which give masses of about 2210 m_e, are distributed in a reasonable manner. $\phi_{\max}$ and $\phi_{\min}$ can be calculated as functions of P, for this experimentally-determined mass, and the resulting curves are shown in Fig. 6. In addition, P can be calculated as a function of ϕ for a fixed value of θ, the angle of emission in the rest system of the V-particle (cf. Fig. 2). The dotted curves in Fig. 6 correspond to values of θ of 60° and 120° and, as shown previously, half of the observed forks should lie between these lines.

The values for fourteen examples with individual masses in the range $(2180-2350)m_e$ are plotted in Fig. 6; in each case a range of

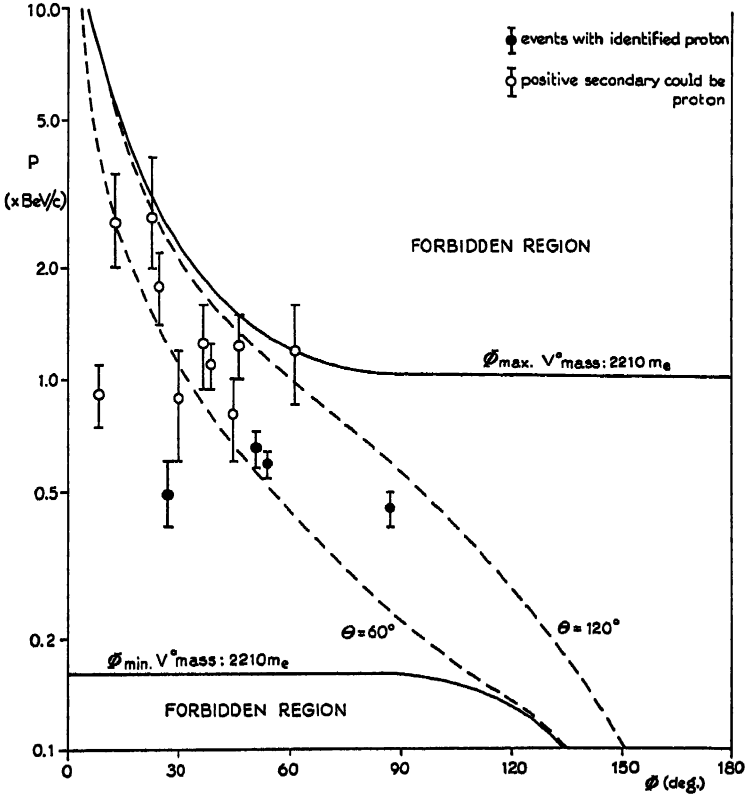

Fig. 6

P values is given, which corresponds to about twice the standard deviation on the individual average values. The forks are distributed in approximately the most probable region of the $P - \phi$ diagram; about half lie between the dotted curves. They are, therefore, a set of forks which may reasonably be explained by the decay of V-particles, of mass 2210 m_e, into protons and π-mesons. When more data are available, the distribution of the values of ϕ for a chosen P could be determined experimentally and compared with the theoretical distribution calculated for the average mass.

It is important to enquire whether the V-particles with masses about 2700 m_e on the same decay scheme are also reasonably probable forks for their particular mass. The $P - \phi$ plot for these few events is given in Fig. 7, the dotted curve shows P as a function of ϕ with θ constant and equal to 60°. Three quarters of the forks with mass close to 2700 m_e should lie between the dotted and full curves. In fact, six of the seven forks lie to the left of the dotted curve, that is in a relatively improbable region of the $P - \phi$ diagram. Thus there is evidence that these events may not have followed the assumed decay scheme. Their values of p_+/p_- are all about unity and it is likely that they can be interpreted best as the decay of neutral V-particles into two π-mesons.

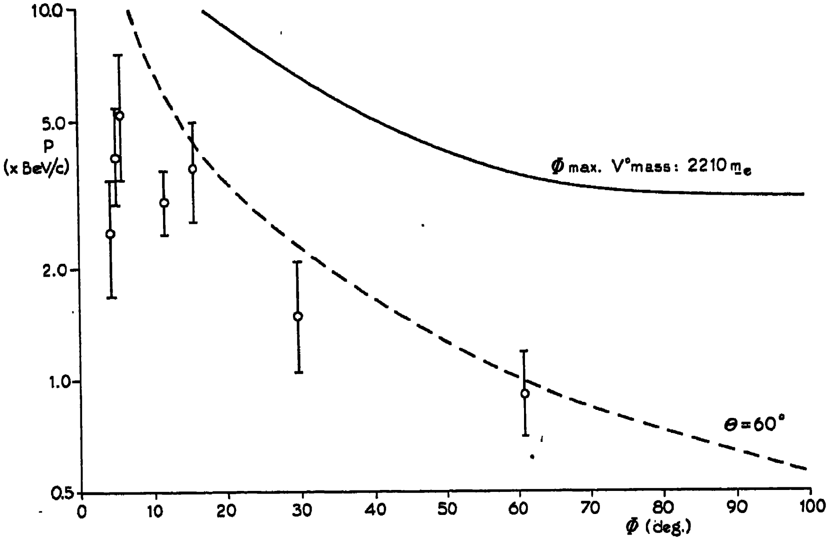

Fig. 7

7.2 The dynamics of the decay scheme: $V_2^0 \rightarrow \pi^+ + \pi^-$

The two mesons are emitted in their centre-of-mass system in the manner described in § 7.1, but the dynamics are simple owing to the symmetrical form of the decay process. For example, the momentum distributions of the positive and negative secondary particles in the laboratory frame of reference are the same, and the average value of the ratio p_+/p_- is unity.

The set of $\phi - \theta$ curves, given in Fig. 8, has been calculated for a mass of 1000 m_e; they are symmetrical about $\theta = \pi/2$. The general properties of the decay scheme can be found from these curves. $\phi_{\max}$ and $\phi_{\min}$ are shown as functions of P in Fig. 9; it may be seen that the intermediate region of Fig. 4 in which all values of ϕ are possible does not occur for the symmetrical decay scheme. The most probable region for the observed forks is close to the curves, on the left above the critical momentum, and on the right below this value.

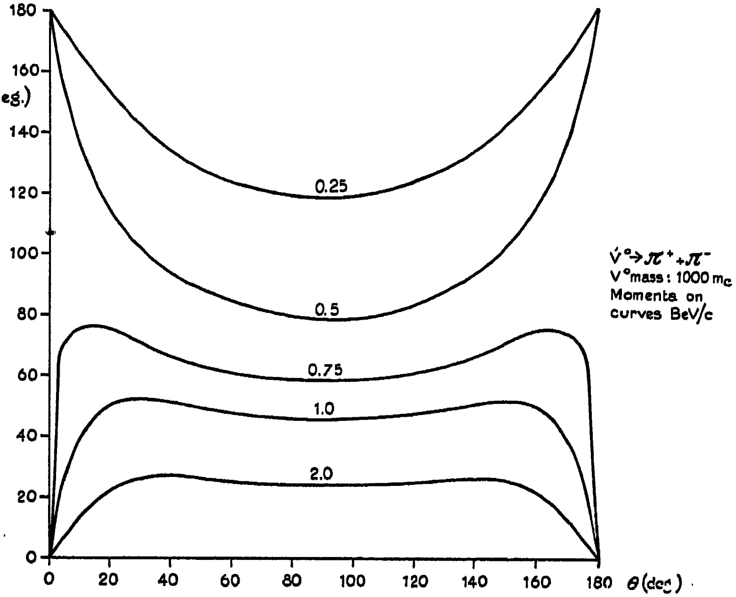

Fig. 8 – Angular relations for the scheme $V_2^0 \to \pi^+ + \pi^-$.

In § 6. 1 it was shown that seven V-particles have high masses when interpreted by the first decay scheme. They can be explained in terms of the second scheme and are plotted in Fig. 9. In addition, five V-events can only be explained by the second scheme; these were discussed in § 6. 2 (Table 9) and the $P - \phi$ values are also plotted in figure 9. Ten of the eleven forks shown in Fig. 9 are located reasonably close to the curve and it is concluded provisionally that they can be explained by the decay of V-particles with mass about 1000 m_e. One point lies in the forbidden region; its calculated mass is about 700 m_e which may be significantly lower than the value of 1000 m_e.

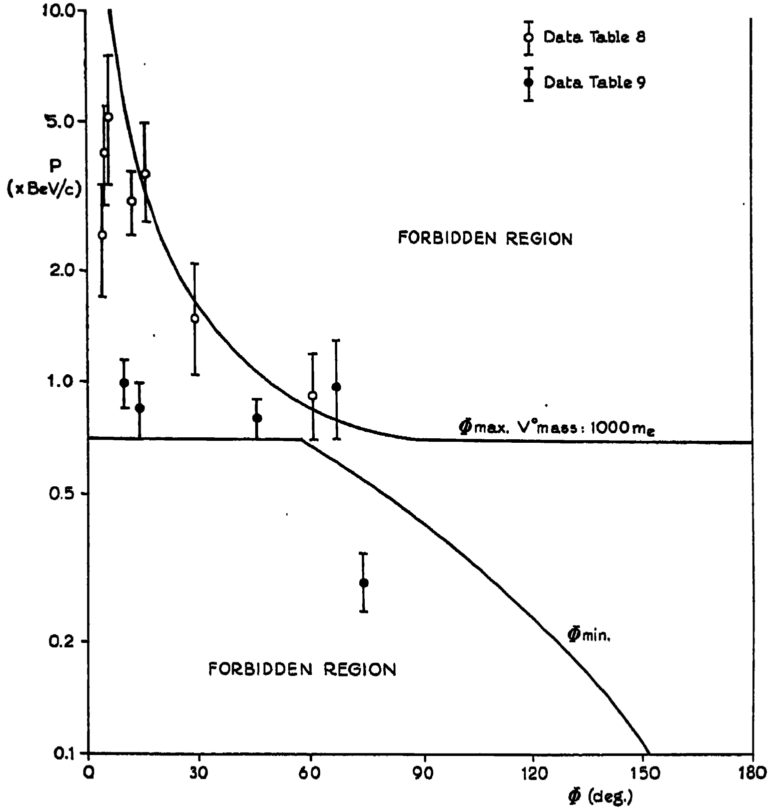

Fig. 9

The detailed study of the dynamics of the two likely decay schemes enables a partial separation of the data between the two schemes to be made. There is considerable evidence for the decay of V-particles into protons and π-mesons and fourteen of the forks, found by the Pic-du-Midi group, fit in well with the scheme. The best mass value is 2210 m_e. In addition, twelve events can be interpreted in terms of the decay of V-particles into two π-mesons. No fork consisting of two identified π-mesons has yet been observed.

8. THE MEAN REST LIFETIME OF NEUTRAL V-PARTICLES

SERIFF *et al.* have made a determination of the rest lifetime of the neutral V-particles. They found the distribution of the decay points along the line of flight of the particles and then made allowance for the variation in path length resulting from the geometry of the cylindrical chamber, and estimated the relativistic time dilatation factor for each event. The data was very limited since the origins could only be found on, at most, nineteen photographs. It is difficult to assess the necessary geometrical corrections and as accurate momentum measurements were not available the relativistic corrections could not have been accurately determined. The mean rest lifetime obtained by this method is quoted as $(3 \pm 2) \times 10^{-10}$ sec. The same procedure can be used with the data of the Pic-du-Midi group and the result is not inconsistent with the wide limits set by SERIFF *et al.* In order to obtain a reliable value of the lifetime the main nuclear interactions must be produced in the chamber. The points of origin of the V-particles are then well determined and the geometrical corrections are much less serious. Fretter has found a value of about $(1.0—2.0) \times 10^{-10}$ sec. for the mean rest lifetime determined from fifteen forks. He assumed the second decay scheme and made an approximate determination of the relativistic time dilatation correction from the geometry of each fork.

These values of the lifetime can only be very approximate since the workers were not able to divide the observed forks reliably between the different decay schemes. If the results described in § 7 are correct, there may well be two quite different V-particles with different masses and lifetimes, rather than one neutral V-particle with two alternative modes of decay.

9. CONCLUSIONS

Altogether more than 100 forks, due to the decay of neutral V-particles, have been observed in cloud chambers and one similar event has been found in a photographic emulsion. The discovery of one neutral V-shaped track was reported by Rochester and Butler in 1947, about the same time as the discovery of the π-meson by LATTES, OCCHIALINI and POWELL [1947]. In the last four years, however, the properties of the π-meson have been exhaustively examined and are now known in considerable detail. There appear to be at least three reasons why knowledge of the V-particles has developed so slowly. Firstly, the particles are much less frequently produced than π-mesons; SERIFF *et al.* deduced that the neutral V-particles number about 3 % of the ionizing particles produced in penetrating showers. Secondly, V-particles have only been found in appreciable numbers in cloud chambers, when they are operated under difficult conditions at high altitudes. Finally, they have a lifetime which is neither very short nor very long; this complicates considerably the study of the decay processes. If the lifetime were about 10^{-12} sec., or even shorter, the decay processes of the V-particles could be studied with ease in photographic emulsion; on the other hand, if the lifetime were appreciably longer than 10^{-9} sec., the V-particles would frequently decay almost at rest. All the well-understood decay processes can be observed frequently when the particles are almost at rest.

The analysis of the properties of the neutral V-particles found before April 1st, 1951, can be summarised as follows:

9.1 Not more than 10 % of the neutral V-shaped tracks can be interpreted by processes other than the spontaneous decay of hitherto-unknown particles.

9.2 The secondary particles cannot all be identified. Protons and negative mesons, most probably π-mesons, have been found. Evidence for the occurrence of positive particles lighter than protons has been obtained, but no positive mesons have been identified.

9.3 Preliminary investigations are consistent with the assumption that the decay processes involve only the two charged secondary particles. Serious difficulties are encountered when investigating the orientation of the forks with respect to their origins; additional and more accurate measurements are needed.

9.4 At least two decay schemes are needed to explain all the observed forks:

$$V_1^0 \rightarrow p^+ + \pi^- \quad \text{(scheme (3))}$$

and

$$V_2^0 \rightarrow \pi^+ + \pi^- \quad \text{(scheme (4))}.$$

The scheme:

$$V_1^0 \rightarrow p^- + \pi^+,$$

which is symmetrical with the first decay scheme (3), might be expected. Five slow proton secondaries have been observed, but no slow negative protons have been found. This may be evidence that the negative proton is not created in a symmetrical manner with the proton.

9. 5 The Pic-du-Midi group has studied in detail twenty-six neutral V-particles. An analysis has been made which enables fourteen forks to be explained by the first scheme. The average mass value obtained is $2210\,m_e$. The remaining twelve events can probably be explained in terms of the second scheme and have a mass of about $800\,m_e$. There is thus strong evidence for the existence of at least two different neutral V-particles.

9. 6 The fact that a fairly consistent set of mass values has been found may give support to the conclusions in § 9. 3. If the decays each involve a third, neutral, secondary particle, then the mass values already calculated will all be too small. The number of events contributing to the two sets of mass values is very small, and a reliable statistical procedure has not yet been used to test whether the values are consistent with a single average, or are really distributions over a range of values, as would be expected if a three-body decay is treated as a two-body decay. Many more events, very accurately measured, will be required before this type of argument can be used with confidence.

9. 7 Early measurements of the mean rest lifetime of the neutral V-particles give values between 10^{-10} sec. and 5×10^{-10} sec. The two different neutral V-particles may have very different lifetimes.

Finally, it is useful to consider some of the future developments that may be expected. The detailed discussion of the properties of the V-particles, as distinct from the V-shaped tracks, depends on the assumption discussed in § 9. 3. Clearly it will be necessary to study the basis of this assumption and to plan future experiments accordingly. The consequences of the decay of V-particles into three secondary particles must be considered. The theoretical treatment of this type of process is very complex and cannot be made in detail without recourse to fundamental theory. Two types of V-shaped tracks have been observed; if there are only two secondaries, they can be explained by two different decay schemes. These two schemes could be extended to apply to one V-particle with two modes of decay, viz.

$$V^0 \rightarrow p^+ + \pi^- + \pi^0$$

and

$$V^0 \rightarrow n^0 + \pi^- + \pi^+$$

If these schemes operate it should, eventually, be possible to detect the neutrons and π°-mesons by finding interactions, which point back to the apexes of the forks, in lead plates.

It will also be necessary to obtain many more forks with long secondaries, which can be measured with considerable precision, and also to obtain more forks with identifiable secondaries. The existence of neutral V-particles has been established, but as yet very few of their properties are known, even approximately. Very many experiments will be carried out during the next few years, in order to settle the numerous queries about their properties which can already be posed.

PART II

THE DECAY OF HEAVY CHARGED PARTICLES

10. THE DECAY OF τ-MESONS

During the first experiments with electron-sensitive photographic plates exposed on the Jungfraujoch, **Brown** *et al.* [1949] found a very unusual event, a mosaic of which is reproduced in Plate XIII. There are two stars, A and B, linked by track π. The probability of the two centres being unrelated events is extremely small and may safely be neglected. The range of track k in the emulsion exceeds $3000\,\mu$ and the grain density increases progressively towards A. Near A, the track is indistinguishable from that of a singly-charged particle at the end of its range; particle k must, therefore, have initiated event A. Similarly, particle π initiated event B.

The mass of particle A can be determined from measurements of the grain density as a function of its range. Considerable care was taken to establish that the plate was uniformly developed and that the degree of fading was insignificant. The average number of grains per $10\,\mu$ interval was plotted against the particle range for several proton tracks found in the same plate. A similar curve was constructed for particle k, and its mass determined by making a comparison of its grain density curve with the mean curve for protons. **Brown** *et al.* found the mean mass value of particle k to be $(1080 \pm 160)\,m_e$. A mass of $(1800 \pm 400)\,m_e$ for particle k was obtained from a study of its small-angle scattering; more weight is given to the grain-counting method than to the scattering method.

Track π is characteristic of a π-meson, captured at B. The lengths of the remaining two secondary tracks, a and b, due to singly-charged particles, are respectively $2000\,\mu$ and $116\,\mu$; within statistical fluctuations, both have the same ionization, namely 2.2 times the minimum value. The energies and momenta of these two particles were deduced from the observed grain densities and scatterings, after making various assumptions concerning their masses; for example, they were assumed to have been protons, π- or μ-mesons. The track lengths and ionization measurements indicate that the particles cannot have been electrons if the rise of ionization for high-energy electrons flattens before the value of 2.2 times the minimum value is reached.

There are two possible interpretations of event A, which was produced by particle k; either the latter was captured by a nucleus or it decayed spontaneously. A particle of mass about 1000 m_e at the end of its range could be captured by a nucleus and lead to the ejection of two energetic protons and a π-meson. The energies of the secondaries would be approximately the same as those already obtained assuming particles a and b to have been protons. It is almost certain, however, that the release of such a large amount of energy would have produced the evaporation of the remaining nucleons in the nucleus; in fact, a many-pronged star should have been observed. It seems, therefore, that tracks a and b could not have been due to protons, but they may have been due to π-mesons or μ-mesons. If a and b were π-mesons, their kinetic energies must have been 27 MeV and, for μ-mesons, 37 MeV. These values are small and cannot be reconciled with the absorption of 500 MeV into the nucleus, which would take place if particle k, with a mass of about 1000 m_e, were captured.

The alternative explanation, namely that tracks a, b and π are the secondaries of the spontaneous decay of particle k, can now be considered. BROWN *et al.* determined the relative directions of the three particles, after allowing for the shrinkage of the emulsion, and found them to be coplanar. The direction of any one track makes an angle of less than 4° with the plane of the other two tracks. The errors are due to the fact that track π is very short compared with tracks a and b. These measurements support the conclusion that particle k decayed, almost at rest, into particles a, b and π.

Particle π was almost certainly a π-meson; from its observed range, the energy was found to be 1.04 MeV. From the directions of motion of the three secondary particles and the energy of the π-meson, the momenta of particles a and b are found to be (98 ± 5) MeV/c and (104 ± 5) MeV/c respectively. The grain densities are known, so that the particles can now be identified and are found to be either π- or μ-mesons. The mass of particle k can be calculated for the two most likely modes of decay, which are

$$\begin{aligned} &\mathrm{k} \rightarrow \pi + \pi + \pi \\ \text{and } &\mathrm{k} \rightarrow \pi + \mu + \mu \end{aligned} \tag{9}$$

since the observed grain densities agree best with the assumption that particles a and b are of the same type. The mass values obtained are $985\,m_e$ and $869\,m_e$ respectively.

Finally, the possibility that particle k was not related to events A and B may be considered. The determination of the mass of particle k does not exclude the possibility, as an extreme fluctuation, that the particle may have been a proton which stopped in the emulsion very close to A and was unrelated to particles a, b and π. It is then extremely difficult to explain the event made up of tracks a, b and π, because stars of this type are not found in emulsions. BROWN *et al.* considered several other alternative explanations involving one or more of the tracks having been unrelated to the others, but were not able to find a plausible scheme to explain the event. They concluded that the only reasonable explanation of the whole event is that particle k must have been an unstable particle of mass about $1000\,\mathrm{m}_e$, which initiated events A and B. Charged particles of this type are now called τ-mesons. Since the discovery of BROWN *et al.*, a considerable volume of photographic emulsion, sensitive to fast particles, has been examined, but only two additional events of the same type have been reported, both by HARDING [1950].

The first of the decay events found by Harding was in an electron-sensitive emulsion exposed for 85 days under 3 m. of ice. A heavily-ionizing particle approached a centre, similar to centre A of BROWN *et al.* The multiple scattering of this particle increased towards the star and the grain-density measurements indicate that the particle, referred to as k, almost stopped before it produced the star. The star consists of three tracks with useful lengths of $1300\,\mu$, $420\,\mu$ and $30\,\mu$ respectively.

The event was observed in a plate that had received an exceptionally long exposure. Harding carefully considered the effect of fading, after showing that the plate was developed uniformly. Grain-density measurements were made on protons and μ-mesons, that stopped in the emulsion, and grain density-range curves were drawn. The curve for π-mesons was obtained by interpolation between the two curves. The grain density-range curve for the particle k was always above that for the π-mesons; if k was a π-meson, it must have traversed the emulsion right at the end of the exposure.

The only well-known capture process that could explain the star is that of a π-meson. If particle k is assumed to have been a π-meson, then the energy released in the nucleus was only 150 MeV. Now if the secondaries are assumed to have been protons, then the ionization measurements indicate that their total energy would have been of the order of 500 MeV; therefore the event could not have been initiated by a slow π-meson. The star could be due to the capture of a π-meson if one or two of the secondary particles were electrons. The direct production of electrons in stars has not been observed and so this explanation is very unlikely.

The value of the product, momentum x velocity, for the longest secondary particle is 25 MeV; it was probably a π-meson. The remaining two secondaries are too short to permit reliable scattering measurements, but one shows much less scattering than the longest track. It is clear that, if a π-meson is captured by a nucleus, there is not sufficient energy available to produce even a μ-meson and to provide kinetic energy for two other particles. Harding therefore concluded that the event could not be interpreted as a nuclear capture of a π-meson.

The spatial arrangement of the three secondary tracks was carefully examined again, after allowing for the shrinkage of the emulsion. The normal to a plane containing any two of the tracks was perpendicular to the third within 2°; thus the three tracks were coplanar, as in the event of BROWN *et al.* This provides evidence that particle k decayed spontaneously into only three particles,all singly charged. Harding assumed that the longest secondary was a π-meson and, using the scattering data already referred to, calculated the energy to be 13 MeV. If the other two particles are assumed to be π-mesons then, using the laws of conservation of momentum and energy, the mass of the τ-meson is calculated to be 1040 m_e. If track k is due to a particle of this mass, then the effect of fading must have been very considerable, since its ionization was only slightly above the average for π-mesons in the same plate.

The second event of the same type, observed by Harding, had very short secondary tracks and so no conclusions could be made, beyond noting the fact that the secondaries were approximately coplanar.

The interpretation of the events observed by BROWN *et al.* and HARDING is supported by many detailed arguments and the evidence for the existence of the decay into three mesons is very convincing. This conclusion is of particular interest in view of the work of FRANZINETTI [1950] and FOWLER [1950] who both showed that less than 2 % of all heavily-ionizing particles from stars are τ-mesons unless their lifetime is very short.

11. THE DECAY OF CHARGED V-PARTICLES

11. 1 The first charged V-shaped track

A charged V-shaped track was observed by DAUDIN [1944] in a small cloud chamber without a magnetic field operated at 2000 m. altitude, but the event was not discussed in detail. The angle of deflection was about 10° and the event may well have been a $\pi \rightarrow \mu$ decay (cf. § 11. 3 below) because the particle was probably heavily ionizing.

The first V-shaped track, due to a charged particle, to be investigated in detail, was observed by ROCHESTER and BUTLER [1947] and is shown in Plate II. The incident track (1) follows the general direction of the shower; it is short and unmeasurable and the particle was apparently deflected through 19° in the gas. The charged secondary particle, which subsequently penetrated the 3.4 cm. lead plate without appreciable scattering, was positively charged, and had a measured momentum of (0.77 ± 0.10) BeV/c. There is no obvious blob of ionization at the apex which could be due to a recoil; therefore the fork could hardly have been due to a scattering or to a nuclear interaction in the gas. Rochester and Butler interpreted the event as the decay of a positive particle into one charged particle and one or more neutral particles. Assuming the existence of only two secondaries, they found that the minimum mass of the unstable particle was $(980 \pm 150)\, m_e$.

11. 2 The statistical data on charged V-shaped tracks

SERIFF *et al.* observed four V-tracks due to charged particles among their 11,000 photographs. Three of these unstable particles were produced in nuclear interactions in the 2 cm. lead plate in the cloud chamber. The angles between the primary and secondary tracks were 7°, 15°, 34° and 40° respectively. They do not describe the appearance of the tracks made by the unstable particles; presumably they were all substantially at minimum ionization.

The Pic-du-Midi group has discovered eleven examples of charged decay events, three of which were produced in the lead plate. The tracks of two of the unstable particles were considerably above minimum ionization.

Fretter has observed four charged V-tracks, all produced in the lead plates. The same number has been observed by Bridge and Annis in their multiplate chamber; the incident tracks of two of these are heavily ionizing. In addition, the latter have observed seven heavily-ionizing particles which came to the end of their range in one or other of the lead plates. In each case, a track at minimum ionization was produced from the lead plate.

O'CEALLAIGH [1951] has found a charged V-shaped track in a photographic emulsion during a study of μ-meson decays. The grain density of the secondary track is the minimum value for the particular emulsion.

11. 3 The explanation of the charged V-shaped tracks

SERIFF *et al.* have not reported momentum measurements on their four charged V-shaped tracks; they concluded, however, that the events could only be interpreted as due to the decay of charged particles. One of the secondary particles penetrated the 2 cm. lead plate without interaction and was probably more massive than the electron.

There are at least three possible explanations of the charged V-tracks observed by the Pic-du-Midi group, other than that adopted by Rochester and Butler. The events may be due firstly to nuclear interactions, secondly to scattering and thirdly to well-known decay processes, such as those of the π- and μ-meson. The first explanation appears to be improbable owing to the absence, in every case, of nuclear recoils. In addition, no event, similar to a charged V-shaped track but with evaporation tracks, has been observed. It is unlikely that eleven high-energy stars in the gas would be observed without finding at least one with evaporation tracks. Following the procedure outlined in § 4. 1, an estimate of the expected number of high-energy nuclear interactions in the gas, which are associated with the observed penetrating showers, can be made. The probability of finding one such interaction or star is small. In fact, however, two have been found, but they are different from the charged V-tracks and both have short recoils (cf. § 4. 1).

The observed events can hardly be ascribed to nuclear scattering owing to the absence of recoil tracks. It is easy to show, for several of the measured events, that these recoils would have been visible in the chamber, if the events were due to scattering. If the scattering explanation is correct, then about 400 times as many examples of scattering should have occurred in the lead plate. During the period when the 2 cm. lead plate was in use, three charged V-shaped tracks were observed, thus 1200 particles should have suffered large-angle scattering in the plate. In fact, approximately 120 deflections of greater than 5° were observed in the lead plate. The momenta of these particles have not all been measured; those with momentum less than about 0.3 BeV/c may have been examples of multiple-Coulomb scattering. Thus the observed number of examples of anomalous scattering may not be greater than 60, a very much smaller number than that predicted on the assumption that the charged V-shaped tracks arise from large-angle scattering.

Finally, it is necessary to consider the possibility that the small number of observed events may be explained by well-known decay processes, such as those of π- and μ-mesons. π-Mesons form a considerable fraction of the fast particles in penetrating showers and may be expected to decay in the chamber. An approximate estimate of the number of decays can be made from the known flux of π-mesons, from their lifetime and from reasonable assumptions about their spectrum. The result obtained is that about thirty $\pi \to \mu$ decays are to be expected; many of these, however, will be high-energy events for which the apparent angle of deflection is very small.

The dynamics of the decay scheme:

$$\pi \to \mu + \nu, \tag{10}$$

where ν is a neutrino, are relatively simple and it can easily be shown that, for a given momentum of the π-meson, there will be a

PLATE XIV

THE DECAY OF A SLOW V-PARTICLE

(BRIDGE and ANNIS [1951])

A slow charged particle decayed between the 4th and 5th plates. The chamber was fitted with 8 plates, alternately of lead and aluminium. The ionization of the secondary particle was about twice the minimum value and it made an angle of 90° with the direction of the V-particle. Subsequently the slow secondary entered an aluminium plate above the point of decay. Bridge and Annis considered that it was scattered through a large angle, travelled downwards, and came to rest after penetrating four plates. From the observed range, scattering and ionization, they concluded that the particle was a meson, probably a π-meson if it, in fact, suffered a nuclear scattering.

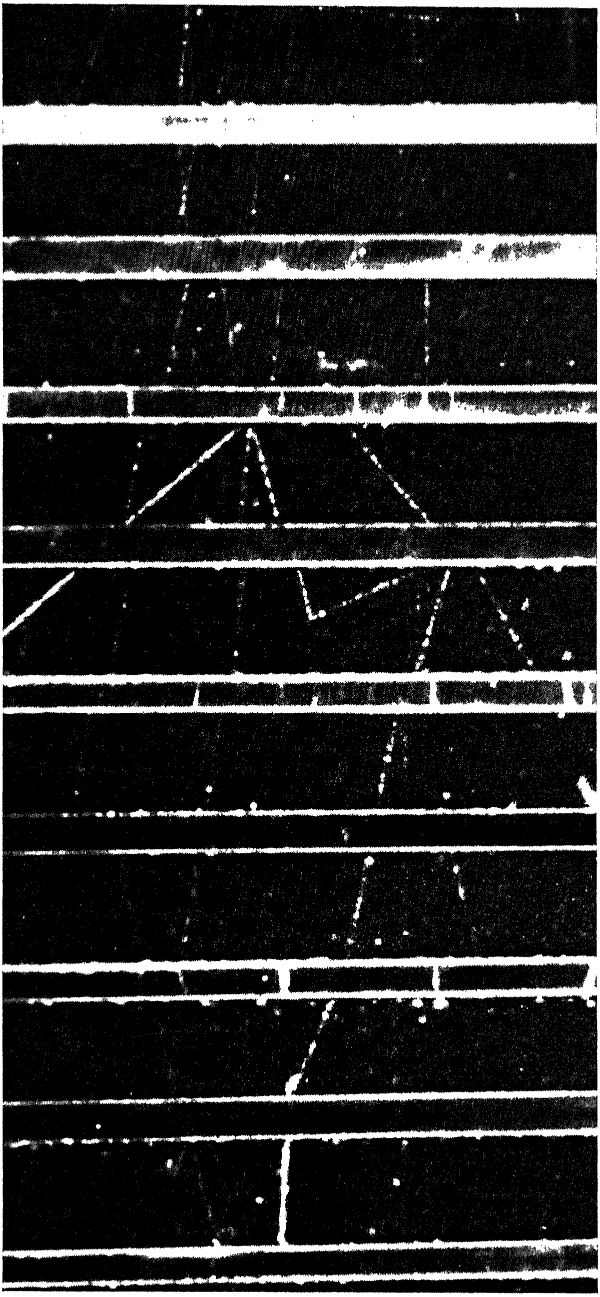

PLATE XV (see § 11. 5)

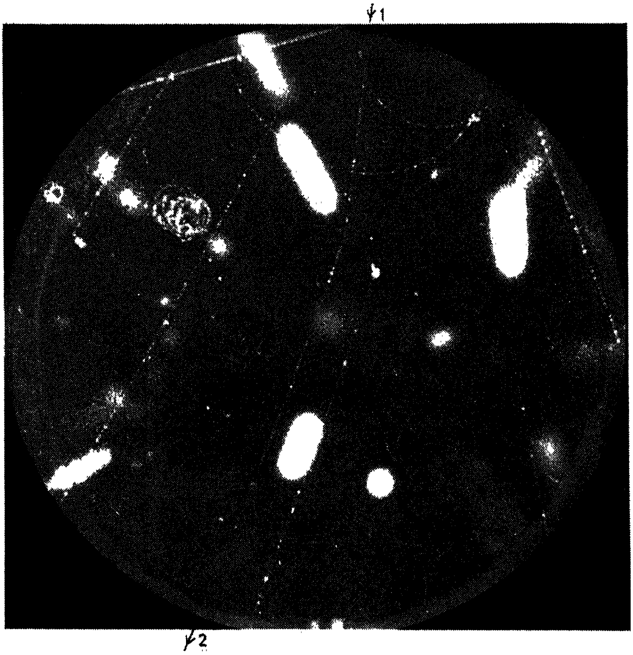

PLATE XVI (see § 11. 5)

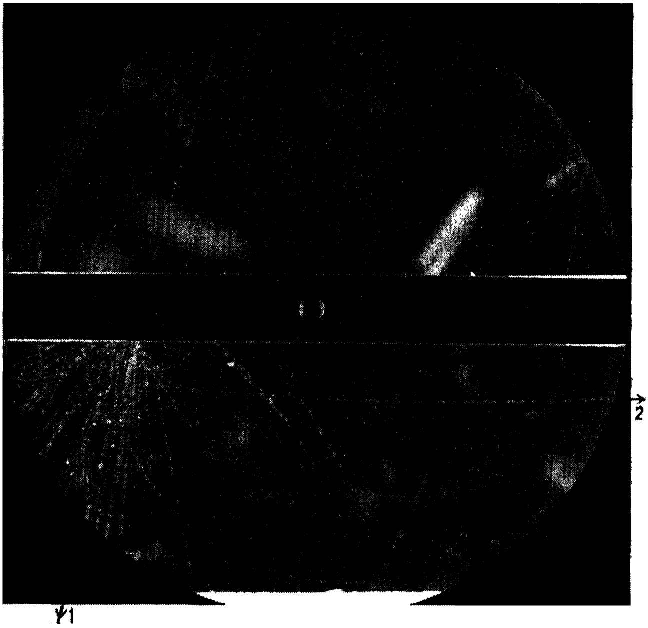

PLATE XV

THE DECAY OF A HIGH-ENERGY NEGATIVE V-PARTICLE

(The Pic-du-Midi group).

This event is similar, except for the sign of the V-particle, to the one obtained by Rochester and Butler in 1947. The momentum of the primary particle cannot be found accurately; it was probably greater than the measured value of 1.4 BeV/c. The momentum of the secondary was 0.7 BeV/c and the angle of deflection 11°. The mass of the V-particle can be calculated, if assumptions are made about the nature of the neutral decay product. Values are given in Table 11 of § 11. 5. For example, if the one neutral secondary was a π-meson, then the mass of the V-particle was about 750 m_e. If the neutral secondary was a V-particle of mass 800 m_e, then the V-particle mass was about 1280 m_e.

PLATE XVI

THE DECAY OF A SLOW NEGATIVE V-PARTICLE

(The Pic-du-Midi group)

A slow particle appeared from a high energy nuclear interaction in the lead plate, and decayed about 2 cm. below the plate. The primary track length is very short and cannot be measured. but the ionization is greater than four times the minimum value. The negative secondary, track (2), makes an angle of 100° with the direction of the primary and has a measured momentum of (0.18 ± 0.02) BeV/c. The minimum and maximum values of the mass of the negative V-particle can be calculated and are given in Table 11 of § 11.5. For example, if the neutral secondary was a π-meson, the V-particle mass was between 900 m_e and 1080 m_e; on the other hand, if the neutral secondary was a V-particle of mass 800 m_e, then the mass of the V-particle was between 1310 m_e and 1440 m_e.

maximum value of θ, the angle between the directions of the π and μ-mesons. This value of θ is given by

$$\sin \theta_{\max} = \frac{0{\cdot}04}{P}, \tag{11}$$

where P (in BeV/c) is the momentum of the π-meson. It can also be shown that the most probable values of θ, for a π-meson with a given P, lie very close to the corresponding $\theta_{\max}$. If the momenta are known, values of $\theta_{\max}$ can be calculated for each of the observed charged V-particles for comparison with the actual values; then, if an observed value is significantly greater than the calculated maximum value, the scheme cannot explain the observed decay. This procedure appears to be the only reliable one for separating the decay of charged V-particles from those of π-mesons but, inevitably, some genuine charged V-shaped tracks will be interpreted as the decay of π-mesons.

The decay of μ-mesons should be very rare in a cloud chamber triggered mainly by penetrating showers in which they can only be produced by the decay of π-mesons. Extensive air showers occasionally triggered the chamber so a few μ-mesons crossed the chamber.

Four of the charged V-shaped tracks found by the Pic-du-Midi group can be explained as π-meson decays and one as a μ-meson decay. Measurements have been made on one or sometimes both tracks of five decay events, which cannot be explained in terms of the well-known decay processes, and are, therefore, interpreted by the decay of charged V-particles.

SERIFF *et al.* observed two charged V-shaped tracks with angles of deflection of less than 20°; unless the unstable particles were of high energy, the forks may have been due to the decay of π-mesons. Two of the charged decay events observed by Bridge and Annis have secondary particles which could be electrons. They considered that these events might have been examples of β-decay or of the decay of μ-mesons. Both of these explanations are improbable.

11. 4 The nature of the secondary particles of charged V-particles

No event, similar to those discovered by BROWN *et al.* and HARDING, has been found in the cloud chamber. All the examples of the decay of a charged particle so far observed in chambers have had only one ionizing secondary particle. No worker has reported finding a heavily-ionizing secondary of a V-particle decay in a magnetic field. One of the observed secondaries penetrated 3.4 cm. of lead and another 2 cm. of lead, both without appreciable scattering and without making electromagnetic or nuclear interactions.

Bridge and Annis have obtained an interesting charged V-shaped track which is shown in Plate XIV. The ionization of the secondary particle is about twice the minimum value and it makes an angle of 90° with the direction of the V-particle, which is itself heavily ionizing. Subsequently, the secondary particle apparently suffered large-angle scattering in the aluminium plate above the point of decay. The particle then penetrated four plates before coming to rest. From the observed range, scattering and ionization, Bridge and Annis concluded that this particle must have been a meson and probably a π-meson, because it suffered a nuclear scattering in the aluminium plate. The particle, however, could not be identified unambiguously before the interaction in the aluminium plate. It is possible that the interaction in the plate was of a more complex type than that suggested by Bridge and Annis; for example, the π-meson may have been produced in the aluminium plate.

The Pic-du-Midi group have made measurements on the component tracks of five V-particle decay events. The measurements are given in Table 10, along with the results obtained by Rochester and Butler for their one event. Several of the tracks are very

TABLE 10

Measurements on six charged V-particles

Event no.	Sign	Measured incident momentum (× BeV/c)	Measured secondary momentum (× BeV/c)	Angle of deflection (deg.)
R & B (1947)	+	too short	0.77	19
1	–	1.1	~ 0.15	24
17	–	too short	0.18	100
40	–	1.4	0.71	11
54	+	1.0	too short	10
61	–	~ 0.2	> 0.15	70

short and near the edges of the chamber, consequently the measured momenta are not very accurate.

The negative secondaries of events 1 and 17 were at minimum ionization and had momenta such that they were undoubtedly lighter than the proton. They could, however, have been mesons or electrons. If all the charged V-events are of the same type, it is reasonable to conclude that the charged secondaries are π-mesons.

It is, as yet, impossible to obtain much significant information about the nature and number of the neutral particles that must take part in the decay of charged V-particles. For simplicity, the data will be analysed on the assumption that there is only one neutral particle involved, but this assumption may have to be discarded when more information becomes available. The most likely neutral particles appear to be neutrons, π°-mesons and neutrinos. The first two could, in principle, be identified by their interactions or by the interactions of their products in lead plates. The existence of neutrinos cannot be discovered by such direct means. There is, however, some evidence, which is discussed in § 11. 5, that the neutral particle may sometimes be a neutral V-particle.

11. 5 The mass of the charged V-particles

The mass of a charged V-particle can be determined in two ways. Firstly, the mass may be calculated from the momentum and ionization, if the latter is appreciably above the minimum value. Secondly, the mass may be calculated from the momenta of the V-particle and its secondary, the angle of emission of the latter and an assumed decay scheme.

O'CEALLAIGH [1951] has observed the decay of a charged V-particle in a photographic emulsion. The unstable particle made a track 4200 μ long before it came to rest and decayed into one charged particle which made a minimum ionization track. The mass of the slow particle can be found from measurements of the grain density as a function of the range and is found to be $(1380 \pm 180)\, m_e$. The mass can also be found from measurements of the small-angle scattering of the particle as a function of its residual range; the value obtained is $(1260 \pm 290)\ m_e$.

The Pic-du-Midi group have observed two slow V-particles (events 17 and 61) in a magnetic field. Unfortunately, both tracks are too short to permit reliable momentum measurements. Bridge and Annis have also observed two heavily ionizing V-particles but, without a magnetic field, it is difficult to determine mass values.

The decay of a charged V-particle into two secondaries is shown diagrammatically in Fig. 10. The mass of the charged V-particle may be calculated using the following equations:

$$\text{(12)} \qquad \begin{aligned} \sqrt{M^2+P^2} &= \sqrt{m_1^2+p_1^2}+\sqrt{m_2^2+p_2^2} \\ p_2^2 &= P^2+p_1^2-2P\,p_1\cos\theta \end{aligned}$$

which can be combined to give *M* explicitly. The principal sources of error are found to be in the momentum measurements.

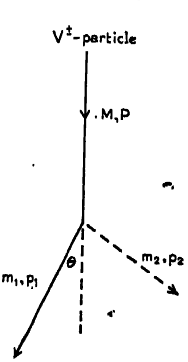

Fig. 10

The first of the Pic-du-Midi events to be described (no. 1, Table 10) is so far unique and provides some information on the nature of the neutral particle produced in the charged decay. This was the first decay photograph obtained on the Pic-du-Midi and unfortunately cannot be reproduced satisfactorily owing to the faintness of the tracks. A negatively-charged particle penetrated the 2 cm. lead plate and decayed in the gas. Subsequently, the decay of a neutral V-particle occurred 1 cm. below the first decay. The Pic-du-Midi group concluded, after making reprojection measurements, that the two decay events were directly related. The plane of the second fork contains the point of decay of the charged V-particle, within measurement error. The simplest explanation of the double decay event is that a neutral V-particle was produced in the charged decay. The momentum measurements on the secondaries of the neutral V-decay are very inaccurate owing to the short track lengths and their poor quality. The data, which are given in Table 9 of § 6. 2, favour the decay scheme of equation (4).

The decay scheme, followed by the negatively-charged V-particle, appears to be of the type

$$\text{(13)} \qquad \mathrm{V}^- \rightarrow \pi^- + \mathrm{V}_2^0$$

where, as far as the actual measurements are concerned, the π-meson can be replaced by a μ-meson. The mass of the neutral

V_2^0-particle is about 800 m_e. It is possible that this particular particle may have had a mass of 2200 m_e (decay scheme of equation (3)). It is clear, from the dynamics of the actual decay, that the momentum of the neutral particle was very much higher than that of the charged secondary. The implication of this asymmetry in the momenta is that the neutral particle was considerably more massive than the charged particle, otherwise the observed distribution of the V-particle momentum between the two secondaries would be improbable.

An alternative, but much less plausible, explanation is that the incident particle interacted in the lead plate and produced two unstable particles, with substantially the same directions, but no other visible particles. The two V-particles then decayed in the gas below the plate. The most likely neutral particles from the charged decay are π°-mesons, neutrons and neutrinos. The various possible explanations of the double-decay event are summarised in Table 11; the approximate mass values are given in row (4).

TABLE 11

The masses of the charged V-particles

(1) Scheme no.	(1)	(2)	(3)	(4)	(5)
(2) Nature of charged secondary	π	π	π	π	π
(3) Nature of neutral secondary	V° ($800 m_e$)	V° ($2200 m_e$)	n°	π°	ν
(4) Mass event 1 ($\times m_e$)	1160	2460	2140	820	790
(5) Mass event 40 ($\times m_e$)	1280	2900	2530	750	660
(6) Mass range event 17 ($\times m_e$)					
Min. mass	1310	2630	2320	900	800
Max. mass.	1440	2740	2420	1060	960
(7) Min. mass event R & B (plate II) ($\times m_e$) . .	1530	2910	2580	1120	1050

The second event (No. 40, Table 10) which can be analysed in terms of the five schemes in Table 11 is reproduced in Plate XV, and is similar, except for sign, to the one obtained by Rochester and Butler. The mass values are listed in row (5).

The third event (No. 17, Table 10) illustrated in Plate XVI, consists of a heavily-ionizing particle from a high-energy nuclear interaction in the lead plate, which decays about 2 cm. below the plate. The point of the decay cannot be seen clearly in a single photograph owing to the confusion introduced by the other particles; it can, however, be seen stereoscopically. The primary track length is short and cannot be measured, but the specific ionization is greater than four times the minimum value. The negative secondary particle makes an angle of 100° with the direction of the primary and has a measured momentum of 0.18 BeV/c. The minimum mass of the charged particle can be calculated, if the particle is assumed to have decayed at rest and if a particular decay scheme is assumed. The maximum value of the mass for the assumed decay scheme can be calculated, if the decaying particle is given the maximum momentum consistent with its observed specific ionization. The minimum and maximum values are given in row (6) of Table 11. If an attempt is made to explain this event as a $\pi \rightarrow \mu$ decay, then the minimum value of the π-meson mass is 630 m_e, an absurdly high value.

The V-shaped track found by O'Ceallaigh is very similar to the cloud-chamber example shown in Plate XVI. The decay occurred at rest and, assuming that the charged secondary was a π-meson, its momentum was found to be 0.28 BeV/c, a rather higher value than that found for the event obtained by the Pic-du-Midi group. If the V-particle decayed into a charged and a neutral π-meson, then its mass was 1260 m_e, but if the neutral particle was a neutral V-particle of mass 800 m_e its mass was 1320 m_e. These values are higher than those obtained by the Pic-du-Midi group for their event, they are not, however, incompatible with the mass found from a study of the track of the V-particle before it came to rest. O'Ceallaigh could not identify the charged secondary particle, which could have been a meson or an electron.

The positively-charged V-shaped track observed by Rochester and Butler cannot be analysed in detail because the momentum of the incident particle is unknown. It is possible, however, to assume any one of the decay schemes (1) to (5) of Table 11 and use the secondary momentum to calculate the minimum possible value of the mass. These minimum values are given in row 7 of Table 11.

The various schemes each give fairly consistent mass values, but with only a few events analysed fully, it is not possible to judge if any one scheme is more consistent than the others. The scheme:

$$V^{\pm} \rightarrow \pi^{\pm} + \pi^{0}$$

gives several mass values which fit quite well with the one direct mass measurement which has been made so far.

11. 6 The mean rest lifetime of charged V-particles

It is impossible to find the lifetime of the charged V-particle from the properties of the very small number of events so far identified. SERIFF *et al.* suggest that the lifetime may be much shorter than the value they obtained for the neutral V-particles. They found twenty-five neutral V-particles from above the chamber and five from the lead plate; at the same time, one charged V-particle came from the lead above the chamber and three from the plate. These figures indicate that the majority of the charged V-particles may have decayed before reaching the chamber, owing to their very short lifetime. The number of events is small and the conclusion may be incorrect if one or two of the charged V-shaped tracks can be explained by the decay of π-mesons rather than by V-particles.

The lifetime of charged V-particles is unlikely to be shorter than 10^{-10} sec., because the Pic-du-Midi group and Bridge and Annis have both observed the decays of several slow V-particles. In fact, the lifetime may be quite long if the event in Plate XVI is similar to the negative τ-meson observed by BUTLER *et al.* [1950]. These workers observed three slow τ-mesons, with a total track length of about 20 cm., which did not decay in the chamber. Bridge and Annis have found seven cases in which a particle entered the chamber from the counter set and apparently stopped in one of the plates. In each case, a single secondary particle, at minimum ionization, emerged from the bottom of the plate. One of the secondary particles traversed about 3 cm. of lead without multiplication. Bridge and Annis concluded that this secondary could not have been an electron and so they could not interpret the event as the decay of a μ-meson. They were of the opinion that some of the other cases cannot have been $\mu \rightarrow e$ decays and concluded that several may have been examples of the decay of slow V-particles. If these conclusions are correct, then the mean lifetime of the charged V-particle cannot be much shorter than 10^{-9} sec.

12. Conclusions

Convincing evidence has been obtained for the existence of unstable charged particles, heavier than π-mesons. It is not yet certain how many of these particles exist and a very considerable amount of work on their properties will be undertaken in future years. The principal conclusions may be summarised as follows:

12. 1 Three examples of the decay of charged particles each into three π-mesons have been observed in photographic emulsions. In two of these the mass of the unstable particle was close to 1000 m_e. One example of the decay of a charged particle into a single charged secondary has been identified in a photographic emulsion. The mass obtained from a study of the track of the unstable particle is $(1260 \pm 290)\ m_e$, possibly a higher value than that obtained by similar measurements on the τ-mesons.

12. 2 About thirty charged V-shaped tracks have been observed in cloud chambers, each involving one charged secondary. It has been shown that momentum measurements must be made before the events can be distinguished from the decay of π-mesons, which are relatively common in penetrating showers. The Pic-du-Midi group have observed seven examples of the decay of charged particles, heavier than the π-meson.

12. 3 Several heavily-ionizing particles have been observed to decay in the gas of cloud chambers. Up to April 1951, however, only two have been observed in a magnetic field and their tracks were too short for momentum measurements to be made.

12. 4 The masses of several charged V-particles have been calculated on the basis of a variety of assumed decay schemes. The choice of decay schemes is influenced by evidence on the nature of the secondary particles; one secondary particle has probably been identified as a π-meson. In one case there is evidence which suggests that the neutral secondary may have been a neutral V-particle, probably the type with a mass of about 800 m_e. If the charged V-particles decay according to the scheme:

$$V^{\pm} \rightarrow \pi^{\pm} + V_2^0,$$

then their mass is within the range (1200—1500) m_e, a rather higher value than that found for the τ-meson. On the other hand, if both secondaries of charged decays are π-mesons, then the V-particle mass is about 1000 m_e.

ACKNOWLEDGEMENTS

The author wishes to thank Professor Carl Anderson, Dr C. O'Ceallaigh, Dr W. B. Fretter and Dr H. S. Bridge for sending details of their work, prior to publication. He is grateful to them and also to Professor C. F. Powell for granting permission to reproduce several of their photographs.

He is particularly indebted to his colleagues in the Pic-du-Midi group, Mr R. Armenteros, Mr K. H. Barker, M. A. Cachon and Mr A. H. Chapman, who obtained the cloud chamber photographs of V-particles on the Pic-du-Midi and carried out much of the detailed analysis. While preparing this article he has had the benefit of many long discussions with Mr K. H. Barker.

Thanks are also due to Professor P. M. S. Blackett for his encouragement and close interest in the work on the Pic-du-Midi and to Dr J. G. Wilson and Dr G. D. Rochester for their helpful criticisms and suggestions.

REFERENCES

ALIKHANIYAN, A. I., A. I. ALIKHANOV and A. WEISSENBERG, 1948, J. Exp. Theor. Phys. U.S.S.R., 18, 301.

ARMENTEROS, R., K. H. BARKER, C. C. BUTLER, A. CACHON and A. H. CHAPMAN, 1951, Nature, Lond., 167, 501.

ASTBURY, P., P. CHIPPENDALE, J. A. NEWTH. and A. B. SAHIAR, 1951. Private communication.

BARKER, K. H. and C. C. BUTLER, 1951, Proc. Phys. Soc., A64, 4.

BLATON, J., 1950, Det Kgl., Danske Vidensk Selskab., Mat-fys. Medd., 24, Nr. 12.

BRIDGE, H. S. and M. ANNIS, 1951, Phys. Rev,, 81, 445.

BROWN, R., U. CAMERINI, P. H. FOWLER, H. MUIRHEAD, C. F. POWELL and D. M. RITSON, 1949, Nature, Lond., 163, 82.

BUTLER, C. C., W. G. V. ROSSER and K. H. BARKER, 1950, Proc. Phys. Soc., A63, 145.

DAUDIN, J., 1944, Ann. Phys., Paris, II, 19, 110.

FORSTER, H. H., 1950, Phys. Rev., 77, 733.

FOWLER, P. H., 1950, Phil. Mag., 41, 169.

FRANZINETTI, C., 1950, Phil. Mag., 41, 86.

FRETTER, W. B., 1951. Private communication.

HARDING, J. B., 1950, Phil. Mag., 41, 405.

HOPPER, V. D. and S. BISWAS, 1950, Phys. Rev., 80, 1099.

LATTES, C. M. G., G. P. S. OCCHIALINI and C. F. POWELL, 1947, Nature, Lond., 160, 453.

LEIGHTON, R. B., S. D. WANLASS and W. L ALFORD, 1951. Private Communication.

LEPRINCE RINGUET, L. and M. L'HÉRITIER, 1946, J. Phys. Radium, (Ser. 8), 7, 66.

LEPRINCE RINGUET, L., H. TCHANG FONG, L. JAUNEAU and D. MORELLET, 1948, C. R. Acad. Sci., Paris, 226, 1897.

O'CEALLAIGH, C., 1951. Private communication.

ROCHESTER, G. D. and C. C. BUTLER, 1947, Nature, Lond., 160, 855.

SERIFF, A. J., R. B. LEIGHTON, C. HSIAO, E. W. COWAN and C. D. ANDERSON, 1950, Phys. Rev., 78, 290.

THOMPSON, R. W., H. O. COHN and R. S. FLUM, 1951, Phys. Rev., 83, 175.

TINLOT, J., 1948, Phys. Rev., 73, 1476.

WAGNER, N. and D. COOPER, 1949, Phys. Rev., 76, 449.

CHAPTER III

COUPLING PROPERTIES OF NUCLEONS, MESONS AND LEPTONS

BY

LOUIS MICHEL

Institute of Theoretical Physics, Copenhagen

INTRODUCTION 127
1. THE PHYSICS OF PARTICLES 127
2. π-MESONS AND HEAVIER MESONS 145
3. INTERACTION BETWEEN FOUR FERMIONS 159
4. POSSIBLE COUPLING SCHEMES 176
5. CONCLUSION 182
REFERENCES 185

INTRODUCTION

With the discovery of the neutron (Chadwick [1932]) and the positon (Anderson [1932]), all nucleons and leptons that we now know had been observed (the existence of the neutrino was assumed from β^--radioactivity). The first successful quantum mechanical description of a non-electromagnetic interaction between elementary particles was given by Fermi [1934] for β^--radioactivity; Wick [1934] in the same year showed the direct extension to the newly discovered β^+-radioactivity. However, this interaction was much too small to explain nuclear forces. The meson hypothesis of Yukawa [1935] removed this difficulty, and suggested the coupling scheme between elementary particles according to Figure 1; it was then natural to classify particles as nucleons, mesons and leptons.

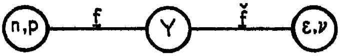

Fig. 1. Coupling scheme before 1947

The theory predicted (Tomonaga and Araki [1940]) the absorption of negative mesons by nuclei, and this was verified in experiments with lead and iron, but Conversi *et al.* [1945, 47] showed, unexpectedly, that most negative mesons stopped in carbon decay. The validity of the scheme was then doubtful, and the discovery of the π-meson (Lattes *et al.* [1947]) destroyed it completely.

More recently, numerous schemes have been proposed (see for instance, surveys of the question in different years: Rosenfeld [1948b] and Yukawa [1949]). Even the problem of nuclear forces has not yet been solved in terms of meson fields, and several new reactions, some involving new particles (π°-mesons, heavy mesons), have been discovered in 1950.

1. THE PHYSICS OF PARTICLES

Any physical result is based on experimental data and theoretical hypothesis, and it is necessary to know fully its bases in order to appreciate its value and the limits of its validity. In the present state of physics, with the obvious specialization of physicists, it is often very difficult for experimental and theoretical people to know the exact significance and implications of their mutual discoveries. It is necessary for experimental cosmic ray workers to have right and precise ideas of the theoretical concepts they have to use to make qualitative deductions, (quantitative calculations are left to the theoreticians, and, moreover, form the weakest part of the theory !). In this paper it seems useful, after a short summary of experimental data on particles, to give a review of the framework of the theory as it is currently in use, and to show what is the basis of the main laws and theorems (conservation laws, Furry's theorem etc.) useful for the qualitative study of reactions and couplings between elementary particles. This, together with the trite, but essential, specification of units, is the aim of the present section.

1. 1 Experimental data

Experimentally, particles are at once classified into charged and neutral particles. Neutral quanta (photons, π°-mesons) have strictly no charge, while within experimental accuracy (a few per cent.) charged particles have all the same amount of electric charge, with both signs of charge for electrons and mesons. This amount is supposed to be strictly the same for all charged particles, and this implies that neutrons and neutrinos have strictly no charge. Only for electrons has each charge conjugate state been named — negaton and positon. Particles are further experimentally characterized by their rest-mass. Table 1 gives the list of mass values and the notation used in this paper, and numerical results given by authors will be corrected by taking into account these values if necessary. Latest references of experimental data are indicated; see also POWELL's [1950] review on mesons.

There are mesons heavier than π-mesons; the existence of these particles is certain, but their masses are not yet known with any accuracy. The properties of these particles will be studied in § 2. 5 and § 2. 6 under the titles: "Neutral V-mesons" and "Charged V-mesons and τ-mesons". We shall not, however, consider here varitrons (see DAUDIN [1950] for a critical survey) nor the photographic plate evidence of decays attributed to them (Alikhaniyan *et al.* [1949]).

Other characteristic properties of free particles: mean life, magnetic moment and spin, will be reviewed separately for each of them.

TABLE 1

Particle	Mass notation	Mass value	Experimental data	
ε electron	m	unit		
ν neutrino	ν	0	< 0.002	Curran *et al.* [1949]
μ μ-meson	μ	213	210 ± 4	Smith *et al.* [1950]
			215 ± 4	Retallack, Brode [1949]
			212 ± 4	Peyrou, Lagarrigue [1950]
π { $\pi^{\pm}$-meson	$\varkappa$	271	271.4 ± 2.5	Moyer Harwell Conf. [1950]
π°-meson	$\varkappa'$	261	261 ± 4	
n, p nucleon	M	1837		
Difference $M_n - M_p$		2.53	2.53 ± 0.025	Robson [1951]
			2.535 ± 0.012	Hornyak *et al.* [1950]

1.2 Theoretical methods

Many authors have attempted to develop fundamental theories giving the number of elementary particles, their rest-masses, and so on .... Others have tried to describe some particles as constituted of several other "elementary" particles (generally a pair of fermions). However, up to now the only far reaching attempt for the description of the properties of particles is the field theory: the wave function of a field satisfies equations defined for a given value of the spin, and which contain the mass of the particle as a parameter. Essays have been made for describing particles with several states of mass, but until now only particles with one mass and one value of spin have been widely used for explaining or forecasting experimental data, the values of spin being restricted to 0, $\frac{1}{2}$ and 1. An excellent report on non-interacting field theory has been given by Pauli [1941], since when no essential progress has been made on the subject. For fields in interaction, formal and substantial progress has been made since 1948 (see papers of Tomonaga, Schwinger, Feynmann, Dyson and so on), but it is more or less restricted to electrodynamics.

The only relativistic equation for spin $\frac{1}{2}$ particles that has been widely used is the Dirac equation. There are two possibilities for describing spin 0 particles: the wave function can be either a scalar, S, or a pseudoscalar, P; this is also true for spin 1 particles, the wave function being either a vector, V, or a pseudovector, A. In the following we shall indicate these four possibilities for bosons by the letters S, V, A, P.

Charged particles are described by imaginary wave functions satisfying gauge invariant equations; imaginary wave functions are also necessary to describe neutral particles with a magnetic moment: their wave functions are directly coupled with the electromagnetic field, and not with the potential, and therefore gauge invariance is not imposed. In both cases there are two states of the particle, with opposite charge (for charged particles) and opposite magnetic moments (for spin $\neq 0$ particles). Most physicists believe in the existence of negative protons and antineutrons, but this question can ultimately only be solved by experiment[1].

Photons and π^0-mesons are described by real wave functions; it is not yet known whether neutrinos must be described with two states (called in the following "neutrino" and "antineutrino") or only one state (see § 3. 1 for discussion) as is possible with the Dirac equation (Majorana [1937]); in this case the wave function is real if a convenient representation of Dirac's matrices is used: $\widetilde{\alpha} = \alpha^* = \alpha$, $\widetilde{\beta} = \beta^* = -\beta$. In the following, we shall refer to fermions with only one state as "Majorana particles".

It must be emphasized that there is actually no theoretical distinction between "kinds" of particles; the isotopic spin formalism allows one to speak of protons and neutrons as the same particle, the nucleon; electrons and neutrinos as the same particle, the lepton; but this is only a more condensed way of writing, and it does not correspond to a deeper theoretical concept[2].

---

[1] Searches for negative protons have up to now led to negative results. However, they have mainly been based on the study of β^--radioactive nuclei emitting delayed neutrons (since $M_n + m > M_p$), Broda *et al.* [1947] Sun [1949], Scott and Titterton [1950], and in this case the theory forbids the spontaneous emission of negative protons, as was pointed out by the last authors (see also Michel [1950b]). We would expect the main source of antinucleons to be pair production of nucleon-antinucleon in the very energetic events of cosmic rays; they will disappear by annihilation.

[2] It seems possible, for fermions, to distinguish between "kinds" of particles by the anticommutation of the wave functions of the "same" kind

For the study of coupling properties between particles we shall study "reactions" between these particles; a reaction is defined by the nature and the "charge conjugate state" of the involved particles and by the set **M** of the values of the dichotomic variable M for each particle: $M = -1$ when the particle is absorbed, and $M = 1$ if the particle is emitted. In the following we shall also use the dichotomic variables L and K: if Ce is the charge of the particle, for a charged particle $L = C$, for a neutral particle with a magnetic moment L is a function of its sign (here it will be chosen as the opposite of this sign because of the neutron), and for a neutral particle without magnetic moment (photons, probably π°-mesons and perhaps neutrinos) L is arbitrary. K is defined by $K = LM$. A given reaction can be characterized by **L** and **M**, these notations representing the two sets of values of L and M for each involved particle.

1. 3 The conservation laws

The conservation laws summarised below, with the exception of the last, apply also in classical theory. They are expressed by group invariance, this condition restricting the number of possible terms in the Lagrangian. The information given by the application of these laws is absolutely independent of the particular hypothesis for the interactions between particles and even of the imperfect state of the theory. All physicists apply them in the same order for excluding impossible cases, but the selection rules due to the two last laws have not been well known.

Conservation of charge: invariance under gauge group. This can be expressed for a reaction between n particles by

$$\Sigma M_i C_i = 0 = \Sigma' K_i \tag{1}$$

Σ' indicating summation over the charged particles only.

Conservation of momentum and energy: invariance under Lorentz displacement group. If $\mathbf{k}_i$ is the four vector momentum-energy of the i^{th} particle, the law is: $\Sigma M_i \mathbf{k}_i = 0$.

---

of particles and the commutation of the wave functions of particles of "different" kind: see, for instance, NISHIJIMA [1950] who deduces certain selection rules for decay from such a distinction. But it can easily be shown that these two ways of writing are equivalent.

Conservation of angular momentum. This law requires that the number of fermions involved in a reaction must be even. For a given system of particles we shall call J its total angular momentum: it is the sum of the angular momenta and the spins.

A system of two bosons with opposite momenta cannot have all possible values of J in the following three cases:

(a) For two photons, $J \neq 1$: LANDAU [1948], YANG [1950a], PEASLEE [1950], and STEINBERGER [1949b] quotes also WIGNER for this result.

(b) For two identical spin 0 bosons, J cannot be odd (see for instance PEASLEE [1950]).

(c) For one photon and one spin 0 boson, $J \neq 0$.

Conservation of parity. This law has no classical correspondence, its importance was shown by WIGNER [1927].

We can decompose the Lorentz group $\mathfrak{L}$ of transformations into $\mathfrak{L} = (1 + T)(1 + R)\mathfrak{L}_+^\uparrow$ (see, for instance, BHABHA [1949]) where T changes x, y, z, t into $x, y, z, -t$ and R changes x, y, z, t into $-x, -y, -z, t$. Invariance under the group $\mathfrak{L}_+^\uparrow$ gives the conservation of angular momentum. Time has an absolute orientation for us, therefore all physical laws cannot be invariant under T, the reversal of the time direction (however, this non-invariance under T may be limited to statistical mechanics). But, outside biology, we cannot in nature make any distinction between right-handed and left-handed frames of reference; therefore no physical law allows us to distinguish between the two kinds of frame, and they must all be invariant under transformations $R\mathfrak{L}_+^\uparrow$ exchanging two frames of different kind, i.e. they must be invariant under the group $1 + R$. However, wave functions do not need to be invariant for R, thence the possible distinction between S and P mesons, V and A mesons.

Here we shall give the results of parity conservation only in the case of the spontaneous decay of a particle into integral spin particles; there is no need to specify which is the initial particle and which particles are secondaries. Decay is forbidden for the following sets:

$$SSP,\ PPP,\ SSA,\ PPA,\ SPV,\ SSSP,\ SPPP,$$

(see PEASLEE [1950] for the decay into two spin 0 mesons; MICHEL [1951] for all cases)[3].

These results are very fundamental, and the only hypothesis made for their validity is that there are only scalar coupling constants (no pseudoscalar coupling constants: see § 1. 6 and § 3. 6).

1. 4 Coupling between fields

The field equations mentioned in § 1. 2 are deduced by a variational principle from a Lagrangian which contains quadratically the field variables or, bilinearly, these variables and their first derivatives[4]. This Lagrange function must be a scalar. The field variables ψ of non-interacting fields can, by quantization, be decomposed into plane waves which describe creation and annihilation of particles when they are applied to a state vector. There are interactions between the fields when there are, in the Lagrangian, terms formed with the ψ's (or the first derivatives of one of them) of different fields. Field equations are deduced in the same way, but they cannot be solved exactly; an approximate method must be used, generally the perturbation theory where the coupling terms are considered as small and their presence perturbing only the ψ's of free fields. This is why we can still speak in terms of particles, of their creation and their annihilation[5].

We use the notation $\psi_i^{K_i} = \psi_i$ if $K_i = -1$, and $= \psi_i^*$ if $K_i = 1$; we can define a coupling between fields by **K**, the set of values of the K_i in the interaction terms of the Lagrangian; this coupling can contain several terms if it is possible to form several independent scalars with the involved $\psi_i^{K_i}$ or the first derivatives of one of these $\psi_i^{K_i}$. The coefficient of each term is a coupling constant. The Lagrangian must also contain for any term which is not self conjugate, its hermitian conjugate; these conjugate terms correspond to the sets $-\mathbf{K}$ of the values of K_i. With the Majorana representation of Dirac matrices (see § 1. 2) and appropriate notations, the K defined here are identical with the K defined in § 1. 2; therefore the possible "first order" reactions **L**, **M** for a given coupling satisfy

---

[3] The list of those sets has been given by FUKUDA *et al.* [1950a] who found for them no Lorentz invariant terms of the S-matrix in particular lowest order perturbation calculations; see also papers of ONEDA, OZAKI and SASAKI quoted in § 2. 5.

[4] It is not impossible, indeed, to have a Lagrangian containing higher derivatives of the field variables, and the equations would then be partial differential equations of higher order, but the physical solutions taken are still restricted to plane waves for non-interacting fields.

[5] All the theoretical numerical results we shall use are obtained with this weak coupling method; there are other methods: strong coupling theory, more or less phenomenological methods for multiple meson production (Heisenberg, Fermi) etc., but they are not applied to the whole problem of coupling between particles. The first question to be answered is: can the usual theory give an acceptable solution to this problem? We restrict this paper to the ordinary weak coupling theory.

$$L_iM_i = K_i \quad \text{or} \quad L_iM_i = -K_i \tag{2}$$

We shall call a "class" the set of all possible first order reactions of a coupling $\pm \mathbf{K}$.

Now the operator which transforms the function representing the initial state into that representing the final state, i.e. the S-matrix or the perturbation Hamiltonian, is developed in increasing powers of the coupling constants, and a very intuitive and useful graphical representation of the perturbation theory has been introduced by Feynmann and Dyson [1949]. The physical reaction can be considered as the result of a sequence of "first order" reactions (each represented by a vertex of the graph); these intermediary reactions are virtual, and the particles absorbed in those reactions have been emitted by a previous one, if they are not the initial particles themselves. In the graph, virtual particles are represented by lines joining two vertices, real particles by lines touching only one vertex.

Example 1. We consider the two couplings *f* and *e* responsible for the first order reactions:

$$f,\ p^+ \to p^+ + \pi^\circ; \quad e,\ p^+ \to p^+ + \gamma.$$

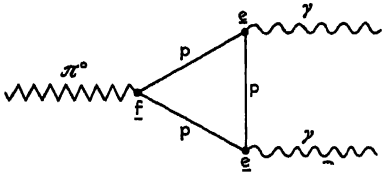

Fig. 2 Graph of $\pi^\circ \to 2\gamma$

The three successive virtual reactions $\pi^\circ \to p^+ + p^-$, $p^- \to p^- + \gamma$, $p^+ + p^- \to \gamma$, give the real reaction $\pi^\circ \to 2\gamma$, and the graph of the processes is given in Fig. 2; an alternative for the second virtual reaction is $p^+ \to p^+ + \gamma$ and gives the same graph.

Example 2. A graph can be composed of disconnected parts; here is an example. The atomic masses of A^{40}_{18}, K^{40}_{19}, Ca^{40}_{20} are respectively 39.9755, 39.9756, 39.9751 (ROSENFELD [1948a]), therefore the β^--decay of A^{40}_{18} is not possible, but the virtual reaction:

$$\mathrm{n}\ (\text{of } A^{40}_{18}) \to \mathrm{p}^+\ (\text{of } K^{40}_{19}) + \varepsilon^- + \nu$$

followed by the reaction:

$$\mathrm{n}\ (\text{of } K^{40}_{19}) \to \mathrm{p}^+\ (\text{of } Ca^{40}_{20}) + \varepsilon^- + \nu$$

gives a real reaction:

$$2\mathrm{n}\ (\text{of } A^{40}_{18}) \to 2\mathrm{p}^+\ (\text{of } Ca^{40}_{20}) + 2\varepsilon^- + 2\nu.$$

The graph of this reaction is given in Fig. 3. If the neutrino is a "Majorana" particle (see § 1. 2), one can have either the graph of Fig. 3 or the graph of Fig. 4, corresponding to the reaction

$$2\mathrm{n}\ (\text{of } A^{40}_{18}) \to 2\mathrm{p}^+\ (\text{of } Ca^{40}_{20}) + 2\varepsilon^-;$$

but if the neutrino has two states ("neutrino" and "antineutrino") only the graph of Fig. 3 is possible, as is easily seen.

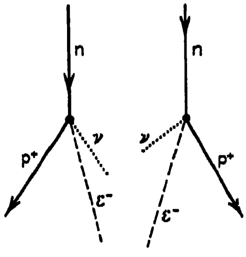

Fig. 3. Graph of $2\mathrm{n}\,(\text{of } A^{40}) \to 2\mathrm{p}^+\,(\text{of } Ca^{40}) + 2\varepsilon^- + 2\nu$

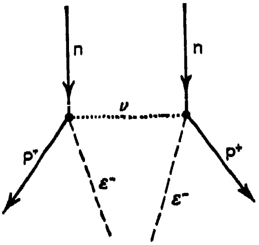

Fig. 4. Graph of $2\mathrm{n}\ (\text{of } A^{40}) \to 2\mathrm{p}^+\ (\text{of } Ca^{40}) + 2\varepsilon^-$

The number of vertices in a graph gives the "order" n of the phenomenon; this means that its probability is proportional to a homogeneous polynomial of degree $2n$ in the coupling constants involved [6].

It follows from the principles of perturbation theory that the graphs of minimum n for a process give the main contribution, and the graphs with larger n give only higher order (sometimes called "radiative") corrections.

From this formal study of coupling we deduce easily that the existence of a reaction **M, L** implies the existence of reactions **—M, L** (reversibility in microphysics), **M, —L** (charge conjugation) [7] and all the reactions (virtual or real) which have the same or opposite **K** ($\mathrm{K}_i = \mathrm{L}_i \mathrm{M}_i$) from the observed one.

1. 5 Couplings commonly used

All possible couplings of the theory are not used for calculations; nearly all authors avoid the use of derivatives of Dirac wave functions and of imaginary and pseudoscalar coupling constants. A rapid review of the other (used and unused) possibilities is given here.

It is possible to form five invariants with two Dirac wave functions $\psi_1^{\mathrm{K}_1}$ and $\psi_2^{\mathrm{K}_2}$. With the Majorana representation (see § 1. 2) of the matrices, these invariants can be written $\psi_1^{\mathrm{K}_1} F_i \psi_2^{\mathrm{K}_2}$: $i = 1$ yields a scalar s'', $i = 2$ the four components of a vector v'', $i = 3$ the six independent components of a skew tensor t'', $i = 4$ the four components of a pseudovector a'', $i = 5$ a pseudoscalar p''. Among the 16 matrices F, 10 are symmetrical and 6 antisymmetrical; in the Majorana representation they are distributed so that

$$\tilde{F}_i = -\theta_i F_i \text{ with } \theta_i = 1, -1, -1, 1, 1. \tag{3}$$

---

[6] Particle lines can only join at a vertex, therefore it is not coherent with the theory to use such a graph, for instance, for the coupling responsible for the reaction $\mu^- \rightarrow \varepsilon^- + \nu_+ + \nu_-$ (ν_+ and ν_- are the two states of the neutrino), as was suggested by OGAWA and KAMEFUCHI [1950a] for making possible the reaction $\mu^- \rightarrow \varepsilon^-$ (in the presence of other particles intervening in the rest of the graph and assisting energy-momentum conservation).

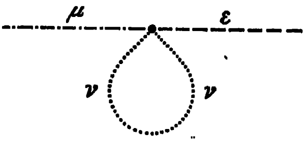

[7] There is a complete symmetry between charge conjugate states of a particle; a correct use of Dirac's hole theory cannot give different results when one permutes the role of the holes and the particles.

If the two ψ^{K} are identical, from the anticommutation relations we immediately deduce:

$$(4)\qquad \psi^{\mathrm{K}}F_i\psi^{\mathrm{K}} = \tfrac{1}{2}\psi^{\mathrm{K}}(F-\widetilde{F})\psi^{\mathrm{K}} = \tfrac{1}{2}(1+\theta_i)\psi^{\mathrm{K}}F_i\psi^{\mathrm{K}} \text{ i.e. } v'' = t'' = 0.$$

There is an arbitrary factor in the F_i's; it can be removed in the coupling constants and it is then possible to have all the F hermitian:

$$(5)\qquad F_i^{\dagger} = F_i$$

With the wave functions s, v, a, p of S, V, A, P bosons (see § 1. 2) and with the vector $\partial_\mu = \partial/\partial x,\ \partial/\partial y,\ \partial/\partial z,\ \partial/\partial t$, it is possible to form four other invariants $v'_s,\ t'_v,\ t'_a,\ a'_p$.

Case 1. Coupling between one boson field and one fermion field. (a) charged fermion field: the boson field must be neutral, and we suppose that it is described by a real function. The only possible form of the coupling terms (see § 1. 4) is

$$(6)\qquad C = f_i\varphi_i\cdot\psi^{\mathrm{K}}F_i\psi^{-\mathrm{K}} + \text{h.c.}$$

where "·" indicates a scalar product, φ either the boson wave function or its first derivatives and "h.c." the hermitian conjugate. Using equation (5), equation (6) can be written:

$$(7)\qquad C = (f+f^*)\varphi\cdot\psi^{\mathrm{K}}F\psi^{-\mathrm{K}},$$

and we are left with only the real part of the coupling constant; in other words, in this case the coupling constant must be real. C is also charge conjugate, since (see equation (3)),

$$(8)\qquad C = \tfrac{1}{2}\varphi_i\cdot(f_i\psi^{\mathrm{K}}F_i\psi^{-\mathrm{K}} - f_i\psi^{-\mathrm{K}}\widetilde{F}_i\psi^{\mathrm{K}}) = \\ = \tfrac{1}{2}\varphi_i\cdot(f_i\psi^{\mathrm{K}}F_i\psi^{-\mathrm{K}} + \theta_i f_i\psi^{-\mathrm{K}}F_i\psi^{\mathrm{K}});$$

on account of the Majorana representation of matrices[8], the second term is deduced from the first by changing **K** into $-\mathbf{K}$ (this changes **L** into $-\mathbf{L}$, see § 1. 2 and § 1. 4) which is the charge conjugation, but we note that the coupling constants are multiplied by θ_i. This important result will be used in § 1. 9.

---

[8] The Majorana representation of Dirac's matrices does not restrict the validity of the formalism; if it is not used, one has to introduce for charge conjugation a matrix C (see PAULI [1941]), the wave function of the Majorana particle is no longer real but there is imposed a more complicated condition, ... everything is, of course, equivalent, but written in a more complicated way. The Majorana representation is more convenient for all covariant calculations. Nevertheless the Dirac representation is much more used: historically it was the first, and it is more convenient for non-relativistic calculations (separation into large and small components).

We can now list all possible terms. There are eight. For scalar mesons: $f_S \varphi \psi^{\mathrm{K}} F \psi^{-\mathrm{K}} = f_S ss''$ and $\lambda f_S' \partial_\mu \varphi \cdot \psi^{\varkappa} F_2^{\mu} \psi^{-\varkappa} = \lambda f_S' v_S' \cdot v''$, these will be noted Ss and Sv; for vector mesons: $f_V v \cdot v''$ and $\lambda f_V' t_V' \cdot t''$, noted Vv and Vt; for pseudovector mesons: $f_A\, a \cdot a''$ and $\lambda f_A' t_A' \cdot t''$, noted Aa and At; for pseudoscalar mesons: $f_P\, pp''$ and $\lambda f_P' a_P' \cdot a''$, noted Pp and Pa· We have multiplied the coupling constants f' (of the coupling terms containing derivatives of the meson wave function) by $\lambda = \hbar/\varkappa c$, the wave length of the meson; then f and f' have the same dimensions since ∂_μ has the dimension of the reciprocal of a length.

If the boson field were described by an imaginary wave function, only the real part would be significant (as for f in equation (7)); for this reason neutral mesons are described by neutral wave functions. From these theoretical considerations they must have no magnetic moment.

(b) neutral fermion field. If this is represented by an imaginary wave function, we can form exactly the same couplings as in (a); this is done for the neutron. There is another possibility with f imaginary as well as the wave function; because of equation (4), this is only possible for s, a, and p couplings. If the fermion is a Majorana particle, there is only one possibility which can be deduced from any of the previous cases by omitting the useless K; equation (4) shows that there are no Sv, Vv, Vt, At couplings, and thus a Majorana particle cannot be coupled with vector mesons or with photons.

Case 2. Coupling between one boson field and two fermion fields. It would be significant here to use imaginary coupling constants, but it is possible by means of the isotopic spin formalism (see § 1. 8) to write the coupling terms in a form identical to Case 1(a), and if we restrict ourselves to this form we obtain the same limitations as for Case 1(a).

Case 3. Coupling between four fermion fields. Five invariants can be formed with the first two fields: s_1'', v_1'', t_1'', a_1'', p_1'', and five other invariants with the remaining two fields: s_2'', v_2'', t_2'', a_2'', p_2'';

by scalar products it is then possible to form five scalars J_i where $J_1 = s_1'' s_2'' + \text{h.c.}$; $J_2 = v_1'' \cdot v_2'' + \text{h.c.}$ etc.... For this kind of coupling we shall use the notation g for the coupling constants, and the most general coupling is a linear combination of five terms:

$$C = \Sigma g_i J_i. \tag{9}$$

It is possible here to take the g imaginary, and this possibility is discussed in § 1. 6, but in this paper the g will be taken as real.

One can show the following properties for the J (MICHEL 1950a): if the order of the ψ^{K} in the J_i is changed, the new J_i are linear combinations of the old ones (see FIERZ 1937); if two (or more) ψ^{K} are identical, there are only three (or one) independent J_i: this result will be used in § 3. 2.

1. 6 Couplings not commonly used

(a) Couplings with derivatives of the fermion fields. Such a coupling was used for β-decay by KONOPINSKI and UHLENBECK [1935]; it was a direct coupling between n, p, ε, ν and it contained the first derivative of the neutrino wave function. It was put forward to fit experimental data, but it has since been rejected in the light of better experiments. No study has been made of meson-nucleon coupling involving derivatives of the nucleon wave functions. Some cases would be identical with the usual couplings, but most of them would give quite different results. Such couplings, with derivatives of nucleon wave functions, have probably not been used for the historical reason of correspondence with electrodynamics.

(b) Use of pseudoscalar coupling constants is allowed for the same reason as the use of pseudoscalar or pseudovector wave functions: the observable results are even functions only of coupling constants and of wave functions. Then, the coupling constants are formally written in the same way but their meaning is different. The first use of a pseudoscalar coupling constant was made (although not of intent) by FERMI [1934] in his paper on β-decay (direct coupling between four fermions); KONOPINSKI and UHLENBECK [1935] using scalar coupling constants found the same result as Fermi except for the terms containing the neutrino mass (which correspond to a change of sign of the neutrino mass), a discrepancy which has been explained by RACAH [1937]: this result can be shown to be quite general. There are no essentially new results if scalar g and pseudoscalar $\hat{g}$ coupling constants are used in the same coupling, but their interference will give terms of the form $g\,\hat{g}\,\Delta$, where Δ is the only pseudoscalar which can be formed with four particles: it is the determinant of the four components of the four **k** fourvector momentum-energy of the particles; for four free particles $\Delta = 0$ on account of energy-momentum conservation $(\Sigma \mathrm{M}_i \mathbf{k}_i = 0)$; for bound particles, inside a nucleus, for instance, these terms may give important results. Modifications to the transformation law for Dirac wave functions under space reflexions have been proposed by Jarkov [1950] and Yang and Tiomno [1950]; these can be shown to be strictly equivalent to the possibility of using pseudoscalar ocupling constants. Such a use has been proposed practically by Schoenberg [1941]; there is no longer any distinction between scalar and pseudoscalar meson, vector and pseudovector meson. A spin 0 meson can have four coupling terms with nucleons: those already labelled *Ss*, *Sv*, *Pa*, *Pp*, while a spin 1 meson can have the four coupling terms *Vv*, *Vt*, *At*, *Aa*. In other words, spin 0 mesons can have properties of both *S* and *P* mesons, spin 1 mesons those of both *V* and *A* mesons (see calculations from Enatsu [1950]), but no other new physical effects occur when $\Delta = 0$. As we pointed out in § 1. 3, the use of pseudoscalar coupling constants would modify the form of results due to parity conservation.

(c) Imaginary coupling constants. We have seen in which cases coupling constants can be imaginary. It is easy to show that different observable results are obtained only for the terms containing the product of different coupling constants of the same coupling (as defined in § 1. 2, for instance *Ss* and *Sv*, or the five $g_i J_i$). One can for instance have instead of the expression $g_i g_j E_{ij}$ for real g, the expression $|g_i| \cdot |g_j| \cdot E_{ij} \cos \theta$, θ being the phase difference between g_i and g_j in the complex plane. Thus, the use of imaginary coupling constants. when it is allowed, would introduce more arbitrary constants (phase differences) which would eventually decrease the importance of interference between the different terms of the same coupling; moreover, the domain of validity of Furry's theorem (see § 1. 9) would be modified.

In the following we shall use for the purposes of our discussion only the commonly used couplings of § 1. 5 and neglect the possible couplings described in the present subsection. Theory might be saved by the introduction of more arbitrary constants, but one has first to try the simplest hypotheses for fitting experimental data. We therefore explicitly make the following simplifying hypotheses for coupling: coupling constants scalar and real, derivatives of fermion wave functions excluded.

1. 7 Units

The best system of units for theoretical studies of coupling becomes apparent during computations. The method of introducing coupling constants f and f' in § 1. 5 is formally similar to the use of Heavyside units in electrodynamics, where $e^2/4\pi\hbar c = 1/137$. It is now usual to use the natural system of units where $\hbar = c = 1$, in which the product of a mass by a length is a pure number. Since $\hbar/mc = 3.85\ 10^{-11}$ cm in c.g.s. units, (electron mass, m) (1 cm) $= 1/(3.85\ 10^{-11})$. If $\varkappa$ is the mass of a nuclear (integral spin) meson, $(1/\varkappa)\partial_\mu$ is dimensionless (see § 1. 5, here $\lambda = 1/\varkappa$) and f' as well as f and e is dimensionless. In this system, the values of f^2, f'^2 and e^2 are the values of the pure numbers $f^2/\hbar c$, $f'^2/\hbar c$ and $4\pi/137$.

Now we can express the dimensions of every quantity by a power of length or of mass by multiplying it by the requisite powers of $\hbar$ and c; here we choose mass, and, for instance, time has the dimensions $(\text{mass})^{-1}$. We have already chosen (§ 1. 1 table 1) the mass of the electron as our mass unit, and it is also the unit of energy and momentum. In the system where $\hbar = c = m = 1$, the unit of length is $3.85\ 10^{-11}$ cm (the Compton wavelength of the electron) and the unit of time $1.28\ 10^{-21}$ sec. (i.e. $\hbar/mc^2$); thus we multiply the values of time expressed in this system of units by $1.28\ 10^{-21}$ to bring them to seconds.

In the c.g.s system the g constants are expressed in ergs.cm^3. The pure number, $(g/mc^2)(\hbar/mc)^{-3}$, used by many physicists (see for instance Bethe [1947, p. 99]), is evidently their value in the system $\hbar = c = m = 1$.

1. 8 Isotopic variable

This name, proposed by Rosenfeld [1948a, p. 51], is better than the more usual "isotopic spin". As we pointed out in § 1. 3 this formalism is only a more condensed way of writing, which allows one formally to write the coupling of a charged and/or a neutral boson with two fermion fields (generally two nucleons or two leptons) in the same form as the interaction of one boson field with one fermion field (§ 1. 5).

(a) charged meson field ϕ, proton field ψ_p, neutron field ψ_n; coupling,

$$C = f[\phi^* \cdot (\psi_n^* F \psi_p) + \phi \cdot (\psi_p^* F \psi_n)]. \tag{10}$$

Let us write $\phi = \phi_1 + i\phi_2$ with ϕ_1 and ϕ_2 real, and $\psi = \begin{pmatrix}\psi_n \\ \psi_p\end{pmatrix}$, and let us define the four hermitian matrices:

$$\tau_0 = \begin{pmatrix}1 & 0\\ 0 & 1\end{pmatrix}, \ \tau_1 = \begin{pmatrix}0 & 1\\ 1 & 0\end{pmatrix}, \ \tau_2 = \begin{pmatrix}0 & -i\\ i & 0\end{pmatrix}, \ \tau_3 = \begin{pmatrix}1 & 0\\ 0 & -1\end{pmatrix}. \tag{11}$$

Equation (10) can then be written (with $f_1 = f_2 = f$, and $\sigma = 1,2$):

$$C = \sum_\sigma f_\sigma \, \phi_\sigma \cdot (\psi^* \tau_\sigma F \psi). \tag{12}$$

(b) neutral meson coupled with the proton and neutron fields by the coupling constants f_p and f_n. Let us define $f_3 = \frac{1}{2}(f_n - f_p)$ and $f_0 = \frac{1}{2}(f_n + f_p)$. The coupling term:

$$C' = f_n \phi \cdot (\psi_n^* F \psi_n) + f_p \phi \cdot (\psi_p^* F \psi_p), \tag{13}$$

can be written as in equation (12) with σ taking the values 0 and 3. With σ taking the values 1, 2, 3, 0 all these coupling terms can be condensed into the form of equation (12) with the condition $f_1 = f_2$ only. The extension to the f' is obvious.

1. 9 Furry's theorem

This theorem applies to the graphs containing closed loops of fermions. For instance, let us take the graph of Fig. 2. It represents elements of the S-matrix proportional to $f\,e^2$. We have seen (§ 1. 4, example 1), that this graph represents two possible alternatives obtained from each other by exchange of p^- and p^+. Because of the charge conjugation of the formalism, this shows that the values of the corresponding terms of the S-matrix are obtained from each other by the exchange of e, f and $\theta_2 e$, $\theta_i f$, ($\theta_2 = -1$, see equations (3), (8)), therefore if f is the constant of one of the couplings Sv, Vv, Vt, At, the sum of the terms represented by this graph is equal to 0 (since $1 + \theta_i = 0$).

Now it is easy to show for a reaction between real bosons through intermediary fermion fields, that when these real bosons introduce an odd number of couplings of given kinds, any graph contains at least one closed loop of fermion lines with an odd number of these couplings (because virtual particles introduce only an even number of couplings of any kind, and any partition of an odd integer contains at least one odd integer). Thence Furry's theorem:

*T*1. A reaction between neutral bosons through one intermediary fermion field is forbidden if the total number of v and t couplings is odd.

However, we must emphasize the following restriction: only one coupling term is allowed for S and A bosons; V and P bosons can have both their coupling terms (Vv and Vt, Pp and Pa) since they are equivalent for this theorem, evidently Vv and Vt or Pp and Pa of the *same* meson are only counted as one. This theorem was proved by Furry [1937] for electrodynamics, and its evident extension to neutral fields was indicated.

The isotopic variable formalism suggests an extension. The coupling f_3 (see § 1. 8) will be equivalent for this theorem to the v and t couplings, when one exchanges protons and neutrons in the graph considered, since $f_n = -f_p$ for neutral mesons with a pure f_3 coupling ($f_0 = 0$). Therefore, with the supplementary restriction that, for neutral mesons, either f_3 or f_0 are equal to 0, we transform *T*1 into *T*2:

*T*2. A reaction between charged and neutral mesons through the nucleon field is forbidden if the number of f_3, v, t couplings is odd.

This extension of *T*1 was first enunciated by Fukuda and Miyamoto [1949c] (see also van Wyck [1950b]); they pointed out that *T*2 cannot be applied to photons (as *T*1) since for photons $f_n = 0$, i.e. $-f_3 = f_0 = 0$. They also extend *T*1 to the case of neutral mesons interacting with nucleons, but we disagree with their result: it is true that charge conjugation gives *T*1; moreover, to each closed loop of protons we have to add the same closed loop of neutrons, this contribution being deduced from the first by multiplication by $(-1)^x$, x being the number of f_3 couplings.

*T*3. A reaction between neutral mesons through the nucleon field is forbidden if either, the number of f_3 couplings is odd, or, the total number of v and t couplings is odd.

We must emphasize that the selection rules due to Furry's theorem are valid to *any* order of the perturbation calculation.

It is of course possible to extend the theorem to g couplings: for instance, if we consider the direct coupling leptons-nucleons or μ, ν, n, p, we can still apply $T2$, replacing "charged mesons" by "charged mesons, electron-neutrino pairs and μ-meson-neutrino pairs". The coupling constants g do not change by charge conjugation, but the proof of $T2$ is based on the exchange, for the isotopic variable, of n and p, and the exchange of n and p change g_i into $\theta_i g_i$. Therefore the extension of $T2$ is:

$T4$. A reaction between charged and/or neutral mesons and pairs of one charged and one neutral fermion through the nucleon field is forbidden if the total number of v, t, f_3, g_2, g_3 couplings is odd.

For example, the decay of the π-meson can be represented by the graph Fig. 5 from two classes of reactions:

$$\pi^+ + \mathrm{n} \rightarrow \mathrm{p}^+, \quad \mathrm{n} \rightarrow \mathrm{p}^+ + \varepsilon^- + \nu.$$

There are selection rules for this decay (valid to all orders) arising from $T4$, see § 4. 1.

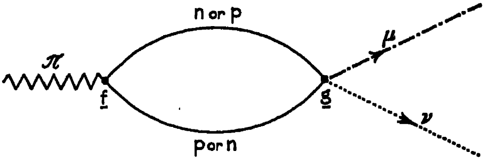

Fig. 5. Graph of $\pi^\pm \rightarrow \mu^\pm + \nu$

1. 10 Equivalence theorem, radiative corrections, renormalization and regularization

It can be shown (Nelson [1941], Dyson [1948], le Couteur and Rosenfeld [1949], Case [1949b]) that in most calculations to the second order in nucleon-meson coupling, the coupling *Pa*, with a coupling constant f'_p, can formally be replaced by a coupling *Pp* with a coupling constant $f_p = f'_p\,(M_n + M_p)/\varkappa$, and the coupling *Sv* (with constant f'_s) replaced by the coupling *Ss* with coupling constant $f_s = f'_s\,(M_n - M_p)/\varkappa$. This property is generally called the "equivalence theorem". It is reasonable to put $M_n = M_p = M$, and then the *Sv* coupling gives no contribution when the equivalence theorem applies (for instance for second order nuclear forces).

In recent years, developments of electrodynamics have been completely successful in explaining the Lamb shift and the anomalous magnetic moment of the electron (Schwinger [1948]); these results were obtained with the ideas of charge and mass renormalization which enable one to separate small physical effects from the divergences inherent in the present state of the quantum field theory. This handling of infinite quantities is quite delicate, and it is only successful in electrodynamics and neutral *Vv* meson theory. Pauli and Villars [1949] have proposed a "safer" and more powerful, but more arbitrary, way of handling these mathematically meaningless quantities: regularization. For many decay processes, the results we shall quote have been obtained with the regularization procedure, but this will always be specified.

One of the simplest radiative corrections in meson theory leads to the magnetic moments of nucleons; for pseudoscalar meson theory, calculations have been carried out (in the lowest order) both with old and recent methods, all give the same result (Luttinger [1949a], Slotnick and Heitler [1949], Case [1948, 1949a], Borowitz and Kohn [1949]), but this result does not fit with experimental data. Luttinger [1949b] however showed that the values of the magnetic moments of n and p can be found for a mixture of *Vv* and *P* mesons, but with very large values of the coupling constants. In any case, these results cannot be a test for meson theories.

On the other hand, results obtained by regularization must not be too firmly "believed" (see §§ 2. 2, 2. 5, 2. 6 and 4. 1): they can be quite different from those obtained by older methods (when these work) and they are sometimes ambiguous. Broadly, regularization has failed in its aim: there is at present no *a priori* method able to handle all divergence difficulties which can be encountered in calculations. As we shall see, many conclusions can be drawn from much safer theoretical grounds.

2. π-MESONS AND HEAVIER MESONS

2. 1 Nuclear forces

π-mesons can safely be identified with the particles of Yukawa's hypothesis for explaining nuclear forces, but the best experimental confirmation of the theory does not come from nuclear forces. Up to now, meson theories have failed to explain high energy nucleon-nucleon scattering. They are not even completely successful for low energy scattering or for the consideration of the constitution of nuclei, but in these cases the particle aspect of the meson is not so important, and these phenomena do not allow one to choose between the various meson theories. Successful attempts to explain "magic numbers" of protons and neutrons in nuclei have used a shell model involving strong spin-orbit coupling. Now only vector mesons can give large spin-orbit interaction between two nucleons, and they would therefore lead to a strong spin-orbit coupling between an "external" nucleon and the core of the nucleus. But the converse argument is not true: the existence of strong spin-orbit coupling (not yet accounted for) in the shell model of nuclei does not necessarily imply the existence of such an interaction between two nucleons; it is actually very doubtful if such a direct relation exists (see notes, added in proof, of CASE and PAIS [1950]).

The most important bearing of nuclear forces on meson theories comes from the equality of n—n, p—p, n—p forces observed for low energy (S wave) scattering and from the study of mirror nuclei. This leads to only two possibilities for the meson theory:

pure neutral theory: couplings given by equation (12) with $f_1 = f_2 = f_3 = 0$; there are only neutral mesons, coupled to protons and neutrons with the same strength $(f_n = f_p = f_0)$;

symmetrical meson theory: in equation (12) put $f_1 = f_2 = \pm f_3$ and $f_0 = 0$; there are charged and neutral mesons, the coupling constants ("mesic" charge of the nucleons) of the neutral meson and of the charged meson have the same absolute value, but for the neutral meson $f_n = -f_p$.

It is not possible to have a mixture of symmetrical and neutral theory with the *same* neutral meson, since then f_n and f_p are different, i.e. n—n and p—p forces are different (see ROSENFELD [1948b] p. 137). Of course one cannot exclude *a priori* a mixture of charged and neutral mesons of different kinds, with coupling constants such that the charge independence of nuclear forces is satisfied in its experimental domain of validity, on the ground that such an hypothesis is unaesthetic! But as we shall see (§ 2. 4), experimental data on $\pi^{\pm}$ and π^0 mesons (without excluding the possible existence of heavier nuclear mesons), outside the field of nuclear forces, are strongly in favour of charged and neutral pseudoscalar mesons.

Pseudoscalar meson theory has particular features, not shared to the same extent by the other theories: relativistic effects and, notably, higher order effects are very important. For the second order interaction between nucleons, the equivalence theorem is valid. However, the numerical values of the coupling constants for the second order still depend on the method of calculation; even the exact solution of the relativistic equations of the deuteron for the second order potential (see VAN HOVE [1949] for this potential) gives a logarithmic divergence (LEVY [1951]). The value of f_p' (*Pa* coupling) necessary to explain low energy scattering and the binding energy of the deuteron is about $f_p'^2 = 0.15$, and this coupling is formally equivalent to *Pp* coupling with $f_p = (2M/\varkappa)f_p'$, which gives for f_p^2 about 40. Now the fourth order interaction between nucleons gives rise to divergences for *Pa* coupling, but it has been calculated for *Pp* coupling by BETHE [1949] and by WATSON and LEPORE [1949], and these authors have shown the importance of the fourth order terms (and terms of still higher order), which decrease the value of f_p^2 to about 4 when they are taken into account.

2. 2 The nature of the π°-meson

The neutral π^0-meson has been observed through its decay products (two photons) since the end of 1949, both in cosmic rays (POWELL, Edinburgh Conf. Nov. 1949) and produced at Berkeley (CRANDALL, MOYER and YORK, American Phys. Soc. meeting, Stanford Dec. 1949); under both conditions it was produced in nucleon-nucleon collisions. The mass has been measured (Table 1) and the mean life evaluated to be between 1 and 5×10^{-14} second (CARLSON *et al.* [1950]). Production by photons on nuclei has also been observed (STEINBERGER *et al.* [1950]). The existence of this particle had been assumed from observations (FRETTER [1948, 1949], CHAO [1949] and others) and from theoretical studies (for example HEITLER and POWER [1947], GREISEN [1948]) of the cosmic ray soft component and of extensive and mixed showers;

see also KAPLON *et al.* [1949] and MARSHAK [1949c] for the observation and study of a very large star (in a photographic emulsion) produced by an energetic α-particle and containing a narrow shower of about 23 charged mesons and 35 γ-rays.

The discovery of the neutral π^0-meson is an important success for the meson theory which had long predicted its existence and its decay into photons. In § 1. 3 we have seen that the conservation of angular momentum forbids the decay of a spin 1 particle into two photons, therefore we conclude that the π^0-meson has spin 0. But the quantitative theoretical results, based on the graph Fig. 2, are not so attractive. Calculations were first made by FINKELSTEIN [1947] for *Pp* mesons, who found a lifetime of 10^{-16} sec. TANIKAWA [1947] using damping theory found 10^{-24} sec. and FUKUDA *et al.* [1949b] showed that some terms were not gauge invariant, and proposed to suppress them. The use of the regularization procedure is very necessary in this case, but the results are ambiguous. FUKUDA and MIYAMOTO [1949a] and STEINBERGER [1949b] have made independent calculations; both give alternative values and they are not completely comparable. Steinberger's results, with the values of M and $\varkappa'$ given in Table 1, give for *Ss* and *Pp* mesons: $\tau_s = f_s^{-2}\,10^{-14}$ sec., $\tau_p = f_p^{-2}\cdot 4\,10^{-15}$ sec.; in both τ is proportional to $\varkappa'^{-3}$. For the pseudoscalar meson τ is too small; however it is not known if the equivalence theorem applies in this case, and the author gives another alternative for *Pa* coupling, where τ is proportional to $\varkappa'^{-7}$ and $\tau\cdot(2Mf'/\varkappa')^2 = 2\,10^{-11}$ sec. One dare not argue from these results concerning the nature of the π^0-meson, (except that *Sv* cannot decay into two photons, being forbidden by Furry's theorem).

There is a possibility of deciding the nature of π^0-mesons which is based only on fundamental laws (parity conservation): for a scalar meson, the two secondary photons will always be polarized in parallel planes, while for a pseudoscalar meson the planes of polarization of the two secondary photons will always be perpendicular. This can be tested by experiment, and YANG [1950b] has proposed to study the angular distribution of pairs produced by these two photons in order to determine the parity (even for S, odd for P) of the π^0-meson.

We shall resume this discussion in § 2. 4, after examining evidence about the nature of the $\pi^{\pm}$-meson.

2. 3 The nature of the $\pi^{\pm}$-meson

The reaction $\pi^- + p^+ \rightarrow n + \gamma$ shows that the π^--meson is a boson. It was pointed out by WENTZEL [1949] that $\pi^{\pm}$-mesons produced in the Berkeley cyclotron might show a polarization effect for star production or for decay into μ-mesons if they have spin 1. Theoretical calculations by FEER [1949b] have been made on the polarization of mesons produced by photons at the energy threshold; here too polarization effects would give information on the nature of the coupling π-meson to nucleon. Anisotropic effects do not seem to have been observed either for artificially produced mesons or for cosmic ray mesons (the latter, however, are probably irrelevant, since polarization effects decrease as energy increases).

An interesting phenomenon for deciding the spin of π-mesons seems to be their production by photons on nucleons. Experiments were first reported by McMILLAN *et al.* [1949a, b]: in the laboratory system, meson production by a dE/E photon energy spectrum (Bremsstrahlung photons) is nearly isotropic between 45° and 135°, and the total cross-section decreases slightly with increasing meson energy. BRUECKNER [1950a] showed from semi-classical arguments as well as from perturbation theory (lowest order) that the experimental distribution is in agreement with calculation for A or P mesons; furthermore a very characteristic feature of spin 1 mesons is the rapid increase of their production cross-section with energy, and thus the properties of a spin 1 $\pi^{\pm}$-meson seem to be incompatible with the experimental data. The ratio of π^-/π^+ production (about 1. 7 in the reported experiments) is also more in favour of a P meson than an S meson (see also ARAKI [1950] and BENOIST-GUEUTAL *et al.* [1950] for this last point). FERRETTI and GALLONE [1950] have proposed the study of the low energy scattering of π-mesons by deuterium as compared with scattering by hydrogen in order to decide the parity of spin 0 mesons. A more decisive experiment, however, is possible. WIGHTMAN [1950] has shown that π^--mesons moderated in hydrogen or deuterium fall into the K-orbit before decaying or being captured, and this has been verified by experiment. Then the capture of a meson by deuterium giving two neutrons:

$$\pi^- + D^+ \rightarrow n + n \tag{14}$$

will be very different for S and P mesons, because of the parity conservation law. If p is the parity of the meson at rest, the parity of the system $D^+ + \pi^-$ (in the K-orbit) is p, since D is even and L the orbital momentum $= 0$; the total angular momentum is therefore $J = 1$ (deuteron spin), and the final state which is formed of two neutrons must also have $J = 1$. According to the exclusion principle this state is odd, and the initial state must therefore also be odd [9], i.e. p is odd, and the meson cannot be scalar if (14) takes place.

The absorption of π^- by deuterium has been observed at Berkeley (Aamodt *et al.* [1950]): among the three possible reactions (14), (15), (16):

$$\pi^- + D^+ \rightarrow n + n + \gamma \tag{15}$$

$$\pi^- + D^+ \rightarrow n + n + \pi^0 \tag{16}$$

(16) does not occur to the limits of experimental accuracy, (15) has been observed directly while (14) has not been observed directly. However, the existence of (14) can be deduced by subtraction, and the branching ratio (14)/(15) calculated in this way is about 2. The most extensive theoretical comparative study of these reactions has been made by Tamor and Marshak [1950]; results depend chiefly on the parity and spin of the meson, and not on more subtle points of meson theories. For S and V mesons the ratio (14)/(15) is respectively 0 and 55, and these two possibilities can be confidently excluded. Only in the case when π^- has spin 0 and the same parity as π^0 is (16) very improbable ((16)/(14) about 10^{-4}), in the other cases: π^- spin 1, or π^- spin 0 while π^- and π^0 of opposite parities, the occurrence of (16) is comparable to that of (15). Therefore, although the existence of an A π^--meson is not strictly impossible, these experiments are strongly in favour of π^- and π^0 both pseudoscalar. Moreover, in this case the equivalence theorem does not apply, and pure Pa and pure Pp coupling give respectively for the ratio (14)/(15), the values 2.1 and 4.1; the second of these seems therefore to be ruled out.

---

[9] A similar argument shows that the existence of the reaction $p^+ + p^+ \rightarrow D^+ + \pi^+$ (see Peterson [1950]), if it is confirmed at the threshold of energy, would be unfavourable to the hypothesis of a scalar π^+-meson. On the other hand, the observation of the angular distribution of the products would give an indication of the spin of the meson, Prentki [1951].

According to recent calculations by CHESTON [1951] the absorption of a π^+-meson by deuterium at sufficiently high energy (25 MeV.) will give $\pi^+ + D^+ \rightarrow 2p^+$ with a not too small cross-section (of the order 10^{-25} cm^2), and the observation of the ratio of the intensities of secondary protons at 90° and 180° (centre of mass system) would lead to a definite conclusion for the spin of the meson, and, in the case of spin 0, for its parity.

2. 4 Are $\pi^\pm$ and π° mesons symmetrical pseudoscalar mesons?

The existence of the reaction: $p^+ + \pi^-$ (in K-orbit) $\rightarrow n + \pi^0$ also shows that if π^- has spin 0, π^- and π^0 have the same parity (application of parity conservation only).

Summing up the discussion, we have seen that:

π^0 has spin 0 (decay into two photons),

π^- cannot be S or V or, very probably, A (absorption by deuterium),

$\pi^\pm$ cannot have spin 1 (slightly decreasing cross-section of meson production by photons with energy).

We therefore conclude that $\pi^\pm$ is probably pseudoscalar, and it is then implied that π^0 is also pseudoscalar. (Several other arguments support the same conclusion.) Then, as we have seen in § 2. 1, the charge independence of nuclear forces requires a symmetrical set of $\pi^\pm$, π^0 mesons.

The comparable production of charged and neutral mesons by nucleon-nucleon collisions in accelerators (CRANDALL *et al.* [1950]) and in cosmic rays (CARLSON *et al.* [1950] give for the production ratio in large stars $N(\pi^0)/N(\pi^\pm) = 0.45 \pm 0.10$) shows that the coupling strengths of charged and neutral mesons are comparable. However, there is one case in which this ratio of production would be expected to be small (about $\varkappa'^2/M^2$) according to the theory: this is meson production by photons on nuclei. But the ratio has been found experimentally to be about 1 for Bremsstrahlung photons from the 320 MeV. accelerator (STEINBERGER *et al.* [1950], STELLER and PANOFSKY [1951]). This experimental result has been discussed by BRUECKNER and WATSON [1950b]. We have already seen how important the contribution of higher terms in symmetrical pseudoscalar meson theory can be for nuclear forces (§ 2. 1); by a consideration of higher order effects for meson production by photons, Brueckner and Watson have shown that pseudoscalar theory (and this theory only, among symmetrical theories) is not necessarily incompatible with experiments.

There is an experiment which, besides a precise determination of the mass $\varkappa'$ of the neutral π-meson, can give more information on its coupling constants; this is the capture of π^--mesons in hydrogen, which has been examined by PANOFSKY *et al.* [1950a, b] at Berkeley. The following reactions have been observed:

(17) $\pi^- + p^+ \rightarrow n + \gamma$

(18) $\pi^- + p^+ \rightarrow n + \pi^0$ (and $\pi^0 \rightarrow 2\gamma$).

From equation (18), it has been found that $\varkappa - \varkappa' = 10.6 \pm 2.0$. The study of these reactions has been carried out by MARSHAK and WIGHTMAN [1949b] (there are several errors, however), OGAWA and YAMADA [1950b] (for spin 0 mesons only), and more extensively by MARSHAK *et al.* [1950]. The branching ratio (18)/(17), observed to be 0.96 ± 0.20, is a function of either f_3 or f_0 (see § 1. 8) of the neutral meson. However the authors have not made calculations for the case of pseudoscalar symmetrical theory. The more refined calculations of AIDZU *et al.* [1950] give for pure *Pp* coupling (symmetrical theory) $f_p^2 = 2.8$ (we have seen in § 2. 1 that nuclear forces give f_p^2 = about 4). The equivalence theorem does not hold in this case. A promising way for deciding between *Pa* and *Pp* coupling is to study the dependence of the cross-section of the π-meson reactions in hydrogen with energy; this was proposed by ASHKIN *et al.* [1950].

What is the value of pseudoscalar symmetrical theory for explaining nuclear forces? For n — p and p — p scattering above 50 MeV., meson theories have not yet explained the experimental data, and this is not surprising if π-mesons are pseudoscalar. In pseudoscalar theory, as we have already stated (§§ 2. 1 and 2. 4), higher order corrections are very large, and it is probably illusory to expect more detailed quantitative results from the weak coupling perturbation method; it is necessary to look for more appropriate methods in meson field theories for relativistic calculations. One may hope that the great importance of the higher order terms of the perturbation theory is directly related to "multiple" meson production in nucleon-nucleon collisions, which received strong experimental support in 1950 from particular stars observed in photographic emulsions, and which can be studied by more phenomenological methods (LEWIS *et al.* [1948], HEISENBERG, FERMI).

2. 5 Neutral V-mesons

The existence of a neutral particle heavier than the π-meson was first reported by ROCHESTER and BUTLER [1947]. Now its existence is well established: the particles are observed, chiefly in cosmic ray penetrating showers, by recognition of the two charged products of decay, which appear as V-shaped tracks in the cloud chamber. For a survey of the status of experimental investigations on these particles and their decay products, we refer to the article by BUTLER in this volume. We observe, however, that it is probably not at present possible to identify the meson secondaries certainly as π-mesons or as μ-mesons. On account of the origin of the V-particles in nuclear events, and their relatively great abundance, it is unlikely (and probably incompatible with the observed smallness of the interaction between μ-mesons and nucleons), however, that μ-mesons are a product of decay of these particles.
V'^0. We shall label V' the particle which would decay according to:

$$V'^0 \to p^+ + \pi^-. \tag{19}$$

V'^0 would have half integral spin, and can be considered as an unstable state of the neutron comparable to those predicted in strong coupling theories (see, for instance, ROSENFELD [1948a] p. 19), or in a theory of particles of several possible rest-masses.
V^0. We similarly denote by V the particle which would decay according to:

$$V^0 \to \pi^+ + \pi^-. \tag{20}$$

The most likely hypothesis is to consider V^0 as a nuclear meson decaying through its nuclear coupling. To explain such a reaction in a coherent way, we must show that other likely reactions due to the same hypothetical coupling are not more probable: these reactions could, very probably, only be decays into two particles:

$$V^0 \to 2\gamma \tag{21}$$

$$V^0 \to 2\pi^0 \tag{22}$$

$$V^0 \to \gamma + \pi^0 \tag{23}$$

$$\text{and even } V^0 \to \varepsilon^- + \varepsilon^+. \tag{24}$$

The conservation laws (§ 1. 3) and Furry's theorem (§ 1. 9) can then give very interesting results: these results are independent of the nature of $\pi^{\pm}$ and of a spin 0 π^0-meson, since (with the restriction only that they do not have both *Ss* and *Sv*, *Aa* and *At* or f_3 and f_0 couplings, see § 1. 9) $\pi^+ + \pi^-$ or $2\pi^0$ introduce an even number of *v*, *t*, and f_3 couplings. Furry's theorem (T2) does not give any selection rules for equation (20) but gives the nature of the coupling of V° (f_3 or f_0); then T3 gives selection rules for equation (22). A summary of the results is given in Table 2.

TABLE 2

Nature of V°	*Ss*	*Sv*	*Vv*	*Vt*	*At*	*Aa*	*Pa*	*Pp*	
(21) $V^0 \rightarrow 2\gamma$	.	T1	A	A	A	A	.	.	
(22) $V^0 \rightarrow 2\pi^0$	.	T3	A	A	A	A	P	P	
(23) $V^0 \rightarrow \gamma + \pi^0$	A	A	.	.	.	T1	A	A	
(24) $V^0 \rightarrow \varepsilon^+ + \varepsilon^-$	T1	?	.	.	.	T1	T1	T1	
(20) $V^0 \rightarrow \pi^+ + \pi^-$	.	?	.	.	P	P	P	P	(spin 0 $\pi^{\pm}$)
	.	?	.	.	.	.	.	.	(spin 1 $\pi^{\pm}$)
Coupling of V°	f_0	f_3	f_3	f_3	f_3	f_0	f_0	f_0	(by T2)

A forbidden by angular momentum conservation
P ,, ,, parity conservation
T ,, ,, Furry's theorem T1, T2, or T3
? ,, in lowest order if equivalence theorem is valid
Order of application: A, P, T and ?.

We see in Table 2 that if $\pi^{\pm}$ had spin 1 and V° were an Aa meson, only reaction (20) would be allowed and all the others would be forbidden. However, we have concluded in § 2. 4 that $\pi^{\pm}$ is probably pseudoscalar. We are then left with two possibilities: V° is either *S* or *V*.

V° *scalar*. The coupling *Sv* forbids (21), (22), (23) and is acceptable. (This coupling is never very attractive to theoretical physicists, because it does not contribute to nuclear forces in the lowest order). The coupling Ss allows decay into 2γ or $2\pi^\circ$. The second decay gives no difficulty, the lifetime for the processes (20) and (22) being roughly equal and twice the apparent lifetime of V°, but we know from the observations on the π°-meson that the decay of a neutral nuclear meson into two photons is very rapid. Even if all charged particles in penetrating showers were $\pi^{\pm}$-mesons, the relative abundance V°/π° is $\geqslant 0.06$; hence, if *F* is the nuclear coupling constant of V°, neglecting the difference of mass of V° and π° (the heavier mesons would be relatively more difficult to produce), we have $F^2/f^2 \geqslant 0.06$. On the other hand, a heavy meson decays more easily into two photons than a lighter meson with the same coupling (in § 2. 2 we have seen that for an *Ss* meson τ is proportional to $\varkappa'^{-3}$); even neglecting this, we find for the two photon decays $\tau_V < \tau_\pi(1/0.06) = 16\ \tau_\pi$, thus there is a difficulty with this hypothesis, since experimentally τ_V is already about 10^4 times larger than τ_π.

V° *vector*. The reaction (23) is also very rapid. We are obliged, for studying this question to rely on quantitative predictions of the theory, but it seems better to draw no conclusions! With the new methods, extensive calculations for all reactions have been made by FUKUDA *et al.* [1950a, b, d] and by ONEDA, OZAKI, SASAKI (see OZAKI *et al.* [1949], ONEDA *et al.* [1950], SASAKI *et al.* [1950] and OZAKI [1950]). The reaction (23) has also been studied by FINKELSTEIN [1947], who gives a lifetime 10^{-18} sec., and by VAN WYCK [1949] for charged mesons (his result corresponds, for neutral mesons, to a lifetime $4.\ 10^{-16}/F^2 f^2$ sec.). We can say from these calculations that (20) is more probable than (23), at least for *V* V°-mesons and *Pp* π°-mesons, but its calculated mean life is too small. The best conclusions from the very interesting and extensive calculations of the Japanese physicists are to be drawn on the value of regularization; many results were divergent and they applied regularization, in some cases the divergence is reduced to zero instead of a finite result and the reaction is forbidden (in this order), in other cases the procedure gives ambiguous results. Moreover, if the regularization procedure is applied to all cases (divergent or finite) it also modifies finite results and leads to more ambiguity. Reaction (24) has been studied by FUKUDA and MIYAMOTO [1949d] and by STEINBERGER [1949b]; it is relatively slower.

Summing up, if reaction (20) is observed with the lifetime 10^{-10} sec., it favours V° being *Sv*, f_3 or *V*(*t* or even *v*), f_3 or even, but much less likely, *Ss*, f_0.

2. 6 Heavier charged mesons, V and τ

The existence of heavier charged mesons has been reported for several years, the first by LEPRINCE–RINGUET and L'HÉRITIER [1944] who measured a meson mass about 1000. Now there is considerable experimental evidence; however these particles appear in three different kinds of phenomena, and for each the experimental data is very scarce. Here is a summary of the data, (for details, see the paper by BUTLER in this volume).

1st kind of events: one charged secondary of decay, observed in the same conditions as V°. We have still less knowledge of $V^{\pm}$ than of V°. The lifetime of the charged particle is probably rather shorter than that of the neutral particle (SERIFF *et al.* [1950]); the charged secondary is probably a π-meson, and mass of about 1000 or 1200 would be consistent with two particle decay.

2nd kind of events: a charged meson at low energy produces a star in a photographic emulsion, among the prongs is a π-meson. The mass of the initial meson is accordingly intermediate between M and $\varkappa$, and is estimated by the authors reporting the three recorded examples (LEPRINCE–RINGUET [1949], WAGNER and COOPER [1949], FORSTER [1950]) to be greater than 700.

3rd kind of events: decay into three charged particles. One case reported by BROWN *et al.* [1949], two by HARDING [1950]. Among the secondaries there is certainly one π^--meson, and the other two particles are probably π-mesons also. If this is so, the kinetic energies of secondaries are measurable in two cases, and an accurate value of mass of the primary follows: about 940 (using $\varkappa = 271$). From the energy and range of the initial particle (3 mm in the event observed at Bristol), the mean life cannot be shorter than about 10^{-11} sec.

The heavy mesons responsible for the second and third kind of events are usually described as τ mesons. The similarity of the first kind of events with the observations on neutral V′-mesons of course suggest the reaction

$$V'^{+} \rightarrow n + \pi^{+}, \tag{25}$$

V'^{+} being an excited state of the proton; since there are some negative V′ particles antinucleons must also be introduced. However, this hypothesis is unable to explain events in the other two categories, while all three kinds of events suggest that $V^{\pm}$ may be a nuclear meson. Is it possible to explain these different events in a single scheme? The hypothesis of the reaction

$$V^{\pm} \to \pi^{\pm} + \pi^{\circ} \tag{26}$$

would lead to difficulties, since then the reaction

$$V^{\pm} \to \pi^{\pm} + \pi^{\pm} + \pi^{\mp} \tag{27}$$

involving one more meson would be less probable and not observed. The existence of (27) implies the existence also of

$$V^{\pm} \to \pi^{\pm} + 2\pi^{\circ} \tag{28}$$

which can be used to explain events of the first kind. Since it is understandable that decays with only one charged particle may be missed or not identified in photographic emulsions (and some observations have been reported which could be interpreted as (28)), it would be noteworthy if events (28) had been identified in the cloud chamber without the detection of reaction (27), which would be equally probable.

However, the Manchester group (ARMENTEROS *et al.*, reported by BLACKETT at the Harwell conference 1950) has obtained one cloud chamber picture suggesting

$$V^{\pm} \to V^{\circ} + \pi^{\pm} \tag{29}$$

while BRODE stated at the same conference that he also had obtained evidence supporting this reaction. It is then conceivable to identify the three kinds of $V^{\pm}$ decay as due ot the same particle, if (26) is forbidden while (27), (28) and (29) are allowed. Furry's theorem gives this result with the restriction only that $\pi^{\pm}$ and π° form a symmetrical theory (see § 1. 8).

Table 3 is drawn up with the supplementary hypothesis that π-mesons are pseudoscalar (§ 2. 4). It shows that if we accept (27) for $V^{\pm}$, this meson cannot decay into two particles according to (26) but only according to (29). It shows that the $V^{\pm}$ meson must be either a P (pseudoscalar) or an Aa meson. If it is P, the reaction

$$V^{\pm} \to \pi^{\pm} + \gamma \tag{30}$$

is forbidden. One can expect that (since $V^{\pm}$ is probably less strongly coupled with nucleons than π), (27) is only a little slower than (29) and so the three kinds of event could be attributed to the same particle. Calculations have been carried out for the

TABLE 3

Nature of V	*Ss*	*Sv*	*Vv*	*Vt*	*At*	*Aa*	*Pa*	*Pp*
(26) $V^{\pm} \to \pi^{\pm} + \pi^0$	T2	.	.	.	P	P	P	P
(29) $V^{\pm} \to V^0 + \pi^{\pm}$	P	P	T2*	T2*	T2	.	.	.
(27) $V^{\pm} \to \pi^{\pm} + \pi^{\pm} + \pi^{\mp}$	P	P	T2	T2	T2	.	.	.
(28) $V^{\pm} \to \pi^{\pm} + 2\pi^0$								
(30) $V^{\pm} \to \pi^{\pm} + \gamma$	A	A	.	.	.	.	A	A

A forbidden by angular momentum conservation,
P forbidden by parity conservation,
T2 forbidden by Furry's theorem; T2* also forbidden by parity conservation if V is scalar.

reactions of Table 3 by Power [1949] (*P* mesons only), Fukuda *et al.* [1950b, c, d], Oneda *et al.* [1950] and Ozaki [1950]; since the calculations are divergent they require regularization and all authors find coherent values which can agree with experiment (10^{-10} to 10^{-11} sec.) for the lifetime of (27); the decay (30) into a meson and a photon is very rapid when it is allowed (see § 2. 5 and also Power [1949] and Fukuda and Miyamoto [1950d]), and this rules out the possibility $V^{\pm}$ pseudovector. But when $V^{\pm}$ is pseudoscalar, even the reaction

$$V^{\pm} \to \pi^{\pm} + 2\gamma \tag{31}$$

would be a little more rapid than (28): by a factor 2 according to Power [1949] (see also van Wyck [1950a]). As we have seen in § 2. 5, there are important difficulties for V° decay (and also for (29)) if these calculations using regularization are taken too seriously. There is another difficulty: the τ-meson of the third kind of event appears to have a mass about 950, which gives for V° and $V^{\pm}$ smaller mass values than those commonly reported.

Summing up, we can say that the hypothesis of a charged *P* (or even *Aa*) meson of mass about 1000 is not ruled out for explaining *all* experimental data, up to now, on heavy charged mesons. There are also arguments for the existence of nuclear mesons heavier than π-mesons from the study of nuclear forces[10]; however, relativistic calculations on neutron-proton scattering (MICHEL, 1950, unpublished) at the second order of perturbation show that a mixture of scalar or vector (Vv) V°-meson and of pseudovector (Aa), or pseudoscalar $V^{\pm}$-meson (according to the results of §§ 2. 5 and 2. 6, but with more arbitrary masses) and of symmetrical pseudoscalar π-meson cannot fit the experimental data on n — p scattering at 90 MeV (see also MARTY and PRENTKI [1950a], MARTY [1950b]), but it must be remembered that even relativistic calculations are not reliable at the second order for pseudoscalar meson theory.

3. INTERACTION BETWEEN FOUR FERMIONS

3. 1 The neutrino

The existence of the neutrino was postulated by PAULI to preserve the existence of the conservation laws (momentum, energy and angular momentum) in β-decay. Up to now the neutrino has escaped detection, i.e. no neutrino induced effects have been observed[11]. It is possible to make an energy-momentum balance for a few β-activities (see CRANE [1948] for a review of the search for the neutrino): the (not yet very precise) experimental relations between the missing momentum and energy can be satisfactorily explained by the emission of a zero rest mass particle, which is called neutrino. Angular momentum conservation requires for it spin $\frac{1}{2}$.

When a π-meson decays into a μ-meson, some energy and momentum are also missing; this can be satisfactorily explained by the simultaneous emission of a zero rest mass particle.

---

[10] For instance, the range of nuclear forces at low energy corresponds to a heavier mass (about 330) than those of $\pi^{\pm}$ and π^{0} mesons, and this may point to a contribution of heavier mesons with attractive sign (ROSENFELD at the Harwell Conference). From high energy data, JASTROW [1951] has proposed the existence of a short range repulsive core in the nuclear potential, which also could be an effect of heavier mesons. Unhappily, these arguments are contradictory!

[11] Cross-sections for neutrino induced β-decay are of the order 10^{-44} cm^2. However, it is possible that such an effect will in time be detected with the always increasing sources of neutrinos constituted by the large piles (PONTECORVO, lecture at Manchester, 1949).

O'CEALLAIGH [1950] has searched for effects induced by this particle along its path and has shown that it cannot be a photon.

When a μ-meson decays to one electron, the lacking energy and momentum cannot be explained by the simultaneous emission of one particle, since the secondary electrons of μ-decay at rest have a continuous spectrum of energy between 0 and 55 Mev. (see LEIGHTON *et al.* [1949], LAGARRIGUE and PEYROU [1951] and also for qualitative work STEINBERGER [1948, 1949a] and DAVIES *et al.* [1949]). On the other hand, when the electron is emitted with maximum energy, the particle (or particles) capable of carrying away the missing energy and momentum must have negligible rest mass (or rest masses). Therefore μ-meson decay can be coherently explained by the emission of an electron and two zero rest mass particles. The nature of these particles has been investigated by several physicists, and the work of HINCKS and PONTECORVO [1950] has shown that they are not photons (observed photons are shown to be created by Bremsstrahlung of the electrons).

Since, in these three decays the emission of neutral particles with zero rest mass "characterized" by the absence of detectable effects is assumed, the simple hypothesis is that they are in each case the same particle, the already named neutrino. This assumption implies that the μ-meson is a fermion like the electron, and that the π-meson is a boson, in agreement with the other experiments on π-mesons (§ 2. 3) and on μ-mesons (CHRISTY and KUSAKA [1941]).

We have seen in § 1. 2 that there are two theoretical possibilities for spin $\frac{1}{2}$ neutral particles: they can be described either with two "charge conjugate" states or with only one (Majorana particle). The existence of a magnetic moment for the neutrino would eliminate the second possibility. The experiment of NAHMIAS [1935], according to BETHE's [1935] calculations, gives for the neutrino magnetic moment an upper limit of 1/5600 Bohr magneton (see also BARRETT [1950] who gives a smaller cross-section for neutrino interaction with atomic electrons, but for less energetic neutrinos). We have seen (§ 1. 4) that if the neutrino is a Majorana particle, double β-decay is possible without the emission of neutrinos (Fig. 4). This was first pointed out by FURRY [1939], who also showed that the double β-decay without the emission of neutrinos is about 10^{10} times more rapid than the other possibility (Fig. 3).

FIREMAN's [1949] experiment was in favour of the rapid process (Fig. 4), but all other more recent experiments do not support it (INGHRAM and REYNOLDS [1949, 1950], LEVINE *et al.* [1950], LAWSON [1951]). Except for μ-meson decay, in all the following there is theoretically no possible distinction between the two alternatives; reactions will be written without distinguishing the two possible states of the neutrino.

3. 2 μ-meson decay

It can easily be shown that:

$$\mu^{\pm} \rightarrow \varepsilon^{\pm} + \nu + \nu \tag{32}$$

cannot be implied by the existence of any known reaction. This will appear very clearly in § 4. The indirect coupling (μ, ν)—π—(ε, ν) would probably be the most rapid; calculations can be made from our knowledge of the lifetime of the π-meson for the two spontaneous decays:

$$\pi^{\pm} \rightarrow \mu^{\pm} + \nu \tag{33}$$

$$\pi^{\pm} \rightarrow \varepsilon^{\pm} + \nu. \tag{34}$$

Measurements of the lifetime $\tau_{\pi\mu}$ of equation (33) have been made by RICHARDSON [1948] $0.89 < \tau < 1.42$; MARTINELLI and PANOFSKY [1950] $1.80 < \tau < 2.13$; KRAUSHAAR *et al.* [1950] $1.32 < \tau < 1.98$; CHAMBERLAIN *et al.* [1950] $2.47 < \tau < 2.77$ (values given in units 10^{-8} sec.)[12]. The decay (34) has not yet been observed, and so a lower value of its mean life can be given, $\tau_{\pi\varepsilon} > 10^{-6}$ sec. (according to the results of FRIEDMAN and RAINWATER [1951], see also POWELL [1950]). Therefore the lifetime of the μ-meson for decay (32) through a virtual π-meson would be much too great (to be measured in months!). We are thus led to the hypothesis of a direct coupling between the four fermions μ, ε, ν, ν. We have seen in § 1. 5 that the most general (used) coupling is a linear combination of five terms $g_i J_i$. Calculations have been made for some particular couplings by TIOMNO *et al.* [1949a] and for the general coupling by MICHEL [1949][13].

---

[12] Authors seem to consider only statistical errors, and to neglect possible systematic errors.

[13] In both papers the effect of the acceleration of the electric charge,

Michel's results are as follows: if E is the energy of the electron, $1 \leqslant E \leqslant W = (\mu^2 + 1)/2\mu$, the energy spectrum is given, (omitting negligible terms), by

$$P(E) = (1/24\,\pi^3)\mu E(E^2 - 1)^{\frac{1}{2}}(WQ_1 - EQ_2) \tag{35}$$

where Q_1 and Q_2 are two quadratic forms of the g. The mean life of the meson is $\tau_\mu = 2.15 \pm 0.07 \times 10^{-6}$ sec. (CONVERSI and PICCIONI [1946]), and gives the condition:

$$\int_1^W P(E)dE = 1/\tau_\mu. \tag{36}$$

If we suppose that only one g is $\neq 0$, this condition gives its value, of the order 10^{-12} (or 10^{-49} erg. cm^3); this is also the magnitude of the Fermi constant, as was pointed out by KLEIN [1948]. We shall study this interesting fact in § 3. 3. For the comparison of equation (35) with experimental data, (36) gives the scale of each theoretically possible curve. It is easy to see that (36) imposes a linear condition between Q_1 and Q_2, and therefore the whole family of theoretical curves depends only on a linear parameter ϱ (a function of the g_i); all the curves pass through a single point (at $E = 3W/4$) and sweep a certain area when ϱ takes all possible values. The agreement with experimental data is very satisfactory (see MICHEL [1950a] and LAGARRIGUE and PEYROU [1951]), the experimental curves of Leighton *et al.* and Lagarrigue and Peyrou pass through the imposed point and are shaped like the theoretical curves. Of course, other hypotheses can fit the experimental data, (see TIOMNO [1949c] where the μ-meson is assigned spin 0 and a new spin 0 neutral particle is introduced), but the hypothesis studied here is the simplest, for it does not involve any new particle, and it assumes the simplest possible coupling.

Now we have to distinguish between two cases: (i) the two emitted neutrinos in μ-meson decay are distinguishable (one "neutrino" and one "antineutrino" are emitted, probably with opposite magnetic moment); (ii) the two emitted neutrinos are

---

carried successively by the meson and by the electron, has been neglected. This will probably lead to the emission of a photon with energy a few per cent of the electron energy, according to the preliminary results of ABRAGHAM and HOROWITZ [1951], and is negligible for the following discussion (compare FEER [1949a] who makes calculations for a two particle decay of the μ-meson, or HANAWA and MIYAZIMA [1950] for $\pi - \mu$ decay).

identical and must satisfy the Pauli exclusion principle. From the remark in the last paragraph of § 1. 5, we know that in case (ii) there are only three independent J_i (when the order $\mu, \varepsilon, \nu, \nu$ is chosen for the wave functions in the J_i, equation (4) shows that $J_2 = J_3 = 0$), and in this case the area swept by all possible curves is smaller than, and included within, the area for case (i). If the experimental curves had been in the part of the area (i) outside the area (ii), it would have proved that there are two (charge conjugate) states of the neutrino, but this is not the case, and the experimental curve certainly lies in the common area.

Knowledge of the spectrum gives the value of the linear parameter, ϱ, i.e. a quadratic relation between the g. This is important only if other restricting hypotheses are made, as in § 3. 3.

3. 3 The radioactivity of the neutron

The fact that the same coupling constant could explain both β-radioactivity and μ-meson decay is attractive. When meson theory was developed, and the (wrong) meson and its instability discovered in cosmic rays, β-radioactivity was explained through a virtual meson (see Fig. 1), and the (earlier) direct coupling went out of fashion. However in the present state of affairs there are difficulties in describing β-radioactivity through intermediary virtual nuclear mesons (see § 4. 3), and on the other hand we have seen in § 3. 2 strong arguments for a direct coupling between $\mu, \varepsilon, \nu, \nu$, in order to explain μ-meson decay. The similarity of the coupling strength with that of β-radioactivity invites a closer comparison between these two phenomena.

The study of β-radioactivity is not quantitatively simple because n and p are not free particles but are bound in the initial and final nuclei, except in the case of neutron decay. The large production of neutrons in piles has now made a study of the radioactivity of the neutron possible (SNELL *et al.* [1950], ROBSON [1950, 1951]).

We shall therefore directly compare the decay (32) with

$$(37) \qquad \mathrm{n} \rightarrow \mathrm{p}^{+} + \varepsilon^{-} + \nu,$$

explaining them by the same coupling $g_i J_i$. From the remark in the last paragraph of § 1. 5, we know that the J_i depend on the order in which the four wave functions are written in these expressions; more precisely, if we do not pay attention to the permutations of this order which change only the sign of the J_i, we have only to specify how the four wave functions are paired with each other by the two operators F_i. For β-radioactivity it is natural to have the two nucleons (n, p) with one operator, and the two leptons (ε, ν) together. Since reaction (32) has a common pair (ε, ν) with reaction (37), we are led to compare the pair (μ, ν) with the nucleons (n, p). Passing from the case n $\leftrightarrow \nu$, p $\leftrightarrow \mu$ to the case n $\leftrightarrow \mu$, p $\leftrightarrow \nu$ changes only the sign either of g_2 and g_3, or of g_1, g_4 and g_5[14].

With this chosen order, a pure g_5 or a pure g_1 interaction for μ-meson decay seems ruled out by experimental data. The next subsection will also be devoted to β-radioactivity, we need at the moment only the two following preliminary results concerning the nature of the interaction.

A pure g_5 (the socalled "pseudoscalar") interaction is ruled out[15]. Because of the low energy of the nucleons, the dependence of the lifetime in β-radioactivity on the g is quite different for g_5 and for the other coupling terms, and for a pure g_5 interaction the lifetime depends chiefly on the change of the kinetic energy of the nucleon during the decay. This variation of kinetic energy is quite irregular among the different nuclei, and it would lead to quite irregular values of "$F\tau$" (for a definition of $F\tau$, see equation (39)). Moreover, this variation is small in the case of the neutron as compared with other nuclei, and a value of g_5 based on the lifetime of some families of nuclei would give a neutron mean life of several days or months (about 10^4 too long).

The neutron decay spectrum, as far as it is known, is of the allowed shape; knowledge of the shape of spectrum for an allowed transition gives a quadratic relation between the g when one uses a linear combination of the five terms $g_i J_i$. This was done first by FIERZ [1937], who found, besides the main term responsible for the shape of the allowed spectrum, the term $\pm(g_1g_2 - 3g_3g_4)/E$, where E is the energy of the electron and $\pm$ refers to $\beta^{\pm}$-decay. This term would seriously modify a part of the allowed spectrum, and would then be in contradiction with experimental data, if it were more than a few per cent of the main term. In the following it will be neglected.

---

[14] Different authors use different conventions for the sign of the J_i, since there are no theoretical reasons for the choice of this sign (and even of the relative phases of the $g_i J_i$ if one does not reject the use of imaginary coupling constants). Therefore comparison of results in different papers sometimes involves a change of sign of some g. Here, the signs of the J_i have been implicitly defined by the notation of § 1. 5.

[15] This was kindly pointed out to me by Dr KOFOED-HANSEN; see also MARSHAK [1949a] footnotes 8 and 11.

With these two remarks on the nature of the coupling, the condition corresponding to equation (36) is, for the case of the neutron:

$$(g_1^2 + g_2^2 + 3g_3^2 + 3g_4^2) = (2\pi)^3/4F\tau_n \tag{38}$$

where F is the integral of the energy distribution, $(1 \leqslant E \leqslant W)$:

$$F(W) = \int E_1^W (E^2 - 1)^{\frac{1}{2}} (W - E)^2 \, dE. \tag{39}$$

We see that for the neutron the product $F\tau$ depends only on the coupling constants. For complex nuclei it also depends on the nuclear matrix element, the product $F\tau$ is therefore the criterion for the classification of nuclei according to their β-decay. (Of course the charge Ze of the nuclei cannot be neglected for not too small Z, then F is a more complicated function of E and Z and is different for β^+ and β^- decays.) In Table 1 we have given $W = 2.53$ and the corresponding value of F is 1.63; (it must be noted that for the neutron F is very sensitive to the value of W, the older value of which, (2.47), gives $F = 1.39$).

For μ-meson decay we saw (§ 3. 2) that two cases must be considered. We now make comparison with these.

(i) *distinguishable neutrinos.* The relation (36) is written

$$g_1^2 + 4g_2^2 + 6g_3^2 + 4g_4^2 + g_5^2 = 6\,(2\pi)^3/(\tfrac{1}{2}\mu)^5\tau_\mu = (2\pi)^3/2280\ \tau_\mu, \tag{40}$$

(it happens to be independent of the order of the particles in the J_i). Among all possible direct couplings there is one remarkable one: it is the determinant made with the four indices of the four wave functions (it is therefore invariant under any permutation of the order of the four particles); it was first proposed by CRITCHFIELD and WIGNER [1941], and in the notation of this paper it is defined by

$$g_1 = -g_4 = g_5 = g_0, \text{ and } g_2 = g_3 = 0. \tag{41}$$

With the value $\tau_\mu \doteq 2.15 \times 10^{-6}$ sec., equation (40) gives $g_0 = 3.3 \times 10^{-12}$ (or 1.5×10^{-49} erg.cm³), and for the mean life of the neutron (from equation (38))

$$\tau_0 = 18.8 \text{ min.} \tag{42}$$

This value is quite acceptable. For the study of the other possible couplings, we define λ by

$$\tau_n = \lambda\tau_0 = 18.8\,\lambda \text{ min.} \tag{43}$$

According to the experiments of SNELL *et al.* [1950], and of ROBSON [1950], the "half-life" τ_n' of the neutron is between 10 and 25 minutes; i.e. the mean life $\tau_n = \tau_n'/\ln 2$ is between 14 and 36 minutes, the corresponding values of λ being $0.75 < \lambda < 1.92$. The experimental determination of λ will give (from equations (38) and (40)) the following quadratic relation between the g:

$$(2 - 3\lambda)g_1^2 + (8 - 3\lambda)g_2^2 + 3(4 - 3\lambda)g_3^2 + (8 - 9\lambda)g_4^2 + 2g_5^2 = 0, \tag{44}$$

(the terms discarded in this formula are less than 3 % of those kept).

(ii) *identical emitted neutrinos.* The values of g_0 and τ_0 are not changed, but equation (44) is replaced by:

$$\left\{\begin{aligned} &\tfrac{3}{4}(1 - 4\lambda)g_1^2 + 3(2 - \lambda)g_2^2 + 9(1 - \lambda)g_3^2 + 3(2 - 3\lambda)g_4^2 + \tfrac{3}{4}g_5^2 \\ &+ g_1(2g_2 - 3g_3 - 2g_4) + 4g_2g_4 + g_5(\tfrac{1}{2}g_1 + 2g_2 + 3g_3 - 2g_4) = 0 \end{aligned}\right. \tag{45}$$

It is remarkable that mean lives differing by a factor 10^9 can be explained by the same coupling. We have then to make assumptions about the nature of the (admitted) direct coupling terms g_iJ_i responsible for the β-decay of nucleons (this is the object of the next subsection), and then test, using equations (35), (36) and (44) or (45), the hypothesis of common coupling between $(\mu, \nu)(\varepsilon, \nu)$ and $(\mathrm{n}, \mathrm{p})(\varepsilon, \nu)$.

3. 4 Nature of the coupling of β-radioactivity

We suppose a direct coupling, and note (§ 3. 3) that:

(46) g_5 cannot be much larger than the other g,

and FIERZ's [1937] term must be small; here we shall assume:

$$g_1g_2 = 0 \qquad g_3g_4 = 0. \tag{47}$$

For complex nuclei Fierz's term is $\pm(A\,g_1g_2 - B\,g_3g_4)$, where A and B are functions of the nuclear matrix elements: since A/B varies with the nuclei, the smallness of Fierz's term implies g_1g_2 and g_3g_4 separately small.

Now we must proceed from the simplest hypothesis: can a single g give a satisfactory interaction? Historically, this question was first raised for the g_2 ("vector") interaction, that proposed by FERMI [1934]. Using the isotopic variable formalism (see § 1. 8), let us write ψ and ψ^* the initial and final states of the nucleon field, and φ and φ^* the corresponding functions of the lepton field. Because of the low velocity of the nucleons, the density of the interaction Hamiltonian reduces to

$$h = g_2J_2 = g_2(\psi^*\psi)(\varphi^*\varphi). \tag{48}$$

For nuclei, ψ^* and ψ differ from zero only inside the nucleus, neglecting the Coulomb field of the nucleus, φ and φ^* are normalized plane waves describing the free leptons. Their wave lengths are much larger than the radius of the nucleus, and so inside the nucleus $\varphi^*\varphi$ is nearly constant and equal to 1. If the nucleus changes its spin and/or its parity during the transition, the initial and final states are orthogonal, and therefore

$$\int h\,dv = g\int\psi^*\psi\,dv = 0. \tag{49}$$

It is easily seen that the g_1J_1 term gives the same result. Therefore β-decay of nuclei is allowed for g_1 or g_2 interaction only if

$$\Delta I = 0,\ \text{no} \tag{50}$$

(I, spin of nucleus, "no" means no change of parity). Even with the same spin and parity, the initial and final states of the nucleus can have quite different structures (change in super multiplet, WIGNER [1939]) then $\int J_2\,dv$ is small compared with unity, these transitions are called "unfavoured allowed". However, for nuclei having the same structure ("mirror" nuclei) this term can have nearly its maximum value.

When equation (49) is satisfied, the main contribution for the transition comes from neglected terms, (a) the term in g_2J_2 proportional to the velocity, which gives a contribution of about 1 % when the main term is $\neq 0$, and (b) the first term of the development of $(\varphi^*\varphi - 1)$, which gives about the same contribution. Terms (a) and (b) give the main contribution to the "first forbidden" transitions, and (a) still gives an allowed shape for the spectrum. If these terms are also equal to zero, one must consider the second term of the exponential ($\varphi^*\varphi-1$) or the product of the first forbidden terms to get the main contribution to the "second forbidden" transitions, and so on . . . (see KONOPINSKI [1943] for a general survey of β-radioactivity).

As we said in § 3. 3, the value of $F\tau$ is the criterion for recognizing the degree in which a transition is forbidden. We have the value of F for the neutron, and therefore for the neutron

$$F\tau_0' = 1275, \tag{51}$$

τ_0 has been defined in equation (42), and since $F\tau'$ the relative half-life is more widely used than $F\tau$ the relative mean life, we recall here that

$$\tau_n' = \lambda\tau_0' = 13\,\lambda \text{ min.} \tag{52}$$

Many nuclei are known with $F\tau'$ of some 10^3. Few spins of nuclei (chiefly of unstable nuclei) and still fewer parities have been determined experimentally, but other theoretical considerations can give this information (shell structure for nuclei has had great success). One of the best established theoretical rules is:

(53) "nuclei with even numbers of both n and p have spin 0"

and these nuclei have even parity.

Several examples are known of "allowed" transitions between nuclei for which we would have expected $\Delta I = 1$. A historic transition is

$$\mathrm{He}^6 \rightarrow \mathrm{Li}^6 + \varepsilon^- + \nu; \tag{54}$$

He^6 has spin 0 according to (53) while Li^6 has spin 1 (measured by MANLEY and MILLMAN [1937]), but $F\tau' = 590$, the smallest value known! (All values of $F\tau'$ given here, except that of the neutron, have been calculated by TRIGG and are given by HORNYAK *et al.* [1950]). This and other transitions led GAMOW and TELLER [1936] to propose, instead of a g_2 interaction, a g_3 or g_4 ("tensor" or "pseudovector") interaction, since the corresponding selection rules for allowed transitions would then be

$$\Delta I = 0 \text{ or } \pm 1 \text{ (except } 0 \leftrightarrow 0\text{), no.} \tag{55}$$

There have, however, been some difficulties, according to theoretical expectations, for these G—T selection rules also. A well known example is

$$(56) \qquad Be^{10} \rightarrow B^{10} + \varepsilon^- + \nu,$$

expected to be very similar to reaction (54), since there is one α-particle more in each nucleus, but here $F\tau' = 7.9 \times 10^{13}$. Spin measurements for B^{10} give 3, and so $\Delta I = 3$. On this basis, MARSHAK [1949a] made a theoretical study of the spectrum of this reaction, and predicted a unique possible shape for the spectrum; this has been well confirmed by experiments (it also necessitates G—T selection rules if the theoretical prediction of even parity for B^{10} is reliable). Other cases of uniquely predicted spectra have also been well verified, notably for the family found since 1949, chiefly among fission products: Y^{91}, Y^{90}, Sr^{89}, Sr^{90}, Sr^{91} ... (see WU [1950] for general survey); this family has β-decay, according to shell structure predictions, $\Delta I = 2$, yes; and this imposes G—T selection rules. Another difficult case is

$$(57) \qquad C^{14} \rightarrow N^{14} + \varepsilon^- + \nu,$$

of the same form as (54) and (56). C^{14}, an even-even nucleus has spin 0 (see (53)) and even parity, the spin of N^{14} has been measured and found $= 1$ while its parity is expected to be even; the transition is therefore expected to be allowed, but $F\tau' = 9.3 \times 10^8$, too high even for an unfavoured allowed transition. (GERJUOY [1951] has proposed measurements of the parity of N^{14} since an odd parity would solve the difficulty; on the other hand, the ground state of N^{14} is a mixture of $^3S_1$ and $^3D_1$; the difficulty would be solved if the contribution of the ^3S part is negligible, for instance, destroyed by interference).

The β-radioactive O^{14} discovered by SHERR *et al.* [1949] is the mirror nucleus of C^{14}. The structures of C^{14} and O^{14} are: an α-particle + all $P_{3/2}$ states filled + a pair of $P_{1/2}$ neutrons (for C^{14}) or of $P_{1/2}$ protons (for O^{14}). The higher energy of O^{14} is due to a larger Coulomb interaction. There is also an excited state of N^{14}, denoted here $^*N^{14}$, which also has the same configuration (α-particle + all $P_{3/2}$ states filled + one $P_{1/2}$ neutron and one $P_{1/2}$ proton), see Fig. 6, and the Coulomb energy calculations fit very well with the data. SHERR *et al.* [1949] found that O^{14} decays to the state $^*N^{14}$, they observed the 2.3 Mev. γ-ray and found for the Fτ' of O^{14} the value 3000, which is normal for an allowed transition between mirror nuclei. The three nuclei C^{14}, $*N^{14}$, O^{14} have spin 0 and the same parity (even), but $0 \leftrightarrow 0$ transitions are forbidden for G—T selection rules (55) and allowed, on the contrary, by the Fermi selection rules (50) (see Hornyak *et al.* [1950]). The transition $O^{14} \rightarrow N^{14}$ (ground state) has not been observed, and this gives for the corresponding Fτ' the value 2.10^6, difficult to explain with G—T selection rules; however, this is not a new difficulty since the expected Fτ' of this reaction must be about 10^9, i.e. the value of the Fτ' for the identical reaction (57).

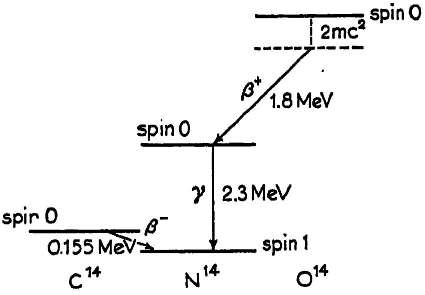

Fig. 6. C^{14}, N^{14}, $*N^{14}$, O^{14} nuclei

Must we admit a mixture of F (Fermi) and G—T selection rules? According to equation (47), the only possible mixtures are: g_1, g_3; g_2, g_3; g_2, g_4; g_1, g_4, and if a third term is assumed it can only be g_5. The necessity of such a mixture has been claimed by Longmire *et al.* [1949] for the reaction

$$Cl^{36} \rightarrow A^{36} + \varepsilon^- + \nu. \tag{58}$$

The spin of Cl^{36} has been measured and found = 2; no γ-rays are observed, and therefore the transition is into the ground state of A^{36} which is expected to have spin 0, according to (53), and even parity. The authors say that no calculated spectra for $\Delta I = 2$, "no" (and even "yes") will fit the experimental curve. They interpret this by a mixture of g_1, g_3; g_2, g_4 or even g_2, g_3 but not g_1, g_4. From the published curves it does not seem to be altogether convincing that a pure g_2 or g_3 coupling is ruled out, but in any case the conclusions, that *either g_2 or g_3 are necessary* and that any mixture of g_1, g_4, g_5 is ruled out, seem well established. More recent study, LANGER and MOFFAT [1951], for the decay of Cs^{137}, expected $\Delta I = 2$, also rules out any combination of g_1, g_4, g_5. A pure g_3 interaction could explain this spectrum, but the decay of O^{14} has ruled out pure G—T selection rules.

There is still another kind of experiment which can give information on the nature of the coupling terms; it is the experiments on the recoil of the nucleus which give information on the angular correlation between the emitted electron and neutrino (BLOCH and MØLLER [1935]). Theoretical calculations have been made by HAMILTON [1947] for allowed and first forbidden transitions on the hypothesis of only one coupling term. The following is the correlation function for neutron decay and for the most general coupling satisfying conditions (46) and (47):

$$(59)\quad \begin{cases} C(\theta) = 1 + av\cos\theta, \\ \text{with } a = (-g_1^2 + g_2^2 + g_3^2 - g_4^2)/(g_1^2 + g_2^2 + 3g_3^2 + 3g_4^2), \end{cases}$$

(θ is the angle between the two leptons, v is the electron velocity in c units). For complex nuclei the corresponding formula is given by equation (50) in DE GROOT and TOLHOEK [1950]. (See also TOLHOEK's thesis for proposed experiments on the polarization of β-rays to give more information on the nature of the interaction). A review of experimental data has been given by CRANE [1948]; experiments are still difficult and the results sometimes contradictory (for example, difficulties arise when the source is on solid material). Recent experiments with a gaseous source, He^6, performed by ALLEN *et al.* [1949] give an a which can be from 0 to $-1/3$ or $-1/2$; a result which seems to be against a mixture of g_2 and g_3. Very recently, systematic calculations of forbidden decays with the general direct coupling (linear combination) have been announced by TRIGG [1951].

Summing up, we see how recent and still inconclusive the experimental data are which allow us to make hypotheses on the nature of the terms of the (direct) coupling responsible for β-radioactivity. To-day, the best hypothesis seems to be a mixture of g_1, g_3 or g_2, g_4 or even perhaps g_2, g_3; but there are still difficulties not overcome by the theory. However, the situation is very promising: better recoil experiments and more precise determinations of the neutron half-life can be expected, more measurements of spin (and even of parity) together with improvements of the shell model will permit fruitful analysis of forbidden spectra; transitions with ΔI equal to the degree of forbiddeness, will give information on the mixture of coupling terms. We can already say that the good experimental agreement with uniquely predicted spectrum shapes for allowed and for some forbidden transitions, and also K-capture lifetimes (not reviewed here) are strong verification of the hypothesis of coupling terms of the form $g_i J_i$ (with the g_i constants and not a function of the energy, as happens for some coupling terms with an intermediate virtual meson as in Fig. 1 scheme). Further, the introduction in the J's of derivatives of the wave functions (as proposed by KONOPINSKI and UHLENBECK [1935] for explaining inaccurate experimental data) are completely ruled out.

3. 5 The capture of μ-mesons by nuclei

We noted in the introduction that μ-meson capture was observed in Pb and Fe, but not in light nuclei. Since this behaviour was unexpected (for nuclear mesons!), many experiments were carried out with various materials from Be to S, by SIGURGEIRSSON and YAMAKAWA [1947, 1949], VALLEY [1947], TICHO [1947a, 1948b, c], NERESON [1948], KISSINGER and COOPER [1948], TICHO and SCHEIN [1947b, 1948a], VALLEY and ROSSI [1948]. It was discovered by the last four authors that while the lifetime of the μ^+-meson was constant, the lifetime of the μ^--meson decreases with increasing Z (charge of nucleus); the quantitative results verified the theoretical predictions of WHEELER [1947] who showed that the μ^--meson first falls into a Bohr orbit of the nucleus and then must be captured without electron emission (see also WHEELER [1949]) with a lifetime of capture $\tau_c \sim Z^{-4}$, giving the μ-meson an apparent mean life:

$$\tau = \left(\frac{1}{\tau_c} + \frac{1}{\tau_\mu}\right)^{-1}. \tag{60}$$

Since τ_μ (for decay into electron) is independent of Z, τ_c can be given by:

$$\tau_c = \tau_\mu (Z_0/Z)^4 \tag{61}$$

where, from experiments, Z_0 has been found to be about 11.

That the μ-meson falls into a Bohr orbit of the nucleus was directly shown by the observation of the photons it emits during its jumps to lower quantum number orbits, CHANG [1949]; (HINCKS [1951] gives, for the total energy of the γ-rays emitted for each meson, about 15 MeV). How is the meson captured from the lowest orbit? No nuclear explosions are observed [16], and this rules out the hypothesis of transfer of all the meson rest energy to the nucleus. We must therefore assume that a light neutral particle is emitted, carrying away most of the available energy (about 90 MeV). No high energy photons have been observed (PICCIONI, [1948]) and it is natural to identify this neutral particle with the neutrino (PONTECORVO, [1947]) as we have already done in three processes (§ 3. 1) where energy (and momentum and also angular momentum) is missing; this hypothesis avoids the introduction of a new particle and it is coherent, since it gives spin 1/2 for the μ-meson.

We have therefore to assume the reaction

$$\mu^- + p^+ \rightarrow n + \nu. \tag{62}$$

Even with the emission of the 0 rest-mass neutrino, the neutron receives a non-negligible energy (about 10 to 20 MeV). Such an excitation of the nucleus has been studied by TIOMNO and WHEELER [1949b] and ROSENBLUTH [1949], who showed that the most probable event is the loss of one neutron or sometimes two. GROETZINGER and MCCLURE [1948], SARD *et al.* [1948, 1949], have detected these neutrons by coincidence methods. More recent experiments give quantitative results for the number of emitted neutrons by captured mesons: 1.90 ± 0.24 (CROUCH, [1951], 1.40 ± 0.30 (CONFORTO and SARD, [1951]).

What is the nature of the coupling responsible for reaction (62)? This reaction can be explained from the two classes of reactions

$$p^+ + \pi^- \rightarrow n \text{ and } \pi^- \rightarrow \mu^- + \nu. \tag{63}$$

by the graph of Fig. 7 (virtual π-meson). The value of the coupling constants f and $\check{f}$ are determined from nuclear forces and from the lifetime of the π-meson; LODGE [1948], PUPPI [1948, 1949], LEE *et al.* [1949], TAKETANI *et al.* [1949] have shown that these values of f and $\check{f}$ give quantitative agreement with the experimental data for the reaction (62). On the other hand, reaction (62) can be attributed to a direct coupling between n, p, μ, ν, and as has been pointed out by these authors, and by TIOMNO and WHEELER [1949b], the necessary coupling strength is about the same as for β-radioactivity (by a direct coupling) and for μ-meson decay: 10^{-12} (i.e. 10^{-49} ergs.cm.^{3}).

---

[16] μ-mesons can produce nuclear disintegrations (EVANS and GEORGE [1949], see also COCCONI and COCCONI–TONGIORGI [1951]) but this is another phenomenon due to the (probably electromagnetic) interaction of the nuclei with fast, instead of bound, μ-mesons.

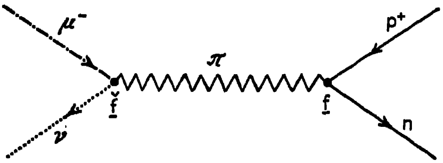

Fig. 7. Graph of $\mu^- + p^+ \rightarrow n + \nu$

3. 6 Universal direct coupling between four fermions?

Is it only fortuitous that a direct coupling with the same strength (within experimental results) can explain β-radioactivity, μ-meson decay and μ-meson capture by nuclei? It is natural to make the hypothesis that the *same* coupling is responsible for the three kinds of phenomena and this has been proposed independently by PUPPI [1948, 1949], LEE *et al.* [1949], TIOMNO and WHEELER [1949b]. Of course, the final decision lies with experiment, and we shall discuss some consequences of this hypothesis in § 4. 1; however, since such a decision is pending we can look for the "meaning" of this hypothesis of the *same* coupling between different kinds of particles.

As we emphasized in § 3. 2, when defining the coupling terms between four fermions we have at least to pair them. The natural pairing established in § 3. 2, i.e. (p, n), (ε, ν) and (μ, ν) is now confirmed by the interaction (p, n)(μ, ν). The situation is illustrated by Fig. 8: between each two of the three pairs of fermions exists the same direct coupling g (g represents the set of the constants g_i of this coupling). This introduces the concept of a correspondence between the different known fermions. Such a correspondence between (μ, ν) and (ε, ν) suggests that μ and ε are two states of the same particle, but the comparison with nucleons is less inspiring!

Another point of view is to admit this interaction as general between any set of four fermions. Since we cannot any longer fix the order of the four wave functions in the coupling terms, we have to choose the only interaction invariant by any permutation of this order, the Critchfield and Wigner [1941] interaction g_0 defined in (41). Moreover, it is of course necessary to give some selection rules forbidding non-observed couplings. Such a proposal has been made by Yang and Tiomno [1950c] by introducing for the different fermion wave functions different transformation laws under space reflexions R (see § 1. 3), ψ is transformed into ψ' with

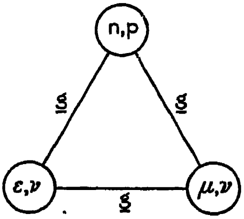

Fig. 8.

$$\psi' = \eta\beta\psi. \tag{64}$$

In the commonly used formalism, $\eta = i$ (or $-i$) and it is the same for all fermions. Here the possible values of: L, —L; i, —i(L = ± 1, according to the charge conjugate state of the particle, has been defined in § 1. 2) are distributed among the different kinds of fermions and then the authors can lay down a fundamental principle: "Between any four fermions, not all of the same kind, there exists a direct coupling g_0, if the product of their four η is 1 and the K (= LM defined in § 1. 2) of fermions of the same kind are equal". (Of course, electric charge must be conserved, i.e. from equation (1) the sum of the K's of charged particles must be = 0.) But as we pointed out in § 1. 6, the law (64) instead of the usual one is equivalent to the introduction of pseudoscalar coupling constants, and since it is not possible for the Yang and Tiomno formulation to have the equivalent of the use of both kinds (scalar and pseudoscalar) of coupling constants for the same coupling, we already know that their formulation does not differ physically (provided the neutrino mass = 0) from the ordinary formalism. The authors have expressed their choice of couplings in a very elegant way (one sentence only) but for that they have sacrificed the natural elegance of the commonly used formalism (for them $\psi^*\beta\psi$ for nucleons can be a scalar, but then $\psi\beta\psi$ is a pseudoscalar, and the formulation of parity conservation becomes more inelegant); and, this being the main point, their interesting proposal does not give a deeper insight into the present theory. From their choice of coupling the authors implicitly assume that the two neutrinos emitted in μ-meson decay are identical, and that the direct coupling responsible for the class of reaction:

$$(65) \qquad \mu^+ + \varepsilon^- \rightarrow \mu^- + \varepsilon^+$$

exists; but neither assumption can be tested by actual experiments (the cross-section of (65) is 10^{-40} cm.^{2} per electron for the observed μ-mesons).

The basic physical test for the existence of a universal interaction between different groups of four fermions is the validity of g_0 (Critchfield–Wigner) interaction. We have indicated (§ 3. 2) the resulting neutron mean life, and have also noted experimental evidence against it in § 3. 4. Further, the experimental energy spectrum of electrons from μ-meson decay (see MICHEL, [1950a], p. 1371, for the comparison of the results of LEIGHTON *et al.* [1949] with the theoretical curve, and the excellent discussion by LAGARRIGUE and PEYROU [1951] of their own data and those of LEIGHTON *et al.*) is not in favour of the g_0 interaction.

4. POSSIBLE COUPLING SCHEMES

4. 1 Coupling scheme (1)

The fact that a single direct coupling between any two of the following pair of fermions (p, n), (μ, ν), (ε, ν) is consistent with all data considered so far is very attractive and its consequences must be studied. Besides this coupling we have the π-meson-nucleon coupling and the not yet studied consequences of the total scheme, the indirect couplings π-(μ, ν) and π-(ε, ν), (see Fig. 9). In this scheme, there is a complete symmetry of coupling when μ and ε are exchanged and it seems that $\pi \rightarrow \varepsilon + \nu$ will in any case be more rapid than $\pi \rightarrow \mu + \nu$. However, calculations have been carried out by STEINBERGER [1949b] (some selection rules are wrong), RUDERMAN and FINKELSTEIN [1949], SASAKI *et al.* [1949] (V and

P π-mesons only) and by Nakamura *et al.* [1950]. Furry's Theorem (T4 in § 1. 9) applies and forbids many possibilities and the equivalence (E) theorem (§ 1. 10) also applies; seven other cases (marked X in Table 4) have matrix elements = 0 (at least for the lowest order). For non-forbidden cases, the results are divergent (logarithmically with the new methods). However, if we consider only one coupling (either f or f', see § 1. 5) for spin 1 mesons and only one term g_i of the two direct coupling terms giving allowed decay (this is not necessary for A π-mesons); the ratio $\tau_{\pi\mu}/\tau_{\pi\varepsilon}$ is of the form

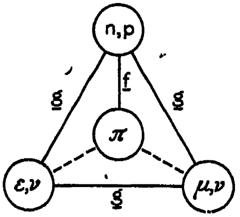

Fig. 9. Coupling scheme (1)
---- indirect coupling.

TABLE 4

$g \backslash \pi$	Ss	Sv	Vv	Vt	At	Aa	Pa	Pp
g_1	5.7	T4	T4	T4	T4	X	X	X
g_2	T4	E	4.4	4.4	X	T4	T4	T4
g_3	T4	E	2.7	2.7	2.4	T4	T4	T4
g_4	X	T4	T4	T4	T4	4.4	1.3×10^{-4}	1.3×10^{-4}
g_5	X	T4	T4	T4	T4	X	5.7	5.7

(66) $$\tau_{\pi\mu}/\tau_{\pi\varepsilon} = \zeta\, \mathfrak{R}/\mathfrak{R},$$

where both $\mathfrak{R}$ represent the same divergent integral. Mathematically (66) is not defined, and, on account of the imperfect state of the theory, theoretical physicists have to apply a procedure to $\mathfrak{R}$ (regularization, cut-off) in order to get a finite result. Then $\tau_{\pi\mu}/\tau_{\pi\varepsilon} = \zeta$ and this is independent of the procedure. Table 4 gives the value of ζ; for a pseudoscalar π-meson and g_4 coupling ζ is very small (10^{-4}). The symmetry of the scheme for μ, ε is therefore no longer a difficulty for a P $\pi^{\pm}$-meson and for any combination of terms containing g_4 (but not g_5) for the direct coupling. But this result is not really quantitative since the calculations give rise to divergences; regularization gives a much too long lifetime (10^{-2} sec.) for $\tau_{\pi\mu}$, and although $\mathfrak{R}$ is only logarithmically divergent, its value is very sensitive to the choice of a cut-off value. A "normal" cut-off value gives the right order of lifetime of about 10^{-8} sec.[17].

We can also see if this coupling scheme is coherent with our conclusions on $V^{\pm}$-mesons (if these heavy mesons are nuclear mesons; no question arises here about V°-mesons). $V^{\pm}$ can decay by the same indirect coupling as $\pi^{\pm}$, into $\mu^{\pm}+\nu$ or $\varepsilon^{\pm}+\nu$. We were left in § 2. 5 with only two possibilities for V:

(a) $V^{\mp}$ is pseudoscalar (*Pp* or *Pa*); $\tau_{\nu\mu}/\tau_{\nu\varepsilon} \sim 10^{-4}$; and (see NAKAMURA *et al.* [1950]),

$$\tau_{V\mu}/\tau_{\pi\mu} = (f^2/F^2)(\varkappa_\pi/\varkappa_V)^3; \tag{67}$$

inserting the estimated values of §§ 2. 4 and 2. 5, $\tau_{V\mu}/\tau_{\pi\mu} = (100/3) \cdot (1/4)^3 \approx \frac{1}{2}$, $\tau_{V\mu}$ is of the order 10^{-8} sec., and the reaction $V^{\pm} \rightarrow \mu^{\pm}+\nu$ cannot be observed instead of reaction (29) which is more rapid.

(b) $V^{\pm}$ is pseudovector (*Aa* coupling); $\tau_{V\mu}$ and $\tau_{V\varepsilon}$ are of the same order of magnitude, but in this case the lifetimes are much longer than for *S* V-mesons, according to Nakamura *et al.*, and from the formula of these authors it is easy to see that there are no difficulties ($\tau_{V\mu} \sim 10^{-8}$ sec.).

Summing up, the coupling scheme of Fig. 9 is quite satisfactory for the present state of the theory and in agreement with actual experimental data. The only trouble is that the value of $\tau_{\pi\mu}$, although reasonable, is ambiguous since it is given by divergent calculations, but this cannot be an argument against the existence of the scheme. Equally, while this scheme is very elegant, since it introduces only two different couplings, this elegance is not an argument for its existence. However, it is natural to adopt and test first the simplest hypothesis, i.e. this scheme (1) for coupling properties of particles. It requires a pseudoscalar $\pi^{\pm}$-meson, and this is in agreement with the discussion in § 1. 3. It requires also the g_4 term for the direct coupling, and $g_5 = 0$. Then we are led to a direct coupling with two terms in g_2 and g_4 according to the discussion in § 3. 4. These qualitative consequences will probably soon be tested by experiments.

---

[17] Ruderman and Finkelstein have to take a very large cut-off value because they choose f^2 (*Pp* coupling of π-meson) about ten times too small (see value in § 2. 1). Nakamura *et al.* say that *Pv* coupling is better because they choose $f = f'$ instead of applying the equivalence theorem, valid here, or taking the values of f and f' given in § 2. 1.

4. 2 Coupling scheme (2), an alternative to scheme (1)

We noted in § 3. 5 the agreement between the calculated and observed μ-meson capture when it is described by an indirect coupling (Fig. 10), f, $\check{f}$, the value of $\check{f}$ being determined from π-decay to $\mu + \nu$. We can therefore replace scheme (1) by scheme (2) and then we are no longer obliged to compare $\tau_{\pi\mu}$ and $\tau_{\pi\varepsilon}$ directly and to restrict π to be a P-meson. However, since the calculation of $\tau_{\pi\varepsilon}$ in this scheme leads to divergent results, we cannot draw final conclusions, and from a reasonable cut-off it seems doubtful if charged π-mesons could have any other coupling than Aa or P, their decay into electrons being otherwise too rapid. From other experimental results we have seen that there is very strong presumption that π-mesons are indeed P mesons. Then the coupling scheme (2) introduces one more different coupling (i.e. at least one more coupling constant) without giving (with the present state of the theory) the possibility of a better fit of experimental data. At present, there seems to be no reason to reject scheme (1) in favour of scheme (2).

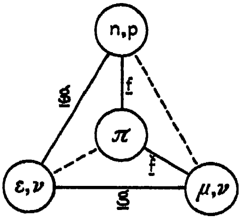

Fig. 10. Coupling scheme (2)
----- indirect coupling.

4. 3 Is direct coupling necessary for β-radioactivity?

β-radioactivity through an intermediate virtual nuclear meson was studied by Yukawa *et al.* [1938b], Sakata [1941b] and Rozental [1941a, 1945]. As we saw in § 3. 4, the actual experimental accuracy (by drawing the linear plots of spectra) rejects all terms which are not of the form $k_i J_i$ where k_i are constants. When there is only one meson coupling term, there are no interference terms and the indirect coupling is of the required form, giving for the constant k_i,

(68) $$k = f\,\check{f}\,a/\varkappa^2,$$

a being a factor $(\frac{1}{2}\sqrt{2}) \leqslant a \leqslant 2$, dependent on the nature of the meson. The equivalent direct coupling for *Ss* mesons is g_1, for *Vv* mesons g_2, for *Vt* or *At* mesons g_3, for *Aa* or *Pa* mesons g_4, and for mesons g_5.

The lifetime $\tau_{\pi s}$ is given (except for *Pa* and *Sv* mesons) by

(69) $$1/\tau_{\pi s} = a'\check{f}^2\varkappa/4\pi$$

with $a' = 1$ for *Ss* or *Pp* mesons, $= 2/3$ for *Vv* or *Aa* mesons, $= 1/3$ for *Vt* or *At* mesons. For *Pa* or *Sv* mesons,

(70) $$1/\tau_{\pi s} = m^2 f'^2/4\pi\varkappa$$

(for calculations of $\tau_{\pi s}$ see YUKAWA *et al.* [1938a], BETHE and NORDHEIM [1940], CHANG [1942], and for all cases SAKATA [1941a]). We know the value of k and the magnitude of f, it is therefore possible, by eliminating $\check{f}$ between (68) and (69) or (70), to find the value of $\tau_{\pi s}$. For *Pa* (or *Sv*) mesons,

(71) $$\tau_{\pi s} = 4\lambda \cdot 10^{-6} \text{ sec.}$$

(λ has been defined in (43)), and for the other cases

(72) $$\tau_{\pi s} = \tfrac{1}{2}\,a\lambda \cdot 10^{-10} \text{ sec.},$$

i.e. it is $\varkappa^2/a$ times smaller. (This result is essentially the object of ROZENTAL's [1941b] paper where it was shown that the lifetime of the cosmic ray meson was only compatible with *Pa* mesons!). Therefore only *Pa* charged π-mesons can be acceptable for coupling scheme (3) (see Fig. 11).

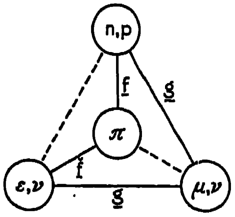

Fig. 11. Coupling scheme (3)
---- indirect coupling.

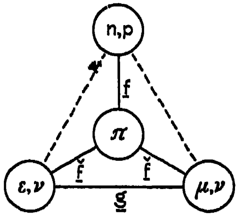

Fig. 12. Coupling scheme (4)
---- indirect coupling.

Moreover, in this case (MARTY and PRENTKI [1948], LOPES [1948]) if π-mesons have the same coupling $\check{f}'_{\nu}$ with (μ, ν) and (ε, ν), we have $\tau_{\varepsilon\nu} \gg \tau_{\mu\nu}$ [18] and therefore, as in § 4. 2, a possible alternative to scheme (3) is scheme (4) (Fig. 12).

If π is pseudoscalar (as is likely, see § 2. 3), in schemes (3) and (4) the indirect coupling for β-radioactivity is equivalent to a g_4 direct coupling (n, p)(ε, ν); this gives the G—T selection rules. However, we have seen (§ 3. 4) that the Fermi rules seem also necessary at least for the O^{14} decay, and also probably for some forbidden shape spectra which can be explained only by a mixture of Fermi and G—T interactions, g_1, g_3 or g_2, g_4 or even g_2, g_3. Therefore a direct coupling g_2 must be added or, if one wants to avoid this direct coupling, one has to postulate the existence of another charged nuclear meson giving an indirect coupling equivalent to g_2. It must therefore be a vector meson, and according to § 2. 6 it cannot be the $V^{\pm}$-meson. The lifetime of this postulated meson X (rest mass $\varkappa$) for the process $X \rightarrow \varepsilon^{\pm} + \nu$ would be

$$t = 1.6 \times 10^{-10} f^2/\varkappa^5 \text{ sec.,} \tag{73}$$

where f is its nuclear coupling. Of course if f is small enough and/or $\varkappa$ is large enough, this meson would not be observable!

4. 4 Summary

It is to be expected that we shall soon have more knowledge of the nature of the V and V′ mesons, and also on the terms of the β-radioactivity direct (or equivalent indirect) coupling. The coupling scheme (1) will be ruled out if this interaction is not g_2, g_4 (other mixtures compatible with the scheme are forbidden in the discussion § 3. 4), or if π-mesons are not pseudoscalar (but this is most unlikely).

When the nature of the terms of the interaction for β-radioactivity (direct) coupling are known more precisely, it will be possible, by the study (still in progress) of the μ-meson decay spectrum, to determine whether this spectrum can be satisfactorily accounted for by the same coupling terms. It now seems more difficult to visualize μ-meson capture experiments decisive for the choice of coupling schemes.

---

[18] For the equivalence of the direct coupling (n, p) (μ, ν) and the indirect coupling π-(n, p) and π-(μ, ν) we did not distinguish between *Pa* mesons and the other possibilities because the ratio of $\tau_{\pi\mu}$ is then no longer χ^2/a but only $\chi^2/\mu^2 a \approx 1.7/a$.

5. CONCLUSION

At present, the study of the coupling properties of particles is only descriptive. Physicists observe and classify couplings in much the same way as botanists do species! No essentially new ideas (outside electrodynamics) have been successfully put forward since Fermi's β-radioactivity and Yukawa's mesons, now over fifteen years old. Predictions from these ideas have been very helpful, but not completely so, as was expected.

Meson theories have had great success, but this is outside the field of nuclear interaction. Nuclear physics has developed quite independently of meson theories (for instance, the droplet model, shell structure, and the phenomenological potential for nucleon-nucleon interaction), and even for the simple nucleon-nucleon interaction meson theories fail at high energy. However the discovery of the π°-meson, so badly needed for meson theories of nuclear forces, was a notable success, and its decay into two photons gives more confidence to the application of hole theory for nucleons. The $\pi^\pm$ and π°-mesons are probably pseudoscalar, and experiments now in progress with artificially created mesons (mainly concerning interactions with hydrogen and deuterium) may be expected soon to give a still better answer to the question, and allow one to decide in favour of *Pa* and/or *Pp* coupling for this symmetrical pseudoscalar set of mesons.

Today, direct coupling seems necessary for β-radioactivity, and experimental agreement is satisfactory (the main difficulty is C^{14}). The study of spectra with forbidden shape (conjugated with spin measurements), of electron neutrino angular correlation, of neutron decay, etc. should fairly soon allow one to specify which terms $g_i J_i$ form the direct coupling. It is for μ-meson decay however, in the present state of affairs, that direct coupling is absolutely necessary and gives perfect agreement with experiment.

As long as coupling scheme (1) is not ruled out, it is remarkable that one may be able to explain all interactions between particles by adding only one coupling to the already known nuclear, electromagnetic and gravitational interactions.

Especially for the problem of coupling properties of particles, many answers are pending because in these cases the theory cannot give reliable quantitative results. Too often in the literature the existence of these particular cases is claimed to be excluded because of such difficulties [19]; it seems necessary to recall (as did ROSENFELD [1950]) Fresnel's sentence: "La Nature se joue de nos difficultés analytiques".

The opposite attitude is no better. The elegance of a theory is no guarantee of its applicability to natural phenomena. Since elegance cannot be decisive in accepting or rejecting a theory, it cannot be significant as a criterion for the choice of alternatives within the arbitrariness of a theory (as the choice of coupling [20] here). Experiments give the final answer. Of course one has to make and test first the simplest hypotheses (with the least possible arbitrariness). But only a completed theory can be put in an elegant form; theories in evolution are necessarily unsatisfactory, and this is true for the present theory of elementary particles which, (besides the lack of a successful intermediate coupling method) probably breaks down at very short distances or at very high energies. The realistic point of view of regularization could have been a solution, since it emphasizes the necessity of treating all fields together, but it failed (see, for instance, PAIS and UHLENBECK [1950]).

However, the future is very promising; new heavy particles (V and/or V′) have been discovered in cosmic rays and may soon be produced artificially. These probably have some bearing on the unsolved problems of nuclear forces. Finally, the techniques of observation of very high energy nuclear events have been greatly developed, and will offer important data for testing improvements or fundamental modifications of the theory of the interactions between particles. Cosmic rays will for many years be our only source of such events.

---

[19] This has even been invoked against the existence of direct coupling because of the $\sim r^{-5}$ second order *static* interaction potential between any two of the involved fermions!

[20] As, for instance, the symmetry principle of DE GROOT and TOLHOEK [1950]; this principle restricts the direct coupling of β-radioactivity to a mixture of either g_2, g_3 or g_1, g_4, g_5.

ACKNOWLEDGEMENTS

I am very grateful to Professor Niels Bohr for his kind hospitality. I wish to thank Professor Rosenfeld, Dr Mottelson, Dr Kofoed–Hansen and all the physicists of the Copenhagen Institute for Theoretical Physics and of the University of Manchester for many stimulating discussions.

I am indebted to the French Service des Poudres, whose generosity and understanding have made possible my stays abroad.

REFERENCES

Aamodt, L., J. Hadley and W. Panofsky, 1950, Phys. Rev., 80, 282.

Abragham, A. and J. J. Horowitz, 1951. Private communication.

Aidzu, K., Y. Fujimoto, N. Fukuda, S. Hayakawa, K. Takayanagi, G. Takada and Y. Yamaguchi, 1950, Progr. Theor. Phys., 5, 931.

Allen, J. S., H. R. Paneth and A. H. Morrish, 1949, Phys. Rev., 75, 570.

Alikhaniyan, A. I., E. M. Samoilovich, I. I. Gurevich and K. P. Babayan, 1949, J. Exp. Theor. Phys., 19, 667.

Anderson, C. D., 1932, Science, 76, 238.

Araki, G., 1950, Progr. Theor. Phys., 5, 507.

Armenteros, R., K. H. Barker, C. C. Butler, A. Cachon and A. H. Chapman, 1951, Nature, Lond., 167, 501.

Ashkin, J., A. Simon and R. E. Marshark, 1950, Progr. Theor. Phys., 5, 634.

Barrett, J. H., 1950, Phys. Rev., 79, 907.

Benoist-Gueutal, P., J. Prentki and J. Ratier, 1950, J. Phys. Radium, 11, 553.

Bethe, H. A., 1935, Proc. Camb. Phil. Soc., 31, 108.

Bethe, H. A. and L. W. Nordheim, 1940, Phys. Rev., 57, 998.

Bethe, H. A., 1947, Elementary Nuclear Theory. (New York; John Wiley and Sons).

Bethe, H. A., 1949, Phys. Rev., 76, 191.

Bloch, F. and C. Møller, 1935, Nature, Lond., 136, 911.

Bhabha, H. J., 1949, Rev. Mod. Phys., 21, 451

Borowitz, S. and W. Kohn, 1949, Phys. Rev., 76, 818.

Broda, E., N. Feather and D. H. Wilkinson, 1947, Phys. Soc. Camb. Conf. Report, p. 114.

Brown, R., U. Camerini, P. H. Fowler, H. Muirhead, C. F. Powell and D. M. Ritson, 1949, Nature, Lond., 163, 82.

Brueckner, K. A., 1950a, Phys. Rev., 79, 641.

Brueckner, K. A. and K. M. Watson, 1950b, Phys. Rev., 79, 187.

Carlson, A. G., J. E. Hooper and D. T. King, 1950, Phil. Mag., 41, 701.

Case, K. M., 1948, Phys. Rev., 74, 1884.

Case, K. M., 1949a, Phys. Rev., 76, 1.

Case, K. M., 1949b, Phys. Rev., 76, 14.

Case, K. M. and A. Pais, 1950, Phys. Rev., 80, 203.

Chadwick, J., 1932, Nature, Lond., 129, 312.

Chamberlain, O., R. F. Mozley, J. Steinberger and C. Wiegand, 1950, Phys. Rev., 79, 396.

Chang, T. S., 1942, K. Danske Vidensk. Selsk. Mat.-fys. Medd., 19, no. 10.

Chang, W. Y., 1949, Rev. Mod. Phys., 21, 167.

Chao, C. Y., 1949, Phys. Rev., 75, 581.

Cheston, W. B., 1951, Phys. Rev., 82, 335.
Christy, R. F. and S. Kusaka, 1941, Phys. Rev., 59, 414.
Cocconi, G. and V. Cocconi–Tongiorgi, 1951, Phys. Rev., 82, 335.
Conforto, A. M., R. D. Sard, 1951, Phys. Rev., 82, 335.
Conversi, M., E. Pancini and O. Piccioni, 1945, Phys. Rev., 68, 232.
Conversi, M., E. Pancini and O. Piccioni, 1947, Phys. Rev., 71, 209.
Conversi, M. and O. Piccioni, 1946, Phys. Rev., 70, 859.
Crandall, W. E., B. J. Moyer and H. F. York, 1950, Phys. Rev., 78, 89.
Crane, H. R., 1948, Rev. Mod. Phys., 20, 279.
Critchfield, L. and E. Wigner, 1941, Phys. Rev., 60, 412.
See also L. Critchfield, 1943, Phys. Rev., 63, 417.
Crouch, M. F., 1951, Phys. Rev., 81, 164.
Curran, S. C., J. Angus and A. L. Cockcroft, 1949, Phys. Rev., 76, 853.
Daudin, J., 1950, J. Phys. Radium, 11, 25.
Dyson, F. J., 1948, Phys. Rev., 73, 929.
Dyson, F. J., 1949, Phys. Rev., 75, 486 and 1736.
Davies, J. H., W. O. Lock and H. Muirhead, 1949, Phil. Mag., 40, 1251.
Enatsu, H., 1950, Progr. Theor. Phys., 5, 102.
Evans, J. and E. P. George, 1949, Nature, Lond., 164, 21.
Feer, D. B., 1949a, Phys. Rev., 75, 731.
Feer, D. B., 1949b, Phys. Rev., 76, 306.
Fermi, E., 1934, Z. Phys., 88, 161.
Ferretti, B. and S. Gallone, 1950, Phys. Rev., 77, 153.
Fierz, M., 1937, Z. Phys., 104, 553.
Finkelstein, R. J., 1947, Phys. Rev., 72, 415.
Fireman, L., 1949, Phys. Rev., 75, 323.
Forster, H. H., 1950, Phys. Rev., 78, 92.
Fretter, W. B., 1948, Phys. Rev., 73, 41.
Fretter, W. B., 1949, Phys. Rev., 76, 511.
Fretter, W. B., 1951, Phys. Rev., 82, 294.
Friedman, H. L. and J. Rainwater, 1951, Phys. Rev., 81, 644.
Fukuda, H. and Y. Miyamoto, 1949a, Progr. Theor. Phys., 4, 347.
Fukuda, H., Y. Miyamoto, T. Miyazima and S. Tomonaga, 1949b, Progr. Theor. Phys., 4, 385.
Fukuda, H. and Y. Miyamoto, 1949c, Progr. Theor. Phys., 4, 389.
Fukuda, H. and Y. Miyamoto, 1949d, Progr. Theor. Phys., 4, 391.
Fukuda, H., S. Hayakawa and Y. Miyamoto, 1950a, Progr. Theor. Phys., 5, 283.
Fukuda, H., S. Hayakawa and Y. Miyamoto, 1950b, Progr. Theor. Phys., 5, 352.
Fukuda, H. and Y. Miyamoto, 1950c, Progr. Theor. Phys., 5, 147.
Fukuda, H. and Y. Miyamoto, 1950d, Progr. Theor. Phys., 5, 148.
Furry, W. H., 1937, Phys. Rev., 51, 125.
Furry, W. H., 1939, Phys. Rev., 56, 1184.
Gamow, G. and E. Teller, 1936, Phys. Rev., 49, 895.
Gerjuoy, E., 1951, Phys. Rev., 81, 62.
Greisen, K. I., 1948, Phys. Rev., 73, 521.

Groetzinger, G. and G. W. McClure, 1948, Phys. Rev., 74, 341.

de Groot, S. R. and H. A. Tolhoek, 1950, Physica, 16, 456.

Hamilton, D. R., 1947, Phys. Rev., 71, 456.

Hanawa, S. and T. Miyazima, 1950, Progr. Theor. Phys., 5, 459.

Harding, J. B., 1950, Phil. Mag., 41, 405.

Heitler, W. and S. Power, 1947, Phys. Rev., 72, 266.

Hincks, E. P. and B. Pontecorvo, 1950, Phys. Rev., 77, 102.

Hincks, E. P., 1951, Phys. Rev., 81, 313.

Hopper, V. D. and S. Biswas, 1950, Phys. Rev., 80, 1098.

Hornyak, W. F., T. Lauritsen, P. Morrison and W. A. Fowler, 1950, Rev. Mod. Phys., 22, 291.

Inghram, M. G. and J. H. Reynolds, 1949, Phys. Rev., 76, 1264.

Inghram, M. G. and J. H. Reynolds, 1950, Phys. Rev., 78, 822.

Jarkov, K. B., 1950, J. Exp. Theor. Phys., 20, 492.

Jastrow, R., 1951, Phys. Rev., 81, 165.

Kaplon, M. F., B. Peters and H. L. Bradt, 1949, Phys. Rev., 76, 1735.

Kissinger, C. W. and D. Cooper, 1948, Phys. Rev., 74, 349.

Klein, O., 1948, Nature, Lond., 161, 897.

Konopinski, E. J. and G. E. Uhlenbeck, 1935, Phys. Rev., 48, 7.

Konopinski, E. J., 1943, Rev. Mod. Phys., 15, 209.

Kraushaar, W. L., J. E. Thomas and V. P. Henri, 1950, Phys. Rev., 78, 486.

Lagarrigue, A. and C. Peyrou, 1951, J. Phys. Radium, to be published and C. R. Acad. Sci., Paris, 233, 478.

Landau, L. D., 1948, Dokl. Akad. Nauk. SSSR., 60, 207.

Langer, L. M. and R. J. D. Moffat, 1951, Phys. Rev., 82, 333 and 635.

Lattes, C. M. G., G. P. S. Occhialini and C. F. Powell, 1947, Nature, Lond., 160, 453.

Lawson, J. S., Jr., 1951, Phys. Rev., 81, 299.

Le Couteur, K. J. and L. Rosenfeld, 1949, Phil. Mag., 40, 151.

Lee, T. D., M. Rosenbluth and C. N. Yang, 1949, Phys. Rev., 75, 905.

Leighton, R. B., C. D. Anderson and A. J. Seriff, 1949, Phys. Rev., 75, 1432.

Leprince-Ringuet, L. and M. l'Héritier, 1944, C. R. Acad. Sci., Paris, 219, 618.

Leprince-Ringuet, L., 1949, Rev. Mod. Phys., 21, 43.

Levine, C. A., A. Ghiorso and G. T. Seaborg, 1950, Phys. Rev., 77, 296.

Levy, M., 1951, Proc. Roy. Soc. A, to be published.

Lewis, H. W., J. R. Oppenheimer and S. A. Wouthuysen, 1948, Phys. Rev., 73, 127.

Lodge, A. S., 1948, Nature, Lond., 161, 809.

Longmire, C., C. S. Wu and C. H. Townes, 1949, Phys. Rev., 76, 695.

Lopes, J. L., 1948, Phys. Rev., 74, 1722.

Luttinger, J. M., 1949a, Phys. Rev., 75, 309.

Luttinger, J. M., 1949b, Phys. Rev., 75, 1277.

McMillan, E. M. and J. M. Peterson, 1949a, Science, 109, 438.

McMillan, E. M., J. M. Peterson and R. S. White, 1949b, Science, 110, 579.

Majorana, E., 1937, Nuovo Cim., 14, 171.

Manley, J. H. and S. Millman, 1937, Phys. Rev., 51, 19.

Marshak, R. E., 1949a, Phys. Rev., 75, 513.

Marshak, R. E. and A. S. Wightman, 1949b, Phys. Rev., 76, 114.

Marshak, R. E., 1949c, Phys. Rev., 76, 1736.

Marshak, R. E., S. Tamor and A. S. Wightman, 1950, Phys. Rev., 80, 765.

Martinelli, E. A. and W. K. H. Panofsky, 1950, Phys. Rev., 77, 464.

Marty, C. and J. Prentki, 1948, J. Phys. Radium, 9, 147.

Marty, C. and J. Prentki, 1950a, C. R. Acad. Sci., Paris, 230, 54.

Marty, C. and J. Prentki, 1950b, C. R. Acad. Sci., Paris, 230, 1508.

Michel, L., 1949, Nature, Lond., 163, 959.

Michel, L., 1950a, Proc. Phys. Soc., A63, 514 and 1371.

Michel, L., 1950b, Nature, Lond., 166, 654.

Michel, L., 1951, to be published.

Nahmias, M. E., 1935, Proc. Camb. Phil. Soc., 31, 99.

Nakamura, S., H. Fukuda, K. Ono, M. Sasaki and M. Taketani, 1950, Progr. Theor. Phys. 5, 740.

Nelson, E. C., 1941, Phys. Rev., 60, 830.

Nereson, N., 1948, Phys. Rev., 73, 565.

Nishijima, K., 1950, Progr. Theor. Phys., 5, 187.

O'Ceallaigh, C., 1950, Phil. Mag., 41, 838.

Ogawa, S. and S. Kamefuchi, 1950a, Progr. Theor. Phys., 5, 311.

Ogawa, S. and E. Yamada, 1950b, Progr. Theor. Phys., 5, 503.

Oneda, S., S. Sasaki and S. Ozaki, 1950, Progr. Theor. Phys., 5, 165.

Ozaki, S., S. Oneda and S. Sasaki, 1949, Progr. Theor. Phys., 4, 524.

Ozaki, S., 1950, Progr. Theor. Phys., 5, 373.

Pais, A. and G. E. Uhlenbeck, 1950, Phys. Rev., 79, 145.

Panofsky, W. K. H., L. Aamodt and H. F. York, 1950a, Phys. Rev., 78, 825.

Panofsky, W. K. H., L. Aamodt, J. Hadley and R. Phillips, 1950b, Phys. Rev., 80, 94.

Pauli, W., 1941, Rev. Mod. Phys., 13, 203.

Pauli, W. and F. Villars, 1949, Rev. Mod. Phys., 21, 434.

Peaslee, D. C., 1950, Helv. Phys. Acta, 23, 845.

Peterson, V. Z., 1950, Phys. Rev., 79, 407.

Peyrou, C. and A. Lagarrigue, 1950, J. Phys. Radium, 11, 666.

Piccioni, O., 1948, Phys. Rev., 74, 1754.

Pontecorvo, B., 1947, Phys. Rev., 72, 247.

Powell, C. F., 1950, Rep. Phys. Soc. Progr. Phys., 13, 350.

Power, S., 1949, Phys. Rev., 76, 865.

Prentki, J., 1951, C. R. Acad. Sci., Paris, 232, 940.

Puppi, G., 1948, Nuovo Cim., 5, 587.

Puppi, G., 1949, Nuovo Cim., 6, no. 3.

Racah, G., 1937, Nuovo Cim., 14, 322.

Retallack, S. G. and R. B. Brode, 1949, Phys. Rev., 75, 1716.

Richardson, J. R., 1948, Phys. Rev., 74, 1720.

Robson, J. M., 1950, Phys. Rev., 78, 311.

Robson, J. M., 1951, Phys. Rev., 81, 297.

Rochester, G. D. and C. C. Butler, 1947, Nature, Lond., 160, 855.

Rosenbluth, M. N., 1949, Phys. Rev., 75, 532.

Rosenfeld, L., 1948a, Nuclear Forces (Amsterdam: North-Holland Publishing Co.)

Rosenfeld, L., 1948b, Rep. Solvay Conf.

Rosenfeld, L., 1950, Progr. Theor. Phys., 5, 519.

Rozental, S., 1941a, K. Danske Vidensk. Selsk. Mat.-fys. Medd., 18, no. 7.

Rozental, S., 1941b, Phys. Rev., 60, 612.

Rozental, S., 1945, K. Danske Vidensk. Selsk. Mat.-fys. Medd., 23, no. 11.

Ruderman, M. and R. Finkelstein, 1949, Phys. Rev., 76, 1458.

Sakata, S., 1941a, Proc. Phys.-Mat. Soc., Japan, 23, 283.

Sakata, S., 1941b, Proc. Phys.-Mat. Soc., Japan, 23, 291.

Sard, R. D., W. B. Ittner, A. M. Conforto and M. F. Crouch, 1948, Phys. Rev., 74, 91.

Sard, R. D., A. M. Conforto and M. F. Crouch, 1949, Phys. Rev., 76, 1134.

Sasaki, S., S. Oneda and S. Ozaki, 1949, Science Rep. Tohoku Univ., 33, 77.

Sasaki, S., S. Oneda and S. Ozaki, 1950, Progr. Theor. Phys., 5, 25.

Schoenberg, M., 1941, Phys. Rev., 60, 468.

Schwinger, J., 1948, Phys. Rev., 73, 416.

Scott, J. M. C. and E. W. Titterton, 1950, Phil. Mag., 41, 318.

Seriff, A. J., R. B. Leighton, C. Hsiao, E. W. Cowan and C. D. Anderson, 1950, Phys. Rev., 78, 290.

Sherr, R., H. R. Muether and M. G. White, 1949, Phys. Rev., 75, 282.

Sigurgeirsson, T. and K. A. Yamakawa, 1947, Phys. Rev., 71, 319.

Sigurgeirsson, T. and K. A. Yamakawa, 1949, Rev. Mod. Phys., 21, 124.

Slotnick, M. and W. Heitler, 1949, Phys. Rev., 75, 1645.

Smith, F. M., W. H. Barkas, A. S. Bishop, H. Bradner and E. Gardner, 1950, Phys. Rev., 78, 86.

Snell, A. H., F. Pleasonton and R. V. McCord, 1950, Phys. Rev., 78, 310.

Steinberger, J., 1948, Phys. Rev., 74, 500.

Steinberger, J., 1949a, Phys. Rev., 75, 1136.

Steinberger, J., 1949b, Phys. Rev., 75, 1180.

Steinberger, J., W. K. H. Panofsky and J. Steller, 1950, Phys. Rev., 78, 802.

Steller, J. S. and W. K. H. Panofsky, 1951, Phys. Rev., 81, 649.

Sun, K. H., 1949, Phys. Rev., 76, 1266.

Taketani, M., S. Nakamura and M. Sasaki, 1949, Phys. Rev., 76, 852.

Tamor, S. and R. E. Marshak, 1950, Phys. Rev., 80, 766.

Tanikawa, Y., 1947, Progr. Theor. Phys., 2, 31.

Ticho, H. K., 1947a, Phys. Rev., 72, 255.

Ticho, H. K. and M. Schein, 1947b, Phys. Rev., 72, 248.

Ticho, H. K. and M. Schein, 1948a, Phys. Rev., 73, 81.

Ticho, H. K. and M. Schein, 1948b, Phys. Rev., 74, 492.

Ticho, H. K. and M. Schein, 1948c, Phys. Rev., 74, 1337.

Tiomno, J., J. A. Wheeler and R. R. Rau, 1949a, Rev. Mod. Phys., 21, 144.

Tiomno, J. and J. A. Wheeler, 1949b, Rev. Mod. Phys., 21, 153.

TIOMNO, J., 1949c, Phys. Rev., 76, 856.
TOMONAGA, S. and G. ARAKI, 1940, Phys. Rev., 58, 90.
TRIGG, G. L., 1951, Phys. Rev., 82, 325.
VALLEY, G., 1947, Phys. Rev., 72, 772.
VALLEY, G. and B. ROSSI, 1948, Phys. Rev., 73, 177.
VAN HOVE, L., 1949, Phys. Rev., 75, 1519.
VAN WYCK, C. B., 1949, Proc. Phys. Soc., A62, 697.
VAN WYCK, C. B., 1950a, Proc. Phys. Soc., A63, 350.
VAN WYCK, C. B., 1950b, Phys. Rev., 80, 487.
WAGNER, N. and D. COOPER, 1949, Phys. Rev., 76, 449.
WATSON, K. and J. V. LEPORE, 1949, Phys. Rev., 76, 1157.
WENTZEL, G., 1949, Phys. Rev., 75, 1810.
WHEELER, J. A., 1947, Phys. Rev., 71, 320.
WHEELER, J. A., 1949, Rev. Mod. Phys., 21, 132.
WICK, G. C., 1934, Atti. Accad. Naz. Lincei., 19, 319.
WIGHTMAN, A. S., 1950, Phys. Rev., 77, 521.
WIGNER, E., 1927, Göttingen Nachr., p. 375.
WIGNER, E., 1939, Phys. Rev., 56, 519.
WU, C. S., 1950, Rev. Mod. Phys., 22, 386.
YANG, C. N., 1950a, Phys. Rev., 77, 242.
YANG, C. N., 1950b, Phys. Rev., 77, 722.
YANG, C. N. and J. TIOMNO, 1950, Phys. Rev., 79, 495.
YUKAWA, H., 1935, Proc. Phys.-Mat. Soc. Japan, 17, 48.
YUKAWA, H., S. SAKATA and M. TAKETANI, 1938a, Proc. Phys.-Mat. Soc. Japan, 20, 720.
YUKAWA, H., S. SAKATA, M. KOBAYASI and M. TAKETANI, 1938b, Proc. Phys.-Mat. Soc. Japan, 20, 720.
YUKAWA, H., 1949, Rev. Mod. Phys., 21, 474.

CHAPTER IV

THE NATURE OF PRIMARY COSMIC RADIATION

BY

B. PETERS

Department of Physics, University of Rochester

INTRODUCTION 193

1. THE STUDY OF HEAVY PRIMARY PARTICLES IN NUCLEAR EMULSIONS 195

2. NUCLEAR INTERACTIONS AND ENERGY MEASUREMENTS 202

3. THE FLUX AND ENERGY SPECTRUM OF PRIMARY COSMIC RAY NUCLEI 216

4. THE CHEMICAL COMPOSITION OF PRIMARY COSMIC RADIATION 228

5. THE COMPOSITION OF PRIMARY COSMIC RADIATION AND THE PROBLEM OF ITS ORIGIN 233

REFERENCES 241

INTRODUCTION

In recent years it has become feasible to study directly the high energy particles which enter our atmosphere from outer space. Progress in this field is largely due to the development of stratosphere balloons which permit extended observations in the top layers of the atmosphere. As a result of measurements carried out at altitudes above 25 km, with counter telescopes, cloud chambers, ionization chambers and especially photographic emulsions, it has been established that primary cosmic rays consist of nuclei of many of the chemical elements known on earth. The relative abundance of nuclear species appears to be closely related to the abundances of elements in the visible universe as deduced from the spectra of stars and planetary nebulae and from the composition of meteoric material.

A few years ago there was little direct information on the primary particles responsible for the complicated nuclear and electromagnetic effects occurring in the atmosphere. Originally one attributed these effects to very penetrating electromagnetic radiation entering from outer space. In 1927—1929 J. Clay demonstrated that the intensity of cosmic rays on the earth's surface decreased with decreasing geomagnetic latitude; he thereby proved that, since it was affected by the earth's magnetic field, the incoming radiation must consist of particles carrying an electric charge. After the motion of charged particles in the magnetic dipole field of the earth had been studied, mainly by Störmer, Lemaitre and Vallarta, one could, on the basis of the observed asymmetry between particles entering from the East and West, conclude further that most if not all primary particles must carry positive charge. Without introducing unknown particles a decision had to be made between protons and positrons. By means of counter telescopes, SCHEIN *et al.* [1941] showed that most of the particles near the top of the atmosphere which can penetrate several centimetres of lead will not multiply in traversing the lead absorber; they do not initiate the cascade showers typical of high energy electronic radiation.

Since that time it has been generally accepted that the primary cosmic radiation consists of protons. Later work has shown that in first approximation this conclusion was correct. With the help of balloon-borne ionization chambers (Hulsizer [1949]) and cloud chambers (Critchfield *et al.* [1950]), the possible contribution of electrons to the primary radiation was successively reduced to less than ¼ % at geomagnetic latitude 55° N. corresponding to a flux of less than 4 electrons $\sec^{-1} m^{-2} \text{sterad}^{-1}$.

The possibility that the primary cosmic ray beam may contain nuclei of heavier elements was pointed out by several authors (Alfvén [1939]; Swann [1943]). An increase in the efficiency of low pressure counters with altitude was observed by Pomerantz in 1947 and, although these results remained unpublished until 1949, they may be considered to represent the first experimental indication for the presence of fairly energetic particles of charge $Z > 1$ at high altitudes.

In a stratosphere balloon flight, Freier *et al.* [1948a] observed the tracks of very heavy nuclei of large penetrating power in nuclear emulsions exposed above 90,000 feet. They showed that some of these nuclei could not have been produced by protons in the atmosphere since charge estimates based on the diameter of the column of developed silver along the track indicated that they were much heavier than air nuclei. They also showed that the number of such nuclei decreased with increasing absorber thickness much faster than the primary proton component and therefore could not be produced by incident protons. From these facts it was concluded that heavy nuclei were part of the primary cosmic ray beam, and an approximate value of the flux was given. While the main conclusions were confirmed by later experiments the initial estimates of the charge of heavy nuclei were much too high. The nuclei observed in the original experiment belonged to elements of atomic numbers between magnesium and iron. Later, investigations showed that lighter nuclei, especially helium were present in significant numbers.

Although the total number of nuclei heavier than protons constitute only about 15 % of the cosmic ray beam, their influence on the interpretation of cosmic ray phenomena in the atmosphere is nevertheless considerable, since they

(i) represent 30—35 % of the incoming nucleons

(ii) carry perhaps 30 % of the incident cosmic ray energy, and
(iii) provide about 50 % of the ionization in the upper layers of the atmosphere.

Also it is possible that the very high energy events in cosmic radiation, the extensive Auger showers carrying energies up to 10^{17} eV or even higher, are connected with heavy nuclei rather than protons.

Apart from its effect on the interpretation of cosmic ray phenomena in the atmosphere, the detailed study of the chemical composition and the energy spectrum of the heavy primary component provides data relevant to the unsolved question of the origin of cosmic radiation and information on the relative abundance of elements which can be compared with cosmic abundance data obtained from meteorites and from spectroscopic analysis of starlight. Some of these questions will be discussed in §§ 4 and 5. Here one should only point out that the mere existence in the primary beam of heavy nuclei with many BeV of energy makes it very unlikely that the acceleration of cosmic ray particles occurs in a violent nuclear catastrophe as has sometimes been suggested. The relatively loose structure of a large nucleus could not be expected to stay together in such a rapid accelerating process.

Heavy nuclei in the stratosphere have now been observed not only with photographic emulsions but also with cloud chambers (FREIER *et al.* [1948b]), low pressure Geiger counters (POMERANTZ *et al.* [1949]), proportional counters (SINGER *et al.* [1950]) and scintillation counters (NEY *et al.* [1951]). However, most of the quantitative results so far have been obtained with nuclear emulsion techniques. A description of these techniques as far as they apply to the study of heavy particles will therefore be given in the next section.

1. THE STUDY OF HEAVY PRIMARY PARTICLES IN NUCLEAR EMULSIONS

1. 1 Tracks produced by heavy nuclei

Fig. 1 shows the track of a non-relativistic iron nucleus which comes to rest in the emulsion.

Fig. 2 shows the last part of a track due to a nucleus of oxygen. In both pictures one sees the increase in the density of secondary electron tracks (δ-rays) as the particle slows down and approaches the end of its range. As the velocity decreases further, the δ-rays become shorter since the energy which a particle of velocity v can transfer to an electron is limited to $W_{\max} = 2m_e v^2$. Finally the track begins to thin down as the nucleus begins to capture orbital electrons leading to a reduction of its effective charge.

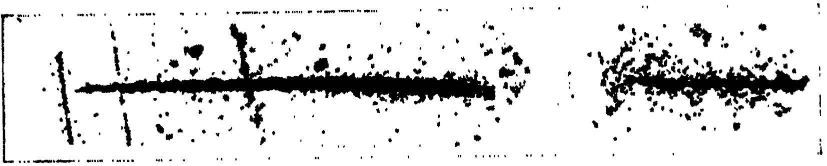

End of Track

Residual Range
1.3 gms./cm^2

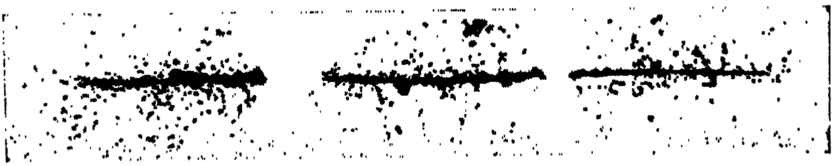

Residual Range
2.6 gms./cm^2

Residual Range
15 gms./cm^2

Residual Range
22 gms./cm^2

Fig. 1 – Track of a primary nucleus of charge $Z = 26 \pm 2$. The particle enters a stack of plates with an energy of 62 BeV and comes to rest in the emulsion of the 33rd plate after traversing 35 gm.cm^{-2} of glass.

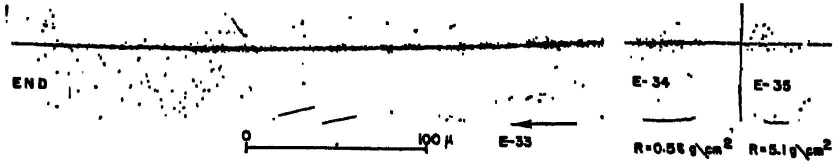

Fig. 2 – Track of primary oxygen nucleus. The particle enters the stack of plates with an energy of 15 BeV and comes to rest in the emulsion after traversing 5.4 gm.cm^{-2} of glass.

All these characteristics of tracks ending in the emulsion may be used to estimate the charge of the nucleus and have been employed by PERKINS [1950] to identify heavy splinters emitted in nuclear explosions. The δ-ray density is a function both of the charge and the velocity of the nucleus, but the position on the track where the density reaches its maximum value depends on the velocity alone. Since, as will be shown in § 1. 2, the residual range of a nucleus of a mass M and a given velocity is proportional to M/Z^2 (if one neglects the region in which the effective nuclear charge is reduced by electron capture) the charge can be obtained from the distance between the δ-ray maximum and the end of the track. A correction, however, is necessary if the residual range is not large compared to the "thin-down" length L in which the nucleus captures electrons. The cut-off point beyond which all δ-rays are shorter than a given value is again a function of velocity only. If this point is determined the residual range will again permit an estimate of the charge.

Finally the "thin-down" length L as a function of charge can be estimated from a simple model assuming that electron capture in a particular shell occurs when the velocity of the nucleus equals the orbital velocity of the electrons. Perkins gives the approximate relation $L = 0.7\,Z^2$ where L is measured in microns.

In practice all these methods are useful only for estimating the charge within a factor 2, since neither can the "thin-down" length be accurately determined nor is the number of δ-rays in short sections of the track sufficient to locate accurately the density maximum or the position of cut-off.

1. 2 Charge determination of heavy primary nuclei

The identification of the charge of primary cosmic ray nuclei is based on measurements of their specific ionization. In photographic emulsions this involves a careful measurement over an appreciable track length of either the density of developed silver grains along the trajectory or the δ-ray density, i.e. the number of electrons ejected in the ionization process with sufficient energy to produce appreciable secondary ionization.

The pulse height distribution in scintillation counters and the response of low pressure counters or proportional counters inserted into a counter telescope have also been used to determine specific ionization loss of heavy nuclei. Apart from difficulties of distinguishing pulses due to heavy particles from pulses due to nuclear explosions in the counter or the counter walls, the accuracy of values obtained for the specific ionization is still inferior to the accuracy obtainable in photographic emulsions. For this reason most of our information on the charge spectrum of primary nuclei is at present based on emulsion work.

The theoretical calculations of the specific energy loss of charged particles traversing matter carried out by Bohr, Bethe, Bloch and others (see HEITLER [1944, p. 218]) lead to a relation between range and energy which is in good agreement with experimental results. To a close approximation the formula may be written as:

$I_Z = Z^2 \varphi(v)$ where Z is the charge of the particle and $\varphi(v)$ is a function of its velocity only. The residual range $R_{M,Z}$ of a particle of mass M and charge Z is then given by:

$$R_{M,Z} = \int_0^E \frac{dE}{I_Z} = \frac{M}{Z^2}\psi(v) \tag{1}$$

and therefore

$$I = Z^2 F\left(\frac{RZ^2}{M}\right). \tag{2}$$

The known specific ionization loss of protons of a given range determines the function F and permits us to construct a curve of I vs. R for nuclei of any mass or charge. Such a graph is shown in Fig. 3.

The relation between specific ionization and grain density depends of course on the sensitivity of the particular emulsions used, and has to be obtained by calibrating each set of plates with identifiable particles of known energy.

Measurements of grain density, and therefore specific ionization, will uniquely identify the nucleus if its range is known or if the change in ionization can be measured between two points of the trajectory separated by a known amount of absorber, or if the energy and therefore the residual range can be deduced from the multiple Coulomb scattering of the particle in the emulsion. Grain density alone will identify the nucleus if it is known to possess relativistic energies. It is therefore easier to obtain the charge spectrum of primary radiation at low latitudes where relativistic energies are required to penetrate the earth's magnetic field, because for those particles grain density is only a function of charge and not of both charge and velocity.

The method of measuring specific ionization loss by δ-ray counting is quite similar to the grain counting method except that the δ-ray density does not depend strongly on the sensitivity of the particular emulsion used provided this emulsion is able to register tracks of electrons with more than about 50 KeV energy. A formula for the number of electrons emitted in the ionization process with energies between W_1 and W_2 is given by BRADT *et al.*

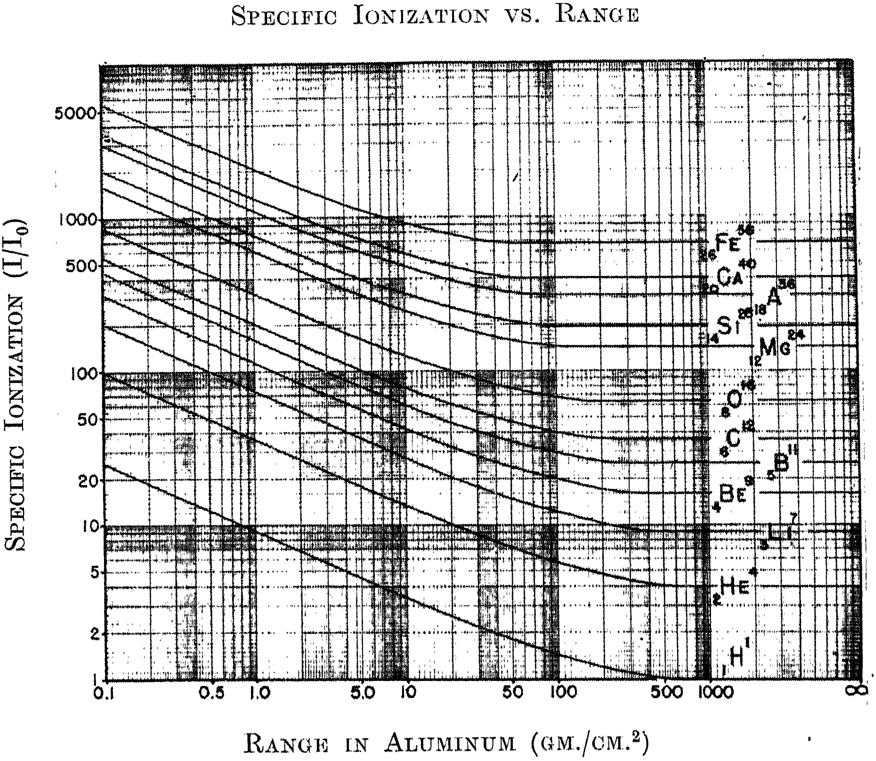

Fig. 3 – Specific ionization loss of different nuclei in units of the minimum ionization loss of singly charged particles is plotted against their range in aluminum.

[1948] based on the cross-section for elastic scattering of electrons in the Coulomb field of a nucleus calculated by MOTT [1929]. Mott's formula contains both terms which are quadratic and cubic in the charge Z, but the cubic term introduces only a few percent correction for $Z < 30$. The number of fast electrons and therefore the number of visible δ-rays depends otherwise on the velocity of the nucleus only and, making use again of the arguments given above, the δ-ray density N will be given by:

$$N = Z^2 G\left(\frac{RZ^2}{M}\right). \tag{3}$$

Thus the δ-ray density N for any particle can be obtained as a function of range if it is known for α-particles or other identified nuclei. Fig. 4 gives the δ-ray density for different nuclei as a function of their range. Since both theoretically and experimentally the δ-ray density is very nearly proportional to $1/v^2$ we can also write:

$$\frac{Nv^2}{Z^2} = \text{constant} = A \tag{4}$$

where A depends, of course, on the geometric criteria which are

δ-Ray Density vs. Range

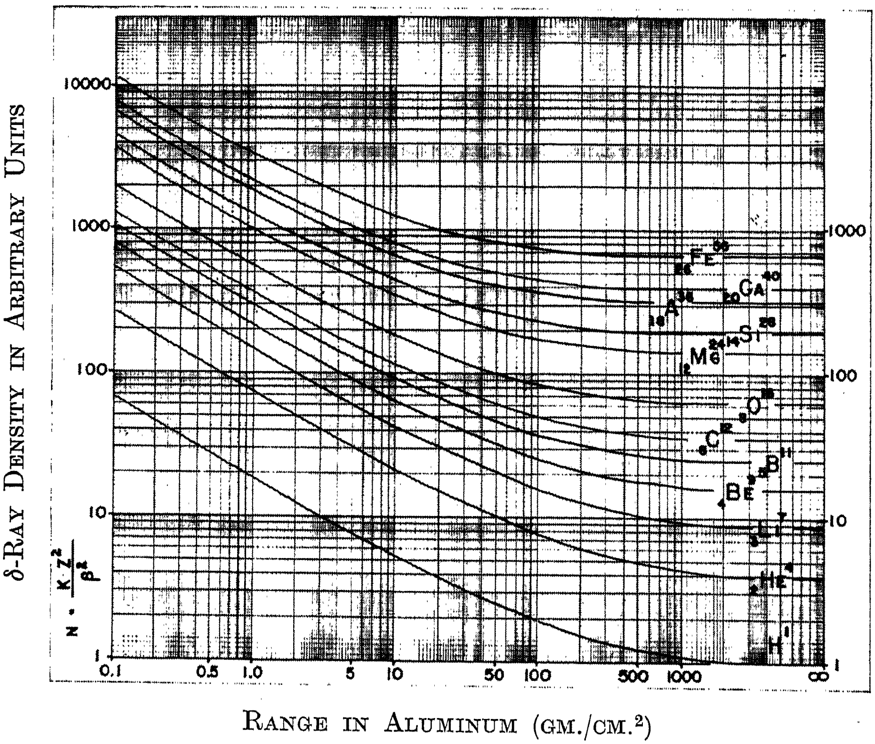

Fig. 4 – The number of δ-rays in arbitrary units is plotted for different nuclei as a function of their range in aluminum.

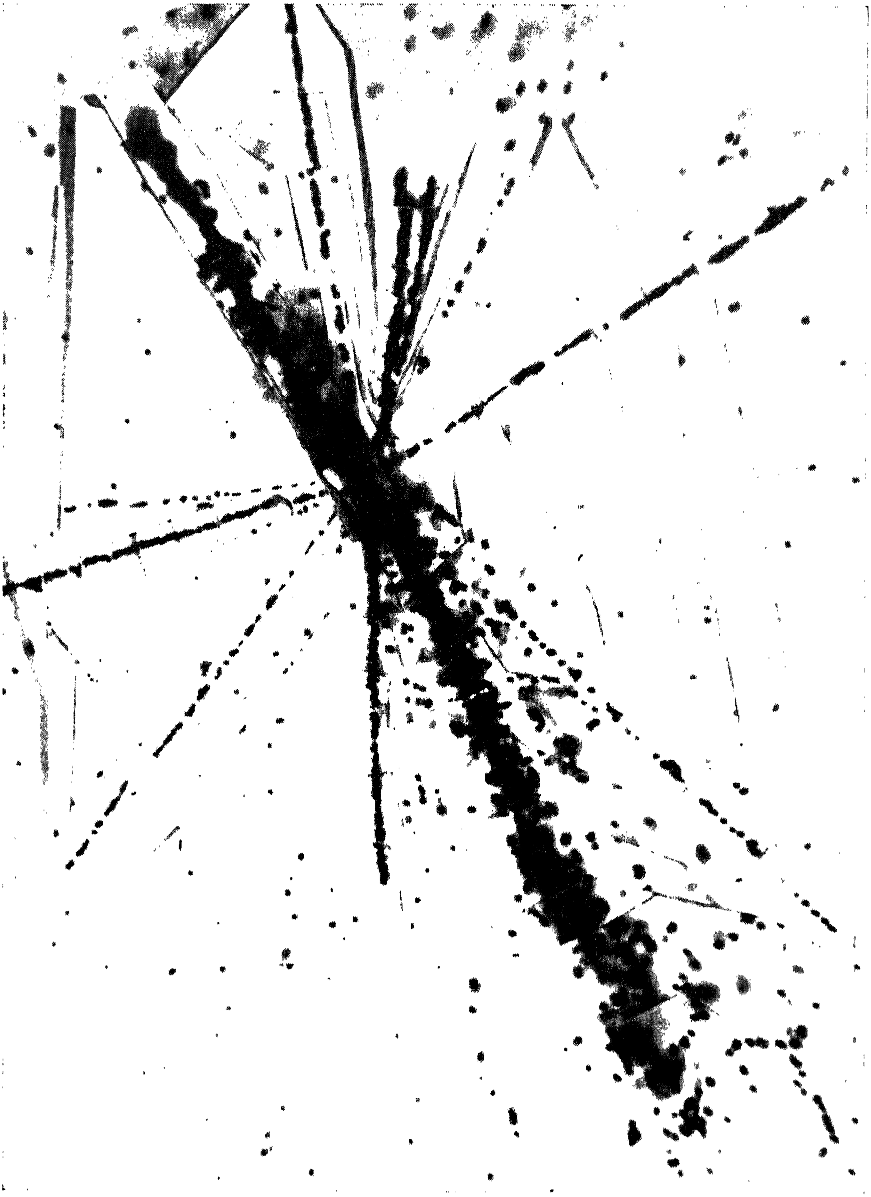

A nucleus of iron is completely destroyed in a collision with a nucleus of the emulsion. At least 30 mesons are produced.

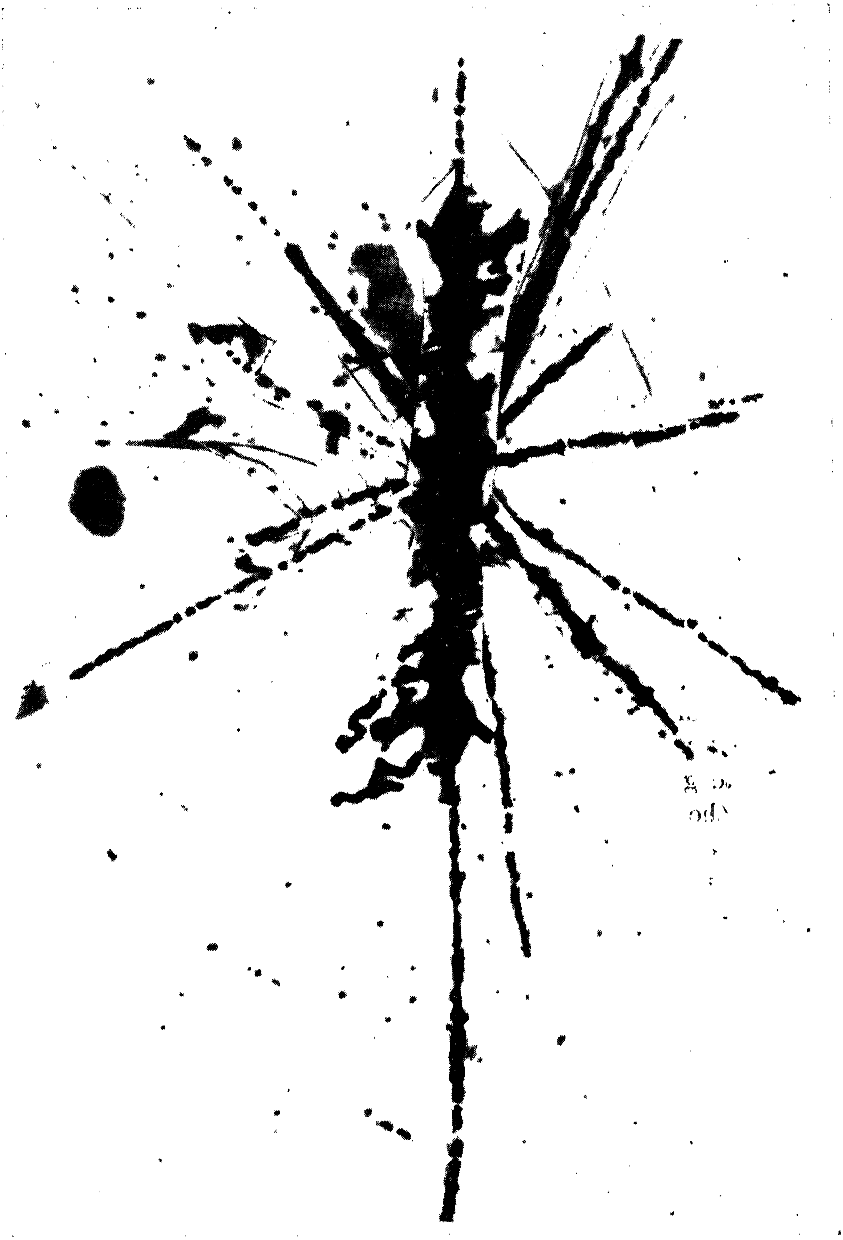

An iron nucleus produces a star in the emulsion and proceeds undeviated without any appreciable loss of charge.

employed for counting δ-rays of different lengths and orientation.

Again, if the energy of the particle is in the relativistic range, δ-ray density alone is sufficient to identify the particle; otherwise additional information is required such as the range of the particle or the rate of change of δ-ray density with range or the energy as deduced from multiple Coulomb scattering.

Since the background of slow electrons in nuclear emulsions exposed in the stratosphere is usually not negligible, it is necessary to correct the δ-ray count for background in the case of nuclei of charge $Z < 8$.

Comparing the methods of grain counting and δ-ray counting we find that both have advantages and disadvantages. δ-rays are difficult to count because of the large variation in length and the strong scattering of the electron tracks. The strict maintenance of initially arbitrary criteria as to the length and orientation of the δ-rays to be included in the counting requires experience, and introduces a subjective element, which limits the accuracy obtainable to 15—20 %. The advantage of the method lies mainly in the fact that it gives reasonably good results over wide ranges of specific ionization such that tracks with ionization between 30 and 1000 times minimum ionization can be measured in the same emulsion. For fast nuclei of charge $Z < 6$ the δ-ray method becomes very inaccurate, since the δ-ray density approaches the value given by the background of slow electrons in the emulsion. δ-ray counting involves the use of fairly sensitive emulsions in which the fuzzy appearance of their tracks makes it easy to recognize heavy nuclei, and makes the detection probability very nearly equal to unity.

The method of grain counting is much more accurate and objective and permits measurement of specific ionization with an error of less than 5 %. It is, however, necessary to employ emulsions of low sensitivity in order to obtain well separated grains along the track of a heavily ionizing particle. An emulsion of given sensitivity will permit good measurements over a range of 10 to 15 in specific ionization only and therefore cover only a small part of the primary spectrum in a single plate. It also becomes difficult to identify a given track as due to a heavy nucleus since δ-rays will not be visible in emulsions of low sensitivity. This last difficulty can be avoided by combining sensitive and insensitive emulsions in closely packed, well aligned, stacks. Heavy particle tracks can then easily be located in the sensitive plate and traced into the insensitive emulsion where grain density measurements are carried out. Table 1 given by Bradt *et al.* [1950c] shows that complete resolution of neighbouring elements is possible, and that therefore the chemical analysis of the primary cosmic ray beam can be carried out by these methods.

TABLE 1

Grain counts for successive 1000 *micron intervals for five tracks traced through several insensitive plates*

Track no.	B 403	568	B 12	B 416	408
Element	carbon	nitrogen	oxygen	neon	magnesium
	265	391	403	555	726
	266	359	390	553	722
	283	307	394	572	737
	251	353	465		
	257	347	385		
	275	348	393		
		350	394		
		351			
Average grains/ 1000 μ	266	351	404	560	728

2. Nuclear interactions and energy measurements

2.1 Different types of nuclear interaction

In order to interpret the nuclear events produced by complex nuclei incident on a target nucleus, it is convenient to consider first the case where the target nucleus is a proton and then look at the event in the more familiar reference system where the proton is moving and the complex nucleus is at rest.

When a proton is incident on a heavy nucleus, a nuclear explosion or "star" is produced. The charged fragments are usually divided into four different categories according to their charge and energy:

(a) Shower particles causing "light tracks". These consist of singly charged particles of high energy with near minimum ionization. Fowler [1950] has shown that more than 75 % of these particles are π-mesons, the remainder mostly protons.

They appear only in collisions involving energies in excess of ~ 1 BeV. and increase in multiplicity as the energy increases. As many as 60 shower particles have been observed to arise from an incident proton whose energy was estimated to exceed 3×10^{12} eV (SCHEIN [1951]). The tracks are usually collimated in the forward direction, the degree of collimation increasing with multiplicity.

(b) Fragments producing "grey tracks". These consist mostly of protons in the energy range from about 20 MeV to 200 MeV with a small admixture of heavier nuclei. The tracks are not collimated but are preferentially emitted in the forward hemisphere. These particles are probably the result of the nucleonic cascade started by the incident proton.

(c) Evaporation tracks consisting of about equal numbers of protons and α-particles with energies of a few MeV and some heavier fragments whose charge rarely exceeds that of a carbon nucleus. The angular distribution of these tracks is spherically symmetrical.

(d) Recoil fragments. This is the part of the target nucleus which has escaped destruction in the collision and has cooled down by the evaporation of α-particles, protons and neutrons. A recoil fragment is almost always present if the target nucleus was heavy. It produces a very short track rarely exceeding a few microns in length.

The appearance of some of these categories of tracks will change if we transform to a coordinate system where the heavy nucleus is moving at high velocity:

(a′) The appearance of the shower particles will not be modified since they consist mostly of mesons produced in nucleon-nucleon encounters. The velocity of the reference system in which the two colliding nucleons have equal and opposite momenta is not changed by the interchange of target and projectile.

(b′) Depending on the velocity of the incident heavy nucleus the group of "grey" tracks will be shifted towards somewhat higher average energies and stronger collimation.

(c′) Evaporation tracks will now appear as a highly collimated beam of protons, α-particles and some heavier fragments with energies per nucleon nearly equal to that of the incident nucleus.

(d′) The recoil fragment appears now as the original incident nucleus, reduced in charge but undeflected and with undiminished velocity.

If the collision occurs not between a heavy nucleus and a proton but between two heavy nuclei the situation is further complicated. All eight categories of tracks may appear. Also, since the number of nucleon-nucleon interactions is greatly increased, the destruction of both nuclei will in general be more complete. The number of shower particles may become very high and at the same time the number of grey tracks will increase at the expense of evaporation tracks and recoil fragments. This is illustrated by the fact that while evaporation particles and recoil fragments are nearly always present in the collision between a proton and a heavy nucleus, only 40 to 50 % of collisions between heavy nuclei result in the narrow showers of protons, α-particles and heavy fragments which denote evaporation of the incident nucleus.

Plate I shows a collision between a primary iron nucleus and (presumably) a silver or bromine nucleus in the emulsion, leading to the complete destruction of both. The number of fragments is close to 100 and considerations of charge conservation show that at least 30 to 50 mesons are present. Almost all tracks are due to singly charged particles of high velocity. In spite of the large number of mesons which must be present, there is only moderate collimation of shower particles, indicating that the high multiplicity is not due to very high energy of the incident nucleons but rather to a large number of nucleon-nucleon collisions at intermediate energies. The absence of a narrow cone of heavy fragments or α-particles in the forward direction shows that the incident nucleus was completely disintegrated.

Fig. 5 shows the collision between a nucleus of $Z = 10 \pm 1$ and a target nucleus which is most probably a proton. No mesons are produced. The incident nucleus evaporates into fragments of charge 3 and 6 or 7. A third track caused by a proton of about 200 MeV may be due to the target nucleus. The heavy fragments are still observed after penetrating several glass plates and have relativistic velocity.

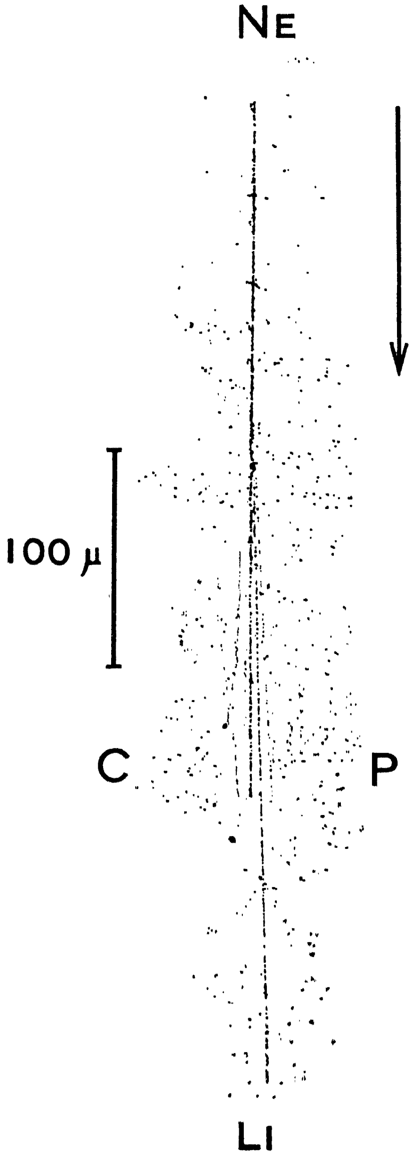

Fig. 5 – A neon nucleus collides with a proton and breaks up into a nucleus of lithium and a carbon (or nitrogen) fragment.

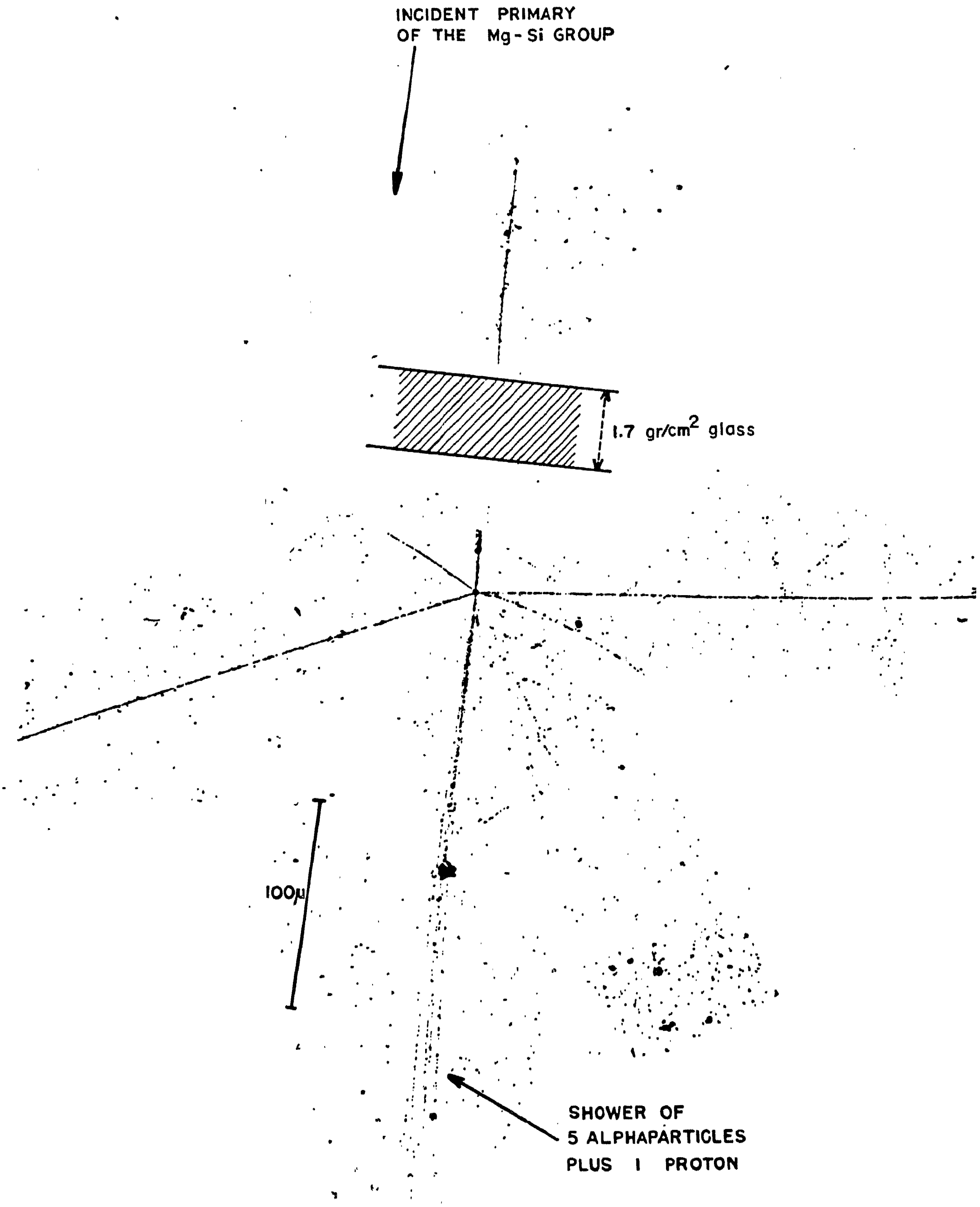

Fig. 6 – A nucleus of the Mg-Si group collides with a nucleus of the emulsion. The narrow shower consisting of one proton and 5 α-particles is believed to be due to the evaporation of the primary nucleus which had been excited in the collision. The other particles emerging from the star are considered to be fragments of the target nucleus.

Fig. 6 illustrates the clear separation between the evaporation tracks of the incident nucleus and the other star fragments. The incident nucleus has a charge $Z = 12$ to 14, its evaporation products are represented by a narrow cone containing five α-particles and one proton, all of relativistic energies. The average angle between the α-particles and the shower axis is 0.03 radian. A similar event is shown in Fig. 7 where a nitrogen nucleus gives rise to a narrow shower containing three α-particles; the angles between the tracks are of the order of 10^{-3} radian.

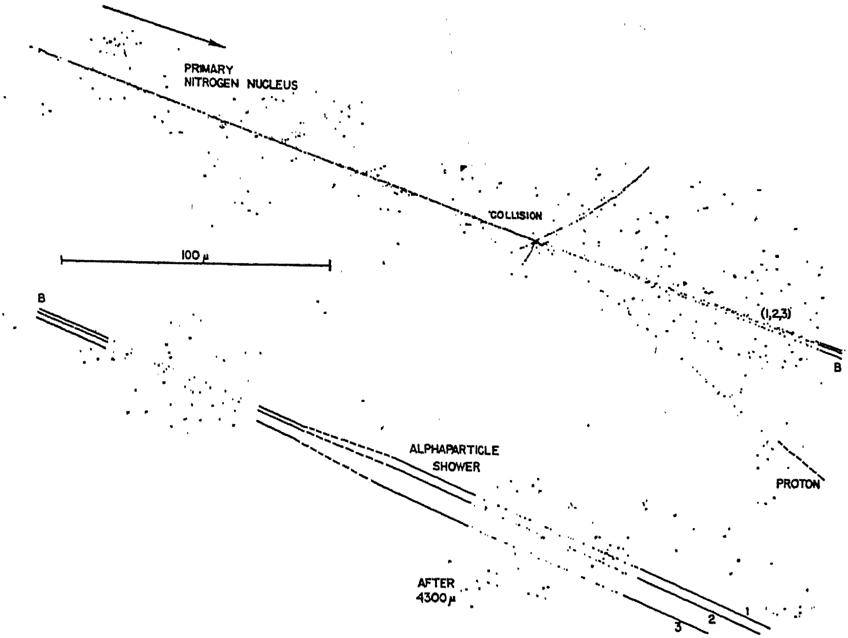

Fig. 7 – A nitrogen nucleus collides with a nucleus of the emulsion. The collision was probably a glancing collision in which the charge of the incident nucleus was reduced by one unit. The excited carbon residue subsequently disintegrated into 3 α-particles which in the laboratory system are emitted in a narrow cone in the forward direction.

Plate II illustrates a collision in which the incident nucleus escapes almost undamaged. The original charge of about 20 is reduced by not more than 2 units. Fig. 8 illustrates the collision of an α-particle of energy $10^{12} - 10^{13}$ eV with a silver or bromine

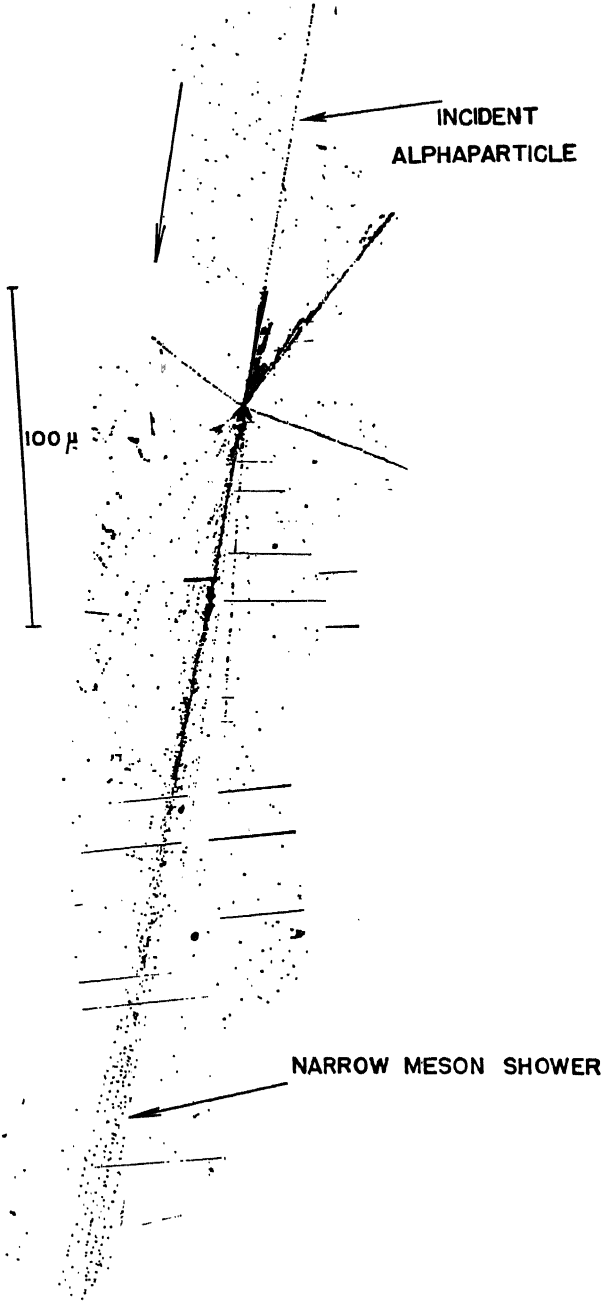

Fig. 8 - A primary α-particle of energy $10^{12}-10^{13}$ eV gives rise to 56 shower particles most of which are mesons. 23 of the shower particles are concentrated in a narrow core. Production of high energy electron-positrons in the core is interpreted as due to γ-rays from the decay of a comparable number of neutral mesons.

nucleus in the emulsion. The total number of charged mesons is larger than 50. Twenty-three shower particles are concentrated in a narrow core which also contains an approximately equal number of high energy γ-rays attributed by Bradt *et al.* [1950b] to the decay of neutral mesons produced in the encounter.

2. 2 Mean free path for nuclear collisions

By exposing large stacks of photographic plates carefully aligned, it is possible to trace the trajectories of heavy nuclei over appreciable distances and therefore study the frequency of collisions leading to complete or partial destruction of the nucleus in some absorber separating the emulsions.

Taking as criterion for a collision that the charge of the nucleus emerging from the absorber must be reduced by at least two units, Bradt *et al.* [1950a, c] obtained the collision mean free path in glass and Kaplon *et al.* [1951] in brass, for four groups of nuclei. Their results are represented in Table 2.

TABLE 2

Atomic Number	Number of Collisions observed		λ (gm. cm^{-2}) glass	λ (gm.cm^{-2}) brass
	in glass	in brass		
$Z = 2$	20	5	50	80
$3 \leqslant Z \leqslant 5$	5	—	47.5	—
$6 \leqslant Z \leqslant 9$	59	43	34.5	58.5
$10 \leqslant Z \leqslant 26$ ($Z_{\text{average}} \sim 14$)	47	26	25.5	49

The corresponding cross-section can be represented by the empirical formula:

$$\sigma = \pi(r_1 + r_2 - 2\Delta r)^2 \tag{5}$$

where the subscripts refer to the two colliding nuclei,

$$r = 1.45 \times 10^{-13} A^{1/3} \text{ cm. and}$$
$$\Delta r = 0.85 \times 10^{-13} \text{ cm.}$$

This formula may be interpreted as a cross-section which is smaller than the geometric cross-section because of the small overlap of nuclear volumes which may occur before strong interaction takes place. Since glass contains mostly the light nuclei oxygen and silicon, the same formula should be applicable for calculating the collision cross-section in air. The corresponding mean free paths are then given by:

Atomic number	λ_a(gm.cm^{-2})
$Z = 2$	44.5
$3 \leqslant Z \leqslant 5$	32.0
$6 \leqslant Z \leqslant 9$	27.0
$10 \leqslant Z \leqslant 26$ ($Z_{\text{average}} \sim 14$)	21.0

It follows that, even at an altitude of 90,000 feet, corresponding to 15 gm. cm^{-2} of residual atmosphere, there is already an appreciable reduction of the flux of heavy nuclei at large zenith angles and a shift in the charge spectrum towards lower atomic number. This shift is due partly to the smaller collision cross-section of lighter nuclei, partly to the addition of fragments from the break up of heavier nuclei and partly to the higher ionization losses of the heavier nuclei. Correcting for the absorption of primaries in nuclear collisions it was shown that at high latitude the angular distribution of heavy particles at balloon altitudes corresponds to an incident flux which is isotropic at the top of the atmosphere.

Conversely, if isotropy at the top of the atmosphere is assumed, the mean free path for destruction of heavy nuclei in air can be obtained from the angular distribution below the top. This method was used by DAINTON *et al.* [1950] to obtain a mean free path in air from the angular distribution of heavy particles at 68,000 feet (52 gm.cm^{-2}). The charge spectrum obtained by these authors shows that at an altitude of 68,000 feet most of the particles of charge $Z > 10$ have already been eliminated by nuclear collisions. Their value for the mean free path of 28 gm.cm^{-2} refers to particles which belong mainly to the carbon, nitrogen, oxygen group and is therefore in very good agreement with the value calculated from collision cross-section of these nuclei in glass.

2. 3 Energy determination for non-relativistic nuclei

If the particle comes to rest in a stack of photographic plates its range in addition to its specific ionization is measured, and charge and energy are determined simultaneously (§ 1. 2). Energy determination is also possible if the particle is sufficiently slow to exhibit an increase of ionization along its path. KAPLON *et al.*

[1951] measured the energy spectrum of particles with charge $Z \geqslant 6$ in the range from 0.35 to 0.7 BeV/nucleon by this method. The spectrum was obtained from the range distribution of particles in a large stack of horizontal emulsions separated by brass absorbers.

As the energy increases, most particles will undergo nuclear collisions before they slow down and very few particles will be found whose range can be measured. Using the collision mean free paths of § 2. 2 one finds that less than 10 % will reach the end of their range if the particle energy exceeds:

0.425	BeV/nucleon	for Helium
0.74	,,	for Oxygen
0.91	,,	for Silicon
1.05	,,	for iron

Different techniques are therefore required to measure the energy spectrum above these values.

Up to energies of a few BeV/nucleon one can use the methods developed by GOLDSCHMIDT *et al.* [1948], OCCHIALINI [1949] and others, who measured the multiple Coulomb scattering of particles traversing nuclear emulsions. The track is divided into equal cell lengths and the angle between sagittas or tangents in neighbouring cells is measured. The mean scattering angle is given by

$$\alpha = \frac{KZ}{\beta p} t^{1/2}$$

where Z, β, p are the charge, velocity and momentum of the scattered particle and t is the cell length employed. The constant K depends mainly on the scattering material and the definition of the mean scattering angle, it is however, also a slowly varying function of the cell length t. CORSON [1950] determined K for nuclear emulsion. He defined α as the mean angle between successive sagittas projected into the plane of the emulsion. The cell length employed was 100 μ. Single large scatterings were omitted from the determination of α if they exceeded four times the mean scattering per cell lengths. With this definition he measured

$$\alpha = (0.26 \pm 0.01)^\circ \text{ for 100 MeV electrons}$$

and 100 μ cell lenghts.

Using the experimental value, the scattering angle for heavy nuclei becomes

$$\alpha = \frac{4.5 \times 10^{-4}}{\beta p_0} t^{1/2} \left(\frac{Z}{M}\right) \tag{6}$$

where α is the scattering angle in radians between successive sagittas projected into a plane containing the track,

$Z/M \sim \frac{1}{2}$ is the charge to mass ratio for heavy nuclei,
t is the cell length in units of 100 μ,
$\beta = v/c$ is the velocity and
p_0 is the momentum per nucleon in units of BeV/c.

The smallest measurable scattering is determined by the finite length of track in the emulsion, by distortion of the emulsion, by imperfections of the microscope stage and by reading errors due to the finite size of grains. The highest energy which can at present be measured is of the order of 2 BeV/nucleon, although occasionally an exceptionally long track may permit the measurement of somewhat higher energies.

2. 4 Energy determination for relativistic nuclei

Energies from 1 BeV/nucleon to approximately 100 BeV per nucleon can be measured by making use of the narrow showers containing α-particles and recoil fragments which are produced in the collision of heavy primary particles and represent the evaporation tracks of the incident nucleus. Illustrations of such showers were given in § 2. 1. Before describing how these measurements are carried out, it is useful to discuss the kinematics of these showers in order to show that the angle of divergence of the shower particles can be used to obtain an energy estimate as well as an upper limit on the energy of the incident particle, and that all shower particles have nearly the velocity of the incident nucleus.

Although in many cases (see Fig. 6) the evaporation shower is clearly separated from the rest of the particles emitted in a collision, it cannot be ruled out that mesons with relativistic energies will sometimes appear in the shower core. We limit ourselves therefore, to shower particles of charge $Z > 1$. In high energy collisions these fragments will have relativistic energies in the laboratory system. Since relativistic multiply charged fragments are not emitted in ordinary stars we can safely assume that they represent particles evaporated from what remained of the incident nucleus after the collision had taken place. Almost all these shower particles are α-particles which should have the same angular distribution and energy spectrum in the rest system of the incident nucleus as the evaporation α-particles from stationary target nuclei since they are produced in identical processes.

Evaporation α-particles have been studied by many observers and are known to be emitted isotropically. LE COUTEUR [1950] and others have discussed their energy spectrum. Their average energy lies between 10—15 MeV and particles above 30 MeV are rare.

The root mean square angle which the shower particles in the laboratory system make with the direction of motion is simply related to their mean kinetic energy in the rest system:

$$\sqrt{\langle\theta^2\rangle} = \left(\frac{\langle T\rangle M}{3\,p_0^2}\right)^{1/2}. \tag{7}$$

Here $<T>$ is the average kinetic energy of the α-particles in the rest system, M is the proton mass and p_0 is the momentum per nucleon of the incident particle. Using 12 MeV for the average α-particle energy one obtains for incident particles of high energy:

$$\sqrt{\langle\theta^2\rangle} = \frac{0.06}{\varepsilon_0} \tag{8}$$

where θ is measured in radians and ε_0 is the total energy per nucleon of the incident particle in BeV. Comparing this value with (6) one sees that multiple Coulomb scattering will change the opening angles of the shower by less than 10 % over a distance of 10 cm. The angles between the shower particles can therefore be measured with very high precision by measuring the separation of tracks in two successive plates separated by several centimetres. Angles of the order of 10^{-4} radian can easily be measured and therefore energy estimates for the incoming particle could be made up to $\sim$ 600 BeV/nucleon.

If the shower contains only two or three α-particles the estimate could be quite wrong since in the rest system all the α-particles may accidentally be emitted in the forward or backward direction close to the direction of motion or because they may all have energies much smaller than the assumed average energy of 12 MeV. Both effects would decrease the opening angle in the laboratory system and lead to an overestimate of the energy. However, as the multiplicity of α-particles increases the danger of gross overestimate decreases rapidly.

If we assume that none of the α-particles are emitted in the rest system with more than 30 MeV, the largest observed angle of any shower particle with respect to the axis gives an upper limit for the energy of the incident particle. The largest possible angle in the laboratory system is given by:

$$\varepsilon_0 \tan \theta_{\max} = \beta_{\max} (\beta_0^2 - \beta_{\max}^2)^{-1/2}$$

or

$$\theta_{\max} \approx \frac{0.12}{\varepsilon_0}. \tag{9}$$

Since $\theta_{\max} \geqslant \sqrt{<\theta^2>}$ it follows that while the energy can be overestimated from the angular aperture of the shower it cannot be underestimated by more than a factor 2.

In the laboratory system the velocities of all α-particles are nearly the same and equal to that of the incident nucleus. If ε, ε' denote the energy per nucleon of an α-particle in the laboratory system and the rest system respectively, ε_0 the energy per nucleon of the incident particle; and ϑ the angle at which the α-particle is emitted in the rest system, then

$$\varepsilon = \varepsilon' \varepsilon_0 + \sqrt{(\varepsilon')^2 - 1}\,\sqrt{\varepsilon_0^2 - 1}\,\cos\vartheta. \tag{10}$$

For $\varepsilon_0 \gg 1$ and $\varepsilon' - 1 \leqslant 8 \times 10^{-3}$ corresponding to the maximum α-particle energy of 30 MeV, the difference in the energy per nucleon of the α-particles and the incident nucleus is limited by:

$$\frac{|\varepsilon - \varepsilon_0|}{\varepsilon_0} \leqslant 13\,\%$$

the most probable energy spread being less than half this value.

The homogeneity in energy of all the shower particles makes it possible to measure the energy of the incident nucleus by measuring multiple Coulomb scattering of the α-particles in the shower.

In order to make scattering measurements in the energy range between 1 to 100 BeV/nucleon it is necessary to reduce the reading error by using large cell lengths and to avoid the error arising from the distortion of emulsions and inaccuracies of the microscope stage. The first can be accomplished by using large stacks of nuclear emulsions separated by several mm of absorber and tracing the shower particles through distances of 10 to 20 cm. Inaccuracies in the stage are eliminated by measuring only the relative scattering of the particles, i.e. measuring their relative separation in successive plates. The effect of distortion in the emulsion can be avoided by measuring the distances between tracks at the point where they enter the glass of the plate.

In the absence of scattering the distances between tracks should increase linearly between evenly spaced plates. Errors arise from relative tilt and rotation of successive plates and small unknown differences in plate spacing. Errors due to tilt and rotation can be made negligible by careful construction. Since the spurious scattering due to variation in plate spacing is proportional to the angle of divergence of the tracks and since for cell lengths of $\sim$1 cm. the true scattering angle is of the order of 3 % of this opening angle, the plate spacing must be known with an accuracy better than ½ %. The required accuracy is independent of the energy to be measured since the error is proportional to the opening angle and the spurious scattering as well as the true scattering is for a given cell length inversely proportional to the particle energy. The error arising from variations in plate spacing can be eliminated in the statistical treatment of the data, since unlike the random scattering it changes simultaneously all distances between the shower particles by the same percentage.

The method of using the relative scattering of evaporation α-particles in order to determine the energy of heavy nuclei has been used by KAPLON *et al.* [1951].

Table 3 summarizes their first results.

The first column gives the charge of the primary nucleus, the next columns:

the nature of the shower particles of charge $Z > 1$,
the cell lengths employed,
the number of cells available for measurement,
the energy per nucleon determined from scattering,
the energy estimate from the r.m.s. angle of the shower particles based on two different values for the average α-particle energy in the rest system,
and the upper limit of the energy based on the largest occurring angle, $\theta_{\max}$.

TABLE 3

Energy of Heavy Primary Nuclei Determined from their Break-up Products

Primary	Shower particles	Cell length mm	No. of cells	Energy from scattering (BeV/nucleon)	Energy from opening angle (BeV/nucleon) for <T>:		Upper limit of energy from opening angle (BeV/nucleon)
					12 MeV	10 MeV	
Ca^{20}	Be^{4} + 6α	27.0	6	32.0	25.0	22.6	37.0
Fe^{26}	B^{5} + 3α	21.4	2	25.5	32.0	29.1	49.0
O^{8}	Be^{4} + 2α	10.4	2	21.0	17.0	15.4	33.0
Mg^{12}	4α	13.7	2	4.3	5.3	4.8	10.0
O^{8}	3α	10.3	4	4.1	5.9	5.4	12.0
C^{6}	3α	10.5	5	3.7	8.0	7.2	18.0
S^{16}	N^{7} + 2α	10.9	4	3.4	3.4	3.0	4.3
Si^{14}	4α	5.2	2	3.3	4.0	3.6	8.0
O^{8}	3α	5.6	2	0.95	1.4	1.2	3.4
Mg^{12}	N^{7} + 2α	5.2	4	0.93	1.0	0.85	2.1
Si^{14}	4α	5.7	2	0.90	1.6	1.40	2.8
Fe^{26}	Mg^{12} + 2α	5.6	4	0.80	1.4	1.20	3.2
Ne^{10}	4α	5.4	2	0.54	0.62	0.53	1.5
S^{16}	O$^{8}_{*}$ + 4α	10.0	2	0.30	0.40	0.34	0.95

* The range of this fragment shows that its energy lies between 0.33 and 0.37 BeV/nucleon.

It is seen that the estimates based on the angular aperture of the shower are in fair agreement with the values obtained from scattering.

3. THE FLUX AND ENERGY SPECTRUM OF PRIMARY COSMIC RAY NUCLEI

The determination of the number of primary protons entering the atmosphere is complicated by the fact that they cannot easily be distinguished from secondary high energy protons produced in collisions in the upper atmosphere. This difficulty is not eliminated if the flux is measured outside the atmosphere by telescopes carried in rockets. Secondary protons are leaving the atmosphere and may even return again after being bent by the earth's magnetic field at large distances. That this effect is appreciable was shown by VAN ALLEN *et al.* [1950] who obtained a counting rate at a height of about 100 km which increased strongly with zenith angle. They observed an angular distribution $I_{(\theta)} = I_{(0)} (1 + 0.6 \sin \theta)$, and attributed the excess at large angles to the atmospheric albedo which may be expected to increase with zenith angle. The vertical flux I_0 represents an upper limit rather than a true value for the primary flux. PERLOW [1951] has demonstrated this by showing that at geomagnetic latitude 41° N even at rocket altitudes part of the vertical counting rate is due to electrons of moderate energy and perhaps to protons whose energy is lower than the magnetic cut-off energy of primary protons at this latitude.

The difficulty of distinguishing primary from secondary particles is not as serious in flux determinations of the heavy primary component. Sometimes collisions in the upper atmosphere will completely destroy these nuclei. At other times part of the heavy nucleus may escape strong interaction with the target nucleus and survive the collision but, if it survives, the residual nucleus with its evaporation products will proceed undeviated in the original direction and cannot leave the atmosphere. Hence at sufficiently high altitudes one measures the true primary flux of the heavy component.

At present most flux measurements on primary heavy nuclei have been made with photographic emulsions at geomagnetic latitudes between 55° and 30° N. In recent months counter equipment designed for the detection of heavy nuclei and measurement of specific ionization has been developed and will no doubt result in more accurate flux values in the near future.

In determining the flux of particles entering the top of the atmosphere from observations carried out below 10—20 gm.cm^{-2} of air several corrections are necessary:

a) The destruction of nuclei in the residual atmosphere has to be taken into account. Since the mean free path for nuclear collisions can be determined directly (as shown in § 2. 2), this correction can be made with fair accuracy.

b) The number of light nuclei will be increased by fragments of heavier nuclei making collisions in the upper atmosphere. This correction is small for α-particles but not for the much rarer elements of charge $Z < 6$. Especially when examining the absence or presence of a particular element of low abundance in the primary cosmic ray beam, this effect has to be considered.

c) At high latitudes particles may enter whose energies are insufficient to penetrate the residual atmosphere above the detector.

In order to penetrate to an atmospheric depth of 15 gm.cm^{-2} the energy of the primaries must exceed

.13 BeV/nucleon for α-particles
.28 BeV/nucleon for Oxygen
.37 BeV/nucleon for Magnesium
.60 BeV/nucleon for Iron

Thus at a latitude $\lambda = 54°$ where the cut-off energy for heavy nuclei is 0.35 BeV/nucleon, the low energy spectrum of particles of charge $Z > 12$ can only be studied at altitudes exceeding 30 km.

3.1 The flux of primary alpha-particles

Helium is, next to hydrogen, by far the most abundant element in the primary cosmic ray beam. The flux of this component has been studied in emulsions (Goldfarb *et al.* [1950]), with proportional counters (Perlow [1951]) and with scintillation counters (Ney [1951]). Data closely related to the flux of primary α-particles have also been obtained with low pressure counters by Singer [1949, 1950] and by Pomerantz *et al.* [1949].

All these measurements are complicated by the fact that the number of secondary particles which have the same specific ionization as primary α-particles is appreciable even at high altitudes. A true flux determination requires therefore not only a measurement of the specific ionization but also an energy measurement to determine whether the particle energy exceeds the geomagnetic cut-off value or is at least sufficiently high to exclude most secondary particles.

Goldfarb tried to distinguish primary helium nuclei from secondary particles by plotting number of particles *vs.* grain density in emulsions exposed under 10—15 gm.cm^{-2} of residual air. A sharp peak in the distribution is obtained at a value of grain density corresponding to four times minimum ionization. From the number of particles in this region of grain density he subtracted a background of secondary particles extrapolated from the number of tracks whose grain density fell outside the peak. Fig. 9 and 10 show the number of tracks obtained at two different latitudes plotted against the specific ionization K in units of minimum

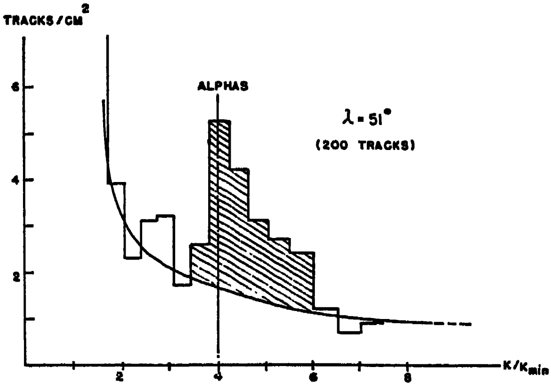

Fig. 9 – Frequency distribution of particles of a given specific ionization K/K_{min} as obtained by grain count observed at geomagnetic latitude $\lambda = 51°$. The peak at $K/K_{\text{min}} = 4$ is attributed to primary α-particles. Since at that latitude all α-particles are admitted whose energy exceeds 0.5 BeV/nucleon the peak is broadened towards larger values of K/K_{min}.

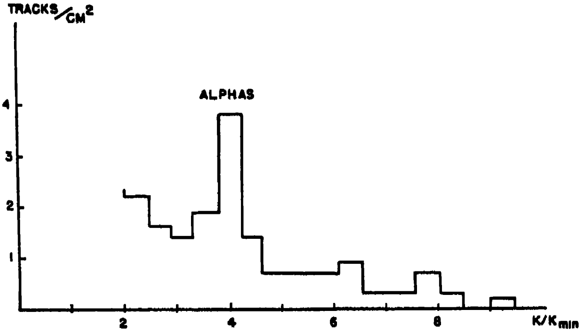

Fig. 10 – Frequency distribution of particles of a given specific ionization K/K_{min} as obtained from grain counting, observed at geomagnetic latitude $\lambda = 30°$. Since at that latitude α-particles are only admitted if their energy exceeds 3.5 BeV/nucleon a sharp peak is produced by the primary helium component at $K/K_{\text{min}} = 4$.

ionization $K_{\min}$. Based on a collision mean free path for α-particles in air of 50 gm.cm^{-2}, he obtains the flux values

$$340 \pm 120 \ \alpha\text{-particles m}^{-2}\,\text{sec}^{-1}\,\text{sterad}^{-1} \text{ at } \lambda = 51^\circ \text{ N}$$

$$80 \pm 30 \ \alpha\text{-particles m}^{-2}\,\text{sec}^{-1}\,\text{sterad}^{-1} \text{ at } \lambda = 30^\circ \text{ N}$$

The large probable error in these flux values is mainly due to the uncertainty in the number of secondary particles of equal ionizing power which have to be subtracted.

At an altitude corresponding to $\sim$ 15—20 gm.cm^{-2} of residual atmosphere, the correction for relativistic α-particles which are fragments of heavier nuclei colliding in the air above is not very large. The nuclei of charge $Z > 2$ constitute less than 10 % of the α-particle flux and less than half of these will have suffered collisions in the first 15—20 gm.cm^{-2} of air. We may expect that per collision the number of fast α-particles produced in air is the same as produced in collisions in glass. This number has been measured and is

0.45 fast α-particles per collision for particles of charge $6 \leqslant Z \leqslant 9$

0.70 fast α-particles per collision for particles of charge $Z \geqslant 10$.

Secondary α-particles from this source will therefore contribute less than 3 % to the flux values given above.

Additional measurements at $\lambda = 30^\circ$ were carried out counting only particles which in addition to the correct ionizing power had a range in glass sufficient to establish their relativistic energy. The new flux value obtained was: 60 ± 10 particles m^{-2}sec^{-1}sterad^{-1}.

The value at $\lambda = 51^\circ$ should be compared with the value 280 ± 8 particles m^{-2}sec^{-1}sterad^{-1} obtained by NEY *et al.* [1951] at $\lambda = 55^\circ$. Their values are based on the pulse height distribution of a scintillation counter inserted into a counter telescope.

POMERANTZ [1949] estimates that about one third of the incident primary particles are helium nuclei.

At $\lambda = 41^\circ$ PERLOW [1951] used a proportional counter inserted into a rocket borne counter telescope and obtained a value of 140 ± 30 α-particles m^{-2}sec^{-1}sterad^{-1}.

At the same latitude SINGER [1949, 1950] measured the efficiency of a low pressure counter inserted into a rocket borne telescope and compared its efficiency to that obtained from mesons at sea level. He interpreted the efficiency ratio of 1.30 ± 0.15 as due to a mixture consisting of 80 % singly charged relativistic particles and 20 % helium or heavier nuclei.

At $\lambda = 0°$ Singer obtains with the same apparatus an efficiency ratio of 1.0 ± 0.2 consistent with a primary beam consisting of protons only. However both α-particles and heavier nuclei whose energy exceeds the magnetic cut-off at the equator have been identified in photographic plates and heavy nuclei have been found in plates exposed at the equator. The value of the helium flux at $\lambda = 0°$ must therefore await further clarification.

The available data for α-particle flux have been collected in Table 4.

TABLE 4

Flux of primary helium nuclei

Geomagnetic latitude	Particles ($m^{-2}sec^{-1}sterad^{-1}$)
$\lambda = 30°$	60 ± 10
$\lambda = 41°$	140 ± 30
$\lambda = 51°$	340 ± 120
$\lambda = 55°$	280 ± 8

Since the α-particle component constitutes a large fraction of the incident nucleons, it seems very desirable to increase the accuracy of these values by counter measurements at different latitudes.

3. 2 The flux of primary nuclei of charge $Z > 2$

The three lightest nuclei in this group: lithium, beryllium and boron are rare in the primary beam. In photographic emulsions their detection is difficult because they have to be sorted out from a large background of secondary tracks of equal ionizing power. Their identity can be established by a combination of grain counting and scattering measurements or by establishing that their range exceeds that of α-particles of equal ionizing power.

In Ney's scintillation counter arrangement pulses corresponding in height to the passage of such particles are mostly due to nuclear disintegrations produced in the counter.

Because the number of primary Li, Be, B nuclei is small while at the same time they frequently occur as fragments in nuclear collisions of heavier primaries, the contribution from collisions in the atmosphere accounts for a sizeable fraction of such nuclei below 20 $gm.cm^{-2}$ of atmosphere.

At present only measurements at geomagnetic latitude $\lambda = 30°$ are available (Bradt *et al.* [1950c]). These measurements are consistent with the complete absence of such nuclei in the primary beam, and yield an upper limit of 0.4 particles $m^{-2}sec^{-1}sterad^{-1}$.

Primary particles of charge $Z \geqslant 6$ are easily detected in photographic emulsions. Their flux was measured below 15—20 $gm.cm^{-2}$ at latitudes $\lambda = 55°, 51°, 41°, 30°$, and the results are given in Table 5.

TABLE 5

Flux of primary nuclei of charge $Z > 2$

Geom. latitude	particles $m^{-2}sec^{-1}sterad^{-1}$		
	$3 \leqslant Z \leqslant 5$	$6 \leqslant Z \leqslant 9$	$Z > 10$
$\lambda = 55°$	?	15 ± 1.5	4.5 ± 1.0
$\lambda = 51°$	?	12 ± 3	3.5 ± 0.7
$\lambda = 41°$	?	5.8 ± 0.7	2.5 ± 0.5
$\lambda = 30°$	$\leqslant 0.4$	3.4 ± 0.5	1.0 ± 0.3

At latitude 55°, below 10 $gm.cm^{-2}$ of air, Ney *et al.* [1951] obtained flux data from the pulse height distribution of a scintillation counter. Their values:

$$16. \pm 2 \text{ particles } m^{-2}sec^{-1}sterad^{-1}, \quad 6 \leqslant Z \leqslant 8$$
$$4.3 \pm 1 \text{ particles } m^{-2}sec^{-1}sterad^{-1}, \quad Z \geqslant 9$$

are in close agreement with the values obtained in photographic emulsion.

The low energy part of the CNO group at $\lambda = 55°$ has been further investigated by measuring the range distribution of those particles which came to rest by ionization loss. It was found that about 20 % of these incident nuclei have energies between 0.3 and 0.45 BeV/nucleon and another 20 % have energies between 0.45 and 0.7 BeV/nucleon. Similar range measurements have been carried out for particles of charge $Z \geqslant 10$ in the energy range from

0.6 to 1.3 BeV/nucleon. The results have been included in Fig. 11.

DAINTON *et al.* [1950] measured at $\lambda = 54°$ the flux of particles with energy sufficient to reach a stack of plates at an altitude corresponding to 52 gm.cm^{-2}. Their flux value is 13 particles m^{-2}sec^{-1}sterad^{-1} of charge $Z \geqslant 6$. Since 70 % of the particles observed at the higher altitudes have sufficient energy to penetrate to this depth, their value is in agreement with other measurements.

INTEGRAL ENERGY SPECTRUM OF PRIMARY COSMIC RAYS

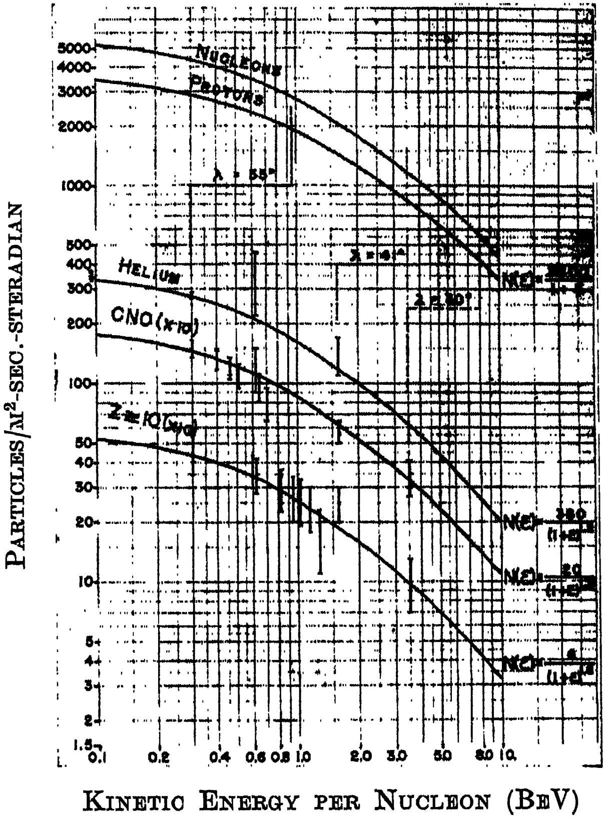

Fig. 11 – Integral energy spectrum of different components of cosmic radiation. The curve for protons was drawn such as to give the observed total primary flux at each latitude.

3. 3 The low energy cut-off for heavy primary nuclei

It is obvious that any high energy ion which traverses a small amount of atmosphere (< 1 mg) will be completely stripped of its orbital electrons. It is however important in connection with the origin of these particles to know whether this stripping occurs in the upper layers of the atmosphere or whether the particles are already stripped outside of the atmosphere and approach the earth as bare nuclei.

If they arrive completely stripped such that their charge to mass ratio $Z/M = \frac{1}{2}$ outside the earth's atmosphere, particles at a given latitude can only arrive if their momentum per nucleon exceeds the value $p_c/2$ where p_c is the cut-off momentum for protons at this latitude.

For instance at $\lambda = 54°$ heavy particles, if they arrive completely stripped, would have a minimum energy of 0.35 BeV/nucleon. This corresponds to a minimum range for carbon and oxygen nuclei of 28 and 21 gm.cm^{-2} respectively. If the particles had retained one of their K-electrons when entering the earth's magnetic field the corresponding ranges would be 15 and 12 gm.cm^{-2} respectively. Bradt *et al.* [1949] found at latitude $\lambda = 54 - 55°$ no carbon or oxygen nuclei with ranges between 15 and 20 gm.cm^{-2} but an appreciable number with ranges between 20 and 40 gm.cm^{-2}. This shows that at least the light particles have lost all electrons before entering the atmosphere.

At the same latitude very heavy nuclei like iron would only penetrate 6.8 gm.cm^{-2} if their energy is 0.35 BeV/nucleon. Observations at altitudes corresponding to less than 5 gm.cm^{-2} of residual atmosphere would be required to establish whether these particles also arrive completely stripped or whether particles with less than 0.35 BeV/nucleon are admitted. Such altitudes are not accessible to balloons at present. Nevertheless it seems fairly certain that very heavy particles also arrive without any electronic shells. This follows from the observation that no slow heavy nuclei have been found at $\lambda = 30°$ where the cut-off energy for bare nuclei in 3.5 BeV per nucleon and that the lowest energies observed so far at $\lambda = 41°$ correspond exactly to the cut-off value for bare nuclei (1.6 BeV/nucleon).

It seems therefore safe to assume that the latitude effect can be used to establish the energy spectrum for nuclei of any charge value.

3. 4 Time fluctuations in the flux of heavy nuclei

All the flux values of Table 5 have been obtained in daylight flights. Recently LORD *et al.* [1950] have reported large time fluctuations in the heavy particle flux at $\lambda = 55°$, probably correlated with time of day. The number of particles whose δ-ray density corresponds to more than 100 times the ionization of a singly-charged relativistic particle was found to be smaller by a factor of 2.5 in two flights carried out at night time, compared to the corresponding number in day flights. At latitude 54° these particles consist of heavy primaries of charge $Z \geqslant 10$ and the more numerous low energy nuclei of the carbon, nitrogen, oxygen group. It is not known yet whether the observed fluctuations are confined to the low energy primaries or extend over all energy ranges. The experiment is difficult because the number of low energy primaries are very sensitive to the geomagnetic and the atmospheric cut-off and the observed number depends therefore critically not only on the height of the balloons but also on their drift in the north-south direction.

A much smaller time fluctuation of heavy primary particles was also observed by NEY *et al.* [1951] at the same latitude. These workers found, between 10.30 a.m. and 3 p.m., an increase of 35 % in the counting rate of particles whose specific ionization exceeded 16 times the minimum value. At the same time the counting rate of particles with minimum ionization stayed constant within 3 %.

3. 5 The energy spectrum of primary cosmic rays

In addition to the information obtained from the variation of flux with geomagnetic latitude, range measurements have furnished some data in the low energy region and scattering measurements in the high energy region. The results obtained from the range distribution of particles of charge $Z \geqslant 6$ at $\lambda = 55°$ have already been mentioned. Large horizontal sheets of emulsion were inserted between absorbers and exposed at altitudes corresponding to 20 gm.cm^{-2}. On the assumption that the cross-section for nuclear collisions in the absorber does not depend on the energy of the primary particle, the observed range distribution of particles coming to rest by ionization can be transformed into an energy distribution at the top of the atmosphere.

Energy determinations at higher energy were made by measuring the relative scattering of α-particle fragments in the narrow "evaporation" showers as described in § 2. 3.

Heavy primaries incident on a stack of horizontal emulsions separated by brass plates were followed through the stack; the energy was determined for all those giving rise to narrow α-particle showers.

Examples of such energy determinations were given in Table 3. Since there is a close correspondence between the energy values obtained from the relative scattering of the α-particles and those obtained from the mean square opening angle of the shower, the results of both kinds of measurement can be combined. Most of the primaries whose energy has been measured in this way have charge $Z \geqslant 12$.

Only if we assume that the number of evaporation α-particles produced in a collision between heavy nuclei is, at energies above about 1.5 BeV/nucleon, independent of energy and depends only on the size of the nuclei and the impact parameter, do such measurements determine the differential energy spectrum of heavy nuclei above 1.5 BeV/nucleon. This assumption, while not unreasonable, cannot at present be proved.

The difficulty could perhaps be avoided by using absorbers of low atomic number between emulsions. If the absorber contains a large amount of hydrogen the probability of obtaining in a given collision a narrow α-particle shower will be greatly increased and may approach unity for all energies above 1 BeV/nucleon.

The data discussed in §§ 3. 1 and 3. 2 can be represented by an energy spectrum which is identical for all heavy primaries in the energy range from 0.35 to $\sim$ 10 BeV/nucleon. The number of particles $m^{-2}sec^{-1}sterad^{-1}$ with kinetic energy per nucleon in excess of ε (BeV) is then given by:

$$N(\varepsilon) = \frac{K}{(1+\varepsilon)^{1.2}} \tag{11}$$

where $K = 380$ for Helium
$K = 20$ for Carbon, Nitrogen, Oxygen
$K = 6$ for particles of charge $Z \geqslant 9$.

In order to account for the total primary flux as measured by the vertical counting rate of telescopes above ~ 15 gm.cm^{-2} of residual atmosphere (WINCKLER *et al.* [1950]) we must assume for the proton component in the same energy range a spectrum which falls off somewhat more slowly:

$$N(\varepsilon) = \frac{K_p}{1+\varepsilon} \tag{12}$$

where $K_p = 3800$.

Fig. 11 shows the integral energy spectrum for protons, helium, CNO and heavier nuclei. It shows also the total number of nucleons incident with energies larger than ε. The experimental points are indicated on the graph.

In order to obtain the total primary flux as a function of latitude we have to add the flux of protons whose momentum exceeds the cut-off value p_c to the flux of heavy particles whose momentum per nucleon exceeds the value $p_c/2$. The proton energy spectrum and intensity in Fig. 11 has been so chosen as to give a total primary flux at each latitude in agreement with the values given by Winckler.

There are then 3630 nucleons m^{-2}sec^{-1}sterad^{-1} incident on the atmosphere with energies between 0.35 and 8 BeV. They carry a total energy of 8000 BeV m^{-2}sec^{-1}sterad^{-1} or an average energy of 2.2 BeV/nucleon. Of these nucleons

66 % are due to protons
26 % due to helium
5 % due to carbon, nitrogen, oxygen
3 % due to particles of charge $Z \geqslant 9$

These percentages represent also very nearly the relative amounts of energy carried by each component.

The contribution of the heavy primary components to the sea level cosmic ray intensity cannot as yet be determined. The total latitude effect at sea level amounts to only 14 %; therefore 86 % of all sea level mesons must be produced by the latitude insensitive part of the primaries that is by protons of energy larger than ~ 15 BeV and heavy nuclei of energy larger than ~ 6.6 BeV/nucleon. The composition of the primary radiation above these energies is still unknown.

It is interesting to note that within the accuracy of the measurements all heavy primary particles seem to have the same velocity spectrum.

This fact permits a test of various hypotheses concerning the accelerating mechanism of primary particles and will be further discussed in § 5.

4. THE CHEMICAL COMPOSITION OF PRIMARY COSMIC RADIATION

4. 1 The charge spectrum between latitudes $\lambda = 55°$ and $\lambda = 30°$

In §§ 2 and 3 we have divided the heavy component of primary radiation into four groups: α-particles, the group comprising lithium, beryllium and boron; the carbon, nitrogen and oxygen group and the heavy group containing elements up to charge $Z \sim 26$. From the data in Table 1 (§ 1. 2) it is, however, apparent that under favourable conditions the atomic number of primary nuclei can be determined with much greater precision, and that it is in fact possible to determine separately the flux for each element in the primary beam. Such a detailed analysis has not been carried out as yet. Nevertheless the charge determinations given by Bradt *et al.* [1950a, b] permit one to distinguish some of the finer features in the charge spectrum.

Fig. 12 gives a histogram of 422 heavy primary particles ($Z \geqslant 6$) observed under 15 gm.cm^{-2} of atmosphere. Results obtained at

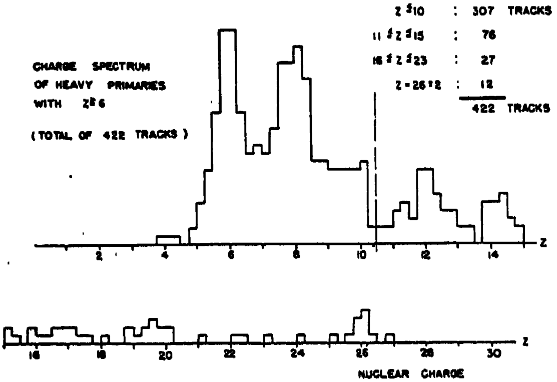

Fig. 12 – Charge spectrum of primary nuclei ($Z \geqslant 6$) observed under 15 gm.cm^{-2} of atmosphere at $\lambda = 55°$ and 30°. The charge determinations were based on the δ-ray density of the tracks.

geomagnetic latitudes $\lambda = 55°$ and $\lambda = 30°$ have been combined, since within the accuracy of the charge measurements the relative intensity of all elements seemed to be identical. The charge values represented in this histogram were obtained by δ-ray counting. Fig. 13 shows a similar charge spectrum of particles observed at $\lambda = 30°$ under 20 gm.cm^{-2} of residual atmosphere. Here the analysis has been extended to include particles of charge $3 \leqslant Z \leqslant 5$ and the charge values were obtained by grain counting in under-developed emulsions as described in § 1. 2. This technique results in a higher dispersion for elements of atomic number below silicon. The black and shaded areas in the histogram represent the result of a systematic survey including all particles traversing a given plate in the stack; the shaded area represents nuclei identified as fragments from heavier nuclei which have undergone collisions in the stack before they reached the particular plate in which the survey was carried out. The open square represents additional particles observed in a less systematic manner.

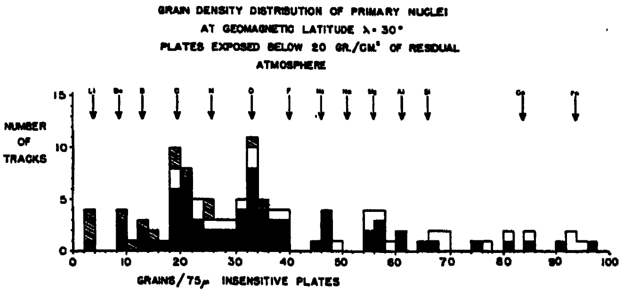

Fig. 13 – Charge spectrum of primary nuclei $Z > 2$ observed at geomagnetic latitude $\lambda = 30°$. The charge determination was based on the grain density of tracks in emulsions of low sensitivity.

Both spectra show that at least up to silicon the distribution of elements is not a smoothly varying function of atomic number and that elements of even charge are more abundant than their immediate neighbours of odd charge. They both terminate abruptly at elements of charge 26—28. No nucleus heavier than iron, cobalt or nickel has been identified among nearly one thousand particles whose charge has been measured. However a few nuclei of higher charge have been reported by other authors (Freier *et al* [1948]; Sörensen [1949]; Fong [1950]).

The elements carbon and oxygen are definitely present in very nearly equal abundance and represent the strongest component next to hydrogen and helium. The occurrence of neon, magnesium, silicon and iron seems also well established. They appear in comparable numbers. The nuclei between silicon and iron cannot as yet be identified. In the measurements represented in Fig. 13 a primary nucleus had on the average to traverse 15 $\mathrm{gm.cm^{-2}}$ of glass in addition to 20 $\mathrm{gm.cm^{-2}}$ of air in order to reach the plate in which the survey was made. This affects the spectrum in two ways:

(a) A smaller proportion of the very heavy nuclei will be observed because their cross-sections for destruction by nuclear collisions are greater than that of the carbon oxygen group. This effect is largely compensated for if one includes the open squares of the less systematic survey.
The elements carbon and oxygen are therefore each approximately eight times as abundant as the elements neon, magnesium, silicon and iron.

(b) Particles will appear among the lighter elements which are fragments of heavier nuclei partially destroyed in the upper atmosphere. Since the particles had to traverse approximately equal amounts of air and glass, this contribution will for each element be approximately equal to the shaded area which represents fragments produced in the glass.

The effect on particles of charge $Z \geqslant 10$ will be negligible, because very heavy collision fragments are rare, and because the number of nuclei large enough to produce such heavy splinters is small.

The correction is small for carbon and oxygen because of their relatively large abundance. On the other hand the lithium, beryllium and boron nuclei must almost all be attributed to collisions in the air. This is indicated by the fact that in Fig. 13 the black and shaded areas are nearly equal. Not only do such nuclei arise with large probability as splinters in nuclear collision but also, being lighter than carbon and oxygen, they can arise from the most abundant component of the heavy nuclei. We must conclude from Fig. 13 that their flux at the top of the atmosphere at $\lambda = 30°$ is either zero or at most 10 % of the flux of carbon and oxygen nuclei [1].

Insufficient resolution makes it as yet uncertain whether nitrogen and fluorine occur in the primary beam; they may be hidden in the tail of the strong carbon and oxygen peaks. Oxygen collisions in the upper atmosphere could be responsible for most of those nitrogen nuclei which because of exceptionally long track length could definitely be identified. The abundance of nitrogen and fluorine could however, hardly be greater than one third of the carbon or oxygen abundance.

4.2 Comparison of the cosmic abundance of elements with their abundance in primary cosmic rays

Present knowledge about the relative abundance of chemical elements in the universe is based on the study of the spectra of stars and planetary nebulae, on the absorption of light in interstellar space and on the chemical analysis of meteorites, the earth's atmosphere and its crust. There is a remarkable similarity between the relative abundances of non-volatile elements in meteorites and in the solar atmosphere, as well as between abundances of elements obtained from the spectrum of the sun and that of other astronomically unrelated stars and planetary nebulae. Although the composition of the interior of stars and of the vast amounts of finely divided matter between stars is still largely unknown, the observed similarities in the results derived by different methods and from different sources suggest a more or less uniform chemical composition of the universe and have led several authors to compile cosmic abundance tables.

For our comparison we shall use the values given by Brown [1949], who discusses the assumptions underlying the construction of his table of cosmic abundances and the uncertainties involved in estimating the abundance of various elements. We shall compare these abundances with the composition of the primary cosmic ray beam in the velocity interval corresponding to 0.3 to ~ 10 BeV/nucleon. As shown in § 3. 4 the composition stays reasonably constant in this interval which contains the bulk of the primary radiation. It is perhaps more natural for the purpose of this comparison to use the composition of the primary beam in a given velocity interval rather than the composition incident at a given magnetic latitude.

---

[1] Dainton *et al.* recently reported a large flux of primary lithium, beryllium and boron nuclei at geomagnetic latitude $\lambda = 54°$. They concluded that some of the particles whose observed δ-ray density corresponded to a specific ionization larger than nine times minimum showed too small a Coulomb scattering to be attributed to slow doubly charged particles and some of the particles whose ionization exceeded thirty-six times minimum too large a scattering to be attributed to fast carbon nuclei. Although these measurements were made at a different latitude than those of Bradt *et al.* it nevertheless seems that the different techniques used by the two groups of authors lead to contradictory results.

Table 6 lists the most abundant elements in the universe as well as the corresponding abundances of these elements in the cosmic radiation. The cosmic ray values for the relative flux of hydrogen, helium, carbon and oxygen are known with about 25 % accuracy. The values for neon, magnesium, silicon and the group around iron are probably correct within a factor of two as are most of the values for cosmic abundances.

TABLE 6

Abundance in universe according to H. Brown

Z Element	atoms per 10^5 atoms of hydr.		abundance in cosmic radiation	
1 Hydrogen	100,000		100,000	
2 Helium	10,000		10,000	
8 Oxygen	63	132	260	520
7 Nitrogen	46		?	
6 Carbon	23		260	
10 Neon	2.6–70		30	
26 Iron	5		30	
14 Silicon	2.9		30	
12 Magnesium	2.5		40	
All other elements $Z \leqslant 30$	2.7		30	
All elements $30 < Z \leqslant 92$	4×10^{-3}		< 1	

The relative abundances of elements in the universe and in primary cosmic radiation are surprisingly similar. Except for nitrogen whose intensity in the cosmic ray beam is as yet unknown, abundant elements in cosmic rays are the elements of the highest abundance in the universe. The hydrogen to helium ratio, the carbon to oxygen ratio and the ratios between the most abundant elements of $10 \leqslant Z \leqslant 26$ are the same within the experimental error. Compared to helium, the CNO group, as well as the group of elements of charge $10 \leqslant Z \leqslant 26$, seem somewhat stronger in cosmic rays than in the universe. While the iron-nickel group is strong, elements of charge $Z > 30$ are extremely rare in both columns of Table 6.

A satisfactory theory of the origin of cosmic rays will have to account for this similarity of composition as well as for the similarity of the velocity spectrum of different nuclear species, discussed in § 3. It may therefore be useful to consider whether some information on the origin can be derived from our present knowledge of primary cosmic radiation. Because our knowledge of primary radiation is still incomplete, such a discussion will necessarily have to be preliminary and tentative.

5. THE COMPOSITION OF PRIMARY COSMIC RADIATION AND THE PROBLEM OF ITS ORIGIN

The chemical composition of the primary radiation as it enters the earth's atmosphere will not necessarily be identical with the chemical composition which prevails in the region in which it originates.

The process in which the atoms are accelerated may favour some components with respect to others and therefore result in a beam whose composition is quite different from the composition of the source region. A further modification may occur between the time the particles are accelerated and the time when they arrive at the atmosphere. Such a modification would occur if the accelerated particles had to traverse appreciable amounts of matter during their journey through space and therefore suffered nuclear collisions resulting in partial or complete breakup. The similarity between universe abundances and the chemical composition of the radiation hitting the earth is therefore not trivial and could be accidental.

We shall first consider the question whether the chemical composition of the primary radiation as observed on earth is similar to the composition of the beam which was accelerated at the source or whether it has been modified by nuclear collisions in the interstellar medium. If an energetic heavy nucleus collides with a proton in the interstellar gas it will disintegrate into protons, neutrons, α-particles and heavier fragments and most of these disintegration products will proceed with nearly undiminished velocity. The collision products (including the neutrons which decay into protons) will therefore themselves become components of the primary radiation as observed on earth. We may inquire whether the chemical composition of the primary radiation contains any evidence for such breakup products.

Let us assume that particles of various atomic numbers are continuously being injected by some source in the galaxy and that they are retained in the galaxy by suitable magnetic fields until they are destroyed by nuclear collisions with interstellar hydrogen. The heavier nuclei will eventually be disintegrated by successive collisions into protons which will then be removed from the cosmic ray beam by inelastic collisions. If this picture is correct the composition of the primary radiation will reach some equilibrium and will consist of a mixture of the elements which are injected and of their collision products. The observed composition permits us to calculate the rate of production of each element at the source if we know its cross-section for collision with protons and the type of fragments which result from such a collision.

Since the cross section and fragmentation of nuclei colliding with fast protons is known from the study of stars in photographic plates we can attempt to calculate the rate of production at the source. The equilibrium condition requires that

$$\frac{dN_i}{dt} = 0 = F_i - \frac{N_i}{\tau_i} + \sum_{j>i} p_{ij} \frac{N_j}{\tau_j}. \tag{13}$$

Here N_i are the number of nuclei of element "i" in the primary beam.

F_i is their number injected per unit time.

τ_i is their average life-time in the proton gas.

p_{ij} is the probability that the collision between a proton and a nucleus of element "j" will lead to a fragment of element "i".

The summation is carried out over all nuclei heavier than element "i" ($j > i$). Since the lifetimes τ_i are inversely proportional to the collision cross-sections σ_i, the equation can be written

$$N_i = F_i \tau_i + \sum_{j>i} p_{ij} N_j \frac{\sigma_j}{\sigma_i}$$

and

$$\frac{F_i}{F_k} = \frac{N_i \sigma_i - \sum\limits_{j>i} p_{ij} N_j \sigma_j}{N_k \sigma_k - \sum\limits_{j>k} p_{kj} N_j \sigma_j}. \tag{14}$$

All quantities on the left are known from the measurements of the primary flux or can be estimated from the production of stars by fast protons and an analysis of their fragments.

Such a calculation made by BRADT *et al.* [1950a, c] shows that a reasonable fit with the observed abundance of elements in the primary beam is obtained only if nuclei of the CNO group and of the group $Z \geqslant 10$ are accelerated at the source in the ratio of about 2 : 1 and that the rate of injection (F) is zero or very small for all other nuclei. In particular most of the protons and α-particles in the primary beam should be fragments from heavier nuclei.

But even if we neglect the contribution of fragments from heavy nuclei to the observed proton component, the ratio of the number of protons injected at the source to the number of injected nuclei of charge $Z \geqslant 10$ cannot be very large; it must be smaller than their ratio in the observed beam multiplied by the ratio of their collision cross sections.

If we assume that the collisions in interstellar space are mostly collisions with hydrogen, the collision cross-section for nuclei of charge $Z \geqslant 10$ is nearly equal to the geometric area or approximately $\sigma_A = 7 \times 10^{-25}$ cm². The cross-section corresponding to the elimination of protons from the primary cosmic ray beam is smaller than the total collision cross-section, because only those collisions are effective in which both nucleons emerge with greatly reduced energy. We shall assume $\sigma_p \leqslant 2 \times 10^{-26}$ cm².

According to § 3. 5 the ratio of protons to nuclei of charge $Z \geqslant 10$ in the primary radiation is $N_p/N_A = \frac{3800}{6}$. The ratio of protons to heavy nuclei injected at the source should therefore be

$$\frac{F_p}{F_A} \leqslant \frac{N_p \cdot \sigma_p}{N_A \cdot \sigma_A} \approx 18.$$

Therefore if collisions play an important part in the history of the primary particles, we must devise an accelerating mechanism which strongly favours the acceleration of heavy particles and injects very few of the light nuclei in spite of their overwhelming abundance in the universe.

A similar calculation shows that the number of lithium, beryllium and boron nuclei produced in interstellar collisions with hydrogen or with heavier atoms would be so large that even if none were accelerated at the source, they should be approximately as abundant in the primary beam as the carbon, nitrogen, oxygen group. Because of their extremely low cosmic abundance, a lithium, beryllium and boron component in the primary beam would almost certainly have to be attributed to collisions in interstellar space.

Thus a large primary flux of nuclei of charge $3 \leqslant Z \leqslant 5$ would indicate:

(a) that we are on earth observing a mixture of particles accelerated at the source and their fragments produced in interstellar space,

(b) that the accelerating mechanism at the source is strongly selective in favouring the acceleration of heavy elements compared to the much more abundant hydrogen and helium nuclei,

(c) and that the close agreement between the cosmic abundance of elements and their relative number in the cosmic ray beam impinging on the atmosphere is largely accidental.

On the other hand, if, as indicated by the measurements of Bradt *et al.*, Li, Be and B nuclei are either absent or very rare in cosmic radiation, one may conclude that the chemical composition of the primary radiation has not been appreciably modified since it left the source and that the composition of the cosmic ray beam reflects the chemical composition of the source region [2].

If we can be sure that the primary particles observed at the top of the atmosphere are particles originally accelerated at the source and not collision fragments of heavier nuclei, the abundance of the noble gases, particularly of neon and argon becomes of great interest. Their cosmic abundance as derived from spectra is very uncertain. In Brown's table the abundance of these elements was obtained by extrapolation from the abundance of neighbouring nuclei. Their appearance in the cosmic ray beam may confirm the validity of this extrapolation. Ionized neon and argon have been observed in some stars and in planetary nebulae but have not been found in the sun or in solar flares. The question of the abundance of these elements in the primary beam is therefore of great significance in discussing the origin of cosmic rays.

---

[2] See however footnote page 41. In view of the existing discrepancy in experimental results no decision between these two possibilities can at present be made.

Next we may attempt to use our information on the composition and energy spectrum of cosmic ray nuclei to obtain some information about the mechanism by which they were accelerated.

In § 3. 4 it is shown that nuclei of atomic weight between 40 and 60 with total kinetic energies of at least 10^{11}—10^{12} eV form a measurable part of cosmic radiation. The acceleration process must therefore be of such a nature as to be capable of imparting to a complex and relatively loosely bound nuclear structure an energy which is very large compared to the binding energy of its constituent parts. This makes it almost certain that the particles do not derive their energy from some catastrophic nuclear event. The suggestion that cosmic ray particles obtain their energy from spontaneous annihilation of atoms in interstellar space (MILLIKAN *et al.* [1942]) or from the annihilation of matter and antimatter (KLEIN [1944]) could not easily be reconciled with the observation of complex nuclei of high energy.

An entirely different accelerating mechanism has been suggested by FERMI [1949]. In his theory the particles derive their energy from the kinetic energy of interstellar matter by colliding with the magnetic fields assumed to be attached to highly ionized gaseous clouds travelling in our galaxy. As Fermi points out, this mechanism is not capable of accelerating heavy nuclei unless they have already obtained very large energies by some different acceleration process. For instance the energy of an iron nucleus has to exceed 3×10^{11} eV before it can be further accelerated by such a process. Such an accelerating mechanism discriminates therefore very strongly against nuclei heavier than protons. and seems to be hard to reconcile with the observed composition of the primary beam.

An electrostatic or electromagnetic accelerating mechanism seems preferable since it does not discriminate so strongly against heavier elements. If we assume such a mechanism we note first of all that the relative number of particles of different elements entering the accelerating process is proportional to the relative number of ions and not to the relative number of atoms in the source region. Unless the source region is very hot or very rarefied the ratio of ions to neutral atoms will depend in an extremely sensitive way on the ionization potential of a particular element and we might expect that elements whose ionization potential is low will be prominent in the cosmic radiation, while those with high ionization potential, particularly the noble gases should be negligible by comparison. From Table 6 we see that this is not the case. The elements helium, oxygen, magnesium and neon for example occur in ratios comparable with their cosmic abundance ratio, although their ionization potentials range from 7.6 eV for magnesium to 21.5 eV for neon and 24.5 eV for helium. The chemical composition of primary radiation therefore suggests that all atoms, even those of noble gases, are ionized in the source region, or that noble gases are not originally accelerated ionized but produced later as fragments from accelerated nuclei suffering collisions in interstellar matter. If the latter alternative were correct we should, however, also observe nuclei of lithium, beryllium and boron as pointed out earlier in this section.

Apart from the fact that only ionized atoms can enter the accelerating process we would expect that an electrostatic or electromagnetic accelerating process should favour protons over heavier ions because of their higher charge to mass ratio.

On the other hand the charge to mass ratio of all particles heavier than protons is very nearly the same once they are completely stripped of electrons. If the main part of the accelerating process occurs after this stripping has taken place, the velocity spectrum of all nuclei from helium to iron should be identical. As shown in Fig. 11 a single velocity spectrum for the heavy component is indicated by the measurements available at present.

It would be very important to know whether this equality of the velocity spectra holds accurately for all heavy nuclei in all energy ranges. Let us assume for instance that, as in the process suggested by Fermi, the acceleration takes place in our galaxy over very long periods until the particle finally suffers a nuclear collision in the interstellar material. In this case, because of their larger collision cross-section, very large nuclei would spend less time in the accelerating process and fewer should reach very high energies. The velocity spectrum would therefore, as pointed out by Fermi, fall off faster for heavy than for lighter nuclei. If this is not the case we have to assume that the acceleration takes place in a much shorter time.

Let us now assume an electromagnetic accelerating process which produces cosmic ray particles in a time short compared to the time between nuclear collisions in interstellar matter. Such a process would produce the same velocity spectrum for all heavy nuclei provided the main part of the acceleration occurs after the particles have lost all their electrons and have achieved the same charge to mass ratio. The subsequent traversal of interstellar matter should not destroy the similarity of velocity spectra for particles of different mass, at least in the high energy region. This follows if we assume that the cross-section for nuclear collisions in interstellar matter is proportional to the geometric area of the nucleus and independent of its energy. Elimination of particles by nuclear collisions will therefore reduce the intensity of the large nuclei compared to the lighter ones without affecting the shape of the spectrum. The energy loss due to ionization produced in interstellar matter should only affect the similarity of the spectra in the non-relativistic region, because the amount of energy loss which a nucleon can suffer before undergoing nuclear collisions is relatively small. If we assume a specific ionization loss of 4.7 Z^2 MeV gm.cm^{-2} in interstellar hydrogen gas for a relativistic particle of charge Z, and if we assume a cross-section σ for collision with protons equal to the geometric area of the heavy nucleus, the energy loss by ionization per nucleon and per mean free path is given by

$$d\varepsilon = \frac{4.7\,Z^2}{A} \cdot \frac{M_p}{\pi r_0^2 A^{2/3}} \approx 34.5\,Z^{1/3}\,\text{MeV}$$

where M_p is the proton mass and $r_0 = 1.5 \times 10^{-13}$ cm. Thus the energy per nucleon which a particle can lose by ionization before it is destroyed by a collision with protons in the interstellar gas is a slowly varying function of Z and is even for nuclei as heavy as iron only of the order of 100 MeV. The traversal of interstellar gas should therefore not destroy any initial similarity of the velocity spectrum for nuclei of different mass if their energy exceeds about 1 BeV/nucleon. In the low energy region of the spectrum, however, the effect of an absorbing gas layer becomes important and since it depends on the nuclear charge, it may destroy an initial similarity.

Present data on the low energy part of the spectrum are not yet accurate enough to permit such an analysis. A more detailed study of the intensity and energy spectrum of each of the elements represented in the cosmic ray beam, in particular the spectrum at low energies, seems necessary to provide further guidance for the development of a satisfactory theory of the origin of cosmic rays.

REFERENCES

ALFVÉN, H., 1939, Nature, Lond., 143, 435.

BRADT, H. L. and B. PETERS, 1948, Phys. Rev., 74, 1828.

BRADT, H. L. and B. PETERS, 1949, Phys. Rev., 76, 156.

BRADT, H. L. and B. PETERS, 1950a, Phys. Rev., 77, 54.

BRADT, H. L., M. F. KAPLON and B. PETERS, 1950b, Helv. Phys. Acta, 23, 24.

BRADT, H. L. and B. PETERS, 1950c, Phys. Rev., 80, 943.

BROWN, H., 1949, Rev. Mod. Phys., 21, 625.

CORSON, D. R., 1950, Phys. Rev., 80, 303.

CORSON, D. R., April 1951, Washington Mtg. Am. Phys. Soc.

CRITCHFIELD, C. L., E. P. NEY and S. OLESKA, 1950, Phys. Rev., 79, 402.

DAINTON, A. D. and D. W. KENT, 1950, Phil. Mag. 41, 963.

FERMI, E., 1949, Phys. Rev., 75, 1169.

FONG, H. T., May 1951, Thesis, Université de Paris.

FOWLER, P. H., 1950, Phil. Mag., 41, 169.

FREIER, P., E. J. LOFGREN, E. P. NEY, F. OPPENHEIMER, H. L. BRADT and B. PETERS, 1948a, Phys. Rev., 74, 213.

FREIER, P., E. J. LOFGREN, E. P. NEY and F. OPPENHEIMER, 1948b, Phys. Rev., 74, 1818.

GOLDFARB, L., H. L. BRADT and B. PETERS, 1950, Phys. Rev., 77, 751.

GOLDSCHMIDT–CLERMONT, Y., D. T. KING, H. MUIRHEAD and D. M. RITSON, 1948, Proc. Phys. Soc., 61, 183.

HEITLER, W., 1944, The Quantum Theory of Radation, 2nd ed. (Oxford University Press).

HULSIZER, R., 1949, Phys. Rev., 76, 164.

KAPLON, M. F., B. PETERS, H. L. REYNOLDS and D. M. RITSON, 1951, Phys. Rev. (in press).

KLEIN, O., 1944, Ark. Mat. Astr. Fys., 31A.

LE COUTEUR, K. J., 1950, Proc. Phys. Soc., A63, 259.

LORD, J. J. and M. SCHEIN, 1950, Phys. Rev., 80, 304.

MILLIKAN, R. A., H. V. NEHER and W. H. PICKERING, 1942, Phys. Rev., 61, 397.

MOTT, N. F., 1929, Proc. Roy. Soc., A124, 425.

NEY, E. P. and D. M. THON, 1951, Phys. Rev., 81, 1068.

OCCHIALINI, G. P. S., 1949, Nuovo Cim. 6, Suppl., 413.

PERLOW, G. J. and L. R. DAVIS, 1951. Private communication.

PERKINS, D. H., 1950, Proc. Roy. Soc. A203, 399.

POMERANTZ, M. A. and F. L. HEREFORD, 1949, Phys. Rev., 76, 997.

SCHEIN, M., W. P. JESSE and E. O. WOLLAN, 1941, Phys. Rev., 59, 615

SCHEIN, M., 1951. Private communication.

SINGER, S. F., 1949, Phys. Rev., 76, 701.

Singer, S. F., 1950, Phys. Rev., 80, 47.
Sörensen, S. O. C., 1949, Phil. Mag. 40, 947.
Swann, W. F. G., 1943, J. Franklin Inst., 236, 1.
Van Allen, J. A. and A. V. Gangnes, 1950, Phys. Rev., 78, 50.
Winckler, J. R., T. Stix, K. Dwight and R. Sabin, 1950, Phys. Rev., 79, 656.

CHAPTER V

RECENT DATA ON GEOMAGNETIC EFFECTS

BY

H. V. NEHER

Norman Bridge Laboratory of Physics,
California Institute of Technology

INTRODUCTION 245
1. AN OUTLINE OF THE THEORY OF GEOMAGNETIC EFFECTS 246
2. COSMIC RAYS IN THE ATMOSPHERE 254
3. DATA ON GEOMAGNETIC EFFECTS 262
4. CORRELATION OF GEOMAGNETIC EFFECTS 288
5. ENERGY DISTRIBUTION OF THE PRIMARY RADIATION 297
6. SOME CONCLUSIONS ON THE GROSS BEHAVIOUR OF COSMIC RAYS IN THE ATMOSPHERE 304
7. SUMMARY 311
REFERENCES 313

INTRODUCTION

Since the early experiments in the period of 1927 to 1932, definitely establishing the first evidence that at least part of the primary cosmic radiation consisted of electrically charged particles, more and more evidence has been accumulated which strongly suggests that nearly all, if not all, of the primary energy is brought in by charged particles. Not only are they electrically charged but there is strong evidence that the primary particles carry only a positive charge. The kinds and numbers of these primary particles is the subject discussed by Peters in this volume. Their energy distribution and some of their interactions with the atmosphere on which they impinge are the main subjects of this article.

It so happens that approximately two-thirds of all the energy brought to the earth by cosmic rays is carried by particles that are measurably influenced by the magnetic field of the earth. Hence, by studying the various geomagnetic effects one might hope to determine some of the properties of the primary radiation and, in addition, find some of the gross behaviour of the radiation as it reacts with the atmosphere through which it passes.

Although, in a broad sense, most of the properties of cosmic ray interaction with the atmosphere change with latitude, i.e. change with the energy of the primary particles, we shall limit the present discussion to the over-all behaviour of the absorption processes. Since, in the north (or south) temperate latitudes, where most cosmic ray research is done, the magnetic field of the earth lets in nearly all of the primary particles, while at the equator the low energy particles are removed, the most fruitful location to study nuclear reactions initiated by cosmic ray particles is where the major part of the research is taking place at the present time.

While the magnetic field of the earth acts as a magnetic analyzer for the incoming charged particles, its resolution is rather poor. This therefore places a severe burden on the instruments used, to attain the required information on the primary radiation. There is the added complication that cosmic rays show random secular variations with time, and while these are small at or near sea-level, they are frequently troublesome when conclusions are to be drawn from precise measurements. Such fluctuations are much more pronounced at high altitudes and high latitudes. The study of these fluctuations, however, promises to be fruitful in the future in yielding information as to the origin of the particles themselves.

Geomagnetic effects such as the east-west effect at the equator can be studied at one location and difficulties due to fluctuations, as mentioned above, can be minimized by the correct experimental procedure, but there is considerably more difficulty connected with finding a satisfactory latitude effect at high altitudes because of the distances involved. At least a partial solution to this problem has been met by using an airplane equipped to fly at high altitudes, as will be discussed later.

1. AN OUTLINE OF THE THEORY OF GEOMAGNETIC EFFECTS

We shall discuss in this section the main results which have been arrived at from calculations dealing with the behaviour of electrically charged particles moving in the magnetic field of the earth.

STÖRMER [1930] was originally interested in the paths of charged particles in the earth's magnetic field in connection with his studies of the aurora borealis. Later, EPSTEIN [1931] and, particularly, LEMAITRE and VALLARTA [1933, 1936a, b] and VALLARTA [1935], added greatly to our understanding of the behaviour of charged particles in the field of a magnetic dipole. For a discussion more complete than here given the reader is referred to an article by JOHNSON [1938] and a recent book by MONTGOMERY [1949].

1.1 The earth's magnetic field

For the main analysis of the effect of the earth's magnetic field on the paths of charged particles, the field external to the earth is represented by a dipole, located at its centre, of magnetic moment 8.1×10^{25} gauss cm. A harmonic analysis of the local field at the surface of the earth at different latitudes and longitudes fixes the direction of the axis of this main dipole. The points where this axis emerges from the earth are called the geomagnetic poles and are located at 78.5° N, 69.0° W and 78.5° S, 111.0° E. The geomagnetic equator thus is tilted 11.5° with respect to the geographic equator and crosses it at 159° W and 21° E. Geomagnetic latitude is computed from the geomagnetic equator as follows: Let Λ be the geographic latitude of the point in question, Ω its geographic longitude, then, by spherical trigonometry, the geomagnetic latitude λ is given by:

$$\sin \lambda = \cos 78.5° \cdot \cos (\Lambda - 69.0°) + \sin 78.5° \sin \Omega$$

Tables giving λ in terms of geographic position are given by McNish [1936].

A detailed study of cosmic rays has indicated departures from the behaviour expected in the field of a symmetrically located dipole. Bartels and Chapman [1940,. p. 651] have made a more careful analysis and find that the field external to the earth can be best represented by a main dipole situated at 342 km from the centre of the earth and whose axis emerges from the earth at 80.1° N, 82.7° W and at 76.3° S and 121.2° E. The most satisfactory treatment, however, for cosmic ray work is to treat the symmetrical case and then determine corrections that need to be made for a given latitude and longitude.

1. 2 Application of Liouville's theorem

Important in the analysis of geomagnetic effects in cosmic rays is an application of Liouville's theorem. This subject has been discussed by Lemaitre and Vallarta [1933] and by Swann [1933]. It is first assumed that cosmic rays come uniformly from all directions in space. The application of Liouville's theorem then implies that for a given momentum the numbers of charged particles crossing unit area per unit solid angle per second is the same in all accessible regions and directions whether the magnetic field is present or not. We shall see presently that at a given geomagnetic latitude on the earth, certain regions of the sky are inaccessible to charged particles with less than a certain momentum. For locations and directions that *are* accessible for particles of this momentum, there will be the same intensity just above the atmosphere as at great distances from the earth.

1. 3 Units of energy and momentum

Before discussing the application of the Störmer theory of allowed directions, to cosmic ray particles, something should be mentioned concerning appropriate units. Since the curvature of a charged particle moving in a magnetic field is a measure of its momentum, ROSSI [1940] has suggested that, for cosmic ray phenomena, momentum be measured in terms of electron volts divided by the velocity of light. The unit of velocity is taken as the velocity of light. Thus, an electron with 1 BeV of energy has a momentum, p, of 1 BeV/c, since its rest mass energy is small compared with its total energy. For a particle of rest mass m_0, unit charge and momentum p, the energy of motion is

$$(1) \qquad W = [(pc)^2 + m_0^2 c^4]^{1/2} - m_0 c^2.$$

If the unit of pc is taken as 1 BeV, the energy of motion of a proton becomes

$$(2) \qquad W = [(pc)^2 + 0.87]^{1/2} - 0.93.$$

If the particle carries Z units of electric charge, then for the light elements, with the exception of hydrogen, a particle of atomic weight A has an energy of motion per nucleon given approximately, by

$$(3) \qquad \frac{W}{A} = \left[\frac{1}{4}\left(\frac{pc}{Z}\right)^2 + 0.87\right]^{1/2} - 0.93$$

in units BeV. The quantity p/Z is the momentum of the particle per unit charge measured in BeV/c. Particles with the same value of $p/Z = ev/Zc$ thus have the same radius of curvature in the same magnetic field.

1.4 Application of Störmer's theory

The theory developed by Störmer gives the lowest momentum for which a given direction at a given latitude is accessible. From the application of Liouville's theorem cited above, particles with momenta larger than this minimum can also come in at this latitude and direction.

As an example, consider the situation at the geomagnetic equator. Here, the Störmer theory gives a value of 14.9 BeV/c for the minimum momentum that a singly charged particle must have to come in at the zenith. All particles with momenta less than this are excluded from the zenith. The boundary between excluded regions and allowed regions for 14.9 BeV/c particles at the equator is, in the simple Störmer theory, a vertical, north-south plane.

As the momentum of the incoming particle decreases, the zenith angle in the east-west plane which divides the allowed from the forbidden directions swings toward the west for positively charged particles until such particles are just cut out completely at the western horizon if their momenta are less than 10.1 BeV/c.

For zenith angles z in the east-west plane at the geomagnetic equator, let z be positive for angles measured toward the east and negative for those measured toward the west. Then, for positive, singly-charged particles of momentum $p = ev/c$, directions are forbidden to those particles whose momentum is less than that given by the following expression:

$$\sin z = 2\left(\frac{59.6}{p}\right)^{1/2} - \frac{59.6}{p}. \tag{4}$$

For negatively charged particles, z is to be replaced by $-z$ and the allowed directions are on the eastern side.

As one proceeds north or south from the geomagnetic equator, the least allowable momentum at the zenith decreases. According to Störmer's theory, the least permissible momentum a particle must have to come in vertically at latitude λ is given by

$$p = 14.9 \cos^4 \lambda \text{ in BeV/c.} \tag{5}$$

Again, for particles with momenta greater than this, they arrive at the vertical with the same intensity as in outer space, while positive particles with a momentum equal to this are excluded for all zenith angles in the east-west plane from the vertical to the eastern horizon, but can come in with full intensity from the zenith to the western horizon.

1.5 Modifications to Störmer's theory

The above, very briefly, are some of the main conclusions arrived at by applying Störmer's theory with the help of Liouville's theorem, to the magnetic field of the earth. While it contains many of the essential features, Lemaitre and Vallarta [1936a, b] have shown that, when the problem is examined in more detail, there are directions excluded for certain particles that the simple Störmer theory allows to enter.

To an observer at a given location on the earth, the sky may be divided into the following regions, (a) the Störmer cone within which no particles of a given momentum can enter, (b) the main cone within which all particles of the given momentum may enter, (c) the penumbra, lying between the Störmer and main cones, within which there are alternate bands of permitted and excluded regions, and (d) the shadow cone which is due to particles that intersect the earth. This latter region lies near the horizon toward the north or south pole and is of the most importance at large zenith angles.

The region of the penumbra is very difficult to calculate. It is of most importance at the lower latitudes. At high latitudes the simple Störmer theory should apply. Also, in the east-west plane at the equator the main cone and the Störmer cone coincide so that here also the simple Störmer theory applies.

Lemaitre and Vallarta [1936b] have calculated the effect of the penumbra and the shadow cone for various directions at the equator and their results are given in Figure 1. The lines plotted are the orthogonal projections of the boundaries to the cones of allowed directions for particles of given momenta. Thus, consider the line marked 14.9 BeV/c. It passes through the zenith and then

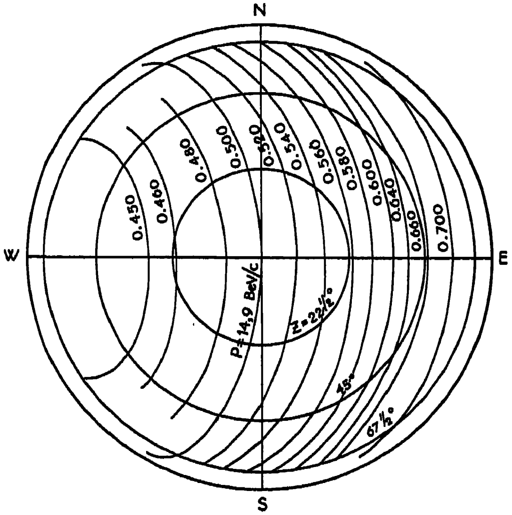

Fig. 1 – The orthogonal projections of the boundaries to the cones between permitted and forbidden regions at the geomagnetic equator, for positively charged particles. The curves are drawn for given values of momentum measured in Störmer units, r_0. The relation between this unit and momentum is given by, $p = 59.6\ r_0^2$ in BeV/c, for the case of the earth.

bends toward the west, crossing the zenith angle of 45° at 15° west of north (or south). Referring again to Liouville's theorem we infer that, at the top of the atmosphere, a counter telescope pointed in the direction indicated by this line should count the same for all zenith angles.

1. 6 Corrections for eccentricity of dipole

There are two important corrections that need to be made to the results obtained by considering the magnetic field external to the earth as due to a dipole situated at its centre. Since the actual magnetic field of the earth can best be represented by a dipole situated about 340 km from the centre of the earth a first correction must be made for the fact that the magnetic field varies along the magnetic equator. The effect of this eccentric dipole on cosmic ray phenomena was calculated first by Vallarta. We may find the approximate correction on the momentum of the particles involved as follows: the momentum required to reach the earth varies inversely with the square of the distance from the dipole. Hence, if α is the eccentricity of the dipole $= 340/6370 = 0.053$ rad., ω the longitude of the meridian plane containing the axis of the dipole and the centre of the earth, then the correction to the momentum at longitude Λ along the geomagnetic equator is given by,

$$\frac{\Delta p}{p} = 2\alpha \cos(\Lambda - \omega). \tag{6}$$

The dipole is nearest the surface of the earth at $\omega = 161.8°$ E and farthest away at 18.2° W. Thus, we might expect the cosmic ray intensity at a given depth in the atmosphere to vary along the geomagnetic equator, reaching a maximum at 18.2° W and a minimum at 161.8° E. The real field of the earth, however, reaches a minimum more nearly at 100° E and it is in this latter region that Millikan and Neher [1935, 1936] found cosmic rays at sea level to be a minimum. The maximum of the cosmic ray intensity along the geomagnetic equator seems to occur very close to 18° W.

The second correction to the eccentric dipole, as pointed out by Neher [1935] and Lemaitre [1937] is due to the fact that the meridian plane passing through the centre of the earth does not coincide with the plane passing through the dipole. The zenith angle calculated for a given minimum momentum of incident particle from theory is measured from the line passing through the observer and the dipole. In terms of the quantities given in Eq. (6) above, the correction in momentum for angles measured from the vertical has been shown by JOHNSON [1938] to be given by

$$\frac{\Delta p}{p} = \tfrac{1}{2}\,\alpha \sin (\Lambda - \omega) \tag{7}$$

for the vertical direction at the equator. Thus, the total correction for these two anomalies becomes

$$\frac{\Delta p}{p} = 2\alpha \,[\cos (\Lambda - \omega) + \tfrac{1}{4} \sin (\Lambda - \omega)]. \tag{8}$$

In the region of 80° W geographic longitude, i.e., near the coast of Peru, $(\Lambda - \omega)$ has a value of about 240°. Hence, here we would expect a correction to the minimum momentum at the vertical of about -8 %. Further, Eq. (8) has a maximum at $(\Lambda - \omega) = 15°$. Thus, the maximum and minimum occur on the geomagnetic equator at 15° farther west than one would expect from the simple effect of the distance from the dipole. The maximum change in the minimum momentum of particles at the vertical at the equator is, from Eq. (8) $\pm$ 11 %. The result on cosmic rays of this change in momentum for changes in longitude at a given geomagnetic latitude gives rise to the so-called longitude effect.

While the above gives very closely the correct result, a more careful analysis, considering the way the surface magnetic field of the earth changes, gives a slightly different result. Using available maps showing lines of equal horizontal intensity of the earth's magnetic field near the coast of Peru we find that the effective angle between the vertical and the line to the dipole is 4° instead of the geometrical value of 3°. A more exact treatment by VALLARTA [1935] of the effect of the distance to the dipole gives a value very close to that calculated above. The final result arrived at is, that at the vertical in Peru, charged particles are required to have a minimum momentum of 13.5 BeV/c. In southern India a similar study shows that the corresponding minimum is 17.0 BeV/c. These two values are of importance in the analysis that follows.

For directions other than the vertical in Peru, 4° have been subtracted from all zenith angles and the corresponding values of the minimum momentum calculated from Eq. (4). The results are shown in Fig. 2. They should give the expected behaviour of the charged particles since in the east-west plane at the equator there is no effect of the penumbra or of the shadow of the earth. Later we shall have occasion to use these results.

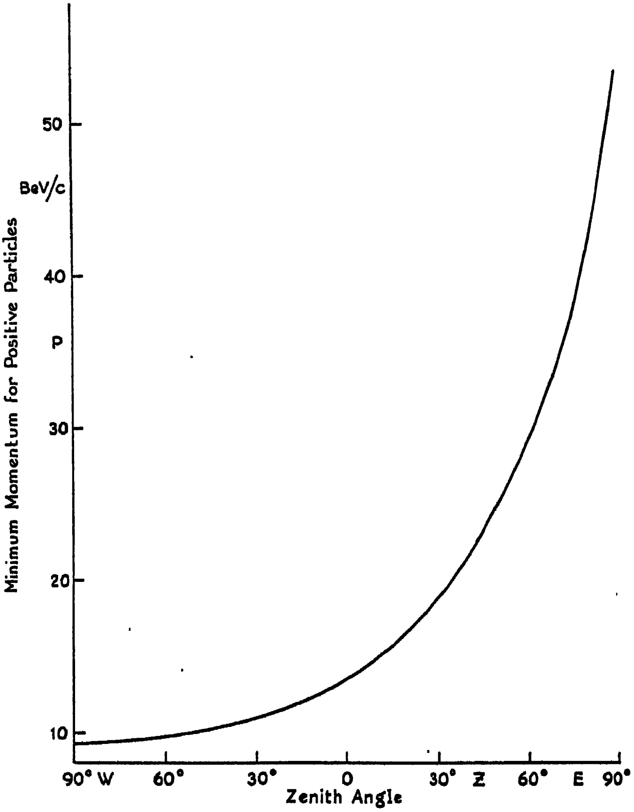

Fig. 2 - The minimum permissible momentum for positively charged particles in the East-West plane at the geomagnetic equator as a function of zenith angle. Corrections for eccentricity and tilt of the earth's magnetic field have been made as they apply to longitude 80° W.

1. 7 Definition of geomagnetic effects

Since all known properties of cosmic rays change with altitude, experiments on geomagnetic effects must be carried out at a particular depth in the atmosphere to be meaningful. If μ represents the particular quantity under investigation, then we would usually like to know the coefficient defined as

$$\beta = \frac{1}{\mu}\frac{\partial\mu}{\partial\nu}$$

when all other variables are held constant. The quantity ν will depend upon the particular geomagnetic effect under investigation. These are 5 in number, as pointed out by JOHNSON [1938]; namely (a) the latitude effect, (b) the longitude effect, (c) the zenith angle effect at a given azimuth, (d) the azimuth effect at a given zenith angle, and (e) the magnetic moment effect due to changes in the magnetic field. Thus, the coefficient β, for the latitude effect of the radiation at the vertical becomes

$$\beta = \frac{1}{j_\perp}\frac{\partial j_\perp}{\partial\lambda}.$$

We shall limit the discussion that follows to the first four effects. Changes due to variations in the magnetic moment of the earth are entangled with those due to different kinds of magnetic storm effects and will not be discussed here.

Frequently, however, our interest lies in the total relative change in the particular effect under investigation. Thus, for the latitude effect we usually take the relative change between a high latitude, where no further change occurs as one goes closer to the pole, and the equator. For the zenith angle, or east-west effect, we shall follow JOHNSON [1935] and take the difference between the westerly and easterly directions at the same zenith angle and divide by the average of the east and west values to arrive at a measure.

2. COSMIC RAYS IN THE ATMOSPHERE

2.1 Units of cosmic ray intensity

In the atmosphere we shall denote by j the number of charged particles per unit solid angle per second crossing unit area perpendicular to their direction of motion. Near sea level at latitudes greater than 45° one finds experimentally the following approximate dependence on zenith angle z,

$$j = j_\perp \cos^2 z \tag{9}$$

where $j_\perp$ is the intensity in the vertical direction.

The total number of charged particles crossing a unit horizontal area per unit time will then be

$$J = \int j \cos z \, d\omega \tag{10}$$

where the integral is extended over the upper half sphere. The total flux of charged particles across a sphere of unit area will be

$$J_0 = \int j \, d\omega. \tag{11}$$

Above the atmosphere where the incoming particles have suffered almost their complete bending by the earth's magnetic field but where they have not yet had a chance to react with the atmosphere, there are quantities similar to the above. We shall designate these by the superscript °. Thus, the unidirectional primary intensity will be designated by j° and the total number of charged particles crossing a unit horizontal area in unit time will then be

$$J^\circ = \int j^\circ \cos z \, d\omega. \tag{12}$$

j° will depend, especially near the equator, on the zenith angle z and azimuth angle ϕ.

The numerical values of j, J, and J_0 at sea-level as determined with cosmic-ray telescopes with and without lead absorber between the counters are given in Table 1 as quoted by Rossi [1948].

TABLE 1

Values of the vertical intensity, $j_\perp$, the flux through a unit horizontal area, J, and the flux across unit sphere, J_0, for sea level

No Absorber	15 cm lead	Units	Observer
1.14×10^{-2}	0.83×10^{-2}	$\text{cm}^{-2}\text{sec}^{-1}\text{sterad}^{-1}$	Greisen [1942]
1.79×10^{-2}	1.27×10^{-2}	$\text{cm}^{-2}\text{sec}^{-1}$	Quoted by Rossi [1948]
2.41×10^{-2}	1.68×10^{-2}	$\text{cm}^{-2}\text{sec}^{-1}$	

2. 2 Relation of intensity in the atmosphere to that above the atmosphere

Present evidence indicates that the particles that are incident on the top of the atmosphere which give rise to cosmic ray phenomena are atomic nuclei of very high energies. For every particle incident, a whole progeny of other particles arise. If directions were preserved, the intensity measured by a cosmic ray telescope would indicate m times as many particles in a given direction and position in the atmosphere as were incident on top in the same direction, provided the density of the particles from a single primary was such that the chance of two or more of its secondaries passing through the telescope was small. The quantity m would be the overall multiplicity which, for an extended shower, might run into thousands lower in the atmosphere.

The evidence is that directions for the more penetrating progeny are preserved quite well. The same applies to a lesser degree to the more absorbable part. Later we shall compute the numbers of primary particles, and since we know the counting rate of telescopes throughout the atmosphere, we shall have a means of calculating the overall multiplicity, m.

2. 3 Are there any primary electrons in cosmic rays?

In the analysis that follows in § 5, it is assumed that those primary particles which cause cosmic ray phenomena are all positively charged. Experiments by HULSIZER [1949] on bursts indicate that at 51° N an upper limit to the number of electrons compared with the total primary particles is 6 %. CRITCHFIELD, NEY and OLEKSA [1950], using cloud chambers at 90,000 to 100,000 feet, find that not more than 0.2 % of the primaries at 55° N can be electrons. We shall then feel justified in assuming that no electrons are contained in the primary cosmic rays, and since we know of no stable negatively charged particles other than electrons, we shall assume also the complete absence of negatively charged particles.

2. 4 Correlation between measurements taken with ionization chambers and counter telescopes

If the total number of particles crossing a sphere of unit area is known at any place in the atmosphere and the ionization, I, within that sphere is measured when it contains, say, one atmosphere of air, then the specific ionization or the average number of ion pairs formed per unit length is given by

$$\bar{\sigma} = \frac{I}{J_0}. \tag{13}$$

This assumes no effect of the walls. In the case of sea level measurements, we may take the value of $J_0 = 1.68 \times 10^{-2}$ particles $\text{cm}^{-2} \cdot \text{sec}^{-1}$ from Table 1 as measured through 15 cm. of lead. For the ionization at sea level we may take the value given by MILLIKAN and NEHER [1936] of $I = 1.75$ ion pairs $\text{cm}^{-3}\,\text{sec}^{-1}\,\text{atm}^{-1}$ of air under an average of 11 cm. of lead. If we decrease this by 3.5 % to arrive at the value that would have been obtained for an added 4 cm. of lead, we find a value of

$$\bar{\sigma} = \frac{1.69}{0.0168} = 100 \text{ ion pairs per cm of path.}$$

This value of specific ionization is somewhat greater than that found by counting individual ions along tracks obtained in cloud chambers. However, it is known that the ions which are readily counted do not represent the full energy loss of the ionizing particle. A considerable fraction of the energy of the particle goes into the formation of δ-rays which may form blobs in a cloud chamber, and the number of ions formed in such a region is very difficult to ascertain. Assuming an average energy loss of 32 eV per ion pair, the above value of 100 ion pairs cm^{-1} in air at normal pressure and temperature would give a total loss in one atmosphere of 2.5 BeV.

If we try to find a similar value for the case of no lead shield at sea level we may take the value of MILLIKAN and NEHER [1936] of $I = 2.88$ ions $\text{cm}^{-3}\,\text{sec}^{-1}\,\text{atm}^{-1}$ of air. This, however, is undoubtedly high due to the transition effect from air to iron, since the wall of the ionization chamber had an average wall thickness of about 8 mm. of steel. It is estimated that the increase due to this amount of steel at sea level is approximately 5 %. We find, then, for the average specific ionization for all particles at sea level, using the value of J_0 with no absorber, from Table 1,

$$\bar{\sigma} = \frac{2.74}{0.0241} = 114$$

ion pairs per cm. of path in air at normal pressure and temperature.

If we apply this same principle to the determination of the specific ionization at a height in the atmosphere corresponding to 310 gm cm^{-2}, we may take the data of BOWEN, MILLIKAN and NEHER [1938] of 92 ion pairs $\text{cm}^{-2}\,\text{sec}^{-1}\,\text{atm}^{-1}$ of air taken with a thin wall (0.5 mm. of steel) ionization chamber at 51° N and compare it with counter telescope data and the zenith angle dependence found by **Biehl**, **Neher** and **Roesch** [1949]. The vertical intensity was measured as 0.240 particles $\mathrm{cm}^{-2}\,\mathrm{sec}^{-1}$ sterad^{-1}, while the zenith angle dependence was found to be

$$j = j_{\perp} \cos^{1.7} z$$

at this altitude and latitude. We find the total flux through a sphere of unit area at this altitude to be

$$J_0 = 2.32\, j_{\perp} = 0.558 \text{ par. cm}^{-2}\,\text{sec}^{-1}.$$

Hence, the average specific ionization per particle at 50° N and at 30,000 feet will be

$$\bar{\sigma} = \frac{92}{0.558} = 165 \text{ ion pairs cm}^{-1}\text{ atm}^{-1} \text{ of air.}$$

A similar computation based on data from the same two papers above gives for the average specific ionization at the equator $\bar{\sigma} = 146$ ions cm^{-1} per atmosphere of air at 310 gm cm^{-2} air pressure [1].

For the case of lead absorber at 30,000 feet, **Biehl**, **Neher** and **Roesch** [1949] took zenith angle data with 10.4 cm. of lead with a counter telescope at 48° N and at the equator. (Data at this latter place unpublished.) A zenith angle dependence in the former case close to $\cos^{1.3} z$ was found, and in the latter, very close to $\cos z$ in the direction of constant momentum. On later flights from 64° N to the equator **Biehl** and **Neher** took data with an ionization chamber shielded with 11 cm of lead at the same altitude. (Data from 40° to 64° N published, [1950]). The ionization found at 51° N was 30.5 ions $\mathrm{cm}^{-3}\,\mathrm{sec}^{-1}\,\mathrm{atm}^{-1}$ of air, while at the equator this had dropped to 16.2. Thus, the latitude effect without lead absorber, at 30,000 feet, in the total ionization is 36.1 %, while with the 11 cm. of lead it is 47 %.

The results of these data reduced to the same thickness of lead (2 % per cm. of lead with the counter telescopes) are collected in Table 2.

The values given in Table 2 for no lead absorber calculated from data taken with thin-walled ionization chambers and Geiger

---

[1] This increase of the ionization of the particles with altitude was first called to the attention of the author by J. A. van Allen in a private communication.

TABLE 2

Values of specific ionization at 51° N and at the equator without and with lead shield

	30,000 ft.		Sea Level
	50° N	Equator	41° N
No lead.	165	146	114
11 cm lead.	157	117	100

counters probably give a relatively true measure of the ionization along the paths of the particles. For the case of lead absorber, there will be many and varied kinds of reactions with the lead around the ionization chamber, giving rise to showers, stars and other nuclear reactions which do not affect the counter telescope. From the work of SIMPSON, URETZ [1949] and others, it is known that such nuclear events have a much larger latitude effect than the total radiation. The evidence from Table 2 is that, at the equator at 30,000 ft., the radiation that can penetrate 11 cm. of lead is similar to that found at sea level.

We may find the average effective specific ionization throughout the atmosphere by correlating the readings of a thin-walled ionization chamber with a counter telescope, both covering all depths in the atmosphere and data taken at the same latitude. As discussed by NEHER and PICKERING [1942], the area under the vertical coincidence counter curves is proportional to the vertical energy incident at the top of the atmosphere, provided the following assumptions are made: (a) secondaries produced along the path of the incident particle do not diverge appreciably from the direction of the primary; (b) the passage of several secondaries, from the same event, through the counters simultaneously is a relatively rare event; (c) the contribution to the observed counting rate of showers, arising from primaries making a large angle with the vertical, can be neglected. If the radiation is isotopic at the top of the atmosphere, the total energy may be obtained by multiplying the energy per cm^2 per sec per steradian by the factor π.

The proportionality constant connecting the energy dissipated in the atmosphere in the form of ions, as measured with an ionization chamber, and the area under the telescope curve, is the average specific ionization of the charged particles. Hence, if h is the depth in the atmosphere, we may, for isotropic radiation at the top of the atmosphere, write

$$\bar{\sigma} = \frac{1}{\pi} \frac{\int_{\infty}^{0} I(h)\, dh}{\int_{\infty}^{0} j_{\perp}(h)\, dh} \tag{14}$$

where $I(h)$ is the ionization at a depth h in the atmosphere and $j_{\perp}(h)$ is the vertical intensity at a depth h in the atmosphere.

Using the areas under the ionization curves as given by BOWEN, MILLIKAN and NEHER [1938], and the areas under counter curves as given by NEHER and PICKERING [1942], and by BIEHL, NEHER and ROESCH [1949], we arrive at the values given in Table 3 for the average specific ionization throughout the atmosphere at the locations given.

TABLE 3

Location	Mag. Lat.	Area Under Counter Telescope Curve	Area Under Ionization Curve	$\bar{\sigma}$
Saskatoon	60° N	162	9.10×10^4	180
Omaha	51° N	157	8.73	177
San Antonio	38° N	139	7.08	162
Peru	0°	103	4.8 *†	150
Bangalore	3° N	91	4.1 †	143

Units of counter telescope area are (particles $\text{cm}^{-2}\text{sec}^{-1}\text{sterad}^{-1}$).($\text{gm.cm}^{-2}$).
Units of ionization area are (ions $\text{cm}^{-3}\text{sec}^{-1}$ (atm of air)$^{-1}$).(gm.cm^{-2}).
Units of $\bar{\sigma}$ are ions cm^{-1} (atm of air)$^{-1}$.

* This value was obtained by knowing the ionization at 30,000 feet in Peru, and then multiplying all ordinates of the Madras-Bangalore ionization curve by a constant factor to obtain a fit.

† These two values have been increased by 7 % each to allow for the different effective energy range of primaries covered, compared with counter telescopes. JOHNSON [1938] has discussed the corrections that must be applied to ionization curves to find the effective minimum momentum of the primary particles that would be comparable with counter telescopes at the same latitude. Assuming a reasonable energy distribution of the primary particles, and weighting them according to the solid angles given in Fig. 1, Johnson finds that the effective vertical minimum momentum at the equator should be increased by 2 BeV/c from the vertical value. From Fig. 32, this corresponds to a change in total energy of about 7 %.

Values of $\bar{\sigma}$ against minimum momentum of the primary particles are plotted in Fig. 3. The evidence is that, as the energy of the primary increases, the average ionization of the resultant charged particles decreases. It is possible that, for the highest energy primaries, the average value of the ionization of their progeny throughout the atmosphere would approach the sea level value.

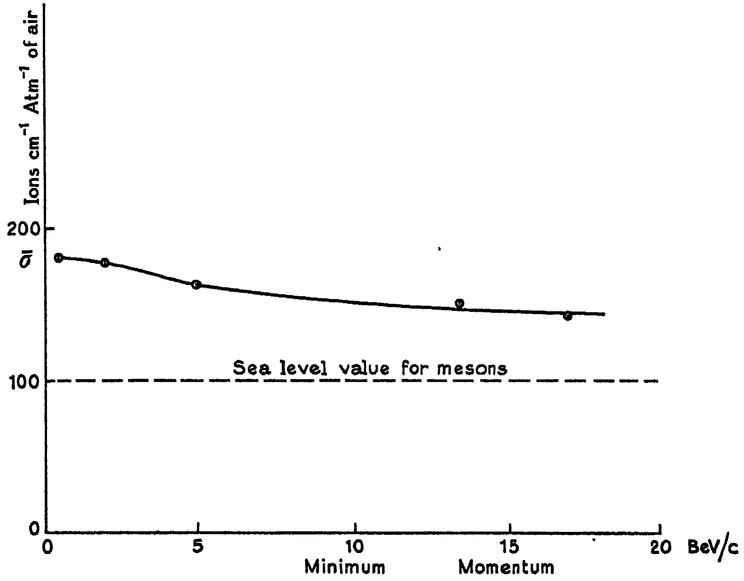

Fig. 3 – The average specific ionization for charged particles throughout the atmosphere as a function of the minimum momentum of the incident particles

The values of $\bar{\sigma}$ given in Fig. 3, should perhaps be regarded more as a quantity connecting the readings of ionization chambers and counters, rather than as a true measure of specific ionization along the paths of the particles. Two effects at least will tend to make this quantity larger than otherwise; (a) stars and small showers will add to the ionization more than to the counter telescope; (b) scattering will decrease the rates recorded by the vertically directed telescopes below what they otherwise would be.

It should be pointed out that, because of this change of specific ionization with energy of the primary, a Gross transformation of ionization curves at different latitudes will not give the true relative behaviour of counter telescopes at these latitudes.

3. DATA ON GEOMAGNETIC EFFECTS

3.1 Introduction

The main analysis which follows depends primarily on the results of BIEHL, NEHER and ROESCH [1949] obtained on an airplane flight at an air pressure of 310 gm cm^{-2} from 64° geomagnetic north to the geomagnetic equator along longitude 80° W. This trip covered the times given in Table 4.

TABLE 4

Flight No.	Route	Time	
4	Inyokern–Chicago	May 26, 1948	0334–1004*
5	Chicago–54° N–Tampa	May 29, 1948	1146–2100
6	Tampa, Florida–Panama . . .	June 2, 1948	1522–2334
7	Panama–Lima, Peru	June 4, 1948	0945–1839
8	Above Peru.	June 6, 1948	1505–2130
9	Lima–Panama.	June 8, 1948	1537–2324
10	Panama–Tampa	June 9, 1948	1738–0130
11	Tampa–Chicago	June 10, 1948	2044–0328
12	Above Illinois & Wisconsin . .	June 12, 1948	1758–0118
13	St. Louis–Inyokern	July 1, 1948	1405–2240

Greenwich Civil Time.

In each case where a break in the trip occurred, the procedure was to return to the latitude where the preceding stage had ended and connect the data with overlapping points.

In addition to the flight along a constant longitude, a high altitude flight was made to an air pressure of 235 gm. cm^{-2} over the equator. The advantages to be gained by using data collected on such a trip are:

(a) Similar equipment was used, and this equipment could be, and was, constantly intercompared.

(b) The same equipment was used to collect data as a function of (1) latitude, (2) altitude, (3) zenith angle, (4) azimuth angle.

(c) A repetition of the experiments could be made on the return trip to check the constancy of the apparatus and the constancy of the quantities being measured.

(d) Effects of fluctuations in the primary radiation could be minimized by the short times involved.

In addition, where counter telescopes were used, the counter areas were such that the statistical errors were small, even though the times were short due to the speed of the plane and the relatively short time it could remain aloft.

In studying geomagnetic effects, it might be supposed that the ideal would be to go to the top of the atmosphere in order to measure the primary radiation itself, yet there is an advantage in being down in the atmosphere beyond the effects of circulating particles which have been trapped in the earth's magnetic field or are scattered upward from the atmosphere. The importance of this "albedo" effect is unknown at present, but probably exerts little influence at the altitudes where these flights were made.

Because of the wide variety of experiments performed, under the controlled conditions of temperature and pressure that existed in the airplane, and the wide range of latitude covered in a relatively short time, it became possible for the first time to make an analysis of the different geomagnetic effects using data collected with similar apparatus which could be frequently intercompared.

3.2 Description of the apparatus

It was deemed desirable on this flight to collect as much data as possible with due consideration for space available in the airplane (a B-29 with pressurized compartments). In all, eight telescopes were in continuous operation. These consisted of three trays of

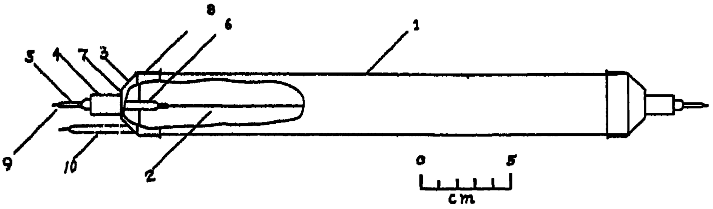

Fig. 4 Light weight Geiger counter: 1. Metal cylinder is formed from copper-plated steel sheet, 0.025 cm. thick. The joint is a lock seam that is silver soldered together simultaneously with joints 7 and 8; 2. Tungsten wire, 0.0025 cm. dia.; 3. Copper-plated steel caps; 4. Metal eyelet containing glass bead; 5. Glass-sealing metal tube through which tungsten wire is threaded; 6. Glass covering to metal tube; 7, 8. Silver soldered joints; 9. Tube is pinched when wire is taut, then silver soldered; 10. Tubulation consisting of copper tubing pinched to a feather edge to seal. Weight of complete counter is 90 gm.

8 counters per tray. The separation between outer trays was 80 cm., while the effective area of each tray was about 600 cm^2. The design of the counters themselves is shown in Fig. 4. The total number of counters in operation at one time was 152.

Four trays were mounted in three of the frameworks used, so that the top three trays could be used as one telescope, and the bottom three as another. The centre two trays were thus common to these two telescopes. Two other frame works contained three counter trays each, and were completely independent of each other.

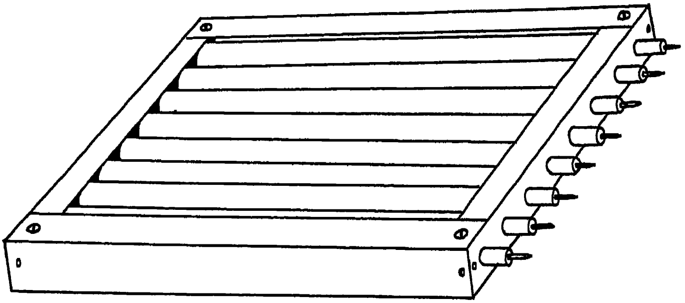

Fig. 5 – Eight counters were mounted rigidly in a framework to form a sensitive area of 600 cm^2. Three of these trays were used to count triple coincidences. The weight of each tray was 850 gm.

Two of the telescopes containing four trays were mounted along the centre of the B—29, as shown in Fig. 6, and could be rotated about a horizontal axis. Their size was such that when turned horizontally they just touched the inner wall of the pressurized compartment. One of these telescopes contained 10.2 cm. of lead between the lower two trays, while the other had 20.3 cm. of lead in a similar location. Thus, the top three trays in each case constituted a telescope with no lead absorber, while one had 10.4 cm. lead absorber (including the iron box) and the other 20.8 cm. of lead. Since the heading of the plane going to and from the equator was always nearly geomagnetic south or north, these frameworks could be pointed geomagnetic east or west by rotating them on their mountings about a horizontal axis.

The size of the trays and their separation resulted in a half angle θ_0, in one plane of 16° and 20° in the other. In the telescopes which were tilted, the counters were mounted so that the 16° angle was in the vertical plane. An inclinometer with a pointer was mounted on the side of the two frames that could be rotated. The graduated scale read to $\pm \frac{1}{4}°$ and the sensitivity of the bubble was such that $\frac{1}{4}°$ could be detected easily. No difficulty due to vibration, roll or pitch of the plane was experienced in reading the position of the bubble. The automatic pilot held the plane on a very level, straight course, except on two occasions, when storms were encountered. Scaling circuits were used where necessary to reduce the randomness and average rate of counting to values where a negligible number of counts would be missed by the registers used. All circuits were dipped in hot paraffin to avoid effects of moisture in the tropics.

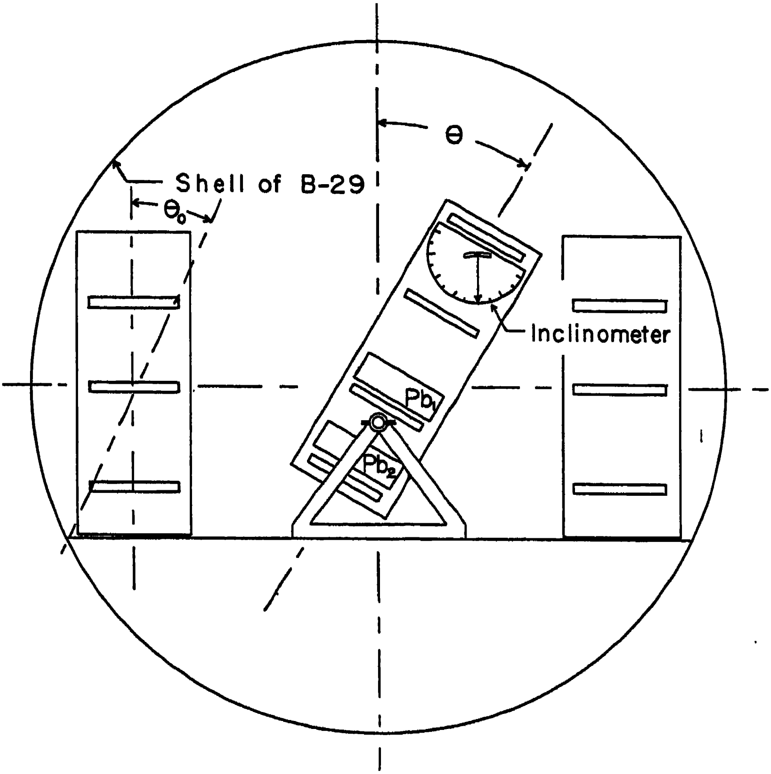

Fig. 6 – Disposition of cosmic-ray telescopes in pressurized section of the airplane.

A 35 mm. camera was used to photograph, at intervals of one minute, the faces of the registers, a clock and pertinent information written on a small card.

3. 3 Experiments performed

Most of the experiments listed below were performed during one trip of a B—29 to Lima, Peru, and return. On a subsequent trip some of the experiments were repeated. These were in substantial agreement with those made before. Other flights were made within the United States and Canada to study the behaviour of the radiation at 30,000 to 33,000 ft. between 40° and 64° geomagnetic north. The equipment in all flights was essentially the same. Some modification was made in the circuits on the later flights, but otherwise there was little difference in the experimental arrangements.

The following experiments pertinent to the present discussion were performed:

A. On the latitude effect from 64° geomagnetic north to the equator continuous measurements were made both going and coming.

1. Vertical radiation: two independent telescopes; no added absorber.
2. Vertical radiation: one telescope; 10.4 cm. lead absorber.
3. Vertical radiation: one telescope; 20.8 cm. lead absorber.
4. Total radiation: continuously recording ionization chamber [2]. No added absorber.
5. Total penetrating radiation: continuously recording ionization chamber [2] inside a 11 cm. lead absorber.
6. East-west effect at 45°: two independent telescopes; no added absorber.
7. East-west effect at 45°: one telescope; 10.4 cm. lead absorber.
8. East-west effect at 45°: one telescope; 20.8 cm. lead absorber.

---

[2] These ionization chambers were those used in the surveys of MILLIKAN and NEHER [1936]. They are spherical in shape with a 3 mm. steel wall and a 2.5 × 2.5 cm^2 steel band around the centre and lying in a vertical plane. The average thickness of iron is close to 8 mm.

B. East-west and azimuthal effects at the geomagnetic equator.
   1. East-west effect at 30,000 ft. (310 $gm.cm^{-2}$) with no lead and with 10.4 and 20.8 cm. lead absorbers.
   2. Azimuthal effect measured every 30° at 36,000 ft. (235 $gm.cm^{-2}$ air pressure) with no lead, 10.4 and 20.8 cm. of lead at zenith angles of 22½°, 45° and 67½°.

C. Other experiments performed.
   1. Counting rates *vs.* air pressure were taken with all telescopes turned vertically at nearly all times when the plane was ascending. The rate of ascent was such that good records without lead, with 10.4 cm. lead and with 20.8 cm. lead were obtained.
   2. Longitude effect at 30,000 ft from 110° W to 90° W along geomagnetic latitude 41° N.

3. 4 Internal calibrations

All telescope data were adjusted by suitable correction factors to read what set No. 1 (one of the unshielded telescopes) would have read in the same circumstances. These calibration factors were determined as follows: on several occasions, both on the ground and in the air, the four telescope sets with no added absorber were measuring the same radiation while the cosmic ray intensity was constant for a sufficient length of time to yield an accurate ratio between the counting rates. There is no significant difference between the two methods of comparing the rates.

For the calibration of the telescopes containing lead, data taken in the plane while on the ground were used. These data gave the counting rate with the lead removed but with the iron boxes which held the lead still in place. An experiment in which iron sheets were inserted between the trays of the unshielded telescopes gave the necessary correction for the iron boxes.

The results of the internal comparisons are shown in Table 5.

TABLE 5

n (Set No.)	ϱ	n (Set No.)	ϱ
1	1.000	6	1.000 ± 0.007
3	0.979 ± 0.004	7	1.037 ± 0.006
4	0.981 ± 0.007	8	1.011 ± 0.006
5	1.037 ± 0.009	9	1.019 ± 0.016

The values are the ratios of set No. 1 to set *n*. The indicated probable errors are those computed from statistical errors in the calibration. The above comparison gives a good experimental check of the similarity of the geometries of the various telescopes.

3. 5 Corrections to the telescope readings

The following corrections need to be considered:

A. Accidental counting rates
B. Dead time of the counters
C. Effect of side showers
D. Finite opening of the telescopes
E. Absorption in the counter walls and walls of the plane.

Other corrections due to variations in the height of the plane, efficiency of the recording circuits, variations in the zenith angle of the east-west sets, etc., were negligible.

Accidental counting rates were corrected for in the usual way. The main contribution was from the real double coincidence rate between two of the trays and the single counting rate of the third tray. This correction was never more than —1.5 %.

Correction for dead time of the counters was somewhat more important. Using the individual counting rates of the Geiger tubes this correction was determined in the laboratory. It amounted to +4.0 % at the northern latitudes and +2.6 % at the equator.

The correction for side showers was important for the telescopes without lead absorber. To gain information on the importance of this correction a fourth tray of counters was mounted opposite the middle tray and just beyond the line where real triple coincidences could take place. At the northern latitudes at 30,000 ft. the counting rate with the side tray so placed was 44 per minute, when the telescope was vertical, compared with 800 per minute when the telescope was operated in the usual way. When tipped over at 45° the rate with the centre tray to the side was 29 per minute. At the equator this went down to 20 per minute. The fact that this shower rate has the same latitude effect as the total intensity means that the showers are not of the extended variety which show no latitude effect.

To gain further information on side showers the telescopes were turned horizontally. Because of the finite opening of the telescopes, particles coming in at zenith angles from 74° to the horizon would be counted from each end when in this position. Assuming mass absorption for these particles that could penetrate the 10 or 20 cm. of lead in the telescopes, the counting rate due to these low angle particles could be estimated. Thus, at northern latitudes at 30,000 ft., the average of the counting rates with the telescopes containing 10 and 20 cm. of lead was 21 per minute. Fourteen per minute could be accounted for as due to these nearly horizontal particles. The remainder, or 7 per minute, we estimate is due almost entirely to extended showers. The evidence, then, is that the telescopes with lead between trays were so well protected that the small side showers were largely eliminated.

For the telescopes without lead the counting rates when horizontal were 102 per minute at the northern latitudes. Of these, 26 per minute could be accounted for by real triple coincidences due to particles from 74° to the horizon. The remainder, or 76 per minute, we assume are due to side showers.

For other zenith angles we can make an estimate of the effect of side showers from the data on the counting rate with the centre tray displaced. This side shower effect will be due mostly to one of the shower particles passing through two of the trays and another shower particle passing through the third. This effect will increase as the centre tray is moved into line with the other two. Assuming that these small showers have the same zenith angle distribution as the total radiation, one can calculate the way in which the measured shower rate depends on the position of the centre tray.

In the above way we arrive at the scheme given in Table 6.

TABLE 6

Total correction in counts per minute due to side showers for telescopes with no lead absorber for zenith angle, z.*

Latitude	$Z = 0$	$22\frac{1}{2}°$	45°	$67\frac{1}{2}°$	90°
50°	100 ± 10	92 ± 10	85 ± 15	80 ± 15	76 ± 10
0°	66 ± 7	61 ± 7	57 ± 10	53 ± 10	50 ± 7

* No correction is made for local side showers for telescopes with lead absorber.

The probable errors are estimates based on the uncertainties of applying shower data to our particular geometry.

In making the correction due to the finite opening of the telescope, it was assumed that to a first approximation the variation of the counting rate over the mouth of the telescope for any one zenith angle could be approximated by assuming the mass absorption law to hold, and then using absorption curves obtained in the vertical direction in the atmosphere. A double graphical integration was made for each zenith angle, and for the telescopes without and with lead. The results of some cases for no lead are given in Table 7.

TABLE 7

Corrections to be applied to zenith angle data for finite opening of telescope. No lead absorber

Zenith Angle	48° North (310 gm. cm^{-2})	0° (230 gm. cm^{-2})		
		N-S Plane	West	East
	%	%	%	%
0°	0.0	0.0	0.0	0.0
22½°	1.0	0.1	0.3	0.2
45°	− 2.0	1.1	1.1	0.6
67½°	−23	− 8.0	− 8.1	− 9.5

No correction has been applied for the five wall thicknesses of the counters or for the skin of the plane, both of which the particles needed to penetrate to be counted. The former totalled 1.6 gm.cm^{-2} of iron, and the skin of the plane added another 1 gm.cm^{-2} of aluminium. The effect of adding iron between the trays near sea level is given in Fig. 7. The slope of the line is 2.0 ± 0.2 % gm^{-1} cm^{2} of iron. These data cannot be applied directly at 30,000 ft. because of the different composition of the radiation.

The corrections which have been made have been gone into rather extensively because of their importance in reducing the data. A summary of the corrections made to the original data is as follows:

A.	Accidentals	Maximum of — 1.5 %
B.	Dead time of Counters	,, ,, + 4.0 %
C.	Side Showers	
	No lead absorber	,, ,, —13.0 % at vertical
	With lead absorber	,, ,, 0.0 %
D.	Finite aperture (except at 67½°)	,, ,, 2.0 %.

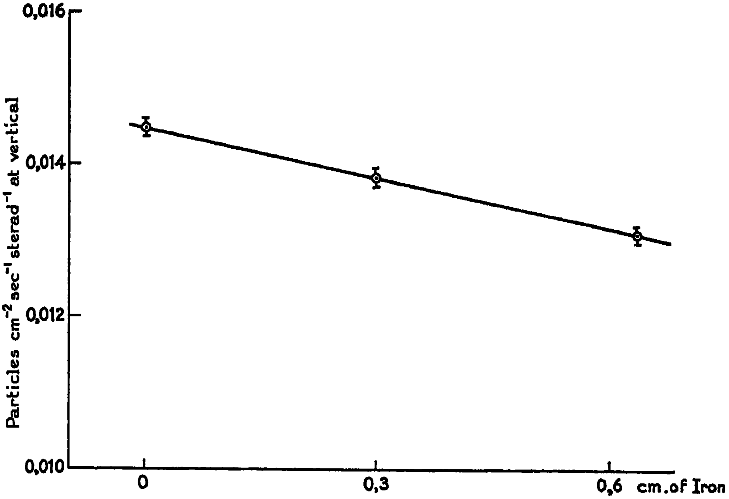

Fig. 7 – Adding sheets of iron between the trays near sea level (2500 ft elevation) gave an absorption of 2.0 ± 0.2 percent $gm^{-1}cm^{-2}$.

3. 6 Reduction to absolute values

After reducing the readings of each telescope to what No. 1 would have read under the same conditions, as given in Table 5, the corrections discussed above were applied. These values were then multiplied by an appropriate factor to reduce the rates to an absolute value. R. A. MONTGOMERY [1949] has made an accurate determination of the absolute value of the intensity of cosmic rays at sea level and in Pasadena with the counters here used. He found a value of $j_\perp = 0.0116$ ionizing particles cm^{-2} sec^{-1} $sterad^{-1}$ at the vertical at sea level. This is slightly higher than the value given by Greisen in Table 1 above.

Comparing our geometry with that used by Montgomery on the one hand, and by placing our telescopes outdoors and assuming cosmic rays had not changed in the 3 or 4 months intervening on the other, we found that the constants necessary to reduce our values to absolute values determined these two ways differed by 1.5 %. We therefore took the average, or a multiplying factor of 3.43×10^{-4} to reduce our counts min^{-1} to counts cm^{-2} sec^{-1} $sterad^{-1}$.

3. 7 Experimental results

Figures 8 and 9 give the experimental data obtained on the latitude effect along longitude 80° W at 30,000 ft. (310 gm.cm^{-2} air pressure) (a) at the vertical, (b) at 45° W and (c) 45° E without lead absorber and with 10.4 cm. and 20.8 cm. of lead between the second and third trays of counters. These data have had no corrections applied except to reduce all readings to what set No. 1

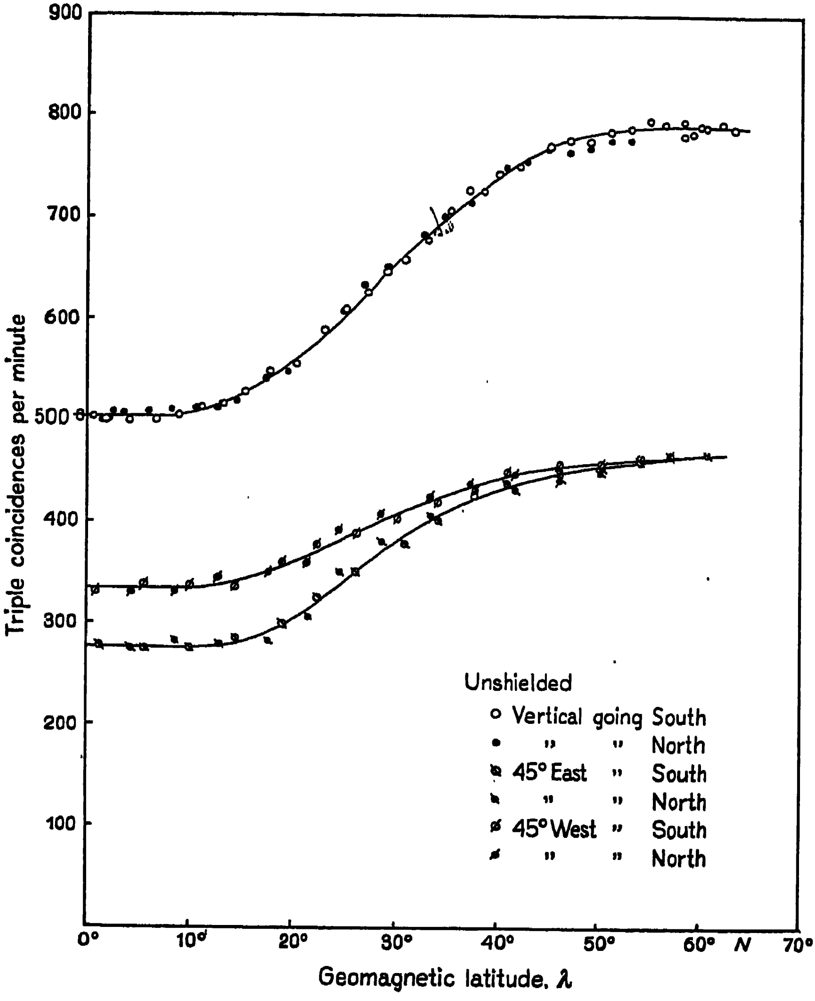

Fig. 8 – Latitude effect of the total radiation at the vertical, 45° West, and at 45° East with no absorber. No corrections applied.

would have read under the same circumstances, as given in Table 5. The vertical data with no lead are the averages for two independent telescopes. The data at 45° east and west with no lead are also the averages for two independent telescopes. The procedure followed on the flight was as follows: the two observers (Biehl and Neher) would swing the two telescopes first 45° E, then 45° W, leaving them in a given position for 10 minutes. Since these frameworks also contained the telescopes with lead absorber, the data with lead at 45° E and W also represent alternating values.

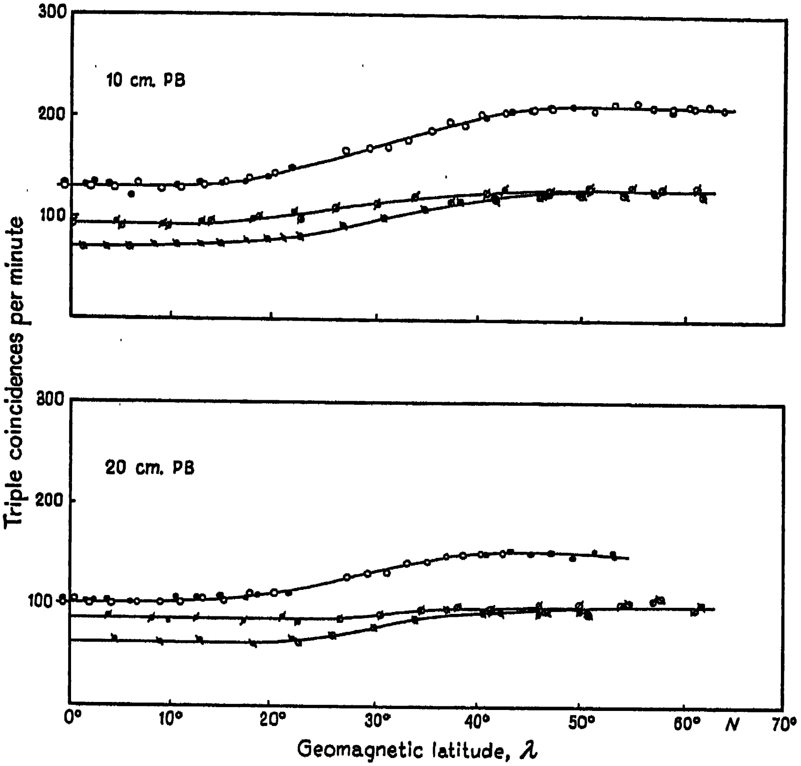

Fig. 9 – Latitude effect at the vertical, 45° West and 45° East, for that part of the radiation that can penetrate 10.4 and 20.8 cm. of lead. No corrections applied.

The statistical errors of each plotted point in Figs. 8 and 9 are no greater than the diameters of the points themselves. In the case of the vertical telescopes with no lead, each point represents the average for a 30 minute time interval. Thus, at northern latitudes each point has a statistical error determined by about 50,000 counts.

The data given in Figs. 8 and 9 were then corrected as explained in section 4.5 and reduced to absolute values of particles cm^{-2} sec^{-1} sterad^{-1}. Figs. 10 and 11 represent the data so reduced. In Table 8 some numerical values are given for definite latitudes, both before any corrections were applied and after such corrections were made and the data reduced to absolute values.

TABLE 8

Telescope data at 310 *gm.cm*$^{-2}$ *air pressure*

Geo-magnetic Latitude λ	Vertical			45° W			45° E			Remarks
	No Lead	10.4cm Lead	20.8cm Lead	No Lead	10.4cm Lead	20.8cm Lead	No Lead	10.4cm Lead	20.8cm Lead	
60° N	788	212	153	466	127	100	466	127	100	Uncorrected counts per minute
0°	503	128	102	335	93	86	277	71	63	
60° N	0.243	0.0738	0.0529	0.134	0.0436	0.0343	0.134	0.0436	0.0343	Corrected and reduced to particles cm^{-2} sec^{-1}steradian^{-1}
0°	0.153	0.0443	0.0350	0.098	0.0321	0.0295	0.077	0.0246	0.0218	

After applying corrections explained in section 4.5, values in upper half of table are multiplied by $3.43 \times 10^{+4}$ to reduce to particles cm^{-2} sec^{-1} steradian^{-1}

To find the importance of the change in longitude on intensity measurements at 30,000 feet altitude, the airplane flew along a constant geomagnetic latitude of 40.8° N from 112° W to 90° W. Shown in Fig. 12 are the data obtained with the unshielded ionization chamber as a function of longitude. On the basis of the eccentricity of the dipole as discussed in § 1, it is possible to calculate the expected dependence on longitude at this elevation, from the known dependence on latitude of the same instrument when the momentum range covered was the same. The expected value at 100° W was calculated to be — 0.29 % per degree change in longitude compared with the measured value —0.24. (See: BIEHL and NEHER [1950]).

The above information makes it very desirable to state the

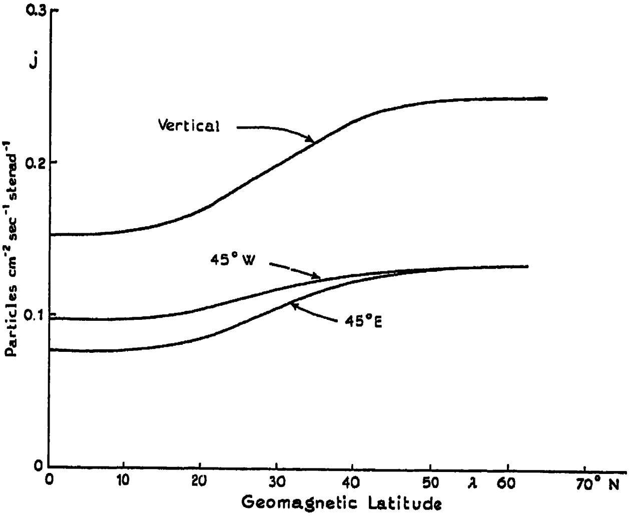

Fig. 10 – Data of Fig. 8 after corrections have been applied and reduction made to absolute values.

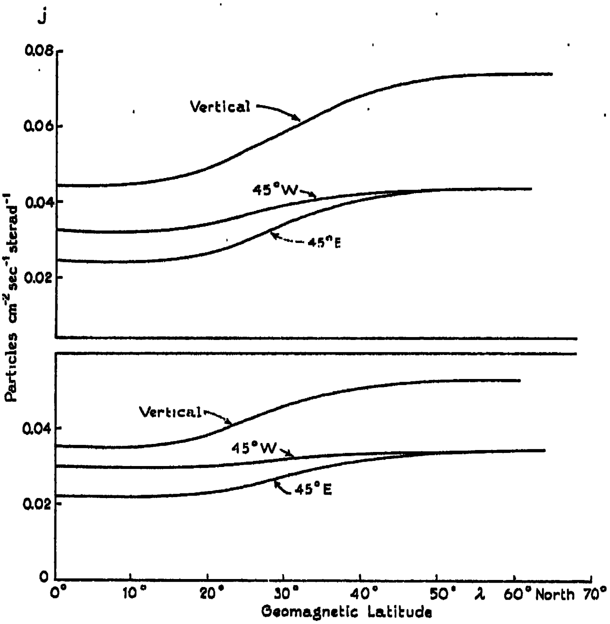

Fig. 11 – Data of Fig. 9 after corrections have been applied and reduction made to absolute values.

longitude as well as the latitude where such experiments are made. The ionization and counter telescope data obtained at two different longitudes on several flights are shown in Figs. 13 and 14. The differences in the two curves taken at the two different longitudes are consistent with the change with longitude shown in Fig. 12.

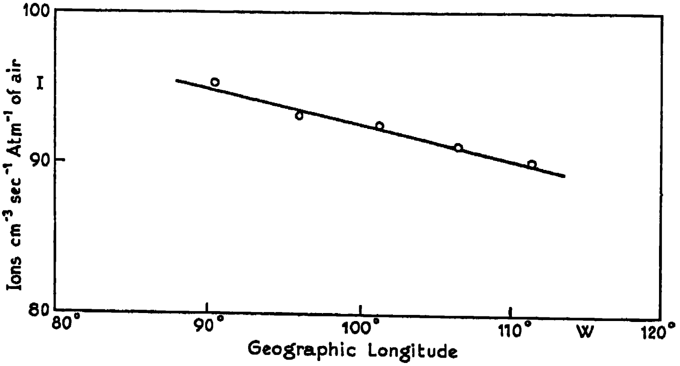

Fig. 12 – The longitude effect at 310 gm.cm^{-2} air pressure (30,000 ft.) at 40.8° N.

The next geomagnetic effect for which data were obtained was on the dependence of counting rate on zenith angle in the east-

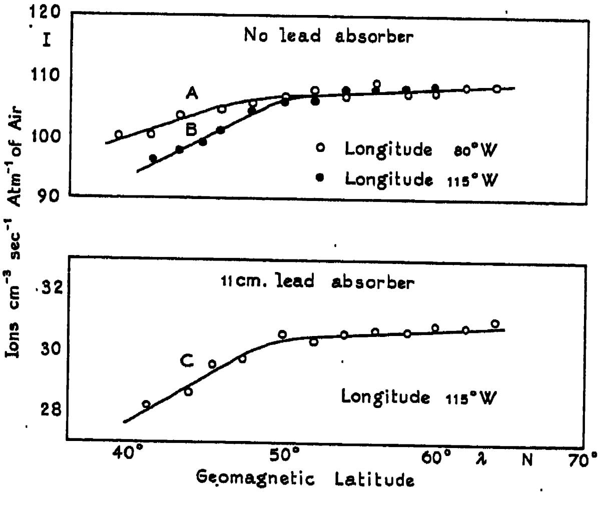

Fig. 13 – The latitude effect at two different longitudes. A and B taken with unshielded ionization chamber; C taken with 11 cm. lead shield.

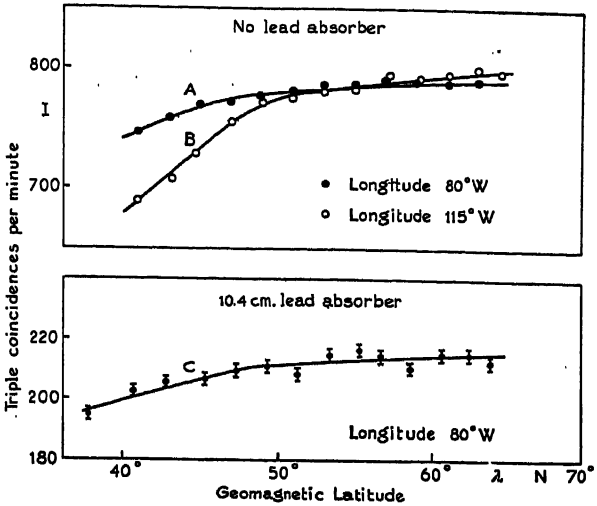

Fig. 14 – Latitude effect at the vertical using counter telescopes. A and B taken with no added absorber; C taken with 10.4 cm. lead between second and third trays.

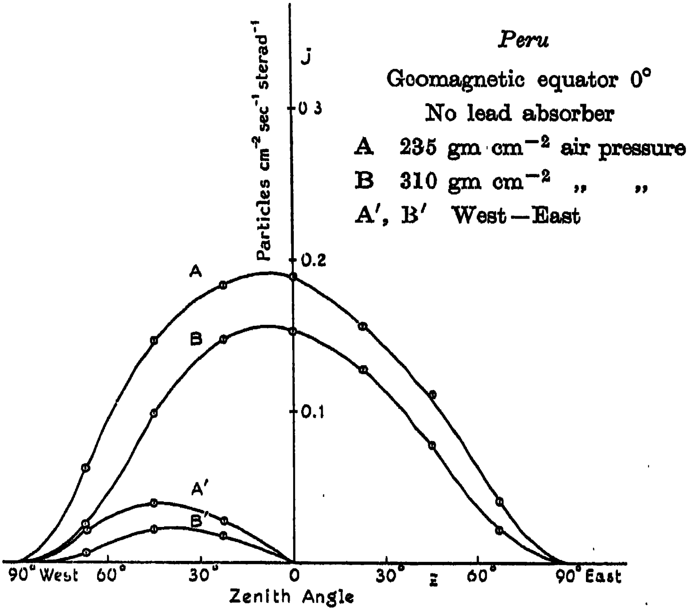

Fig. 15 – Zenith-angle dependence in the East-West plane at two different elevations over Peru with no lead absorber.

west plane at the equator. This is generally known as the east-west effect. In this case, data were taken not only at 310 gm. cm^{-2} air pressure, but also at 235 gm.cm^{-2}. In Figs. 15, 16 and 17, these data are given for no lead absorber and with 10.4 and 20.8 cm. of lead absorber. All corrections have been applied, including those for finite opening of the telescopes. In Table 9 are given the numerical values of the counting rates both at 310 and 235 gm.cm^{-2} air pressure.

TABLE 9

Particles cm^{-2} sec^{-1} steradian^{-1}

Telescope data in east-west plane at equator

Zenith Angle / Added Absorber	Vert-ical	22½°W	22½° E	45°W	45° E	67½°W	67½° E	Remarks
0 cm. lead	0.153	0.146	0.128	0.098	0.077	0.025	0.0190	310 gm.cm^{-2} air pressure
10.4	0.0443	0.0450	0.0340*	0.0321	0.0246	0.0147	0.0117	
20.8	0.0350	0.0364	0.0307	0.0295	0.0218	0.0117	0.0105	
0 cm. lead	0.188	0.183	0.156	0.149	0.111	0.061	0.0405	235 gm.cm^{-2} air pressure
10.4	0.0530	—	—	0.0444	0.0316	0.0217	0.0160	
20.8	0.0424	0.0445	0.0369	0.0395	0.0276	—	—	

* This particular datum is for 27½°.

Some values of the percentage west excess taken from Table 9 are listed in Table 10. These are computed in the usual way of

TABLE 10

Per cent East-West effect over Peru

Calculated from $2(j_W-j_E)/(j_W+j_E)$

Absorber	Zenith Angle			Remarks
	22½°	45°	67½°	
0 cm. lead	13.1	23.3	27	310 gm. cm^{-2} air pressure
10.4	17.0	27.6	23	
20.8	17.0	30.4	11	
0 cm. lead	16.0	29.1	40	235 gm. cm^{-2} air pressure
10.4	—	33.0	30	
20.8	18.6	35.4	—	

The statistical probable errors involved in the above values are approximately ± 7 % for 22½° and 67½° and ± 5 % for 45°.

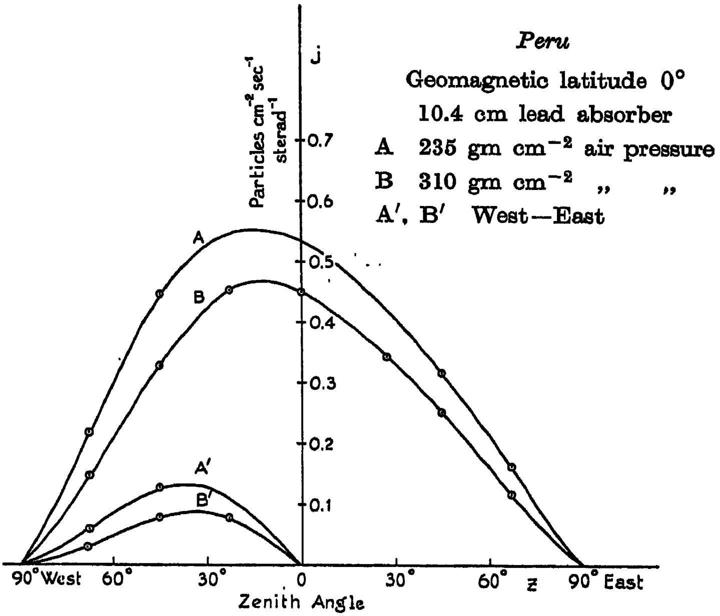

Fig. 16 - Zenith-angle dependence in the East-West plane at two different elevations over Peru with 10.4 cm. lead absorber.

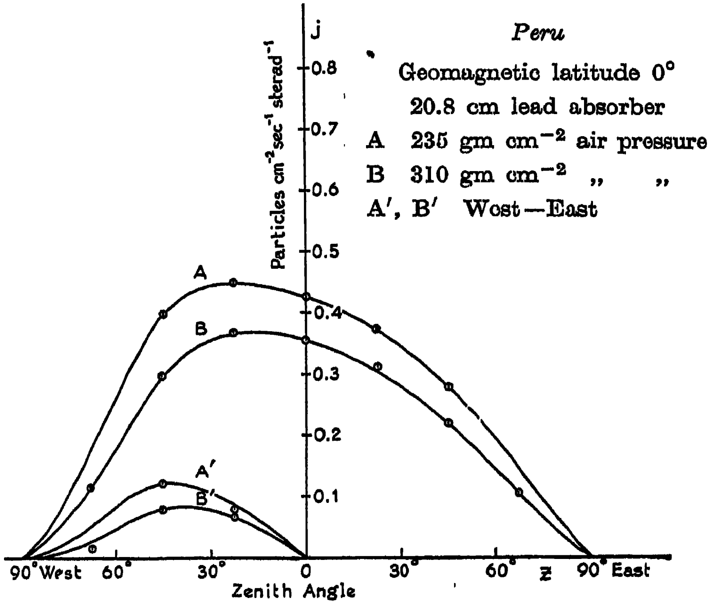

Fig. 17 - Zenith-angle dependence in the East-West plane at two different elevations over Peru with 20.8 cm. lead absorber.

taking the difference between the westerly and easterly values at a given angle and dividing by the average for the east and west. For the higher elevation (235 gm.cm^{-2}) the percentage west excess is plotted as a function of zenith angle, in Fig. 18.

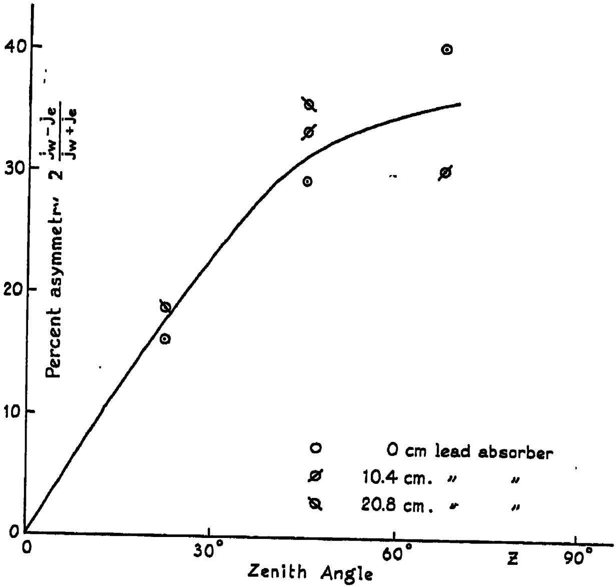

Fig. 18 – Percent asymmetry at 235 gm.cm^{-2} air pressure (36,000 ft). at the geomagnetic equator as a function of zenith angle.

The smaller value of the percentage west excess at 67½° with 20.8 cm. of lead at 310 gm.cm^{-2} is probably due to the higher energy primaries necessary for their secondaries to penetrate the greater thickness of atmosphere and lead. These primaries show less east-west asymmetry. At still larger zenith angles the east-west effect should approach zero since the primaries that can penetrate the greater depth are not affected by the earth's magnetic field.

The last geomagnetic effect for which data were obtained on the flight to Peru, i.e., along longitude 80° W, is on the dependence of counting rate on azimuth angle for given zenith angles at the geomagnetic equator. The data taken with no lead absorber, 10.4 cm. and 20.8 cm. of lead are given in Figs. 19 and 20 when no corrections have been applied. After making the corrections for

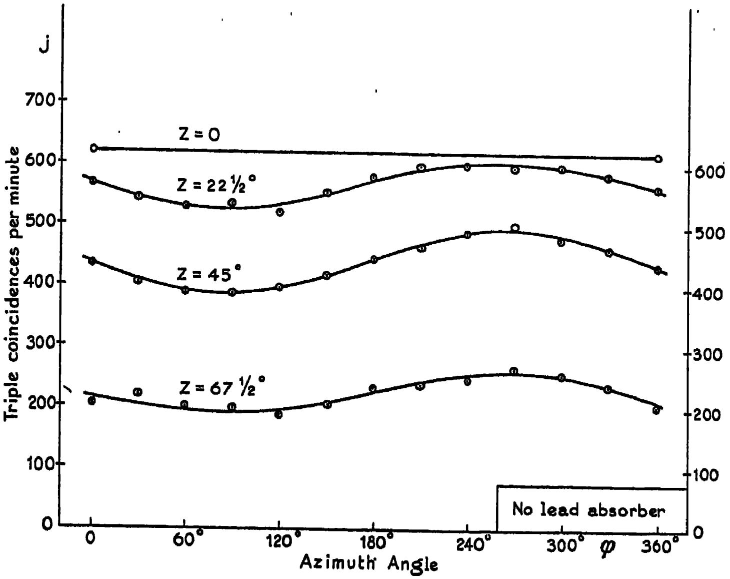

Fig. 19 – Azimuth-angle effect for several zenith angles at 235 gm.cm⁻² over Peru with no lead absorber. No corrections applied.

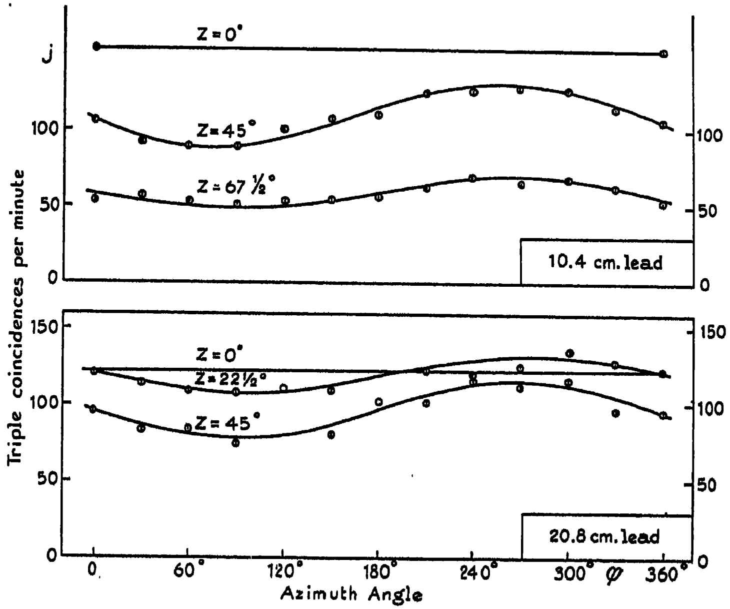

Fig. 20 – Azimuth-angle effect for several zenith angles at 235 gm.cm⁻² over Peru with 10.4 and 20.8 cm. lead absorber between second and third trays of counters. No corrections applied.

accidentals, efficiency, side showers and finite opening of the telescopes and then reducing to absolute values, the results given in Figs. 21 and 22 are obtained. Each point for the case of no lead at zenith angle 45° has a statistical probable error of ± 0.7 %, while for the telescopes with lead the probable error is about ± 2% for the same angle.

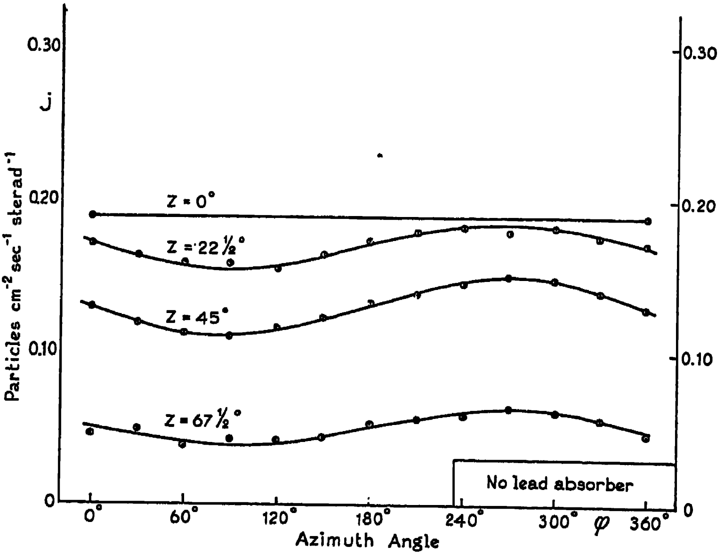

Fig. 21 – Data of Fig. 19 after corrections have been applied and reduction made to absolute values.

It is interesting that the azimuthal angle effect may be represented empirically, within the experimental uncertainties, by a sinusoidal function. Thus at 235 $gm.cm^{-2}$ at the equator over Peru we find the best fit to the experimental points is given by the relations in Table 11 where ϕ is the azimuth angle measured from the north.

TABLE 11

Empirical representation of azimuth angle data at the geomagnetic equator over Peru at 235 $gm.cm^{-2}$. Values are in particles cm^{-2} sec^{-1} $steradian^{-1}$

Absorber	Zenith Angle		
	22½°	45°	67½°
0	$0.174 - 0.014 \sin \phi$	$0.130 - 0.019 \sin \phi$	$0.052 - 0.010 \sin \phi$
10.4 cm lead	——	$0.0374 - 0.0062 \sin \phi$	$0.0193 - 0.0030 \sin \phi$
20.8 cm lead	$0.0412 - 0.0038 \sin \phi$	$0.0330 - 0.0058 \sin \phi$	——

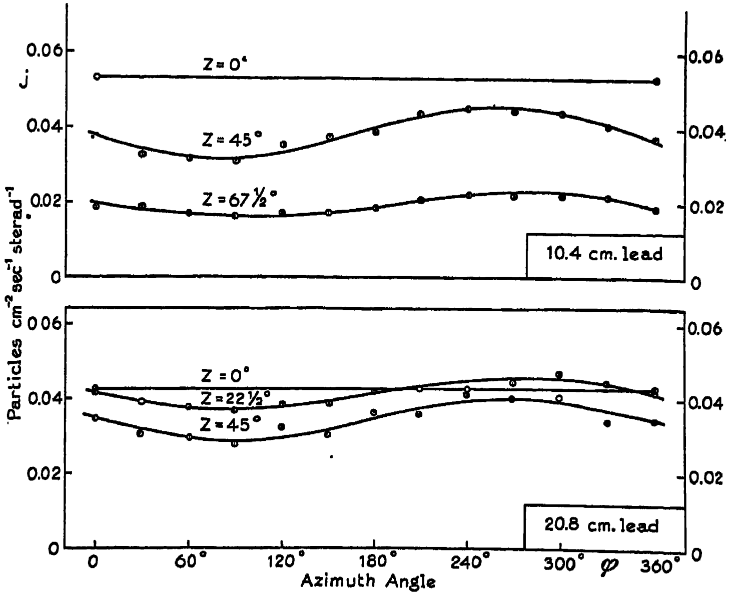

Fig. 22 – Data of Fig. 20 after corrections have been applied and reduction made to absolute values.

In addition to the above, further data were taken that are pertinent to the discussion that follows. As indicated previously in § 3.3, the telescopes were turned vertically while gaining altitude from the various airports. The rate of rise was such that quite satisfactory data were obtained. In particular in Figs. 23 and 24 are plotted the results for the airport north of Chicago at geomagnetic latitude 53° N. These data have all been corrected and reduced to absolute values. The agreement between the values here obtained and those taken in the summer of 1947 with nearly identical telescopes by Biehl, Montgomery, Neher, Pickering and Roesch [1948] should be pointed out. We then obtained 0.234 particles cm^{-2} sec^{-1} sterad^{-1} with no lead absorber at 310 gm.cm^{-2} air pressure using free ballons at Rapid City, South Dakota (λ_{mag} = 53° N) as compared with the present value of 0.240 after all corrections have been made.

Other data on the zenith angle distribution, both at the northern latitude and at the equator, will be useful. While going between California and Chicago, the plane flew along geomagnetic latitude 48° N. This gave a good opportunity to measure the zenith angle distribution in the north-south plane. No dissymmetry within the accuracy of the data was found. The reduced data without and with absorber are plotted in Fig. 25. Of particular importance here is the evidence at large zenith angles for scattering of the radiation.

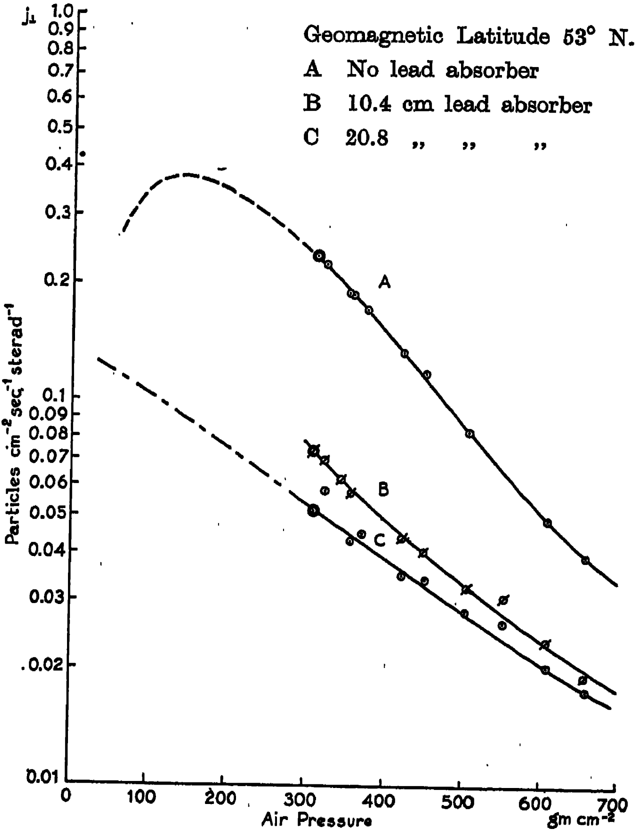

Fig. 23 – Intensity *vs.* air pressure at geomagnetic latitude 53° N with and without lead absorber. Extension to curve A is from balloon flights at Omaha, (Biehl, etc. [1948]); extension to curve C is from data due to Schein using 18 cm. of lead as quoted by D. J. X. Montgomery [1949]. The double circled points are from averages over long periods of time.

Plotted also in Fig. 25 are the values one obtains for the vertical direction for the same intervening mass of air. To make the comparison between the two sets of data clearer the corresponding values are given in Table 12.

TABLE 12

Intensity at several zenith angles compared with intensity at the vertical for the same mass of intervening air

Absorber	Zenith Angle								Remarks
	0°	Vertical	22½°	Vertical	45°	Vertical	67½°	Vertical	
0	0.237	0.237	0.204	0.202	0.131	0.120	0.035	0.021	48° N. 310 gm. cm^{-2}
10.4 cm. lead	0.0735	0.0735	0.0655	0.0642	0.0463	0.0440	0.018	0.013	
20.8	0.0525	0.0525	0.0484	0.0484	0.0325	0.0342	0.012	0.011	
0	0.188	0.188	0.172	0.177	0.135	0.136	0.055	0.040	Equator. 235 gm.cm^{-2}
10.4 cm. lead	0.0530	0.0530	—	0.050	0.040	0.041	0.020	0.019	
20.8	0.0424	0.0424	0.041	0.040	0.035	0.035	—	0.016	

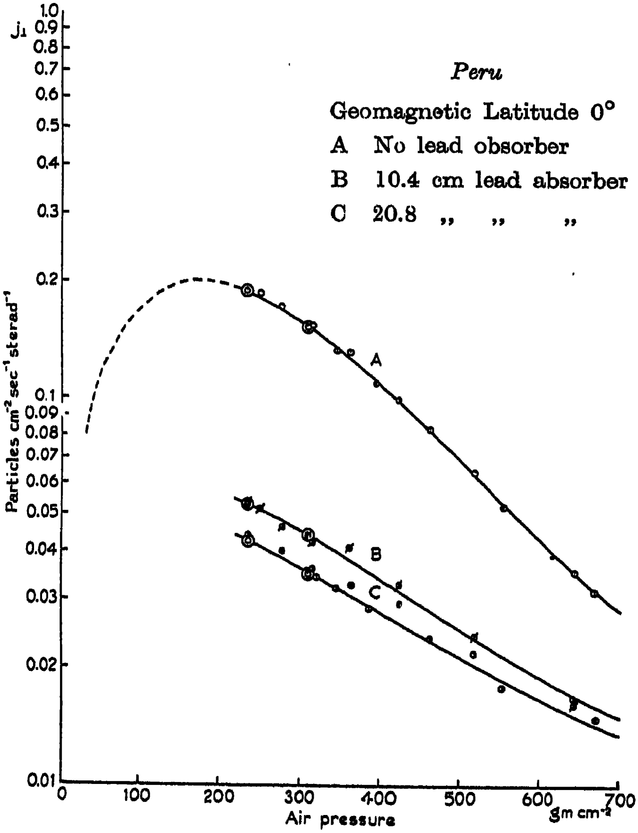

Fig. 24 – Intensity *vs.* air pressure at geomagnetic 0° with and without lead absorber. Extension to curve A is from balloon flights at Bangalore, India, (NEHER and PICKERING [1942]). The double circled points are from averages over long periods of time.

The data given in the lower half of the table are taken from Figs. 21 and 22 for those particular azimuth angles where, according to the calculation of Vallarta *et al.* given in Fig. 1, the same minimum momentum is required for a particle to penetrate the earth's magnetic field. (See discussion in § 1. 5). These values, then, represent a true zenith angle dependence since in these directions the same numbers of particles, with the same momentum distribution, are incident on the top of the atmosphere in all cases. In Fig. 26 are plotted these data at the geomagnetic equator over Peru at an air pressure of 235 gm.cm^{-2}.

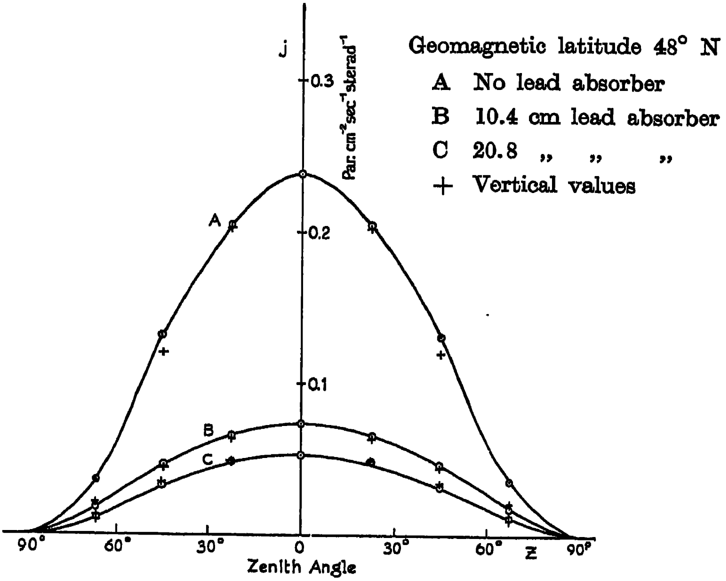

Fig. 25 – Zenith-angle dependence in the North-South plane at 310 gm.cm^{-2} at geomagnetic latitude 48° N. The vertical values are taken from Fig. 23 for the same mass of intervening air.

There is good agreement, using no lead absorber at 22½ ° to the vertical, with the intensity measured at the vertical through the same mass of intervening air. The discrepancy between the two becomes progressively worse at the larger zenith angles and is more pronounced at 48° N than at the equator. At 67½°, the measured intensity at 48° N is 67 % higher than at the vertical through the same mass of air. At the higher altitude at the equator the value at 67½° is 37 % larger than at the vertical through the same mass of air. The situation with lead absorber is considerably better, the discrepancy being 10 % at 48° N and 5 % at the equator, both at a zenith angle of 67½°.

It is believed that here is good evidence for the effects of scattering, for more particles will be scattered into the regions of low

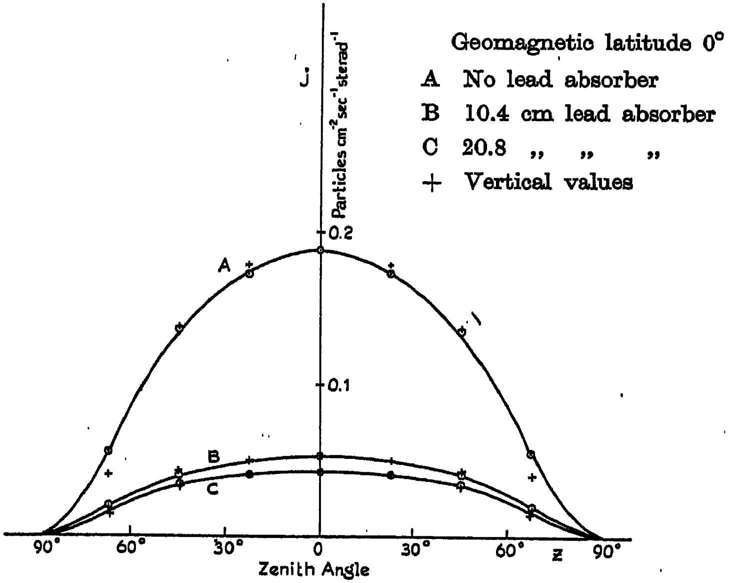

Fig. 26 -- Zenith-angle dependence at the geomagnetic equator at 235 gm.cm-^{2} air pressure, in the direction of constant minimum momentum. The vertical values are taken from Fig. 24 for the same mass of intervening air.

intensity, i.e., at large zenith angles, than are scattered out and this effect will be more pronounced for the lower energy particles that are counted by the telescopes with no lead absorber. In the case of lead absorber the decrease in intensity that would be expected at the larger zenith angles due to decay of the μ-mesons seems to be nearly compensated for by the effect of scattering.

Further evidence for the effects of scattering can be gathered from the latitude curves for 45° E and 45° W as given in Figs. 8 and 9. The unshielded telescope at 45° E shows an increase in intensity soon after the vertical curve starts to rise as one goes north. However in the case of lead absorber the telescopes pointing

45° E show much less increase with new energy coming in from the west and the vertical as one goes north. This again we interpret as due to the scattering of low energy secondary particles through relatively large angles.

4. CORRELATION OF GEOMAGNETIC EFFECTS

4. 1 Introduction

Several attempts have been made in the past to correlate the various geomagnetic effects to see if the known experimental data could be fitted into a consistent scheme. In particular the attempts of JOHNSON [1938] and JANOSSY (Cosmic Rays, Oxford [1948], p. 308) should be mentioned. These authors took their own data or those of others and with the help of the calculations of Störmer, Lemaitre, Vallarta *et al.* on the effect of the magnetic field of the earth on charged particles, tried to tie together, for example, the latitude effect with the east-west effect. These attempts were more or less successful. They suffered partly because of lack of experimental data which in some cases were collected from different authors or a lack of definite calculations on the behaviour of charged particles in the magnetic field of the earth. At the lower latitudes, as pointed out previously, these calculations become exceedingly laborious due to the complexity of the penumbra. VALLARTA [1948] has summarized the most important results of the calculations in a recent paper. The curves there given bring out very well the uncertainties in the calculations at the lower latitudes.

In the following correlation of the various geomagnetic effects we shall take the experimental evidence cited previously, that no more than 0.2 % of the primaries can be electrons, to mean that no appreciable number of negatively charged particles are in the primary radiation. We shall assume in addition that no neutral radiation such as neutrons or photons are among the primary particles. Thus we shall take the primary radiation to consist entirely of positive particles. This being so, all of the geomagnetic effects should be related and, in fact, we shall use this assumed relationship to help solve the problem worked on by Vallarta *et al.* of determining the effect of the magnetic field of the earth on charged particles.

We shall use the calculations of Vallarta *et al.* at the geomagnetic equator as correct for a starting point. In the east-west plane where no penumbra or shadow effect exists these calculations should be free from reasonable doubt. There is somewhat less certainty with the calculations in other azimuths at the equator but the effects of the penumbra and shadow cones are small until one reaches large zenith angles. We therefore shall take the dependence of the minimum momentum of the primary particles on zenith angles as given by Fig. 2 as correct and shall take also the azimuth angle dependence as given by Fig. 1 as correct after making the necessary corrections for eccentricity of the dipole and tilt of the earth's magnetic field in Peru as explained in § 1. 6.

We shall further, for the immediate purpose, use the data from the telescopes with the lead absorber in correlating the various geomagnetic effects since these seem to be more nearly free from effects of scattering. Combining Liouville's theorem with the experimental evidence that with lead absorber the mass absorption law appears to hold together with the assumption that the primary radiation consists only of positively charged particles, we conclude that: if at a certain latitude, longitude, air pressure, azimuth angle and zenith angle a certain intensity of particles is measured that can penetrate the lead absorber, then, if the same intensity is measured at some other latitude, longitude, air pressure, azimuth angle, and zenith angle for the same mass of intervening air, the primary radiation incident on the top of the atmosphere is the same.

4. 2 Correlation of latitude effect and zenith angle effect with the calculations of Vallarta et al.

The zenith angle effect as given in Fig. 26 is for a telescope pointed in the direction of the constant momentum boundary as explained previously. The ratio of these values for the same zenith angle taken in the east-west plane to those in this constant momentum direction is then different from unity only because of the different primary momentum range included. In Fig. 27 this ratio is plotted not as a function of zenith angle, but of the least allowable momentum in the east-west plane for that particular direction as obtained from Fig. 2. The data are for the average of 10 and 20 cm. of lead taken at the atmospheric pressures of 235 and 310 gm.cm^{-2}. The values at 310 gm.cm^{-2} are computed from data, some of which have not been heretofore published. A slightly greater asymmetry is shown at the higher altitude as mentioned previously. In the calculations that follow a linear relation is assumed between this ratio and the mass of absorbing air for the limited ranges of air mass involved.

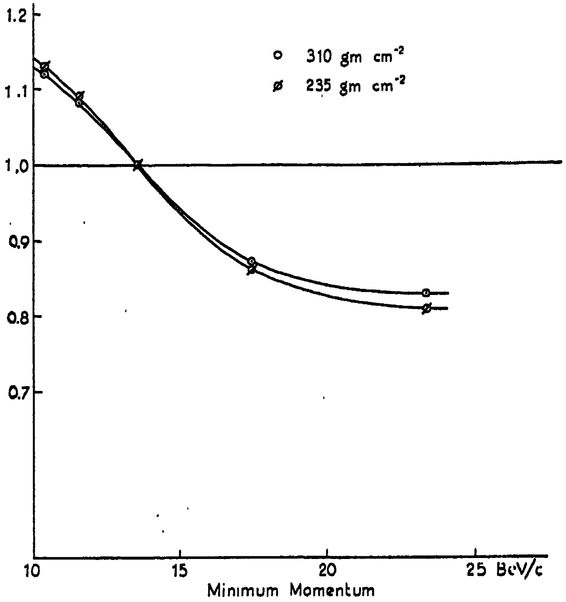

Fig. 27 – Ratio of intensity in the East-West plane at the equator to that in the direction of constant minimum momentum, for the same mass of intervening air, as a function of minimum momentum of the incident particles. Average for 10.4 and 20.8 cm. lead.

Assuming only positive primary particles, we must expect the same relative increase in the latitude effect at the vertical as we go away from the equator, shown in Figs. 9 and 11, as is shown in Fig. 27 when the momentum range covered is the same. We thus have sufficient information to solve parametrically for the minimum momentum of the primary particles *vs.* geomagnetic latitude. This has been done as shown in Fig. 28 down to a minimum momentum of 10.3 BeV/c or a latitude of 22.5° N and has not been carried farther because of the increasing importance of atmospheric absorption.

Plotted in the same figure are the two limiting curves given in the summary by VALLARTA [1948]. The curves here are plotted on a momentum basis and are corrected for tilt and eccentricity of the earth's magnetic field. The upper broken curve gives the calculated momentum a particle must have in the vertical direction at the geomagnetic latitude given by the abscissa, above which all momenta are allowed by the earth's magnetic field. The lower broken curve gives the least momentum a particle must have in order to penetrate the earth's magnetic field in a vertical direction at the geomagnetic latitude given by the abscissa.

The experimental curve has been extended to higher latitudes by gradually dropping down to the lower curve, following the instructions given by Vallarta.

The next comparison we shall make with the calculations of Vallarta *et al.* is using the latitude effect at 45° as given by Figs. 9 or 11. Again, using the average values for 10 or 20 cm. of lead,

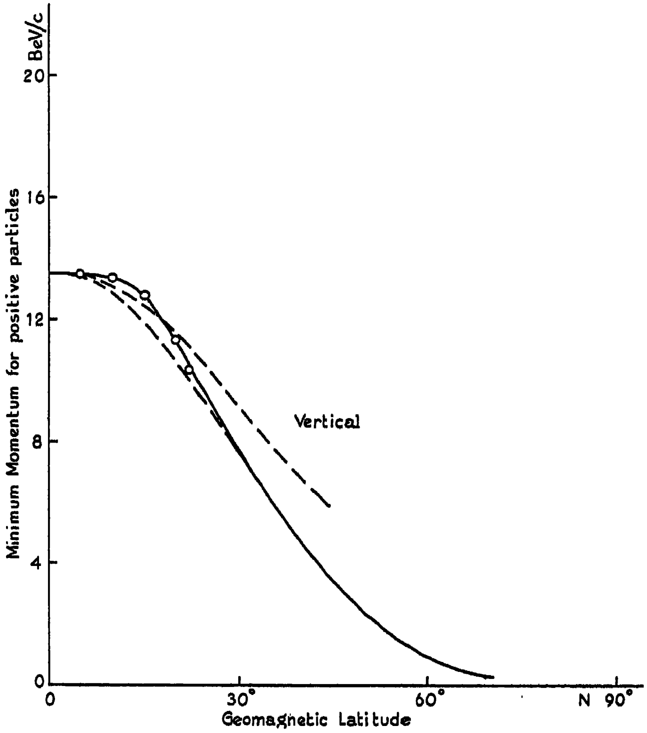

Fig. 28 – Experimentally derived dependence of minimum momentum *vs* geomagnetic latitude at the vertical. Dashed curves are those given by VALLARTA [1948].

we find that since the intensity, when the telescopes are pointed at zenith angle 45° E at latitude 31° N is the same as when pointed 45° W at the equator, the same momentum range must be covered by the 45° E telescope when carried from 31° N to the equator as is covered by the telescope sweeping across the sky in the vertical plane at the equator from 45° W to 45° E.

Solving parametrically the two experimental curves of relative counting rate *vs.* geomagnetic latitude, and relative counting rate *vs.* momentum as given in Fig. 27, we arrive at the results shown by the dots in Fig. 29 for minimum momentum *vs.* geomagnetic latitude for the case of zenith angle 45° E. The point at 10° N indicates the same minimum momentum as 0°. This is due to the fact that no increase with geomagnetic latitude is found at 45° E with either lead telescope up to 10° N.

At 31° N the minimum momentum at 45° E is the same as for the equator at 45° W as shown experimentally by the same intensities. We can carry the comparison of the experimental results with calculations to higher latitudes by noting from the lead curves of Figs. 9 or 11 that, beginning with 0° and 31° N there is a latitude, where toward the west the intensity is the same as at another latitude toward the east. From what has been said previously, this means that the minimum momentum must be the same in the two cases. In Table 13 pairs of latitudes are given at which these intensities become equal for the average of 10 and 20 cm. of lead absorbers.

TABLE 13

Pairs of latitudes at which the intensity at 45° W becomes equal to that at 45° E. Average of 10 and 20 cm. of lead

0 and 31° N	30 and 37.5° N
15 and 31.5° N	35 and 41.5° N
20 and 33.0° N	40 and 45.5° N
25 and 34.2° N	45 and 51.0° N

These pairs of points have been plotted in Fig. 29 and shown by the circles. In plotting these we start first with the previous point at 31° N and extend the 45° E curve in such a manner that the corresponding points lying on the 45° W curve gradually drop down to the lower of the two extreme curves (shown dashed) given by VALLARTA [1948].

The above experimental solution to the problem of the behaviour of charged particles in the magnetic field of the earth leans heavily on the theoretical calculations of Störmer, Vallarta and others. What we have done here is to try to determine experimentally the behaviour in those regions where the calculations are very laborious and have not in general been carried out.

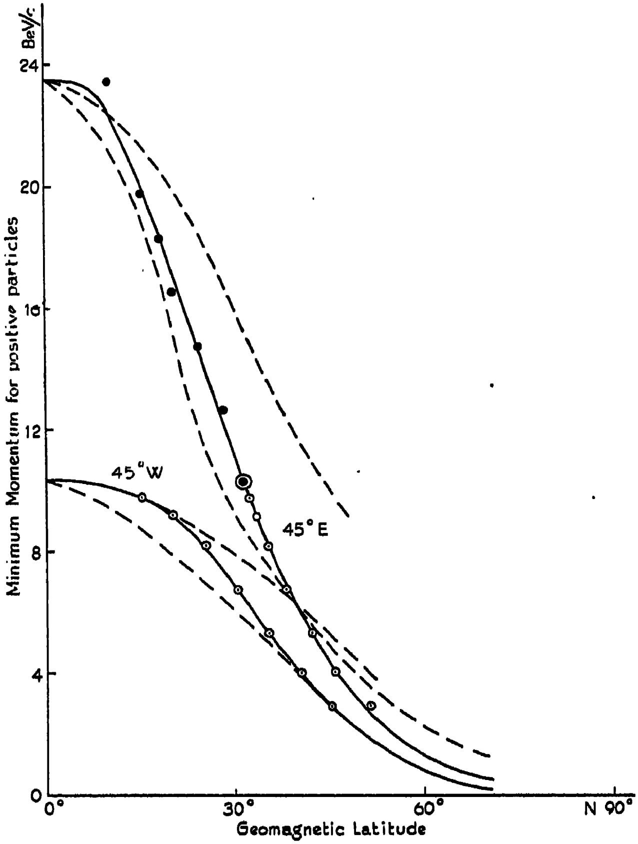

Fig. 29 – Experimentally derived dependence of minimum momentum *vs* geomagnetic latitude at 45° East and 45° West. Dashed curves are those given by VALLARTA [1948].

It should be remarked that these curves have been strictly determined only along longitude 80° W and are not applicable directly to other longitudes. However, using the corrections for eccentricity and tilt of the earth's magnetic field, as discussed in

§ 2. 6, and with the help of calculations of Vallarta it should be possible to predict the behaviour at other longitudes. It will be noticed that all of the experimental curves tend to lie above the upper curve given by Vallarta at the low latitudes. This may be due to the peculiar variation of the earth's magnetic field along this particular longitude.

4. 3 Correlation of azimuthal effect with zenith angle effect at the equator

In Fig. 1 the calculated boundaries of the cones for particles of minimum momentum are plotted as given by LEMAITRE and VALLARTA [1936]. We have already used these calculations for the boundary of that cone which passes through the vertical to find the zenith angle dependence for particles of the same momenta.

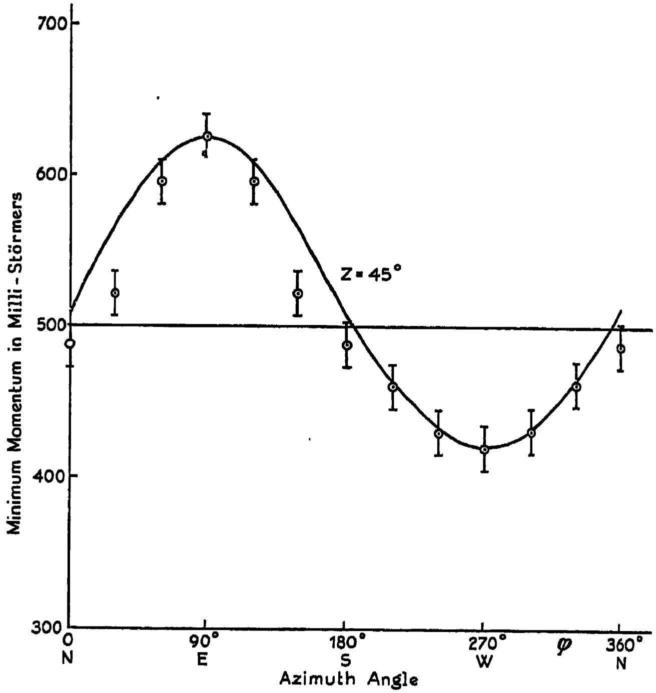

Fig. 30 – Comparison of the measured azimuthal effect at zenith angle 45° with the results given in Fig. 27 permits a determination of minimum momentum *vs* azimuth angle. The curve is from calculations of LEMAITRE and VALLARTA [1936b] as given in Fig. 1.

We can make a detailed comparison at other zenith angles by using the experimental values given in Fig. 27 and the azimuthal curves given in Figs. 20 and 22. Again we solve the two curves parametrically and find the relation between minimum momentum and azimuth angle. The comparison of these results with the calculations of Lemaitre and Vallarta is shown in Fig. 30 where we have used only the data with lead absorber and for zenith angle 45°. Suitable corrections to the ordinate of the calculated curve have been made to allow for eccentricity of the earth's dipole and tilt of the magnetic field. It is apparent that with due regard for the experimental errors involved there is satisfactory agreement between the calculations and experimental values.

4. 4 Correlation of latitude, zenith angle and longitude effects

When the telescopes that pointed 45° E were carried from northern latitudes to the equator, the minimum momentum range covered for the primaries was 1 to 23 BeV/c. This includes the momentum range covered by particles just able to get in at the vertical in going from Peru (13.5 BeV/c) to southern India (17.0 BeV/c). Actually the azimuth experiment at the equator at 22½° to the vertical also covered this momentum range. In Fig. 31 we have

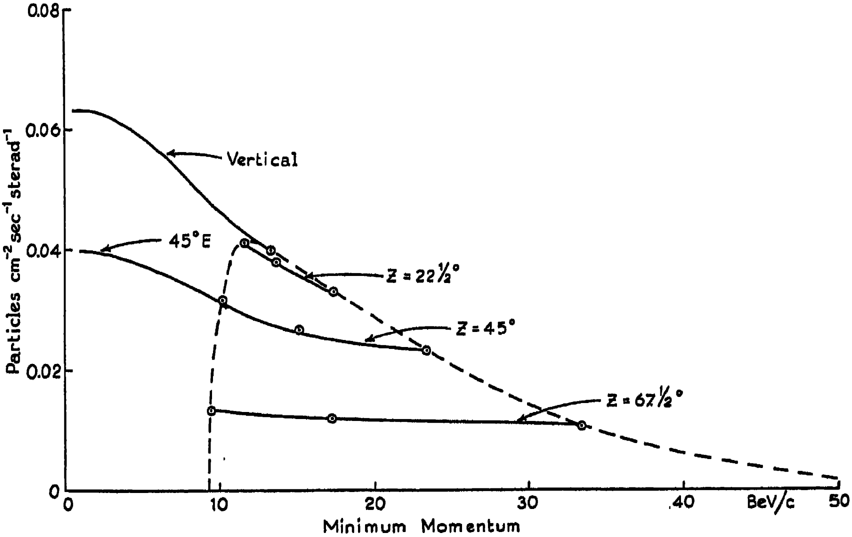

Fig. 31. – Using the results of Figs. 2, 28 and 29, it is possible to plot intensity *vs* minimum momentum for the latitude and azimuth-angle effects.

plotted the intensity as measured through the average of 10 and 20 cm. of lead as a function of minimum momentum as determined from Figs. 28 and 29, for not only the experiments on the latitude effect but for the azimuthal effect as well. The smoothed curve at 45° E, for example, covers the momentum range 1 to 23 BeV/c, while the azimuth experiment at the same altitude and zenith angles covers the range 10.3 to 23 BeV/c. The experimental points for the azimuth experiment are shown. It is really not surprising that the agreement between the two sets of data is so good for we have determined the values of minimum momentum *vs.* latitude and azimuth angle in such a way as to give agreement.

A further test of the above results, however, is to compare the longitude effect found between India and Peru with the change in intensity shown in Fig. 31 between the same momentum ranges. From the zenith angle data at $22\frac{1}{2}°$, corresponding to an air pressure of $310 \sec 22.5° = 335$ gm.cm^{-2}, we find a 13 % decrease in going from 13.5 to 17 BeV/c. Now the latitude effect in the total radiation and in the penetrating part is nearly the same. Hence, assuming the radiation responsible for the longitude effect to be of the same nature we would expect a 13 % change at this air pressure in going from Peru to India either with or without lead absorber. It is difficult to compare this figure with existing experimental data since similar flights have not been made in Peru and India. However a comparison of the counter telescope readings taken at this height over Peru and given in Fig. 24 is certainly not in disagreement with the data published by NEHER and PICKERING [1942].

Another comparison can be made through a greater mass of air. From Fig. 31 we find for the momentum range 13.5—17 BeV/c a change in intensity at $67\frac{1}{2}°$ of 5 %. At $67\frac{1}{2}°$ the mass of air along the axis of the telescope is 810 gm.cm^{-2}. Millikan and Neher at sea level, or 1030 gm.cm^{-2}, found a longitude effect with ionization chambers of 4 %. This latter figure would certainly be higher if taken at 810 gm.cm^{-2} with a counter telescope, but we may say nevertheless that within the experimental errors there is satisfactory agreement.

4. 5 Summary of correlation of geomagnetic effects

The calculations of Störmer, Lemaitre, Vallarta *et al.* on the paths of charged particles in the magnetic field of the earth have shown the general behaviour to be expected in the several geomagnetic effects found in cosmic rays. In case the primaries are all of one sign of charge, their calculations in conjunction with Liouville's theorem make the problem of cosmic ray interpretation much simpler than if there were a mixture. Experimental evidence points to a negligible percentage of negative particles. We have therefore assumed that only positively charged particles are contained in the primary radiations. A corollary of this is that all of the geomagnetic effects are related. We have therefore turned the problem around and tried to determine how, for example, the minimum momentum for entrance of the charged particles at several zenith angles changes with geomagnetic latitude. This we have done with the help of the theoretical calculations and have, in fact, assumed that they are correct in the east-west plane at the equator. The evidence is that the experimental measurements on the geomagnetic effects are consistent within the experimental errors and that the theoretical calculations can be fitted with experiment to make an overall consistent scheme.

5. ENERGY DISTRIBUTION OF THE PRIMARY RADIATION

5. 1 Introduction

A number of attempts in the past have been made to determine the energy distribution of the primary particles. This first became possible with the balloon flights of BOWEN, MILLIKAN and NEHER [1938] at several different geomagnetic latitudes. These flights, however, covered rather wide ranges in latitude. Especially large was the jump between San Antonio, Texas and Madras, India. Balloon flights with counter telescopes were made by NEHER and PICKERING [1942], MILLIKAN, NEHER and PICKERING [1944] and BIEHL, MONTGOMERY, NEHER, PICKERING and ROESCH [1948] at closer intervals of latitude. A correlation between the readings of counter telescopes and ionization chambers as discussed in § 2. 4 now permits the former to be used for purposes of energy determination.

5. 2 Normalization of counter telescope curves

From the data taken with the vertical telescopes on the flight at 30,000 ft. to Peru along longitude 80° W, it is possible to redraw the balloon telescope counter curves in such a manner as to agree with the airplane data at 310 gm.cm^{-2} air pressure, as given in Fig. 10. To do this, all curves at a particular latitude were multiplied by a constant factor to affect this coincidence. This procedure is thought to be justified (a) by the fact that curves taken at stations close together in latitude are closely similar; (b) if the adjustment involves correcting for changes in the primary radiation, such changes will affect the whole curve more or less by the same percentage; (c) the fitting is done rather high up on the curves (in the case of the curve at Omaha, 60 % of the way to the maximum) and (d) the adjustment was in all cases only a few per cent. Such adjustment in principle, at least, will have the effect of eliminating instrumental errors and fluctuations in the primary radiation. The balloon counter curves so normalized are shown in Fig. 32. Here we have picked out certain of the balloon flight curves from those available as being the most consistent for the flights made at a given station and also for being well spaced in latitude.

TABLE 14

Location	Geo-magnetic Latitude	Min. Energy at Vertical for Proton in BeV*	Counts cm^{-2} sec^{-1}sterad^{-1} × gm.cm.$^{-2}$	BeV cm.$^{-2}$ sec^{-1} sterad^{-1}
Saskatoon . .	60° N	0.4	162	0.774
Omaha . . .	51° N	1.4	157	0.740
Ft. Worth . .	42° N	3.2	147	0.660
Acapulco. . .	25° N	8.7	122	0.508
Peru	0°	12.6	103	0.413
Peru (45° E) .	0°	22 (45° E)	84	0.310

*) Because of the method used to adjust the curves taken at the stations in the first column on the left, these energy values are for these particular geomagnetic latitudes at longitude 80° W.

In Table 14 is given a list of stations with their geomagnetic latitudes, the values of the minimum energy for protons permissible at the vertical as calculated from Fig. 28 using Eq. 1, and the areas under certain selected counter telescope curves. The value for Peru (45° E) was obtained by taking the two points at 45° E at 235 and 310 gm.cm^{-2} air pressure and constructing a curve that passed through these points. The position of the maximum and the slope of this curve could be estimated by knowing how these quantities changed with the momentum of the incident particles.

In calculating the area in BeV $\mathrm{cm}^{-2}\,\mathrm{sec}^{-1}\,\mathrm{sterad}^{-1}$, the values of specific ionization as taken from Fig. 3 were used, together with a value of 32 eV per ion pair. In Table 15 the differences in the areas between adjacent stations are given and these are plotted as a histogram in Fig. 33 for the energy limits given in Table 14. The ordinates, then, represent the energy per cm^2 per second being brought into the earth by particles whose energy lies between E and $E + dE$. By Liouville's theorem, this is also the energy distribution in space. (The reasons for assuming protons only will be discussed later).

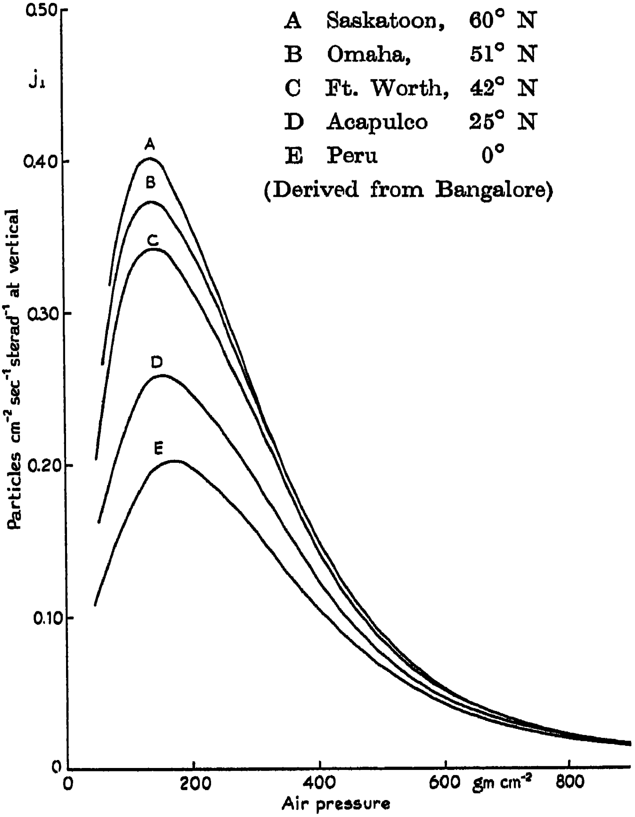

Fig. 32 – Former balloon counter telescope curves are normalized to present airplane data at 310 $\mathrm{gm.cm}^{-2}$ air pressure.

TABLE 15

Stations	Δ area, BeV $\mathrm{cm}^{-2}\ \mathrm{sec}^{-1}\ \mathrm{sterad}^{-1}$
Saskatoon–Omaha . . .	0.034
Omaha–Ft. Worth . . .	0.080
Ft. Worth–Acapulco . .	0.155
Acapulco–Peru.	0.095
Peru–Peru (45° E) . . .	0.103

The blocks given in Fig. 33 are obtained from differences of curves and are therefore subject to considerably more error than the curves themselves. Further, the limiting energy for the particular station is also subject to some error. In comparing the present energy distribution with that given by BOWEN, MILLIKAN and NEHER [1938] using their data from thin-walled ionization chambers, it is seen that the general shape is the same. The chief difference is in the abscissa.

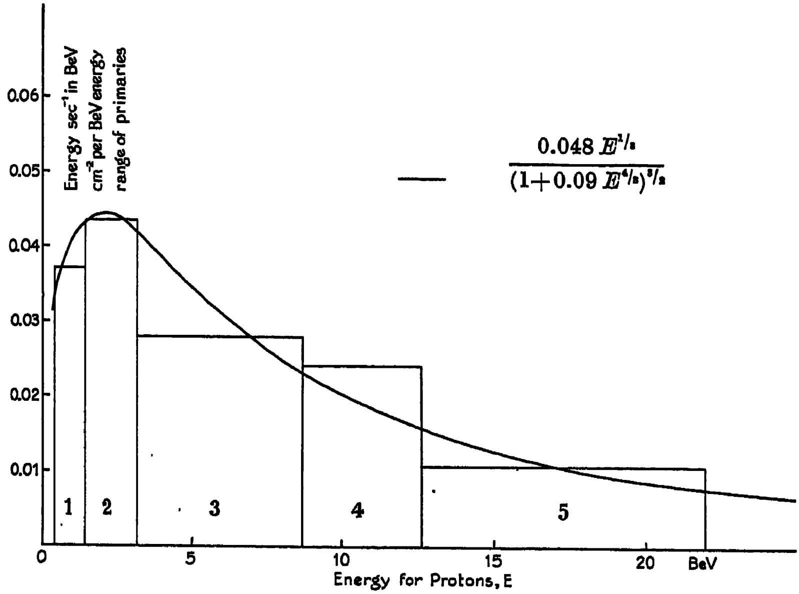

Fig. 33 – Histogram of differences in areas under counter telescope curves. Smooth curve is an empirical energy distribution.

5. 3 Empirical relations

It would be desirable to find an empirical expression that would represent the experimental data as well as possible. A simple power law such as E^{-n} obviously cannot represent the situation at low energies; hence it seems necessary to go to a more complicated expression. One that seems to fit the situation the best is given by

$$EN(E) = \frac{0.048\,E^{1/3}}{(1+0.09\,E^{4/3})^{3/2}} \tag{14}$$

in BeV cm^{-2} sec^{-1} sterad^{-1} per BeV energy range. This curve is plotted in Fig. 33.

The numbers distribution is therefore, $N(E)$ and the number of particles with energies greater than E is given by $\int_0^\infty N(E)dE$. This integral has been evaluated graphically and the results are given in Fig. 34.

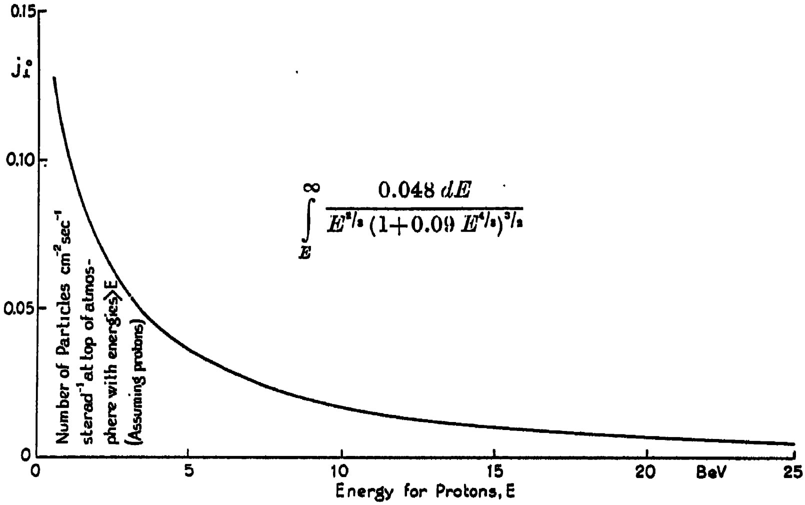

Fig. 34 – Intensity of incident particles *vs* energy, assuming only protons.

In justification of Eq. (14) the following may be cited:

(a) The expression may be integrated directly and gives a total energy for all particles of 0.418 BeV cm^{-2} sec^{-1} sterad^{-1} at the vertical in Peru. The experimental value is 0.413 as seen from Table 14.

(b) A similar integration for Bangalore gives 0.35 as against the experimental value 0.34.

(c) From 0.4 BeV to ∞ it gives 0.787 as compared with 0.774 for Saskatoon.

(d) It gives a dependence on E of $E^{-2.67}$ for the differential number distribution at very large E. This is within the limits of the exponent found by HILBERRY [1941] to be necessary to explain extended showers.

(e) It gives an effective dependence on E of $E^{-1.1}$ for the integral number spectrum in the range 2 to 12 BeV. This is the distribution found necessary by VAN ALLEN and SINGER [1950] to explain their results using rockets.

(f) It gives a ratio in the total number of particles at 50° N and 30° N of 3.4 compared with the value of 3.5 found for all primaries by BRADT and PETERS [1950].

While the above distribution agrees well with the relative values found with rockets above the atmosphere by van Allen and Singer, their absolute value is a factor of 2 larger[3]. On the other hand, the presence of heavy nuclei in the primaries means that the calculated value, assuming only protons, will be high since each heavy nucleus brings in for large E more energy by a factor of Z than a proton which is just able to get to the earth at a given latitude. Expressing the ordinates in terms of nucleons instead of protons would be more nearly correct. The chief difficulty in this latter case is that the neutrons get a free ride. However, taking the data given by BRADT and PETERS [1950] that the ratios of protons: α-particles: C, N, O: $Z > 10$ are 78: 20: 0.78: 0.22, we find that if these ratios hold for all latitudes the numbers of particles will be about two-thirds of what there would be with protons only. This makes the discrepancy with the directly measured value of van Allen and Singer even worse. The difficulty may arise from two factors (a) it is known that meson decay involves the loss of energy presumably in the form of neutrinos, and (b) there is an unknown albedo effect above the main part of the atmosphere which may add to the values found with rockets or with instruments sent to high altitudes with balloons.

---

[3] A good summary of values on the primary flux is given by WINCKLER, STIX, DWIGHT and SABIN [1950]. Their own data taken from 90 to 100,000 feet at several latitudes is quite extensive and agrees with that of Singer and Van Allen when extrapolated to the top of the atmosphere in showing a similar factor of 2 at all latitudes.

We shall take the numbers, calculated from protons only, as correct and any future information on the two effects cited above may be used to correct these figures.

5. 4 Consequences of the above distribution of cosmic ray energy

Two features of the energy distribution of the primary cosmic ray particles should be pointed out. The differential energy distribution as shown in Fig. 33 seems definitely to pass through a maximum at 2 or 3 BeV (protons). This characteristic has been pointed out previously and needs to be taken into account in any theory of the origin of cosmic rays or their subsequent behaviour before arriving at the earth. A second feature is the absence of any definite cut-off of the primary radiation at northern latitudes. Thus even though the energy brought in by particles whose energy lies between E and $E + dE$ may go to zero for zero energy, the differential number distribution may still increase as E goes to zero.

There are several experiments besides those cited above that bear on the cut-off of the primary radiation at high latitudes. CARMICHAEL and DYMOND [1939] sent balloons with an ionization chamber to 17 gm.cm^{-2} air pressure at $\lambda = 85°$ N on August 3, 1937. On August 14—17 of that same year, BOWEN, MILLIKAN and NEHER [1938] made flights at Saskatoon, Canada, with ionization chambers having very close to the same wall thickness as that used by Carmichael and Dymond. The two resulting curves, when fitted from 100 gm.cm^{-2} to sea level, show an apparent 5 % latitude effect at the maxima. This may be a true latitude effect, or, as pointed out by CARMICHAEL [1949] may be due to somewhat higher field strengths and consequently a larger fraction of the ions collected from the heavily ionizing particles, in their case. At the most, however, these experiments would permit a latitude effect no greater than 5 % between 60° N and 85° N.

However, POMERANTZ [1950] finds an increase at very high altitudes of 46 % using counter telescopes with and without absorber between geomagnetic latitudes 52° and 69° N. These experiments were performed in the summer of 1949.

That there are large fluctuations in the primary radiation at high altitudes and latitudes is well borne out by the ionization chamber measurements of MILLIKAN, NEHER and PICKERING [1944] made in the summer of 1940. Using the same instruments as used at Saskatoon in 1937 it was found that at Bismarck, N. D., the highest intensity reached was 470 ions $cm^{-3} sec^{-1} atm^{-1}$ of air at 30 $gm.cm^{-2}$ and the curve showed no signs of turning over. This is 25 % greater than the value found at the maximum of the curve for Saskatoon in 1937. This large increase occurred near the top of the atmosphere but there was still some increase as far down as 500 $gm.cm^{-2}$. It is significant, however, that the values in 1940 at San Antonio, $\lambda = 38°$ N, agreed with those of 1936.

If the magnetic field of the sun were responsible for affecting the charged particles that can arrive from infinity, then one might hope to find a diurnal effect (which seems to be lacking) and perhaps a periodic effect depending on the solar sun spot cycle.

6. SOME CONCLUSIONS ON THE GROSS BEHAVIOUR OF COSMIC RAYS IN THE ATMOSPHERE

6. 1 Introduction

Numerous attempts have been made either (a) to predict the individual processes of absorption of the primary radiation in the atmosphere by knowing the over-all or gross behaviour, or (b) to predict the over-all behaviour, knowing the individual processes. Both courses of action have led to many incorrect conclusions in the past. The reasons have been a lack either in sufficient experimental information or in theoretical calculations. The absorption process and the nuclear reactions involved have turned out to be much more complex than originally supposed and, in fact, to involve many entirely new processes. It is true, however, that once the individual processes are known it should, in principle at least, be possible to predict the gross behaviour.

6. 2 Absorption in lead as a function of minimum momentum of the primaries

If lead is added between the counter trays of a telescope (in our case between the second and third from the top) the particles or their charged secondaries that cannot penetrate that thickness of lead will be eliminated. The ratio of those particles that are not so eliminated at a given depth in the atmosphere, to the total number of particles present gives a measure of the penetrating particles present. It might be supposed that this ratio would depend on the momentum of the primary, initiating particle. In Table 16 are given these ratios for given values of minimum momentum of the primary.

TABLE 16

Ratio of penetrating to total charged particles for selected values of minimum momentum of primaries

	2.5 BeV/c	13.5 BeV/c		23 BeV/c
	310 gm cm^{-2}	310 gm cm^{-2}	235 gm cm^{-2}	330 gm cm^{-2}
10.4 cm. lead . .	0.30	0.29	0.28	0.29
20.8 cm. lead . .	0.22	0.23	0.23	0.25

It is evident from these values that the fraction of particles that can penetrate 10 or 20 cm. of lead is not strongly dependent on the energy of the primary particles within the ranges covered. There is some evidence that the higher energy primaries give rise to a somewhat larger fraction of secondaries that can penetrate 20 cm. of lead than the lower energy primaries.

It is of interest to calculate the numbers of penetrating and non-penetrating particles at a given depth in the atmosphere that result from a given number of primaries. This will be done in more detail in the next section for particles of given energies. Let us find the ratio of penetrating to non-penetrating particles at 45° E and 45° W at the equator at a vertical depth in the atmosphere of 235 gm.cm^{-2}. There are incident on the top of the atmosphere, according to Fig. 34, 0.0050 particles cm^{-2} sec^{-1} sterad^{-1} at 45° E at the equator. By the time this radiation has penetrated to 235 cos 45° = 330 gm.cm^{-2} there are 0.079 particles cm^{-2} sec^{-1} sterad^{-1} that cannot penetrate 10 cm. of lead and 0.032 that can, according to Table 9. Thus the non-penetrating (we assume mostly electrons) particles have multiplied up by a factor of 16 and the penetrating particles by a factor of 6.4 (we assume mostly μ-mesons). On the other hand there are incident on the top of the atmosphere, according to Fig. 34, 0.016 particles cm^{-2} sec^{-1} sterad^{-1} at 45° W at the equator. By the time this radiation has penetrated to the same depth, i.e., 330 gm.cm^{-2}, there are 0.095 particles cm^{-2} sec^{-1} sterad^{-1} that cannot penetrate 10 cm. of lead and 0.044 that can. The non-penetrating particles have thus multiplied up by a factor of 6.0 and the penetrating by a factor of 2.7. The ratio of penetrating to non-penetrating (using 10 cm. of lead as a dividing line) is in this case 0.45 while at 45° E the similar ratio from above is 0.40. There is thus some evidence that as the energy of the primary increases the ratio of penetrating particles to non-penetrating at $^1/_3$ atm. decreases.

This trend is consistent with the behaviour of the very high energy primaries that are responsible for the extended showers. For these particles the ratio of penetrating to non-penetrating is of the order of 0.02. (See COCCONI, TONGIORGI and GREISEN [1949]).

6. 3 Multiplicity of charged particles

For every particle incident on the top of the atmosphere there will be a number m of charged particles at some depth in the atmosphere. If dj is the number of particles at a given depth in the atmosphere due to primaries whose energy (again assuming protons) lies between E and $E + dE$ and $dj°$ is the number of primaries in this same energy range, then $m = dj/dj°$ will be the multiplicity due to particles of this energy.

If we consider the data of Fig. 32 and take the intensity as a function of geomagnetic latitude we arrive at the curves of Fig. 35. These give the latitude effect for given depths in the atmosphere for the total radiation.

We next plot these same curves *vs.* minimum energy (for protons) and arrive at Fig. 36. For comparison we plot on this same figure the derived integral number distribution of the primary particles as given originally in Fig. 34. To find the multiplicity we then divide the slope of one by the slope of the other at a given E. The results are shown on a double logarithmic plot in Fig. 37. The sea-level is obtained from the counter telescope data of NEHER and PICKERING [1938] taken on a route passing from Japan to Singapore to Melbourne.

The overall multiplicity rises to a factor of 7 for 10 BeV incident particles, the maximum occurring at a depth of about 150 gm.cm^{-2}. For 10 BeV particles incident on the top of the atmosphere only one in ten results in charged particles that can reach sea-level.

The azimuth experiments at the equator at 310 and 235 gm.cm^{-2} allow extensions of these results to higher energies. These extensions all show a less rapid dependence of m on the energy of the primary particle than the latitude data. Indeed, for very large energy primaries such as are responsible for extended showers, the overall multiplicity at sea level or mountain altitudes must increase about linearly with E. The reason for this is that a considerable part of the energy of the primary must eventually go into the electronic component which (as far as we know), according to shower theory, results in a number of electrons proportional to the energy of the original electron or γ-ray.

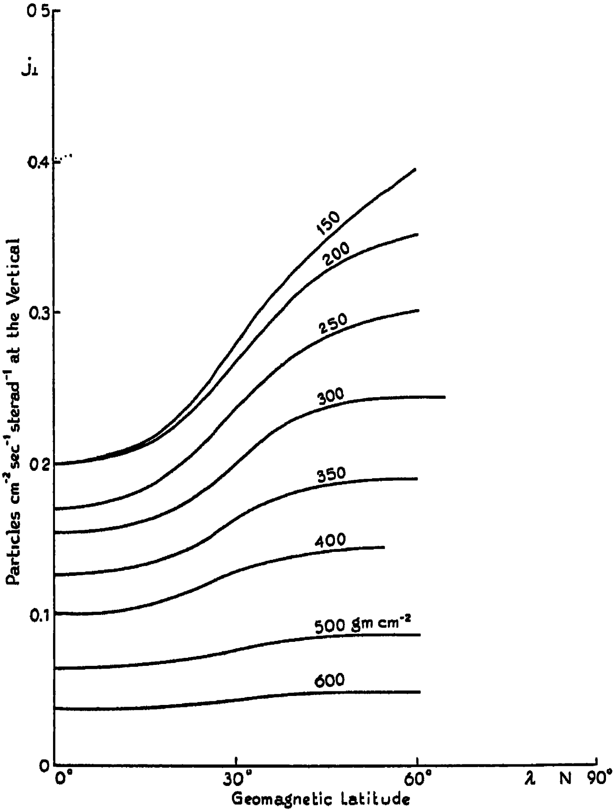

Fig. 35 – Intensity of the ionizing particles at the vertical for certain atmospheric depths. These curves are taken from those of Fig. 32.

Two derived results may be obtained from Fig. 37. The slopes of the lines give the multiplicity as a function of E for a given depth in the atmosphere. For sea level the multiplicity varies as $E^{2.8}$ for the energy range covered. As pointed out above, this rapid dependence of the secondaries, that can reach sea level, on the energy of the parent particles, cannot continue.

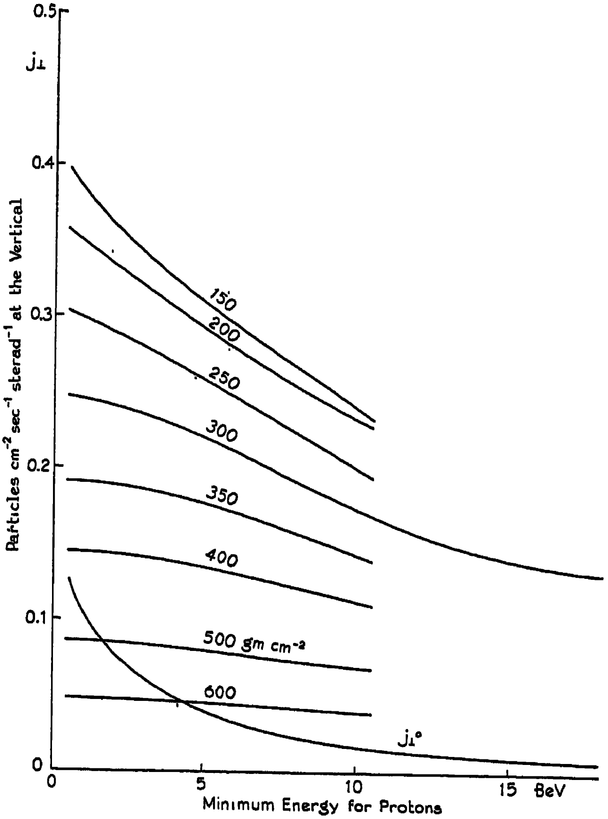

Fig. 36 – Curves of Fig. 35 are plotted as a function of minimum energy (assuming protons) of the incident particles. Curve marked $j^0_\perp$ is the total number of incident particles with energies larger than E as taken from Fig 34. The extension of the 300 gm.cm^{-2} curve is derived from the azimuth data at the equator.

The other derived result is obtained by taking the multiplicity as a function of depth for a given energy of the primary. The results are shown in Fig. 38. Probable extensions of these curves are shown dotted.

The 10 BeV curve has a slope of 138 gm.cm^{-2} at 500 gm.cm^{-2} air pressure. To compare this with other results, we may take the difference between the counter telescope data at Peshawar and Bangalore, India, where the mean energy of the primaries respon-

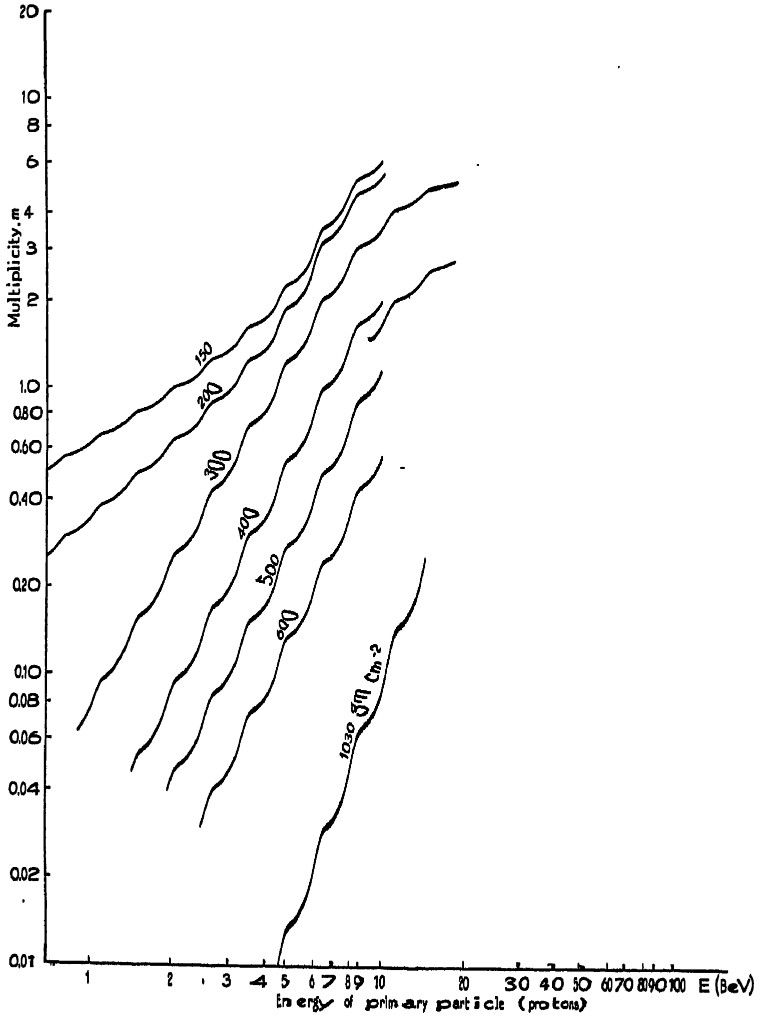

Fig. 37 - Overall multiplicity, *m*, *vs* energy of the incident particles for certain depths in the atmosphere.

sible for this difference is about 13 BeV. The slope of this line when plotted logarithmically is 150 gm.cm^{-2} at this same depth of 500 gm.cm^{-2}.

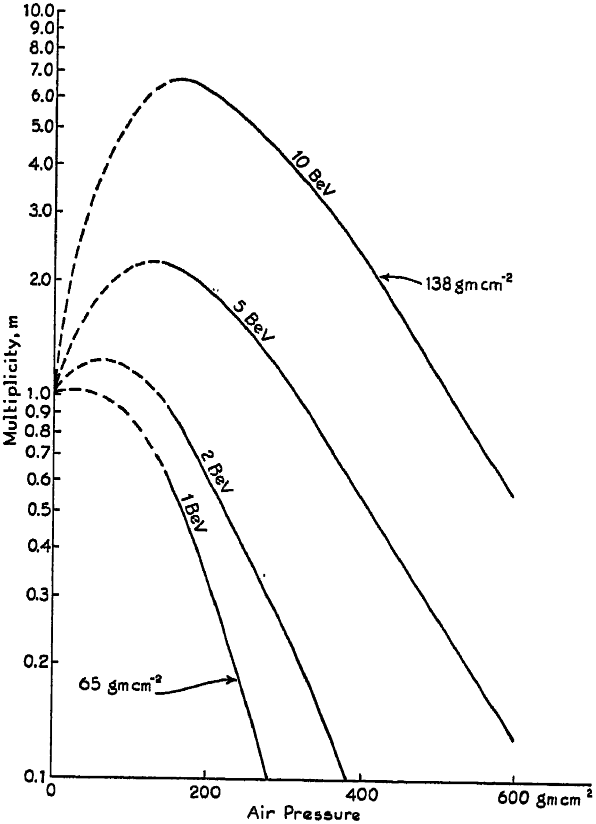

Fig. 38 – Multiplicity *vs* atmospheric depth for definite energies of the primaries (assuming protons). The dashed curves represent probable extensions.

The 1 BeV line shows an absorption of about 65 gm.cm^{-2}. This is close to the mean cross-section for air nuclei. Such a rapid absorption means that few protons of 1 BeV energy will succeed in causing any effect at $^{1}/_{3}$ atmosphere, or below.

If the primary flux as derived from areas under ionization or counter curves is not correct by some factor, the ordinates of Figs. 37 and 38 must be changed accordingly. In particular if the primary flux is that obtained by VAN ALLEN and SINGER [1950] using rockets, then the ordinates of the plotted curves must be decreased by a factor of 2.

6. 4 Consequences of dependence of multiplicity on energy of the primaries

This dependence of the number of secondary particles on the energy of the primary has an important bearing on the percentage west excess found in the atmosphere. Thus the integral number distribution found in § 6. 3 indicates a ratio of 3 to 1 in the total number of primaries at the equator incident at 45° W to those at 45° E. This does not mean a 100 % east-west effect will be measured in the atmosphere. Indeed, if one assumes a multiplicity which depends linearly on E, then the number of secondaries will be proportional to $EN(E)$. This is just Eq. (14). Hence the east-west effect for zenith angle 45° will be, under this assumption:

$$2 \cdot \frac{\int_{10.3}^{\infty} EN(E)\, dE - \int_{23}^{\infty} EN(E)\, dE}{\int_{10.3}^{\infty} EN(E)\, dE + \int_{23}^{\infty} EN(E)\, dE} = 0.40.$$

We would thus expect a 40 % east-west effect at 45° zenith angle. The measured value with no lead absorber at 36,000 feet over Peru was 30 % and with 10 cm. of lead, 33 %. A slightly stronger dependence on the energy of the primaries as indicated by Fig. 37, would bring agreement with the measured values.

The fact that measurements in rockets made by VAN ALLEN and GANGNES [1950] at the equator showed an asymmetry of only 40 %, together with the balloon measurements of WINCKLER and associates [1950], who found an asymmetry of 0.53 at zenith angles 40—60° at 90,000 to 100,000 ft. are good arguments in favour of a rather large albedo, or general background, at or near the top of the atmosphere.

7. SUMMARY

The attempt has been made to correlate a rather large variety of experiments having to do with the behaviour of the incident, charged particles in the magnetic field of the earth. In order to provide the necessary internal consistency, data taken with the same, or similar apparatus only, were used. It is found that the experimental data and the calculations on the behaviour of charged particles in the magnetic field of the earth can be fitted into a consistent scheme. Also, a correlation of counter telescope and ionization data at various latitudes has permitted a more exact redetermination of the energy distribution of the primary particles. This distribution is found to be consistent with rocket flights as far as relative values are concerned, but is low by at least a factor of two in absolute value. Other results are derived for the overall multiplicity of charged particles and the absorption of the radiation in the atmosphere.

REFERENCES

BARTELS, J. and S. CHAPMAN, 1940, Geomagnetism. (Oxford University Press).

BIEHL, A. T., R. A. MONTGOMERY, H. V. NEHER, W. H. PICKERING and W. C. ROESCH, 1948, Rev. Mod. Phys., 20, 360.

BIEHL, A. T., H. V. NEHER and W. C. ROESCH, 1949, Phys. Rev., 76, 914.

BIEHL, A. T. and H. V. NEHER, 1950, Phys. Rev., 78, 172.

BOWEN, I. S., R. A. MILLIKAN and H. V. NEHER, 1938, Phys. Rev., 53, 855.

BRADT, H. L. and B. PETERS, 1950, Phys. Rev., 77, 54.

CARMICHAEL, H. and E. G. DYMOND, 1939, Proc. Roy. Soc., A171, 321.

CARMICHAEL, H., 1949, Proc. Echo Lake Cosmic Ray Symposium, 156.

COCCONI, G., V. C. TONGIORGI and K. GREISEN, 1949, Phys. Rev., 75, 1063.

CRITCHFIELD, C. L., E. P. NEY and S. OLEKSA, 1950, Phys. Rev., 79, 402.

EPSTEIN, P., 1931, Proc. Nat. Acad. Sci., Wash., 16, 658.

GREISEN, K., 1942, Phys. Rev., 61, 212.

HILBERRY, N., 1941, Phys. Rev., 60, 1.

HULSIZER, R. I., 1949, Phys. Rev., 76, 164 (A).

JANOSSY, L., 1948, Cosmic Rays, (Oxford University Press).

JOHNSON, T. H., 1935, Phys. Rev., 48, 287.

JOHNSON, T. H., 1938, Rev. Mod. Phys., 10, 193.

LEMAITRE, G. and M. S. VALLARTA, 1933, Phys. Rev., 43, 87.

LEMAITRE, G. and M. S. VALLARTA, 1936a, Phys. Rev., 49, 719.

LEMAITRE, G. and M. S. VALLARTA, 1936b, Phys. Rev., 50, 49.

LEMAITRE, G., 1937, Nature, Lond., 140, 23.

MCNISH, A. G., 1936, Terr. Mag., 11, 37.

MILLIKAN, R. A. and H. V. NEHER, 1935, Phys. Rev., 47, 205.

MILLIKAN, R. A. and H. V. NEHER, 1936, Phys. Rev., 50, 15.

MILLIKAN, R. A., H. V. NEHER and W. H. PICKERING, 1944, Phys. Rev., 66, 295.

MONTGOMERY, D. J. X., 1949, Cosmic Ray Physics (Princeton University Press).

MONTGOMERY, R. A., 1949, Phys. Rev., 75, 1407.

NEHER, H. V., 1935, Phys. Rev., 47, 417.

NEHER, H. V. and W. H. PICKERING, 1938, Phys. Rev., 53, 111.

NEHER, H. V. and W. H. PICKERING, 1942, Phys. Rev., 61, 407.

POMERANTZ, M. A., 1950, Phys. Rev., 77, 830.

ROSSI, B., 1940, Phys. Rev., 57, 660.

ROSSI, B., 1948, Rev. Mod. Phys., 20, 537.

SIMPSON, J. A., Jr. and R. B. URETZ, 1949, Phys. Rev., 76, 569.

STÖRMER, C., 1930, Zeit. f. Astrophys., 1, 237.

SWANN, W. F. G., 1933, Phys. Rev., 44, 224.

VALLARTA, M. S., 1935, Phys. Rev., 47, 647.
VALLARTA, M. S., 1948, Phys. Rev., 74, 1837.
VAN ALLEN, J. A. and S. F. SINGER, 1950a, Phys. Rev., 78, 819.
VAN ALLEN, J. A. and A. V. GANGNES, 1950b, Phys. Rev., 79, 51.
WINCKLER, J. R., T. STIX, K. DWIGHT and R. SABIN, 1950, Phys. Rev., 79, 656.

CHAPTER VI

THE EQUILIBRIUM OF THE COSMIC RAY BEAM IN THE ATMOSPHERE

BY

G. PUPPI* and N. DALLAPORTA
Institute of Physics, University of Padua
**now at the University of Naples*

INTRODUCTION 317
1. THE PRIMARY COMPONENT AT THE TOP OF THE ATMOSPHERE 317
2. COSMIC RADIATION UNDERGROUND 330
3. COSMIC RAYS IN THE ATMOSPHERE 332
4. THE μ-COMPONENT 336
5. THE ELECTRON-PHOTON COMPONENT 348
6. THE N-COMPONENT 352
7. THE GENETIC RELATION 363
8. HIGH ENERGY EVENTS IN THE N-COMPONENT . . . 364
9. THE π-MESONS 367
10. LOW ENERGY EVENTS IN THE N-COMPONENT 373
11. EXTENSIVE AIR SHOWERS 380
12. ENERGY BALANCE OF THE COSMIC RAY BEAM . . . 380
REFERENCES 388

INTRODUCTION

The purpose of this paper is to give a survey of the problem of the diffusion and of the equilibrium of the various components of the cosmic ray beam in the atmosphere. The subject has been treated from a phenomenological rather than from a theoretical point of view, because many features (for example, the cross-sections for nuclear interactions) are still insufficiently known, so that a comprehensive mathematical treatment cannot at present be satisfactorily carried out. Only the main components of cosmic rays have been discussed; their secondary effects, and also such topics as the geomagnetic effects, extensive showers and nuclear interactions have been either omitted or only mentioned, because they are the subject of detailed analysis elsewhere in this volume.

The authors have reviewed the literature available up to April 1951, but not in a completely systematic manner on account of the limited time at their disposal, and they offer their apologies for any unintentional omissions.

1. THE PRIMARY COMPONENT AT THE TOP OF THE ATMOSPHERE

We begin our analysis with a brief review of the experimental data known with sufficient certainty about the cosmic ray primaries. The importance of such accurate data is not only related to the problem of building up a descriptive picture agreeing with the phenomenology of cosmic rays in the atmosphere, but it is also of interest for various theoretical problems of nuclear physics, especially for the problem of interaction between highly energetic nucleons, for these phenomena cannot at present be experimentally produced in cyclotrons, which are still operating near the limit of inelastic phenomena.

The experimental data we are interested in are related (*a*) to the intensity and form of the primary spectrum, (*b*) to the nature of the particles forming the primary beam. We first discuss data under heading (*a*).

1. 1 Vertical data

As is well known, the terrestrial magnetic field acts on a supposed isotropically distributed primary radiation (VALLARTA, [1948]) approaching the earth, in such a way that it determines at any point at the top of the atmosphere, and for any direction of incidence, a minimum value for the momentum of particles such that particles having greater momentum enter with the same intensity that they would have outside the terrestrial magnetic field (NEHER [1950]), whereas particles of lower momentum (apart from considerations of the penumbra region) are prevented from reaching the earth. This minimum value, or "momentum cut-off" may be approximately taken as the lower limit of the integral spectrum of the incident particles, which is, for a particular kind of particle, a complicated function of latitude, longitude, zenithal and azimuthal angles defining the direction of arrival, as well as of the special parameters relating to the particle origin. This functional dependence may be used for the determination

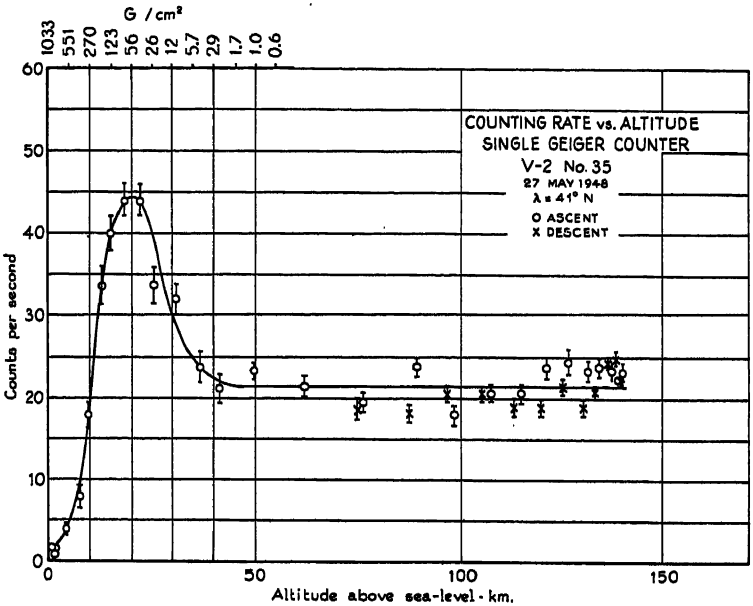

Fig. 1 – Counting rate as a function of altitude for a single Geiger counter carried in a V2 rocket (GANGNES [1949]).

of the primary spectrum using measurements in which the considered cut-off varies in a known manner as a function of one or more of these parameters (zenithal effect, total azimuthal effect and so on). But the experimental evidence least affected by secondary complications (allowance for which is not at all straightforward) is obtained from the latitude effect of the vertical component, which, moreover, has the advantage of being independent of sign for primary spectra having the same form.

Various measurements of the vertical and omnidirectional intensity have been carried out in recent years by means of rockets and balloons, the former allowing the exploration of the atmosphere up to 150 Km (GANGNES *et al.* [1949]; SINGER [1950ab]; VAN ALLEN [1950abc]). It was found that beyond the top of the atmosphere measurements in the vertical direction (SINGER [1950a]) or with detectors inclined at 45° (GANGNES *et al.* [1949]; SINGER [1950b]; VAN ALLEN *et al.* [1950ab]) showed that the omnidirectional intensity measured by a single counter and the directional intensity measured with telescopes of rather poor directional definition rise to a maximum when particles enter the atmosphere, and at high altitudes show a constant value probably corresponding to the primary flux (Fig. 1).

These measurements, although interesting from an inductive point of view, are neither sufficient nor very reliable, because the large opening of the telescopes used, the rolling motion of the rockets and the short time of flight all reduce the precision of the experimental data.

It seems necessary, therefore, also to consider the evidence obtained using balloons, for these observations, although influenced by the interactions of the primaries in the upper layers of the atmosphere (balloons have not reached altitudes higher than about 30 Km), are less affected by statistical errors, being derived over larger time intervals and with telescopes of smaller aperture (POMERANTZ [1950]; WINCKLER *et al.* [1950]). Data on the vertical intensity as a function of latitude, derived from the above mentioned experiments, are summarised in Table 1.

As a control for the absolute value, the directional intensity averaged over all directions in latitude 41° and the directional value obtained by rockets using telescopes inclined at 45° are given in Table 2.

TABLE 1

Geo-magnetic latitude (λ)	Flux of particles cm^{-2}sec^{-1}sterad^{-1}	Cut-off (protons)	Author	Depth
0	0.026 ± 0.001	15. BeV	Winckler 1950	15 gm.cm^{-2}
0	0.027 ± 0.001	15. BeV	Winckler 1950	15 gm.cm^{-2}
0	0.031 ± 0.001	15. BeV	Winckler 1950	15 gm.cm^{-2}
0	0.028 ± 0.004	15. BeV	Van Allen 1950*b*	rocket
20	0.031 ± 0.001	11. BeV	Winckler 1950	15 gm.cm^{-2}
28	0.046 ± 0.001	8.8 BeV	Schein (unpubl.)	15 gm.cm^{-2}
31	0.046 ± 0.0015	8.0 BeV	Winckler 1950	15 gm.cm^{-2}
38.8	0.085 ± 0.003	5.5 BeV	Winckler 1950	15 gm.cm^{-2}
39.5	0.068 ± 0.002	5.3 BeV	Winckler 1950	15 gm.cm^{-2}
41	0.082 ± 0.002	4.8 BeV	Winckler 1950	15 gm.cm^{-2}
41	0.073 ± 0.006	4.8 BeV	Van Allen 1950*b*	rocket
50	0.180 ± 0.02	2.6 BeV	Van Allen 1950*b*	rocket
51	0.22 ± 0.01	2.4 BeV	Winckler and Stroud (unpubl.)	15 gm.cm^{-2}
52	0.17 ± 0.004	2.2 BeV	Pomerantz 1949*b*	top
56	0.23 ± 0.01	1.5 BeV	Winckler 1949	15 gm.cm^{-2}
58	0.29 ± 0.03	1.2 BeV	Van Allen 1950*b*	rocket
69	0.29	0.27BeV	Pomerantz 1950	top

TABLE 2

$I_0 = 0.131 \pm 0.005$ particles sec^{-1}cm^{-2}sterad^{-1}

$I_{45^\circ} = 0.109 \pm 0.006$ particles sec^{-1}cm^{-2}sterad^{-1}

1.2 Secondary processes and asymmetries

Although various experimental results are available on the zenithal and azimuthal effects, they are not yet sufficient to provide a complete picture of the phenomena, because of the various secondary effects which cannot be entirely separated from the principal event. At the top of the atmosphere, the directional intensity as a function of the zenith angle increases with the angle. At latitude 0°, averaging over all azimuthal angles, it is given approximately (van Allen and Gangnes [1950c]) by:

$$J(\theta) = 0.028\ (1 + 0.6 \sin \theta)$$

an unexpected result, for according to geomagnetic theory (Val-

LAERTA [1948]) the variation of the latitude cut-off as a function of zenith angle leads to the expectation that the intensity will decrease with increasing zenith angle. Moreover, measurements of the East-West effect (a consequence of the general azimuthal variation) give far too small a value with reference to that expected from geomagnetic theories on the hypothesis of positively charged primaries initially distributed isotropically.

TABLE 3

Inclined flux data for latitude 0°, 45° *zenith angle*

Azimuthal angle	Particles $\mathrm{cm^{-2}sec^{-1}sterad^{-1}}$	Cut-off (protons)
87°	0.031 ± 0.003	23 BeV
268°	0.048 ± 0.003	11 BeV

Tentative hypotheses of a negatively charged primary have been made on the basis of these results, for it is clear that the presence of negative primaries would reduce the East-West asymmetry and also modify the zenith angle effect. Before discussing the possibility of negative primaries, we will consider the contribution to these effects of the radiation diffused backwards (albedo), and also effects arising from the multiplication of primaries in the residual depth of the atmosphere, which will vary with the latitude cut-off and zenith angle. The possible effect of lateral soft showers has, of course, also to be noted.

The East-West asymmetry, a, is defined by the relation:

$$a = \frac{I_W - I_E}{I_W + I_E}.$$

When, in addition to the primary radiation secondaries are also present, the quantities I_W and I_E must be replaced by $I_W + k_1 I_W$ and $I_E + k_2 I_e$ respectively, where k_1 and k_2 are the mean multiplication coefficients for primaries in collisions with the nuclei of the atmosphere. These mean values are increasing functions of the energy. Since the cut-off in easterly directions is higher than that in the west, it follows that k_2 will be larger than k_1 and, therefore, the asymmetry with respect to that of the primary radiation will be reduced.

The coefficients may be approximately estimated from the transition curves of the vertical component in equivalent latitudes, that is to say in latitudes for which the vertical energy cut-off is respectively equal to that of the East and West components under consideration (WINCKLER *et al.* [1950]). The transition curves have the form shown in Fig. 1.

The problem of the albedo is complicated, and a firm estimate of its contribution to the measurements already discussed would require accurate knowledge of cross-sections and angular distributions which is at present not available. No accurate calculations have, therefore been carried out, but preliminary estimates have been made by SWANN [1950].

1.3 The primary spectrum

Having emphasized the importance of multiplicative processes and of the albedo, the question arises of the way in which these may influence the vertical measurements of intensity upon which our knowledge of the primary spectrum must be based. As we have indicated, however, we are at present unable to make useful progress. It is generally assumed that the data given in Table 1 and incorporated in Fig. 2 are not seriously affected by these corrections, and that therefore the result in Fig. 2 is fairly acceptable up to the maximum cut-off in the vertical direction, about 15 BeV. At higher energies, information on the form of the spectrum can be derived either from data on extensive showers or from measurements of underground absorption. However, this extrapolation is not free from objection, for in the former case the values would strictly depend on the generation model assumed for the showers, and, in the latter, on the behaviour of the cross-sections involved in meson production. If one assumes that the dependence on the chosen model is not sensitive, and that the relevant cross-sections depend only on the fractional energies, it is found that the behaviour of the spectrum deduced from showers appears to be that of a power spectrum of negative exponent about -1.7, while from underground absorption evidence the power spectrum has an exponent -1.6. The energy range in the former case is beyond 10^4 BeV and in the latter case is limited to between 10^2 and 10^3 BeV.

The results for energies between 1 and 15 BeV, i.e., in the range of energy for which the spectrum is fairly well known, may be summarized in the following way:

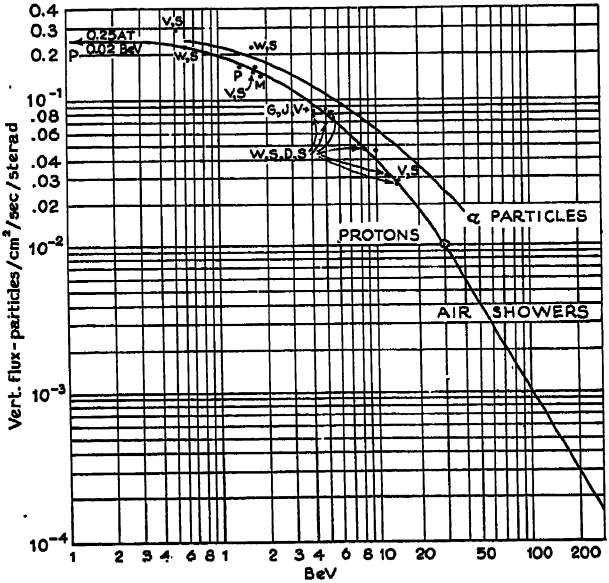

Fig. 2 – Integral number-energy spectrum from flux measurements by various workers at high altitude. The spectrum given by Hilberry for air showers, with $\gamma = 2.7$, is joined to form a continuous curve. (WINCKLER [1950]).

(a) the spectrum may be roughly approximated by a power law of average negative exponent -1.1, but inspection of the curve shows that its behaviour is better represented by the following relation

$$S(E) = \frac{A}{(B+E)^{\gamma}}$$

with the coefficients A and B properly chosen.

(b) at very low energies, ∼ 1 BeV, the form of the spectrum cannot be exactly determined because of instrument cut-offs which are comparable with the energies of the incident particles; however, recent experiments (POMERANTZ [1950]) show that between 50° N and 69° N the intensity filtered through 0.1 — 7.5 cm. of lead and measured at the residual pressure of about 5 gm.cm^{-2} increases by 30 — 40 %.

This result is significant, because it gives a negative answer to the hypothesis of a latitude cut-off on primaries above 50° (COSYNS [1936]), which was attributed to the solar magnetic field

(JANOSSY [1950] p. 300) but at present it does not give much help towards determining the actual form of the spectrum at very low energies.

1. 4 Discussion on the hypothesis of primary electrons

The spectrum of the primary radiation has been derived from experimental evidence concerning the vertical intensity and without any hypothesis on the nature of its components. This is acceptable provided one supposes that one component predominates. This hypothesis is sufficiently close to the truth for most problems we are going to discuss; in fact, experiments have shown that the primaries are essentially protons, together with a certain admixture of heavier nuclei. Before going into details about the accepted primary beam, it is first convenient to discuss the direct and indirect evidence which seems to exclude the existence of a primary electronic component of both signs, or at least, of a negatively charged component.

The hypothesis that the origin of the soft component in the upper part of the atmosphere is different from that of the hard component and is caused by primary electrons of high energy has frequently been assumed, for the cascade theory provides an elegant and helpful theoretical tool by the aid of which, through a proper choice of the spectrum of the incident electrons, it is possible to give a satisfactory account of the electron and photon spectra at any height, for that fraction of the electron-photon component in the atmosphere which remains when the contribution of the secondary soft component generated by the hard component in knock-on and decay processes has been subtracted (BERNARDINI *et al.* [1948]). Besides, the lack of an appreciable East-West asymmetry of the soft component at great heights, which is characteristic of the hard radiation, supported the view that they had an independent origin and suggested the hypothesis of soft primaries formed by an equal number of electrons and positrons (JANOSSY [1950] p. 313).

Finally, a model according to which the electron-photon component might be generated simultaneously with the mesonic component by the primary nucleonic radiation appeared in the past to be very problematic and obscure. However, in the last two years, the picture has been substantially modified and a new phenomenological scheme is supported by the following experimental evidence.

(*a*) Experiments have been carried out in order to give *direct* evidence of the presence of highly energetic primary electrons in the upper part of the atmosphere (HULSIZER and ROSSI [1948]; ROSSI [1949b]). One experiment was based on the frequency of ionization bursts in a lead shielded ionization chamber operated at a height corresponding to a residual pressure of 20 gm.cm^{-2}. The number of particles responsible for an event of the required kind (where at least 80 ionizing secondary particles are necessary) was found to be very low. In this way it has been possible to estimate 11 % as the upper limit for the relative abundance of primary electrons in comparison with the total primary radiation. In this number of electrons, photons are also included because they may produce a similar effect. Another experiment (CRITCHFIELD *et al.* [1950]) was based upon 1625 random expansions of a Wilson chamber operated at a residual pressure of 20 gm.cm^{-2} and containing lead frames within which electrons of energy 1 BeV would originate visible showers. Taking into account both the finite fraction of the residual atmosphere above the experimental arrangement and the linear dimensions and aperture of the apparatus, and on the basis of the observed showers not accompanied by penetrating particles, the authors estimated as the upper limit of electrons, having an energy higher than 1 BeV, 0.2 % of the whole primary flux.

(*b*) The East-West asymmetry of the total radiation and of the hard component has recently been measured at various heights and latitudes by many authors (BIEHL *et al.* [1949]; BARBER [1949]; SCHEIN *et al.* [1948]). The results of those measurements performed with counter telescopes revealed, in contradiction to the earlier work, an East-West asymmetry for the soft component the absolute value of which appears to be a little lower than that of the penetrating component, although it is probable that various correcting factors, like angular scattering due to the generation processes and the effects of the terrestrial magnetic field, are responsible for the observed differences.

(*c*) For completeness, it may be pointed out that evidence against the existence of highly energetic electrons has also been given by investigations on the specific ionization of primaries (SINGER [1949]). The value found is in accordance with a protonic and nuclear composition of the primary radiation, but it is too low if a sensible electronic component is included as a part of the primaries.

A satisfactory model for the prodcution of the electron-photon component in nuclear collisions of the heavy primaries has recently been suggested. This model, the details of which will be discussed later, provides that when highly energetic nuclear collisions occur, not only are charged mesons of both signs produced, but also neutral mesons, which will be indicated as π°. The mean life of π° is much shorter than that of the charged mesons, and of the order of 10^{-14} sec. The neutral meson undergoes decay into two photons.

Summarizing, the hypothesis of primary electrons and even that of any energetic electrons from which the extensive showers are derived are seen to fail in the light of the experiments considered, quite apart from the difficulty, when known processes are considered, of explaining how electrons can acquire energies of the order $10^{15} - 10^{16}$ ev. in interstellar space (FERMI [1949]). On the other hand, the experimentally verified presence of mesons and nucleons in extensive showers (GREISEN *et al.* [1950]; FRETTER [1949]; COCCONI *et al.* [1949b]; MIURA *et al.* [1947]) suggests strongly that these showers also originate in nucleon collisions. The processes whereby mesons, secondary nucleons and electron-photon cascades are generated in primary nuclear encounters are known, and while it is not necessary to exclude the possibility of some contributions to the heavy particles from extensive showers derived from the electron-photon component, such a contribution can hardly be more than secondary.

According to this point of view, (COCCONI [1950]) the generation of an extensive shower should not be considered as qualitatively different from those events which generate the main electron-photon component and the μ-component. The only difference would be a mere instrumental one, in the sense that only when very concentrated events are detected is it possible to verify that coherence in the origin of the various components which represents the general phenomenon.

1. 5 Discussion on the hypothesis of negative primaries

The low value of the azimuthal effect at high altitudes, may still arouse the suspicion that there is some contribution to the primaries from an unspecified negative component, which, since electrons (see § 1.4) and unstable particles for obvious reasons are both clearly excluded, would have to be supposed to be, at least on our present knowledge, negative protons, the existence of which seems to be possible on the lines of a formalism similar to that of Dirac. If negative protons are supposed to behave at relatively high energies as do ordinary protons and neutrons, i.e. if they produce mesons through nuclear collisions and only at lower energies undergo the annihilation process, since at sea-level there is a considerable positive excess in the meson component, it seems an acceptable conclusion that the fraction of these negative protons cannot be very large. Since the primary charge is distributed over a rather limited number of charged mesons (about 4) having both signs, it is easy to deduce that the absolute value of the positive excess (about 25 %) is in agreement with the hypothesis that the whole primary radiation is formed by positively charged particles. Of course, this conclusion refers to that part of primaries which generate mesons. On the basis of a detailed research on the East-West effect of the positive excess, it should be possible to reach more definite conclusions, although the effect of the terrestrial magnetic field on the particles makes the interpretation of the experimental data rather complicated (see § 4. 4).

According to the experimental evidence thus far available, the East-West effect of the positive excess can be explained completely on the basis of the deflection caused by the terrestrial magnetic field (GROETZINGER and MCCLURE [1950]) acting on the μ-particles, and this supports the conclusion that the contribution to the primaries due to negative protons is really insignificant.

Further information may be derived from the analysis of the total azimuthal effect of the penetrating component at sea-level. As has been pointed out by VALLARTA [1939], the penumbra phenomenon on the primary spectrum at intermediate latitudes gives supporting evidence about a fine azimuthal structure for the intensity of the hard component, which is, according to observations, localized into the NW quadrant for positively charged particles.

1. 6 Heavy nuclei in the primary radiation

The existence of a considerable fraction of heavy nuclei having a charge greater than 1 (Bradt and Peters [1950a]) has been established in the primary radiation. The primary nature of these particles is proved by the fact that the experimentally determined charge may be higher than that of air nuclei; moreover, the abundance of the heavy nuclei has been found to be strongly dependent on the transversed atmospheric layer as well as on the geomagnetic latitude at which they are observed. An accurate examination of this evidence allows the conclusion that these nuclei enter individually, and completely stripped of electrons (Bradt and Peters [1950a]) into the earth's magnetic field, which effectively acts upon them.

The problem of the presence of heavy nuclei and that of their relative abundance is strictly related to the problem of the origin of the cosmic radiation and it is hoped that the solution of the former question will shed light on the latter, although at present neither accurate experimental data nor detailed theories are available, so that definite conclusions cannot be drawn. The only conclusion that can be reached at present is that the relative abundance of heavy nuclei is comparable with the relative abundance of the elements in the universe (for instance, the appreciable abundance of iron and the probable absence of some elements like Be, B, Li).

The information about heavy nuclei which is of interest in the phenomenology of the cosmic radiation in the atmosphere is the relative abundance of other nuclei with reference to protons and the energy spectrum. In the following table the intensity of particles of different kinds is given at geomagnetic latitude 30° (Bradt and Peters).

TABLE 4

Data on the primary flux at 30° *N. latitude*

Nuclei	particles $m^{-2}sec.^{-1}sterad^{-1}$	% of particles	nucleons $m^{-2}sec.^{-1}sterad.^{-1}$	% of nucleons
Proton	356	79.0	356	45.0
Helium	90	20.0	360	45.3
C, N, O. . . .	3.5	0.78	49	6.2
$Z > 10$	1.0	0.22	28	3.5
TOTAL. . . .	450.0	100.00	793	100.0

The number of incident nucleons bound in heavy nuclei is about one half of the total number of particles and it follows that almost one half of the nucleons in the atmosphere are derived from the heavy component. In particular, 25 % of the nucleons in the primary radiation are neutrons.

Information on the form of the spectrum may be based on the latitude effect. From experimental data at different latitudes (Vallarta [1950]) the value 1.64 for the exponent of the power spectrum has been derived, which is, in the energy band considered, not very different from that for protons (Winckler [1950]). However, the value reported above should not be considered definite.

Because of collisions with atmospheric nuclei, the heavy particles are broken up and give rise to fragments of smaller size and to free nucleons. The mean free path which characterizes these collisions depends on the kind of colliding nuclei; and decreases as the atomic number increases. This supports the approximate derivation of the cross-sections concerning this kind of collision by adding the square of the radii of the incident nucleons and of the air nucleus. The collision cross-section has the following form:

$$\sigma = \pi(r_n + r_a - 2\Delta r)^2$$

where r_n and r_a are, respectively, the radius of the colliding particle and of the air nucleus and Δr is a correction factor which takes into account the inefficiency of glancing collisions ($\Delta r \sim 0.85 \; 10^{-13}$ cm.).

The values of range which have been experimentally obtained are in close agreement with those calculated with this formula, as is shown in Table 5:

TABLE 5

Range of heavy nuclei in air (*gm.cm*$^{-2}$)

Z	6—8	10—18	∼ 26
Experimental . .	35 ± 5	25 ± 5	19 ± 6
Theoretical . . .	(34)	(25)	(18)

The table shows that the heavy component is very rapidly absorbed as compared with the proton component, the mean free path of which is 60 gm.cm^{-2} (while the attenuation of protons is even slower, with range ∼ 120 gm.cm^{-2}).

A very prominent day-night effect of the order of 100 % (LORD and SCHEIN [1950a]) has been reported for heavy nuclei of $Z > 2$, which supports the conclusion that in these phenomena the sun has an important influence, and this daily variation would affect the secondary components. The estimation of the influence of this effect leads to the same order of magnitude (3 %) for the daily effect, which is observed on the μ-component at sea-level.

2. COSMIC RADIATION UNDERGROUND

The intensity of the cosmic radiation has been measured at various depths, underwater and in mines, down to depths greater than 1400 m. of water.

Measurements have been carried out with ion chambers, Wilson chambers and coincidence counters. Because of the relatively great intensity of local effects, experiments which impose directional conditions on the accepted beam are to be preferred.

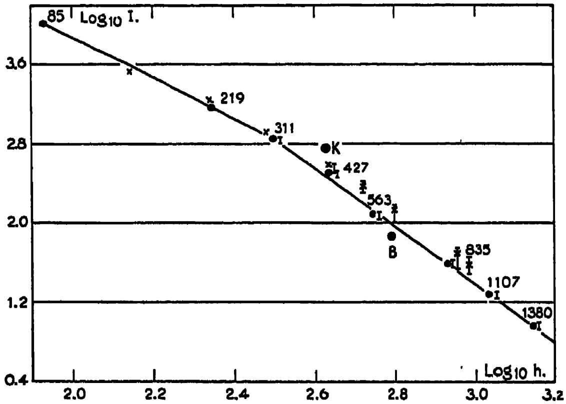

Fig. 3 – Decrease of cosmic ray intensity in rock (m.w.e.). • Clay and Gemert, × Wilson, •K Kolhorster, ·B Barnothy and Forro.

From coincidence measurements, the behaviour of intensity as a function of depth is given by the graph, Fig. 3, which has been interpreted by supposing that the intensity decreases with depth according to a power law, the exponent of which is approximately 1. 7 between 0 and 300 m. of water, and — 2. 7 between 300 m. and 1400 m. of water. It follows that the curve appears to change at a point roughly corresponding to 300 m. water. Several explanations have been proposed in order to explain this circumstance; in particular, a plausible interpretation based on the phenomena responsible for the generation of the μ-component (Greisen [1948] and [1949]) has been advanced (see § 9. 3).

The primary penetrating component must be assumed to be almost entirely composed of energetic ionizing μ-particles. The following experiments support this conclusion:

(*a*) the absorption curves versus depth have been compared with those obtained under layers of lead (V. C. Wilson [1939]). The ionizing nature of the primary component has been tested by the fact that both curves are identical with reference to a given value of depth expressed in gm.cm^{-2}. It has also been convincingly demonstrated that the presence of secondaries consisting of a hypothetical non-ionizing component (Barnothy and Forro [1939, 1940]) should be ascribed (Miesowicz *et al.* [1950]) to a residual radio-activity generated by low energy gamma-rays.

(*b*) Wilson chamber experiments (V. C. Wilson and Hughes [1943]; Tiffany and Hazen [1950]) have confirmed that the vertical beam is formed only by μ-particles and by the electron-photon component in equilibrium with them; furthermore, no evidence has been obtained about physical events which could not be interpreted on the basis of the well-known model according to which, through bremsstrahlung and knock-on processes, the electron-photon component comes into being. The secondary electron-photon showers become more and more dense as greater depths are considered, because at great depths only very energetic particles arrive; the ratio of the soft to the hard component therefore increases with depth.

Experiments with photographic plates, which are particularly sensitive to certain phenomena of the propagation of the beam underground, have substantially confirmed the previous description; in addition they have allowed the detection of particular details such as the production of stars by μ-particles in flight (George and Evans [1950]) and at the end of their range (George and Evans [1951]). In the former case, the star production has presumably to be ascribed to electromagnetic interaction, and in the latter to a Fermi interaction.

These phenomena have been mentioned only for the sake of completeness and in this paper they will not be taken further into consideration.

3. Cosmic rays in the atmosphere

The available data concerning the cosmic radiation incident from outer space on the top of the atmosphere, and those concerning the component detectable underground, have been accounted for by a simple description of the phenomena occurring in these two regions; but much more complicated problems have to be solved when the phenomena are studied in the intermediate region, that is to say in the atmosphere. In fact, because of the nucleonic interaction with the nuclei of the atmosphere, the primaries falling on the earth give rise to many different secondary components, which are differently absorbed in the atmospheric layers; the absorption is strictly dependent on the nature of the particles and on their energy, so that only a little below ground level the least absorbable component alone may be detected, i.e. the μ-component, to which the whole of the underground events should be ascribed.

Before discussing the main problem concerning the equilibrium of the cosmic rays in the atmosphere, that is, the genetic relation among all the secondary components, it is convenient to analyse the experimental evidence thus far obtained concerning the main secondary components and also to point out some doubtful factors the explanation of which would be of great importance in the completion of our present experimental knowledge.

The phenomenological distinction between the "hard" and the "soft" component with reference to the layer of lead they can penetrate has been followed since the pioneering researches on cosmic rays. Now, in the former "hard radiation", the μ-component, the nucleonic and the π-components have to be distinguished. The last two of these are usually considered together as the "N-component", because actually the π-component cannot be clearly distinguished from the nucleonic. The "soft" component, on the contrary, is formed by a preponderant fraction of photons and electrons and also by smaller fractions of mesons and slow protons, which are stopped in thin absorbing layers.

Since the most reliable data thus far available generally refer to measurements at sea-level, we shall first take into account the sea-level data concerning each component. The three principal components, the μ, the electron-photon and the N-component, will then be described in that order.

The μ-component can be considered as the best known, and some of the data referred to it are the only ones which are likely to be retained as really accurate in the whole field of cosmic rays; furthermore, its diffusion in the atmosphere is perfectly interpreted on the basis of well-known phenomena.

The diffusion through the atmosphere of the electron-photon component is well understood from the theoretical standpoint, but data on its behaviour are scarce in recent literature so that it may be considered as still not well defined. On the other hand, data on the N-component are very numerous, but are not of a decisive kind, for the interactions originated by it do not allow a detailed description on theoretical lines.

3.1 Experimental data at sea-level

Measurements of the intensity of the ionizing component are made with coincidence counter telescopes; the deduction of the absolute value is dependent on the estimate of the effective geometrical cross-section of the experimental arrangements used and of the efficiency of the counters (MONTGOMERY [1949]; POMERANTZ [1949b]); spurious coincidences and the contribution of lateral showers must also be evaluated (GREISEN [1943]) and allowed for.

We shall take into consideration only experiments reported in the last two years; the reader is referred to the ROSSI review [1948] for information on researches performed before 1948.

The value of the vertical intensity of the ionizing component under 167 gm.cm^{-2} lead, at a latitude 50° N and at a pressure of 740 mm. has been given by Greisen, $(0.82 \pm 0.01) \cdot 10^{-2}$ cm^{-2}sec^{-1} sterad^{-1}. This value, quoted by Rossi, has been confirmed in counter experiments: for example, POMERANTZ [1949b] obtained the value (0.82 ± 0.01) under 157 gm.cm^{-2} lead at 52° N and at the pressure of 756 mm., and KRAUSHAAR [1949], with 138 gm.cm^{-2} lead obtained (0.887 ± 0.005). We shall consider as acceptable with accuracy of a few per cent the value $I_v = 0.83 \times 10^{-2}$

$cm^{-2}sec^{-1}sterad^{-1}$ for the vertical intensity I_v at sea-level and at northern latitudes.

The statistical precision indicated by the various authors is not really significant because discrepancies of the same order of magnitude between different experimental values should actually be expected if random variations of cosmic ray intensity are taken into account.

The value chosen by Rossi for the total intensity, on the basis of Greisen's measurements is $(1.14 \pm .01) \cdot 10^{-2} cm^{-2} sec^{-1} sterad^{-1}$, which is in fairly good agreement with the following values: $(1.18 \pm .01) \cdot 10^{-2}$ at latitude 40° N. and 760 mm. pressure (MONTGOMERY [1949]), and $(1.24 \pm .01) \cdot 10^{-2}$ at latitude 52° N., 756 mm. pressure under 4.4 gm.cm. of counter wall (POMERANTZ [1949b]). Assuming tentatively Montgomery's value to be correct, and subtracting from it the value of the penetrating component, one obtains the value $0.35 \cdot 10^{-2}$ $cm^{-2}sec^{-1}sterad^{-1}$ for the vertical intensity of the so-called soft component; this value includes not only the usual components, but also all particles of total range less than 157 — 167 $gm.cm^{-2}$.

The contribution of low energy particles may be calculated by determining the fraction of them which is stopped per $gm.cm^{-2}$ in lead. This quantity may be determined by several methods using counter arrangements. In Fig. 4, the top telescope (AB) selects particles having a range larger than a certain value, R; an absorber, S, placed close below the top telescope stops that fraction of particles the range of which initially was included between R and $R + \Delta R$. Another group of counters (C) may be used in the following ways:

(i) in coincidence with group (AB); on evaluating the difference between events of type (AB) and those of type (ABC), the number of particles stopped in S is obtained.

(ii) in anticoincidence with group (AB); from the number of events (AB — C) the number of particles stopped in S is obtained directly.

(iii) in delayed coincidence with group (AB); from the number of events (AB + C), the number of μ-particles which, brought to rest in S give rise to decay particles detected in (C), is immediately deduced.

From the values obtained by these three methods, it is possible to derive the number of particles having initial range between R and $R + \Delta R$ which are stopped per gm.cm^{-2} in S.

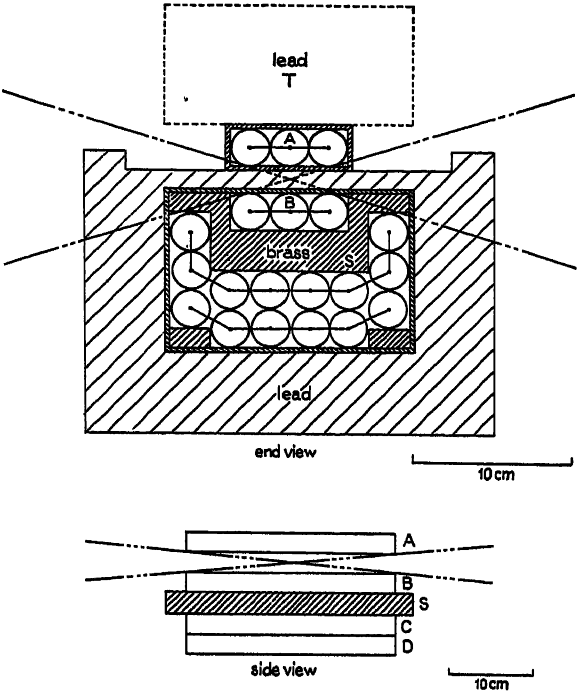

Fig. 4 – Experimental arrangement (Sands).

The results obtained by these methods are not in good agreement, for they depend upon different geometrical configurations; in particular the method of delayed coincidence gives, for reasons not well understood, values which are consistently lower than those obtained by the other two methods. Considering values obtained by several different methods, (Rossi [1948], Sands [1950], Conversi [1950]) we adopt the value 5.5×10^{-6} cm^{-2}sec^{-1} sterad^{-1} per gm.cm^{-2} of air, that is, 4.5×10^{-4} of the vertical intensity. Moreover, since 157 — 167 gm.cm^{-2} of lead correspond to about 80 gm.cm^{-2} air, the correction term will be 0.05×10^{-2} cm^{-2}sec^{-1}sterad^{-1}, supposing that in this region the range spectrum is flat (Rossi [1948]). Hence:

$$I_{\text{soft}} = \{1.18 - (0.83 + 0.05)\}\, 10^{-2} = (0.30)\ 10^{-2}\ \text{cm}^{-2}\,\text{sec}^{-1}\,\text{sterad}^{-1}.$$

This residual fraction, rapidly absorbed in up to 10 or 15 cm. lead consists mainly of electrons with a few slow protons.

4. THE μ-COMPONENT

In the preceding section, we reported values of the vertical intensity of the μ-component at sea level and in northern latitudes. The directional intensity is a function of various parameters related to the geomagnetic coordinates (λ, χ) and to the coordinates (ϑ, φ) defining the direction of incidence with reference to the vertical and the magnetic North.

All of these more or less complicated functional dependences are usually condensed into groups of effects: the latitude effect, the longitude effect, the East-West effect and the total azimuthal effect. Each of these effects can be related to the others, (NEHER [1950]), and they together strongly support the hypothesis that the particles observed are descended from positively charged primaries. With reference to the problem of the equilibrium of the cosmic ray components, we are mainly interested in the variation of the vertical intensity with height, and in the energy distribution of particles.

4. 1 Intensity-height distribution

At 4500 m. above sea-level (616 $gm.cm^{-2}$) under 157 $gm.cm^{-2}$ and 167 $gm.cm^{-2}$ lead, the absolute value of the intensity has been found to be respectively $(1.90 \pm 0.03) \cdot 10^{-2}$ (POMERANTZ [1949b]) and $(1.88 \pm 0.03) \cdot 10^{-2}$ (GREISEN [1948]). The ratios between the values at sea-level and those obtained at 4500 m. are respectively 0.443 ± 0.009 and 0.437 ± 0.007, in good accord with the value 0.44 ± 0.04 found by ROSSI, HILBERRY and HOAG [1940].

Determinations at higher altitudes in airplanes and balloons (POMERANTZ [1949a]) allow the plotting of typical intensity-height curves (Fig. 5) for the ionizing radiation filtered through various absorbing layers.

It appears that the total radiation passes through a maximum at about 200 $gm.cm^{-2}$ pressure, whereas the radiation filtered through layers thicker than 6 cm. lead does not show a maximum [1].

---

[1] See, however VIDALE and SCHEIN, Phys. Rev. 81, 1065 (1951); similar results have been obtained by BHABHA and by DYMOND (private communications). Editor.

The position of the maximum is connected with the secondary component derived from the hard component, while the absence of it for μ-particles should be related to the spectrum at formation of π-mesons, ancestors of the μ-particles. Since the μ-particles do not interact with the nuclei of the atmosphere, and their absorption is only by ionization and by decay to electrons, it follows that there is no close relation between μ-particle production and their apparent absorption, while, of course, such a relation would exist for a component rapidly absorbed.

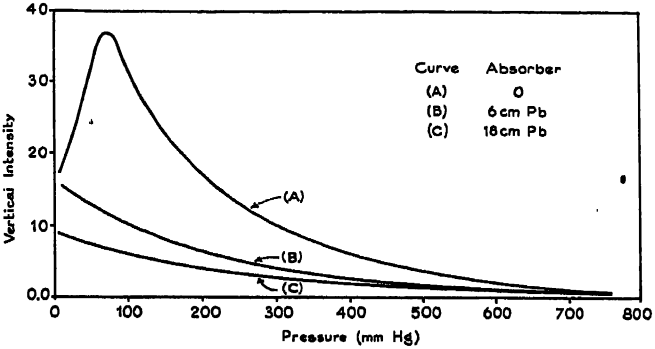

Fig. 5 – Intensity *vs* altitude curves with 0, 6, and 18 cm. of lead. The points of Schein and Allen, with 18 cm. lead, have been fitted to the others at 760 mm. Hg, in conjunction with absorption measurements at sea level. (POMERANTZ [1949a]).

This is well shown, since while the electron-photon component in the intermediate atmosphere (between 400 and 700 gm.cm^{-2}, where, on the one hand, the transition effect of the high atmosphere is not very important, and on the other, the production of electron-photon secondaries by the hard component and in equilibrium with it is still negligible), has an absorption length 123 gm.cm^{-2}, the μ-component has one of 340 gm.cm^{-2}, in spite of the fact that both are derived from the nucleonic component of absorption length 125 gm.cm^{-2}.

Low energy μ-particles are probably always locally generated for at these energies the short mean life (2.2×10^{-6} sec.) does not undergo the relativistic time dilation which determines the behaviour of the high energy particles. Fig. 9 shows the relative efficiency of production of the various levels of the atmosphere above that at which the low energy particles are detected. It follows that direct measurements of this component allow the rate of production to be determined. Sands' data (SANDS [1950]) on meson production may be represented by an exponential law of absorption length 125 gm.cm^{-2}. On comparing these measurements with those of the spectrum at sea-level where generation has practically ceased, and supposing that the particles undergo only slowing down processes and spontaneous decay, it is possible to deduce (SANDS [1950]) a distribution function (Fig. 6), which is given by

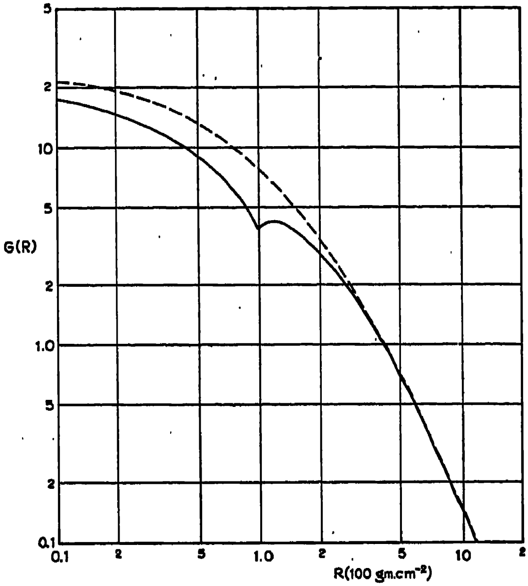

Fig. 6 – Range distribution of μ-meson at production (Sands).

$$S(x, t) = G(x) \exp(-t/R) \tag{1}$$

with reference to unit intervals of time and path.

In order to have an adequate analytical representation for the function $G(x)$, one assumes as trial functions:

$$G(x) = \begin{cases} x_0^{-\gamma}, & x \leqslant x_0 \\ x^{-\gamma}, & x \geqslant x_0 \end{cases}; \quad G(x) = \frac{A}{(B+x)^\gamma}$$

and linear combinations of them. By integration of equation (1) the total number of μ-particles generated in the atmosphere is (SANDS [1950]):

$$N = 0.4\ \mathrm{cm^{-2}sec^{-1}sterad^{-1}},$$

and their total energy:

$$W = 2.95\ m_0c^2\ \mathrm{cm^{-2}sec^{-1}sterad^{-1}},$$

or 7.4 m_0c^2 per μ-particle.

4. 2 The spectrum at sea-level

It has already been pointed out that the energy spectrum at sea-level is accounted for in terms of the production spectrum, the slowing down effects and μ-particle decay in the atmosphere from the point of generation down to the level of observation.

According to a unidimensional model, the spectrum is given by the diffusion equation

$$\frac{\partial\mu}{\partial t} = \beta \cdot \frac{\partial\mu}{\partial\varepsilon} - \frac{b}{t\varepsilon}\mu + S(\varepsilon, t), \tag{2}$$

where $b = \mu c/\tau_0 H$, $S(\varepsilon, t)$ is the production function, $\beta = 1$ is the constant ionization loss per "Heitler unit", $H = 8$ Km. is the

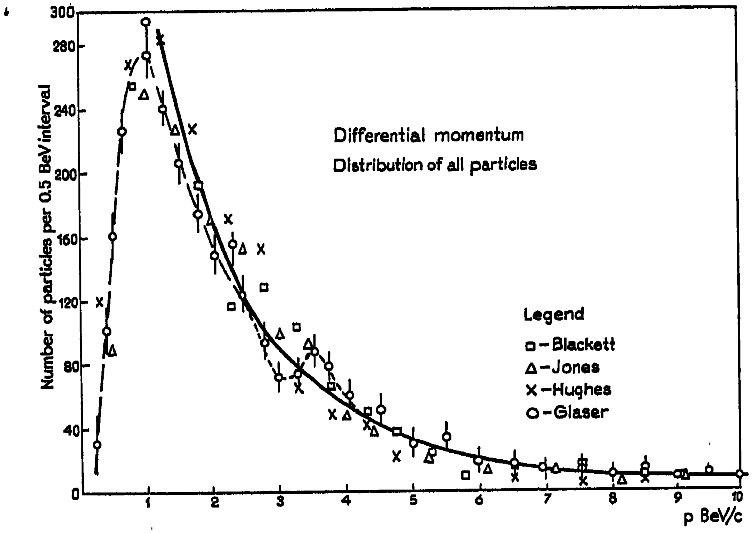

Fig. 7 – Differential momentum spectrum at sea level (GLASER [1950]). The broken curve shows the data before correction for instrumental cut-off. A possible anomaly at 3 BeV/c is shown dotted.

height of the homogeneous atmosphere; and τ_0 is the mean life at rest of the μ-particles. The behaviour described by (2) is in accordance with the experimental data of Figs. 7, 7a and 8.

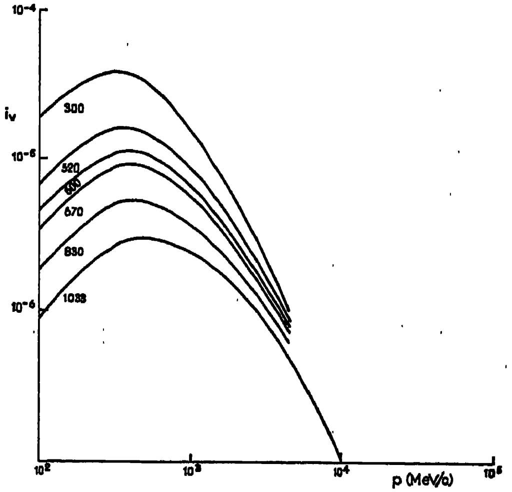

Fig. 7a – Differential momentum spectra of μ particles. $i_v \cdot [\text{cm}^{-2}\text{sec}^{-1}\text{sterad}^{-1}(\text{MeV/c})^{-1}]$.
Figures on curves are of atmospheric depth in gm.cm^{-2}.

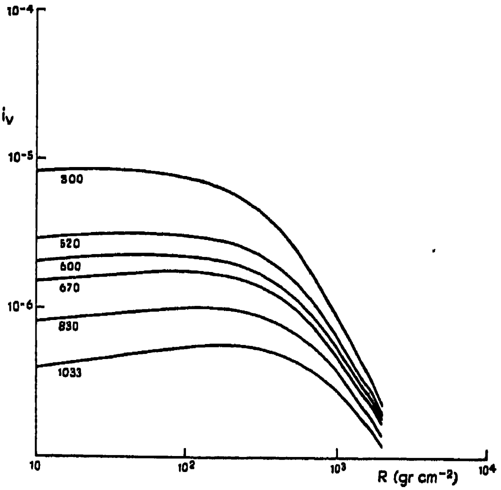

Fig. 8 – Differential range spectra of μ particles. i_v (gm^{-1}sec^{-1}sterad^{-1}).
Figures on curves are of atmospheric depth in gm.cm^{-2}.

The flat form of the range spectrum at low energies is essentially determined by decay, as becomes clear if one considers the probability of survival of μ-particles having different energies and generated at various depths, and the efficiency of μ-particle production at different depths (Fig. 9). For low energies at sea-level, in spite of the attenuation of the process of μ-particle formation through the atmosphere, the effect of decay is so strong that only particles locally generated or, at least, generated in the lowest atmospheric layers, are detected in large numbers. With increasing energy, however, the preferential region for the production of particles able to arrive at sea-level moves rapidly towards the high atmosphere. This behaviour determines the very flat maximum of the differential spectrum.

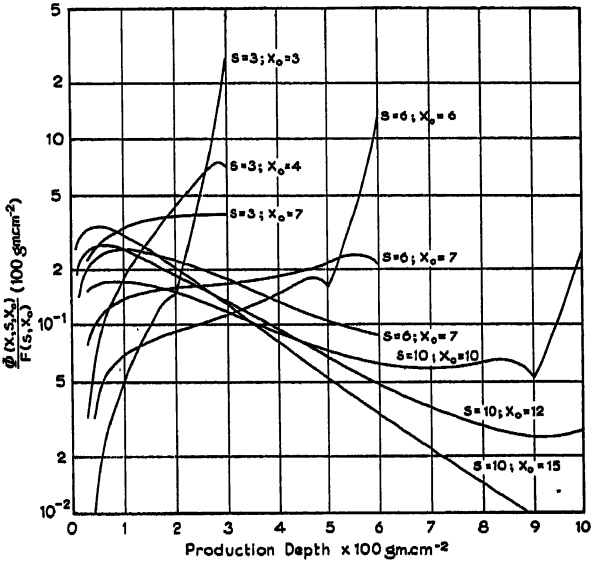

Fig. 9 – Production efficiency at various depths for μ mesons observed at a depth s with residual range $R = (x_0 - s)$, (Sands).

With reference to higher energies, the spectrum at sea-level is in fairly good accord with the production spectrum; an anomaly has been reported to occur at about 2.5 BeV (BLACKETT [1937]) or at 3 BeV (GLASER *et al.* [1950]). Although further experiments are necessary, confirmation of this anomaly would mean that some essential feature of the phenomenon had been neglected.

Finally, the spectrum region concerning very high energy (~ 70 BeV) can be investigated not only at sea-level (Glaser *et al.* [1950]), but also underground, where experiments are much more easily carried out, and where the only conspicuous phenomenon originated by the propagation of the μ-particle beam is the slowing down by ionization and by radiation. As previously noted, it has been found in this way that the differential spectrum is then a power law with negative exponent about —2.7.

4.3 The positive excess

It has been known since the pioneering researches of Anderson and Neddermeyer [1934] and Blackett [1937], and confirmed by many workers, that at sea-level positively charged particles predominate over the negatively charged ones. This circumstance is closely related to the preponderance of positively charged primaries from which, through the π-meson intermediate stage, the μ-particles are generated. Although answers to detailed questions concerning the positive excess have not yet been given, the effect is now satisfactorily interpreted in its essential features.

Investigations on the positive excess have been carried out with Wilson chambers and counter systems; most of the measurements are integral ones, i.e., measurements performed on broad energy bands, but fairly accurate data on the differential effect have been derived, so that the examination of the positive excess as a function of energy can be made.

In Table 6, recent integral determinations are expressed in terms of the ratios:

$$r = \frac{\text{number of particles } (+)}{\text{number of particles } (-)} \text{ and } \delta = 2\,\frac{N_+ - N_-}{N_- + N_+}.$$

TABLE 6

	$r = {}^+/_-$	δ	Energy interval (BeV)
Brode [1950] . . .	1.32 ± 0.02	0.28 ± 0.02	1.0 – 2.5
Quercia [1950] . .	1.26 ± 0.01	0.23 ± 0.01	> 0.5
Glaser [1950]. . .	1.26 ± 0.06	0.23 ± 0.06	—
Glaser [1950]. . .	1.2 ± 0.2		> 10

In the preceding table we have also included the values obtained by **Brode** [1950], whose counter arrangement was most sensitive at about 1.5 BeV, but over so broad a band of energies that it is intermediate between arrangements suitable for integral measurements and those designed for differential measurements.

Inspection of the data shows that the value $r = 1.26$ is fairly well fitted by all the experimental results. This value is, moreover, in general agreement with the differential measurements shown in Fig. 10.

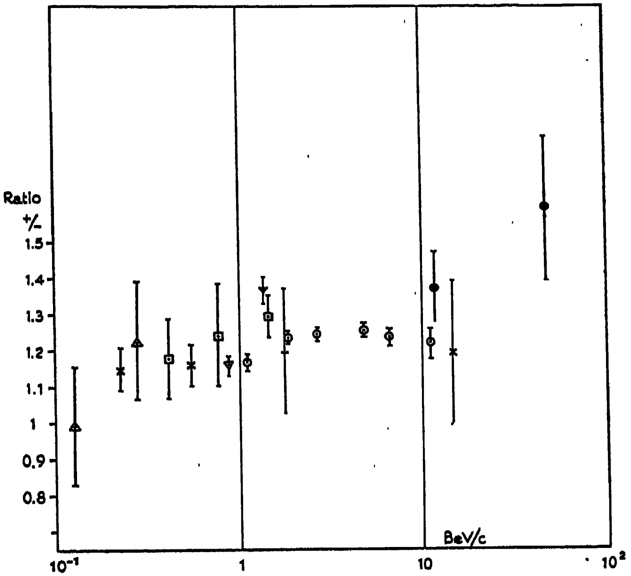

Fig. 10 – Ratio of positive to negative particles at sea level able to penetrate 10 cm. of lead.

△ Conversi, — Leprince Ringuet, ⊙ Owen and Wilson, ▽ Nereson, ▼ Brode, ■ Quercia, Rispoli and Sciuti, ⊡ Bassi, Clementel, Filosofo and Puppi, × Glaser, Hamermesh and Safonov, • Caro, Parry and Rathgeber.

In the following discussion, we shall refer to the measurements by **Owen** and **Wilson** [1951], which are the best available on account of their coherence and statistical precision. At low energies, the differential excess increases with energy up to about 2 BeV/c and then remains practically constant up to momenta of the order 10 BeV/c. Accurate data are not available at higher momenta: Glaser's result is not very significant, being based on very few events, while the values given by CARO *et al.* [1950] may be influenced in an unspecified manner by protons.

Anticipating arguments which will be discussed later (§§ 5, 8, 9), we state the generation model assumed to explain the behaviour of the differential excess at sea-level. We suppose that the primary radiation is absorbed in the atmosphere in more than one inelastic collision, and that the nucleons which are able to give rise to further meson formation in subsequent collisions consist of equal numbers of protons and neutrons. It follows that only that fraction of μ-particles derived from the first collisions is characterized by a positive excess, while the subsequent generations have only the effect of diluting the primary excess. At sea-level, locally generated particles predominate at low energies, and these will not show any appreciable positive excess, but at higher energies, the fraction of μ-particles descending from the first meson-producing collisions becomes larger, the dilution of the primary excess shrinks and approaches a limit which is roughly determined by the ratio of the mean free path and the absorption path of the whole nucleonic component. These arguments explain the increase of the positive excess up to energies of the order 2 BeV. The further behaviour, concerning particles scarcely influenced by meson decay, depends closely upon the positive excess distribution in the production spectrum, and on particular phenomenological features which are clarified by the diffusion theory of the N-component.

These conclusions may be developed in a more rigorous manner by choosing the following two generation functions:

$$\text{(I)} \qquad S_1(\varepsilon, t) = G(\varepsilon) \exp(-t/\Lambda),$$

concerning particles derived from the first generating collisions, which is governed by the mean free path for inelastic collisions of the nucleonic component, and

$$\text{(II)} \qquad S_2(\varepsilon, t) = G(\varepsilon) (\{\exp(-t/\mathrm{R}) - \exp(-/t\Lambda)\},$$

which is expressed as the difference between the total distribution function and that concerning the first generating collisions.

On introducing, for generality, the function $\Delta(\varepsilon)$ describing the positive excess distribution in the spectrum of the first generation, and taking into account the survival factor with reference to decay and to loss by ionization, Heitler's method leads easily (BASSI [1949]) to the following expression for the differential positive excess at height t and for energy η.

$$(3) \qquad \delta = \frac{\int_0^t \Delta(\eta - z)\, e^{-\frac{z}{\Lambda}} \left(\frac{z}{\eta - z}\right) G(\eta - z)\, dz}{\int_0^t e^{-\frac{z}{l}} \left(\frac{z}{\eta - z}\right)^{b/\eta} G(\eta - z)\, dz}$$

It is thus possible to infer that particles deriving from the first generating collision and detected at sea-level with energies not larger than 1 BeV, have been generated with energies approximately included between 2.5 and 3.5 BeV. The observed excess does not seem to be a very sensitive function of the distribution of the excess in the spectrum of the first generation, provided the distribution is a slowly varying function. Information on this subject may be derived from the values of the positive excess at high energies. Supposing for simplicity that, with reference to the considered energy band, the excess is uniformly distributed, the following relation is immediately found:

$$\Delta = \frac{1}{N} \frac{R}{\Lambda}$$

where N is the mean number of particles generated by an incident nucleon and Λ is the mean free path. Since N is known, ($N = 4$) as well as Λ, it is possible to calculate with reference to different energies the fraction of μ-particles generated in the first collisions, detected at sea-level, and the excess Δ which should be expected as a consequence of the dilution of the primary excess.

Taking the μ-particle production in different layers of the atmosphere from Sands' data (SANDS [1950]), and choosing the value $\Lambda = 55$ gm.cm^{-2} (geometrical m.f.p. in air), one gets the values of Table 7.

TABLE 7

Energy (BeV)	0	0.4	1.0	10
Fraction from first collision . . .	0.14	0.21	0.27	0.44
Fraction from successive collisions	0.86	0.79	0.73	0.56
δ	0.06	0.11	0.15	0.25

These values are fairly well fitted by experimental data; however, they should be a little diminished at low energies to take into account the slight neutron excess of the nucleonic component in collisions after the first (see § 10). Since this excess favours the production of μ-particles negatively charged, it follows that when ε approaches zero the excess will tend to a negative value.

Experimental values for higher energies agree well with the limiting value 0.25, which is obtained by extrapolating the results concerning low energies and which depends, in our present approximation, exclusively on the total number of μ-particles generated per incident nucleon. Moreover, the problem concerning high energies is much more complicated both because the quantities N and R are functions of the energy and because the possibility of a non-uniform excess distribution along the spectrum of the first generation should be taken into account. Since none of these parameters can be exactly specified, we shall assume for the positive excess the following asymptotic relation:

$$\delta_{\text{asymp.}} = \Delta(\varepsilon) \frac{\int_0^\infty \exp(-t/\Lambda)\, dt}{\int_0^\infty \exp(-t/R)\, dt} \to \Delta(\varepsilon) \frac{\Lambda}{R}.$$

Concerning the excess distribution in the generation spectrum at the first collision, it must be noted that different theoretical models of generation can lead to different distributions of the differential excess; for example, a theoretical picture of plural production in the sense of Heitler and Janossy leads to a uniform distribution (Caldirola [1949]), whereas models of multiple production lead to a distribution varying either with the inverse square root of the energy (Heisenberg [1949]; Cini and Wataghin [1950]) or with the inverse third root of the energy (Lewis *et al.* [1948]). Experimental data show that the dependence of the primary excess with energy is in any case a slowly varying function.

Finally, for the low energy band, our approximations concerning μ-particles arriving vertically and detected at sea-level may be used to investigate the behaviour of the positive excess as a function of altitude. As is indicated by several experiments, the positive excess in the low and intermediate layers of the atmosphere is a slowly varying function of height; Brode [1950] has found the same results at sea-level and at 3650 m.; QUERCIA *et al.* [1950] at 88, 3500, 5100 and 7300 m.; BASSI [1951] at 2000 m.; previous experiments by BERNARDINI *et al.* [1945] give similar results.

4. 4 Asymmetries of the positive excess

The examination of data for particles arriving in inclined directions requires a special treatment because the positive excess we have previously discussed, which depends directly on the production processes, varies with the ratio between negatively and positively charged particles, and so on the zenithal and azimuthal angles and on the particle energy; furthermore, it must depend on the trajectory of positively and negatively charged particles in the terrestrial magnetic field. On taking into account not only the energy loss by ionization and by μ-particle decay, but also distortions caused by the earth's magnetic field, one obtains values which are continuous functions of the direction of incidence.

The available data refer to the East-West plane and include measurements of the total asymmetry, which, at higher altitudes, depends (JOHNSON [1941]) on the excess at generation, and also measurements of pure positive excess.

TABLE 8

Inclined positive excess in the $E-W$ plane

Reference	Zenith angle	δ_W	δ_E	Altitude (gm.cm^{-2})
Groetzinger [1950]	24°	0.25 ± 0.03	0.12 ± 0.03	680
do.	24°	0.19 ± 0.01	0.09 ± 0.01	1030
do.	58°	0.53 ± 0.03	-0.20 ± 0.02	680
do.	58°	0.28 ± 0.03	-0.04 ± 0.03	1030
Quercia [1950] . .	60°	0.22 ± 0.01	-0.07 ± 0.01	680
Padova group [1951]*	45°	0.41 ± 0.02	-0.01 ± 0.02	1030

* Unpublished.

These data show that in the East-West plane, the excess varies from positive to negative values as the zenith angle varies from West to East. This experimental evidence is perfectly interpreted (GROETZINGER and MCCLURE [1950]; QUERCIA *et al.* [1950]) on the lines of the preceding argument. On comparing the excess of particles having travelled the same path, it is found that the values of excess due to generation are in good accordance with the vertical data.

None of the results thus far known imply the existence of a fraction of negatively charged primaries and, therefore, all the data on the positive excess in northern latitudes, indirectly support the assumption that cosmic ray primaries are positively charged particles.

5. THE ELECTRON-PHOTON COMPONENT

As we have noted, the experimental data on this component are at present meagre, a fact which is understandable if one considers that the soft component is detected by its effects, or more precisely, by certain events incited by it, the most important of which are electron-photon showers generated in the absorbers, bursts in ionization chambers shielded with a small thickness of lead, and finally, gamma-rays of low energy. If these phenomena are considered as events identifying the electron-photon component, it is evident that by means of relative measurements at different heights and latitudes, the behaviour of this component as a function of the above-mentioned parameters can be investigated. An example is provided by experiments on the frequency of Rossi showers in the atmosphere, from which information on the electron-photon component at high and intermediate energies are derived (JANOSSY [1950] p. 235), and by those concerning the frequency of low energy gamma-rays (BERGSTRAHL and SCHRODER [1951]). Difficulties arise when attempts are made to deduce the intensity of the soft component from the frequency of the indicative events, as is necessary, for instance, to disentangle the effects of the energy spectrum and of the relative percentage of electrons and photons. The phenomena originated by the soft component in an absorber are so complex and intricate that such an induction appears to be extremely difficult and not without objections, so that our present knowledge about these two problems is very deficient.

Because of these difficulties, the intensity of the soft component is generally obtained by means of a "difference-method", based upon indirect measurements: the intensity of the soft component is obtained, according to this method, by subtracting the intensity of the penetrating component from the intensity of the total ionizing component. This kind of measurement allows the determination of the intensity of the soft component as a function of height and of latitude, and the results derived agree with experimental data from the previously mentioned experiments (Fig. 11).

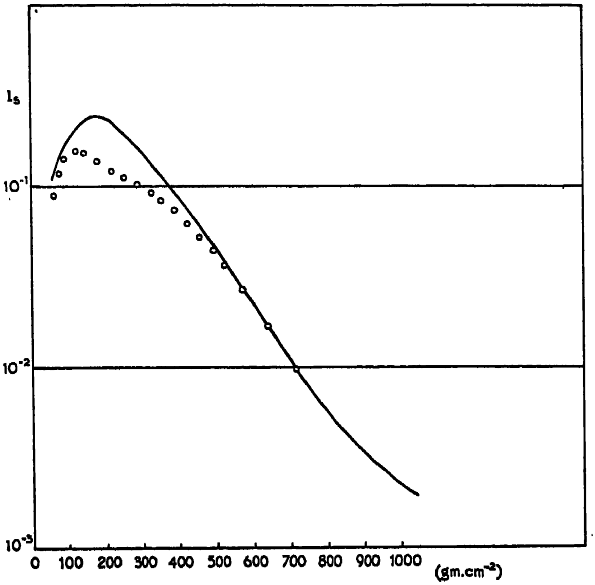

Fig. 11 – Intensity *vs* altitude curve for the soft component.
——— Rossi, ○ ○ ○ ○ Pomerantz.

5. 1 The total intensity-height distribution

We have seen (§ 2) that the soft component underground is in equilibrium with the μ-component because the former is generated by the latter in knock-on and Bremsstrahlung processes and by μ-particle decay. Above sea-level similar phenomena should be expected to occur; consequently the electron-photon component derived from the μ-component should be in equilibrium with it, and should therefore increase with height approximately as does the generating component. This roughly happens up to about 2000 m. altitude, but at greater heights the soft component increases much more rapidly, as is shown either by Greisen's value, $(5.28 \pm 0.10) \cdot 10^{-2}\text{cm}^{-2}\text{sec}^{-1}\text{sterad}^{-1}$ (Greisen [1948]) for the total intensity at 4500 m. above sea-level (measured under 1.7 gm.cm^{-2}), by Pomerantz' value $(4.43 \pm 0.07) \cdot 10^{-2}$ cm^{-2}sec^{-1}sterad^{-1}, under 4.4 gm.cm^{-2} (POMERANTZ [1949b]) and by data at higher altitudes. We may note also values concerning the growth of the soft component between 955 gm.cm^{-2} and 383 gm.cm^{-2} (BARBER [1949]):

Ratios of intensity at 955 *and* 383 *gm.cm*$^{-2}$

Showers	Soft component (difference)	Hard component	Total
28.3	29.0	3.83	10.8

where we also compare the ratio deduced from the difference method with that obtained from the detection of characteristic events (showers). At 660 gm.cm^{-2} the soft component reaches the same intensity as the hard component, it continues to increase up to a maximum occurring at about 200 gm.cm^{-2} pressure, and subsequently decreases at higher altitudes. This behaviour, which may be deduced from Rossi's data, has been confirmed by recent measurements (Fig. 4) (ROSSI [1948]). All these circumstances show clearly that, in addition to the soft component which is secondary to the meson component, there exists another electron-photon component having a quite different origin.

The propagation of a soft component is exclusively based on electromagnetic interactions and is outlined by cascade theory from which may be determined the average number of electrons and photons in a given energy band and at a given depth of any absorber, and originated either by primary electrons or by primary photons. It is found that, by means of the alternating processes of radiation by collision and pair production, the number of electrons and photons increases up to a certain depth of the aborber, where it reaches a maximum, and then decreases because the particles suffer continuous energy loss and from a certain limit downwards their energy becomes insufficient for the generation of other particles through the above-mentioned processes.

This behaviour predicted by the theory has been satisfactorily verified by experiments performed with thick absorbers, especially with lead. As we have already pointed out, it was once believed that a similar cascade process initiated by energetic primary electrons should also be involved in the propagation of the soft component through the atmosphere considered as an absorber, but this hypothesis is actually in contradiction with direct evidence, (see § 1. 4) and moreover, it seems to conflict with many detailed features such as the position of the maximum in the atmosphere, which should, on the primary electron model, be at a depth greater than that at which it is actually observed. But the new experiments (§ 1. 4) support the hypothesis that the ancestors of the electron-photon cascade are photons generated through the decay of neutral π-mesons. Since π° mesons are generated by the nucleonic component through the whole atmosphere, the number of available photon ancestors falls off exponentially with height, and so, according to the new point of view, the maximum of the soft component must be localized in the region where the first collisions of the nucleonic component occur.

5. 2 The latitude effect

It is beyond the aim of this paper to discuss in detail the experimental data on the asymmetries of the soft component with respect to the hard one. For completeness, we note that for both components these asymmetries have the same sign and the same order of magnitude; moreover, they increase with height as is to be expected according to geomagnetic theory based on the assumption of a unique charged primary component (SCHEIN *et al.* [1948]; BIEHL *et al.* [1949]; BARBER [1949]). Similar behaviour was found valid also for the latitude effect (SIMPSON [1948]), i.e., it increases with height in the same manner both for the soft component and for the hard, and for both of these the latitude effect is smaller than that of total ionization and of neutron intensity. All these features are explicable, since in the intermediate and low atmosphere both the soft and the hard components are coherent because of the equilibrium existing between them and because, in the upper part of the atmosphere, the soft component is generated simultaneously with the hard by events which, being equally distributed in energy, have also approximately the same directional distribution.

5. 3 The energy spectrum; the ratio of electrons to photons

The analysis of the electron-photon component at various heights is still largely an open problem. The relevant experimental data can be classified into two groups: (*a*) ratio of electrons to photons; (*b*) the energy spectrum. ROSSI [1949a] succeeded in delineating the main features of an energy spectrum for high energy electrons at 3300 m. altitude on the basis of observations made with Wilson chambers (HAZEN [1944]) and with ion chambers (BRIDGE *et al.* [1947]). The integral spectrum, which is valid only for energies higher than 1 BeV, seems to follow a power law of negative exponent the value of which is between 1. 6 and 2. 0. In order to get more detailed information on the photon-electron component, experiments have been made which, however, exclusively concern primary photons (ROSSI and JANOSSY [1939]; NERESON [1942]; TRUMPY [1943]) originating cascades in a lead absorber of variable thickness; the cascade electrons leaving the absorber being detected by counter coincidences. The number of electrons from different thicknesses depends, according to the cascade theory, on the photon spectrum incident on the absorber; it follows that such a spectrum can be deduced from the observed frequency of appearance of at least one electron, of at least two electrons, and so on.

The experimental data lead, on the basis of Arley's analysis (ARLEY [1948]) to a photon energy spectrum which can be approximated as follows:

$$F(E_0)\,dE_0 = \begin{cases} \alpha \cdot A \cdot \dfrac{dE_0}{E'}, & 0 \leqslant E \leqslant E'; \quad E' = 200 \text{ Mev} \\ A \left(\dfrac{E'}{E_0}\right)^{1+\gamma} \dfrac{dE_0}{E'} & E > E'; \quad \gamma = 1 \cdot 5 \end{cases}$$

Unfortunately, in this case the predictions of cascade theory are not clearly defined and, moreover, depend on the assumptions made concerning correlations among events through which the multiplication of the electron-photon component occurs (Poisson, Furry, Polya's distribution). Any definite conclusions, therefore, appear to be problematical. However, now that the generation of the soft component in the atmosphere is fairly well understood (§ 6) and that direct experimental evidence on the cascade theory are actually available (BLOCKER *et al.* [1950]; CROWE and HAYWARD [1950]), it is worthwhile to emphasise that the problem might well now once more be systematically studied.

6. THE N-COMPONENT

In traversing matter, the μ-component gives rise to phenomena which, for various energies, present the same features (ionization and decay) and which are, therefore, always recorded by the same methods. The N-component, on the contrary, initiates events which, because of different aspects presented at different energies, are detected in different ways using arrangements sensitive to more or less restricted bands of the energy spectrum.

Passing from high to low energies, the most reliable method for recording the nucleonic component at very high energies is by the detection of extensive and penetrating showers generated in air. The differentiation between these two kinds of events is, of course, a phenomenological one, in the sense that when the former events occur, the soft component is recorded and when the latter occur, the penetrating component is recorded, but this distinction ultimately rests on the different energy ranges concerned in the two kinds of event (§ 11).

At lower energies, say a few BeV, local penetrating showers, generated within the absorbing layers of the apparatus, may be detected with counter arrays, cloud chambers and ion chambers, while the photographic plate, which detects the N-component through the nuclear disintegration stars formed in the emulsion becomes of importance in this energy range. The plates have their greatest efficiency between 1 BeV and 200 MeV, being in this range practically the only detector for the N-component. This technique is not suitable for systematic researches of events occurring at very high energies because these are rare and moreover, the development of the event in the plate does not bring clearly into evidence its physical features. At low energies, on the contrary, the limit of applicability of this method is reached at an energy of about 100 MeV, corresponding approximately to stars having the lowest number of ionization prongs allowing of their identification (this number is usually 3 because stars with 2 prongs may easily be confused with other events and have not yet been systematically investigated (MERLIN and PIERUCCI [1951])). Stars formed by highly ionizing prongs can be recorded not only by plates but also by unshielded ionization chambers, where they appear as bursts.

Below 100 MeV there is a gap extending down to very low energies, in which none of the known techniques are suitable. The only way to obtain information about this low energy region is perhaps the investigation of low energy single tracks in the nuclear plates, but unfortunately, only very few data are available (LATTIMORE [1949]). Below this gap, information on very low energies, of the order of a few eV, can be obtained with BF_3 counters, which allow detection of thermal neutrons. Since the cross-section for $n_0^1 + B_5^{10} \rightarrow \alpha_2^4 + Li_3^7$ varies inversely with energy, the sensitivity of the method is localized at the lowest limit of the spectrum. The data thus derived provide the only useful indication which can complete our knowledge about the low energy tail of the spectrum.

The classification of the nuclear events is essentially based on estimates of total energy of secondaries, with reference to their number and kind, the individual energies, angular divergence, etc. It follows that much of the information on the energy of the primaries of these events is indirect, except in high energy events which can be related to the latitude effect. As we have already seen, the vertical cut-off caused by the terrestrial magnetic field concerns a range of energy included between 1 and 15 BeV; therefore, events not affected by the latitude effect all derive from primaries having an energy greater than this maximum limit. For lower energies, the absorption and the multiplication of the nucleonic component in the atmosphere complicate the latitude effect. We begin the discussion on the behaviour of the nucleonic component by examining the data concerning these two effects.

6.1 Absorption and latitude effect

The data on the latitude effect are listed in Table 9, which has been divided into three sections, each referring to a different energy range of the radiation responsible for the nuclear event under consideration, irrespective of the particular technique used. In the first section, highly energetic events are listed; they are greatly influenced by the effects of the first collision because of the range of the secondaries and here the latitude effect is seen to be practically absent. In the third section we indicate events initiated by particles the majority of which can be considered of secondary origin, mainly at high altitudes. The latitude effect is large, but its interpretation depends on detailed investigation of the diffusion of the nucleonic component in the atmosphere. Finally, in the second section we have reported conditions which have to be considered as an intermediate stage between the two cases above stated.

TABLE 9

Latitude effect

Reference	Residual pressure gm.cm^{-2}	λ_1	λ_2	$I_{\lambda_1}/I_{\lambda_2}$
(I) > 10 BeV *extensive showers*				
Biehl [1949].	320	64°	0°	1.0
10 – 30 BeV				
Walsh [1950]	310	55°	20°	1.12
Walsh [1950]	383	55°	20°	1.12
(II) ~ 1 BeV				
McMahon [1950]. . . .	300	55°	20°	1.17
McMahon [1950]. . . .	300	55°	20°	1.32
(III) order eV or MeV				
Staker [1950]	120	55°	20°	2.9 neutrons
Conversi [1950]	320	60°	0°	3.7 protons ~ 0.5 BeV
McMahon [1950]. . . .	300	55°	20°	1.96 bursts ~ 0.4 BeV
Salant [1950]	15	57°	31°	4.3 stars
Yagoda [1949*a*]	670	50°	0°	7. stars
Yagoda [1949*a*]	1030	50°	0°	6. stars

Data on the absorption of the nucleonic component in the atmosphere are summarized in Table 10. As in the preceding table, we group in different sections, irrespective of the technique used,

TABLE 10

Absorption of the nucleonic component

Reference	Latitude	Residual pressure gm.cm^{-2}	Absorption length gm.cm^{-2}
(I) > 10 BeV			
Stinchcomb 1950	40°	675	74
Walsh 1950	55°	300	112
	20°	383	140
Hazen 1949	35°	700	80
Meyer 1949.	25°S	900	103
Tinlot 1948	53°	270	118
Wataghin 1947	25°S	370 – 440	101

TABLE 10 (continued)

Reference	Latitude	Residual pressure gm.cm^{-2}	Absorption length gm.cm^{-2}
(II) 1 BeV–10 BeV			
protons			
McMahon 1950	55°	280–380	125
	20°	300–380	135
neutrons			
McMahon 1950	55°	280–380	143
	20°	300–380	143
local showers			
Fretter 1949	38°	730–1030	123
Cocconi 1949*a*.	40°	260	133
	50°	710	133
Janossy 1945	54°	1030	116
Walker 1950	40°	710	100
(III) 10 MeV–1 BeV			
Bernardini 1950*a*	45°	680	135
Lord 1949	51°–56°	15	148
Yagoda 1949*b*	48°	15	143
	50°	1000	143
George 1949	46°	680	150
bursts (*unshielded chamber*)			
Rossi 1948	45°	270–1000	138
Whyte 1950	0°–35°	90	150
counters			
Conversi 1950	5°–60°	300	150
bursts (*shielded chamber*)			
McMahon 1950	55°	280–380	157
	20°	300–380	198
Forster 1950	30°	420–230	125
(IV) < 150 MeV			
Forster 1950	30°	270–720	133
Lattimore 1949	46°	680–1030	190
(V) ~ eV			
Simpson 1948	53°	200	160
	0°	600	191
Yuan 1948	40°	55	156

results of experiments referring to similar energy ranges. Unless otherwise stated, the absorption paths R are defined by:

$$f \sim \exp(-t/R)$$

where f is the relative frequency of occurrence of the events studied. The absorption path R increases as the energy of the events decreases, a feature discussed in § 12. 3 below.

Noting particularly data of a single author, the absorption path for a certain energy range generally increases as latitude decreases, while the latitude effect increases with height.

6. 2 Absolute intensity of the nucleonic component

The absolute intensity of the nucleonic component can be derived from data from a variety of detecting methods. According to Rossi, an estimate of the intensity of the ionizing fraction with energy > 400 MeV can be obtained at any height in the atmosphere, assuming that at the top of the atmosphere the whole ionizing component consists of protons and developing from this datum an exponential curve of slope 155 gm.cm. Anderson's data, obtained from measurements of the positive excess in a cloud chamber for much smaller energies (up to about 80 MeV), agree fairly well with the values deduced from the above curve. In the first two sections of Table 11 we have collected these data. In the last three sections of the table data on measurements of single tracks of slow protons in nuclear plates, disintegration stars and, finally, slow neutrons (using BF_3 counters) are listed. The data for slow protons are in good accord with other estimates of the ionizing fraction, for they refer only to a very narrow energy band (about 20—30 MeV).

Data on stars allow only an indirect estimation of the nucleonic particles producing them, because knowledge of the production cross-section is involved, but assuming a value equal to the geometrical section the intensity of the generating component is given in Table 12, referred in all cases to altitude 3600 m (680 gm.cm^{-2}). The considerable differences between values in this table probably mainly come from differences of development and perhaps of scanning efficiency; if this is so, the largest values must be considered the most reliable. Since stars are produced by neutrons as well as by protons, and because (see § 9) the neutron

TABLE 11

Absolute intensity of the N-component

Reference	Residual pressure gm.cm^{-2}	Intensity
(I) $>$ 10 BeV		
Hazen 1949	730	$1.1\ 10^{-5}\ \text{cm}^{-2}\text{sec}^{-1}\text{sterad}^{-1}$
Walsh 1950	0	< 0.03
(II) 400 MeV—10 BeV		
Rossi 1948	200	$1.15\ 10^{-2}\ \text{cm}^{-2}\text{sec}^{-1}\text{sterad}^{-1}$
	300	$1.05\ 10^{-2}$
	600	$1.\ \ 10^{-3}$
	1030	$2.\ \ 10^{-3}$
(III) Slow protons		
Rossi 1948	200	$2.4\ 10^{-2}\ \text{cm}^{-2}\text{sec}^{-1}\text{sterad}^{-1}$
	300	$1.05\ 10^{-2}$
	600	$0.95\ 10^{-4}$
	1030	$3.\ \ 10^{-5}$
Lattimore 1949	680	$16.5\ \text{cm}^{-3}\text{day}^{-1}$
Rossi 1948	300	$1.7\ 10^{-5}\ \text{cm}^{-2}\text{sec}^{-1}\text{sterad}^{-1}\text{MeV}^{-1}$
Conversi 1950	300	$3.\ \ 10^{-5}$
(IV) Stars		
George 1950	1030	$1.46\ \text{cm}^{-3}\text{day}^{-1}$
Bernardini 1950*a* . . .	680	14.2
Lattimore 1949	670	16.4
Lord 1951	660	22.
	105	1610.
	15	2390
Addario 1950.	15	1960
Salant 1950	12	2000
(V) Slow neutrons		
Davis 1950	250	$8.2\ 10^{-3}$ captures $\text{sec}^{-1}\text{gm}^{-1}$
	200	$1.5\ 10^{-2}$
Yuan 1951	200	$1.7\ 10^{-2}$
	250	$1.2\ 10^{-2}$
	400	$4.8\ 10^{-3}$
	600	$1.3\ 10^{-3}$

component is probably three to four times more intense than the proton component in the energy range corresponding to the most conspicuous star production, the data thus derived agree as well as is to be expected with those given above.

Finally, the number of slow neutrons, which must be supposed to result from nuclear disintegrations, must be in equilibrium with the stars. The mean number of evaporated neutrons per star should be given by the comparison of the absolute number of neutrons with the number of stars generated in air, which is easily obtained supposing that the ratio of the cross-sections in air and in emulsion is given by the ratio of the geometrical sections. This comparison will be made in § 10. 3.

TABLE 12

Intensity of the star producing radiation

Reference	Residual pressure gm.cm^{-2}	Stars cm^{-3} day^{-1}	Stars cm^{-3} day^{-1} reduced to 680 gm.cm^{-2}	Intensity of radn. cm^{-2}sec^{-1}	
				Total	protons
George 1950 . . .	1030	1.46	18.5	5.41 10^{-3}	1.35 10^{-3}
Bernardini 1950*a*.	680	14.2	14.2	4.16 10^{-3}	1.04 10^{-3}
Lattimore 1949 .	670	16.4	15.1	4.48 10^{-3}	1.12 10^{-3}
Lord 1951	660	22	18.9	5.53 10^{-3}	1.38 10^{-3}
	105	1610	26.45	7.73 10^{-3}	1.93 10^{-3}
	15	2390	20.63	6.03 10^{-3}	1.51 10^{-3}
Addario 1950. . .	15	1960	16.9	4.95 10^{-3}	1.24 10^{-3}
Salant 1950 . . .	12	2000	16.9	4.94 10^{-3}	1.23 10^{-3}

6. 3 The spectrum of the nucleonic component [2]

The spectrum of the nucleonic component may be determined either from the spectrum of formation of nucleons in the atmosphere or from the frequency of interactions produced by incident particles of different energies. Apart from certain features of the unstable component (π-mesons), the spectra of generating and generated particles should be in equilibrium in the atmosphere, and closely related by the cross-sections of the various processes of nuclear collision.

---

[2] Quite recently, direct determinations made by different authors in various ways have made it possible to construct vertical proton momentum spectra at different altitudes which appear to be reliable and give good evidence of the behaviour of the nucleonic component for low energies. These data are given in Fig. 11a. Towards the upper momentum region of the diagram the form of the spectra at all altitudes can probably be approximated by a power law: (Mylroi and Wilson [1951]), $Cdp/p^{2.8}$.

The experimental picture actually available is not yet complete. In fact, the detailed behaviour of the secondary fraction of the N-component can only be followed experimentally to energies about 1 BeV (Brown *et al.* [1949]; Camerini *et al.* [1949]) and therefore information on an intermediate range of energies alone can be derived. The spectrum of protons, which we do not know quanti-

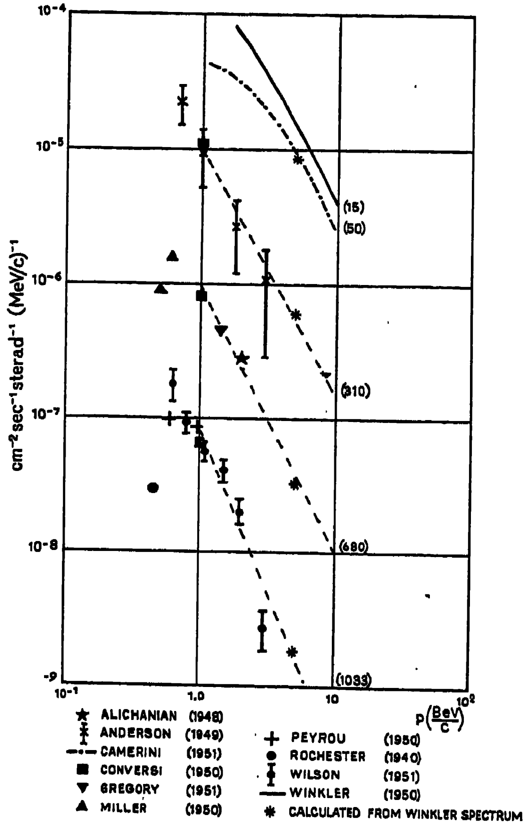

Fig. 11a

tatively, decreases rapidly with energy in qualitative agreement with the behaviour of the primary spectrum, and hence with the hypothesis, which has often been advanced, (§ 9), that the primary spectrum remains valid for secondaries in the propagation through the atmosphere. However, we note in this connection, the presence of deuterons and tritons of intermediate energy which are absent from the primary spectrum (Lord *et al.* [1949]; Bradt and Peters [1950b]).

Observations of the spectrum of the generating nucleonic component are difficult because direct determinations of the energy of the ionizing particles responsible for a nuclear event cannot be performed up to high energies (particularly with simultaneous identification of the nature of the particle). Indirect estimation of primary energy from total energy of the generated particles can only be regarded as a lower limit. The deduction of the spectrum concerning the generating particles from the frequency of the events depends essentially on knowledge of the cross-sections, which is confused, since neither the nuclear transparency nor the inelasticity of the whole process are known. The cross-sections are experimentally directly determined only in the limited energy range within which the cyclotrons can work (up to 400 MeV); outside this range, they have to be inferred.

In addition there is a limited amount of data on the region of extremely high energies where the estimation of the primary energy is based on the angular divergence of secondaries (Lord *et al.* [1950b]), although the result in these examples is only to order of magnitude.

In spite of reservations, nuclear events in photographic emulsions provide information which for many purposes can usefully replace the actual spectrum data, especially when attention is confined to relative measurements such as comparison between heights, the problems of angular distribution and so on. The most suitable indications of energy are either the number and type of star prongs observed or the total energy, which can be determined to good approximation at moderate energies and which appears to be an increasing function of the average number of prongs (Barton *et al.* [1951]). The star frequency as a function of the number of prongs may be approximated by simple laws, e.g.,

$$f = A \exp(-Kn)$$

or, as function of the total energy, by laws of the type:

$$f' = B \cdot E^{-s}$$

6. 4 The ratio of neutrons to protons

A further important datum is provided for various energy ranges by the relative number of protons and neutrons which together form the greater part of the nucleonic component. The co-existence with the ionizing component of a non-ionizing one, equally capable of nuclear interactions, in particular, of the formation of penetrating showers, has long been known from experiments with Geiger counters and cloud chambers; more detailed data have been obtained by nuclear plates.

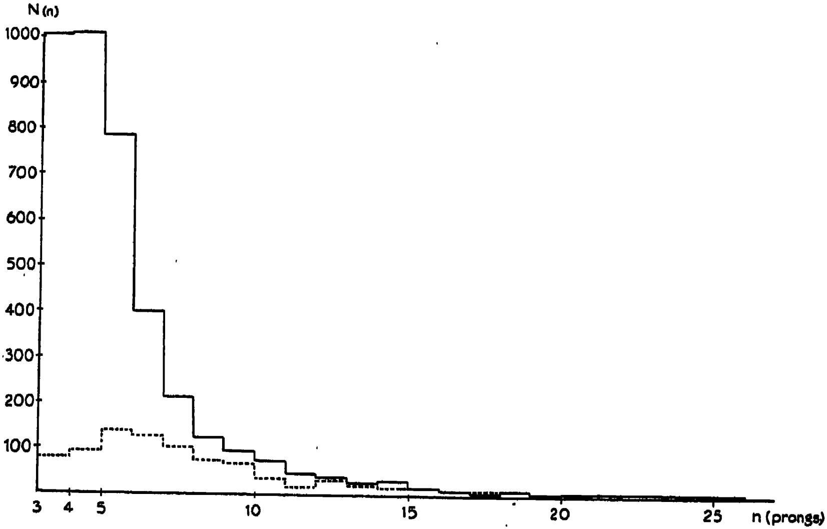

Fig. 12 – Relative number of stars with more than n heavily ionizing prongs, generated by non-ionizing primaries (full line) and by ionizing primaries (broken line). Altitude, 3500 m.

The results obtained by experiments carried out in the low atmosphere (3500 m.) are represented by the curves of Fig. 12. (BROWN *et al.* [1949]). At high energies, the number of stars generated by protons is about equal to the number of stars generated by neutrons; at low energies, however, the latter is much the greater, the protons being reduced to about 20% of the total; this datum is a minimum limit for protons because only when the primary is sufficiently energetic (~ 1.5 times minimum of ionization; 400 MeV for protons) and, therefore, clearly identifiable, can the stars generated by them be classified. The stars actually generated by ionizing particles of lower energy might be classified as produced by non-ionizing primaries; but this fraction cannot be estimated easily and the data relating to the low energy region are, therefore, not fully significant.

The behaviour observed at 3500 m. is substantially valid also in the upper atmosphere, except for a gradual increase at high energies of the percentage of events due to protons (CAMERINI [1949]), evidently caused by the residue of primaries becoming more important as height increases.

It seems plausible that protons and neutrons are equally multiplied in the atmosphere and that at low energies neutrons predominate only because they do not lose energy by ionization.

The ratio N/P between the two components will be variable with the energy, and its value, which depends on energy losses by ionization and on the exchange of charge during interactions with air nuclei, increases as the energy decreases; tentatively it may be represented by the function

$$N/P = \frac{E^2}{E^2-(Mc^2)^2}\cdot$$

where E is the total energy and Mc^2 the rest energy of the nucleons.

7. THE GENETIC RELATION

The main problem of the equilibrium in the atmosphere is based on the genetic relationship existing among all the different components of the cosmic rays. It is convenient to survey the problem in order to indicate how a correct judgment can be reached on available data. Apart from direct evidence, mainly obtained by cloud chambers and nuclear plates, the principle criteria concern the behaviour of each component as a function of the following three parameters: (*a*) energy; (*b*) height; (*c*) latitude. These three criteria, apparently equally indicative for the problem under consideration, have not all the same generality, for they involve certain hypotheses implicitly assumed. For example, to regard a similarity of latitude effect as a genetic relationship involves the hypothesis of a unique primary component. Similarity of spectrum may be ascribed to special features of form of the cross-sections (which become very restricted if, as is often assumed, the form of the secondary spectrum is similar to that of the primary). Moreover, going back to the effective generation functions of the various components, similarity of behaviour with height can be used only supposing that no preferential and distinct bands of production for the various components exist. It appears, however, in spite of these reservations, that the various hypotheses are actually well satisfied, so that the above similarity criteria may be applied with confidence. All the components which are undoubtedly of secondary origin and which we have examined, satisfy these criteria.

This circumstance, together with the direct, although qualitative, evidence allows the description of the genetic relation existing among all the different components. In the primary component, the heavy nuclei which have a rather short mean free path (~ 30 gm.cm^{-2}), are rapidly destroyed and broken down to three-fourths protons and one-fourth neutrons, the latter, on the average, being less energetic than the former. Thus, for our purpose, the precise primary composition is not of great importance, and it is only necessary to assume that the first collision occurs, on the average, at a depth slightly smaller than that which would be expected for protons, and, that the charge per nucleon instead of 1, is a little smaller.

We have noted (§ 1) that the total intensity of the cosmic rays, which is constant at altitudes greater than 55 Km. (21 gm.cm^{-2}), increases rapidly as the height decreases and it reaches a sharp maximum at about 56 gm.cm^{-2}. Evidently, the existence of this maximum is to be ascribed to the processes which generate π-mesons through collisions of primary nucleons against air nuclei. There exist typical illustrations of these events both in nuclear plates and in cloud chambers (star: BRADT *et al.* [1950c]; mixed showers: GREGORY and TINLOT [1951a and 1951b]; FRETTER [1949]; BROWN and McKAY [1950]) in which the complete phenomenology of the generating processes may be seen. We shall distinguish between events occurring at high energies and events occurring at low energies and discuss the two problems separately.

8. HIGH ENERGY EVENTS IN THE N-COMPONENT

When interaction occurs, energetic secondaries appear in beams of ionizing particles around the prolongation of the primary direction, and at the minimum of ionization. It has further been definitely established that these charged particles are accompanied by neutrons, since secondary interactions are found to be initiated more or less equally by ionizing and non-ionizing particles, and by π°-mesons detected by the electron pairs through the photons into which they decay. The ionizing particles are partly π-mesons and partly protons, but in addition there exist also smaller fractions of nucleon fragments of larger mass. The percentage of π-mesons, the direct determination of which is essentially based on photographic plate work (Brown *et. al* [1949]) lies between 50 and 80% of the total number of particles. These sprays of secondary particles have a multiplicity which is probably an increasing function of the primary energy; although the law of multiplicity is at present not known, it is assumed that the dependence does not vary very rapidly with primary energy.

8. 1 Multiple and plural processes

From a theoretical point of view, an important problem is whether meson production is a plural or a multiple event, i.e., whether several mesons are simultaneously ejected from a nucleus because of the collision between the incident proton and a single nucleon in it, or whether they are successively ejected in a cascade of collisions of the incident proton against many nucleons of the nucleus.

Experimental resolution of this question could only come from some particularly remarkable events observed in nuclear plates or cloud chambers; the former would provide more reliable statistics, but unfortunately the conclusions thus derived are generally invalidated by the fact that the main contribution to nuclear interaction cross-sections comes from the heavy nuclei (Ag, Br) of the emulsion and therefore, in order to obtain an evident demonstration of multiple production, the number of ionizing particles should be so high that at present only very few examples could possibly be considered (Lord *et al.* [1950b]; Bradt *et al.* [1950c]). Recent evidence obtained by Osborne [1951] seems to confirm the existence of events which may be accounted for only in terms of multiple production, at least with respect to primaries in the range 1.8 BeV. On the contrary, in experiments in a Wilson chamber, it is possible (Fretter [1950]) to induce events in an absorber of very low atomic number (Li, $Z = 3$) and then a much smaller number of ionizing tracks would be considered as supporting the multiple production process. In the atmosphere, however, multiplicity will not be very significant, and so, from a phenomenological point of view, the controversy is not of great importance.

8.2 Diffusion of the high energy N-component

The diffusion of the nucleonic component in the atmosphere depends essentially on the cross-sections for meson production. No experimental data are available, but only more or less legitimate hypotheses, the most trustworthy of which is based on similarity with bremsstrahlung emission by substitution of the meson field for the Coulomb field, and π-mesons for photons. On the basis of this theoretical parallelism:

(*a*) the total cross-section for meson production at high energies approaches asymptotically to a constant value,

(*b*) the differential cross-sections are exclusively functions of the fractional energies defined by the ratio of the energy loss in meson production to the incident energy.

HEITLER and JANOSSY [1949] on the basis of the hypothesis of plural production have integrated the diffusion equation:

$$\frac{\partial S(E,x)}{\partial x} = -aS(E,\varkappa) + \int_0^\infty S(E,\varepsilon,\varkappa)\, w\left(\frac{\varepsilon}{E+\varepsilon}\right) \frac{d\varepsilon}{E+\varepsilon}$$

(where $a = \int_0^1 w(r)dr$ is the total cross-section, $w(r)$ is the differential cross-section, E the primary energy and ε the energy loss), assuming, as initial conditions,

$$S(E,O) = \begin{cases} \dfrac{E_0^\gamma}{E^{\gamma+1}} & E > E_0 \\ O & E < E_0 \end{cases}.$$

They find the following relation between S and the depth t:

$$S(E,x) = S(E,O)\exp(-aw_{\gamma+1})x,$$

where

$$w_{\gamma+1} = \int_0^1 w(r)\,(1-r)^\nu\, dr.$$

This calculation depends essentially upon the two assumptions (*a*) and (*b*) above, but it is largely independent of other hypotheses.

The theory may be extended to multiple production of mesons and to non-catastrophic collision, that is, to conditions when secondary nucleons have energy sufficient for these also to take part in meson-forming collisions. The introduction, however, of an initial spectrum other than a pure power spectrum, is much more difficult. The calculation taking as initial condition the form of the real primary spectrum, has not yet been carried out.

These considerations have a certain importance as indicating that details of nuclear collisions cannot be deduced from the general behaviour alone of the nucleonic component. If the spectral form is maintained at various heights (as experimental data seem to confirm) and if the absorption has really an exponential behaviour, we have support for the reliability of postulates (*a*) and (*b*), but these results do not reveal any more detail on the cross-sections and on the elementary collisions, or on the relative percentages of mesons and nucleons.

9. THE π-MESONS

The generation of π-mesons in nuclear collisions may be considered as the main event of the whole phenomenology of cosmic rays, because the two components most important from an experimental point of view, the μ-component and the electron-photon component, are both derived from π-mesons. Positive and negative π-mesons, after a very short mean life ($\sim 10^{-8}$ sec.), decay into a μ-particle and a neutrino (LATTES *et al.* [1947]):

$$\pi^{\pm} \rightarrow \mu^{\pm} + \nu.$$

In addition, neutral mesons are produced in nuclear events; their mean life is not yet well established, but seems to be much shorter than that of the charged mesons ($< 5\ 10^{-14}$ sec.). The π°-mesons decay to a pair of photons:

$$\pi^{\circ} \rightarrow h\nu + h\nu.$$

It follows that the π-mesons may be considered as a link between the primary component and the secondary components; it is from this point of view and not as a notable component that they are considered in this paper, for their very short life makes their detection in the atmosphere difficult, and their direct contribution to observable effects small.

Data concerning π-mesons are listed in Table 13.

TABLE 13

π-meson constants

$M_{\pi\pm} = (275.2 \pm 2.5)\ m_0$	Panofsky 1951
$M_{\pi^0} = (264.6 \pm 3.2)\ m_0$	Panofsky 1951
$\tau_{\pi+} = (\ 2.54 \pm 0.1)\ 10^{-8}$ sec	Jacobson 1951

9. 1 The generation spectrum of charged π-mesons

Considering first charged mesons, only very energetic ones ($E \geqslant 50$ BeV) have a significant probability of avoiding decay in the atmosphere and of giving rise to effects influencing the measurements either of the barometric effect or of the spectrum of the μ-component underground (see §§ 2 and 9. 3). On the other hand, the direct experimental recognition of π-mesons essentially operates at relatively low energies, and all other phenomenological data concerning π-mesons are inferred from π-mesons generated in condensed materials (so that the whole path from the point of generation down to the point of observation is caused to be entirely inside the condensed material, for the mean life of π-mesons, although short, is by no means comparable with the slowing down time in a condensed material).

In addition to the direct evidence in plates, the direct creation of π-mesons in nuclear events has been demonstrated by Piccioni's experiment (PICCIONI [1950]) on local showers and based on the details of negative π- and μ-particle capture into nuclei (CONVERSI *et al.* [1947]), and also, up to now only at low energies, in experiments on artificial creation. Experiments have also demonstrated the production of mesons by photon bombardment but not yet directlyby electrons (WHITE *et al.* [1950]; POWELL [1950]). The creation of mesons from photons is confirmed by the production of π-mesons underground in the electromagnetic interaction between μ-particles and nucleons (see § 2), that is to say, in the interaction of nucleons with the virtual photon field of the energetic μ-particles.

The most complete material actually available on the production of π-mesons by the nucleonic component is given by the generation spectrum (Fig. 13) obtained in photographic plates down to about

50 MeV, where the spectrum is presumably almost flat; it begins to decrease with energy according to a power law having negative exponent about — 3/2 up to an energy of 1.4 BeV, and at still higher energies with exponent becoming about — 5/2, a result which is also confirmed indirectly. The behaviour of this spectrum agrees excellently with the generation function of the μ-particles,

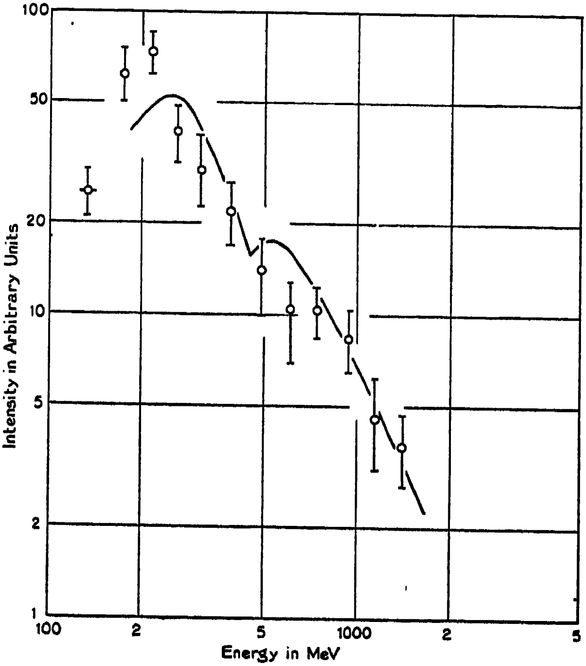

Fig. 13 – Differential distribution in total energy of mesons ejected from stars. The curve is Sands' calculated spectrum. (Camerini [1950]).

which has been previously examined; this conclusion is justified by the almost direct relation existing because of decay between the π-mesons and the μ-particles. Calculations which in the theory of Heitler and Janossy allow the description of the diffusion of the nucleonic component, have been extended to predict the generation spectrum of the π-meson component (Clementel [1950]). With this hypothesis, the π-meson spectrum is similar to that of the nucleonic component, because of the form of the cross-sections used.

9.2 Relation between the spectra of π-mesons and μ-particles

Tentative attempts may be made to trace back the generation spectrum of π-mesons by an inverse argument starting from the known spectrum of the μ-particles, for energies of 100 MeV — 1 BeV. The relation between the generation spectrum of the π-mesons and the distribution function of the μ-particle spectrum is direct and depends on a Lorentz transformation. The inverse transformation will, therefore, allow us to trace back the generation spectrum of the π-mesons from the μ-particle distribution function. When large energies are considered, the ratio between the energy of the π-mesons and the energy of the particles is a constant (about 1.27), and one can immediately infer the identity of the two spectra, already verified in the case of intermediate energies; in corresponding zones of both spectra, there are suspicious irregularities, which, because of their appearance in a rather low part of the spectrum (where a single energy of the π-meson gives rise to a considerable range of energies for the μ-particles) would be expected to be thoroughly smoothed down in the spectrum of the μ-particles as compared with that of the π-mesons (Ascoli [1950]).

At low energies, the relation between the two spectra is more complicated, for a description based upon an equation of unidirectional diffusion is no longer adequate.

9.3 Diffusion equation for π-mesons

The problem of the diffusion of the π-component itself is significant only at such high energies (in the upper part of the atmosphere of the order of some 10 BeV) that the π-meson will have a not negligible probability of avoiding decay in a geometrical path. The interaction theoretically predicted between π-mesons and nuclei, treating π-mesons as the agent of nuclear forces, is not experimentally well verified, because much of the data are inconsistent. However, some clarification comes from recent work on artificial production of π-mesons (Bernardini *et al.* [1950b]; White *et al.* [1950]; Powell [1950]), in terms of nuclear interactions having a mean free path λ comparable to the geometrical path; the effect of this interaction is a nuclear event accompanied by production of high and low energy particles with no significant difference from the other nuclear events already described. Then, since at the energies concerned losses by ionization are negligible, the diffusion equation which can be considered uni-dimensional in the above range is:

$$\frac{\partial \pi}{\partial t} = -\left\{\frac{1}{\lambda} + \frac{\beta}{t\varepsilon}\right\}\pi + S_\pi(\varepsilon, t).$$

An equation of this kind has already been used (GREISEN [1948]) to interpret the variation of the μ-particle integral spectrum underground in terms of the competition between the spontaneous decay processes (expressed by the term $-(\beta/t\varepsilon)\cdot\pi$) and the nuclear absorption (expressed by the term $-(1/\lambda)\pi$) in that part of the atmosphere where the μ-particles were generated (see § 2). It is easily seen that if $\lambda = R$ i.e., the π-component follows the same absorption law as the nucleonic component, the region where the change in the μ-component spectrum occurs corresponds to a depth which can be approximately calculated on the basis of the following relation:

$$\beta = K\frac{1+\gamma}{\gamma}h.$$

If the π-meson mean life is 2.10^{-8} sec., the exponent γ of the generation integral spectrum 1.6, and if the ratio of energies, K, of the π-meson and the μ-particle at high energies is 1.25,

$$h = 300 \text{ m.w.e.}$$

as is observed. It must be pointed out that this outline does not provide a zenith angle anomaly corresponding to the change of the exponent of the integral spectrum, that is, the zenith angle effect is given at any altitude by

$$M(0) = M(0) \cos 0.$$

Equations of the kind

$$\frac{\partial \pi}{\partial t} = \beta\frac{\partial \pi}{\partial \varepsilon} - \left\{\frac{1}{\lambda} + \frac{\beta}{t\varepsilon}\right\}\pi + S'_\pi(\varepsilon, t)$$

in which the energy losses by ionization are also considered, are used in order to investigate the diffusion of π-mesons in condensed materials. In these conditions, the behaviour of π-mesons should be strongly characteristic of the nature of their nucleonic interaction. If this occurs strongly, the absorption of the π-mesons is similar to that in cascade multiplication; on the other hand, when weak nuclear interactions occur ($\lambda \to \infty$) π-mesons are essentially absorbed in range. Unfortunately, the experimental evidence available at present does not allow a more detailed discussion.

The preceding equation can evidently be used in order to set up the diffusion equation for highly energetic μ-particles (GARELLI and WATAGHIN [1950]), in which the μ-particle decay, their losses by ionization and the generation function deriving from the π-meson decay will be included.

9.4 Neutral π°-mesons

Little information is yet available about the π°-spectrum, for the mean life does not allow a spectrum to be obtained directly as in the case of the $\pi^\pm$-mesons. Moreover, since events occur as if photons were directly generated in nuclear collisions, what will be important is the determination of the generation function of the gamma-photons $f(E)$, which presumably will decrease exponentially with altitude in the same way as the nucleonic component and therefore with a law of the kind:

$$f(E) \exp(-t/R)$$

where R represents the absorption path of the nucleonic component. This generation function will lead at any altitude to the electron-photon component, the behaviour of which should be predicted by knowledge of the generation function alone. The generation spectrum of the primary photons has recently been obtained by examining the electron pairs on plates exposed at high altitudes (CARLSON *et al.* [1950]) and it has been found to coincide with the spectrum expected from the decay of π°-mesons (Fig. 14), under the reasonable hypothesis that their generation spectrum is formally similar to that of the π^+-mesons. Since the theory of the electron-photon cascade is reliable, it should be possible to determine with sufficient accuracy the general behaviour of the electron-photon component at different depths. Unfortunately, the experimental picture is not suitable for a detailed comparison because there are not enough experimental results on the spectrum of the electron-photon component.

The various processes of generation of penetrating particles from photons, which we have reported for completeness sake, are not important from the point of view of the equilibrium of the various components in the atmosphere, except perhaps for nuclear photo-disintegrations, which may be responsible for a certain number of low energy stars.

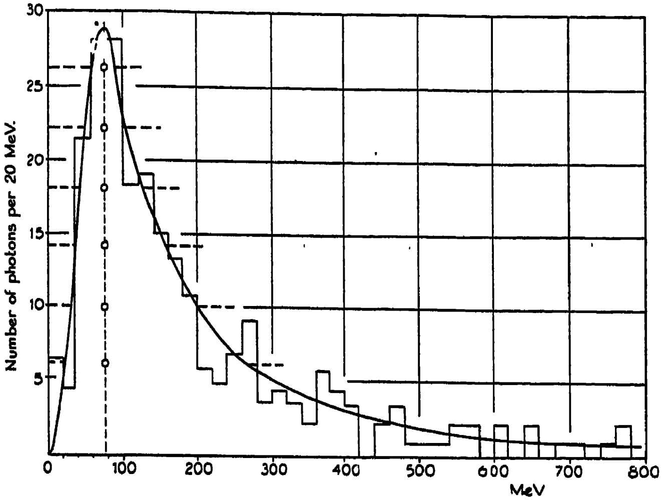

Fig. 14 – Spectrum of γ-radiation at 70,000 feet. The full line is that giving the best fit with the experimental results, and the mass of π^0 is deduced from it. (Carlson, 1950).

9. 5 τ and V-particles

In addition to neutral and charged π-mesons, other kinds of particle are now considered in the cosmic ray phenomenology; these, too, are presumably produced by nuclear interactions. The present state of knowledge concerning these particles is given in the second paper of this volume (BUTLER), from which it will be clear that these particles cannot at present be taken into account in the general atmospheric equilibrium. Although their appearence will certainly alter to some extent the picture already outlined, it seems most improbable that their intrusion will be quantitatively important.

10. LOW ENERGY EVENTS IN THE N-COMPONENT

In nuclear collisions, in addition to streams of collimated energetic particles, particles of intermediate and low energy are also produced, distinguishable by their different ionizing power and penetration; the majority of these particles are nucleons and heavier nuclear fragments. The low energy particles (*a*) have an energy distribution reaching its maximum at about 15 MeV in accordance with the evaporation theory of the nucleus; the more energetic particles (*b*), on the contrary, which are less frequent, are generally considered either as the recoil nucleons of inelastic processes or as caused by knock-on collisions, that is, by collisions occurring close to the surface of the nucleus so that the secondary particles can immediately escape without giving rise to other phenomena. While there is a satisfactory model for the evaporation process, based upon the thermodynamic theory of the nucleus excited by the energy gained in an encounter, no detailed model is available for the formation of particles classified under (*b*), which have energy sufficient to give rise to low energy secondary stars. Their importance in the atmosphere is greater than that which might be supposed on the basis of plate evidence, because the percentage of knock-on and recoil nucleons originating in light nuclei is much larger than that associated with the characteristic heavy nuclei of the plates. In this way, a multiplication chain of disintegration stars is possible, which is the essential feature of the low energy nucleonic component.

For the quantitative problem of this diffusion, we note that the distinction between the components of high and low energy has a clear physical basis. The high energy events which lead to the generation of π-mesons exhibit a large coefficient of inelasticity so that the absorption coefficient appears to be remarkably constant at these energies. On the other hand, scattering experiments with artificially accelerated particles show that at low energies (about 100 MeV) the losses inside nuclei caused by elastic collisions with the nuclear material are very high, so that nuclei of intermediate atomic weight are practically opaque to nucleons. From the former case the cross-section for inelastic losses probably decreases rapidly below about 1 BeV, and reaches at about 300 MeV the extremely small values obtained in measurements by the cyclotron groups. The energy losses, however, due to elastic collisions inside the nuclear matter increase as the energy decreases. It is therefore to be expected that in the band from about 200 MeV up to about 1 BeV there is a relatively transparent region for nucleons, in the sense that a nucleon having energy about 0.5 BeV, when it strikes a nucleus, will lose a relatively small fraction of its energy. This fact justifies the phenomenological distinction between high and low energies, and allows us to consider the low energy nucleonic component for some purposes as secondary. This view is further supported by the presence of a transition effect (Freier *et al.* [1949]) of the secondary component in the upper atmosphere, shown in the frequency of small stars.

The nucleonic component of intermediate energy has not a well defined character. It undoubtedly contributes to the formation of low energy stars (Bernardini *et al.* [1950a]), but, because of the small value of the cross-section for the relevant energy range, the stars with many prongs and with slow mesons form only a small fraction, and do not allow useful estimates about primary energy.

10. 1 Equilibrium between stars and neutrons

The multiplication of stars, one from another, is due to the fact that from each star there are derived, on average, a certain number of particles having energy still sufficiently high to be capable of giving rise to a new star. This happens until the energy of the star is reduced to about 100 MeV. In the meantime, the ratio of protons to neutrons is becoming rapidly smaller, for the former are quickly slowed down by ionization which does not affect the latter. It follows that the majority of nuclear events at low energies are caused by neutrons. The definite predominance of neutrons begins at the energy for which the proton range in air is of the same order as the mean free path for nuclear collisions, (Ferretti, [1949], Budini and Dallaporta, [1950]).

Below the limit of about 100 MeV, the chain of nuclear reactions passes over into the low energy sequence (Bethe *et al.* [1940]) in which only neutrons have a part. These neutrons, which suffer a continuous diminution of energy in elastic collisions, are converted in a path of about 90 gm.cm^{-2} (Davis [1950]) into thermal neutrons, isotropically distributed and detectable in BF_3 counters; finally they are captured by nitrogen nuclei. It is interesting to compare the frequency of the capture events, which in the intermediate atmosphere are in equilibrium with the acts of generation, and the frequency of the nuclear evaporations from which the neutrons are derived.

This comparison can be carried out if one can trace back from the frequency of stars detected in an emulsion to the frequency of stars occurring in air, but the argument is made somewhat uncertain because the ratio between the mean cross-sections for star production in emulsion and in air is not experimentally known: it is generally assumed to have the same magnitude as the ratio of the corresponding geometrical sections, which are defined by the nuclear radii:

$$r = r_0 A^{1/3} \qquad r_0 = 1.37 \cdot 10^{-13} \text{ cm.}$$

Experimental determinations seem either roughly to confirm this result (SALANT *et al.* [1950]) or bring into evidence (HARDING [1949]) results which could be better interpreted by assuming for light elements a cross-section relatively higher than that calculated for heavy elements on the basis of the above relation, but the uncertainty of the numerical factor to be brought in makes it preferable to assume the relation to be valid.

If $\bar{A}_{\text{em}} = 30$ is the average atomic number and $\bar{\sigma}_{\text{em}} = 45.10^{-26}$ cm^2 the average geometrical cross-section for photographic emulsion, and $\bar{A}_{\text{air}} = 14.6$ and $\bar{\sigma}_{\text{air}} = 35.10^{-26}$ cm^2 the corresponding values for air, and putting ϱ for the density of emulsion, one gets immediately:

$$N_{\text{air}}(\text{gm}^{-1}\,\text{sec}^{-1}) = \frac{1}{\varrho}\frac{\bar{A}_{\text{em}}}{\bar{A}_{\text{air}}}\frac{\bar{\sigma}_{\text{air}}}{\bar{\sigma}_{\text{em}}}\frac{1}{8.64.10^4} N_{\text{em}}(\text{cm}^{-3}\,\text{day}^{-1})$$
$$= 4.8\;10^{-6}\, N_{\text{em}}(\text{cm}^{-3}\,\text{day}^{-1}).$$

If Harding's factor for light elements had been taken into account, we would have found a rather higher value for the conversion modulus, say 6.10^{-6}.

From the data of an earlier section (see § 5.3), the behaviour of stars with height can be deduced and hence the behaviour with height of the radiation which generates them. Since the generating radiation essentially consists of nucleons, it should be expected to increase with height according to the Gross function (JANOSSY [1950] p. 138). The Gross function:

$$G(t) = 2\pi \int_0^{\pi/2} \exp\{-(t/R \cos\theta)\} \sin\theta \, d\theta,$$

is not very different from an exponential at depths which are large compared with the directional absorption path, i.e., at sea-level or mountain altitudes; but in the upper part of the atmosphere the difference between the Gross function and an exponential is considerable. Therefore, if stars are indicative of constant efficiency for detection of the nucleonic component in the upper part of the atmosphere, one would expect the number of stars to increase much more rapidly than is found at sea-level. But stars are by no means reliable indicators of the nucleonic component generating them, because there is certainly a large energy band from about 0.5 BeV up to 2 BeV in which nuclei are fairly transparent to nucleons. In this region, therefore, the generation of a visible star is a relatively more improbable event than either in the low or high energy regions. This circumstance, together with definite absence of very low energy nucleons (<1 BeV) in the primaries and with the fact that nucleons of this energy are generated abundantly in the atmosphere by more energetic nucleons, justifies the existence of a transition effect in the atmosphere for small stars having few prongs (the excitation energy of which is some 100 MeV) (LORD [1951]; FREIER *et al.* [1949]). The cut-off of the primary spectrum in the upper part of the atmosphere determines an effect which is opposite to that due to the increase of the Gross function relative to an exponential; this fact leads to an approximate compromise, which certainly is only rough, assuming that the increase of nuclear evaporations is, except in the highest atmosphere, a simple exponential function of absorption path, 140 gm.cm^{-2}. Then, normalizing to data at sea-level and on mountains,

$$N_{\mathrm{em}} = 2500 \exp(-t/140)\ \mathrm{cm}^{-3}\ \mathrm{day}^{-1}$$

where t indicates the depth of the atmosphere (in gm.cm^{-2}) from the top downwards. According to our previous discussion, this result may be expressed in terms of stars in air:

$$N_{\mathrm{air}} = 0.012 \exp(-t/140)\ \mathrm{gm}^{-1}\ \mathrm{sec}^{-1}$$

The results are summarized in Fig. 15.

From these values we can also derive the total number of stars generated per second in a vertical column of the atmosphere having unit cross-section (1 cm^2); thus:

$$N_{\mathrm{air}} = 2\ \mathrm{cm}^{-2}\mathrm{sec}^{-1}$$

This number agrees perfectly with a result recently obtained (YUAN [1951]) according to which the total number of neutrons generated per second in a 1 cm^2 column of air is

$$n_{\mathrm{air}} = 7.1\ \mathrm{cm}^{-2}\mathrm{sec}^{-1}$$

Comparison of these two values yields a value of 3.5 slow neutrons per star. It is extremely probable that these slow neutrons are almost exclusively produced in the evaporation processes, and their number is not in disagreement with experimental determinations.

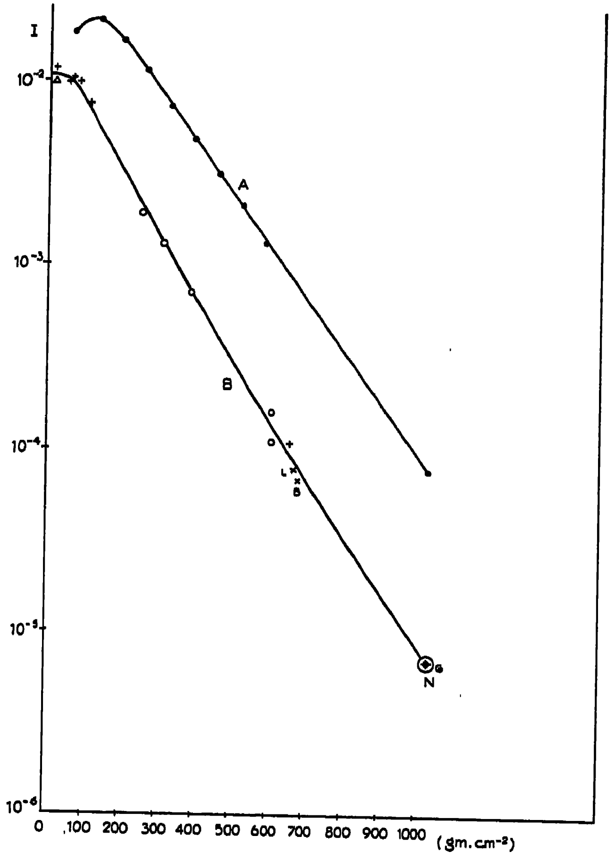

Fig. 15 – Intensity *vs* altitude curves for A: slow neutrons, and B: stars and bursts. (neutron captures and star intensities in units $\mathrm{sec}^{-1}\mathrm{gm}^{-1}$ air. • Yuan, ∘ Bridge, + Lord, L × Lattimore, B × Bernardini, G × George, △ Addario. $\underset{N}{\odot}$ Normalization point for bursts.

Another interesting comparison consists in the determination of the ratio between the above total number of disintegrations and the total number of primary particles incident on the top of the atmosphere. Indicating with J the average intensity of the primaries incident on the top of the atmosphere, the total flux will be πJ and therefore the required ratio will be

$$N_{\text{air}} / \pi J$$

It is reasonable to take

$$J \sim 0.1 \text{ cm}^{-2} \text{ sec}^{-1} \text{ sterad}^{-1}$$

and hence the ratio is about 7, in accordance with Bernardini'- estimate (BERNARDINI *et al.* [1950a]) of low energy secondary nus cleons generated in the atmosphere.

It follows that about 7 nuclear events occur in the atmosphere for every primary incident nucleon. This again emphasizes that the component which generates the majority of nuclear evaporations is a secondary one, more slowly absorbable and derived from the nucleonic component of high energy which, on the contrary, is absorbed rapidly in a few inelastic collisions. The stars with many relativistic prongs may be considered as indicative events of the high energy nucleonic component; a confirmation of these arguments is provided by the fact that the decrease of these energetic events in the atmosphere is more rapid (ADDARIO and TAMBURINO [1949]) than that of low energy events.

Finally, the values calculated either for the frequency of evaporations or for the frequency of slow neutrons may be used in order to estimate the fraction of energy flux transferred by the primary component and dissipated in the atmosphere in evaporation processes.

If the number of neutrons is doubled in order to take into account the charged particles also, and if the energy of 35 MeV is ascribed to every evaporated particle (BERNARDINI *et al.* [1950a]), one gets the total result of ~ 160 MeV $\text{cm}^{-2}\text{sec}^{-1}\text{sterad}^{-1}$, which is not very different from that estimated by ROSSI [1948] on the basis of much less certain experimental data. The value of 245 MeV dissipated per star in the evaporation process, and calculated from the preceding data, is rather uncertain for the light elements (N, O) under consideration, but this estimate cannot be greatly improved;

moreover, the evaporation process is not the only cause of energy dissipation, because the emission of heavier particles, gamma-quanta etc., should be taken into account.

11. EXTENSIVE AIR SHOWERS

All the components of the beam, which have up to now been considered separately, are found altogether in the complex events called extensive showers.

These showers, which were at first treated as simple electron-photon cascades, contain, in addition, penetrating particles among which all the known particles can probably be identified. The hypothesis that they are generated by primary electrons of extremely high energy ($> 10^{15}$ eV) is not now accepted in the light of the arguments given in § 1.4 and one must consider the penetrating particles as the residue of the generating agent from which, in ways which have already been described, the electron-photon component is derived. It is of interest, on the more recent work, to note why the electron-photon component has, in the extensive showers, the conspicuous development observed, which is not shown by lower energetic events such as the penetrating showers of Wataghin and Janossy (JANOSSY [1950]), which we have already discussed. We must suppose that a certain number of charged and uncharged π-mesons are generated in every nuclear interaction. At moderate energies the charged π-mesons decay into μ-particles and therefore they contribute only to the penetrating component; but at very high energies, they will interact with the nuclei before decaying, and will in this way be replaced, partially by π°-mesons, which will contribute to increase the soft component with respect to the hard. A quantitative analysis of this mechanism is not yet possible.

12. ENERGY BALANCE OF THE COSMIC RAY BEAM

The sum of the preceding data, although incomplete from many different points of view, is nevertheless sufficient to allow a preliminary evaluation of the whole balance of the propagation of the cosmic ray beam through the atmosphere to be made. The most important problems concern the flux of energy dissipated as a whole by the cosmic ray beam in the atmosphere and underground, together with the relative percentage of neutral and charged mesons generated in nuclear collisions, and the variation of the absorption path, for the nucleonic component, with energy.

12. 1 Flux measurements

Regarding energy dissipation, ROSSI [1948] obtained for the vertical beam a total value of 695 MeV cm^{-2}sec^{-1}sterad^{-1} by adding the contributions of the various components in all the different absorbing processes. This value must be corrected as shown in Table 14, in order to take into account, on the basis of our present knowledge, the decay of a μ-particle into an electron and two neutrinos (STEINBERGER [1949]; ANDERSON *et al.* [1949]; DAVIES *et al.* [1949]) and also the decay of a π-meson into a μ-particle and a neutrino.

TABLE 14

	Rossi	Revised
Collision loss of μ in atmosphere . .	62	62 MeV cm^{-2}sec^{-1}sterad^{-1}
Collision loss of μ underground . .	37	37
Collision loss of N-rays	52	52
Collision loss of electrons	285	285
Sum of above collision losses . . .	436	436
Sum corrected for angular spread .	480	500
Neutrino loss (decay of μ)	95	127
Neutrino loss (decay of π)		78
Energy loss in nuclear disintegrations	120	160
TOTAL	695	865 MeV cm^{-2}sec^{-1}sterad^{-1}

The estimate of the neutrino losses is based on the following data:

Total energy which goes to π-mesons	367 MeV cm^{-2}sec^{-1}sterad^{-1}
Total energy which goes to μ-particles	289
Difference, to $\pi-\mu$ decay neutrinos	78

Energy dissipated as decay products of μ	190 MeV cm^{-2}sec^{-1}sterad^{-1}
Energy going to decay electrons	63
Difference, to $\mu-e$ decay neutrinos	127

The above values have been computed using the constants:

$$\begin{aligned} m_\pi &= (274 \pm 6)\, m_0 \quad m_\pi c^2 = 145 \text{ MeV} \\ m_\mu &= (215 \pm 6)\, m_0 \quad m_\mu c^2 = 110 \text{ MeV} \end{aligned} \Bigg\} \quad \frac{m_\pi c^2}{m_\mu c^2 + T} = 1.27.$$

Let us examine first of all whether it is possible to confirm the total values listed in Table 14 in any other way. Considering the general description of all the components, it is apparent that the primary energy is completely dissipated either in the generation of charged and neutral π-mesons, in inelastic collisions, or by the production of a low energy nucleonic component responsible for nuclear evaporations. The energy necessary for the production of charged π-mesons may be reckoned on the basis of Sands' data [1950] concerning the production spectrum for μ-particles, while the energy dissipated in the production of π°-mesons may be evaluated as the total energy of the soft component (excluding that of secondary origin) generated by conversion photons the spectrum of which is known. Furthermore, the energy loss by ionization of the N-rays and the energy loss in nuclear disintegrations must be taken into account, and these can be derived from the values listed in Table 14. One thus obtains the values given in Table 15; it is interesting to note that there is satisfactory agreement between the new total and the previous one, so the analysis we have carried out appears to be confirmed.

TABLE 15

Energy which goes into charged mesons .	375 MeV cm^{-2}sec^{-1}sterad^{-1}
Energy which goes into neutral mesons. .	190
Collision loss of N-rays	52
Energy loss in nuclear disintegrations. . .	160
Correction for angular spread	62
TOTAL	839 MeV cm^{-2}sec^{-1}sterad^{-1}

If there are no gaps in our present knowledge about secondary processes incited by the primary radiation, and if all the events dissipating energy in an unobservable manner (for example, neutrinos) have been identified, then the total obtained above must be equal to the energy flux transferred by the primary component into the upper part of the atmosphere. On the basis of the energy spectrum and of the structure of the primary component, it is possible to calculate directly this flux and to compare it with the dissipation estimates just given. From the data given in § 2, one obtains a value for the inward flux of $\sim$ 1600 MeV cm^{-2} sec^{-1}sterad^{-1} in northern latitudes ($\sim$ 50° North), which is very much greater than the value obtained in Tables 14 and 15.

A direct comparison of total ionization measurements throughout the atmosphere provides a datum on the dissipated energy, and the energy flux thus calculated brings into evidence the same disagreement. The ratio between the omnidirectional and vertical measurements which are respectively concerned with the energy flux calculated on the basis of the flux of particles, and with the energy dissipated by ionization, effectively indicates that a larger amount of the omnidirectional flux than of the vertical flux is lost. This indicates that the disagreement is confined, in a predominant way, to phenomena of moderate energy and essentially at the top of the atmosphere. Probably the greatest uncertainty is restricted to low energy nuclear events which escape direct control, although possibly also to events of a still unknown nature.

We shall conclude this analysis by fixing for computational purposes two primary spectra of the form already indicated in § 1.

One of them has been derived from flux measurements (Winckler *et al.* [1950]) and is chosen to give the best fit. The other one appears as reduced, with respect to the former, at the low energies in order to account for the value of the energy dissipated in the atmosphere, and to account for the integral spectrum for the primaries of extensive showers (Williams [1948]). If the energy E is expressed in BeV, the spectra are of the form:

$$N_1\,(\geqslant E) = 0.4\,(E + 1.1)^{-1}\ \mathrm{cm}^{-2}\mathrm{sec}^{-1}\mathrm{sterad}^{-1} \qquad 1 \leqslant E \leqslant 15$$

and

$$\mathrm{N}_2\,(\geqslant E) = 1.75\,(E + 3.4)^{-1.75}\ \mathrm{cm}^{-2}\mathrm{sec}^{-1}\mathrm{sterad}^{-1},$$

where on the right hand side we have indicated the particle flux assuming protonic primaries.

The reduced spectrum (N_2) is justified not only by the values of the energy dissipated in the atmosphere but also by the hypothesis, already mentioned in § 1, (Winckler *et al.* [1950]), that the flux measurements at 15 gm.cm^{-2} of residual atmosphere are appreciably affected by secondary radiations. A correction up to 20 % near the equator is certainly due to the reproduction of the primary in this 15 gm.cm^{-2}, as can be demonstrated by extrapolating the measurements which have been reported at zero depth of the atmosphere. Lateral showers and the albedo will probably contribute another 20 % (Winckler). Of course, the choice of the reduced spectrum is somewhat arbitrary, but it is reasonable to hope that it is not far from true values. The relation between the integral spectrum and the energy flux for a determinate inferior cut-off on the spectrum, is immediately found:

$$W(\geqslant E) = N(\geqslant E)\,\frac{\gamma}{\gamma-1}\left(E + \frac{B}{\gamma}\right).$$

12.2 Ratio between neutral and charged π-mesons

Let us now consider the second question, that is the evaluation of the ratio between the number of π°-mesons and of charged π-mesons ejected in nuclear disintegrations, therefore, the ratio between the generation spectra of the electron-photon component and of the μ-component in the atmosphere.

We shall briefly mention the more or less direct results available. By examination of high energy nuclear events on photographic plates and in cloud chambers, it is possible to determine directly the ratio between the production frequencies of ionizing particles of high energy and of electron pairs derived from π-mesons. On the basis of the assumption that 80 % of the charged particles of high energy ejected in nuclear events are mesons of both signs, this estimate follows, taking into account the conversion probability for photons in emulsion. This estimate gives the values listed in Table 16.

TABLE 16

Author	Ratio	Method
Carlson [1950] . .	0.45 ± 0.10	plates
Bradt [1950c] . .	0.39 ± 0.13	plates

Further information is provided in an indirect way, but still based on single elementary phenomena, by considering (Camerini [1951]) the energetic balance between the primary energy and the sum of the energies concerning the various secondary components for nuclear disintegrations due to inelastic collisions of a charged incident particle. Supposing that in the events treated only $\pi^\pm$- and π°-mesons, recoil nucleons and evaporation particles are generated, and that the neutrons and protons are of comparable distribution, it is possible to obtain by difference the energy available for the production of the π°-mesons and, hence, the ratio (charged)/(neutral) mesons (assuming similar production spectra for both kinds of meson); one finds in this way for the ratio $\pi^\circ/\pi^\pm$ the value: 1.1 ± 0.2.

In addition to these direct estimates based on the investigation of single events, in which particles come into being, there are indirect data based on the analysis of the components generated in the atmosphere by charged and neutral mesons respectively, that is the μ-component and the electron-photon component; ROSSI [1949a] estimates the value 289 MeV $cm^{-2}sec^{-1}sterad^{-1}$ for the total energy dissipated by the electron-photon component. But, since the electron-photon component is partially seondary to the μ-component in the knock-on and decay processes, and since the μ-particles lose in decay an energy equal to 190 MeV $cm^{-2}sec^{-1}sterad^{-1}$, one third of which is transferred to an electron and two-thirds to neutrinos, one obtains for the total energy dissipated by the electron-photon component (apart from secondaries) 222 MeV $cm^{-2}sec^{-1}sterad^{-1}$.

Supposing, further, that the electron-photon component, not secondary to the hard component, is generated only through the conversion of π°-mesons, we find the value 222 MeV $cm^{-2}sec^{-1}$ $sterad^{-1}$ for the energy going into π°-mesons in the atmosphere. The corresponding datum for charged π-mesons is deduced from the value of the energy transfer to the μ-component, taking into account that in the conversion $\pi \rightarrow \mu + \nu$ the ratio between the energy of the π-meson and the average energy of the μ-particle is equal to 1.27. Thus the energy going into $\pi^\pm$-mesons is 357 MeV $cm^{-2}sec^{-1}sterad^{-1}$, and the ratio of neutral to charged mesons is 0.60 ± 0.15. If, following Rossi, an average statistical precision of 25 % is assigned to the measurements of the electron photon component, this estimate does not differ significantly from the preceding ones.

A more detailed and somewhat less indirect analysis could be made still taking into account the two components under consideration, but supposing them to be generated by two sources emitting respectively $\pi^\pm$- and π°-mesons, the former with spectrum:

$$B \exp(-t/R)\, f(E)\, dE\, dt,$$

and the latter

$$A \exp(-t/R)\, f(E)\, dE\, dt.$$

By means of the well-known diffusion equations of the two components generated in this way, it is possible to determine the ratio A/B from the intensity data in the atmosphere.

All the estimates of the ratio $\pi^\circ/\pi^\pm$ seem not incompatible with a value of 0.75, which is to be expected from the symmetrical theory of nuclear forces. If it is assumed that mesons are the particles which, according to meson theories, represent the field quanta of nuclear forces and which in bremsstrahlung at high energies appear as real particles, they are also responsible for the phenomena at lower energies, where the field of force plays a part as nuclear link and as elastic scatterer for nucleons. At low energies this interaction can be described in terms of a virtual exchange between neutral and charged mesons among pairs of nucleons. Charged and neutral mesons correspond respectively to two fields, the "charged field" and the "neutral field". The ratio of the intensity of these two fields, which can vary from theory to theory, is equal to $\frac{1}{2}$ in the symmetrical theory, which seems to have been definitely confirmed, at least up to an energy of 200—300 MeV. This would mean that the field radiated at high energies as charged and neutral mesons gives unaltered the relative numbers of the two kinds of particle of which it consists, as referred to the static field describing the low energy interaction.

12. 3 Variation with energy of the absorption length of the N-component

Finally, we discuss the third question stated in § 12: The quantity "absorption path" undoubtedly undergoes a systematic variation with the energy of the detected events. With reference to nuclear events the energy of which is of the order 10 BeV, the absorption path seems to approach the value corresponding to the geometrical section of air nuclei; for those events by which the majority of mesons diffused in the atmosphere are generated it gradually increases up to about twice the value of the geometrical path, and afterwards, for slow neutrons, the absorption path increases as the energy decreases until it reaches paths extending to 2.5 to 3.5 times that defined by the geometrical section. The essential feature related with this gradual increase of the absorption path may be identified in the different manner according to which the energy of the N-component in the various nuclear events is degraded. According to the hypothesis that the geometrical path effectively represents a minimum, a path close to the geometrical path signifies that the energy is almost completely degraded at each collision, or that the absorption is practically catastrophic, whilst a path long with respect to the geometrical path brings into evidence that the energy is only slowly absorbed. As support for this picture one may refer to the experimental results, still however inadequate, concerning the ratio of the two kinds of particle generating these events, i.e. protons and neutrons. If the absorption path is considerably longer than the geometrical path, it is to be expected that the ratio exclusively depends on the manner in which protons and neutrons are reproduced, and on the way in which they are absorbed during their propagation in the atmosphere. In this case, except near the top of the atmosphere, the residue of primaries has a very weak influence. On the other hand, if the absorption path has a value very close to that of the geometrical path, and therefore the absorption is approximately catastrophic, then at various depths of the atmosphere only the residue of the primary which has avoided collisions with air nuclei down to that level will be observed. The experimental evidence actually seems to indicate that in the atmosphere the nucleonic component of moderate energy is formed of approximately equal numbers of protons and neutrons and that the latter are far more numerous than protons at low energy because of the different energy losses; while, finally, experiments show that in the intermediate atmosphere the primaries of highly energetic events are charged particles the number of which is compatible with the primary residue if protons are approximately as numerous as π-mesons.

Further experimental data are required in order to convert these arguments into a consistent physical picture.

ACKNOWLEDGEMENTS

The authors are grateful to all the staff of the Padua Institute for the interest and encouragement given to them; in particular, to Dr D. Cadorin, A. Coen, C. Ceolin, I. Fontana and Dr M. Merlin for valuable help in reading the proofs and assistence in numerical calculations. They are also particularly indebted to Dr Claudio Villi, who translated the text into English.

Finally, the authors wish to acknowledge the helpful criticism and suggestions given in the preparation of this article by Prof. B. Rossi and Dr. J. G. Wilson.

REFERENCES

Addario, M. and S. Tamburino, 1949, Phys. Rev., 76, 983.

Addario, M. and S. Tamburino, 1950, Phys. Rev., 80, 749.

Anderson, C. D. and S. Neddermeyer, 1934, Int. Conf. Phys. London, 177.

Anderson, C. D., R. B. Leighton and A. J. Seriff, 1949, Phys. Rev., 75, 1466.

Arley, N., 1948, Stochastic Processes 2nd. ed.,(New York: Wiley and Sons).

Ascoli, G., 1950, Phys. Rev., 79, 812.

Barber, W. C., 1949, Phys. Rev., 75, 590.

Barnothy, J. and M. Forro, 1939, Phys. Rev., 55, 870.

Barnothy, J. and M. Forro, 1940, Phys. Rev., 58, 844.

Barton, J. C., E. P. George and A. C. Jason, 1951, Proc. Phys. Soc., A64, 175.

Bassi, P., E. Clementel, I. Filosofo and G. Puppi, 1949, Nuovo Cim., 6, 484.

Bassi, P., 1951, Nuovo Cim., 8, 469.

Bergstrahl, T. A. and C. A. Schroder, 1951, Phys. Rev., 81, 244.

Bernardini, G., M. Conversi, E. Pancini, E. Scrocco and G. C. Wick, 1945, Phys. Rev., 68, 109.

Bernardini, G., B. N. Cacciapuoti and R. Querzoli, 1948, Phys. Rev., 73, 335.

Bernardini, G., G. Cortini and A. Manfredini, 1950a, Phys. Rev., 79, 952.

Bernardini, G., E. T. Booth and S. J. Lindenbaum, 1950b, Phys. Rev., 80, 905.

Bethe, H. A., S. A. Korff and G. Placzek, 1940, Phys. Rev., 57, 573.

Biehl, A. T., H. V. Neher and W. C. Roesch, 1949, Phys. Rev., 76, 914.

Blackett, P. M. S., 1937, Proc. Roy. Soc. A159, 1.

Blocker, W., R. Kenney and W. K. H. Panofsky, 1950, Phys. Rev., 79, 419.

Bradt, H. L. and B. Peters, 1950a, Phys. Rev., 77, 54.

Bradt, H. L. and B. Peters, 1950b, Phys. Rev., 80, 943.

Bradt, H. L., M. F. Kaplon and B. Peters, 1950c, Helv. Phys. Acta, 23, 24.

Bridge, H., B. Rossi and R. Williams, 1947, Phys. Rev., 72, 257.

Brode, R. B., 1950, Phys. Rev., 78, 92.

Brown, R. H., U. Camerini, P. H. Fowler, H. Heitler, D. T. King and C. F. Powell, 1949, Phil. Mag., 40, 862.

Brown, W. W. and A. S. McKay, 1950, Phys. Rev., 77, 342.

Budini, P. and N. Dallaporta, 1950, Nuovo Cim., 7, 230.

Caldirola, P., 1949, Nuovo Cim., 6, 565.

Camerini, U., T. Coor, J. H. Davies, P. H. Fowler, W. O. Lock, H. Muirhead and N. Tobin, 1949, Phil. Mag., 40, 1073.

Camerini, U., P. H. Fowler, W. O. Lock and H. Muirhead, 1950, Phil. Mag., 41, 415.

Camerini, U., 1951, as quoted by Carlson.

Caro, D. E., J. K. Parry and H. D. Rathgeber, 1950, Nature, Lond., 165, 688.

Carlson, A. G., J. E. Hooper and D. T. King, 1950, Phil. Mag., 41, 701.

Cini, M. and G. Wataghin, 1950, Nuovo Cim., 7, 135.

Clementel, E., 1950, Nuovo Cim., 7, 109.

Cocconi, G., 1949a, Phys. Rev., 75, 1074.

Cocconi, G., V. Cocconi–Tongiorgi, and K. Greisen, 1949b, Phys. Rev., 76, 1020.

Cocconi, G., 1950c, Phys. Rev., 79, 1006.

Conversi, M., E. Pancini and C. Piccioni, 1947, Phys. Rev., 71, 209.

Conversi, M., 1950, Phys. Rev., 79, 749.

Cosyns, M., 1936, Nature, Lond., 137, 616.

Critchfield, L., E. P. Ney and S. Oleksa, 1950, Phys. Rev., 79, 402.

Crowe, K. M. and E. Hayward, 1950, Phys. Rev., 80, 40.

Davies, J. H., W. O. Lock and H. Muirhead, 1949, Phil. Mag., 40, 1250.

Davis, W. O., 1950, Phys. Rev., 80, 150.

Fermi, E., 1949, Phys. Rev., 75, 1169.

Ferretti, B., 1949, Nuovo Cim., 6, 379.

Forster, H. H., 1950, Phys. Rev., 78, 247.

Freier, P., E. P. Ney and F. Oppenheimer, 1949, Phys. Rev., 75, 1451.

Fretter, W. B., 1949, Phys. Rev., 76, 511.

Fretter, W. B., 1950, Phys. Rev., 80, 921.

Gangnes, A. V., J. F. Jenkins Jr. and J. A. van Allen, 1949, Phys. Rev., 75, 57.

Garelli, C. M. and G. Wataghin, 1950, Phys. Rev., 79, 718.

George, E. P. and A. C. Jason, 1949, Proc. Phys. Soc., A62, 243.

George, E. P. and J. Evans, 1950, Proc. Phys. Soc., A63, 1248.

George, E. P. and J. Evans, 1951, Proc. Phys. Soc., A64, 193.

Glaser, D. A., B. Hamermesh and G. Safonov, 1950, Phys. Rev., 80, 625.

Gregory, B. P. and J. H. Tinlot, 1951a, Phys. Rev., 81, 667.

Gregory, B. P. and J. H. Tinlot, 1951b, Phys. Rev., 81, 675.

Greisen, K., 1943, Phys. Rev., 63, 323.

Greisen, K., 1948, Phys. Rev., 73, 521.

Greisen, K., 1949, Phys. Rev., 76, 1718.

Greisen, K., S. P. Walker and W. D. Walker, 1950, Phys. Rev., 80, 535.

Groetzinger, G. and G. W. McClure, 1950, Phys. Rev., 77, 777.

Harding, J. B., 1949, Nature, Lond., 163, 440.

Hazen, W. E., 1944, Phys. Rev., 65, 67.

Hazen, W. E., C. A. Randall and O. L. Tiffany, 1949, Phys. Rev., 75, 694.

Heisenberg, W., 1949, Zeit. für Phys., 126, 569.

Heitler, W. and L. Janossy, 1949, Proc. Phys. Soc., A62, 474.

Hulsizer, R. I. and B. Rossi, 1948, Phys. Rev., 73, 1402.

Jacobson, M., A. Schulz and J. Steinberger, 1951, Phys. Rev., 81, 894.

Janossy, L. and G. D. Rochester, 1945, Proc. Roy. Soc., A183, 187.

JANOSSY, L., 1950, Cosmic Rays, 2nd edition (Oxford Univ. Press).
JOHNSON, T. H., 1941, Phys. Rev., 59, 11.
KRAUSHAAR, W. L., 1949, Phys. Rev., 76, 1045.
LATTES, C. M. G., G. P. S. OCCHIALINI and C. F. POWELL, 1947, Nature, Lond., 160, 453.
LATTIMORE, S., 1949, Phil. Mag., 40, 394.
LEWIS, H. W., J. R. OPPENHEIMER and S. A. WOUTHUYSEN, 1948, Phys. Rev., 73, 127.
LORD, J. J., M. SCHEIN and M. VIDALE, 1949, Phys. Rev., 76, 171.
LORD, J. J. and M. SCHEIN, 1950a, Phys. Rev., 78, 484.
LORD, J. J., J. FAINBERG and M. SCHEIN, 1950b, Phys. Rev., 80, 970.
LORD, J. J., 1951, to be published.
MCMAHON, A. J., B. ROSSI and W. F. BURDITT, 1950, Phys. Rev., 80, 157.
MERLIN, M. and O. PIERUCCI, 1951, Nuovo Cim., 8, 528.
MEYER, H. A., G. SCHWACHHEIM, A. WATAGHIN and G. WATAGHIN, 1949, Phys. Rev., 76, 598.
MIESOWICZ, M., L. JURKIEWICZ and J. M. MASSALSKI, 1950, Phys. Rev., 77, 380.
MONTGOMERY, R. A., 1949, Phys. Rev., 75, 1407.
MURA, A., G. SALVINI and G. TAGLIAFERRI, 1947, Nuovo Cim., 4, 10.
MYLROI, M. G. and J. G. WILSON, 1951, Proc. Phys. Soc., A64, 404.
NEHER, H. V., 1950, Phys. Rev., 78, 674.
NERESON, N., 1942, Phys. Rev., 61, 111.
OSBORNE, L. S., 1951, Phys. Rev., 81, 239.
OWEN, B. G. and J. G. WILSON, 1951, Proc. Phys. Soc., A64, 417.
PANOFSKY, W., L. AAMODT and J. HADLEY, 1951, Phys. Rev., 81, 565.
PICCIONI, O., 1950, Phys. Rev., 77, 1.
POMERANTZ, M. A., 1949a, Phys. Rev., 75, 69.
POMERANTZ, M. A., 1949b, Phys. Rev., 75, 1721.
POMERANTZ, M. A., 1950, Phys. Rev., 77, 830.
POWELL, C, F., 1950, Rep. on Progr. in Phys., 13, 350.
QUERCIA, I. F., B. RISPOLI and S. SCIUTI, 1950, Nuovo Cim., 7, 715.
ROSSI, B. and L. JANOSSY, 1939, Rev. Mod. Phys., 11, 279.
ROSSI, B., N. HILBERRY and J. B. HOAG, 1940, Phys. Rev., 57, 461.
ROSSI, B., 1948, Rev. Mod. Phys., 20, 537.
ROSSI, B., 1949a, Rev. Mod. Phys., 21, 104.
ROSSI, B. and R. I. HULSISER, 1949b, Nature, Lond., 163, 246.
SALANT, E. O., J. HORNBOSTEL, C. B. FISK and J. E. SMITH, 1950, Phys. Rev., 79, 184.
SANDS, M., 1950, Phys. Rev., 77, 180.
SCHEIN, M., V. H. YNGVE and H. L. KRAYBILL, 1948, Phys. Rev., 73, 928.
SIMPSON, J. A., 1948, Phys. Rev., 73, 1389.
SINGER, S. F., 1949, Phys. Rev. 76, 701.
SINGER, S. F., 1950a, Phys. Rev., 77, 729.
SINGER, S. F., 1950b, Phys. Rev., 80, 47.
STAKER, W. P., 1950, Phys. Rev., 80, 52.
STEINBERGER, J., 1949, Phys. Rev., 75, 1136.

Stinchcomb, T. G., 1950, Phys. Rev., 80, 479.
Swann, W. F. G., 1950, Phys. Rev., 78, 243.
Tiffany, O. L. and W. E. **Hazen**, 1950, Phys. Rev., 77, 849.
Tinlot, J. H., 1948a, Phys. Rev., 74, 1197.
Trumpy, B., 1943, K. Danske Vidensk. Selsk. Mat.-fys. Medd., 1943, 20, 6.
Vallarta, M. S., 1939, Rev. Mod. Phys., 11, 239.
Vallarta, M. S., 1948, Phys. Rev., 74, 1837.
Vallarta, M. S., 1950, Phys. Rev., 77, 419.
Van Allen, J. A. and A. V. **Gangnes**, 1950a, Phys. Rev., 78, 50.
Van Allen, J. A. and S. F. **Singer**, 1950b, Phys. Rev., 78, 819.
Van Allen, J. A. and A. V. **Gangnes**, 1950c, Phys. Rev., 79, 51.
Walker, W. D., 1950, Phys. Rev., 77, 686.
Walsh, T. G. and O. **Piccioni**, 1950, Phys. Rev., 80, 619.
Wataghin, G., 1947, Phys. Rev., 71, 453.
White, R. S., E. M. **McMillan** and J. M. **Peterson**, 1950, Phys. Rev., 78, 84.
Whyte, G. N., 1950, Phys. Rev., 78, 630.
Williams, R. W., 1948, Phys. Rev., 74, 1689.
Wilson, V. C., 1939, Phys. Rev., 55, 6.
Wilson, V. C. and D. J. **Hughes**, 1943, Phys. Rev., 63, 161.
Winkler, J. R., W. G. **Stroud** and T. J. B. **Shanley**, 1949, Phys. Rev., 76, 1012.
Winkler, J. R., T. **Stix**, K. **Dwight**, R. **Sabin**, 1950, Phys. Rev., 79, 656.
Yagoda, H. and N. **Kaplan**, 1949a, Phys. Rev., 75, 339.
Yagoda, H., N. **Kaplan** and C. H. **Conner**, 1949b, Phys. Rev., 76, 171.
Yuan, L. C. L., 1948, Phys. Rev., 74, 504.
Yuan, L. C. L., 1951, Phys. Rev., 81, 175.

CHAPTER VII

OBSERVATIONS OF COSMIC RAYS UNDERGROUND AND THEIR INTERPRETATION

BY

E. P. GEORGE

Birkbeck College, University of London

INTRODUCTION 395

1. THE DEPTH-INTENSITY RELATION: ABSORPTION MEASUREMENTS 395
2. CLOUD CHAMBER EVIDENCE CONCERNING THE NATURE OF THE RADIATION 403
3. THE DEPTH-INTENSITY RELATION: THEORETICAL . . 408
4. TIME VARIATIONS; TEMPERATURE COEFFICIENTS . . 418
5. STARS AND SLOW MESONS IN EMULSIONS 424
6. SLOW NEUTRONS 436
7. UNDERGROUND SHOWERS 438
8. IONIZATION BURSTS. 444
9. PENETRATING PAIRS OF PARTICLES 448

REFERENCES 450

INTRODUCTION

The number of investigations of underground phenomena of cosmic rays is really quite small when compared with the large number of papers published concerning the radiation above ground. Over the last three years, only 10 out of 520 cosmic ray papers in the Physical Review dealt with underground observations. The subject is one therefore that the physicist can hope to grasp in its entirety. In the following I shall attempt to give a connected account of the main features of the radiation so far observed below ground, and to show that a reasonably consistent interpretation can be given in terms of the behaviour of the cosmic ray μ-mesons.

I propose to begin with a discussion of the variation with depth of the cosmic radiation below ground, and the evidence provided by cloud chamber studies concerning the nature of the radiation. Then we shall see to what extent the depth-variation can be understood in terms of our present knowledge concerning the production spectrum of the π-mesons in energetic nuclear collisions of the primary radiation, and the decay of the π-mesons into μ-mesons. After that I propose to review and discuss more specific phenomena under their separate headings: fluctuations, stars, showers, and bursts, finally mentioning the cloud chamber studies of the penetrating pairs discovered underground by Braddick and Hensby. These latter events are not well understood and should prove to be one of the lines along which development may be expected in the future.

1. THE DEPTH-INTENSITY RELATION; ABSORPTION MEASUREMENTS

1. 1 Depth-intensity relation, experimental

The first measurements at large depths were made in 1925, when **MILLIKAN** and his collaborators started a series of observations with ion chambers lowered into snow fed lakes [1925, '26, '28, '31]. These authors showed that even under 80 m. water the ionization current was finite and still decreasing with depth. These early measurements gave the first indication of the extremely high energies possessed by cosmic ray particles. Similar work by REGENER [1931], using a high-pressure ion chamber, extended the measurements down to 260 m. In order to guard against the effect of any change of the radioactive content of the water with depth, Regener surrounded his ion-chamber with a "wall" of surface water 1m thick. The radioactive background is particularly troublesome in ion chambers operated at great depth and, in the following, use will therefore only be made of observations carried out with telescopes of Geiger counters in coincidence.

The earliest counter measurements were performed by REGENER [1931] who recorded the counting rate of a single counter lowered into Lake Constance. The observations at the largest depths were not reliable, in view of the large background that had to be subtracted. Soon after this, KOHLHÖRSTER [1933, '34], using a vertical telescope of counters in coincidence, extended the measurements to 1,000 m. During the years 1937/39, a series of more reliable measurements down to a depth of 1400 m. was made with counter telescopes by EHMERT [1937] in water, by CLAY [1937, 1939a, b] in water and in a coal mine, and by WILSON [1938] in a mine. The measurements were extended to 3000 m. by MIYAZAKI [1949], where the intensity is 3×10^{-6} of that at sea-level. In Fig. 1, the logarithm of the intensity reported by these authors is plotted against the logarithm of the equivalent depth expressed in metres of water. In addition the single points obtained at various depths by several other authors are given. All the results have been normalised to unity at sea-level.

No attempt has been made to draw a line through these points. so that the reader may get an unbiased view of the results. Several authors have fitted two straight lines of differing slopes of their results plotted in this way, the junction between the two lines occurring near 300 m. Above this so-called "knee", the slope is given as 1.8, and below it as approximately 2.8 (EHMERT [1937], WILSON [1938], CLAY and GEMERT [1939]). Up to the "knee", the radiation was assumed to consist of μ-mesons, but beyond it a qualitative change was thought to take place. Wilson and also Clay have suggested that the radiation at the greatest depths consists of protons, while Barnothy and Forro have favoured neutrinos. A theoretical explanation of the knee has also been given by Greisen [1948].

However, looking at the points in Fig. 1, they would appear rather to fall on a continuous curve, concave to the depth axis. There seems to be no evidence for a "knee" in the curve. The "knee" may perhaps be attributed to the experimental physicist's desire to plot his results on a straight line graph; in this case one line would not do and so two were pressed into service! Given that two straight lines are to be drawn through the points of Fig. 1, then they would naturally meet at about 300 m., since this is near the middle of the graph.

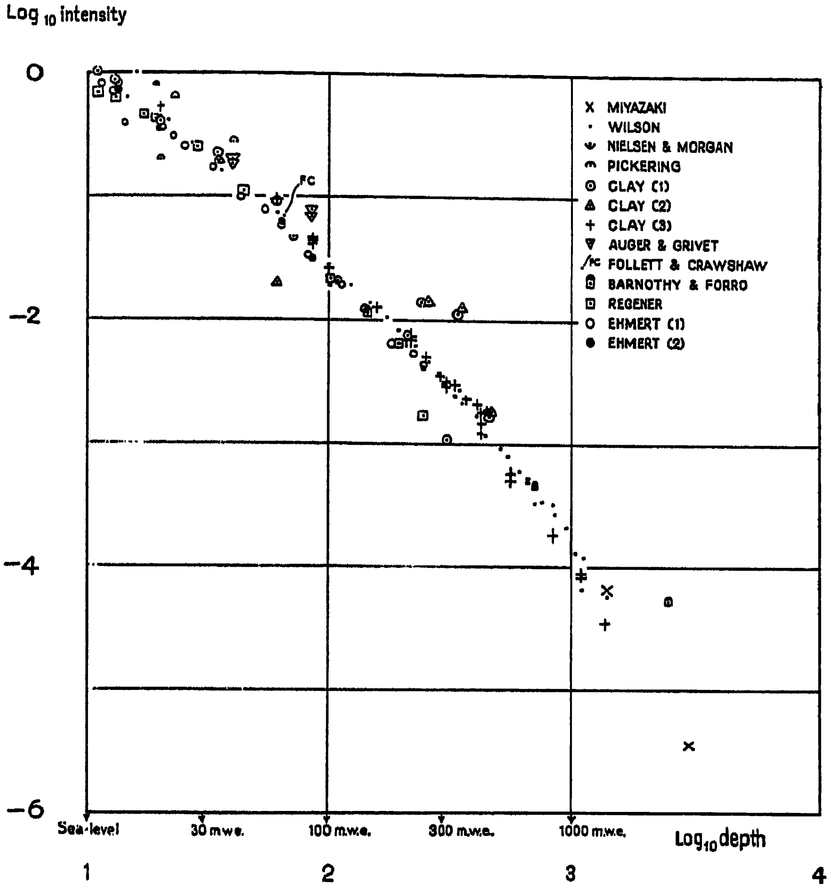

Fig. 1 Intensity — depth curve. (Experimental points).

We will return to this question of the intensity at various underground depths at the end of this section, and will convert the relative intensities of Fig. 1 to an absolute scale of particle flux. Before doing this we must consider one or two other relevant features.

1. 2 Absorption measurements

It is now generally accepted that most of the penetrating component at sea-level consists of μ-mesons, although recently, Mylroi and Wilson [1951] have shown that approximately 1 % consists of protons. Underground, the incident protons will be rapidly absorbed, leaving only the μ-mesons. The μ-mesons will produce energetic electrons by various processes, discussed more fully below, and hence we must expect to find a soft electronic component present underground, secondary to the μ-mesons. Furthermore, since the main energy loss of the mesons is due to ionization, the absorption in lead should agree with that calculated from the depth curve with a simple change of absorber thickness scale.

Most of the measurements carried out below ground, with absorbers placed in counter telescopes, fit in with this simple picture, but there are some that do not. In Table 1, the main features of the results of the authors in the former group are presented. The proportion of soft component has been obtained in the usual way, by extrapolating the absorption curve with more than 10 cm. Pb back to zero thickness. At a given depth,

TABLE 1

Absorption measurements below ground

Author.	Depth, metres water equivalent	Soft component % of total	Absorber, and maximum thickness used,
Wilson, V.C. [1938] . .	30	5	Pb, 1 m.
Auger & Meyer [1938] .	30	10	
Nielsen & Morgan [1938]	60	20	Pb, 50 cm.
George [1946]	60	10	Pb, 50 cm.
Randall *et al.* [1950] . .	850		Pb, 95 cm.
Tiffany & Hazen [1950]	850	40	Pb, 6 cm.
Randall & Hazen [1951]	850	30	Pb and C.

the estimates of the soft component do not agree particularly well, but there appears to be a slow increase in the relative amount of soft component with depth. This increase of the proportion of soft component is confirmed by shower measurements underground (§ 7. 1). It is also consistent with the expected behaviour of μ-mesons, since their mean energy increases with depth (§ 7. 1). Since the electrons will in general be produced at distances less than a few cascade units above the telescopes, the proportion of soft component recorded will be strongly influenced by the geometry of the apparatus, and it is likely that the discrepancies in Table 1 at a fixed depth can be explained along these lines. In the experiments of Tiffany and Hazen, the identification of the soft component was rendered more certain by observations in a cloud chamber containing lead plates in the path of the telescope.

All the authors in Table 1 found that the absorption in lead at thickness greater than 10 cm. was consistent with that calculated from the depth curve. V. C. Wilson obtained the same absorption curve whether the lead was placed in or above the counter telescope, and concluded that the radiation at 30 m. depth consisted of ionizing particles. A similar conclusion was reached at 850 m. by Tiffany and Hazen, who were able to set an upper limit of 3 % on the amount of neutral radiation causing telescope coincidences by way of secondary charged radiation. These authors placed a cloud chamber above a telescope, covering its solid angle of acceptance. In 97 % of the relevant pictures a normal ionizing particle was seen in the chamber.

Quite different conclusions have been reached by **Barnothy** and **Forro** [1939, 1940, 1948]. These authors carried out a series of observations at a depth of approximately 1000 m.w.e., summarised in their 1948 paper. Using a 3-fold telescope, the ratio of the frequencies of 3-fold coincidences to the 2-fold coincidences of the extreme counters, was found to be very small, of the order 0.05, whereas in a similar experiment with a 4-fold telescope, the ratio of 4-fold to 3-fold coincidences was found to be of the order 0.9. From this result they concluded that the greater part of the cosmic radiation at 1000 m. consisted of a neutral or thinly ionizing radiation with an efficiency of about 5 %. By rotating the telescope they showed that this neutral component was isotropic, and they suggested that it might be identified with the neutrinos arising from μ-meson decay, supporting their argument by pointing out that the observations were made beyond the "knee" of the depth curve.

With two different 3-fold telescopes, they investigated the absorption curve in lead up to about 1 m. The results obtained in the later experiment are drawn in Fig. 2. The line drawn by them through their points is shown dotted in Fig. 2. The alleged maxima at M_1 and M_2 were taken to indicate that two groups of charged secondary particles, with ranges ~ 10 cm. and 20 cm. lead respectively, were produced by the neutral component. The absorption curve obtained earlier also showed these large fluctuations but the maxima occurred at 50 and 80 cm. instead of 20 and 56 cm. lead. The full line in Fig. 2 is the expected curve based on the work given in Table 1.

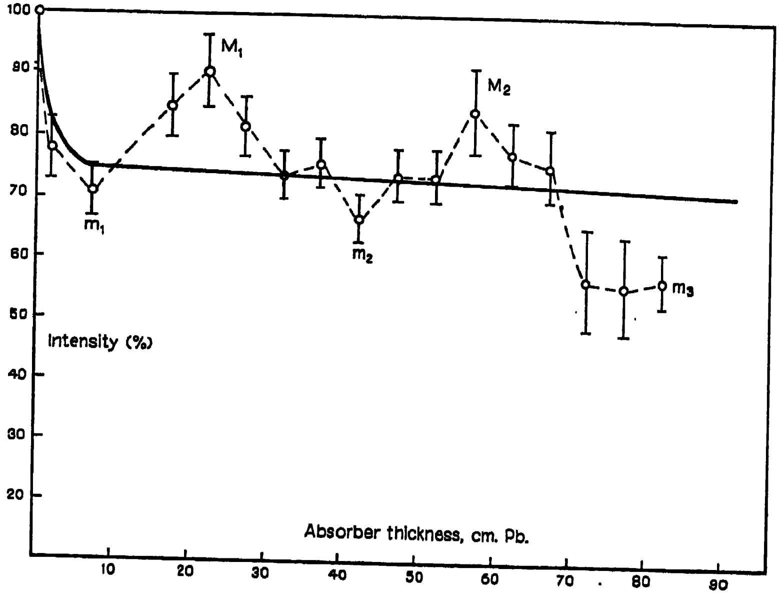

Fig. 2 – Absorption curve in lead at 1000 m. according to Barnothy and Forro
– – – – Line drawn by B. and F.
——— Results of other workers.

MIESOWICZ *et al.* [1951] recorded 2, 3 and 4-fold coincidences in a telescope at depths 540 and 660 m. They confirmed the observations of Barnothy and Forro, but came to different conclusions. According to Miesowicz and his coworkers, the counter coincidences at these depths are caused by two components: (i) an ionizing radiation discharging counters with 100 % efficiency and vertically collimated, and (ii) an isotropic radiation discharging counters with low efficiency and strongly absorbed in lead. Miesowicz *et al.* concluded that this second component, responsible for a large fraction of the 2-fold coincidences in both Barnothy and Forro's observations and their own, was simply γ-radiation from local radioactive contamination in the surrounding earth. This explanation seems highly probable.

1. 3 Angular distribution of the penetrating radiation

Only three investigations have been made of the distribution in angle of the underground radiation. Expressing the angular dependence as $\cos^n \theta$, the values of n obtained at various depths are given in Table 2.

TABLE 2

The exponent in the angular distribution

Follett & Crawshaw [1936]	Randall & Hazen [1951]	Bollinger [1950]
Depth, m.w.e. 60	850	1700
Exponent, n. 2	2.8 ± 0.1	3.0

If the penetrating particles below ground are μ-mesons, then on account of the high energies required to penetrate the loss of particles by decay will be negligible. Then assuming an isotropic primary radiation, the exponent in the angular distribution should be equal approximately to the slope of the intensity depth curve of Fig. 1, since, over a limited range, we may express the depth dependence as

$$I(x) = Ax^{-\gamma}$$

and hence

$$I(x, \theta) = I(x \sec \theta, 0) = Ax^{-\gamma} \cos^{\gamma} \theta = I(x, 0) \cos^{\gamma} \theta$$

Tangents to the depth curve have been drawn and the resulting values of γ are displayed as a function of depth in Fig. 3, on which are also plotted the experimental values in Table 2. The agreement is quite good, though more experimental points are needed, particularly at large depths.

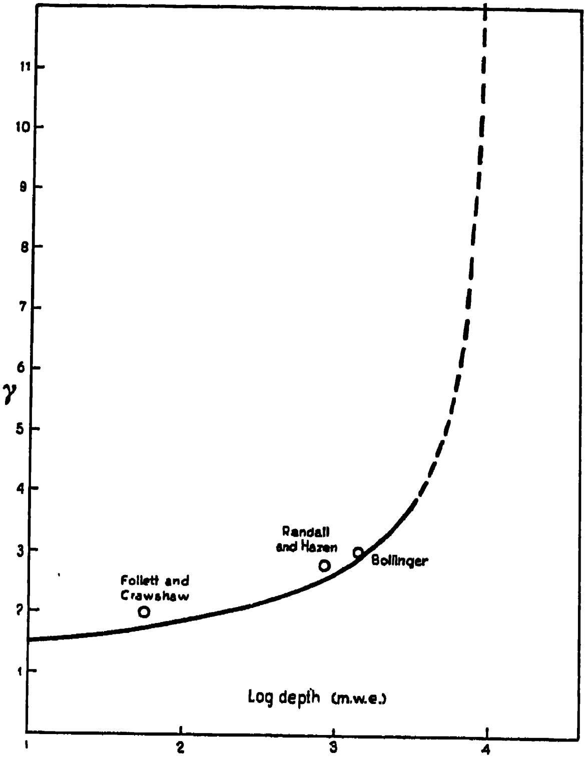

Fig. 3 – γ as a function of depth. Full line from observation, dotted line from Fig. 9. ○, experimental values of angular distribution exponent.

1. 4 Depth-intensity relation, corrected values

Since the angular distribution varies with depth (§ 1. 3), the relative counting frequencies at 2 depths will depend to a certain extent on the solid angle of the counter telescope. Also, the proportion of soft component is not constant. Values of the absolute intensity in the vertical direction, I_v, have been obtained by allowing for the angular distribution (taking the exponent from Fig. 3), subtracting the soft component, and finally normalising to the value of I_v at sea-level given by GREISEN [1942]. The best curve drawn through the experimental results treated in this way is shown in Fig. 4.

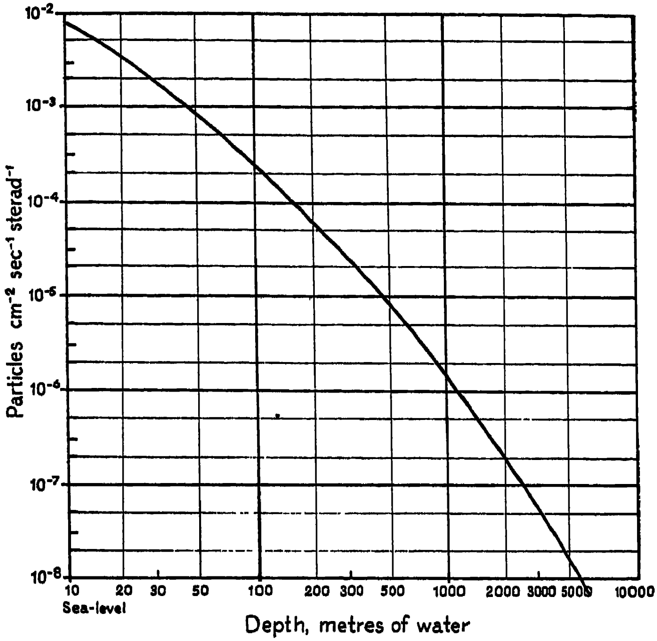

Fig. 4 – Intensity of hard component in vertical direction, in absolute units, as a function of depth.

2. CLOUD CHAMBER EVIDENCE CONCERNING THE NATURE OF THE RADIATION

The work with cloud chambers may conveniently be discussed under the two separate headings: (*a*) the general features of the underground radiation, and (*b*) a study of interactions resulting in secondary penetrating particles. Here we shall only consider observations coming under the first heading, leaving the second until § 8.

2.1 Observations at moderate depths, 20—60 m.

The first cloud chamber observations below ground were carried out by BRADDICK and HENSBY [1939] at a depth of 60 m. A lead plate of thickness either 1.4 or 2.5 cm. was placed across the horizontal diameter of the chamber. Expansions were controlled by a simple telescope consisting of two counters above and one inside the chamber, immediately below the lead plate. The chamber was not operated in a magnetic field.

As at sea-level, a large fraction (80 %) of the pictures showed one single ray penetrating the plate without appreciable deviation, while 6 % of the pictures showed the development of electron cascades in the lead plates. The remaining 14 % were unclassified for various reasons. Most of them showed a penetrating particle accompanied by one or two secondaries, probably electrons, which were absorbed in the lead plate. Apart from the relatively high frequency of penetrating secondary particles, discussed later, the general features of the radiation were very similar to those observed at sea-level.

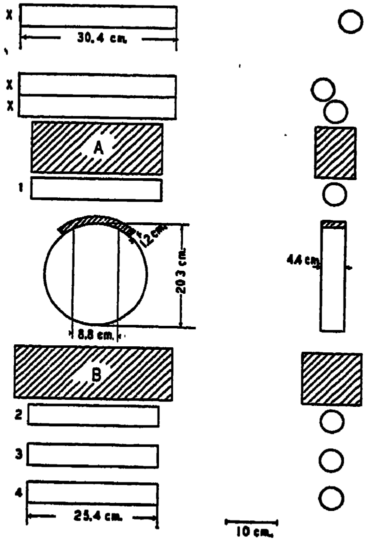

Fig. 5 – Cloud chamber arrangement used by Wilson and Hughes at 71 m.

Cloud chamber observations were also carried out at a similar depth, 71 m., by Wilson and Hughes [1943]. The chamber was mounted between the poles of a 600 lb Alnico permanent magnet, which produced a field of 1250 gauss in the plane of the chamber, enabling reliable momentum measurements to be carried out up to about 1 BeV/c. Three general arrangements were used to control expansions, shown in Fig. 5.

(I) Coincidences of counters 1, 2, 3 and 4, no lead absorber present.

(II) Same as (I) but with 10 cm. lead at B.

(III) Coincidences (1, 2, 3, 4) with 3 to 10 cm. lead at A plus 1.2 cm. on chamber. Counters X, in parallel, light a neon lamp when they discharge in coincidence with (1, 2, 3, 4).

The momentum spectrum of the 364 single tracks long enough for measurement is shown in Table 3 and Fig. 6, tracks showing momenta greater than 10^9 being classified as straight.

TABLE 3

Arrangement	Total tracks	Straight	0.1−1.0 BeV/c		<1BeV/c Total (%)
			+	−	
(I) no Pb.	174	117	22	35	33
(II) 10 cm Pb at B. . .	31	23	5	3	26
(III) 3−10 cm Pb above chamber	159	118	18	23	26
	364				

From Fig. 6 it will be noted that with arrangement (I) there is a marked negative excess at low momentum. This may be understood simply as being due to knock-on electrons. With arrangement (II) the low energy negative excess disappears, there being now no particles with momentum below 210 MeV/c, which agrees well with the momentum for μ-mesons of range 10 cm. lead, 230 MeV/c. Electrons will certainly be excluded by the lead absorbers. The five particles observed with momentum below 500 MeV/c were certainly not protons, since protons in this momentum range would have shown increased ionization.

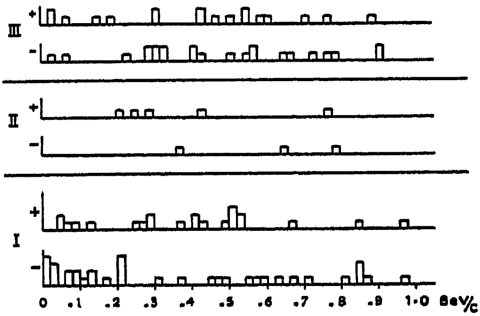

Fig. 6 -- Momentum spectra taken from cloud chamber photographs at 71 m.

The momentum spectrum with arrangement (III) is seen to fall between the spectra observed with arrangements (I) and (II), which is to be expected if the lead block absorbs all the incident low energy electrons but produces some further ones in collisions with the penetrating component.

Analysing the data obtained with counters X and the neon lamps, it was found that in 11 out of 251 coincidences (1, 2, 3, 4) there were no neon lamp flashes. However, on looking at the corresponding cloud chamber pictures, it was found that in no case was there a ray visible whose projection passed through X. In seven pictures, no ray was visible. The chamber did not fill entirely the telescope solid angle, and these seven could easily be accounted for on these lines. Inclined showers were present in two pictures, and the remaining two showed single rays so inclined as to hit the ends of the telescope counters but not counters X. There was no evidence of the production of ionizing particles in the lead block A above the telescope, by a non-ionizing agent. Several knock-on electrons were observed to start in the gas of the chamber, and the numbers were found to agree with the theoretical calculations of Bhabha.

Scattering

The scattering of the penetrating particles in 2 cm. lead has recently been studied by NASH [1951] at a depth of 23 m., using a cloud chamber without magnetic field. The deviation-frequency distribution was found to be consistent with the calculated distribution of multiple Coulomb scattering averaged over the expected energy distribution of the penetrating particles at this depth.

A very small fraction, 0.4 %, of the particles showed deviations greater than 25°, and could not be so explained. A similar result, indicating an anomalous scattering cross-section of the same magnitude, $\sim 10^{-28}$ cm^2/nucleon has been obtained by TRENT [1951] using the apparatus described in § 7. 2.

Specific ionization

The specific ionization of the underground particles was measured by HAZEN [1944] at a depth of 60 m. by drop counting in a cloud chamber with delayed expansion, and compared with similar counts at sea-level. The measured specific ionization was found to be the same at both sea-level and 60 m. depth, while on account of the higher mean energy of the particles below ground, an increase of 15 % above the sea-level value was expected, on the Bethe-Bloch model, for them. However, the later work of HALPERN and HALL [1948] based on the Fermi model predicts a much smaller increase of ionization, and the results of Hazen may be regarded as consistent with the theories of polarization effects.

2. 2 Observations at great depths

A cloud chamber was operated at a depth of 860 m. by Tiffany and Hazen. Their observations are of great interest, for no others have been carried out at any comparable depth, a depth at which counter measurements have been taken, by some authors, to indicate anomalous behaviour of the radiation (BARNOTHY and FORRO [1940]). One bank of counters was placed in the centre of the chamber, which contained four one-inch lead plates with another bank below, and 2-fold coincidences between these trays triggered the expansion mechanism. Of 175 pictures taken with this arrangement, 153 showed a single ionizing particle penetrating the 10 cm. lead in the chamber with no unusual interactions. Eleven of the remaining pictures showed electron showers, leaving 11 blank pictures unexplained. The expected number of accidental coincidences was 6, leaving an upper limit of five, or 3 %, that could be due to non-ionizing particles, though it is probable that these 5 can be explained in other ways.

Another series of observations were carried out with the lower counters moved to a position above the cloud chamber, the other tray remaining in the centre of the chamber. The counter system was now sensitive to electrons as well as to the penetrating component. The results of varying the nature and amount of absorber are shown in Table 4.

TABLE 4

Absorption of electrons from tunnel roof

Absorber gm.cm^{-2}	Penetrating Particles	Electrons	Electrons % of total
9 (Al + Brass.) . . .	108	75	41
22 (Al + Brass.) . . .	100	16	14
66 (Pb, some Al + Brass)	224	9	4

Electronic secondaries were also produced in the chamber and the results are given in Table 5.

TABLE 5

Secondary Electrons Produced in the cloud Chamber

Absorber	Penetrating Particles	Electrons	Ratio electrons/p.p. (%)
Pb	808	170	22
Al	561	128	23
Brass	420	73	17

The corresponding figure at sea-level found by Nassar and Hazen was 6 %. The increase at depth is easily understood in terms of the expected increase in mean energy of the radiation with depth. From this work it may be concluded that at 860 m. depth, the particles causing 2-fold coincidences in a counter telescope are ionizing. The proportion of soft component produced in the roof and in the chamber is significantly higher than at shallower depths. The soft component consists of electrons.

3. THE DEPTH-INTENSITY RELATION, THEORETICAL

From the work reviewed in the preceding two sections, it may be concluded that while there is little direct evidence that the penetrating radiation below ground consists of μ-mesons, there are no observations inconsistent with this assumption. In § 5, evidence of a more positive nature is presented obtained in nuclear emulsions, confirming that at depths down to 60 m., the penetrating component consists of μ-mesons. The intensity-depth curve should therefore be closely related to the momentum spectrum of the penetrating component at sea-level. In order to convert one to the other, it is necessary to make use of the relation between momentum and range, and this we consider first.

3.1 Energy losses of μ-mesons

The following processes leading to loss of energy of μ-mesons will be considered:

(i) ionization.
(ii) bremsstrahlung.
(iii) electron-pair production.
(iv) nuclear disintegration "stars" and showers.
(v) production of penetrating secondary particles.
(vi) Cerenkov radiation.

Usually only the first process is considered. LYONS [1943] considered the second. HAYAKAWA and TOMONAGA [1949] have pointed out the importance of the third. In evaluating the fourth and fifth contributions, results will be used that are given in detail in §§ 5 and 9.

Ionization loss

Following Fermi, the ionization loss may be assumed constant at high energy. For simplicity, we replace the real earth by a hypothetical medium of atomic number, $Z = 10$ and atomic weight $A = 20$. For such a medium, with density about 2, the formulae of Halpern and Hall give for the final steady value of ionization loss at high energy:

$$(1) \qquad (dE/dx)_{\text{ion}} = 2.2 \text{ MeV gm}^{-1}\text{cm}^2$$

Bremsstrahlung

The cross-section for the production of a photon of energy between E' and $E' + dE'$ by a μ-meson of energy E and spin $\frac{1}{2}$ is (CHRISTY and KUSAKA [1941]):

$$(2) \qquad \begin{cases} \sigma(E, E')\, dE' = \\ = \alpha Z^2 r_0^2 (m_0/\mu)^2 \dfrac{16}{3} \left(\dfrac{3E'}{4E} + \dfrac{E'-E}{E}\right) dE' \left[\ln\left(\dfrac{12}{5}\dfrac{E-E'}{E}\right) - \dfrac{1}{2}\right] \end{cases}$$

where $\alpha = 1/137$
$r_0 = e^2/m_0c^2$
$m_0 =$ electron mass
$\mu =$ meson mass $(= 215\, m_0)$.

Multiplying (2) by E' and integrating, we obtain for the energy loss:

$$\begin{aligned}(dE/dx)_{\text{rad.}} &= 4\alpha Z^2 r_0^2 (m_0/\mu)^2 (NE/A) \left[\ln\left(\frac{12E}{5\mu c^2 Z^{1/3}}\right) - \frac{1}{2}\right] \text{gm}^{-1}\text{ cm}^2 \\ &= 1.5 \times 10^{-7} E\,[\ln(E/\mu c^2) - \tfrac{1}{2}] \text{ gm}^{-1}\text{ cm}^2,\end{aligned}$$

where N is Avogadro's number.

This becomes important for energies greater than 100 BeV where it may be expressed simply as follows:

$$(dE/dx)_{\text{rad.}} = 10^{-6}\,E\ \text{gm}^{-1}\ \text{cm}^2. \tag{3}$$

Pair production

The cross-section for the creation of electron pairs by fast charged particles has been given by Bhabha [1935]. Bhabha's formulae for the production of a pair of total energy E' by a μ-meson of energy E may be expressed in the following form, where we write $183\ Z^{-1/3} = a$:

$$\sigma(E, E')dE = \frac{56}{a\pi}(\alpha Z r_0)^2 f(E, E')\,(dE'/E') \tag{4}$$

where

$$f(E, E') = \begin{cases} \ln(E'/m_0c^2)\ln(Em_0/E'\mu), & m_0c^2 < E' < 2am_0c^2 \\ \ln(a)\ln(Em_0/E'\mu), & 2am_0c^2 < E' < (Em_0/\mu) \\ \frac{9}{7}(Em_0/E'\mu)^2\ln(a\mu E'/m_0E), & Em_0/\mu < E' < 2(E/\mu c^2)^2 m_0c^2/a \\ \frac{9}{7}(Em_0/E'\mu)^2\ln(2E/\mu c^2), & 2(E/\mu c^2)^2\, m_0c^2/a < E' < E \end{cases} \tag{5}$$

Multiplying (4), (5) by E' and integrating, we obtain for the energy loss by pair creation:

$$(dE/dx)_{\text{pair}} = \frac{8}{\pi}(\alpha Z r_0)^2 (Nm_0/A\mu)\,\{E\,(\tfrac{9}{16}\ln(a) + $$
$$+ 1 - (m_0/\mu)\ln(2E/\mu c^2)) - \tfrac{14}{9}\mu c^2(\ln(E/\mu c^2) - \ln(2a) + \tfrac{37}{18})\},$$

Substituting numerical values we get approximately:

$$(dE/dx)_{\text{pair}} = 1.6 \times 10^{-6}\,E\ \text{gm}^{-1}\ \text{cm}^2. \tag{6}$$

Observations on the creation of electron pairs by fast cosmic ray particles have been reported by Occhialini [1949] and by Bradt *et al.* [1950]. Hooper, King and Morrish [1951] have been able to confirm approximately the validity of the formulae (4), (5) on which the expression for the energy loss (6) is based.

Nuclear disintegration "stars" and showers

Observations in nuclear emulsions exposed below ground by George and Evans [1950] have suggested that the cross-section for the production of "stars" releasing energy in the limits E', $E' + dE'$ by a μ-meson of energy E is of the form

$$\sigma(E, E')dE' = (2a\sigma_{h\nu}/\pi)(dE'/E') \ln (E/E'), \tag{7}$$

where $\sigma_{h\nu}$ is the photonuclear cross-section, equal to about $2.10^{-28}\mathrm{cm}^2$ (MILLER [1951]). This cross-section is consistent with the observed total cross-section, $\sim 10^{-29}$ cm^2 per nucleon, for the production of stars by fast μ-mesons.

Multiplying equation (7) by E' and integrating, we obtain the following theoretical value for the energy loss by nuclear excitation:

$$\left\{ \begin{aligned} (dE/dx)_{\text{star}} &= 2a\sigma_{h\nu}NE/\pi \\ &= 5.10^{-7}\, E \ \mathrm{gm}^{-1}\mathrm{cm}^2 \end{aligned} \right. \tag{8}$$

Production of penetrating secondary particles

The production below ground of energetic penetrating secondary particles was first noted by BRADDICK and HENSBY [1939]. Subsequent observations by NASH [1951] and WOLFENDALE [1951] have suggested that these events are distinct from those discussed above. This is borne out by the fact that the cross-section for this process turns out to be of the order 4.10^{-29} cm^2 per nucleon, at least four times greater than can be accounted for by the observations on nuclear disintegration stars. It seems clear that this process must lead to loss of energy by the incident μ-mesons, but as yet we have not enough experimental data to give guidance in assessing the numerical value. As a first approximation, we assume that the cross-section varies with energy in a manner similar to that found in the nuclear emulsion work, but that the absolute magnitude is four times greater. This process then gives the energy loss by production of penetrating secondary particles:

$$(dE/dx)_{\text{pen.}} = 2.10^{-6}\, E \ \mathrm{gm}^{-1}\mathrm{cm}^2 \tag{9}$$

On theoretical grounds, GARRELLI and WATAGHIN [1950] considered the energy loss of fast μ-mesons resulting from π-meson production, basing their calculations on the work of SNEDDON and TOUSCHEK [1949]. They arrive at a result very similar to equation (9), and it is possible that their calculations may be related to the process observed by Braddick and Hensby.

Cerenkov radiation

The energy loss as Cerenkov radiation may be written approximately:

$$(10)\qquad (dE/dx)_C = 0.1 \ln (E/10^9) \text{ MeV gm}^{-1}\text{cm}^2$$

where $E > 1$ BeV.

3. 2 The range-energy relation for energetic μ-mesons

Adding together the various contributions (1), (3), (6), (8), (9) and (10), we obtain for the total rate of energy loss at high energies:

$$(11)\qquad dE/dx = a + bE + c \ln (E/10^3),$$

with E in MeV,

$$a = 2.2 \text{ MeV gm}^{-1}\text{cm}^2$$
$$b = 5.1 \times 10^{-6} \text{ gm}^{-1}\text{cm}^2$$
$$c = 0.1 \text{ MeV gm}^{-1}\text{cm}^2.$$

Some representative values derived from equation (11) are given in Table 6 for our hypothetical rock, $Z = 10$, $A = 20$, and for lead.

TABLE 6

Values of dE/dx in MeV $gm^{-1}cm^2$

Energy (BeV)	Ionization		"b" term		Cerenkov	
	Rock	Lead	Rock	Lead	Rock	Lead
1	2.2	1.3	0.005	0.019	0	0
10	2.2	1.3	0.05	0.19	0.2	0.1
100	2.2	1.3	0.5	1.9	0.45	0.2
1000	2.2	1.3	5.	19.	0.7	0.3

It is seen that the term proportional to E in equation (11) becomes as large as the ionization term at energies near 100 BeV, and that at higher energies it becomes dominant. This means that at these high energies it is no longer a good enough approximation to assume a linear relation between energy and range. The loss due to Cerenkov radiation is everywhere a small fraction of the total and is proportional to $\ln E$. We may get a closer approximation to the range-energy relation by assuming the Cerenkov term constant and equal to its true value at $E = 100$ BeV. Then (11) becomes:

$$\left.\begin{aligned} dE/dx &= a + c \ln(100) + bE \\ &= d + bE, \end{aligned}\right\} \tag{12}$$

and this may now be integrated to give the range-energy relation:

$$x = (1/b) \ln(1 + bE/d). \tag{13}$$

This is plotted out in Fig. 7. At low energies the relation is linear, since here ionization is the dominant term, but at energies greater than 100 BeV the increased losses make themselves felt, and the range increases much more slowly with E, showing signs of saturation at a depth of about 10,000 m. There must clearly be a marked effect on the depth intensity relation, which we will now consider.

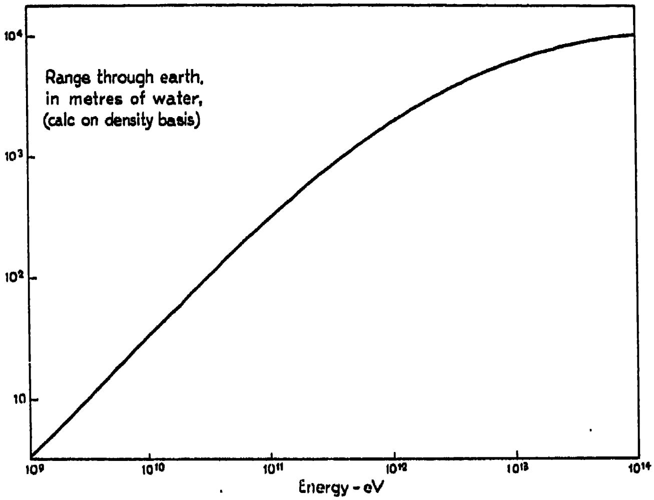

Fig. 7 — Range — energy relation for μ-mesons at high energy.

The values of dE/dx listed in Table 6, are admittedly theoretical figures, though there is experimental justification for each of the detailed processes considered. It would be of great interest to have experimental values of energy loss in absorbers at energies above 100 BeV. This would seem to be within the capabilities of modern cosmic ray spectrographs. There may well be other unknown effects coming into play at these extreme energies which are not envisaged in this report.

3. 3 The energy spectrum at sea-level

The energy spectrum of the particles penetrating 10 cm. lead at sea-level has been measured by CARO, PARRY and RATHGEBER [1950] using a magnetic deviation spectrometer. The apparatus is shown in the insert in Fig. 8. The differential momentum distribution is plotted in Fig. 8 together with the curve derived from earlier measurements by Rossi. The new results fit the curve well except in the high momentum region, where the points fall off faster with increasing momentum. In this region, the spectrum may be represented by a power law with exponent 3.0 ± 0.2. The explanation of the departure from this power law at low momenta in terms of μ-meson decay and the π-meson production spectrum is well known. Beyond 10 BeV/c, the effect of decay is negligible, and we therefore make the following assumptions as a first approach to the interpretation of the depth curve:

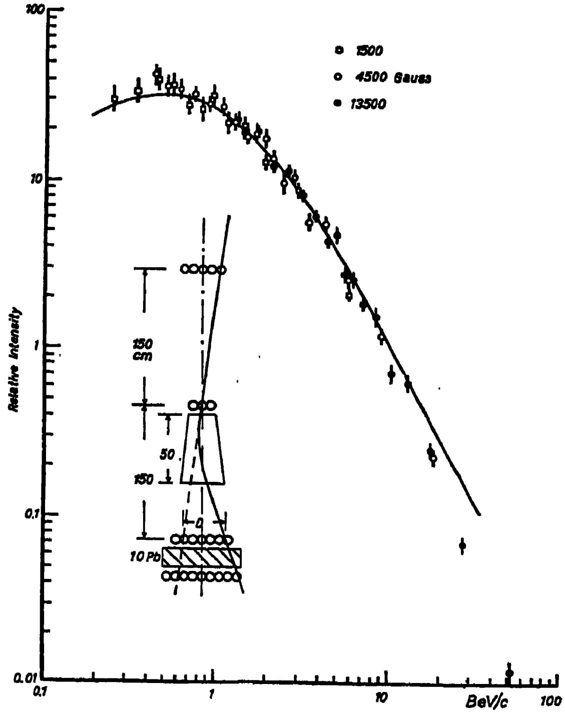

Fig. 8 – Differential momentum spectrum at sea-level of cosmic ray particles able to penetrate 10 cm. of lead (Rathgeber).

(i) substantially all of the penetrating particles at sea-level are μ-mesons.

(ii) the power law spectrum with exponent 3.0 may be extrapolated beyond the upper limit measured by CARO *et al.*

It is then a simple matter to calculate the expected depth-intensity curve using the spectrum in Fig. 8, and the range energy relation (13) and Fig. 7.

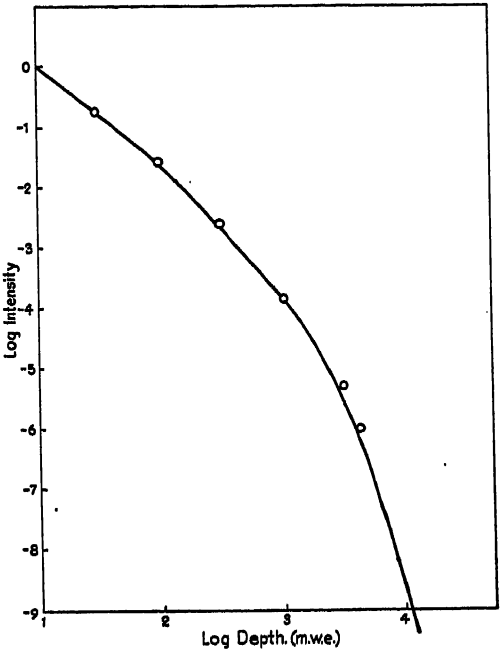

Fig. 9 – Depth—intensity curve, calculated including only increased losses of μ-mesons at high energy.

The result is given in Fig. 9, where some points from the experimental curve, Fig. 4, are reproduced for comparison. The agreement is seen to be quite good down to the greatest depths at which measurements have been made. At depths greater than 1000 m., the increased losses due to pair creation, etc., are appreciable and the calculated curve begins to drop extremely rapidly. According to the results in Fig. 9, for example, the angular distribution at 6000 m. should be proportional to $\cos^6 \theta$. It would be of great value to have many more measurements of the vertical intensity and angular distribution at depths in the region 1 to 10 Km.

3.4 The influence of π-meson interactions

In the above, the depth curve was explained simply by taking the μ-meson spectrum at sea-level from observation, and by making allowance for increasing energy losses, mainly electromagnetic in origin, that become of importance at energies greater than about 100 BeV. We thus successfully avoided introducing π-mesons into the picture. This is hardly justified, since, for example, the mean range before decay of a π-meson of energy 300 BeV is about 15 Km., in other words the whole of the effective atmosphere. At energies near 1 BeV, the nuclear collision cross-section is known to be approximately equal to the nuclear geometric cross-section (CAMERINI *et al.* [1950]). If this were true at 300 BeV, it is clear that a large fraction of π-mesons would suffer nuclear absorption before decay in the atmosphere, with a consequent considerable reduction of the intensity of μ-mesons at this energy. If however, the nuclear interaction of π-mesons were much weaker, as suggested by the damping theory of Heitler, and by other authors, then most of the penetrating particles at sea-level must be π-mesons and not μ-mesons at $E > 300$ BeV. We would then need to know the variation of the nuclear absorption cross-section with energy in order to be able to calculate the depth curve.

Attempts have been made to introduce the influence of π-meson absorption into the explanation of the depth curve, but as yet there is no generally agreed conclusion. The following simple treatment due to GREISEN [1948] brings out the main points. Assume that the π-mesons experience strong nuclear absorption with an absorption length of the order 100 gm.cm^{-2}, equal to that of the primary radiation. The differential equation for the number of π-mesons with given energy is then:

$$dn_\pi/dt = A\exp(-t) - n(1 + B/t), \tag{14}$$

where t is measured in units of 100 gm.cm^{-2}. The first term on the right gives the number produced in dt, and the second the number lost by absorption and decay. $B = 8.10^5\,(m_\pi c/E\tau)$, with m_π, τ the rest mass and lifetime respectively of π-mesons. Thus:

$$B = 1.6 \times 10^{11} E^{-1}.$$

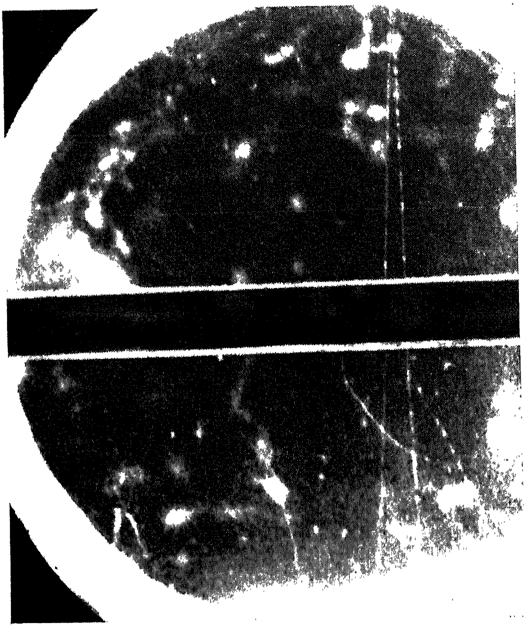

Example of pair of particles each penetrating 2 cm. Pb observed by NASH [1951] at 23 m. depth. The particles diverge from a further Pb plate above the cloud chamber.

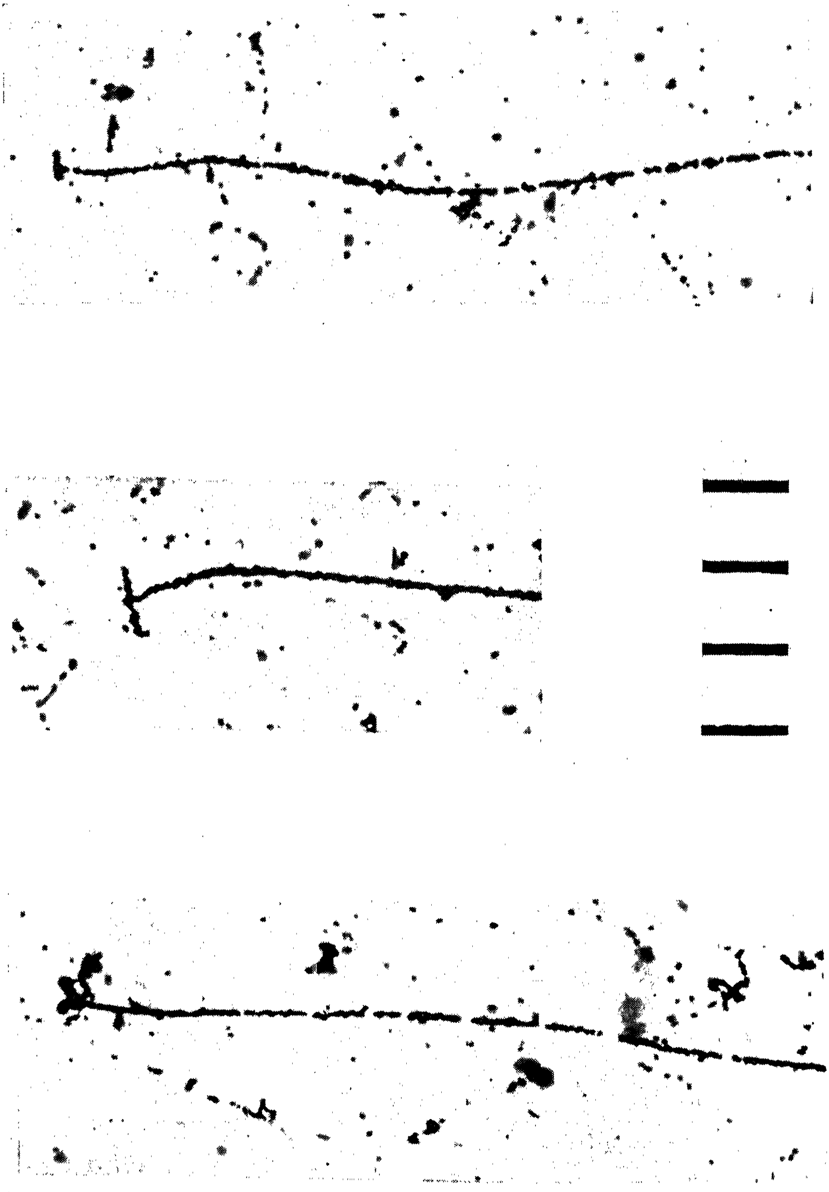

Capture of Negative μ-Meson.

Three examples of mesons stopping in the emulsion and causing small stars of two tracks.

A will be taken proportional to E. The solution of (14) is

$$n_\pi = (At/(B+1)) \exp(-t), \tag{15}$$

and the number of μ-mesons at high energy is

$$n_\mu = \int_0^{10} (Bn_\pi/t)\, dt = BA/(B+1). \tag{16}$$

Taking $\gamma = 3$, the differential spectra at sea-level, $t = 10$, are therefore:

$$\left\{\begin{aligned} n_\pi &= 4.5 \times 10^{-4} E^{-3}\left(1 + \frac{1{\cdot}6 \times 10^{11}}{E}\right)^{-1} \\ n_\mu &= \phantom{4.5 \times 10^{-4}} E^{-3}\left(1 + \frac{E}{1{\cdot}6 \times 10^{11}}\right)^{-1}. \end{aligned}\right. \tag{17}$$

At E about 160 BeV, the power law exponent in the μ-meson spectrum decreases by unity from -3 to -4. The ratio of π-mesons to μ-mesons is $3E/10^{15}$, becoming equal to unity, therefore, at $E = 3.10^{14}$ eV. Assuming only ionization loss of the μ-mesons, GREISEN [1948] suggested that the increasing exponent at great depths could be adequately explained by the increasing steepness of the μ-meson spectrum, equation (17). GARELLI and WATAGHIN [1950] concluded that taking the increased losses at high energy into account together with the effect of π-meson absorption with the geometrical nuclear cross-section gave too rapid a decrease at great depths. They suggested that this provided some evidence showing that the cross-section for the absorption of π-mesons decreased strongly at high energies. This conclusion was based on a π-meson spectrum derived from the Heisenberg-Wataghin model of multiple meson production. It is not yet established that this model is the correct one or whether, by choosing some other spectrum at production, the calculated curve assuming nuclear geometric cross-section and including increased losses at high energy can be fitted to the observed points. Including the μ-meson losses due to bremsstrahlung and pair production, and taking the exponent equal to 2.8, Hayakawa and Tomonaga concluded that the experimental points lay between the limiting curves for the π-meson cross-sections zero and nuclear geometric. It is clear that for resolving this situation, energy spectrum measurements up to say 500 BeV and intensity measurements down to 10 km. would be of the greatest significance. Experiments on both these points are in hand, and we must leave a final decision between the alternatives discussed here to the future.

4. TIME VARIATIONS; TEMPERATURE COEFFICIENTS

In this section the results obtained underground will be discussed. The reader is referred to the following article by Elliot for details concerning the experimental procedure and methods of analysis. Only two systematic studies of the fluctuations below ground have been carried out, by RAU [1939] and by MACANUFF [1951].

4.1 The observations of Rau

Rau used two ionization chambers submerged to a depth of 40 metres in Lake Constance at altitude 395 m. above sea-level. The apparatus was suspended clear of the lake bed by means of a cable slung between local rocks. The depth of immersion could therefore vary only with changes in the surface water level. The water level was found to change with season by as much as 2 metres, being highest in June 1937. During individual runs lasting about 5 days, the change in level was rarely more than 10 cm., corresponding to an intensity change of 0.5 %, and correction of the hourly records for fluctuations in water level was not considered necessary. When differences greater than 10 cm. were found, appropriate corrections were applied only when comparisons between individual runs were made.

Aperiodic variations

An internal temperature effect in the two chambers was not to be expected, and no daily temperature wave could be detected in a thermograph enclosed with the apparatus. Rau concluded that no effect due to external temperature was to be expected, since it would be caused by structural changes of the lower atmosphere, having negligible effect on the radiation under so great a thickness of absorber. Rau found also that atmospheric pressure had no appreciable influence.

In view of the apparent absence of temperature and pressure variations, the measurements were employed directly in subsequent analysis, without correction.

Periodic variations

(i) The annual variation.

The monthly mean values of intensity were reduced to a standard depth of water above the apparatus and plotted as shown in Fig. 10. A pronounced maximum appears in June, the intensity being then about 4 % higher than in winter.

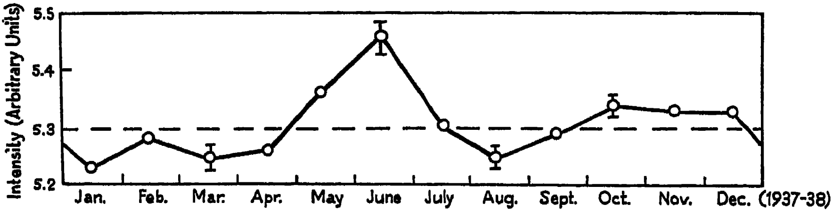

Fig. 10 – Annual variation at 40 m. according to Rau. The deviations indicated are probable errors.

(ii) The daily variation.

The variation of the mean hourly readings (solar time) during the period January 1937—March 1938 is shown in Fig. 11(a). The curve has two maxima, at 9h and 22h Middle European Time, of amplitude 0.2 ± 0.08 %.

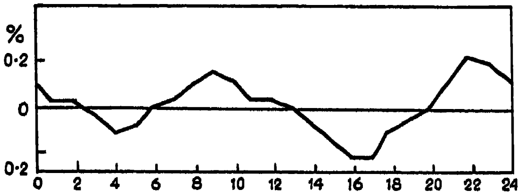

Fig. 11a – The diurnal variation as a function of local time, at 40 m., according to Rau.

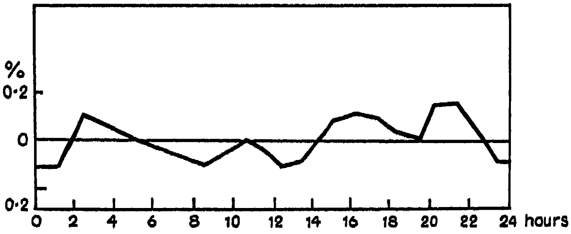

Fig. 11b – The diurnal variation as a function of sidereal time, at 40 m., according to Rau.

The variation with sidereal time is shown in Fig. 11(b). Harmonic analysis of this curve shows that the evidence for a sidereal variation is weak, the amplitude being equal to the statistical error: 0.07 ± 0.07 %.

4. 2 The observations of MacAnuff

Working in the underground laboratory at Holborn Station, London, at a depth of 60 m., MacAnuff [1951] has recorded the coincidence rate in 2 counter telescopes. Each telescope consisted of 3 banks of 15 Geiger counters of dimensions 3.4 × 60 cm. The counting rate of each telescope was ∼ 7000 h^{-1} at this depth, and the number of coincidences was recorded photographically at hourly intervals.

Aperiodic variations

Contrary to Rau, MacAnuff has observed an appreciable barometric effect at 60 m. depth. In Fig. 12 is plotted a typical series of observations showing the variation in number of coincidences per day for the telescopes over a period of 34 days (upper curve). The barometric pressure over this same period is also shown. From this figure, it will be seen that there is obviously a strong correlation

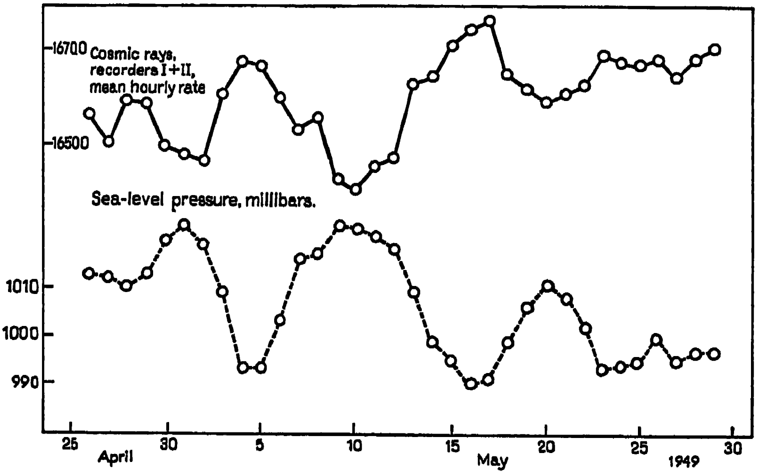

Fig. 12 - Daily mean values of barometric pressure and cosmic ray intensity at 60 m. depth, April & May, 1949. The marked correlation is clearly visible.

with atmospheric pressure. The results for the pressure coefficient at 60 m. depth are:

Barometric coefficient = -0.47 % (cm. Hg)$^{-1}$.
Correlation coefficient = -0.81.

The barometer coefficient is consistent with that expected from the intensity depth curve. At this depth the exponent is approximately 2, and hence the theoretical value is -0.45 % (cm.Hg)$^{-1}$.

Working with similar apparatus at sea-level, **Duperier** [1949] has reported a correlation of the intensity with height of the 100 mb. pressure level, the coefficient being -3.8 % (km.)$^{-1}$. This is explicable in terms of μ-meson decay. At 60 m. depth MacAnuff has found negligible correlation with the height of the 100 mb. or any other pressure level. This is not surprising in view of the increased mean energy, and consequent increased lifetime, of the underground μ-mesons.

MacAnuff has also investigated the correlation with upper air temperatures reported by **Duperier** [1949]. He finds a coefficient of $+0.05$ % per °C. for temperatures in the 100—200 mb layer. This may be compared with Duperier's value at sea-level of $+0.11$ % per °C. **Duperier's** [1951] interpretation of this positive temperature coefficient is in terms of the competition between nuclear absorption and decay of π-mesons, although there is a discrepancy of about 5 to 1 between the calculated and observed values. MacAnuff's underground value is not inconsistent with Duperier's theory.

Forro [1947] has reported that the temperature coefficient at 1000 m. depth is $+0.74 \pm 0.13$ % per °C. Ground level temperatures were employed. In view of the fact that an appreciable number of the counter coincidences appear to have been of local radioactive origin, it is not clear that this coefficient is necessarily a cosmic ray effect. **Hayakawa** *et al.* [1950] have shown that assuming the geometric cross-section for the absorption of π-mesons of all energies, the calculated temperature coefficient at this depth is $+0.16$ % per °C.

Influence of magnetic storms and solar activity

No fluctuations attributable to magnetic storms have been observed below ground. In Fig. 13, the records for two periods

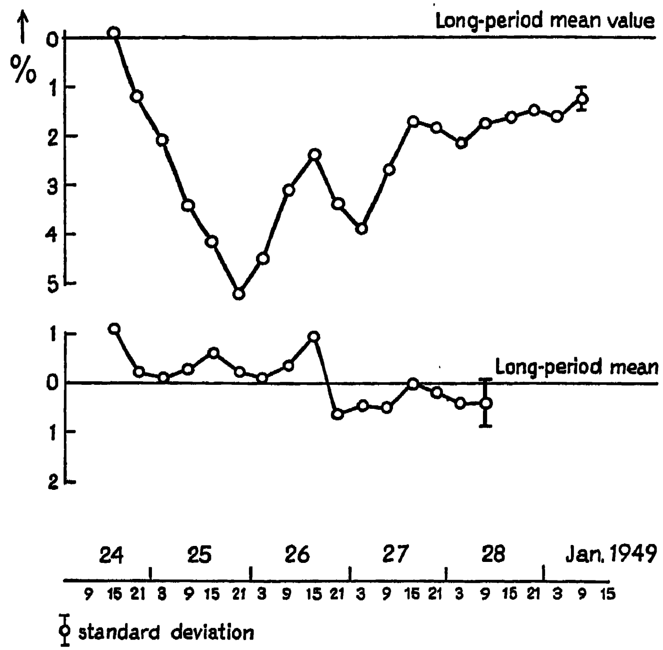

Fig. 13a – Cosmic ray observations with Geiger counter telescopes during period of magnetic disturbance: upper curve, Manchester, at earth's surface, lower curve London, 60 m. underground, Holborn Station.

Standard deviation: $\overset{\top}{\underset{\bot}{\circ}}$

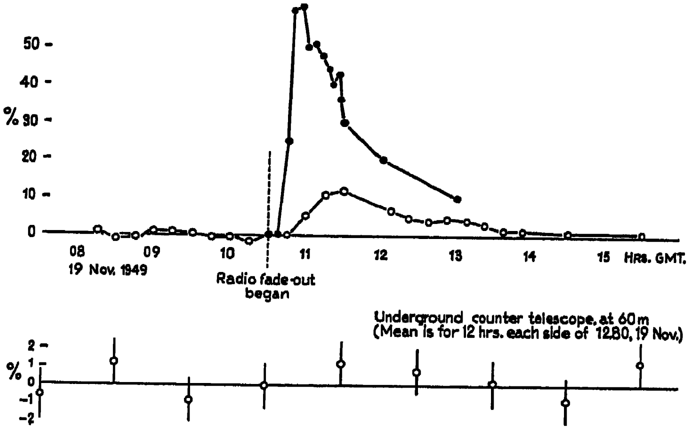

Fig. 13b – Cosmic ray increase, 19th. Nov., 1949.

Above: • Ottawa [Rose, 1950], ∘ Manchester [Dolbear, 1950], both at sea-level. Below: Results 60 m. underground.

are shown when observers at the surface reported large fluctuations. Fig. 13(a) compares readings underground and at Manchester during a magnetic storm on Jan. 25th 1949, and Fig. 13(b), during the solar flare of 19th Nov. 1949. From the large latitude effect of these disturbances it is known that the fluctuations are confined to the low energy primary particles. The absence of any fluctuations below ground confirms this conclusion.

Periodic Variations.

(i) Solar time.

The bi-hourly readings, averaged over a period of one year are shown in Fig. 14(a). There appears to be a small diurnal variation below ground of amplitude about 0.05 % with a maximum at 1600 hrs local time and a minimum at 2400 hrs. The underground results may be compared with the results of Dolbear and Elliot at sea-level, given in Fig. 7 in the next chapter (p. 474). The maxima and minima are seen to occur at the same times, and the amplitude is 0.2 %, 4 times greater than observed below ground. The diurnal curve is discussed by Elliot and in view of the similarity of the curves, the discussion need not be repeated here.

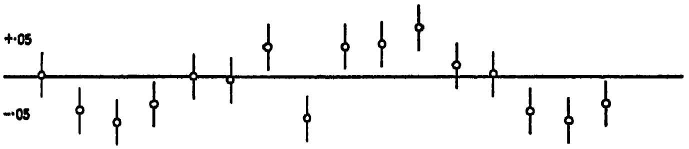

(a) Solar-time variation - Sum of both channels

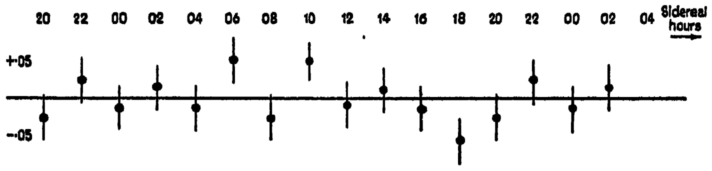

(b) Sidereal variation – Sum of both channels

Fig. 14 – The diurnal variation at 60 m. depth for the sidereal and the solar day.

The statistical accuracy of the underground results is not yet sufficiently great to say very much about the semi-diurnal variation, except that it appears that the amplitude obtained in the present investigation is considerably smaller than that reported by Rau.

(ii) Sidereal time.

The results in Fig. 14(a) have been re-plotted as a function of sidereal time in Fig. 14(b). The points appear to be distributed at random, and it does not appear that the sidereal variation below ground can be as great as 0.02 %.

4. 3 Comparison of observations of Rau and MacAnuff

Apart from their agreement that there is no significant evidence for a sidereal variation, the results of Rau and MacAnuff are not in good accord. Rau reports the absence of aperiodic variations while MacAnuff's results show a marked correlation with the barometer pressure and upper air temperature. Rau reports a large semi-diurnal variation where MacAnuff finds none, while MacAnuff finds an appreciable diurnal variation in contrast to Rau.

MacAnuff's observations were taken under more steady conditions than were Rau's. The counter telescopes were undisturbed for long periods (more than a year), and there were no uncertainties introduced by small changes in the environment. It is possible that some of the discrepancies may be attributed to the use of a counter telescope in one case and ion chambers in the other.

5. STARS AND SLOW MESONS IN EMULSIONS

Nuclear emulsions have been exposed below ground by George and Evans [1950, '51] at various Underground Stations in London at depths down to 60 m., and in a coalmine at depth 600 m. In order to avoid pre- or post-exposure, the plates were prepared, stored and processed below ground, only being brought up to the surface for examination. Up to the present, some 500 cm^3 of emulsion have been searched.

5. 1 Observations of nuclear disintegrations

200 nuclear disintegrations giving rise to "stars" with three or more branches have been observed, of which 18 were in C 2 and the remainder in G 5 emulsions. The stars in G 5 emulsion were classified according to type in the manner described by Brown *et al.* [1949].

The frequency of stars versus depth

The frequency of stars at various depths is given in Table 7.

At the greatest depth, stars are extremely rare and only two have been observed. One of these was a characteristic star produced by negative π-meson capture, showing the emission of three energetic heavy particles, and the other was a small star of type On 3. The results at this depth can only be taken as indicating order of magnitude. At the other depths the σ-meson stars are not included.

TABLE 7

Depth below ground (metres water equivalent)	Stars Observed	Frequency $cm^{-3}day^{-1}$
0	383	1.46 ± 0.07
8	53	0.029 ± 0.004
20	67	0.0066 ± 0.0008
34	36	0.0047 ± 0.0008
60	42	0.0040 ± 0.0006
600	2	$\sim 10^{-4}$

The stars at ground level and above are known to vary exponentially with depth, with an absorption length of approximately 150 $gm.cm^{-2}$. It is generally accepted that the particles producing them are nucleons. It is clear from Table 7 however, that the nucleon component cannot be responsible for the underground stars. This component would give, for example, a star-frequency of 10^{-170} cm^{-3} day^{-1} at 600 m! The frequency of stars below ground varies in the same way as the fast μ-mesons of the hard component (Figure 4), and from this and other arguments George and Evans concluded that the stars were produced by fast μ-mesons.

Classification of stars

At a depth of 8 metres, there is still an appreciable contribution from the nucleon component. The stars observed in G 5 plates at 20 m. and deeper have been grouped together, and Table 8 shows their distribution in star types. This table therefore contains only those stars which are thought to be produced either directly or indirectly by μ-mesons.

The largest star observed had 18 heavy tracks and a "shower" of 8 tracks at minimum ionization. The frequency-distribution of heavy tracks, given in the bottom row of Table 8, is very similar to that observed at sea-level and mountain altitudes.

TABLE 8

Classification of underground stars

Primary (n or p)	Shower Particles	Heavy particles 3	4	5	6	7	8	9	10	11	12	> 12	Total
n	0	16	17	9	5	3	1	1	—	—	1	—	53
p	0	2	6	—	1	—	1	1	—	—	—	13, 18, 20	14
n	1	—	1	1	—	—	—	—	—	—	—	—	2
p	1	7	15	9	2	3	1	1	3	—	—	—	41
p	2	2	—	—	—	1	—	1	—	—	—	—	4
p	3	—	1	1	—	—	—	2	—	—	—	13, 13	6
p	4	—	—	—	—	—	—	—	—	—	1	—	1
p	5	1	—	—	—	1	—	—	—	—	—	14, 15	4
p	6	—	—	—	—	—	1	—	—	—	—	—	1
p	7	—	—	—	—	—	—	—	—	—	—	— —	0
p	8	—	—	—	—	—	—	—	—	—	—	18	1
Total		28	40	20	8	8	4	6	3	0	2	8	127

Stars of type 1*p and "showers"*

Photomicrographs illustrating typical examples of events in this class are shown in Plates III and IV. The single charged particles at minimum ionization in the upper hemisphere visible in both of these pictures are assumed to cause the disintegrations, and since they occur at large depths it is believed that they can only be μ-mesons.

The. 1p stars are then simply regarded as events in which a fast μ-meson is scattered by a nucleon which in recoiling causes the parent nucleus to evaporate. It is possible to obtain a value for the energy of the incident μ-meson as follows. It is assumed that the energy of the recoiling nucleon is all used in forming the star, and its value is estimated from the number of heavy branches, N_h, using the result of Brown *et al.* [1949].

$$E(\text{MeV}) = 37\, N_h + 4\, N_h^2 \tag{18}$$

The angle of scatter may be measured, and this combined with a knowledge of the energy released (18) gives the energy of the incident particle from the conservation of energy and momentum. A series of curves showing the relation between energy and deviation of fast μ-mesons has been plotted for various values of

N_h in Fig. 15. Using these curves, the energies of some 30 μ-mesons causing stars at a depth of 20 m. have been determined, and the results are given in the histogram in Fig. 16. The expected energy distribution, obtained by a slight modification of the μ-meson spectrum described below, is also drawn, and the experimental observations are seen to be consistent with this curve.

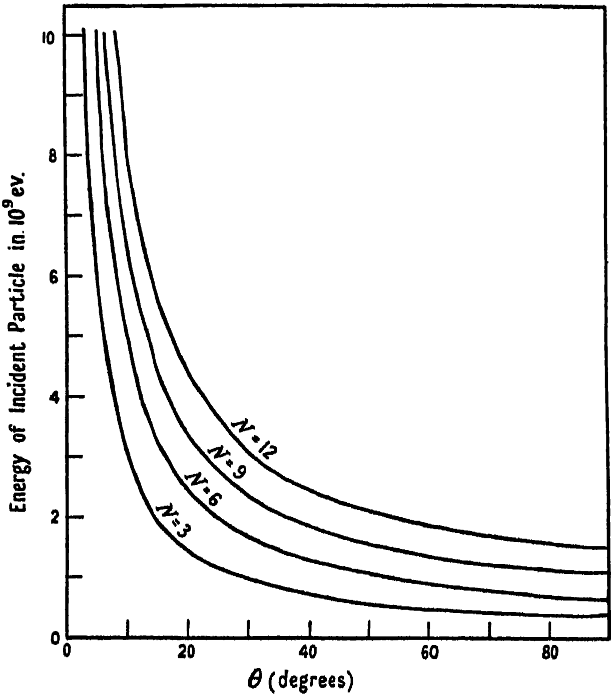

Fig. 15 – Relation between the angle of deflection and energy of the incident particle, for stars produced by the elastic scatter of μ-mesons. Plotted for various values of N, the number of tracks per star.

The nuclear disintegrations associated with "showers" are very similar to those observed at mountain and balloon altitudes. It is known that most of the shower particles in these latter events are π-mesons (Fowler [1950]) and George and Evans assumed that the shower particles observed below ground were also mainly π-mesons. It has now been possible to confirm this in two examples in which the shower particle track was long enough to be the subject of reliable scattering measurements. In both of these cases the particle was identified as a meson, probably a π-meson. Since only seventeen showers have been observed, it is hardly possible to give significant values of their variation with depth, but it can be said that the frequency of showers is approximately the same at 20, 34 and 60 m. This makes it very probable that the showers are also produced by μ-mesons. It is of interest to note that all 17 showers in Table 8 were produced by a charged incident particle. From the observed frequencies of 1p stars and showers at various depths, and the μ-meson flux given in Fig. 4, it is possible to obtain the cross-section for star production by fast μ-mesons as a function of depth. The results are given in the second column of Table 9.

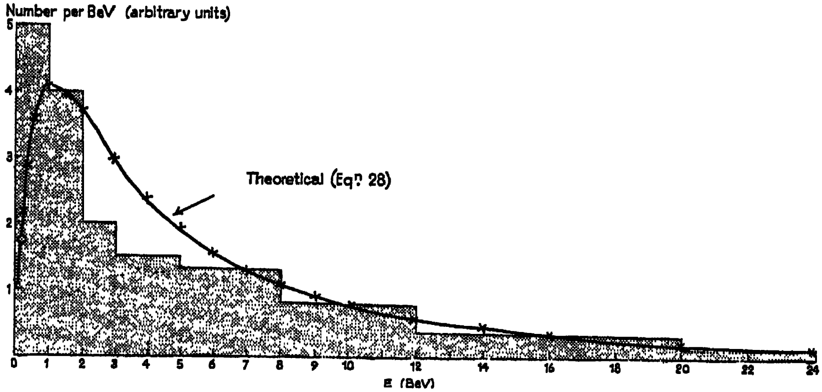

Fig. 16 – Differential spectrum of μ-mesons giving rise to stars of type 1_p at 20 m. below ground.

TABLE 9

Depth (meters water)	Observed cross-section 10^{-30}cm²/nucleon	Calculated cross-section (equ. 27) 10^{-30}cm²/nucleon	Ratio
20	4.2 ± 0.7	2.9	1.45 ± .24
34	4.5 ± 1.2	3.5	1.3 ± .33
60	5.3 ± 1.7	4.1	1.3 ± .4

These values may be interpreted as follows. The cross-section for the production of stars by photons has been measured at Berkeley by MILLER [1951] to be of the order

$$\sigma_{h\nu} = 10^{-28} \text{ cm}^2 \text{ per nucleon.} \tag{20}$$

Thus, following the semi-classical procedure of Williams and Weiszäcker, the cross-section for the production of a star with energy between E' and $E' + dE'$ by a fast μ-meson of energy E is:

$$\sigma(E, E')dE' = (2a\sigma_{h\nu}/\pi)\,(dE'/E')\ln(E/E'), \tag{21}$$

and the total cross-section for the production of stars of energy greater than ε is:

$$\sigma(E, \varepsilon) = \int_{\varepsilon}^{E} \sigma(E, E')\,dE' = (a\sigma_{h\nu}/\pi)\,[\ln(E/\varepsilon)]^2. \tag{21a}$$

Equation (21) is that already used at (7). For the moment, $\sigma_{h\nu}$ is assumed constant. At the depths in question the main energy loss of μ-mesons is in ionization, and the differential energy spectrum may be taken as

$$N(E)\,dE = \frac{2E_0^2}{(E+E_0)^3}\,dE, \tag{22}$$

where E_0 is the ionization loss down to the depth in question. For comparison with observation, the cross-section (21) must be averaged over the μ-meson spectrum, giving:

$$\left\{\begin{aligned} &\bar{\sigma}(E')\,dE' = \int_{E'}^{\infty} N(E)\,\sigma(E, E')\,dE'\,dE = \\ &= (2\,a\sigma_{h\nu}/\pi)\,(dE'/E')\left[\ln\frac{E'+E_0}{E'} - \frac{E_0}{E'+E_0}\right]. \end{aligned}\right. \tag{23}$$

This expression should give the energy distribution of the underground stars, and we will return to this point. Finally, integrating (23) over E', from a lower limit ε of 150 MeV, corresponding to a star of three prongs, we obtain the total theoretical cross-section for star production by μ-mesons underground:

$$\sigma_{\text{theor}} = \int_{\varepsilon}^{\infty} \bar{\sigma}(E')\,dE' = (2\,a\sigma_{h\nu}/\pi)\,F(E_0), \tag{24}$$

where

$$F(E_0) = \int_{\varepsilon}^{\infty} \left[\ln\frac{E'+E_0}{E'} - \frac{E_0}{E'+E_0}\right] dE'/E'. \tag{25}$$

Over a wide range of values of E_0, a close approximation to $F(E_0)$ is

$$F(E_0) = 0.45\,[\ln(E_0/\varepsilon)]^2, \tag{26}$$

and inserting this value, we obtain from equation (24)

$$\sigma_{\text{theor}} = 0.9\,(a\sigma_{h\nu}/\pi)\,[\ln\,(E_0/\varepsilon)]^2. \tag{27}$$

Thus the cross-section should increase slowly with depth. Values calculated from (27), using (20), are given in the third column of Table 9. These are quite close to the observed values, and would be still closer if the photonuclear cross-section had been taken as 1.3×10^{-28} instead of 10^{-28} cm^2. From the above considerations, we may obtain the following theoretical results:

(i) *Energy spectrum of interacting μ-mesons*

This is given by multiplying equations (22) and (21a):

$$N'(E)\,dE = \text{const} \times \frac{[\ln\,(E/\varepsilon)]^2}{(E+E_0)^3}. \tag{28}$$

This is the curve drawn in Fig. 16 showing the energy spectrum of the particles causing 1p stars. It is seen to fit reasonably well.

(ii) *Frequency-depth curve for stars*

Down to about 1000 m., the variation with depth should be

$$S(x) = A \cdot I(x)[\ln\,(ax/\varepsilon)]^2, \tag{29}$$

where $I(x)$ is the meson intensity in Fig. 4. At larger depths, the modification of the μ-meson spectrum would have to be taken into account. In Fig. 17, the observed frequencies are compared with the curve given by equation (29). The agreement is seen to be quite reasonable.

(iii) *Energy spectrum of stars at a fixed depth*

This is given by equation (23). The energy of each of the 1p stars with showers in Table 8 has been calculated as follows. The energy of the heavy particles has been determined from equation (18). To this we have added $(n - 1)$ 960 MeV where n is the number of shower particles. One shower particle has been subtracted as it is assumed that the incident μ-meson continues after producing the star. 960 MeV is the average energy of the shower particles (CAMERINI *et al.* [1950]). The energy distribution of the stars obtained in this way is given in Fig. 18, together with the distribution calculated from equation (23). The agreement is reasonable,

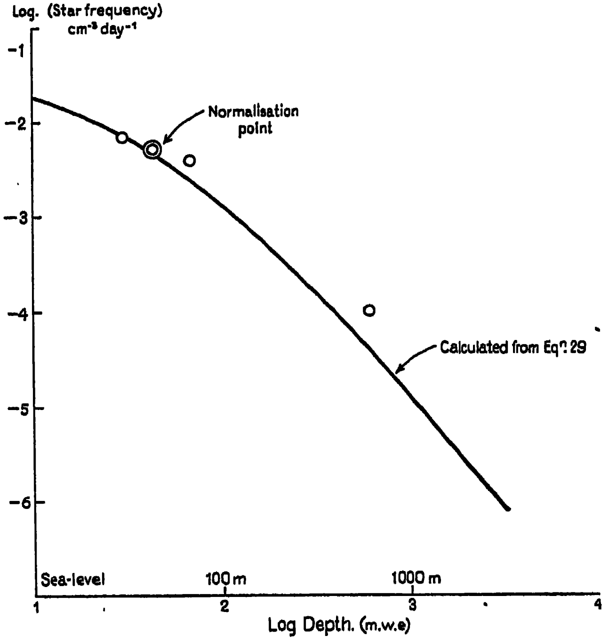

Fig. 17 – Frequency of stars at various depths.

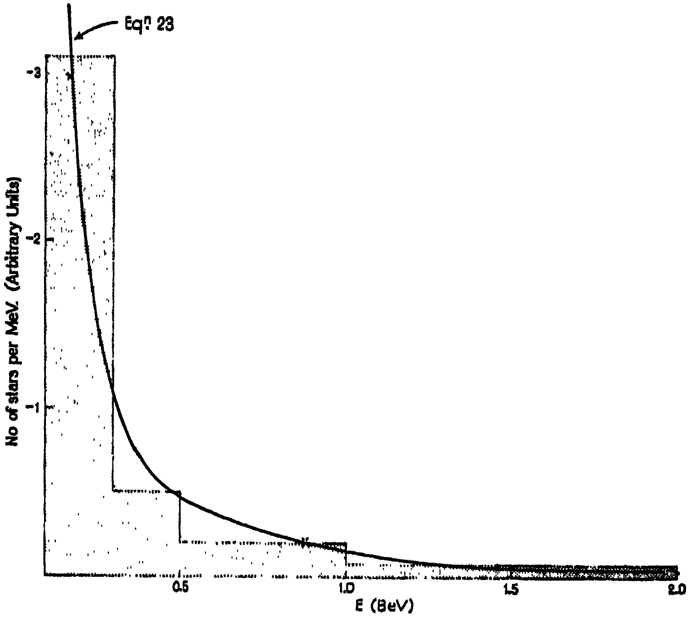

Fig. 18 – Energy distribution of stars type 1p, and "showers".

and the agreement is maintained up to star energies of order 10 BeV. This suggests that the photo-nuclear cross-section remains approximately constant in the energy range 0.1 to 10 BeV. If it changed by an order of magnitude at 10 BeV, the difference would have been detected in the star-energy distribution.

Stars of type On and Op

These may be interpreted as secondary stars produced by neutrons and π-mesons respectively emitted by the stars discussed in the previous section. The required number of energetic neutrons per star is reasonable. Camerini *et al.* [1950] have shown that most of the secondary stars produced by shower particles are of the Op type, and the number of Op stars observed below ground is consistent with the number expected to arise from the shower particles produced there.

5.2 Observations of slow mesons

Mesons of the familiar phenomenological types, π, μ and σ have been observed to come to rest in the emulsions exposed below ground. The number of μ-mesons coming to rest agrees closely with the number calculated by differentiation of the depth-

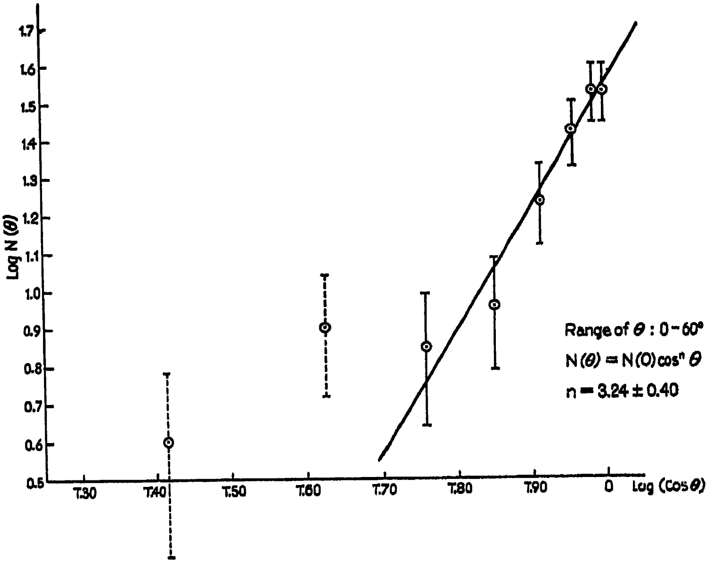

Fig. 19a – Zenith angle dependence of slow cosmic ray μ-mesons at sea-level.

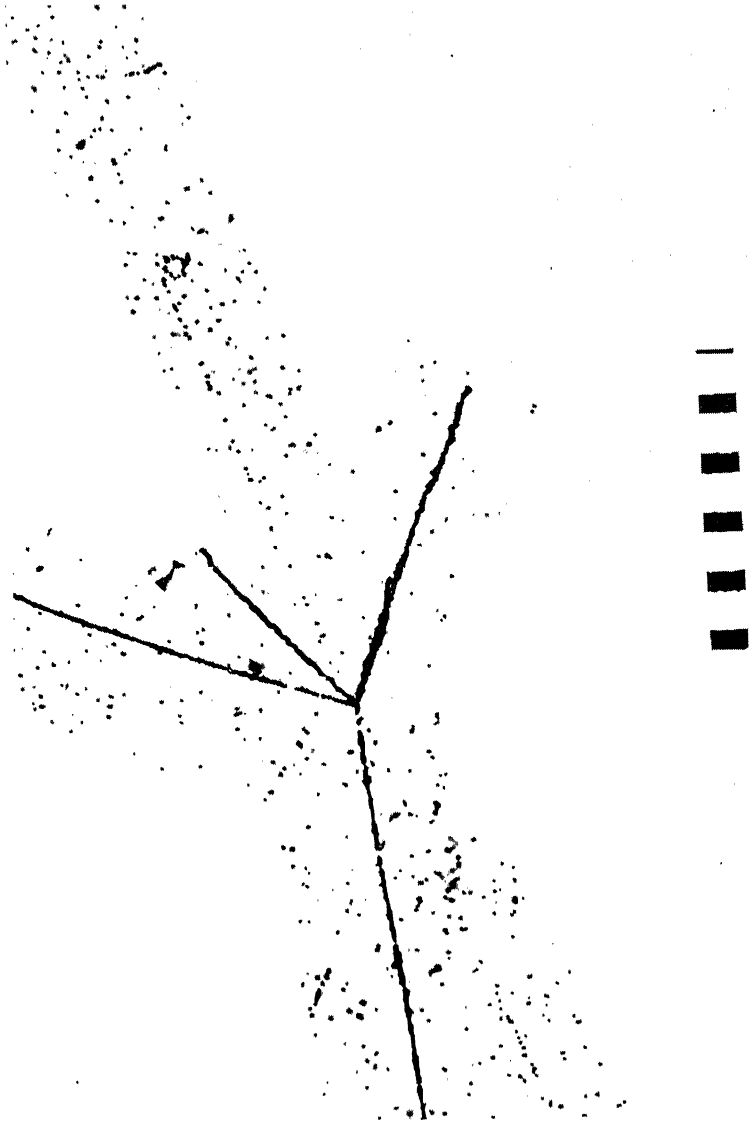

A disintegration produced by a fast charged particle at a depth of 60 m. water. We attribute this type of star to nuclear excitation produced by a fast μ-meson. The electromagnetic interaction between the charge of the μ-meson and neutrons and protons is probably sufficient to account for the observed frequency. In this photograph and also in Plate II the scale shows steps of 10 microns.

Observer: E. P. George.

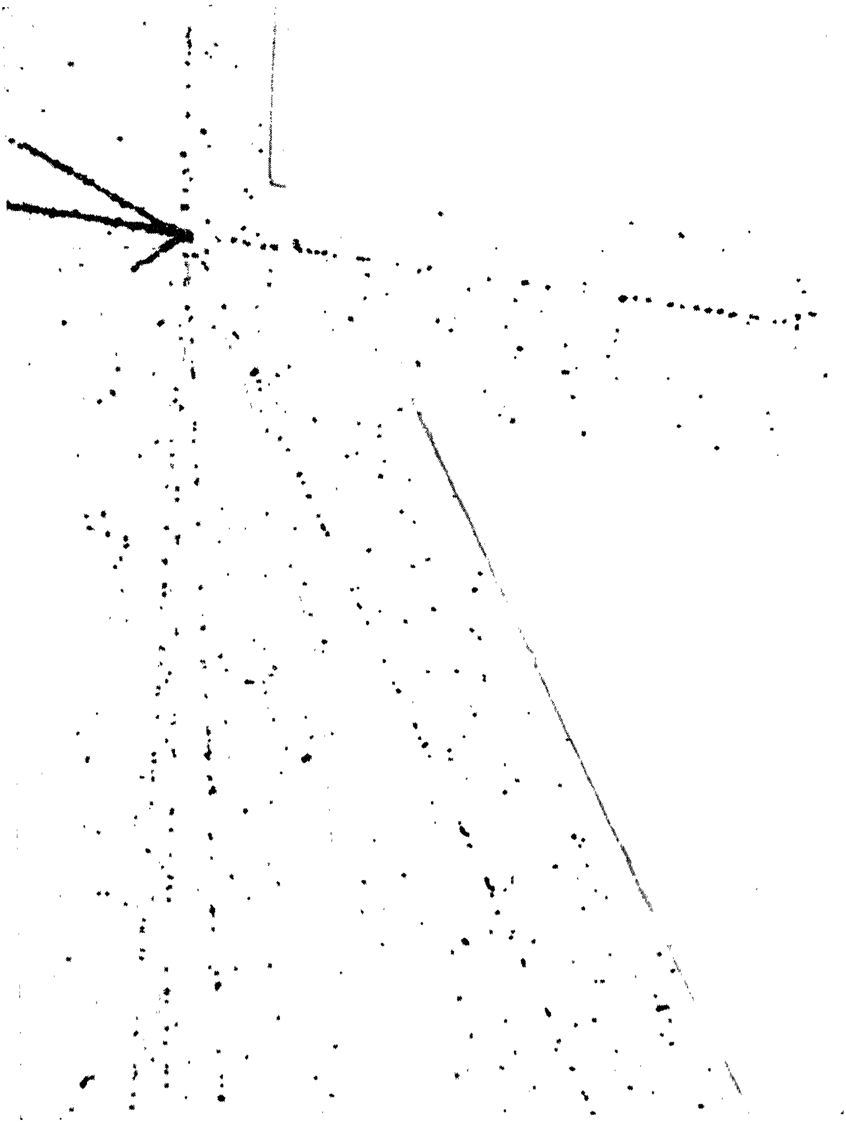

A disintegration produced by a fast charged particle at a depth of 34 m water, and accompanied by a shower of 5 fast particles.

Observer: Mrs. M. H. George.

intensity curve, Fig. 4, and this is perhaps the most definite evidence that at depths down to 60 m., the penetrating component may be identified as μ-mesons.

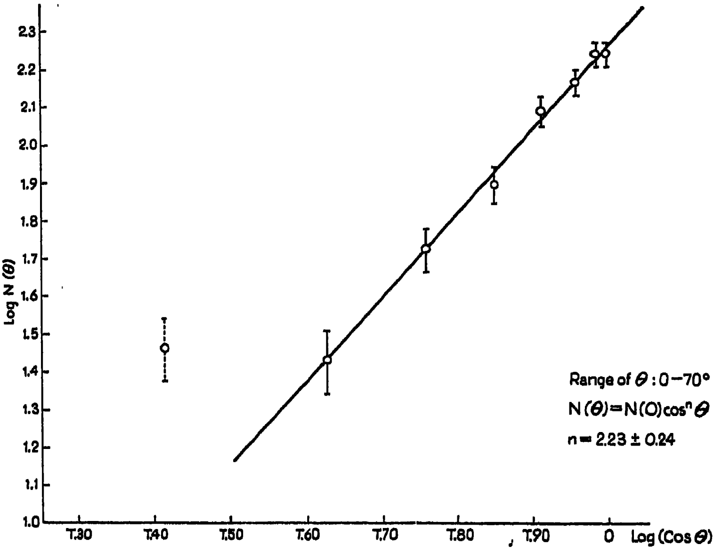

Fig. 19b – Zenith angle dependence of slow cosmic ray μ-mesons underground.

2.6 % of the μ-mesons entered the emulsion from below the horizontal, and these may be explained as arising from the μ-decay of locally produced π-mesons. The angular distribution of the slow μ-mesons has been studied by CREAMER [1951] at sea-level and underground. The distributions are shown in Fig. 19(a) and (b). At angles less than 60°, the distribution may be represented by $\cos^n \theta$, with $n = 3.2 \pm 0.3$ at sea-level and 2.2 ± 0.2 underground. At angles greater than 60° the contribution of the isotropic μ-mesons arising from the decay of π-mesons becomes appreciable. The sea-level exponent agrees well with that found by Kraushaar using a system of Geiger counters.

Ten positive π-mesons showing μ-decay have been observed in the underground emulsions, and this number is consistent with the number expected assuming the "showers" already discussed to be showers of π-mesons, and with the number of upward travelling μ-mesons. Seven of the positive π-mesons entered the emulsion from below the horizontal and three from above.

σ-mesons

Fortysix σ-mesons were observed in the same emulsions, and the frequency distribution of the number of prongs of the σ-stars is given in Table 10. In this table, the expected distribution for an equal number of σ-mesons of the cosmic radiation at mountain and balloon altitudes in the atmosphere is given for comparison (MENON *et al.* [1950]).

TABLE 10

No. of prongs	1	2	3	4	5
Underground σ-mesons .	33	8	5	0	0
σ-mesons at high altitude	15	12	10	6	2

The σ-mesons at high altitude are known to consist almost exclusively of negative π-mesons. From the prong distribution underground, GEORGE and EVANS [1951] concluded that most of the σ-stars below ground were not produced by negative π-mesons but by negative μ-mesons. This conclusion was supported by the following considerations: (*a*) the angular distribution of the σ-mesons was more like that of μ-mesons than that of the positive π-mesons: 40 σ-mesons entered from above and 6 from below the horizontal, (*b*) the frequency of σ-mesons varied with depth below ground in the same way as the μ-mesons. The depth variation is given in Table 11:

TABLE 11

Depth below ground (metres water equivalent)	*Frequency* $cm^{-3}day^{-1}$	
	σ-mesons	μ-mesons
20	0.0032 ± 0.0007	0.098 ± 0.005
34	0.0011 ± 0.0005	0.058 ± 0.004
60	0.0005 ± 0.0003	0.017 ± 0.002

The π-mesons are assumed to come from stars (the shower particles), which, from Table 8 are seen to vary much less rapidly with depth over the range 20 to 60 m. water.

Allowing for a number of negative π-mesons equal in number to the observed number of positive ones, and for the number of negative μ-mesons that come to rest in regions of small atomic number and hence decay into β-particles, the following prong distribution was obtained for the μ-mesons captured:

TABLE 12

No. of prongs	0	1	2	> 2
No. of events (%)	91.4	7.6	1	0

This prong distribution is consistent with that calculated assuming a nuclear excitation of 15 MeV. This figure agrees with that calculated by TIOMNO and WHEELER [1949], assuming a reaction of the form $\mu^- + p \rightarrow n + \mu^\circ$ where μ° is a neutral particle, possibly a neutrino. At this excitation, the nuclear potential barrier favours neutron emission and this would account for the large number of μ-mesons captured without the emission of charged particles. The calculated number of neutrons per μ-capture is 2, and this agrees with the counter observations of SARD *et al.* [1948, 1950] and GROETZINGER and MCCLURE [1948, 1949].

Examples of the 2-pronged stars ascribed to μ-meson capture are shown in Plate II. It is not clear that these events should be classified as stars at all. Assuming them to be examples of nuclear disintegrations, then they are seen to be very different from the 2-pronged disintegrations produced by the capture of negative π-mesons, the emitted charged particles only possessing energies of the order of 1 to 2 MeV.

5. 3 Summary of emulsion work

The picture resulting from the work below ground with emulsions may be summarised as follows. The star frequency shows a rapid decline in the first few metres, characteristic of the nucleon component, thereafter decreases much more slowly like the hard component. The stars at large depths may be explained as arising from nuclear excitation caused by the Coulomb field of the fast μ-mesons as they pass through atomic nuclei. The observed cross-sections are consistent with the photo-nuclear cross-sections measured at Berkeley. Because of the well-known effect of the Lorentz contraction of the Coulomb field with energy, the average μ-meson cross-section increases slowly with depth, causing the star frequency to decrease less slowly than the total intensity. (A similar situation exists for soft cascade showers.) From the frequency of large stars and showers, it appears that the photonuclear cross-section must remain fairly constant up to energies of order 10 BeV. The energy loss arising from the nuclear interaction of fast μ-mesons is small compared with that resulting from direct electromagnetic interactions.

The showers observed below ground have features resembling closely those of similar showers above ground, and are thought to be the production of π-mesons; the frequency of slow π-mesons is also consistent with that calculated assuming that most of the shower particles are π-mesons. Further secondary stars are produced by neutrons and fast π-mesons from the stars directly due to μ-meson collisions, in a manner analogous to the primary and secondary ionization produced by fast charged particles.

At moderate depths, say up to 100 m., most of the stars produced by the capture of slow mesons are caused by negative μ-mesons. The locally produced π-mesons decrease less rapidly than the slow μ-mesons, and at sufficiently great depths, most of the σ-stars will again be produced by π-mesons.

6. SLOW NEUTRONS

Showers of thermal neutrons have been recorded at depths down to 60 m. in Lake Ithaca by COCCONI and COCCONI-TONGIORGI [1951]. The apparatus is sketched in Fig. 20, it consists of a watertight aluminium box containing two banks of six boron trifluoride proportional counters embedded in paraffin wax. Between the counter banks was a lead absorber 45 × 45 × 10 cm. The counters were filled at 1.5 atmospheres, the boron containing 96 % B^{10}.

Events were observed in which m neutrons were recorded within

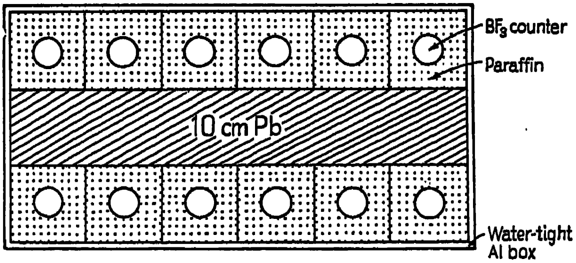

Fig. 20 – Arrangement of BF_3 counters used by Cocconi to study neutron showers.

a short time interval (see COCCONI *et al.* [1950]). Nuclear disintegrations occurring in the immediate vicinity of the counters, resulting in the emission of several neutrons can give rise to the neutron coincidences of the type recorded, and there is no other known process that can do so, hence counter measurements of this type make a powerful addition to the techniques for studying nuclear disintegrations.

Observations were made with and without the lead absorber in place. With the lead removed, the background frequency of occurrence of two or more neutrons was entirely negligible. The results are given as a function of depth in Fig. 21, where $f(m)$ is the frequency of events in which at least m neutrons were recorded, corrected for chance coincidences and background. Below 5 — 10 m. water the contribution to the recorded events due to the nucleon component is negligible, and the absorption curves of the radiation producing the nuclear disintegrations follow the absorption curve of μ-mesons.

Calling ν the number of neutrons produced in each event (m of which are recorded) then the recorded frequency $f(m)$ is related to the true frequency $I(\nu)$ of events with ν neutrons by the relation:

$$f(m) = \sum_{\nu=m}^{\infty} I(\nu)\, P(\nu, m),$$

where $P(\nu, m)$ depends on the efficiency of the counter system for detecting neutrons, determined by separate experiments to be 6.3 %, and a statistical argument based on the characteristics of the recording system, discussed by COCCONI *et al.* [1950]. Assuming that $I(\nu)$ has an exponential form at a given depth, $I(\nu) = Ke^{-a\nu}$, then the value of "a" given by the present data is 0.06. This indicates that the average number of neutrons emitted in the events considered, $\bar{\nu} = 1/a$, is approximately 16, for the disintegrations produced in 10 cm. Pb, and is practically independent of depth. Assuming the events at depth are produced by μ-mesons, the cross-section per nucleon for their production is approximately 10^{-29} cm^2, close to the value deduced from the nuclear emulsion observations.

The average number of prongs of the stars observed in the emulsions was 5, and the number of neutrons per star in lead must be approximately double this value, i.e. $\sim$ 10. In 10 cm. lead it is very possible for secondary stars to be produced by a nucleon cascade process, and the value $\bar{\nu} = 16$ is close to the expected value. The underground results of Cocconi and of George and Evans are thus in good agreement.

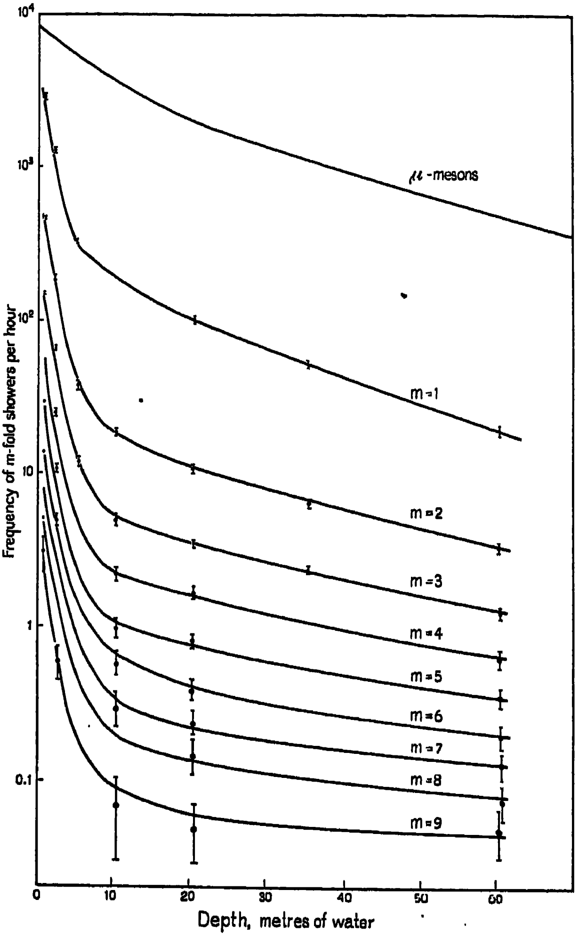

Fig. 21 – Variation of neutron showers with depth, showing the frequency, $f(m)$, of events in which m neutrons were recorded.

7. UNDERGROUND SHOWERS

7.1 Soft showers

The first measurements on showers below ground were made by PICKERING [1935] who observed coincidences between 3 counters arranged at the vertices of a triangle, at depths of 14 and 20 m. The frequency of showers was found to be approximately the same under 0 and 2.2 cm. lead, and Pickering concluded that the thickness of lead giving the maximum frequency of showers decreased rapidly with depth, although later [1937] the results were attributed to the influence of the tunnel roof which was of iron, 20 cm. thick. Underground shower transition curves were studied at 60 and 75 m. by **Follet** and **Crawshaw** [1936] and **Auger** and **Meyer** [1936], who found that there was no pronounced maximum in the curve at 2 cm. lead. This is illustrated in Fig. 22 which shows the transition curve observed by **George** [1941] at 60 m. depth. The absence of the usual maximum at 2 cm. lead will be noted, indicating a large reduction in the relative number of singly incident energetic electrons. The rapid rise up to 2 cm. lead, and subsequent slow decrease of frequency shows that the showers are due to secondaries of some kind with range of the order 2 cm. lead produced by penetrating particles. The observations at this depth may be adequately explained in terms of the knock-on electrons produced by fast μ-mesons.

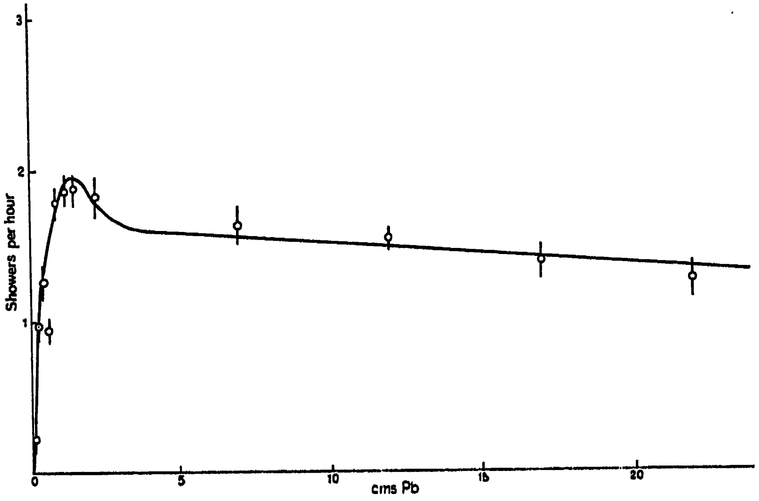

Fig. 22 – Shower transition curve in Pb obtained at 60 m. by George (1941).

The variation of the shower frequency with depth was measured by **Ehmert** [1937] down to 243 m. in Lake Constance, and to 1400 m. in a mine by **Wilson** [1938]. Both authors agree that the showers decrease less rapidly than the vertical intensity with depth. For observations on showers, the vertical telescope used for measuring the total intensity by Wilson was turned through a right angle. In Fig. 23, the ratio of showers to vertical intensity observed by Wilson is shown as a function of depth, normalised to unity at sea-level in order to avoid considerations of counter geometry. The ratio is seen to increase steadily with depth, increasing by a factor of about 4 at 1000 m.

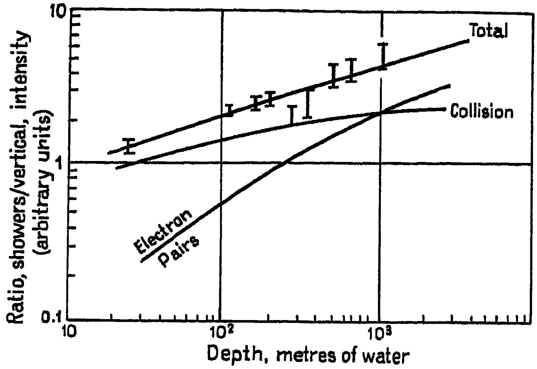

Fig. 23 – Relative shower frequency as a function of depth. The full lines show the contributions of knock-on electron and electron pair production by μ-mesons calculated by Hayakawa and Tomonaga.

The proportion of soft component resulting from knock-on collisions, bremsstrahlung and electron pair production, has been

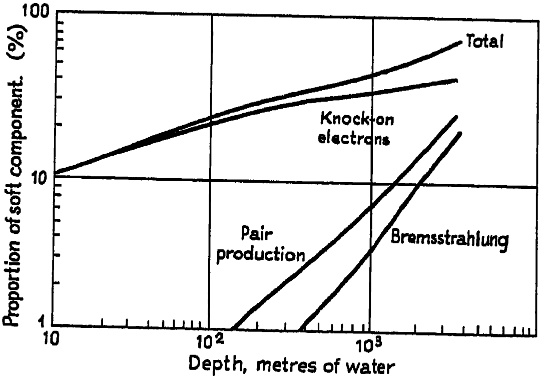

Fig. 24 – The variation with depth of the various contributions to the soft component, calculated by Hayakawa and Tomonaga

considered by HAYAKAWA and TOMONAGA [1949]. Their results are indicated in Fig. 24. As with the energy loss considerations (§ 3), the contributions from pair production and bremsstrahlung become of increasing importance at great depths, bremsstrahlung being less important than pair production.

The theoretical results of HAYAKAWA and TOMONAGA [1949b] for showers of three or more particles are shown as the full lines in Fig. 23. For comparison with Wilson's observations, the theoretical curve has been fitted to the observed points at a depth of 100 m. Pair production becomes an important process at depths of a few hundred metres, and makes the greater contribution below 1000 m. The bremsstrahlung contribution is everywhere much smaller.

7. 2 Penetrating showers

Using a counter system of the Janossy type, GEORGE and JASON [1950] did not observe any penetrating showers at 60 m. in a period of 40 days. A negative result at 23 m. was also reported by HUDSON [1949], who concluded that the coincidences he observed between counters arranged in 3 trays separated by 15 cm. lead could be explained in terms of knock-on electrons.

GEORGE and TRENT [1949, 1951] and MAZE [1950] have reported the existence of penetrating events that cannot be explained by

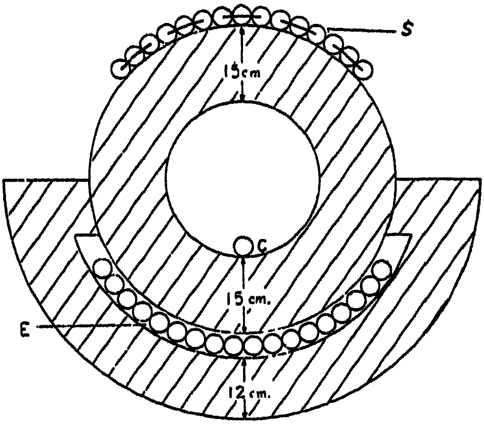

Fig. 25 – Shaded parts represent lead screens. Counter system used at 60 m. by George and Trent to study scattering of μ-mesons, and production of secondary penetrating particles.

the production of secondary electrons. The apparatus used by George and Trent is illustrated in Fig. 25. It is a slightly modified form of that used to study ionization bursts described in § 8. Three-fold coincidences were recorded between any one of the fifteen counters S, counter C and any one of the counters E. Pulses from the counters S and E were fed into a hodoscope unit which indicated the individual counters discharged in bank E and which of the five groups of 3 counters were discharged in S. Events were selected showing two or more counters discharged in E, disregarding those few events in which more than one counter was discharged in S. Some of the records showing two or more adjacent E counters discharged may be explained in terms of secondary electron showers, but multiple events showing a wide separation in the discharged counters in E were interpreted as events of a different nature. In order to reduce the effect of electron secondaries, vertical lead slats 3 mm. thick were introduced between each of the counters in bank E. The results obtained with the lead slats in place are given in Table 13.

TABLE 13

Proportion of multiple events in bank E (%)
No. of intervening undischarged counters in bank E

0	1	2	3	4	5	6
1.51 ± .03	0.16 ± .01	0.065 ± .008	0.026 ± .005	0.022 ± .005	0.032 ± .006	Total 1.81

In the great majority of cases, only 2 counters were discharged in bank E.

Interpreting the events as the production of penetrating secondary particles by the μ-mesons of the penetrating component, the cross-section for the process is found to be 4.10^{-29} cm^2 per nucleon. This is larger than the cross-section for the production of stars, but is similar to that found for the production of penetrating secondary particles by Nash [1951] described in § 9.

The apparatus used by Maze at 30 m. depth is sketched in Fig. 26. At least 5 cm. of lead was between each of the eight counters. All coincidences involving any three or more counters were recorded. Results obtained at sea-level and below ground are given in Table 14.

TABLE 14

No. of counters discharged	Number of events		
	Sea Level 54 hours	Underground 188 hours	Underground 739 hours
3	1277	526	—
4	173	38	163
5	62	2	20
6	24	1	4
7	2	0	0
8	1	0	0

The occurrence underground of combinations of high multiplicity is again in accord with the existence of a penetrating component underground, secondary to the μ-mesons.

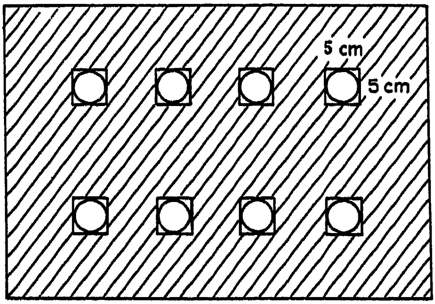

Fig. 26 – Counter arrangement used by Mazo at 30 m. depth.

7. 3 Extensive showers

Extensive showers have been observed at a depth of 60 m. by MacAnuff [1951], who recorded coincidences between three counter banks of area 3000 cm² separated by distances up to 120 metres. In order to reduce accidental coincidences each counter bank consisted of 2 or more trays vertically above each other and in contact, and coincidences between the trays in a given bank were then fed to a further circuit which registered 3-fold coincidences between the banks.

With the banks arranged in a triangle of 6 m. base, observations were made of the effect of covering the banks with 10 cm. lead. The results were

Absorber	3-*fold counts day*$^{-1}$
0	0.67 ± 0.14
10 cm. lead	0.47 ± 0.11

thus indicating that most of the shower particles are penetrating. This may be contrasted to the behaviour of similar apparatus at sea-level, where covering the trays with lead reduces the 3-fold coincidences by a factor of $(50)^{1.5}$ or about 400. The roof of the tunnel was about 1.5 metres above the trays and it was possible that some knock-on electrons could be recorded at this separation, but the results show their contribution must be small. Two of the counter banks were left *in situ*, and the third was moved further away. The banks were unscreened, and the variation of frequency of 3-fold coincidences with distance is given in Table 15.

TABLE 15

Separation of extreme counter banks, m.	6	20	120
3-fold coincidences day^{-1} . . .	0.67 ± 0.14	0.50 ± .08	0.15 ± .05

The events at large separation cannot be explained in terms of the production of secondary particles in the overlying earth. The existence of penetrating particles in the extensive showers at sea-level is well known, where the penetrating particles are thought to consist largely of μ-mesons, and this μ-meson component of the sea-level showers would account for the observations. Since the counter trays were of area 0.3 m^2, the particle density in the recorder showers must be of order 3 m^{-2}. This suggests that with 120 m. separation, the events recorded contained $3\cdot(120)^2$ or about 4.10^4 μ-mesons of mean energy at least 20 BeV.

8. IONIZATION BURSTS

Ionization bursts were first recorded below ground by CHOU [1948] who worked at 60 m. depth, using a small duralumin ion chamber of 12 mm. wall thickness filled with argon to 80 atmospheres. The transition curves obtained in lead and aluminium are shown in Fig. 27. As in the shower transition curve, Fig. 22, the absence of any sharp maximum in the first few cm. of lead will be noted. The integral size-frequency distribution of bursts was found to be of the form $F(N) = AN^{-1.6}$.

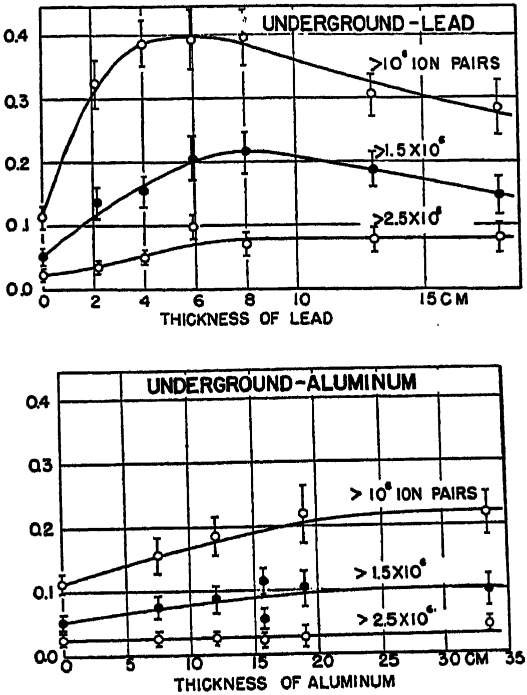

Fig. 27 - Burst transition curves observed at 60 m. by Chou.

Hudson [1949] observed bursts underground at depth 21 m., using 3 cylindrical ion chambers located side by side under 7.5 cm. of lead. Immediately below the chamber were four counters in a triangular arrangement, all of which were required to be discharged. Under this was a second lead shield 15 cm. thick and under this a tray of twelve counters connected to individual neon lamps. The hodoscope was operated whenever a burst of more than 100 electrons occurred in any ion chamber accompanied by a coincidence of the four counters immediately below it.

The results obtained in 788 hours are:

No. of bursts	No. of lower counters discharged				
	0	1	2	3	4
84	55	25	3	1	0

Hudson suggested that the bursts produced by μ-mesons do not contain penetrating particles other than the initiating meson, which may strike the lower tray and give a single count as in 25 cases, or miss the tray as in 55 of the cases. The 4 events with 2 or 3 counters discharged were explained as the effects of knock-on electrons.

From these and other measurements using a system of counters, Hudson concluded that μ-mesons do not with any significant probability interact with nuclei to produce penetrating or "mixed" showers. They produce bursts only by electromagnetic interactions and these bursts do not contain heavy penetrating particles but only electrons and photons.

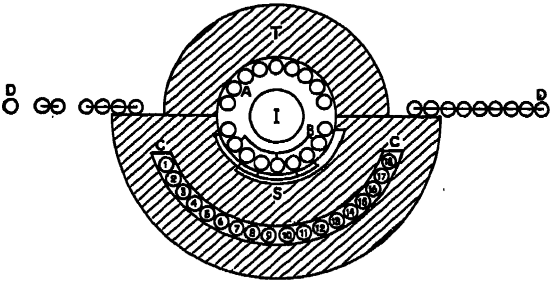

Fig. 28 – Apparatus used at 60 m. by George and Trent to study ionization bursts accompanied by groups of penetrating particles.

Different conclusions were reached by TRENT and GEORGE [1951] working at 60 m. depth. The apparatus used by these authors is shown in Fig. 28. In essentials it is similar to Hudson's arrangement consisting of an ion chamber (the same as that used by Chou) and a bank of nine counters B, connected in 3-fold coincidence. Below B is a bank, C, of eighteen counters, separated by 15 cm. lead. On the occurrence of a burst of 20 or more electrons accompanied by a 3-fold coincidence in B, a hodoscope indicated which counters in banks A and C were discharged. As in Hudson's experiments, the requirement of a 3-fold coincidence in B ensured that bursts due to cascade showers were selected. In a run lasting 1550 hours, with T = 15 cm. lead, 846 bursts were observed, the results relating to the counters discharged in the lower bank were rather similar to Hudson's:

No. of bursts	No. of lower counters discharged					
	0	1	2	3	4	5
846	464	336	33	9	4	0

The distribution in space of the discharged counters is given in Table 16.

TABLE 16

No. of counters discharged in bank C	Events in which all counters were adjacent	Events with 1 intervening undischarged counter	Events with 2 or more intervening	Counters discharged in last column
2	22	8	3	1, 11 7, 17 3, 18
3	2	4	3	14, 16, 18 6, 7, 12 3, 8, 13
4	1	0	3	1, 3, 4, 9 1, 3, 4, 9 7, 12, 14, 18 8, 16, 17, 18

From the frequent occurrence of wide separations between the counters discharged, it was concluded that not all of the events could be attributed to knock-on electrons produced near counter bank C.

Subtracting the events explicable by knock-on electrons, obtained from the measurements described in § 7. 2, it was concluded that 10 % of the bursts observed at 60 m. are associated with penetrating showers containing two or more penetrating particles. Penetrating bursts at mountain altitudes have been explained as being produced by collisions of energetic nucleons resulting in the emission of charged and neutral mesons. The cascade resulting from the photon-decay of the latter accounts for the ionization burst observed. Taking the cross-section for the production of stars associated with "showers" from the nuclear emulsion work described in § 5, and assuming that 1 neutral π-meson is emitted for every 2 shower particles (CARLSON *et al.* [1950]), it is possible to account for the bursts of the mixed shower type observed below ground. George and Trent concluded that only 90 % of the bursts at 60 m. were produced by extra-nuclear Coulomb interactions of μ-mesons, and that the results were consistent with the assumption that about 10 % were due to nuclear excitations produced by μ-mesons resulting in the production of neutral and charged π-mesons.

9. PENETRATING PAIRS OF PARTICLES

In the course of the cloud chamber investigation at 60 m. described in § 2. 1, BRADDICK and HENSBY [1939] obtained five pictures out of a total of 2358 showing two penetrating particles crossing a lead plate in the centre of the chamber without perceptible change in direction and without producing secondaries. In one example the particles also penetrated a further 15 cm. lead above the chamber. They concluded that these photographs showed evidence for the occurrence of pairs of mesons below ground, alternative explanations such as (*a*) random association of independent mesons, (*b*) association of meson and electron or (*c*) association of meson and proton were discussed and shown to be far too improbable to account for the observations. The apparatus was destroyed in 1941. The investigation of these events has been continued by Braddick, Nash and Wolfendale under a thickness of 23 metres of sandstone, near Manchester. Some of the photographs obtained by NASH [1951] were taken with a 4 cm. layer of lead immediately above the chamber. By selecting those events in which the tracks of both penetrating particles diverged from the upper lead absorber, and assuming the events to be produced by the μ-mesons, the cross-section for the production of these events was found to be of the order 5×10^{-29} cm^2 per nucleon .... (30). A typical example is shown in Plate I.

As in the observations of Braddick and Hensby, most of the particles diverged from the overlying rock. Allowing for the apparatus geometry, the number of pairs observed coming from the rock is consistent with that calculated using the cross-section, equation (30).

The following considerations show that these events are different in nature from the "showers" observed in nuclear emulsions. The cross-section per nucleon for the production of "showers" in emulsion is approximately 2×10^{-30} cm^2, which is lower by an order of magnitude than that found from the cloud chamber work. Further, the size frequency distribution of the nuclear emulsion "showers" given in Table 8, shows that 4 out of 17 events consisted of showers of two particles, whereas, in 30 pictures observed by Nash and Braddick and Hensby, the number of related penetrating particles is always two. While particles from some of the showers might have been lost for reasons of geometry, it is difficult to account for all of the discrepancy in this way. This is confirmed by preliminary observations carried out by WOLFENDALE [1951] using a multiplate cloud chamber below ground. Interactions of the penetrating component in the lead plates resulting in the emission of secondary penetrating particles have been observed under conditions of good geometry. Wolfendale finds 15 examples of "pairs" for three of showers containing more than two particles. The cross-section for the production of showers of more than two particles is consistent with that derived from the nuclear emulsion work, here again, however, the number of pairs is greater than the expected value by an order of magnitude.

Thus it seems that μ-mesons produce single secondary penetrating particles by a process that escapes observation in nuclear emulsions. This may indicate that the process is not associated with nuclear disintegrations, for in the searching of the underground emulsions, events consisting entirely of particles at minimum ionization would not have been observed.

ACKNOWLEDGEMENTS

In preparing this report I have drawn freely on many stimulating discussions with my colleagues at Birkbeck College, and take this opportunity to thank them for their part in the clarification of our ideas.

I am very grateful to Dr Cocconi and Dr Bollinger at Ithaca, to Dr Nash and Mr Wolfendale at Manchester for communicating their results prior to publication.

REFERENCES

AUGER, P., and T. MEYER, 1936, C. R. Acad. Sci., Paris, 203.
BARNOTHY, J. and M. FORRO, 1939, Phys. Rev., 55, 870.
BARNOTHY, J. and M. FORRO, 1940, Phys. Rev., 58, 844.
BARNOTHY, J. and M. FORRO, 1948, Phys. Rev., 74, 1300.
BHABHA, H. J., 1935, Proc. Roy. Soc., A152, 559.
BOLLINGER, L. M., 1950, Bull. Am. Phys. Soc., 25, No. 3, 16.
BRADDICK, H. J. J. and G. HENSBY, 1939, Nature, Lond., 144, 1012.
BRADT, H. L., M. F. KAPLON and B. PETERS, 1950, Helv. Phys. Acta, 23, 24.
BROWN, R. H., U. CAMERINI, P. H. FOWLER, H. HEITLER, D. T. KING, and C. F. POWELL, 1949, Phil. Mag., 40, 862.
CAMERINI, U., P. H. FOWLER, W. O. LOCK and H. MUIRHEAD, 1950, Phil. Mag., 41, 413.
CARLSON, A. G., J. E. HOOPER and D. T. KING, 1950, Phil. Mag., 41, 701.
CARO, D. E., J. K. PARRY and H. D. RATHGEBER, 1950, Nature, Lond., 165, 689.
CHOU, C. N., 1948, Phys. Rev., 74, 1659.
CHRISTY, R. F. and S. KUSAKA, 1941, Phys. Rev. 59, 414.
CLAY, J., 1937, Physica, 4, 121.
CLAY, J., 1939a, Rev. Mod. Phys., 11, 134.
CLAY, J. and A. V. GEMERT, 1939b, Physica, 6, 497.
COCCONI, G. and V. COCCONI—TONGIORGI, 1950, Phys. Rev., 79, 768.
COCCONI, G. and V. COCCONI—TONGIORGI, 1951, Phys. Rev., 82, 335.
CREAMER, R., 1951, M. Sc. Thesis, London.
DOLBEAR, D. W. N., 1950, Private communication.
DUPERIER, A., 1949, Proc. Phys. Soc., A62, 684.
DUPERIER, A., 1951, Nature, Lond., 167, 312.
EHMERT, A., 1937, Zeits. f. Physik, 106, 751.
FOLLET, D. H. and J. D. CRAWSHAW, 1936, Proc. Roy. Soc., A155, 546.
FORRO, M., 1947, Phys. Rev., 72, 868.
FOWLER, P. H., 1950, Phil. Mag., 41, 169.
GARELLI, C. and G. WATAGHIN, 1950, Phys. Rev., 79, 718.
GEORGE, E. P., 1941, Ph. D. Thesis, London.
GEORGE, E. P., 1946, Nature, Lond., 167, 296.
GEORGE, E. P. and J. EVANS, 1950, Proc. Phys. Soc., A63, 1248.
GEORGE, E. P. and J. EVANS 1951, Proc. Phys. Soc., A64, 193.
GEORGE, E. P. and A. C. JASON, 1949, Proc. Phys. Soc., A62, 243.
GEORGE, E. P. and A. C. JASON, 1950, Proc. Phys. Soc., A63, 1081.
GEORGE, E. P. and P. T. TRENT, 1949, Nature, Lond., 164, 838.
GEORGE, E. P. and P. T. TRENT, 1951, Proc. Phys., Soc., A64.
GREISEN, K., 1942, Phys. Rev., 61, 212.
GREISEN, K., 1948, Phys. Rev., 73, 521.

Groetzinger, G. and G. W. McClure, 1948, Phys. Rev., 74, 341.
Groetzinger, G. and G. W. McClure, 1949, Phys. Rev., 75, 340.
Halpern, O. and H. Hall, 1948, Phys. Rev., 73, 477.
Hayakawa, S. and S. Tomonaga, 1949a, Progr. Theor. Phys, 4, 287.
Hayakawa, S. and S. Tomonaga, 1949b, Progr. Theor. Phys., 4, 496.
Hayakawa, S., K. Mano and T. Miyazima, 1950, Progr. Theor. Phys., 5, 495.
Hazen, W. E., 1944, Phys. Rev., 65, 259.
Hooper, J. F., D. T. King and A. H. Morrish, 1951, Phil. Mag., 42, 304.
Hudson, D. E., 1949, Proc. Echo Lake Conference.
Kohlhörster, W., 1933, Nature, Lond., 132, 407.
Kohlhörster, W., 1934, Nature, Lond., 133, 419.
Lyons, D., 1941, Phys. Zeits., 42, 166.
MacAnuff, J. W., 1951, Ph. D. Thesis, London.
Maze, R., 1950, C. R., Acad. Sci., Paris, 231, 1295.
Menon, M. G. K., H. Muirhead and O. Rochat, Phil. Mag., 41, 583.
Miesowicz, M., L. Jurkiewicz and J. M. Massalski, 1950, Phys. Rev., 77, 380.
Miller, R. D., 1951, Phys. Rev., 82, 260.
Millikan, R. A., 1925, Nature, Lond., 116, 823.
Millikan, R. A. and G. H. Cameron, 1926, Phys. Rev., 28, 851.
Millikan, R. A. and G. H. Cameron, 1928, Phys. Rev., 31, 163, 921.
Millikan, R. A. and G. H. Cameron, 1931, Phys. Rev., 37, 235.
Miyazaki, Y., 1949, Phys. Rev., 76, 1733.
Mylroi, M. G. and J. G. Wilson, 1951, Proc. Phys. Soc., A64, 404.
Nash, F., 1951, Ph. D. Thesis, Manchester.
Nielsen, W. M. and K. Z. Morgan, 1938, Phys. Rev., 54, 245.
Occhialini, G. P. S., 1949, Nuovo Cim., 6, 413.
Pickering, W. H., 1935, Phys. Rev., 47, 423.
Randall, C. A., N. Sherman and W. E. Hazen, 1950, Phys. Rev., 79, 905.
Randall, C. A. and W. F. Hazen, 1951, Phys. Rev., 81, 144.
Rau, W., 1939, Naturwiss., 27, 803.
Regener, E., 1931, Nature, Lond., 127, 233.
Rose, D. C., 1950, Phys. Rev., 78, 181.
Sard, R. D., W. B. Ittner, A. M. Conforto and M. F. Crouch, 1948, Phys. Rev., 74, 97.
Sard, R. D., W. B. Ittner, A. M. Conforto and M. F. Crouch, 1950, Phys. Rev., 79, 179.
Sneddon, I. N. and B. F. Touschek, 1949, Proc. Roy. Soc., A199, 352.
Tiffany, O. L. and W. E. Hazen, 1950, Phys. Rev., 77, 849.
Tiomno, J. and J. A. Wheeler, 1949, Rev. Mod. Phys., 21, 153.
Trent, P. T., 1951, Ph. D. Thesis, London.
Trent, P. T. and E. P. George, 1951. (in press).
Wilson, V. C., 1938a, Phys. Rev., 53, 337.
Wilson, V. C., 1938b, Phys. Rev., 53, 908.
Wilson, V. C. and D. J. Hughes, 1943, Phys. Rev., 63, 161.
Wolfendale, A., 1951. Private communication.

CHAPTER VIII

TIME VARIATIONS OF COSMIC RAY INTENSITY

BY

H. ELLIOT

The Physical Laboratories, University of Manchester

INTRODUCTION 455
1. VARIATIONS OF ATMOSPHERIC ORIGIN 456
2. THE SOLAR DAILY VARIATION 466
3. THE SIDEREAL DAILY VARIATION 484
4. VARIATIONS ASSOCIATED WITH GEOMAGNETIC AND SOLAR ACTIVITY 492
APPENDIX 511
REFERENCES 512

INTRODUCTION

Systematic measurements of the cosmic ray intensity as a function of time have been made by many workers over the past thirty years and as a result of this work the existence of several distinct variations with time is now well established. These variations may be conveniently divided into two groups, non-periodic and periodic. In the first group are variations due to fluctuations in barometric pressure and atmospheric temperature together with occasional large changes associated with solar flares and magnetic storms. There is also good evidence for the existence of a 27-day recurrence tendency similar to that shown by geomagnetic disturbances.

There are only three periodic variations whose existence can be regarded as certain. The first of these has a period of one year and is almost certainly due to the seasonal variation in atmospheric temperature. The second and third have periods of 24 solar hours and 12 solar hours respectively. In spite of the fact that evidence for a variation with a period of one sidereal day has been sought by many workers since the early days of cosmic ray research, there is still no general agreement as to whether such a variation does or does not exist. A variation with sidereal time is of great importance, since it may be expected to provide a valuable clue to the origin of the radiation.

The investigation of these small periodic variations involves careful observations extended over long periods of time in order that the statistical uncertainties, due to the finite number of particles entering the apparatus in a given time, may be sufficiently reduced. The importance of these purely statistical uncertainties can of course also be decreased by increasing the collecting area of the recording instrument. However even if it were possible to make this area indefinitely large it would still be necessary to extend the observations over a long period in order to smooth out the effects of irregular variations in intensity which are associated with magnetic disturbances and non-periodic variations in pressure and temperature.

Because of the necessity for protracted observations and the inherent complexity of the phenomena to be studied the accumulation and interpretation of the experimental data tends to be a rather slow process. Nevertheless investigations of this kind can be expected to yield valuable information about the origin of the radiation and also about a wide variety of geophysical and heliophysical phenomena.

In the account which follows no attempt has been made to give a detailed survey of the development of the subject but a brief account has been given of the more important contributions during the inter-war period together with a more detailed survey of the results obtained in the last ten years or so.

1. VARIATIONS OF ATMOSPHERIC ORIGIN

1. 1 Atmospheric temperature and μ-meson decay

Measurements of the cosmic ray intensity using ionization chambers[1] have shown that in addition to the well known barometer effect, discovered by MYSSOWSKY and TUWIM in 1928, there is a negative correlation between the intensity and the temperature at ground level. BLACKETT [1938] pointed out that this temperature effect could be explained by the instability of the μ-meson. According to this interpretation, any warming of the atmosphere will increase the height above ground level of the region in which the mesons are produced so that they have a greater chance of decay before reaching the ground, with the result that the intensity is reduced. The magnitude of the effect calculated on this basis was — 0.16 % per °C which was in good agreement with COMPTON and TURNER's [1937] experimental value of — 0.18 % per °C.

BLACKETT also pointed out that the lag in the rise in meson intensity relative to the change in barometric pressure on the approach of a depression (MESSERSCHMIDT and PFORTE [1932]) could be explained on the same basis. Such a depression is generally preceded by a warm air mass so that the rise in temperature tends to offset the increase in intensity due to the decreasing barometric pressure.

HESS [1939] has pointed out that the temperature coefficient deduced from ionization chamber data obtained on the Hafelekar varies with season, the coefficient being about twice as great in winter as in summer. The existence of the variation in magnitude of the temperature coefficient has been confirmed by Hogg [1947], who also finds the coefficient to be about twice as great in winter as in summer. The coefficients obtained by both Hess and Hogg were evaluated using the temperature at ground level. However, it is the mean temperature up to a height of $\sim$ 16 Km., rather than the temperature at ground level, which determines the height of the meson producing layer, and it seems likely that the seasonal variation in the coefficient arises because of the different relation between the mean temperature and the ground level temperature for different seasons.

---

[1] See for example, HESS, GRAZIADEI and STEINMAURER [1935] and COMPTON and TURNER [1937].

A detailed study of the temperature and barometer effects has been made by Duperier [1944] using an unshielded threefold counter coincidence arrangement. He has correlated the total number of coincidences recorded each day with the corresponding mean barometric pressure for the day. The barometer coefficient β_{eB} found in this way has the value 3.45 % per cm. Hg. Duperier pointed out that this barometer coefficient does not represent a simple absorption effect but must include a factor due to meson decay because the height, H, of the meson producing layer is related to the ground level pressure by the hypsometric formula. Thus an increase in either sea-level pressure or mean temperature will in general produce an increase in H. In order to separate the absorption and decay effects Duperier assumed that the day to day variations in intensity are given by the regression equation:

$$(1) \qquad \delta I \quad \beta_1 \delta B + \beta_2 \delta H$$

where δI is the deviation from the mean intensity, δB the deviation from the mean barometric pressure and δH the corresponding deviation for the height of the particular pressure level at which the mesons are supposed to be formed. β_1 is the absorption coefficient and β_2 is the probability of meson decay per unit length of path (the decay coefficient). β_1 and β_2 were determined by substituting in the regression equation the appropriate values of δI, δB and δH. The values of δH were obtained from the radio-sonde observations made by the Meteorological Office.

It is possible to obtain an estimate of the pressure level at which the bulk of mesons reaching sea-level is produced by carrying out a series of multiple correlations between I, B and H for various assumed levels. The partial correlation coefficient between I and H at constant B, written as $r_{IH.B}$ should be greatest for that particular pressure level which is closest to the actual level of production. Duperier found that this correlation coefficient increased steadily as the value of H used was increased and reached its highest value for $H = 16.1$ Km., corresponding to a pressure level of 100 mb. which was the highest level tried. He therefore concluded that the region of meson production was in the neighbourhood of the 100 mb. pressure level or above. This increase with height of the correlation coefficient shows conclusively that it is the mean atmospheric temperature up to ~ 16 Km. rather than that at ground level, which is the controlling influence.

By substituting in the regression equation the day to day changes in height of the 100 mb. isobar Duperier obtained

$$\beta_1 = 2.28\ \%\ \text{per cm. Hg. and}\ \beta_2 = 5.4\ \%\ \text{per Km.}$$

The value for β_1 the absorption coefficient, is in good agreement with the results of direct measurements using absorbers of different thicknesses.

BENEDETTO [1946] has also correlated the meson intensity with the height of different pressure levels and has obtained results which are in rough agreement with those of Duperier. A completely satisfactory comparison of the results is not possible however because of the different procedures which have been followed. Benedetto corrected his data using a barometer coefficient prior to carrying out his correlations with isobaric heights. This considerably complicates matters since, as has been pointed out above, the barometer coefficient is partly due to absorption and partly to decay.

1. 2 The positive temperature effect

DUPERIER [1949] has recently extended his study of the correlation between day to day changes in the meson intensity and the corresponding meteorological changes using a modified arrangement of his original threefold counter set. In its original form the counter array carried no absorbing material so that both mesons and electrons were counted. In the modified arrangement the top two counter trays were placed directly above each other and separated from the lower tray by 25 cm. of lead. The solid angle over which the set was sensitive was therefore considerably less than in the previous arrangement. Five periods of observation were separately analysed comprising respectively 9, 20, 18, 27 and 33 days. The upper air data used were daily means of the radio-sonde observations made at 03, 09, 15 and 21 hours at Larkhill (about 100 km. to the south-west of London) and at Downham Market (about 75 km. to the north-east).

Initially the data were treated in the same way as described in § 1. 1; that is, the partial correlation coefficients between *I*, *B* and *H* were calculated for the 900, 500, 200 and 100 mb. pressure levels. The results are shown graphically in Fig. 1. There is a significant difference between these results and those obtained with the original unshielded arrangement in that the partial correlation coefficient $r_{IH.B}$ does not increase steadily up to the lowest pressure level studied but decreases in value from 200 mb. to 100 mb. On the other hand the partial correlation coefficient between *I* and *B* at constant *H*, written as $r_{IB.H}$ is still increasing up to the 100 mb. layer. Duperier has interpreted this as indicating

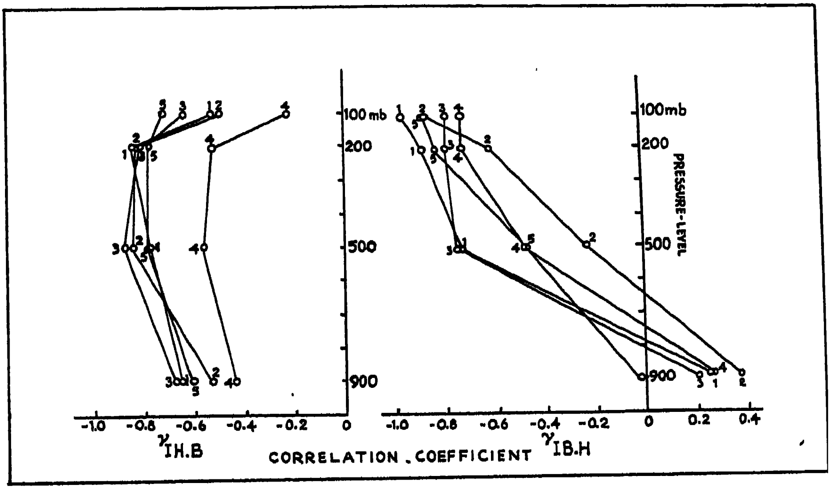

Fig. 1 - (A) Correlation of meson intensity with height of different pressure levels at constant ground pressure. (B) Correlation of meson intensity with ground pressure, at constant height of pressure levels for different pressure levels.

that the regression equation with three variables, (1), does not completely account for the observed changes in the intensity as otherwise both $r_{IB.H}$ and $r_{IH.B}$ should reach their maximum values for the same pressure level, that is, at the level at which the mesons are produced. He therefore concluded that some other variable apart from B and H must be involved. This additional variable was assumed to be the density of the air near a given pressure level P. This density is inversely proportional to the temperature and since it is the temperature which is actually measured by the radio-sonde this is a more convenient variable to use. Accordingly the regression equation now becomes

$$\delta I = \beta_1 \delta B + \beta_2 \delta H + \beta_3 \delta T \tag{2}$$

where the first two terms on the right-hand side have the same meaning as before and δT is the deviation from the mean of the temperature of the layer between P, the chosen pressure level, and $(P + 100)$ mb.

The correlation coefficient between I and T for constant B and H, written $r_{IT.BH}$ was calculated for different pressure levels. A value of $+ 0.68$ was found for the 200—100 mb. layer but there was no significant correlation with the temperature of the 200—300 or 500—600 mb. layers. It was found that all five periods of observation showed a high positive correlation between the meson intensity and the temperature of the 200—100 mb. layer; the mean value found for β_3 was $+ 0.12$ $^0/_0$ per °C.

Duperier therefore concluded that these three variables, the temperature of the air layer between 100 and 200 mb., the barometric pressure and the height of the 100 mb. layer, each exercises a controlling influence on the meson intensity at ground level.

The positive correlation between the meson intensity at ground level and the temperature of the 100—200 mb. layer will be referred to as the *positive temperature effect* in order to distinguish it from the negative temperature effect due to μ-meson decay. This positive temperature effect appears to indicate that the number of mesons at the surface of the earth increases as the air density in the region of production decreases and Duperier has interpreted this as being due to the competing processes of nuclear capture and decay of π-mesons. It is supposed that the π-mesons are produced by the primary cosmic ray particles and then either decay into μ-mesons or are captured in a nuclear encounter. For a π-meson of given energy the probability of capture is proportional to the density of the air along its path so that a low temperature, and therefore a high density, increases the probability of capture and results in a lower intensity of μ-mesons at the ground. Thus if R is the mean free path in $\mathrm{gm/cm^2}$ for a nuclear collision and L is the range in centimetres before decay, the probability of capture is given by $L/(R/\varrho)$ where ϱ is the density of the air. On the other hand the probability of decay into a μ-meson is given by $P = 1 - L\varrho/R$, and the temperature coefficient by

$$a = \frac{dP}{dT} = -\frac{L}{R}\,\frac{d\varrho}{dT}. \tag{3}$$

More recent results (DUPERIER [1951]) show however, that there is a discrepancy between the observed and the calculated temperature coefficients. For instance if the lifetime of the π-meson is taken to be 2.6×10^{-8} sec. and the mean free path for a nuclear interaction to be 60 $\mathrm{gm.cm^2}$ it turns out that the observed temperature effect is about 3 times greater than that calculated on the basis of these values; there is therefore some doubt as to whether this interpretation is correct.

1.3 The seasonal variation

Prior to 1938, work of rather limited accuracy had indicated the presence of a seasonal variation in cosmic ray intensity, most observers agreeing that there was a maximum in winter. FORBUSH ([1938a] and [1939]) analyzed the results of several years ionization chamber data at Cheltenham (U.S.A.), Christchurch (New Zealand), Teoloyucan (Mexico) and Huancayo (Peru). He separated the variation over the year into two parts, a world wide variation of irregular character which he ascribed to geomagnetic activity (see § 4.1) and a twelve monthly wave which was present at all stations except Huancayo. The amplitudes and times of maximum of these waves are given in Table 1 together with the results of a similar analysis of observations on the Hafelekar. All the data have been corrected for variations in barometric pressure.

In each case the cosmic ray variation was found to be very nearly opposite in phase to that for the ground temperature but the temperature coefficient obtained by taking the ratio of the amplitudes varied markedly from station to station (0.19 % per °C for Teoloyucan, 0.13 % per °C for Cheltenham). Because of the variability in the temperature coefficient deduced in this way Forbush did not interpret the seasonal wave as being directly due to atmospheric temperature changes.

TABLE 1

The seasonal variation in cosmic ray intensity

Station	Latitude	Height above sea level	Amplitude	Time of Maximum
Cheltenham	38.7° N	72 m.	1.6 %	January 19
Teoloyucan	19.2° N	2285 m.	1.0 %	January 24
Huancayo	12.0° S	3350 m.	0.0 %	—
Christchurch.	43.5° S	8 m.	0.8 %	July 28
Hafelekar	47.3° N	2300 m.	1.9 %	January 15

GILL [1939] published an independent analysis of the same data as had been used by Forbush. He resolved the seasonal variation into a 12-monthly and a 6-monthly wave and found no significant correlation between monthly means of ground temperature and cosmic ray intensity except at Cheltenham. The amplitudes of the 12-monthly waves differed significantly from those found by Forbush and this is presumably due to the latter having first removed the irregular world wide variation. Gill pointed out that the results could be interpreted as being due to the seasonal temperature changes. The variation in temperature coefficient from station to station is not inconsistent with this interpretation, since it is the mean air temperature up to a height of $\sim$ 16 Km. rather than the ground temperature, which is the controlling influence (see § 1. 1).

VALLARTA and GODART [1939] have suggested an alternative interpretation connected with the solar magnetic field. They assumed a dipole moment of 10^{34} gauss cm^3 for the sun and considered (*a*) the yearly change in heliomagnetic latitude of the earth due to the angle between the sun's dipole and the plane of the ecliptic, (*b*) the periodic change in distance between the earth and the sun (maximum in July, minimum in January) and (*c*) the effect due to the angle between the earth's axis and the plane of the ecliptic. The variation calculated in this way does not, however, agree very well with that found by Forbush and by Gill and this interpretation has received little support.

Some recent observations on the seasonal variation have been made in Manchester (DOLBEAR and ELLIOT [1951]) using threefold counter coincidence sets. Two such sets inclined at 45° to the vertical in the north and south directions were used in order that the directional dependence of the diurnal variation could be studied at the same time. Each counter array contained 35 cm. of lead absorber so that the meson component only was recorded.

The correlation between the daily mean values of the meson intensity, the barometric pressure and the heights of various pressure levels was first investigated using daily records of the barometer reading together with the upper air data obtained from radio-sonde ascents at Liverpool. It was found that the partial correlation coefficient between the daily mean values of the intensity and the height of a particular isobaric level was greatest for the 100 mb. level which was the highest considered.

The decay and absorption coefficients were next evaluated by correlating the daily mean values of the intensity with barometric pressure and the height of the 100 mb. pressure level, using the mean of 16 radio-sonde ascents from four stations in Britain. These correlations were carried out for each of the months in 1949, and for each recorder separately. The mean values obtained for the two regression coefficients were:

Absorption coefficient	(-1.63 ± 0.05) % per cm. Hg.
Decay coefficient	(-5.70 ± 0.23) % per Km.

The seasonal variation was investigated by forming monthly mean values of the intensity and these values are shown plotted in Figure 2 after correcting for the variation in barometric pressure using the absorption coefficient evaluated in the manner described above. It will be seen that the intensity shows a definite decrease in mid-summer amounting to about 2 % and that there is good agreement between the two recorders. The corresponding variations in H_{100}, the height of the 100 mb. layer and T_s, the surface temperature, are shown inverted to make clearer the inverse relationship between these variables and the intensity. These results agree qualitatively with the earlier work using ionization chambers and it is worthy of note that there does not appear to be any directional dependence of the seasonal variation within the accuracy of these measurements.

The monthly values of the intensity plotted in Figure 2 were correlated with the corresponding values of *H* and the correlation coefficients were found to be — 0.94 and — 0.91 for the north and south pointing recorders respectively. The mean value of the decay coefficient, however, was found to be — 3.55 % per Km. which differs significantly from the value — 5.70 % per Km. deduced from the day-to-day correlations with the same data.

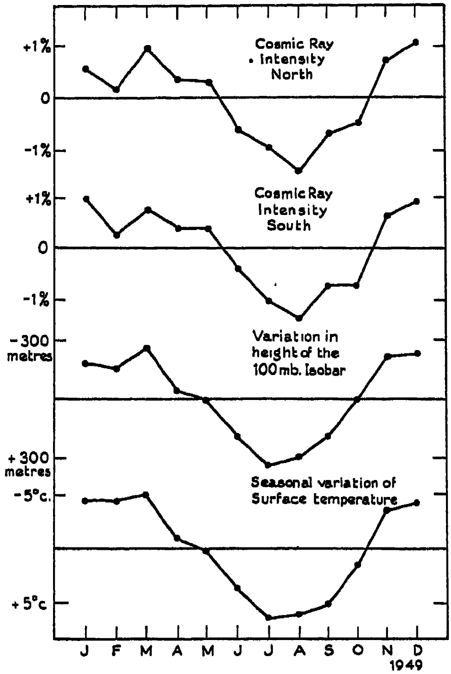

Fig. 2 - The seasonal variation in cosmic ray intensity for North and South directions together with the corresponding variations in height of the 100 mb. isobar and in the surface temperature.

An examination of the data in Figure 2 shows that there are several discrepancies in the behaviour of the intensity when compared with *H*. For example in April and May although *H* has then a value equal to the annual mean the intensity measured by both recorders is 0.5 % above the annual mean; the maximum of H is in July and the minimum of the meson intensity in August. In addition the steep recovery of H to the annual mean in the period September–October is not duplicated in the intensity.

These discrepancies were taken as an indication that some additional variable other than barometric pressure and the motions of the 100 mb. isobar must be taken into account if the annual variation is to be fully explained. This became even more apparent when the monthly mean values of the intensity were corrected for the variation in H using the coefficient — 5.7 % per Km. deduced from the day-to-day correlations. The resulting variation corrected in this way is shown separately for the two recorders in Figure 3.

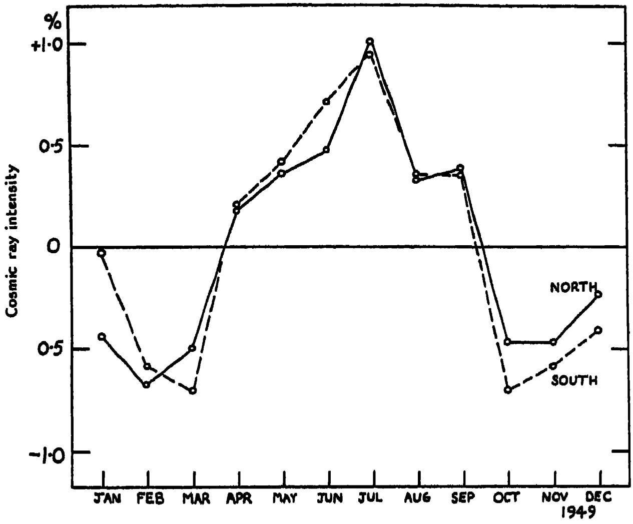

Fig. 3 – The seasonal variation in cosmic ray intensity after correcting for the effect of μ-meson decay.

The decay correction completely reverses the phase of the variation which now shows a maximum in summer. This seasonal wave agrees qualitatively with that found by Rau [1939] with an ionization chamber under 40 metres of water. He found a seasonal variation in the intensity which reached its maximum in June with an amplitude of about 2 %. In this connection it should be pointed out that with the high energy mesons recorded with Rau's arrangement (> 10 BeV) the decay effect was negligible so that no correction for this was required.

Duperier [1949] has suggested that the variation found by Rau may be due to the positive temperature effect and the result shown in Figure 3 can be interpreted in the same way. It therefore appears that in order to explain the seasonal variation we must take into account the positive temperature effect as well as the effect due to the decay of μ-mesons.

2. The solar daily variation

2. 1 Omni-directional measurements

In the period 1911 to 1914 the experiments of Hess and Kolhörster in manned balloons had proved fairly conclusively the existence of a penetrating radiation of extra terrestrial origin and, naturally enough, one of the next problems to be considered was that of locating the source of the radiation. The most direct approach to the problem is that of measuring the intensity of the radiation as a function of time, and in 1923 Kolhörster and Salis working with an ionization chamber on the Jungfrau found an apparent increase in intensity of the radiation when the Milky Way was overhead. This result was clearly of great significance if correct and many workers repeated the measurements in the hope of confirming the existence of the effect. The results obtained were however entirely contradictory, some observers finding variations over the sidereal day of as much as 15 %, others finding none at all.

Lindholm [1928] carried out a series of observations using an ionization chamber and found that whilst the intensity of the radiation did not appear to show any appreciable variation with sidereal time, it did show a variation with local solar time. The maximum intensity occurred in the early afternoon and the minimum at night, the amplitude of the variation being rather less than 0.5 %. Measurements on Mt. Evans by Compton, Bennett and Stearns [1932] also using an ionization chamber, showed a rather similar variation with a time of maximum near noon. Schonland, Delatizky and Gaskell [1937] were able to show, from the results of their measurements made in Capetown during the period 1933—1935, that the amplitude of this solar variation was significantly greater in summer than in winter.

The results of a long series of intensity measurements have been published by LANGE and FORBUSH [1948]. These observations were made with the Model C ionization chamber (COMPTON, WOLLAN and BENNETT [1934]). This chamber is spherical in shape with a volume of about 20 litres and is filled with pure argon to a pressure of 50 atmospheres. In order to reduce the effects of local radioactivity the chamber is surrounded by lead shot equivalent to 10.7 cm. solid lead. The ionization current produced by the cosmic radiation is compensated by ionization produced in a small auxiliary chamber by the γ-rays from a uranium source, and any departure from perfect balance results in the accumulation of either a positive or negative charge on the central collecting electrode. The central electrode is connected to earth for 3 minutes at the beginning of every hour and for the remaining 57 minutes is connected to a Lindemann electrometer. The shadow of the needle of this instrument is projected on to a moving strip of bromide paper, so producing a record of the potential of the collecting electrode which is determined by the cosmic ray intensity. Ionization chambers of this type were installed at Cheltenham (U.S.A.), Huancayo (Peru), Christchurch (New Zealand) and Godhavn (Greenland).

The results collected by Lange and Forbush include detailed records of the bi-hourly mean departures from balance for Huancayo for the period June 1936 to December 1945 together with daily means for each of the four stations over a similar period. In addition annual tables are given of the average diurnal variation for each month, season and year. The diurnal variation data are tabulated for the periods 1936 to 1946 for Huancayo, 1937 to 1946 for Cheltenham, 1936 to 1946 for Christchurch and 1938 to 1946 for Godhavn. All the data have been corrected for variations in barometric pressure.

Figure 4 shows the daily variation for each of the four stations averaged over the period 1939 to 1946 but excluding the years 1942 and 1945 for which the Christchurch records are incomplete. It will be seen that the variation for Christchurch and Cheltenham are similar and have an amplitude of about 0.15 % with a maximum at approximately 3 p.m. The variation for Huancayo has much the same amplitude but the time of maximum is significantly earlier occurring round about mid-day. The amplitude of the variation at Godhavn is smaller than for the other three stations and appears to be rather irregular. The geographic latitudes, geomagnetic latitudes and heights above sea-level of these stations are respectively 12 °S, 0.6°S and 3350 metres for Huancayo

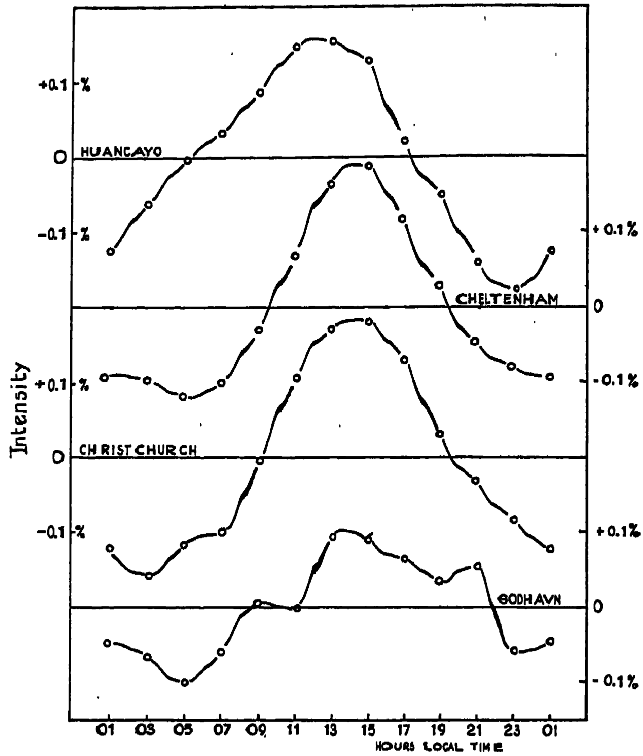

Fig. 4 – The average diurnal variations computed from 8 years ionization chamber data at Huancayo, Cheltenham, Christchurch and Godhavn.

38°.7 N, 50°.1 N and 72 metres for Cheltenham, 43°.5 S, 48°.6 S and 8 metres for Christchurch and 69°.2 N, 79°.9 N and 9 metres for Godhavn.

In dealing with periodic variations of this kind it is often convenient to split them up into their harmonic components. This analysis gives us the Fourier coefficients which we will suppose to be a_1 and b_1, for the 24 hour period, that is to say the first harmonic is given by the expression

$$a_1 \cos t + b_1 \sin t$$

which in turn can be written as $A_1 \sin (t + \varepsilon_1)$ where

$$\mathbf{a}_1 = A_1 \sin \varepsilon_1 \text{ and } \mathbf{b}_1 = A_1 \cos \varepsilon_1$$

The sine wave $A_1 \sin (t + \varepsilon_1)$ can be represented vectorially as shown in Figure 5, where it will be seen that the Fourier coefficients are simply the components of the vector in the two directions at right angles. Plotting the coefficients on the rectangular co-ordinate system shown will therefore give us the end point of the vector so that both its length and phase angle measured anti-clockwise relative to the **b** axis are determined. The maximum of the sine wave $A_1 \sin (t + \varepsilon_1)$ occurs when $t + \varepsilon_1 = \pi/2$ that is to say $t_{\max} = (\pi/2 - \varepsilon_1)$. If a time scale is now inserted on the diagram and is measured in a clockwise direction from the **a** axis such that 360° corresponds to 24 hours the direction of the vector will indicate directly the time of maximum. CHAPMAN has introduced the name *harmonic dial* for a diagram of this kind. Higher harmonics can also be represented on similar dials by inserting the appropriate time scale; thus for the second harmonic of the diurnal variation, 360° would correspond to 12 hours, and so on.

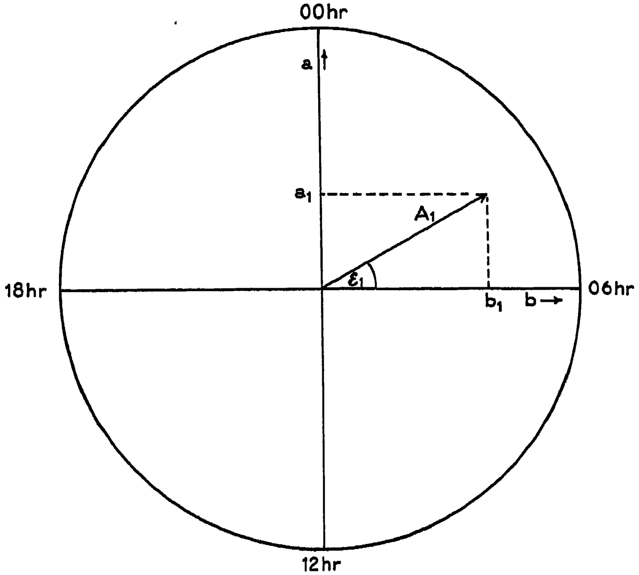

Fig. 5 – Construction of the harmonic dial.

The first harmonics of the daily variations shown in Figure 4 are plotted on a harmonic dial in Figure 6 which shows clearly the difference in phase between the variation at Huancayo and the other three stations. Apart from being situated close to the equator, Huancayo differs from these stations in that its height above sea-level is 3350 metres; consequently it is not possible to say definitely whether we have here an effect arising from the difference in latitudes or from the difference in heights above sea-level. The average for three years ionization chamber data obtained by Hess and Graziadei [1936] on the Hafelekar (2300 metres above sea-level, geographic latitude 47° N) is also shown. Their ionization chamber was shielded by 10 cm. lead and the records extended over the years 1932 to 1934 inclusive, being corrected for both atmospheric temperature and pressure variations. Whilst these results are not directly comparable with the Huancayo data, because of the temperature correction and the difference in time between the observations, they do seem to indicate that at least a part of the discrepancy between the phase of the variation at

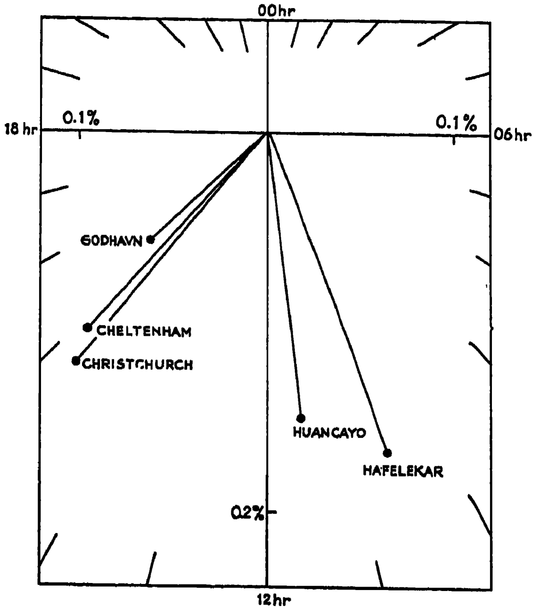

Fig. 6 – Harmonic dial showing the first harmonics of the daily variation at Cheltenham, Christchurch, Huancayo, Godhavn and the Hafelekar.

Huancayo and that at the higher latitude stations is due to the difference in height above sea-level.

HOGG [1949] has published the results of a series of observations made in Canberra using an ionization chamber of volume about 4 litres. The chamber was filled with carbon dioxide at a pressure of ~ 10 atmospheres and was shielded by 10 cm. lead. The observations extended over the period September 1935 to August 1940. The average value for the diurnal variation, after correcting for the variation in pressure, was found to be ~ 0.24 % with a time of maximum close to 1430 h local time. The time of maximum at Canberra is close to that for Christchurch and Cheltenham but the amplitude is appreciably greater than that for the latter two stations.

The diurnal variation is of particular interest because it enables us to obtain some information about the degree of isotropy of the primary flux, and at first sight it might appear that the existence of the solar daily variation itself could be taken as evidence that the primary radiation is not completely isotropic. We know, however, that if data for a large number of days are analyzed there are regular changes over the day in both atmospheric temperature and pressure which must themselves influence the cosmic ray intensity observed at sea-level. Consequently before any information can be obtained about the behaviour of the primaries it is necessary to apply corrections for these effects. Unfortunately the corrections for temperature are both large and uncertain. The temperature is higher during the day than at night and it is to be expected that because of μ-meson decay this will tend to reduce the daytime intensity below that for the night. Since the observed variation shows the intensity to be greatest in the early afternoon correction for this effect will increase the amplitude of the variation.

Corrections of this kind have been applied by DUPERIER [1946] to results covering three years obtained in London, using a three-fold counter coincidence set. The average daily variation corrected for pressure only was found to have an amplitude of 0.244 % with a time of maximum at 1806 h local time. After eliminating the effect of daily variation in temperature, the amplitude became 0.414 % and the time of maximum was advanced to 1618 h. A similar correction has been applied by HOGG to his data and results in a variation with an amplitude of ~ 0.7 %.

In addition to this correction for the effects of μ-meson decay, it would appear that a further correction ought to be made taking into account the positive temperature effect discussed in § 1. 2. This has been discussed by DOLBEAR and ELLIOT [1951], who conclude that it is likely to be even larger than the decay correction. Meanwhile it is sufficient to say that the influence of these factors makes it difficult to link the observed variation at sea-level with that of the primaries outside the atmosphere.

It is possible to overcome much of the uncertainty arising from these effects by using counter telescopes which are arranged symmetrically with respect to the vertical. Thus if two telescopes are set up so that one points to the north at 45° to the vertical and the other to the south at the same angle any changes in atmospheric pressure or temperature will affect both counting rates equally. If the telescopes are located at latitude 45° the north pointing telescope will be directed parallel to the axis of rotation of the earth and the direction in space to which it points will not change as the earth rotates. The south pointing telescope on the other hand is directed into the equatorial plane of the earth and therefore sweeps across the sky as the earth rotates. A non-isotropic distribution of the primary radiation falling on the earth will therefore produce a difference between the daily variations for the two directions. Information can therefore be obtained about the variation in primary intensity by subtracting the variation for the north direction from that for the south. This avoids the necessity for temperature and pressure corrections. The results obtained by using directional counter sets of this kind are described in the next section.

2. 2 Measurements using directional counter arrays

ALFVÉN and MALMFORS [1943] in Stockholm and KOLHÖRSTER [1941] in Berlin have investigated the daily variation with directional counter telescopes. The former workers measured the daily variation for rays arriving at the earth's surface at 30° and 60° to the vertical in the north and south directions. The arrangement used consisted of three counters 50 cm. long and 15 cm. in diameter, mounted on a framework which was turned through 180° about a vertical axis at the end of each hour so that the number of coincidences was recorded in the north and south directions during alternate hours. Records were obtained for a total of 600 complete days during the period February 1939 to August 1941. It was found that the variation showed a definite dependence on direction. For a zenith angle of 30°, for instance, the first harmonic of the daily variation in the north direction had an amplitude of $\sim 0.16\ \%$ with a time maximum of 1330 h. whereas that for the south had a similar amplitude but the time of maximum was shifted to 1900 h.

In discussing these results MALMFORS [1948] points out that the difference between the variations for the two directions cannot be due to any atmospheric effect, since the particles from both the north and south have passed through the same amount of atmosphere under approximately the same conditions. He also shows from model experiments, using a small magnetized sphere (to represent the earth) and an electron beam, that the effect is unlikely to be due to the earth's magnetic field. He concludes that the primary radiation is not isotropic. He points out that this lack of isotropy cannot arise as a result of the deflection of the particles in the solar magnetic field. Only particles of low momentum are likely to be affected by this field and he is able to show from his model experiments that the direction at which such particles arrive in the atmosphere is only slightly dependent on the original direction of the particles outside the earth's magnetic field. This is due to the spiral motion of the particles, a small change in momentum being sufficient to produce a large change in the direction of arrival at the earth's surface. Consequently, if we are to account for the marked difference between the variations for the north and south directions it must be assumed that the lack of isotropy exists for particles of high energy which suffer little deflection in the earth's magnetic field.

Measurements have also been made in Manchester with directional counter arrays (ELLIOT and DOLBEAR [1950 and 1951]). The apparatus used consisted of two counter arrays each array carrying 30 counters arranged in three trays of ten and coincidences were recorded between the three trays in each case. The counters had an effective length of 60 cm. and were 4 cm. in diameter, and the spacing between the trays was 7.5 cm. so that each array counted particles over a rather wide solid angle. The two counter arrays were mounted in boxes on a framework so that one pointed south at 45° to the vertical and the other to the north at the same angle. The framework could be turned about a vertical axis so that the directions of the recorders could be reversed at regular intervals.

The counting rate of each recorder was approximately 50,000 threefold coincidences per hour. The coincidence pulses were fed to scaling units (one for each recorder) which scaled by 100 and the output of these scaling units operated electromechanical counters. These counters, together with a clock and an aneroid barometer, were mounted on a panel which was automatically photographed every fifteen minutes. In order to eliminate any systematic difference between the two recorders they were turned round at fortnightly intervals so that each pointed north and south alternately.

Figure 7 shows the mean daily variation for the north and south directions for a total of 360 days. It is clear from these curves that

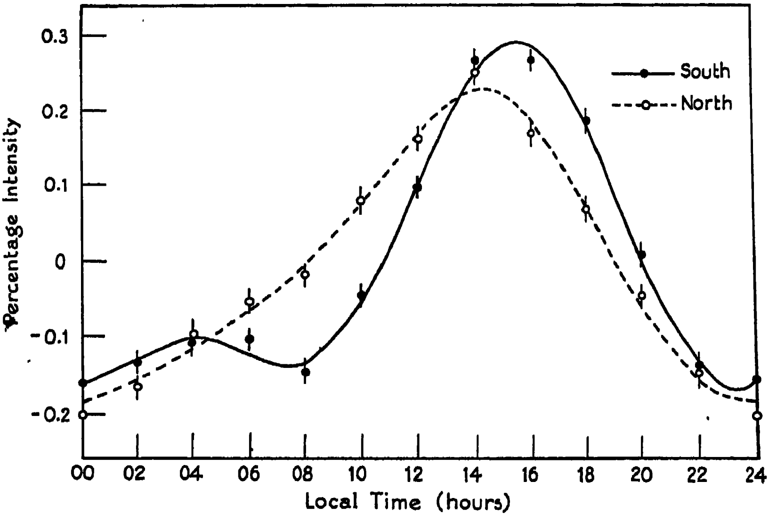

Fig. 7 – The daily variation for the North and South directions at Manchester.

there is a significant difference between the variations in the two directions which is in agreement with Alfvén and Malmfors' results. If the interpretation of this difference in terms of a non-isotropic primary radiation is correct, then as pointed out in the previous section, the difference between the two curves should represent the variation of the incident primary intensity with time of day. The difference curve obtained by subtracting the north variation from that for the south is shown in Figure 8.

Now (Elliot and Dolbear [1950]), it is possible to check this

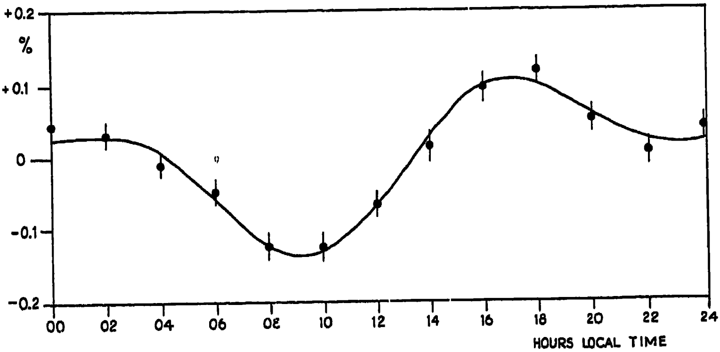

Fig. 8 – Difference curve obtained by subtracting the North variation from that for the South at Manchester.

interpretation in terms of a non-isotropic primary distribution by measuring the daily variation in the east and west directions. Under these conditions the two telescopes scan the same part of the sky in succession as the earth rotates. The difference in time between any particular region of the sky appearing opposite the two telescopes depends on the angle between them. Thus if each telescope is inclined at an angle θ to the vertical this difference in time will be $2\theta/15$ hours. Measurements in the east and west directions have been made in Manchester with the recorders used initially for the north and south measurements described above. With this arrangement the counter arrays were inclined at 45° to the vertical but because of the fall off in intensity with zenith angle the direction of maximum sensitivity actually lay at 25° to the vertical. Consequently for this arrangement $\theta = 25°$ and therefore the primary intensity variation shown in Figure 8 should be displaced 1.7 hours earlier for the east-pointing telescope and 1.7 hours later for the west. The variation shown in Figure 8 can be well represented by the sum of a 24 and a 12 hour wave and can therefore be written as

$$P_1 \cos 2\pi/24(t - t_1) + P_2 \cos 2\pi/12(t - t_2)$$

If we suppose that the part of the daily variation which has its origin in the atmosphere to be given by some function of time $A(t)$ the east variation should be given by

$$\Delta I_E = A(t) + P_1 \cos 2\pi/24\{t-(t_1-1.7)\} + P_2 \cos 2\pi/12\{t-(t_2-1.7)\}$$

and the west variation by

$$\Delta I_W = A(t) + P_1 \cos 2\pi/24\{t-(t_1+1.7)\} + P_2 \cos 2\pi/12\{t-(t_2+1.7)\},$$

the atmospheric component being the same for the two directions since the two telescopes are symmetrical with respect to the vertical. This atmospheric part can therefore be eliminated by taking the difference between the two so that we have

$$\Delta I_E - \Delta I_W = -\{0.86\, P_1 \sin 2\pi/24(t-t_1) + 1.56\, P_2 \sin 2\pi/12(t-t_2)\}$$

This expression for the difference between the east and west daily variations depends on the quantities P_1, P_2, t_1 and t_2 which are all known from the south-north measurements. The only other factor involved is the angle 2θ between the two telescopes which is responsible for the 1.7 hours change in phase. This calculation is based on the assumption that the curve in Figure 8 represents a variation in primary intensity and the truth of this assumption can therefore be checked by comparing the calculated and observed east minus west variations.

The daily variation in the east and west directions measured over a period of 300 days during 1949 is shown in Figure 9 (ELLIOT and DOLBEAR [1951]). The east minus west difference is also shown in the same figure. The points which have been plotted are the observed differences and the curve which has been drawn is that given by the expression deduced above. In view of the close agreement between the observed points and curve calculated from the south-north measurements it seems very likely that the interpretation in terms of a non-isotropic primary radiation is correct.

In order to explain the daily variation completely, it is still necessary, of course, to account for the component $A(t)$ which is supposed to originate as a result of atmospheric effects. As was pointed out above, the decay temperature effect would tend to produce minimum intensity at midday whereas the positive temperature effect would tend to produce a maximum at that time. The resultant variation will therefore depend on the relative magnitudes of these two effects and it may be that the remainder of the variation can be accounted for if the positive temperature effect is sufficiently large to outweigh the decay effect. There is some reason to suppose that this may be so (Dolbear and Elliot [1951]) but the daily temperature variations at great heights are not sufficiently well known to enable a definite conclusion to be reached at present.

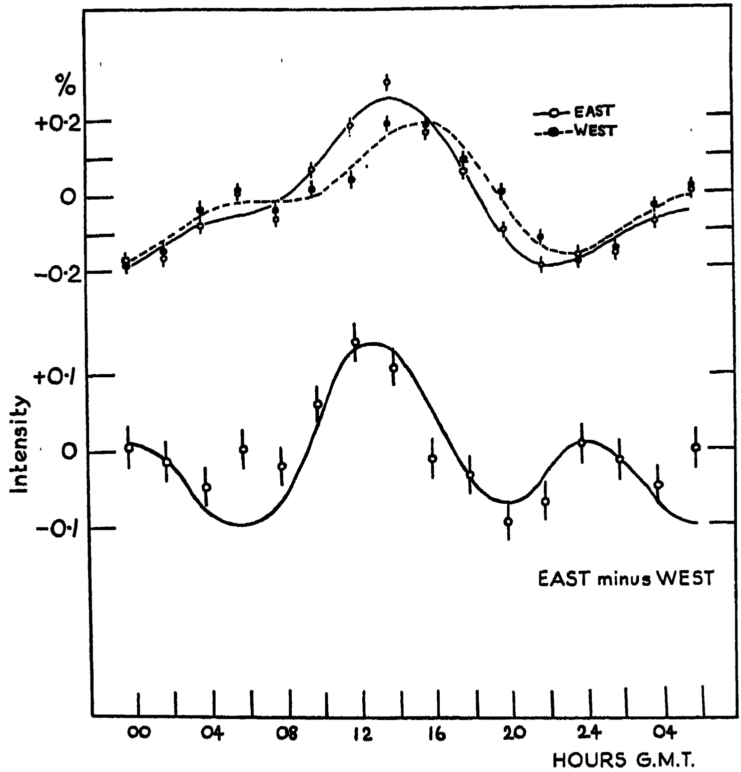

Fig. 9 – The daily variation in the East and West directions and the difference (E-W).

2. 3 The relation between the daily variation and geomagnetic activity

Elliot and Dolbear [1951] have suggested that the non-isotropic primary distribution may be connected with the emission of corpuscular streams by the sun. If the sun has a general magnetic field, then, according to Alfvén [1949], these streams will have transverse electric fields associated with them, due to polarization as a result of the motion of the stream through the solar field. Dolbear and Elliot point out that the direction of the field as seen from the earth will be opposite for streams emitted from the east and west limbs of the sun and that this should lead to a decrease in intensity in the late morning and an increase in the early afternoon if it is assumed that the orientation of the solar dipole is the same as that of the earth. This is in qualitative agreement with the experimental results shown in Figure 8 and rough quantitative agreement is obtained for a solar equatorial field of $\sim$ 8 gauss.

They also suggest that if magnetic disturbances are due to the arrival of a solar stream in the vicinity of the earth the effect of the electric field discussed above should be greatest at the time

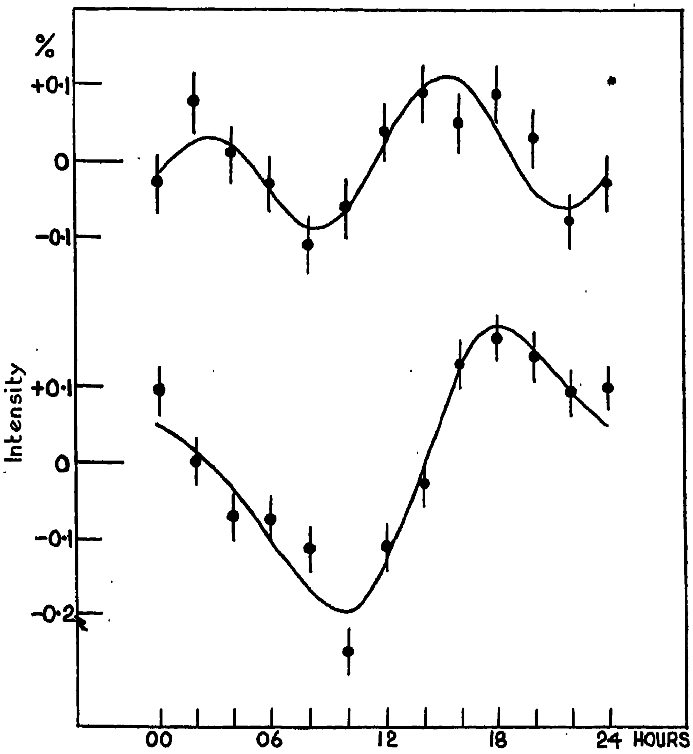

Fig. 10 – The South minus North daily variation and the level of geomagnetic activity; upper curve K $\leqslant$ 17; lower curve K $\geqslant$ 18.

of such disturbances, since the stream will then subtend its maximum solid angle as seen from the earth. With a view to checking this, the data were divided into two groups, one comprising the days on which the sums of the three-hourly K-figures of magnetic activity were $\leqslant 17$ and the other of days for $K \geqslant 18$. The south minus north curves for the two groups are shown in Figure 10 where it will be seen that the variation is indeed greater on disturbed than on quiet days.

This may be connected with the much enhanced daily variation which is sometines observed during the few days immediately following an intense magnetic storm. This effect has been found by SEKIDO and YOSHIDA [1950] and by ELLIOT and DOLBEAR [1951], and is clearly shown in Figure 11 where the hourly values

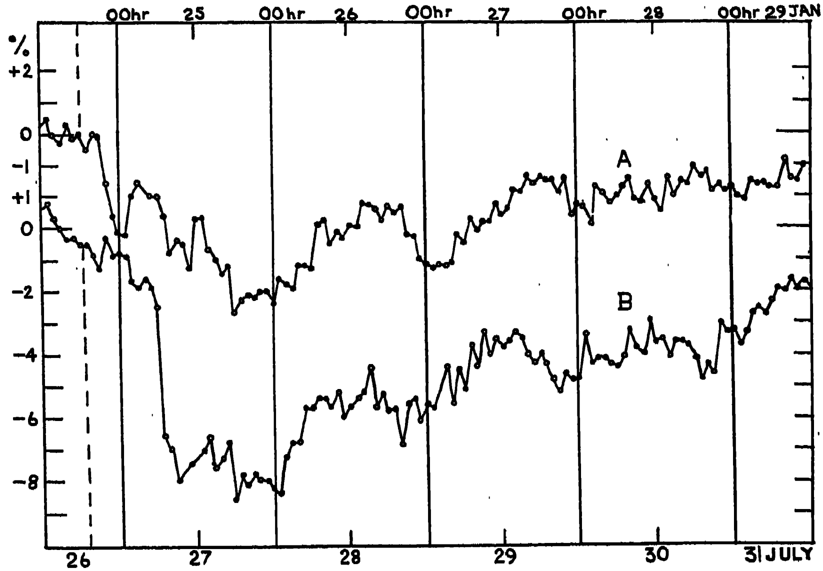

Fig. 11 – The variation in cosmic ray intensity on the days following two geomagnetic storms.

of the cosmic ray intensity in Manchester are plotted for the days following two magnetic storms which began on 26th July 1946 and 24th January 1949 respectively. The values have been corrected to constant barometric pressure.

Figure 12 shows the average diurnal variation for the two days following the magnetic storm of July 26, together with the two days following the storm of Jan. 24. The average variation over 360 days is also shown for comparison. It will be seen that in addition to the increase in amplitude the time of maximum is advanced from 1400 h. to 1200 h. This advance in phase of the daily variation during the days following a storm has also been found by Sekido and Yoshida.

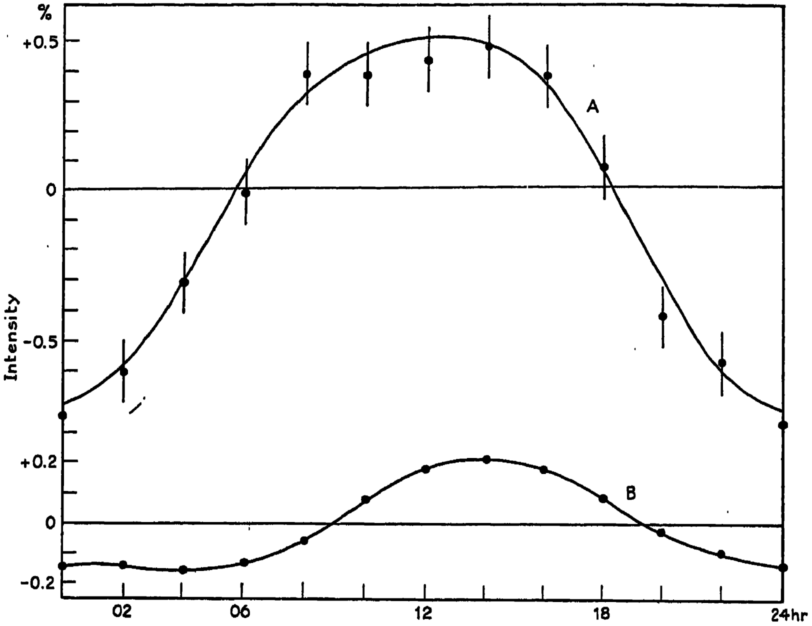

Fig. 12 – (A) Mean daily variation for 26 and 27 January 1949 and 28 and 29 July 1946. (B) average daily variation for 360 days.

2.4 The daily variation at great altitudes

Jánossy [1937] pointed out that if the sun has a magnetic field of the order 50 gauss, it should produce a daily variation in cosmic ray intensity. This variation arises as a result of the rotation of the earth relative to the directions of approach which are forbidden according to the Störmer theory for the motion of charged particles in a dipole field. The amplitude of this daily variation should increase with altitude, since the contribution to the total intensity by particles of low momentum, which are most affected by the solar field, increases with height as absorption effects in the atmosphere become less important.

More recent calculations by Alfvén [1947] and by Kane, Shanley and Wheeler [1949] show that the daily variation is likely to be a good deal smaller than that expected from the simple Störmer theory, because of the effect of particles scattered into periodic orbits in the sun's field by the magnetic field of the earth. This means that the forbidden directions, which would be empty on the simple theory, do in fact carry an appreciable intensity of radiation, and the amplitude of the expected diurnal variation is therefore reduced. Detailed calculations on the phase and amplitude of the variation have been made by Dwight [1950] for two values of the solar magnetic moment, (0.42 and 1.0×10^{34} gauss cm^3) and for different latitudes. Assuming a differential momentum spectrum with exponent — 2.75 he finds that the intensity during the early hours of the morning should be several percent less than at midday. The actual values depend on the value assumed for the solar moment and on the particular latitude.

Measurements of the cosmic ray intensity at 30,000 ft. have been made by Dolbear and Elliot [1950] using a threefold counter coincidence set, and the results show that at this altitude the difference between the day and night intensities is not likely to be greater than 1 %. Bergstralh and Schroeder [1951] using equipment carried aloft by balloons have measured the total ionizing intensity, the γ-ray intensity and the neutron intensity at altitudes up to 75,000 ft. during the two periods 0030 to 0830 h. and 1800 to 2200 h. They find that the difference in intensity is not greater than 1 % for the total ionizing radiation and not greater than 3.5 % for the γ-rays and the neutrons. These figures represent the limits of accuracy attained in each case. According to Dwights's calculations these results indicate that the solar magnetic moment is less than 0.42×10^{34} gauss cm^3 (equatorial field $\sim$ 12 gauss).

2. 5 The semi-diurnal variation

As has been pointed out in the previous section, it is convenient to analyze the solar daily variation into its Fourier components, and it is found that in addition to the 24 hours component there is a significant 12 hours (semi-diurnal) wave. The 12 hour waves for Cheltenham, Christchurch, Huancayo and Godhavn, after correcting for pressure, are shown in Figure 13. It will be seen that the amplitudes of these waves are small, but some workers have found quite large amplitudes. For instance, Rau [1939] using two ionization chambers suspended in a narrow fissure in the rock

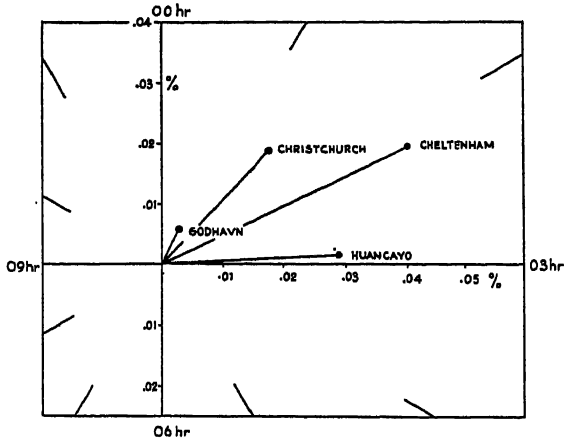

Fig. 13 – Harmonic dial showing the semi-diurnal variations for Christchurch, Cheltenham, Huancayo and Godhavn.

40 metres under the surface of Lake Constance found the solar variation to be primarily semi-diurnal in character with an amplitude of ~ 0.15 %. The times of maximum were 1130 and 2330 h. so that this variation is very nearly in phase with the semi-diurnal variation in barometric pressure. On the other hand Duperier [1945] using an unshielded counter set found a 12 hour wave with amplitude 0.18 % with maxima at 0312 and 1512 h. which is within an hour of being completely out of phase with the barometer variation.

It has been noted by Rau [1940] and by Ehmert [1940] that a semi-diurnal variation in the cosmic ray intensity which is in phase with the barometric variation could be explained on the basis of the theory of atmospheric oscillations outlined by Pekeris [1937 and 1939] and developed in detail by Weekes and Wilkes [1947]. According to this theory the atmosphere has a free oscillation period of 12 hours with the result that the 12 hour barometer variation is magnified by resonance. This oscillation is characterized by a nodal surface at a height of about 30 Km. with the result that the motion of the isobaric surfaces above and below 30 Km. are 180° out of phase. The height of any particular isobar above

30 Km. is a minimum at the time of maximum sea-level barometric pressure. If it is assumed that most of the mesons recorded by Rau's apparatus were produced at some pressure level lying above 30 Km., then because of the decay of the μ-meson the motion of this pressure level should produce a 12 hour variation in the meson intensity in phase with that of the barometric pressure. The atmospheric oscillation theory therefore affords a qualitative explanation of the variation in meson intensity observed by Rau.

The implications of this interpretation have been examined quantitatively by NICOLSON and SARABHAI [1948] and they conclude that this explanation is only possible if the bulk of the mesons is produced at a height of 60 or 70 Km. above sea-level. At this altitude the amplitude of the pressure oscillation, which according to the theory of Weekes and Wilkes increases rapidly with height above the nodal surface at 30 Km., is just sufficient to account for the 12 hour variation in cosmic ray intensity. At 70 Km. however the pressure is about 1/8000 of an atmosphere, and it therefore follows that the primary particles would have to produce a large part of the meson flux in traversing this amount of air. Such an assumption leads to an unreasonably high cross-section for the meson production process compared with the generally accepted figure which corresponds to a mean free path

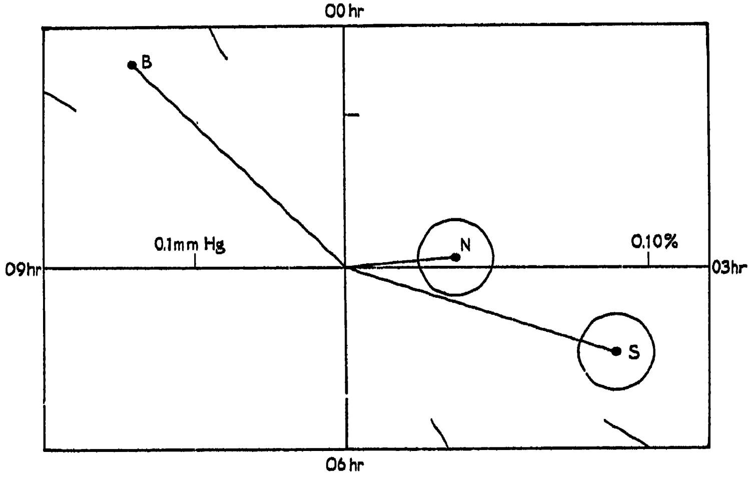

Fig. 14 - Harmonic dial showing the semi-diurnal variation at Manchester for particles arriving from the North and South directions.

for the primaries of $\sim 1/10$ atmosphere. It seems extremely unlikely, therefore, that the semi-diurnal variation observed by Rau can be accounted for in terms of atmospheric oscillations in this way.

Harmonic analysis of the daily variation observed at sea-level using counter telescopes (Elliot and Dolbear [1950 and 1951]) shows that the amplitude of the semi-diurnal wave, like that of the 24 hour wave, is markedly different for particles arriving from the north and south directions as shown by the harmonic dial in Fig. 14. These results show quite clearly that the semi-diurnal variation observed at sea-level, at any rate, cannot be due to the atmospheric oscillations which should produce the same variation irrespective of direction. As was pointed out in the previous section this dependence on direction is apparently due to the non-isotropic primary distribution.

3. THE SIDEREAL DAILY VARIATION

3. 1 Galactic rotation and the cosmic ray intensity

Evidence for a sidereal daily variation has been sought by many workers during the past 25 years but there is still no general agreement as to whether or not such an effect exists. It is true to say, however, that if it does exist it is of exceedingly small amplitude, certainly less than 0.1 % and probably not greater than 0.03 % for the cosmic ray flux at sea-level. The existence or otherwise of a variation of this kind is of importance because of the information it can yield about the origin of the radiation.

The earliest attempts to establish a sidereal variation were made with a view to relating the intensity to the distribution of stars in the galaxy, but the absence of any marked increase at the time of transit of the Milky Way ruled out any simple relation of this kind. Meanwhile Compton and Getting [1935], following a suggestion by Lowry, were able to show that if the radiation originates outside the galaxy, and is isotropic in inter-galactic space, a sidereal variation ought to be produced by the rotation of the galaxy. Because of this rotation the solar system is carried through space with a velocity of ~ 300 Km./sec. relative to the distant galaxies. The direction of motion is towards the constellation Cygnus at $\delta = +47°$, $\alpha =$ 20 h. 40 m. As a result of this motion the energy and intensity of the radiation should be greater on the side of the earth facing the direction of motion than on the opposite side.

Vallarta, Graef and Kusaka [1939] have improved the original calculations of Compton and Getting by taking into account more rigorously the effect of the earth's magnetic field. The effect of the field is to reduce the magnitude of the expected variation since the time of maximum intensity is a function of the momentum of the primaries and consequently, for an incident spectrum covering a wide range of momenta, the variation is to some extent smoothed out. Further, the time of maximum intensity, which would be at 20 h. 40 m. on an unmagnetized earth, is also changed. The results obtained by Vallarta *et. al.* for particles incident vertically at the geomagnetic equator are summarized in Table 2.

TABLE 2

Calculated phase and amplitude of sidereal variation due to Compton–Getting effect

Primary Radiation		Sidereal Time of Maximium	Amplitude in %
Composition	Energy Spectrum		
Positive particles only .	E^{-3}	1320 h	0.17
	e^{-KE}	1800 h	0.24
50 % Positive . . . . 50 % Negative . . .	E^{-3}	0840 h	0.06
	e^{-KE}	2040 h	0.19

3. 2 The separation of solar and sidereal daily variations

Apart from the extreme smallness of the predicted effect the problem of the sidereal variation is complicated by the presence of the solar daily variation. If the amplitude and phase of the solar variation were constant over the year it would present no difficulty, since it could be entirely eliminated by averaging the data for a complete year according to sidereal time. This can easily be seen in the following way. Suppose the data are divided into 12 monthly groups, then the first harmonic of the mean solar variation will be the same for each group. If these harmonics are now plotted on a sidereal harmonic dial they will be represented by 12 equally spaced points on a circle having its centre at the origin of the dial as shown in Figure 15. The points are spaced at 2 hour intervals in a clockwise progression since a sidereal clock gains approximately 2 hours per month on a solar clock. It is clear that the resultant of the 12 vectors, whose end points are represented by the points on the dial, is zero. Exactly the same result would be obtained regardless of the length of interval chosen which could equally well be weekly or bi-monthly. Under these circumstances the presence of a true sidereal variation could be established without difficulty provided the data extend over at least one complete year.

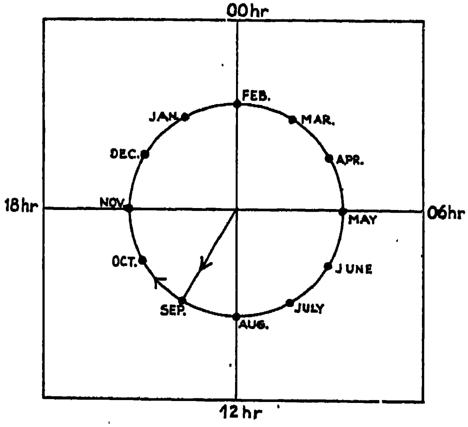

Fig. 15 - Solar daily variation of constant amplitude plotted on a sidereal dial.

If, however, the solar daily variation changes in amplitude over the year the points in Figure 15 will no longer be on a circle and the resultant vector will not in general be zero. This resultant vector will therefore simulate a true sidereal variation although it arises purely as a result of the variation in amplitude of the solar variation. It is known that the amplitude of the solar variation does vary over the year and it will therefore be clear from the above discussion that some caution must be exercised in analyzing data for the presence of a sidereal variation. This problem has been fully discussed by THOMPSON [1939], and he has suggested a method for separating a true sidereal variation from a solar variation which varies in amplitude over the year. The principles upon which the method depends are most easily shown by means of the harmonic dial. Consider first the solar daily variation; if this is of constant amplitude and phase it can be represented by the vector **C** (Figure 16). If a sidereal variation of constant amplitude

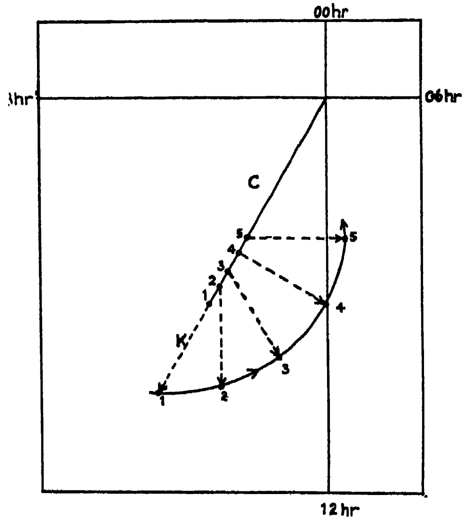

Fig. 16 – Harmonic dial showing combination of sidereal variation and a solar variation which varies in amplitude over the year.

and phase is also present it can be represented as a second vector **K** which will rotate in an anti-clockwise direction about the tip of the vector **C** completing one revolution in a year. The resultant of these two vectors will therefore represent the observed apparent solar diurnal variation at any particular time. If we now suppose that the amplitude of the solar variation itself varies over the year this variation will be represented by a periodic variation in the length of the vector **C**. When this variation is combined with the sidereal vector **K**, the tip of the resultant vector will now describe an ellipse as shown in the diagram. Consequently if the experimental data are divided into monthly groups, for instance, and these groups are subjected to harmonic analysis, the first harmonics when plotted on a harmonic dial should fall in chronological sequence on an ellipse if a true sidereal variation is present.

This method of analysis has been applied by THOMPSON to COMPTON and TURNER'S data [1937] and by FORBUSH [1937a] to ionization chamber data for Cheltenham and Huancayo. No sidereal variation in excess of the experimental errors was found for either of the two sets of data. More recently DUPERIER [1946] has used this method to analyze vertical counter coincidence data in London, extending over a period of three years. The data were divided into bi-monthly groups and corrected for pressure and decay temperature effects. The first harmonics were then found for each group and when these were plotted on a harmonic dial the points were found to lie on an ellipse. From these results Duperier concluded that there was a sidereal variation superimposed on the solar variation. The sidereal wave had an amplitude of 0.21 % with a maximum at 21 hr.

3. 3 Recent experimental results

Hogg [1950] has analyzed five years. ionization chamber data for Canberra using the Thompson method. The data were corrected for pressure and temperature and divided into monthly groups and the first harmonic was calculated for each group. The values obtained were smoothed by averaging the result for each month with that for the preceding and succeeding months. When plotted on a harmonic dial the smoothed monthly points showed a cyclic arrangement about the mean for the year similar to that found by Duperier. The sidereal variation found by Hogg, as a result of this analysis, differs from that found by Duperier, however, in that the amplitude is 0.05 ± .02 % and the time of maximum 0936 h. ± 42 m. If the data are corrected for pressure only slightly different values are obtained, the amplitude being 0.04 ± 0.02 % and the time of maximum 0800 h. ± 42 min. These figures were compared with the results of a similar analysis of the ionization chamber data for Cheltenham, Christchurch and Huancayo. The results as summarized by Hogg are shown in Table 3. (B) indicates the the data have been corrected for pressure only and (B.T) that

TABLE 3

Apparent sidereal variation

Station	Ampl. %	Time of Max. (LST)
London (B.T) . .	0.21 ± 0.02	2100 h
Cheltenham (B) .	0.03	2200 h
Huancayo (B) . .	0.04 ± 0.008	0300 ± 6 m.
Canberra (B.T.) .	0.05 ± 0.02	0936 ± 42 m.
Canberra (B) . .	0.04 ± 0.02	0800 ± 42 m.
Christchurch (B) .	0.04	0806 h

they have been corrected for both pressure and temperature. It will be seen from the table that each set of data shows a sidereal variation of approximately the same amplitude except for London which is very much greater than the rest. The phase, however, shows considerable variation from station to station. In particular the times of maximum for the two stations in the Northern Hemisphere differ by $\sim$ 12 hours from those for the Southern Hemisphere. These features lead Hogg to conclude that these results cannot represent a true sidereal variation and that they are due to some solar effect.

In the above discussion it has been assumed that the amplitude of the solar variation changes with season but the phase remains constant. Given these conditions the Thompson method of analysis should enable an unambiguous separation of the solar and sidereal variations to be made. If however, both the amplitude and phase of the solar vector vary over the year, the solar and sidereal effects cannot be separated by this means. A variation in phase could arise in the following manner. Suppose the solar variation is due to at least two distinct causes, both of solar origin, as seems likely in view of the results given in § 2. 2. The observed variation is then given by the resultant $\mathbf{r}$ of the two vectors $\mathbf{a}$ and $\mathbf{b}$ which represent the variations due to the two different causes. If the amplitudes of $\mathbf{a}$ and $\mathbf{b}$ vary with season then although the phases of these components are constant the resultant $\mathbf{r}$ will in general vary in both phase and amplitude.

It is still possible however to separate the solar and sidereal effects under these circumstances provided observations are available from two stations at the same latitude, one in the southern hemisphere and one in the north. Provided the meteorological conditions are similar, any seasonal variations in amplitude or phase at the two stations will be six months out of phase. Consequently if the data from the two stations are combined any seasonal variation in the solar vector which is due to purely solar causes will be cancelled out and any remaining changes in amplitude and phase should be due to the presence of a true sidereal effect. It should be pointed out that a variation in the solar wave due to the annual change in the sun-earth distance would not be removed by this means, but since any effect of this kind is likely to be very small it can be neglected at any rate to a first approximation.

A second method of approach to the problem consists in using data from a station situated close to the equator where seasonal changes in the solar variation are likely to be small and therefore unlikely to produce a spurious sidereal variation of any appreciable magnitude.

On the basis of these considerations the ionization chamber data for Christchurch, Cheltenham and Huancayo has been examined for evidence of a sidereal variation by Elliot and Dolbear [1951]. The data for Christchurch (Lat. 43.5° S) and Cheltenham (Lat. 38.7° N) have been combined and the average apparent solar variation found for bi-monthly groups of data. The data for Huancayo which is fairly close to the equator (12° S) have also been divided into bi-monthly groups and the first harmonics evaluated for each group. The data used were those published by Lange and Forbush [1948], and they comprised 6 complete years of observations for Christchurch and Cheltenham and 9 years for Huancayo. The results are shown on a harmonic dial in Figure 17 where the points marked (1) correspond to the average for January and February those marked (2) to the average for March and April and so on. It will be seen that for both sets of data the end point of the solar vector shows a progressive anti-

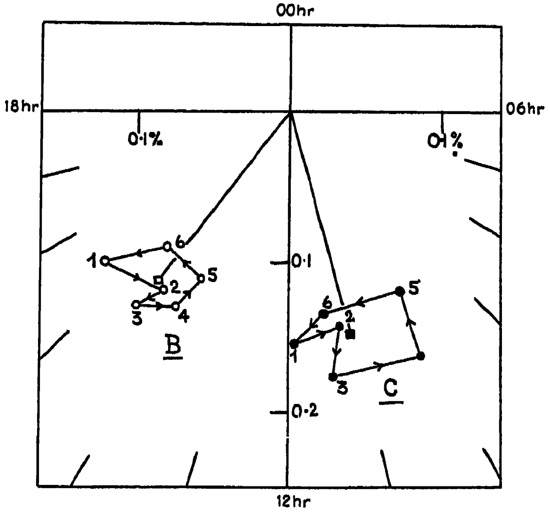

Fig. 17 – Solar time dial showing cyclic arrangement of bi-monthly means of the daily variation at Christchurch/Cheltenham (*B*) and Huancayo (*C*).

clockwise motion about the mean which is to be expected if there is a superimposed sidereal variation. The mean solar vector was then subtracted from the bi-monthly vectors shown in Figure 17 and the residual vectors were transferred to a sidereal dial shown in Figure 18. The mean sidereal variations also are shown together

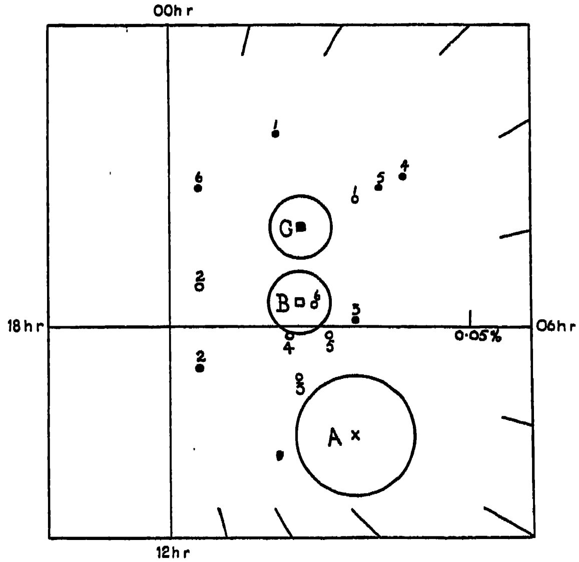

Fig. 18 – Sidereal time dial showing the mean daily variation for Manchester (*A*) Christchurch/Cheltenham (*B*) and Huancayo (*C*). Bi-monthly means are shown as ∘ for Christchurch/Cheltenham and as • for Huancayo.

with their appropriate standard deviation circles. Also shown on the dial is a point obtained by averaging the directional counter coincidence data for Manchester (see § 3. 2) according to sidereal time. With the arrangement used in Manchester it was possible to separate effects due to changes in atmosphere temperature and pressure from those produced by a non-isotropic primary flux by subtracting the daily variation for the north direction from that for the south. Consequently any seasonal changes in amplitude of the solar variation which arise from atmospheric effects could be eliminated. The Manchester point is in fair agreement with the other two and the agreement between the three results gives good grounds for believing that there is a sidereal variation of $\sim 0.02\ \%$ with a time of maximum at about 0500 h. L.S.T.

It is worthy of note that the phase of the variation at Huancayo is almost opposite to that expected from the Compton and Getting effect as calculated by Vallarta, Graef and Kusaka for positive primary particles and assuming that the primary spectrum follows on inverse cube law (see Table 3). This result implies, therefore, that there is either no Compton–Getting effect or that it is masked by something else. If we accept the former alternative as the most likely, it follows that the cosmic radiation must, to a large extent, originate within our own galaxy.

4. VARIATIONS ASSOCIATED WITH GEOMAGNETIC AND SOLAR ACTIVITY

4. 1 Magnetic storms and the cosmic ray intensity

The discovery of the geomagnetic latitude effect by Clay and its confirmation by Compton and his collaborators led to the general acceptance of the belief that the primary cosmic rays are charged particles. Since the latitude measurements showed that the intensity was to some extent controlled by the geomagnetic field it was natural that investigators should also look for variations in the intensity associated with the time variations of the earth's field. Thus MESSERSCHMIDT [1933] found a decrease of $\sim 1\ \%$ during a magnetic storm and STEINMAURER and GRAZIADEI [1933] found an average decrease of 0.3 % for 17 magnetic storms.

The first indication of a world-wide change in cosmic ray intensity at the time of a magnetic storm came in 1937 when Forbush published results from Cheltenham and Huancayo and Hess and Demmelmair for the Hafelekar. A decrease in the intensity of about 4 % occurred at each of these widely separated stations at the time of the great magnetic storm which began on the 24th April, 1937.

Figure 19 shows a similar occurrence reported by FORBUSH [1938b] for a storm beginning on January 16, 1938 when the cosmic ray intensity decreased by some 6 % and there appears to be quite a good correlation between the changes in H (the horizontal intensity of the earth's field) and those of the cosmic ray intensity. Figure 20, however, shows another magnetic storm of comparable magnitude which began on August 22nd, 1937 and which is not accompanied by any significant change in cosmic ray

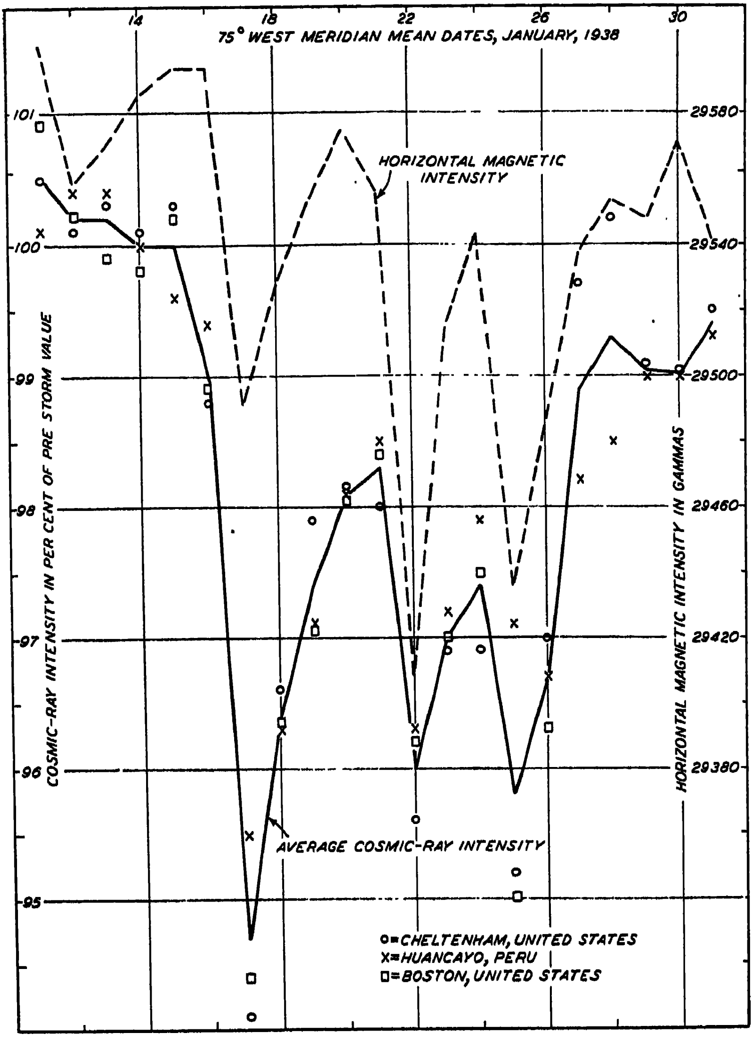

Fig. 19 – Cosmic ray intensity and the magnetic storm of January 16, 1938.

intensity at Huancayo or Cheltenham, although Hogg [1941] claims that a small change occurred at Canberra and Teoloyucan. It is clear that the changes in cosmic ray intensity cannot be directly interpreted in terms of the changes in the magnetic moment of the earth because of this marked difference in the effects of two storms of similar magnitude.

Hogg [1949] has shown that the changes in intensity associated with magnetic storms are invariably decreases and that the course of the disturbance is broadly similar to the storm time variation for *H*. That is to say, the initial decrease in the intensity is fairly sudden, followed by a rather slow recovery to normal which may take many days. He also concludes that the sharp decrease in intensity is delayed by a few hours relative to the onset of the magnetic storm. It is difficult to be quite certain about this since small changes in the intensity may be masked by statistical fluctuations, it seems true to say, however, that the largest changes in the cosmic ray intensity are often delayed relative to the correspondingly large changes in *H*. This can be clearly seen in Figure 21 which shows the variation in cosmic ray intensity in Manchester during the great magnetic storm which began on July 26th, 1946 (Dolbear and Elliot [1947]). It is evident that for this storm there is no detailed correspondence between the behaviour of *H* and the cosmic ray intensity. The increase in intensity on July 25th was associated with a solar flare and will be discussed in § 4. 3.

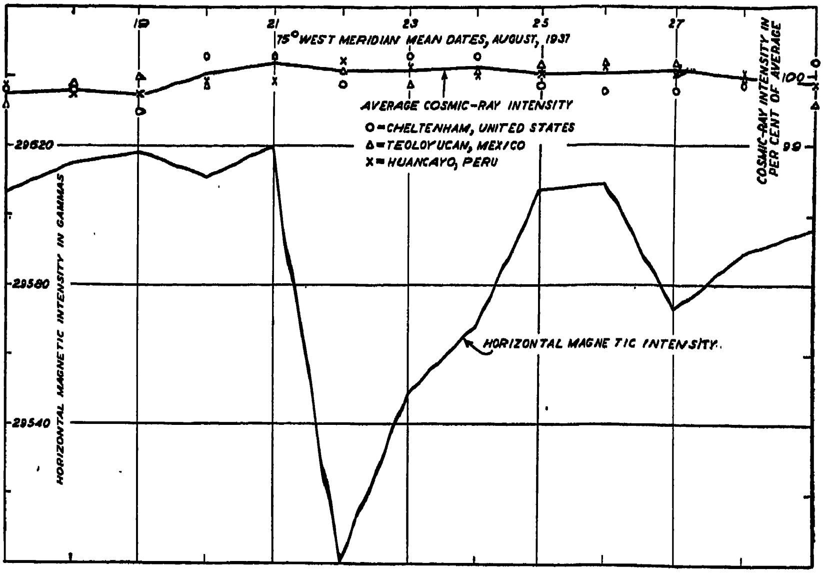

Fig. 20 – Cosmic ray intensity and the magnetic storm of August 21st 1937.

Chapman [1937] has suggested that decreases of cosmic ray intensity can be explained on the basis of a ring current of the kind postulated by Chapman and Ferraro in their theory of magnetic storms. According to this theory, the magnetic storm is due to the arrival in the neighbourhood of the earth of a stream of charged particles (electrons and positive calcium ions) which have been emitted from the sun. On entering the earth's magnetic field this stream, which is neutral as a whole, has currents induced in it and these currents are supposed to produce the short lived initial increase in *H* which generally precedes the main phase of the storm, during which *H* decreases below its normal value. This decrease in *H* during the main phase is ascribed to a ring current which is formed from the ionized stream due to the electrons and calcium ions moving round the earth in opposite directions and with different velocities. The radius of the ring is a few earth radii and the magnetic field of the ring current is opposed to that of

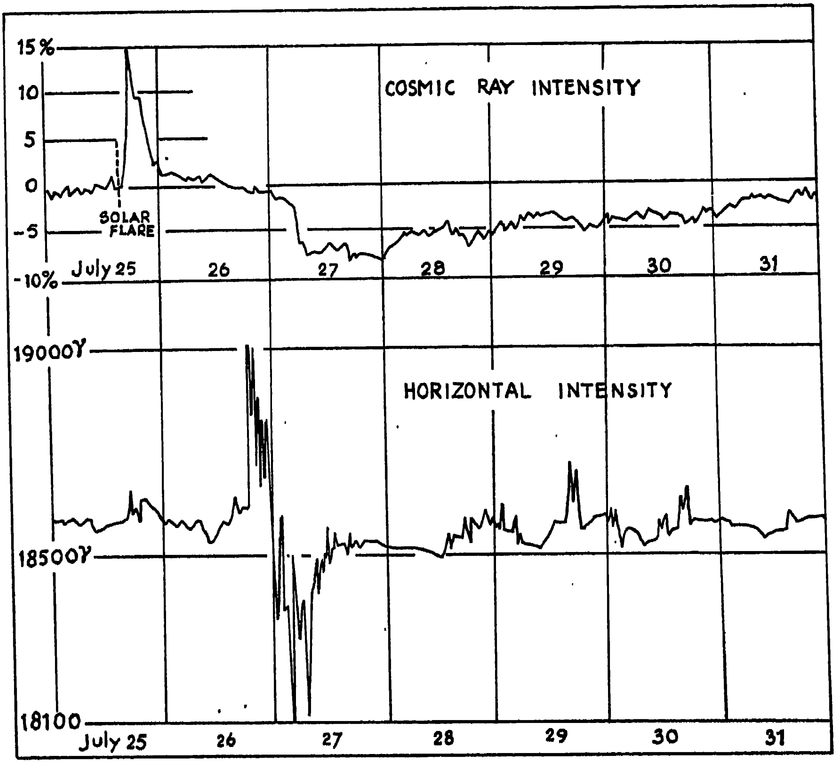

Fig. 21 – Variation in cosmic ray intensity at Manchester at the time of the solar flare of July 25th and the magnetic storm of July 26th 1946.

the earth in the region between the ring and the earth and thus produces the observed decrease in H at the surface of the earth. Outside the ring the earth's field is reinforced by the field due to the ring current. According to Chapman this increase in the field outside the ring deflects away some of the low energy primary cosmic rays so producing the observed decrease in intensity.

FORBUSH [1938] has calculated the radii and current intensities of the ring currents for several occasions on which he observed decreases in the cosmic ray intensity associated with magnetic storms. He concluded that if the radii lay between 2 and 16 earth radii it is possible to account for the observed changes including those magnetic storms which are not accompanied by any appreciable change in cosmic ray intensity. These occasions would correspond to ring currents of relatively low intensity flowing close to the earth. This configuration produces a relatively small change in magnetic moment compared with the change in H and therefore results in only a small change in the cosmic ray intensity although the observed change in H may be quite large.

JOHNSON [1938] has considered the case of a ring current flowing near the earth and has concluded that the magnetic moment of such a current is too small by a factor of 100 to account for the observed changes in cosmic ray intensity. He shows that if the radius of the ring current is very much greater than the radius of the earth this is certainly more favourable from the point of view of obtaining a large change in magnetic moment for a small change in H but it also has the result of producing a greater volume where H is decreased within the ring and where the incoming particles will be most deflected. Consequently if the radius of the ring is made too large the current will produce an *increase* rather than a decrease in intensity. This is borne out by the calculations of HAYAKAWA *et al.* [1950]. They show that the change in cosmic ray intensity produced by the ring current may be either positive or negative depending on whether the radius of the ring is assumed to be greater or smaller than 1.3 earth radii. This calculation was carried out for primary particles having momenta of 15 BeV/c and assuming a ring current of sufficient strength to produce a change of 100 gammas in the horizontal intensity.

These calculations by Johnson and by Hayakawa *et al.* throw some doubt on Chapman's interpretation of the effect in terms of a ring current and indicate that some other factor will probably have to be taken into account. Alfvén [1946 and 1949] has suggested that the decrease in intensity is due to the electric field which arises as a result of the motion of the corpuscular stream through the solar magnetic field. This electric field has already been mentioned briefly in § 2. 3 in relation to the solar daily variation. In order to account for changes of up to 10 % in the intensity, potential differences of the order 10^9 volts are required and this implies the existence of magnetic fields in interplanetary space which are considerably greater than that which could be produced by the solar dipole alone (Alfvén [1949]). Richtmeyer and Teller [1949] have also argued in favour of the existence of these magnetic fields ($\sim 10^{-5}$ gauss), which they suggest are responsible for confining the cosmic radiation to a comparatively small region round the sun of dimensions of the order 0.1 light years.

If electric fields of the magnitude envisaged by Alfvén do in fact exist, it would seem reasonable to expect large increases in the intensity to be produced sometimes during magnetic disturbances. However, decreases only are observed at these times, and although large increases do sometimes occur at the time of solar flares, as will be seen in § 4. 3, these two effects appear to be of quite different origin.

Whatever the mechanism for producing these large changes in intensity may turn out to be, it seems certain that it must have an important bearing on our understanding of magnetic storms and the aurora, and any theory of magnetic storms should be capable of accounting for these changes in cosmic ray intensity if it is to be entirely satisfactory.

4. 2 The 27-day recurrence tendency

It is no wwell known, ((Chree [1913] and Chree and Stagg [1928]), that magnetic disturbances of moderate intensity have a tendency to recur at intervals of 27 days corresponding to the period of rotation of the sun. It is also known that the cosmic ray intensity is to some degree associated with magnetic activity and this has led to a search for recurrence phenomena in the intensity records. The method of analysis which has been used is similar to that originally developed by Chree for his investigation of magnetic disturbances.

The procedure is as follows. The daily mean values of the intensity are first corrected to a constant barometric pressure, and the five days in each month on which the intensity is highest are then selected and the intensity on these days is written down in a vertical column numbered 0. The values of the intensity for the days following these selected zero days are then written down in sequence to the right of column 0 and are given the day numbers $N = 1, 2, 3$, etc. The data for the days preceding the zero day are tabulated in the same way to the left of column 0 and are given the day numbers $N = -1, -2, -3$, etc. The average value of the intensity is then found for each column and this is plotted on a graph against the corresponding day number N. A similar procedure is then followed for the five days in each month on which the intensity is lowest.

An analysis of this kind has been carried out by MONK and COMPTON [1939] for ionization chamber data from Teoloyucan, Mexico. The chamber was shielded by 10 cm. lead and the records extended from April 1937 to October 1938. The results are shown separately for positive and negative day numbers in Figures 22A and 22B together with the differences obtained by subtracting the ordinates for days of low intensity from those of high intensity. Figure 23 shows the final results obtained by folding the difference curves for the preceding days ($N < 0$) on to the succeeding portion of the curve ($N > 0$). These diagrams show quite clearly that there is a tendency for days of high or low cosmic ray intensity to recur at intervals of between 27 and 28 days. Similar results have been obtained by BROXON [1941] for data from Boulder and by HOGG [1949] for Canberra.

Whilst the recurrence interval for cosmic ray intensity appears to be the same as that found by Chree and Stagg for geomagnetic activity the phenomena differ in two respects:

(a) The curves for the geomagnetic data consist of rather sharp peaks with flat portions between them as shown in Figure 24, whereas the cosmic ray intensity shows an almost sinusoidal variation.

(b) The amplitudes of the peaks in geomagnetic activity decrease quite rapidly, each peak being about half the size of its predecessor. The cosmic ray pulses, on the other hand, persist with substantially the same amplitude over at least four intervals.

It should be pointed out that Chree and Stagg in their analysis used daily magnetic character figures which are not a measure of any particular magnetic element but indicate the degree of disturb-

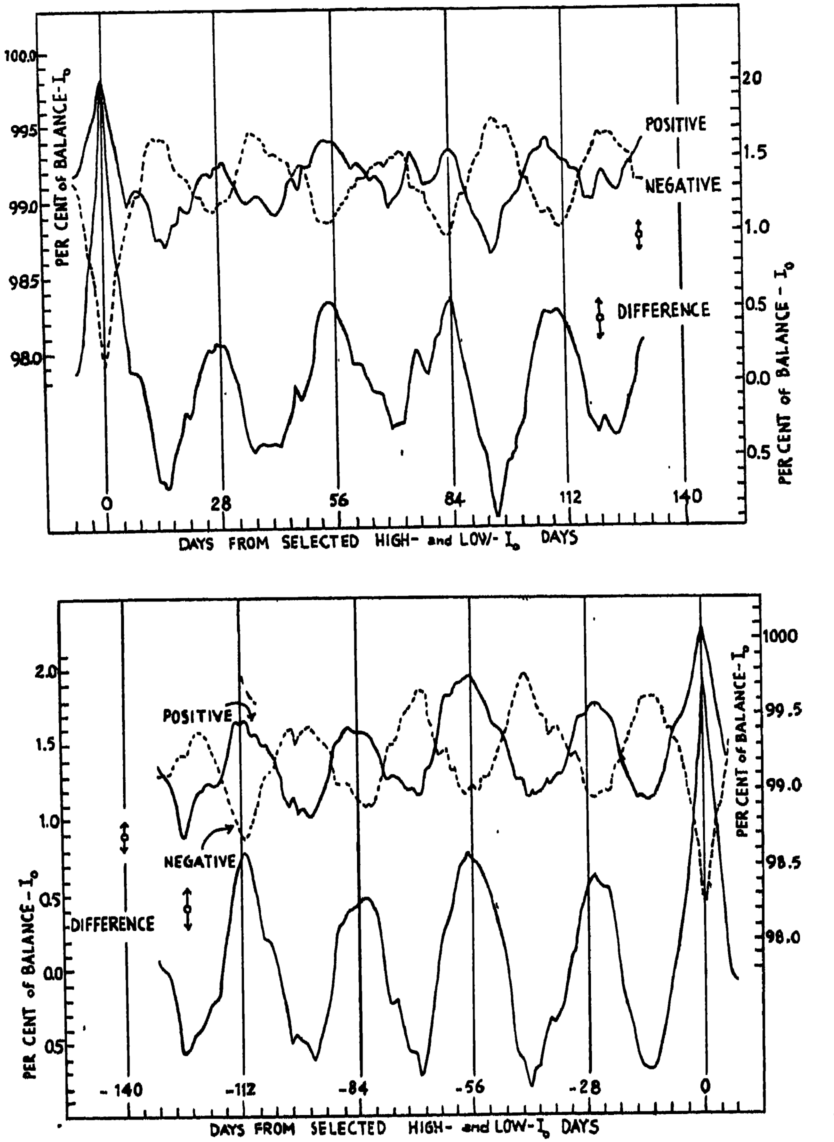

Fig. 22 – 27-day recurrence tendency for days of high and low cosmic ray intensity. (A) days following the zero day (B) days preceding the zero day.

ance. They interpreted the decreasing amplitude of their pulses as being due to a decrease in probability of recurrence the greater the number of intervals considered rather than to a decrease in amplitude of the disturbance itself. That is to say the life of the disturbing influence is not as a rule greater than 108 days and is in general less than this. On this basis the results given above would indicate that the life of the disturbing influence on cosmic ray intensity is long compared with 84 days since there is no appreciable decrease in pulse amplitude over this period. An alternative explanation is that the effect is a truly periodic variation rather than a recurrence phenomenon.

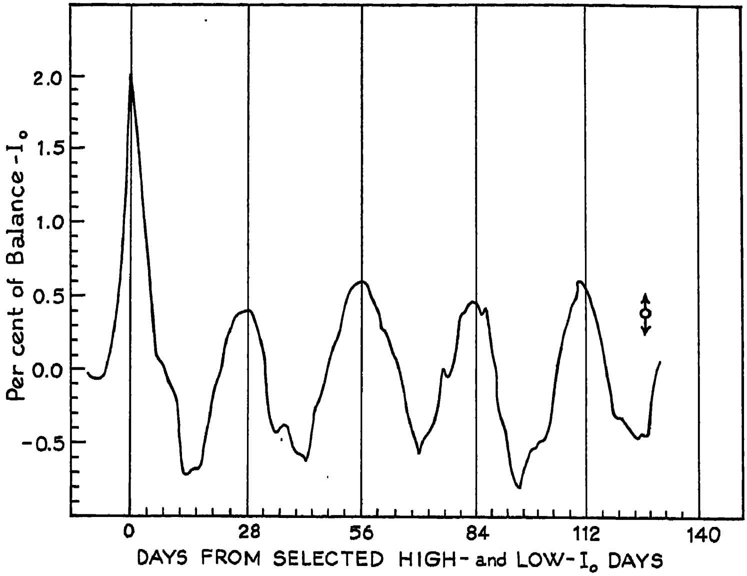

Fig. 23 – Combined difference pulses from Fig. 22A and 22B reversed.

Vallarta and Godart [1939] have pointed out that if the sun's magnetic dipole does not coincide with the solar axis of rotation this should produce a 27 day periodicity in the cosmic ray intensity, since the heliomagnetic latitude of the earth will change with a period of 27 days. Assuming a value of 10^{34} gauss cm^3 for the magnetic moment of the sun, they estimate an amplitude for this variation of 0.2 % at geomagnetic latitude 40° and 0.4 % at geomagnetic latitude 50°.

A truly periodic variation of this kind, as opposed to the recurrence tendency discussed above, has been the subject of a number of investigations. HESS [1936] from an analysis of the ionization chamber data for the Hafelekar found a 27 day periodicity with an amplitude of 0.3 %. KOLHÖRSTER [1939] found a variation with an amplitude of 0.5 % and having a maximum on the 25th day of the rotation according to the BARTELS [1939] numbering system. WAFFLER [1941] and BROXON [1942] have found variations with an amplitude of 0.4 % and 0.2 % respectively. The times of maximum corresponded to the 4th and 5th days of the Bartels' rotation. GHERI and STEINMAURER [1947] have analysed the Hafelekar results using the data for 30 complete solar rotations between Nos. 1410—1488. They found a variation having an amplitude of ~ 0.1 % with a time of maximum on the 3rd day of the rotation. These results all show a certain consistency in that the amplitudes in each case lie within the range 0.1 % to 0.5 % and the times of maximum are within a few days of each other, i.e. on day numbers — 2, + 4, + 5 and + 3 of the rotation.

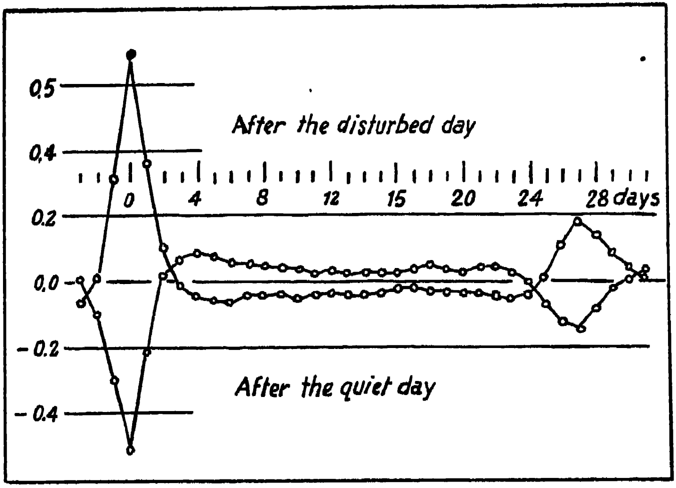

Fig. 24 – The 27-day recurrence tendency in geomagnetic activity.

HOGG [1949] also finds some evidence for a 27 day wave in the Canberra data when these are averaged according to solar rotations. A more rigorous treatment, however, using a harmonic dial on which are plotted the first harmonics of the variation for each individual rotation, fails to confirm the existence of this 27-day wave. The very extensive data used by Hogg in this analysis covered a total of 66 solar rotations (1402—1467). FORBUSH and LANGE [1949] have analyzed some ten years of ionization chamber data and they also find no evidence for a persistent 27-day wave.

In view of the present evidence the existence of a true 27-day periodicity must be regarded as uncertain but there is no doubt that the intensity does show a 27-day recurrence tendency. This recurrence tendency differs in some respects from that for magnetic disturbances and these differences may be taken as a further indication that whilst there is a relationship between cosmic ray disturbances and geomagnetic activity the two are not directly connected.

4. 3 Increases of intensity associated with solar flares

Between February 28 and March 7, 1942 a remarkable series of changes in the cosmic ray intensity were observed simultaneously at a number of widely separated points on the earth. Figure 25 shows these intensity variations as given by LANGE and FORBUSH [1942] for Godhavn (Greenland), Cheltenham (U.S.A.), Christchurch (New Zealand), Teoloyucan (Mexico) and Huancayo (Peru). Similar results have also been published by DUPERIER [1945] for London, EHMERT [1948] for Friedrichshafen, CLAY [1949] for Amsterdam and by BERRY and HESS [1942] for Norfolk (U.S.A.).

It will be seen from Figure 25 that a sudden increase in the intensity occurred at 1400 h. U.T. on the 28th February which was observed at Godhavn, Cheltenham and Christchurch but not at Teoloyucan or at Huancayo. The increase did not occur at Friedrichshafen or Amsterdam, and in London it amounted to less than 1 %.

The increase lasted for a few hours only and was followed on the 1st March by a large decrease of between 8 and 10 % which was observed at all the stations listed above without exception. Following this sharp decrease the intensity recovered slowly towards its normal value over the next five or six days until March 7th when another increase in intensity occurred at all the stations except Huancayo (no record is given for Teoloyucan). The magnitude of this increase varied from 6 % at Christchurch to 30 % at Friedrichshafen maximum intensity being reached at about 0600 h. U.T.

These changes in intensity were associated with an unusually high degree of solar activity and a great geomagnetic storm

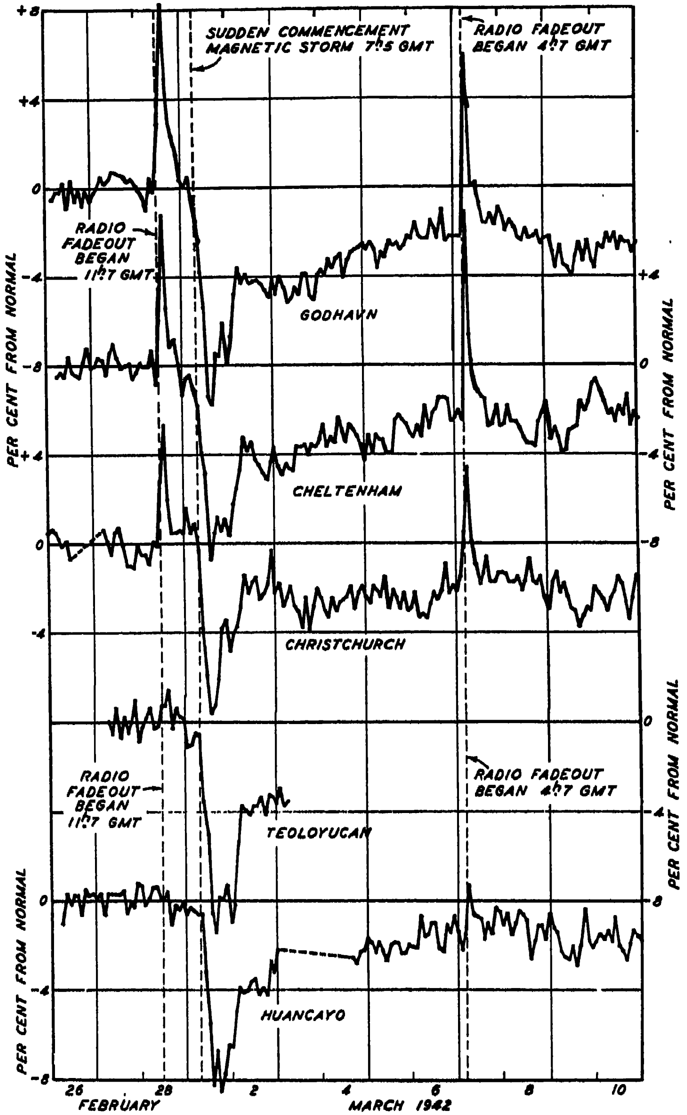

INCREASES OF COSMIC RAY INTENSITY, FEBRUARY 28 AND MARCH 7, 1942

Fig. 25 -- World wide changes in cosmic ray intensity associated with solar and magnetic activity.

(NEWTON [1942]). At this time there was a large group of spots on the sun which, according to the Mount Wilson solar and magnetic data, had a maximum area of 2000 millionths of the sun's hemisphere. The two largest umbrae in the group had opposite magnetic polarities and had a maximum field of about 4800 gauss. At approximately 1200 h. U.T. on the 28th February there occurred a sudden radio fade-out of the kind usually associated with the presence of a solar flare and at about 1240 h. the flare was observed visually in the neighbourhood of the sunspot group which was then about 6 hours prior to transit across the central meridian of the sun at latitude 14° N. This flare was last seen at 1525 h. and it therefore lasted for about 3½ hours. As often happens when an intense flare occurs near the centre of the sun's disc, about a day later, at 0727 h. on March 1st, a geomagnetic storm began. The change in H amounted to $\sim$ 512 gammas and was accompanied by the decrease in cosmic ray intensity. This is clearly a further example of the effect discussed in § 4. 1.

The increase on March 7th seems to have been associated with a radio fade-out which occurred at 0407 h. U.T. on that day, and it seems likely that this was due to a solar flare which was not observed visually. There is no evidence of either a magnetic storm or any further decrease in cosmic ray intensity following this fade-out. It is worthy of note that the increase on March 7th was observed at all the stations mentioned above with the exception of Huancayo. (No record is available for Teoloyucan).

No further increase in intensity of this kind occurred until 1946. On July 25th of that year an intense flare appeared over the large bi-polar sunspot group which was then about 15° E of the central meridian. This flare was observed at Mt. Wilson and also at Edinburgh by ELLISON [1946]. It was first seen by ELLISON at 1620 h. when the line width of H_α was observed to be about 6.5 Å. There then followed a sudden burst of radiation which reached its maximum intensity at 1627 h., the line width at that time being at least 15 Å. This burst lasted only two or three minutes and was followed by a slow decay until at 1820 h. only a few traces remained. This flare was followed by a magnetic storm which began at 1846 h. on July 26th. The cosmic ray intensity recorded in Manchester during this period is shown in Figure 21. It will be seen that a sudden increase of about 13 % occurred shortly after the flare. It is difficult to give a precise estimate of the time at which the increase began, because of statistical fluctuations, but there appears to have been a delay of about 40 minutes between the beginning of the flare and the increase in cosmic ray intensity.

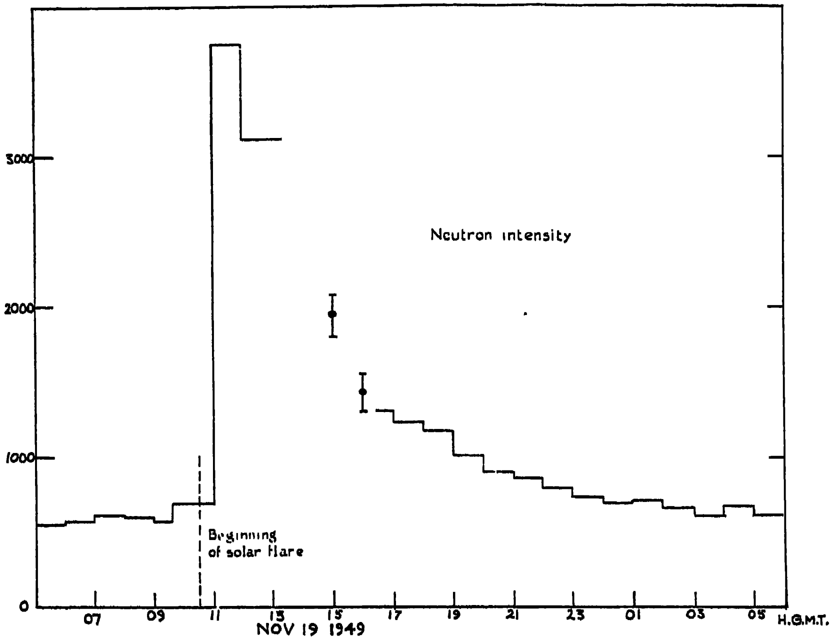

Fig. 26 – Variation in neutron intensity in Manchester at the time of the solar flare of November 19, 1949.

The peak cosmic ray intensity was not reached until about 1½ hours after the flare reached its maximum intensity. A decrease of about 8 % occurred at the time of magnetic storm which followed on the 26th. The changes in intensity on July 25th and 26th were also observed at several other stations [2].

November 19th 1949 was the next, and, at the time of writing, most recent occasion on which a large increase was observed. A radio fade-out began on that day at 1030 h. U.T. and a solar flare was observed at this time in Edinburgh by Ellison and Conway [1950]. The flare began at 1029 h., reached its peak intensity at 1032 h. and then slowly decayed until 1209 h. when all visible radiation ceased. The maximum line width of H_α on this occasion was 22.9 Å, the greatest so far recorded. The flare appeared over a sunspot group at heliographic longitude 70° W and latitude 2° S.

---

[2] See for example Forbush, Phys. Rev. 1946, 70, 771; Clay, Proc. K. Ned. Akad. v. Wet., 1949, 52, 899.

Forbush, Stinchcomb and Schein [1950] reported an increase in cosmic ray intensity at this time amounting to 30 % at Godhavn and 40 % at Cheltenham, whilst at Climax, Colorado (altitude 3,500 m.) the intensity increased by 180 %. The increase at Climax began at 1045 h. U.T. and maximum intensity was reached between 1045 h. and 1100 h. As on the three previous occasions, no increase was observed at Huancayo. From a comparison of the magnitude of the increase at Climax with that at Cheltenham these authors deduced an absorption coefficient of 1/137 $\text{gm}^{-1}\text{cm}^2$ for the particles responsible for the increase. In view of this they concluded that the increase must be due to nucleons rather than mesons which would be absorbed much more slowly.

Observations were also made at this time at Resolute (Lat. 75° N, Long. 95° W) and at Ottawa, using similar counter arrays (Rose [1950]). In Ottawa the intensity increased by 70 % beginning at 1048 h. U.T. and reaching its maximum at 1054 h. At Resolute (geomagnetic latitude 83° N) the increase amounted to only 12 to 15 %, the maximum being reached at 1154 h. U.T. which is about 50 minutes later than at Ottawa.

An increase of about 11 % was observed in Manchester at this time with an unshielded threefold counter coincidence set. This increase, like that recorded at Resolute, was therefore substantially smaller than that observed at Godhavn, Ottawa and the American stations. Furthermore, the time of maximum was about 1130 h. U.T., which again, as at Resolute, was later than that for the other stations mentioned above. Increases ranging between 10 and 20 % were also observed at four stations in Germany (Dieminger *et al.* [1950]), and here again the increase appears to have begun shortly before 1100 h., maximum intensity being reached at approximately 1130 h. Dauvillier [1949] reported an increase of 3.6 % at Bagnères which began at 1130 h. and reached its maximum at 1200 h. U.T. It is clear from these results that there was a delay of approximately half an hour between the times of maximum intensity at Climax and Ottawa on the one hand and Resolute and the European stations on the other. In addition the magnitude of the increase observed in Europe and at Resolute was markedly smaller than that observed at Ottawa, Godhavn and the American stations.

A neutron intensity recorder which was in operation in Manchester at this time showed that the intensity of the neutron component increased to about six times its normal value (ADAMS [1950]). This recorder consisted of two counters, filled with boron trifluoride, operating in the proportional region and placed near the centre of a graphite "pile". It detected neutrons with an incident energy of up to about 10 MeV. The variation in neutron intensity observed at this time is shown in Figure 26 and it will be seen that the maximum rate occurred during the period 1100—1200 U.T. after which the intensity fell gradually to its normal value in about 12 hours. In discussing these results ADAMS and BRADDICK [1950] point out that the most interesting feature of these observations is the very large increase in neutron intensity relative to the ionizing component which increased by only 11 % in Manchester. Whilst fast neutrons from the sun could reach the earth without suffering too great a loss due to decay, it is clear that the increase cannot have been due to primary neutrons from the sun since it persists after sunset. It seems likely that the neutrons are produced in the atmosphere by charged primaries, and Adams and Braddick have pointed out that if the charged primaries are protons with momenta between 2 and 5 BeV/c, any mesons which they produce will be of rather low energy and therefore rapidly absorbed in the atmosphere. Secondary neutrons, on the other hand, are absorbed exponentially and some of them will therefore reach sea-level. Consequently, it is to be expected that an increase in the primary proton intensity in this momentum range would produce a large increase in the neutron intensity relative to the ionizing intensity at sea-level. This assumption of low momentum primaries fits in with the absence of any increase at Huancayo on the magnetic equator where the threshold momentum is about 10 BeV/c.

In addition to the four occasions discussed above, when increases were observed at widely separated points, some observers have reported comparatively large numbers of these occurrences. For instance EHMERT [1948] in Germany observed many such increases in the period 1941—'43, and CLAY [1949] has also observed many. Both of these workers find that a substantial proportion of the increases were associated with solar flares.

LORD, ELSTON and SCHEIN [1950] have reported an increase in the frequency of star production which may have been associated with a solar flare. The increase was observed as a result of a balloon flight which took place between 1840 h. and 2330 h. U.T. on May 11th, 1949, about 24 hours after the occurrence of an intense flare. The number of stars in the photographic plates with 3 to 8 prongs was 50 % above normal. No change in the ionizing component at sea-level has been reported at this time and none was observed at Boulder, Colorado at an altitude of 5,400 ft. (BROXON and BOEHMER [1950]).

Before discussing the interpretation of these increases it is convenient to summarize their most important characteristics which are as follows:

(a) Increases in intensity which are observed simultaneously at widely separated points on the earth are of rather infrequent occurrence. Only four such increases have been observed in the past fifteen years.

(b) The increases are associated with exceptionally intense solar flares and there is a delay of approximately an hour between maximum flare intensity and maximum cosmic ray intensity.

(c) On neither of the four occasions has any appreciable increase in intensity been observed at Huancayo near the geomagnetic equator. This indicates that the primary particles responsible for the increase have momenta less than 10 BeV/c.

(d) On any particular occasion the magnitude of the effect differs for stations at different longitudes.

(e) The magnitude of the effect increases rapidly with height above sea-level.

(f) On the one occasion for which observations are available, the neutron intensity increased very much more than did the ionizing component.

These large increases in intensity are of particular interest since they clearly represent occasions on which particles can acquire energies of up to about 5 BeV somewhere on or in the neighbourhood of the sun. The interpretation of this effect must therefore have an important bearing on any theory of the origin of the cosmic radiation. Several mechanisms have been suggested whereby charged particles might be accelerated to these energies, and they are discussed very briefly below.

ALFVÉN [1946 and 1949] has suggested that the particles are accelerated in the electric fields associated with solar corpuscular streams which are polarized as a result of their motion through the solar magnetic field. This mechanism depends on the existence of a permanent solar magnetic field and has already been mentioned in § 2. 3 in relation to the daily variation.

EHMERT [1948] has pointed out that the particles may be accelerated by the betatron action of the changing magnetic field of a growing sunspot. The possibility of particles being accelerated to cosmic ray energies in this way was first suggested by SWANN [1933]. BAGGE and BIERMANN [1948] have also suggested that the particles may be accelerated in the magnetic fields of sunspots. They suppose the acceleration to be due to the electric field produced by the relative motion of two spots rather than to changes in the intensity of the fields themselves.

MENZEL and SALISBURY [1948] have suggested that low frequency electromagnetic waves may be produced as a result of fluctuations in sunspot magnetic fields brought about by turbulence in the solar atmosphere. This radiation is supposed to have frequencies in the region 1000 to 0.01 cycles/second and to be propagated outwards from the sun. Charged particles are then supposed to be accelerated by the electric fields of these waves. This mechanism has been examined in some detail by MCMILLAN [1950], and he concludes, however, that because of the high conductivity such waves could not be propagated in inter-planetary space although they might exist in a very limited region at the edge of the solar corona.

FORBUSH, GILL and VALLARTA [1949] have pointed out that if the sun has a general magnetic field of ~ 25 gauss, particles of momentum less than 10 BeV/c cannot escape from the surface of the sun except at high latitudes. However, the flares and sunspots associated with the increases in intensity which have been recorded did in fact occur quite close to the equator. In order to explain the emission of particles of this energy from the equatorial region of the sun, they suggest that the magnetic field of a bi-polar sunspot group may produce a "tunnel" by means of which comparatively low energy particles can escape through the general solar field. The existence of this tunnel depends on the relative strengths and orientations of the general dipole field and the sunspot field. These rather special requirements might account for the comparative rarity of the phenomenon.

KIEPENHEUER [1950] has criticised the above suggestions on the grounds that the conductivity close to the surface of the sun is too high for any strong electric fields to exist in the neighbourhood of sunspots, and he favours the view that the electric field is produced well outside the solar atmosphere where the conductivity is much lower. The field is produced in the following way. A corpuscular stream emitted from the neighbourhood of a bi-polar sunspot group at the time of a flare will have currents induced in it such as to maintain the magnetic field inside the stream at its original value. Because of the high conductivity, these currents, once set up, will persist for a long time and the stream can be regarded as being "magnetized". According to Kiepenheuer this magnetized beam will be surrounded by a thin sheet of shielding current formed by ionized interplanetary matter and he estimates that the induced potential difference which causes this current to flow should be of the order $10^{10} - 10^{11}$ volts. He interprets the observed delay of about an hour between the maxima for the flare and cosmic ray intensities as being due to the time of formation and travel of the stream from the chromosphere to the outer regions of the corona where the conductivity is comparatively low and the particles can acquire high energies.

The observational data are at present so limited that they offer little guidance as to which, if any, of these suggestions is likely to be correct but whatever the final interpretation may be, there can be little doubt that it will be of importance for the interpretation also of the more general problems of the origin of cosmic radiation.

APPENDIX

Geographic and geomagnetic co-ordinates of cosmic ray intensity recording stations. (Heights above sea-level are only given when stations are at altitudes greater than 500 m.)

Station	Geographic Latitude	Geographic Longitude	Geomagn. Latitude	Height above Sea level (m.)
Amsterdam . . .	52° N	5° E	54° N	
Bagnères	43° N	0	46° N	550
Boulder	40° N	105° W	49° N	1600
Canberra	35° S	149° E	45° S	800
Cheltenham . . .	39° N	77° W	50° N	
Christchurch . . .	43° S	173° E	49° S	
Climax	39° N	106° W	48° N	3500
Friedrichshafen. .	47° N	9° E	49° N	
Godhavn	69° N	53° W	80° N	
Hafelekar	47° N	11° E	48° N	2300
Huancayo	12° S	75° W	1° S	3350
London	51° N	0	54° N	
Manchester . . .	53° N	2° W	57° N	
Ottawa	45° N	76° W	56° N	
Resolute.	75° N	95° W	83° N	
Stockholm	59° N	18° E	58° N	
Teoloyucan. . . .	19° N	99° W	30° N	2285
Tokyo.	36° N	140° E	25° N	

REFERENCES

Adams, N., 1950, Phil. Mag., 41, 503.

Adams, N. and H. J. J. Braddick, 1950, Phil. Mag., 41, 505.

Alfvén, H., 1946, Nature, Lond., 158, 618.

Alfvén, H., 1947, Phys. Rev., 72, 88.

Alfvén, H., 1949, Phys. Rev., 75, 1732.

Alfvén, H. and K. G. Malmfors, 1943, Ark. Mat. Astr. Fys., 29A, No. 24.

Bagge, E. and L. Biermann, 1948, Naturwiss., 35, 120.

Bartels, J., 1939, Terr. Magn. Atmos. Elect., 44, 411.

Benedetto, F. A., 1946, Phys. Rev., 70, 817.

Bergstralh, T. A. and C. A. Schroeder, 1951, Phys. Rev., 81, 244.

Berry, E. B. and V. F. Hess, 1942, Terr. Magn. Atmos. Elect., 47, 251.

Blackett, P. M. S., 1938, Phys. Rev., 54, 973.

Broxon, J. W., 1941, Phys. Rev., 59, 773.

Broxon, J. W., 1942, Phys. Rev., 62, 508.

Broxon, J. W. and H. W. Boehmer, 1950, Phys. Rev., 78, 411.

Chapman, S., 1937, Nature, Lond., 140, 423.

Chree, C., 1913, Phil. Trans., A212, 76.

Chree, C. and J. M. Stagg, 1928, Phil. Trans. A227, 21.

Clay, J., 1949a, Proc. K. Ned. Akad. Wet., 52, 923.

Clay, J., 1949b, Proc. K. Ned. Akad. Wet., 52, 906.

Compton, A. H., R. D. Bennett and J. C. Stearns, 1932, Phys. Rev., 41, 119.

Compton, A. H., E. O. Wollan and R. D. Bennett, 1934, Rev. Sci. Inst., 5, 415.

Compton, A. H. and I. A. Getting, 1935, Phys. Rev., 47, 817.

Compton, A. H. and R. N. Turner, 1937, Phys. Rev., 52, 799.

Dauvillier, A., 1949, C. R. Acad. Sci. Paris, 229, 1096.

Dieminger, W. *et al.* 1950, J. Atmos. Terr. Phys., 1, 37.

Dolbear, D. W. N. and H. Elliot, 1947, Nature, Lond., 159, 58.

Dolbear, D. W. N. and H. Elliot, 1950, Nature, Lond., 165, 353.

Dolbear, D. W. N. and H. Elliot, 1951. J. Atmos. Terr. Phys. 1, 215

Duperier, A., 1944, Terr. Magn. Atmos. Elect., 49, 1.

Duperier, A., 1945, Proc. Phys. Soc., 57, 468.

Duperier, A., 1946, Nature, Lond., 158, 196.

Duperier, A., 1949, Proc. Phys. Soc., A62, 684.

Duperier, A., 1951, Nature, Lond., 167, 312.

Dwight, K., 1950, Phys. Rev., 78, 40.

Ehmert, A., 1940, Naturwiss., 28, 28.

Ehmert, A., 1948, Z. Naturforsch., 3a, 264.

Elliot, H. and D. W. N. Dolbear, 1950, Proc. Phys. Soc., 63, 137.

Elliot, H. and D. W. N. Dolbear, 1951, J. Atmos. Terr. Phys. 1, 205

Ellison, M. A., 1946, Nature, Lond., 158, 450.
Ellison, M. A. and M. Conway, 1950, Observatory, 70, 77.
Forbush, S. E., 1937a, Phys. Rev., 52, 1254.
Forbush, S. E., 1937b, Phys. Rev., 51, 1108.
Forbush, S. E., 1938a, Phys. Rev., 54, 975.
Forbush, S. E., 1938b, Terr. Magn. Atmos. Elect., 43, 207.
Forbush, S. E., 1939, Rev. Mod. Phys., 11, 168.
Forbush, S. E., 1946, Phys. Rev., 70, 771.
Forbush, S. E., P. S. Gill and M. S. Vallarta, 1949, Rev. Mod. Phys., 21, 44.
Forbush, S. E. and I. Lange, 1949, Phys. Rev., 76, 164.
Forbush, S. E., T. B. Stinchcomb and M. Schein, 1950, Phys. Rev., 79, 501.
Gheri, H. and R. Steinmaurer, 1947, Terr. Magn. Atmos. Elect., 52, 343.
Gill, P. S., 1939, Phys. Rev., 55, 429.
Hayakawa, S. *et al.*, 1950, J. Geophys. Res., 55, 221.
Hess, V. F., 1936, Terr. Magn. Atmos. Elect., 41, 345.
Hess, V. F., H. Graziadei and R. Steinmaurer, 1935, S. B. Akad. Wiss. Wien, 144, 53.
Hess, V. F. and H. T. Graziadei, 1936, Terr. Magn. Atmos. Elect., 41, 9.
Hess, V. F. and A. Demmelmair, 1937, Nature, Lond., 140, 316.
Hess, V. F., 1939, Rev. Mod. Phys., 11, 153.
Hogg, A. R., 1941, Terr. Magn. Atmos. Elect., 46, 51.
Hogg, A. R., 1947, Proc. Roy. Soc., A192, 128.
Hogg, A. R., 1949, Memoirs of the Commonwealth Observatory, Canberra, No. 10.
Hogg, A. R., 1950, J. Atmos. Terr. Phys., 1, 114.
Jánossy, L., 1937, Z. Phys., 104, 430.
Johnson, T. H., 1938, Rev. Mod. Phys., 10, 193.
Kane, E. O., T. J. B. Shanley and J. A. Wheeler, 1949, Rev. Mod. Phys., 21, 51.
Kiepenheuer, K. O., 1950, Phys. Rev., 78, 809.
Kolhörster, W., 1939, Phys. Zs., 40, 107.
Kolhörster, W., 1941, Phys. Zs., 42, 55.
Lange, I. and S. E. Forbush, 1942, Terr. Magn. Atmos. Elect., 47, 331.
Lange, I. and S. E. Forbush, 1948, Carnegie Institution of Washington, Publication 175.
Lindholm, F., 1928, Gerl. Beitr. Z. Geophys., 20, 12.
Lord, J. J., A. W. Elston and M. Schein, 1950, Phys. Rev., 79, 540.
Malmfors, K. G., 1948, Ark. Mat. Astr. Fys., 32A, No. 8.
McMillan, E. M., 1950, Phys. Rev., 79, 498.
Menzel, D. H. and W. W. Salisbury, 1948, Nucleonics, 2, No. 4, 67.
Messerschmidt, W., 1933, Z. Phys., 85, 332.
Messerschmidt, W. and W. S. Pforte, 1932, Z. Phys., 73, 677.
Monk, A. T. and A. H. Compton, 1939, Rev. Mod. Phys., 11, 175.
Myssowsky, L. and L. Tuwim, 1928, Z. Phys., 50, 273.
Newton, H. W., 1942, Observatory, 64, 260.
Nicolson, P. and V. Sarabhai, 1948, Proc. Phys. Soc., 60, 509.

PEKERIS, C. L., 1937, Proc. Roy. Soc., A158, 650.
PEKERIS, C. L., 1939, Proc. Roy. Soc., A171, 634.
RAU, W., 1939, Z. Phys., 114, 265.
RAU, W., 1940, Z. Phys., 116, 105.
RICHTMEYER, R. D. and E. TELLER, 1949, Phys. Rev., 75, 1729.
ROSE, D. C., 1950, Phys. Rev., 78, 181.
SEKIDO, Y. and S. YOSHIDA, 1950, Report on Ionospheric Res. in Japan, 4, 37.
SCHONLAND, B. F. J., B. DELATIZKY and J. GASKELL, 1937, Terr. Magn. Atmos. Elect., 42, 137.
STEINMAURER, R. and H. T. GRAZIADEI, 1933, S. B. Akad. Wiss. Wien, 22, 672.
SWANN, W. F. G., 1933, Phys. Rev., 43, 217.
THOMPSON, J. L., 1939, Phys. Rev., 55, 11.
VALLARTA, M. S. and O. GODART, 1939, Rev. Mod. Phys., 11, 180.
VALLARTA, M. S., C. GRAEF and S. KUSAKA, 1939, Phys. Rev., 55, 1.
WAFFLER, H., 1941, Helv. Phys. Acta, 14, 248.
WEEKES, K. and M. V. WILKES, 1947, Proc. Roy. Soc., A175, 143.

AUTHOR INDEX

Aamodt, L.
1950: ———, J. Hadley, W. Panofsky, Phys. Rev. 80, 282. *150.*
see W. Panofsky.
Abragham, A.
1951: ——— and J. J. Horowitz. Private communication. *162.*
Adams, N.
1950: ——— Phil. Mag. 41, 503. *507.*
1950: ——— and H. J. J. Braddick, Phil. Mag. 41, 505. *507.*
Addario, M.
1949: ——— and S. Tamburino, Phys. Rev. 76, 983. *379.*
1950: ——— and S. Tamburino, Phys. Rev. 80, 749. *358, 359.*
Aidzu, K.
1950: ———, Y. Fujimoto, H. Fukuda, S. Hayakawa, K. Takayanagi, G. Takada, Y. Yamaguchi, Progr. Theor. Phys. 5, 931. *152.*
Alford, W. L.
see R. B. Leighton.
Alfven, H.
1939: ———, Nature, Lond., 143, 435. *194.*
1946: ———, Nature, Lond., 158, 618. *497, 509.*
1949: ———, Phys. Rev. 75, 1732. *477, 497, 509.*
1947: ———, Phys. Rev. 72, 88. *481.*
1943: ———, and K. G. Malmfors, Ark. Mat. Astr. Fys. 29A, no. 24. *472.*
Alikhaniyan, A. I.
1948: ———, A. I. Alikhanov, A. Weissenberg, J. Exp. Theor. Phys. U.S.S.R., 18, 301. *66.*
1949: ———, E. M. Samoilovich, I. I. Gurevich, K. P. Babayan, J. Exp. Theor. Phys. U.S.S.R , 19, 667. *129.*
Alikhanov, A. I.
see A. I. Alikhaniyan.
Allen, J. S.
1949: ———, H. R. Paneth, A. H. Morrish, Phys. Rev. 75, 570. *171.*
see H. R Paneth.
Anderson, C. D.
1932: ———, Science, 76, 238. *127.*
1934: ——— and S. Neddermeyer, Int. Conf. Phys. Lond., 177. *342.*
1949: ———, R. B. Leighton, A. J. Seriff, Phys. Rev. 75, 1466. *381.*
——— ——— *357.*
see R. B. Leighton; A. J. Seriff.
Angus, J.
see S. C. Curran.

Annis, M.
see H. S. Bridge.
Araki, G.
1950: ———, Progr. Theor. Phys. 5, 507. *149.*
see S. Tomonaga.
Arley, N.
1948: ———, Stochastic Processes (New York: Wiley & Sons, 2nd. Ed.) *352.*
Armenteros, R.
1951: ———, K. H. Barker, C. C. Butler, A. Cachon, A. H. Chapman, Nature, Lond., 167, 501. *65, 68, 85, 157.*
Ascoli, G.
1950: ———, Phys. Rev. 79, 812. *370.*
Ashkin, J.
1950: ———, A. Simon, R. E. Marshak, Progr. Theor Phys 5, 634. *152.*
Astbury, P.
1951: ———, P. Chippindale, J. A. Newth, A. B. Sahiar, Private communication. *65, 68, 70.*
Auger, P.
1936: ——— and T. Meyer, C. R. Acad. Sci., Paris, 203, 246. *398, 439.*

Babayan, K. P.
see A. I. Alikhaniyan.
Bagge, E.
1941: ———, Ann. Phys. Lpz. 39, 512. *40, 41.*
1944: ———, Physik. Zeit. 21, 461. *45.*
1948: ——— and L. Biermann, Naturwiss. 35, 120. *509.*
——— *45.*
Barber, W. C.
1949: ———, Phys. Rev. 75, 590. *325, 350.*
Barkas, W. H.
see F. M. Smith.
Barker, K. H.
1951: ——— and C. C. Butler, Proc. Phys. Soc. A64, 4. *68, 83.*
see R. Armenteros; C. C. Butler.
Barnothy, J.
1939: ——— and M. Forro, Phys. Rev. 55, 870. *331, 399.*
1940: ——— and M. Forro, Phys. Rev. 58, 844. *331, 399, 407.*
1948: ——— and M. Forro, Phys. Rev. 74, 1300. *399.*
Barrett, J. H.
1950: ———, Phys. Rev. 79, 907. *160.*
Bartels, J.
1939: ———, Terr. Magn. Atmos. Elect. 44, 411. *501.*
1940: ——— and S. Chapman, Geomagnetism (Oxford Univ. Press) *247.*
Barton, H. M.
1951: ———, E. P. George, A. C. Jason, Proc. Phys. Soc. A64, 175 *361*

- BASSI, P.
  - 1949: ———, E. Clementel, I. Filosofo, G. Puppi, Nuovo Cim. **6**, 484. *345.*
  - 1951: ———, Nuovo Cim. **8**, 469. *347.*
- BENEDETTO, F. A.
  - 1946: ———, Phys. Rev. **70**, 817. *458.*
- BENNETT, R. D.
  - see A. H. Compton.
- BENOIST-GUEUTAL, P.
  - 1950: ———, J. Prentki, J. Ratier, J. Phys. Radium **11**, 553. *149.*
- BERGSTRAHL, T. A.
  - 1951: ——— and C. A. Schroeder, Phys. Rev. **81**, 244. *348, 481.*
- BERNARDINI, G.
  - 1945: ———, M. Conversi, E. Pancini, E. Scrocco, G. C. Wick, Phys. Rev. **68**, 109. *347.*
  - 1948: ———, B. N. Cacciapuoti, R. Querzoli, Phys. Rev. **73**, 335. *324.*
  - 1950: ———, E. T. Booth, S. J. Lindenbaum, Phys. Rev. **80**, 905. *370.*
  - 1950: ———, E. T. Booth, L. Lederman, J. H. Tinlot, Bombay Conf. on Fundamental Particles, *20.*
  - 1950: ———, J. Cortini, A. Manfredini, Phys. Rev. **79**, 952. *19, 42, 44, 46, 48, 356, 358, 359, 375, 379.*
- BERRY, E. B.
  - 1942: ———, and V. F. Hess, Terr. Magn. Atmos. Elect. **47**, 251. *502.*
- BETHE, H. A.
  - 1935: ———, Proc. Camb. Phil. Soc. **31**, 108. *160.*
  - 1937: ———, Rev. Mod. Phys. **9**, 70. *40.*
  - 1940: ———, S. A. Korff, G. Placzek, Phys. Rev. **57**, 573. *375.*
  - 1940: ———, L W. Nordheim, Phys. Rev. **57**, 998. *180*
  - 1947: ———, Elementary Nuclear Theory (New York: John Wiley & Sons) 99. *141.*
  - 1949: ———, Phys. Rev. **76**, 191. *147.*
  - ——— *160.*
- BHABHA, H. J.
  - 1935: ———, Proc. Roy. Soc. **A152**, 559. *410.*
  - 1949: ———, Rev. Mod. Phys. **21**, 451. *132.*
  - ——— *336.*
- BIEHL, A. T.
  - 1948: ———, R. A. Montgomery, H. V. Neher, W. H. Pickering, W. Roesch, Rev. Mod. Phys. **20**, 360. *283, 297.*
  - 1949: ———, H. V. Neher, W. C. Roesch, Phys. Rev. **76**, 914. *258, 260, 262, 325, 351, 355.*
  - 1950: ——— and H. V. Neher, Phys. Rev. **78**, 172. *258, 274.*
- BISHOP, A. S.
  - see F. M. Smith.
- BISWAS, S.
  - see V. D. Hopper.

Bjorklund, R.
1950: ———, W. E. Crandall, B. J. Moyer, H. F. York, Phys. Rev. 77, 213. *12.*
Blackett, P. M. S.
1937: ———, Proc. Roy. Soc., A159, 1. *341, 342.*
1938: ———, Phys. Rev. 54, 973. *456.*
——————— *65, 157.*
Blaton, J.
1950: ———, Det. Kgl. Danske Vidensk Selskab., Mat.-fys. Medd., 24, no. 12. *94.*
Blau, M.
1937: ——— and H. Wambacher, S. B. Acad. Wiss. Wien, 146, 623. *40, 46.*
Bloch, F
1935: ——— and C. Møller, Nature, Lond , 135, 911. *171.*
Blocker, W
1950: ———, R. Kenney, W. K. H. Panofsky, Phys. Rev. 79, 419. *352.*
Bollinger, L. M.
1950: ———, Bull. Amer. Phys. Soc. 25, no. 3, 16. *401.*
Bonnetti, A.
1949: ——— and C. C. Dilworth, Phil. Mag. 40, 585. *51, 53.*
Booth, E. T.
see G. Bernardini.
Borowitz, S.
1949: ——— and W. Kohn, Phys. Rev. 76, 818. *145.*
Bousser, F.
see L. Leprince-Ringuet.
Bowen, I. S.
1938: ———, R. A. Millikan, H. V. Neher, Phys. Rev. 53, 855. *257, 260, 297, 300, 303.*
Braddick, H. J. J.
1939: ——— and G. Hensby, Nature, Lond., 144, 1012. *403, 411, 448.*
see N. Adams.
Bradner, H.
see F. M. Smith.
Bradt, H. L.
1948: ——— and B. Peters, Phys. Rev. 74, 1828. *199.*
1949: ——— and B. Peters, Phys. Rev. 76, 156. *224.*
1950: ——— and B. Peters, Phys. Rev. 77, 54. *209, 228, 235, 302, 328.*
1950: ——— and B. Peters, Phys. Rev. 80, 943. *202, 209, 222, 235, 361.*
1950: ———, M. F. Kaplon, B. Peters, Helv. Phys. Acta, 23, 24. *32, 209, 222, 228, 364, 365, 410.*
see M. F. Kaplon.
Bridge, H.
1947: ———, B. Rossi, R. Williams, Phys. Rev. 72, 257. *354, 380.*
1951: ——— and M. Annis, Phys. Rev. 81, 445. *65, 68, 73, 110, 114, 115, 117, 120.*

BRODA, E.
1947: ———, N. Feather, D. H. Wilkinson, Phys. Soc. Camb. Conf. Rep., p. 114. *130.*
BRODE, R. B.
1950: ———, Phys. Rev. 78, 92. *342, 343, 346.*
——————— *153.*
see S. G. Retallack.
BROWN, H.
1949: ———, Rev. Mod. Phys. 21, 625. *231, 232, 236.*
BROWN, R. H.
1949: ———, U. Camerini, P. H. Fowler, H. Muirhead, C. F. Powell, and D. M. Ritson, Nature, Lond., 163, 82. *65, 105, 107, 108, 109, 114.*
1949: ———, U. Camerini, P. H. Fowler, H. Heitler, D. T. King, and C. F. Powell, Phil. Mag., 40, 862. *6, 360, 362, 365, 424, 426.*
BROWN, W. W.,
1950: ——— and A. S. McKay, Phys. Rev., 77, 342. *19, 364.*
BROXON, J. W.
1941: ———, Phys. Rev., 59, 773. *498.*
1942: ———, Phys. Rev., 62, 508. *501.*
1950: ——— and H. W. Boehmer, Phys. Rev., 78, 411. *508.*
BRUECKNER, K. A.
1950: ———, Phys. Rev., 79, 641. *149.*
1950: ——— and K. M. Watson, Phys. Rev., 79, 187. *151, 152.*
BUDINI, P.
1950: ——— and N. Dallaporta, Nuovo. Cim., 7, 230. *375.*
BURDITT, W. F.
see A. J. McMahon.
BUTLER, C. C.
1950: ———, W. G. V. Rosser and K. H. Barker, Proc. Phys. Soc. A63, 145. *19, 68, 120.*
1951: ——— and K. H. Barker, Proc. Phys. Soc. A64, 4. *19, 21, 25.*
see R. Armenteros, G. D. Rochester.

CACHON, A.
see R. Armenteros.
CALDIROLA, P.
1949: ———, Nuovo Cim., 6, 565. *346.*
CAMERINI, U.
1949: ———, T. Coor, J. H. Davies, P. H. Fowler, W. O. Lock, H. Muirhead and N. Tobin, Phil. Mag., 40, 1073. *360, 363.*
1950: ———, P. H. Fowler, W. O. Lock and H. Muirhead, Phil. Mag., 41, 413. *7, 19, 23, 25, 34, 416, 430, 432.*
1951: ———, J. H. Davies, P. H. Fowler, C. Franzinetti, W. O. Lock, D. H. Perkins and G. Yekutieli, (in press). *7, 16, 23, 25, 28, 35, 36.*

see R. H. Brown.

CAMERON, G. H.
see R. A. Millikan.

CARLSON, A. G.,
1950: ———, J. E. Hooper and D. T. King, Phil. Mag., 41, 701. *12, 147, 151, 372, 373, 384, 448.*

CARMICHAEL, H.
1939: ——— and E. G. Dymond, Proc. Roy. Soc., A171, 321. *303.*
1949: ———, Proc. Echo Lake Cosmic Ray Symposium, 156. *303.*

CARO, D. E.
1950: ———, J. K. Parry and H. D. Rathgeber, Nature, Lond., 165, 689. *344, 414, 415.*

CASE, K. M.
1948: ———, Phys. Rev., 74, 1884. *145.*
1949: ———, Phys. Rev., 76, 1. *145.*
1949: ———, Phys. Rev., 76, 14. *144.*
1950: ——— and A. Pais, Phys. Rev., 80, 203. *146.*

CHADWICK, J.
1932: ———, Nature, Lond., 129, 312. *127.*

CHAMBERLAIN, O.
1950: ———, R. F. Mozley, J. Steinberger and C. Wiegand, Phys. Rev., 79, 396. *161.*

CHANG, T. S.
1942: ———, K. Danske Vidensk. Selsk. Mat.-fys. Medd, 19, no 10. *180.*

CHANG, W. Y.
1949: ———, Rev. Mod. Phys., 21, 167. *173.*

CHAO, C. Y.
1949: ———, Phys. Rev. 75, 581. *12, 147.*

CHAPMAN, A. H.
see R. Armenteros.

CHAPMAN, S.
1937: ———, Nature, Lond., 140, 423. *494, 496.*
————— *476.*
see J. Bartels.

CHESTON, W. B.
1951: ———, Phys. Rev., 82, 335. *151.*

CHIPPINDALE, P.
see P. Astbury.

CHOU, C. N.
1948: ———, Phys. Rev., 74, 1659. *414.*

CHREE, C.
1913: ———, Phil. Trans. A212, 76. *497.*
1928: ——— and J. M. Stagg, Phil. Trans. A227, 21. *497, 499.*

CHRISTY, R. F.
1941: ——— and S. Kusaka, Phys. Rev., 59; 414. *160, 409.*

CINI, M.
1950: ——— and G. Wataghin, Nuovo Cim., 7, 135. *346.*

Clay, J.
1937: ———, Physica, 4, 121. *396.*
1939: ———, Rev. Mod. Phys., 11, 134. *396.*
1939: ——— and A. V. Gemert, Physica, 6, 497. *330, 396.*
1949: ———, Proc. K. Ned. Akad. Wet., 52, 906, 923. *502, 507.*
——————— *193, 492.*
Clementel, E.
1950: ———, Nuovo Cim., 7, 109. *369.*
Cocconi, G.
1949: ———, Phys. Rev., 75, 1074. *356.*
1949: ———, V. Tongiorgi and K. Greisen, Phys. Rev., 75, 1063. *306.*
1949: ———, V. Cocconi–Tongiorgi and K. Greisen, Phys. Rev., 76, 1020. *326.*
1950: ——— and V. Cocconi–Tongiorgi, Phys. Rev., 79, 768. *437.*
1950: ———, Phys. Rev., 79, 1006. *326.*
1951: ——— and V. Cocconi–Tongiorgi, Phys. Rev., 82, 335. *173, 436, 438.*
Cocconi–Tongiorgi, V.
see G. Cocconi.
Cockcroft, A. L.
see S. C. Curran.
Cohn, H. O.
see R. W. Thompson.
Compton, A. H.
1932: ———, R. D. Bennett and J. C. Stearns, Phys. Rev., 41, 119. *466.*
1934: ———, E. O. Wollan and R. D. Bennett, Rev. Sci. Inst. 5, 415. *467.*
1935: ——— and I. A. Getting, Phys. Rev. 47, 817. *484, 485.*
1937: ——— and R. N. Turner, Phys. Rev., 52, 799. *456, 487.*
——————— *492.*
see A. T. Monk.
Cooper, D.
see C. W. Kissinger, N. Wagner.
Coor, T.
see U. Camerini.
Conforto, A. M.
1951: ——— and R. D. Sard, Phys. Rev. 82, 335. *173.*
see R. D. Sard.
Conner, C. H.
see H. Yagoda.
Conversi, M.
1945: ———, E. Pancini and O. Piccioni, Phys. Rev. 68, 232. *127.*
1947: ———, E. Pancini and O. Piccioni, Phys. Rev. 71, 209. *127, 368.*
1946: ——— and O. Piccioni, Phys. Rev., 70, 859. *162.*
1950: ———, Phys. Rev., 79, 749. *335, 355, 356, 358.*
Conway, M.
see M. A. Ellison.

Corson, D. R.
  1950: ———, Phys. Rev., 80, 303. *211.*
Cortini, G.
  see G. Bernardini.
Cosyns, M.
  1936: ———, Nature, Lond., 137, 616. *323.*
Cowan, E. W.
  see A. J. Seriff.
Crandall, W. E.
  1950: ———, B. J. Moyer and H. F. York, Phys. Rev., 78, 89. *147, 151.*
  see R. Bjorklund.
Crane, H. R.
  1948: ———, Rev. Mod. Phys., 20, 279. *159, 171.*
Crawshaw, J. D.
  see D. H. Follett.
Creamer, R.
  1951: ———, M. Sc. Thesis, London. *433.*
Critchfield, L.
  1941: ——— and E. Wigner, Phys. Rev., 60, 412. *165, 175.*
  1950: ———, E. P. Ney and S. Oleksa, Phys. Rev., 79, 402. *194, 256, 325.*
Crouch, M. F.
  1951: ———, Phys. Rev., 81, 164. *173.*
  see R. D. Sard.
Crowe, K. M.
  1950: ——— and E. Hayward, Phys. Rev., 80, 40. *352.*
Crussard, J.
  1950: ———, Bombay Conference on Fundamental Particles. *4, 36, 47, 51.*
Curran, S. C.
  1949: ———, J. Angus and A. L. Cockcroft, Phys. Rev., 76, 853. *129.*

Dainton, A. D.
  1950: ——— and D. W. Kent, Phil. Mag. 41, 963. *210, 223, 231.*
Daudin, J.
  1944: ———, Ann. Phys., Paris, II, 19, 110. *109.*
  1950: ———, J. Phys. Radium, 11, 25. *128.*
Dauvillier, A.
  1949: ———, C. R. Acad. Sci., Paris, 229, 1096. *506.*
Davies, J. H.
  1949: ———, W. O. Lock and H. Muirhead, Phil. Mag., 40, 1250. *160, 381.*
  ——— and D. H. Perkins, (unpublished). *31.*
  see U. Camerini.
Davis, L. R.
  see G. J. Perlow, I. F. Quercia.
Davis, W. O.
  1950: ———, Phys. Rev., 80, 150. *358, 375.*

Dieminger, W.
1950: ——— *et al.* J. Atmos. Terr. Phys., 1, 37. *506.*
Dilworth, C. C.
1950: ———, S. J. Goldsack, Y. Goldschmidt–Clermont and F. Levy, Phil. Mag., 41, 1032. *7.*
see A. Bonnetti.
Dolbear, D. W. N.
1947: ——— and H. Elliot, Nature, Lond., 159, 58. *494.*
1950: ——— and H. Elliot, Nature, Lond., 165, 353. *481.*
1951: ——— and H. Elliot, J. Atmos. Terr. Phys , 1, 215 *463, 472, 477.*
——————— *422.*
see H. Elliot.
Duperier, A.
1944: ———, Terr. Magn. Atmos. Elect., 49, 1. *457, 458.*
1945: ———, Proc. Phys. Soc., 57, 468. *502.*
1946: ———, Nature, Lond., 158, 196. *471, 487, 488.*
1949: ———, Proc. Phys. Soc., A62, 684. *421, 458, 459, 460, 466.*
1951: ———, Nature, Lond., 167, 312. *421, 461.*
Dwight, K.
1950: ———, Phys. Rev., 78, 40. *481.*
Dymond, E. G.
see H. Carmichael.
Dyson, F. J.
1948: ———, Phys. Rev., 73, 929. *144.*
1949: ———, Phys. Rev., 75, 485 and 1736. *134.*

Ehmert, A.
1937: ———, Zeits. f. Physik, 106, 751. *396, 439.*
1940: ———, Naturwiss., 28, 28. *482.*
1948: ———, Z. Naturforsch., 3a, 264. *502, 507, 509.*
Elliot, H.
1950: ——— and D. W. N. Dolbear, Proc. Phys. Soc., A63, 137. *473, 475, 484.*
1951: ——— and D. W. N. Dolbear, J. Atmos. Terr. Phys., 1, 205. *473, 476, 479, 484, 490.*
see D. W. N. Dolbear.
Ellison, M. A.
1946: ———, Nature, Lond., 158, 450, *504.*
1950: ——— and M. Conway, Observatory, 70, 77. *505.*
Elston, A. W.
see J. J. Lord.
Enatsu, H.
1950: ———, Progr. Theor. Phys., 5, 102. *140.*
Epstein, P.
1931: ———, Proc. Nat. Acad. Sci., Wash., 16, 658. *246.*
Evans, J.
1949: ——— and E. P. George, Nature, Lond., 164, 21. *173.*

see E. P. George.

FAINBERG, J.
see J. J. Lord.
FEATHER, N.
see E. Broda.
FEER, D. B.
1949: ———, Phys. Rev., 75, 731. *162.*
1949: ———, Phys. Rev., 76, 306. *149.*
FERMI, E.
1934: ———, Z. Phys., 88, 161. *139, 167.*
1949: ———, Phys. Rev., 75, 1169. *5, 237, 326.*
1950: ———, Prog. Theor. Phys., 5, 570. *5.*
1951: ———, Phys. Rev., 81, 683. *5.*
——————, *153, 238.*
FERRETTI, B.
1949: ———, Nuovo Cim., 6, 379. *375.*
1950: ———, and S. Gallone, Phys. Rev., 77, 153. *149.*
FIERTZ, M.
1937: ———, Z. Phys., 104, 553. *139, 166.*
FINKELSTEIN, R. J.
1947: ———, Phys. Rev., 72, 415. *148, 155.*
see M. Ruderman.
FIREMAN, L.
1949: ———, Phys. Rev., 75, 323. *161.*
FISK, C. B.
see E. O. Salant. ,
FLUM, R. S.
see R. W. Thompson.
FOLLETT, D. H.
1936: ——— and J. D. Crawshaw, Proc. Roy. Soc., A155, 546. *401, 439.*
FONG, H. T.
1951: ———, Thesis, University of Paris. *229.*
FORBUSH, S. E.
1937: ———, Phys. Rev., 51, 1108. *487.*
1937: ———, Phys. Rev., 52, 1254. *487.*
1938: ———, Phys. Rev., 54, 975. *461.*
1938: ———, Terr. Magn. Elect., 43, 207. *492, 496.*
1939: ———, Rev. Mod. Phys., 11, 168. *461.*
1946: ———, Phys. Rev., 70, 771. *505.*
1949: ———, P. S. Gill, M. S. Vallarta, Rev. Mod. Phys., 21, 44. 509.
1949: ——— and I. Lange, Phys. Rev., 76, 164. *502.*
1950: ———, T. B. Stinchcomb, M. Schein, Phys. Rev., 79, 501. *506.*
see I. Lange.
FORRO, M.
see J. Barnothy.

Forster, H. H.
1950: ———, Phys. Rev., 77, 733. *66.*
1950: ———, Phys. Rev., 78, 92. *156.*
1950: ———, Phys. Rev., 78, 247. *356.*
Fowler, P. H.
1950: ———, Phil. Mag., 41, 169. *7, 109, 202, 427.*
see U. Camerini; R. H. Brown.
Franzinetti, C.
1950: ———, Phil. Mag., 41, 86. *109.*
see U. Camerini.
Freier, P.
1948: ———, E. J. Lofgren, E. P. Ney, F. Oppenheimer, H. L. Bradt, B. Peters, Phys. Rev., 74, 213. *194, 229.*
1948: ———, E. J. Lofgren, E. P. Ney, F. Oppenheimer, Phys. Rev., 74, 1818. *51, 195.*
1949: ———, E. P. Ney, F. Oppenheimer, Phys. Rev., 75, 1451. *375, 377.*
Fretter, W. B.
1948: ———, Phys. Rev., 73, 41. *147.*
1949: ———, Phys. Rev., 76, 511. *12, 326, 356, 364.*
1950: ———, Phys. Rev., 80, 921. *365.*
1951: ———, Phys. Rev., 82, 294. *65.*
——————— *68, 70, 73, 86, 110.*
Friedman, H. L.
1951: ——— and J. Rainwater, Phys. Rev., 81, 644. *161.*
Fujimoto, Y.
1949: ——— and Y. Yamaguchi, Progr. Theor. Phys., 4, 468. *44, 50.*
1949: ——— and Y. Yamaguchi, Phys. Rev., 75, 1276. *44.*
1950: ——— and Y. Yamaguchi, Progr. Theor. Phys., 5, 76. *54.*
1950: ——— and Y. Yamaguchi, Progr. Theor. Phys., 5, 787. *44. 48.*
see K. Aidzu.
Fukuda, H.
1949: ——— and Y. Miyamoto, Progr. Theor. Phys., 4, 347. *148.*
1949: ———, Y. Miyamoto, T. Miyazima and S. Tomonaga, Progr. Theor. Phys., 4, 385. *148, 158.*
1949: ——— and Y. Miyamoto, Progr. Theor. Phys., 4, 389. *143, 158.*
1949: ——— and Y. Miyamoto, Progr. Theor. Phys., 4, 391. *133, 155.*
1950: ———, S. Hayakawa and Y. Miyamoto, Progr. Theor. Phys., 5, 283. *129, 151.*
1950: ———, S. Hayakawa and Y. Miyamoto, Progr. Theor. Phys., 5, 352. *155.*
1950: ——— and Y. Miyamoto, Progr. Theor. Phys., 5, 147, 148. *155.*
see K. Aidzu, S. Nakamura.
Furry, W. H.
1937: ———, Phys. Rev., 51, 125. *143.*
1939: ———, Phys. Rev., 56, 1184. *160.*

GALLONE, S.
see B. Ferretti.
GANGNES, A. V.
1949: ———, J. F. Jenkins and J. A. van Allen, Phys. Rev., 75, 57. *318, 319.*
see J. A. van Allen.
GAMOW, G.
1936: ——— and E. Teller, Phys. Rev., 49, 895. *168.*
GARDNER, E.
see F. M. Smith.
GARELLI, C. M.
1950: ——— and G. Wataghin, Phys. Rev., 79, 718. *372, 411, 417.*
GASKELL, J.
see B. F. J. Schonland.
GEMERT, A. V.
see J. Clay.
GEORGE, E. P.
1941: ———, Ph. D. Thesis, London, *439.*
1946: ———, Nature, Lond., 167, 296. *398.*
1949: ——— and P. T. Trent, Nature, Lond., 164, 838. *441, 442.*
1949: ——— and A. C. Jason, Proc. Phys. Soc., A62, 243. *356.*
1950: ——— and A. C. Jason, Proc. Phys. Soc., A63, 1081. *441.*
1950: ——— and J. Evans, Proc. Phys. Soc., A63, 1248. *331, 358, 359, 410, 424.*
1951: ——— and J. Evans, Proc. Phys. Soc., A64, 193. *331, 424, 434.*
see J. Evans, P. T. Trent.
GERJUOY, E.
1951: ———, Phys. Rev., 81, 62. *169.*
GETTING, I. A.
see A. H. Compton.
GHERI, H.
1947: ——— and R. Steinmaurer, Terr. Magn. Atmos. Elect., 52, 343. *501.*
GHIORSO, A.
see C. A. Levine.
GILL, P. S.
1939: ———, Phys. Rev., 55, 429. *462.*
see S. E. Forbush.
GLASER, D. A.
1950: ———, B. Hamermesh and G. Safonov, Phys. Rev., 80, 625. *341, 342.*
GODART, O.
see M. S. Vallarta.
GOLDBERGER, M. L.
1948: ———, Phys. Rev., 74, 1269. *35.*
GOLDFARB, L.
1950: ———, H. L. Bradt and B. Peters, Phys. Rev., 77, 751. *218.*

GOLDSACK, S. J.
see C. C. Dilworth.
GOLDSCHMIDT–CLERMONT, Y.
1948: ———, D. T. King, H. Muirhead and D. M. Ritson, Proc. Phys. Soc., 61, 183. *211.*
1950: ———, Nuovo Cim., 7, 331. *7.*
see C. C. Dilworth.
GRAEF, C.
see M. S. Vallarta.
GRAZIADEI, H. T.
see R. Steinmaurer.
GREGORY, B. P.
1950: ———, B. Rossi and J. H. Tinlot, Phys Rev., 77, 299. *12.*
1951: ——— and J. H. Tinlot, Phys. Rev., 81, 675. *12, 18, 19, 364.*
GREISEN, K.
1942: ———, Phys. Rev., 61, 212. *255, 402.*
1943: ———, Phys. Rev., 63, 323. *333.*
1948: ———, Phys. Rev., 73, 521. *147, 331, 336, 349, 371, 397, 416, 417.*
1949: ———, Phys. Rev., 76, 1718. *331.*
1950: ———, S. P. Walker and W. D. Walker, Phys. Rev., 80, 535. *326.*
——— *271.*
see G. Cocconi, W. D. Walker.
GROETZINGER, G.
1948: ——— and G. W. McClure, Phys. Rev., 74, 341. *173, 435.*
1949: ——— and G. W. McClure, Phys. Rev., 75, 340. *435.*
1950: ——— and G. W. McClure, Phys. Rev., 77, 777. *327, 347.*
DE GROOT, S. R.
1950: ——— and H. A. Tolhoek, Physica, 16, 456. *171, 183.*
GUREVICH, I.
see A. I. Alikhaniyan.

HADLEY, J.
see L. Aamodt, W. K. H. Panofsky.
HALL, H.
see O. Halpern.
HALPERN, O.
1948: ——— and H. Hall, Phys Rev., 73, 477. *407.*
HAMILTON, D. R.
1947: ———, Phys. Rev., 71, 456. *171.*
HANAWA, S.
1950: ——— and T. Miyazima, Progr. Theor. Phys., 5, 459. *162.*
HARDING, J. B.
1949: ———, Nature, Lond., 163, 440. *376,*
1949: ———, Phil. Mag., 40, 530. *46.*
1949: ——— and D. H. Perkins, Nature, Lond., 164, 285. *19, 44, 48.*
1949: ———, S. Lattimore and D. H. Perkins, Proc. Roy. Soc., A196, 325. *42, 44, 46, 48.*

1950: ———, Phil. Mag., 41, 405. *46, 65, 107, 108, 109, 114, 156.*
1951: ———, Phil. Mag., 42, 63. *36.*

HARTZLER, A. J.
1951: ———, Phys. Rev., 81, 323. *19.*

HAYAKAWA, S.
1949: ——— and S. Tomonaga, Progr. Theor. Phys., 4, 287. *409, 440, 441.*
1949: ——— and S. Tomonaga, Progr. Theor. Phys., 4, 496. *409, 440, 441.*
1950: ———, K. Mano and T. Miyazima, Progr. Theor. Phys., 5, 495. *421.*
1950: ——— *et al.*, J. Geophys. Res., 55, 221. *496.*
——— *417.*
see H. Fukuda.

HAYWARD, E.
see K. M. Crowe.

HAZEN, W. E.
1944: ———, Phys. Rev., 65, 67, 259. *352, 406.*
1949: ———, C. A. Randall and O. L. Tiffany, Phys. Rev., 75, 694. *355, 358.*
——— *408.*
see C. A. Randall, O. L. Tiffany.

HEISENBERG, W.
1949: ———, Zeit. f. Phys., 126, 569. *5, 346.*
——— *153.*

HEITLER, H.
——— see R. H. Brown.

HEITLER, W.
1947: ——— and S. Power, Phys. Rev., 72, 266. *147.*
1949: ———, The Quantum Theory of Radiation, 2nd. ed. (Oxford University Press). *198.*
1949: ——— and L. Janossy, Proc. Phys. Soc., A62, 364. *5, 366.*
1950: ——— Helv. Phys. Acta, 23, 417. *5, 21.*
1950: ———, Bombay Conf. on Fundamental Particles. *30.*
1951: ———, Private communication. *30.*
——— *17, 33*
see M. Stotnick; R. H. Brown.

HENRI, V. P.
see W. L. Kraushaar.

HEREFORD, F. L.
see M. A. Pomerantz.

HESS, V. F.
1935: ———, H. Graziadei, R. Steinmaurer, S. B. Akad. Wiss. Wien, 144, 53. *456.*
1936: ———, Terr. Magn. Atmos. Elect., 41, 345. *501.*
1937: ———, A. Demmelmair, Nature, Lond., 140, 316. *492.*
1940: ———, H. Graziadei, Terr. Magn. Atmos. Elect., 41, 9. *470.*

1942: ———, Rev. Mod. Phys., 11, 153. *456.*

HILBERRY, N.
1941: ———, Phys. Rev., 60, 1. *302.*
see B. Rossi.

HINCKS, E. P.
1950: ———, B. Pontecorvo, Phys. Rev., 77, 102. *160.*
1951: ———, Phys. Rev., 81, 313. *173.*

HOAG, J. B.
see B. Rossi.

HOANG–TCHANG–FONG
see L. Leprince–Ringuet.

HODGSON, P.
1949: ———, D. H. Perkins, Nature, Lond., 163, 439. *51.*
1951: ———, Phil. Mag., 42, 267. *52.*

HOGG, A. R.
1941: ———, Terr. Magn. Atmos. Elect., 46, 51. *493.*
1947: ———, Proc. Roy. Soc., A192, 128. *457.*
1949: ———, Memoirs of the Commonwealth Observatory, Canberra, No. 10. *471, 493, 501.*
1950: ———, J. Atmos. Terr. Phys., 1, 114. *488, 489.*

HOOPER, J. F.
1951: ———, D. T. King, A. H. Morrish, Phil. Mag., 42, 304. *410.*
see A. G. Carlson.

HOPPER, V. D.
1950: ——— and S. Biswas, Phys. Rev., 80, 1098. *65, 81.*

HORNBOSTEL, J.
see E. O. Salant.

HOROWITZ, J. J.
see A. Abragham.

HORNYAK, W. F.
1950: ———, T. Lauritsen, P. Morrison, W. A. Fowler, Rev. Mod. Phys., 22, 291. *129, 168, 170.*

HSIAO, C.
see A. J. Seriff.

HUDSON, D. E.
1949: ———, Proc. Echo Lake Conference. *441, 445, 446, 447.*

HUGHES, D. J.
see V. C. Wilson.

HULSIZER, R. I.
1948: ——— and B. Rossi, Phys. Rev., 73, 1402. *325.*
1949: ———, Phys. Rev., 76, 164. *194, 256.*
see B. Rossi.

INGHRAM, M. G.
1949: ——— and J. H. Reynolds, Phys. Rev., 76, 1264. *161.*
1950: ———————————, Phys. Rev., 78, 822. *161.*

ITTNER, W. B.
see R. D. Sard.

JACOBSON, M.
1951: ———, A. Schulz, J. Steinberger, Phys. Rev., 81, 894. *368.*
JAUNEAU, L.
see L. Leprince-Ringuet.
JANOSSY, L.
1937: ———, Z. Phys., 104, 430. *480.*
1945: ——— and G. D. Rochester, Proc. Roy. Soc., A183, 187. *356.*
1948: ———, Cosmic Rays (Oxford University Press). *288.*
1950: ———————— 2nd. edition (Oxford University Press). *324, 348, 380.*
see W. Heitler; B. Rossi.
JARKOV, K. B.
1950: ———, J. Exp. Theor. Phys., 20, 492. *140.*
JASON, A. C.
see E. P. George.
JASTROW, R.
1951: ———, Phys. Rev., 81, 165. *159.*
JENKINS, J. F.
see A. V. Gangnes.
JESSE, W. P.
see M. Schein.
JOHNSON, T. H.
1935: ———, Phys. Rev., 48, 287. *254.*
1938: ———, Rev. Mod. Phys., 10, 193. *246, 254, 260, 288, 496.*
JOHNSON, L.
1941: ———, Phys. Rev., 59, 11. *347.*
JURKIEWICZ, K.
see M. Miesowicz.

KAMEFUCHI, S.
see S. Ogawa.
KANE, E. O.
1949: ———, T. J. B. Shanley, J. A. Wheeler, Rev. Mod. Phys., 21, 51. *481.*
KAPLAN, N.
see H. Yagoda.
KAPLON, M. F.
1949: ———, B. Peters, H. L. Bradt, Phys. Rev., 76, 1735. *148.*
1951: ———, B. Peters, H. L. Reynolds, D. M. Ritson, Phys. Rev. (in press). *209, 210, 215.*
KENNEY, R.
see W. Blocker.
KENT, D. W.
see A. D. Dainton.

KIEPENHEUER, K. O.
1950: ———, Phys. Rev., 78, 809. *510.*
KING, D. T.
see A. G. Carlson; R. H. Brown.
KISSINGER, C. W.
1948: ——— and D. Cooper, Phys. Rev., 74, 349. *172.*
KLEIN, O.
1944: ———, Ark. Mat. Astr. Fys., 31A. *237.*
1948: ———, Nature, Lond., 161, 897. *162.*
KOBAYASI, M.
see H. Yukawa.
KOFOED-HANSEN, O.
——— *164.*
KOHLHÖRSTER, W.
1933: ———, Nature, Lond., 132, 407. *396.*
1934: ———, Nature, Lond., 133, 419. *396.*
1939: ———, Phys. Zs., 40, 107. *501.*
1941: ———, Phys. Zs., 42, 55. *472.*
——— *466.*
KONOPINSKI, E. J.
1935: ——— and G. E. Uhlenbeck, Phys. Rev., 48, 7. *139, 172.*
1943: ———, Rev. Mod. Phys., 15, 209. *168.*
KRAUSHAAR, W. L.
1949: ———, Phys. Rev., 76, 1045. *333.*
1950: ———, J. E. Thomas, V. P. Henri, Phys. Rev., 78, 486. *161.*
——— *433.*
KRAYBILL, H. L.
see M. Schein.
KUSAKA, S.
see R. F. Christy; M. S. Vallarta.

LAGARRIGUE, A.
1951: ——— and C. Peyrou, J. Phys. Radium, to be published. *160, 162, 176.*
see C. Peyrou.
LANDAU, L. D.
1948: ———, Dokl. Akad. Nauk. SSSR., 60, 207. *132.*
LANGE, I.
1942: ——— and S. Forbush, Terr. Magn. Atmos. Elect., 47, 331. *502.*
1948: ———, Carnegie Institution of Washington Publication 175. *467, 490.*
see S. E. Forbush.
LANGER, L. M.
1951: ——— and R. J. D. Moffat, Phys. Rev., 82, 333, 635. *171.*
LATTES, C. M. G.
1947: ———, G. P. S. Occhialini, C. F. Powell, Nature, Lond., 160, 453. *101, 127, 367.*

LATTIMORE, S.
1949: ———, Phil. Mag., 40, 394. *354, 356, 358, 359.*
see J. B. Harding.
LAURITSEN, T.
see W. F. Hornyak.
LAWSON, J. S. Jr.
1951: ———, Phys. Rev., 81, 299. *161.*
LE COUTEUR, K. J.
1949: ——— and L. Rosenfeld, Phil. Mag., 40, 151. *144.*
1950: ———, Proc. Phys. Soc., A63, 259. *42, 44, 48, 49, 213.*
——— *45.*
LEDERMAN, L.
see G. Bernardini.
LEE, T. D.
1949: ———, M. Rosenbluth, C. N. Yang, Phys. Rev., 75, 905. *174.*
LEIGHTON, R. B.
1949: ———, C. D. Anderson, A. J. Seriff, Phys. Rev., 75, 1432. *176.*
1951: ———, S. D. Wanless, W. L. Alford, private communication. *65, 68.*
see A. J. Seriff.
LEMAITRE, G.
1933: ——— and M. S. Vallarta, Phys. Rev., 43, 87. *246, 247.*
1936: ———, Phys. Rev., 49, 719. *246, 249, 294, 295.*
1936: ———, Phys. Rev., 50, 49. *246, 249, 250, 294, 295.*
1937: ———, Nature, Lond., 140, 23. *251.*
——— *193.*
LEPRINCE-RINGUET, L.
1944: ——— and M. l'Heritier, C. R. Acad. Sci., Paris, 219, 618. *156.*
1946: ———, J. Phys. Radium (ser. 8), 7, 66. *65.*
1948: ———, F. Bousser, Hoang-Tchang-Fong, L. Jauneau and D. Morellet, C. R. Acad. Sci., Paris, 226, 1897. *66.*
1949: ———, F. Bousser, Hoang-Tchang-Fong, L. Jauneau, D. Morellet, Phys. Rev., 76, 1273. *30, 66.*
1949: ———, Rev. Mod. Phys., 21, 43. *156.*
LEVINE, C. A.
1950: ———, A. Ghiorso, G. T. Seaborg, Phys. Rev., 77, 296. *161.*
LEVY, F.
see C. C. Dilworth.
LEVY, M.
1951: ———, Proc. Roy. Soc. A, to be published. *147.*
LEWIS, H. W.
1948: ———, J. R. Oppenheimer, S. A. Wouthuysen, Phys. Rev., 73, 127. *5, 153, 346.*
L'HERITIER, M.
see L. Leprince-Ringuet.

LINDHOLM,
1928: ———, Gerl. Beitr. Z. Geophys., 20, 12. *466.*
LOCK, W. O.
1951: ——— and G. Yekutieli, (in press). *19, 20, 29.*
see J. H. Davies.
LODGE, A. S.
1948: ———, Nature, Lond., 161, 809. *174.*
LOFGREN, E. J.
see P. Freier.
LONGMIRE, C.
1949: ———, C. S. Wu, C. H. Townes, Phys. Rev., 76, 695. *170.*
LOPES, J. L.
1941: ———, Phys. Rev., 74, 1722. *181.*
LORD, J. J.
1949: ———, M. Schein, M. Vidale, Bull. Amer. Phys. Soc., 24, no. 4, 16. *356, 361.*
1950: ——— and M. Schein, Phys. Rev., 78, 484. *330.*
1950: ————————————, Phys. Rev., 80, 304. *225.*
1950: ———, J. Fainberg, M. Schein, Phys. Rev., 80, 970. *30, 365.*
1950: ———, A. W. Elston, M. Schein, Phys. Rev., 79, 540. *508.*
1951: ——— to be published. *358, 359, 377.*
—————— *31.*
LOVATI, A.
1950: ———, A. Mura, G. Salvini, G. Tagliaferri, Phys. Rev. 77, 284. *12, 19.*
1951: ———, A. Mura, G. Succi, G. Tagliaferri, Nuovo Cim., 8, 271. *18, 19.*
LOVERA, G.
1947: ———. Ric. Sci. Ricostruz., 17, 2045. *51.*
LUTTINGER, J. M,
1949: ———, Phys. Rev., 75, 309, 1277. *145.*
LYONS, D
1941: ———, Phys. Zs., 42, 166. *409.*

MACANUFF, J. W.
1951: ———. Ph. D. Thesis, Lond. *418, 420, 424, 443.*
MCCLURE, G. W.
see Groetzinger, G.
MCCORD, R. V.
see A. H. Snell.
MCKAY, A. S.
see W. W. Brown.
MCMAHON, A. J.
1950: ———, B. Rossi, W. F. Burditt, Phys. Rev., 80, 157. *355, 356.*
MCMILLAN, E. M.
1949: ——— and J. M. Peterson, Science, 109, 438. *149.*

1949: ——————————— and R. S. White, Science, 110, 579. *149.*

1950: ———, Phys. Rev., 79, 498. *509.*

see R. S. White.

McNish, A. G.

1936: ———, Terr. Mag., 11, 37. *247.*

Majorana, E.

1937: ———, Nuovo Cim., 14, 171. *130.*

Malmfors, K. G.

1948: ———, Ark. Mat. Astr. Fys., 32A, no. 8. *473.*

Manfredini, A.

see G. Bernardini.

Manley, J. H.

1937: ——— and S. Millman, Phys. Rev., 51, 19. *168.*

Marquez, L.

1951: ——— and I. Perlman, Phys. Rev., 81, 953. *51.*

Marshak, R. E.

1949: ———, Phys. Rev., 75, 513. *164, 169.*

1949: ——— and A. S. Wightman, Phys. Rev., 76, 114. *152.*

1949: ———, Phys. Rev., 76, 1736. *148.*

1950: ———, S. Tamor, A. S. Wightman, Phys. Rev., 80, 765. *152.*

see S. Tamor.

Martinelli, E. A.

1950: ——— and W. K. H. Panofsky, Phys. Rev., 77, 464. *161.*

Marty, C.

1948: ——— and J. Prentki, J. Phys. Radium, 9, 147. *181.*

1950: ——— and J. Prentki, C. R. Acad. Sci., Paris, 230, 54. *159.*

1950: ——— and J. Prentki, C. R. Acad. Sci., Paris, 230, 1508. *159.*

Massalski, J. M.

see M. Miesowicz

Maze, R.

1950: ———, C. R. Acad. Sci., Paris, 231, 1295. *441, 442.*

Menon, M. G. K.

1950: ———, H. Muirhead and O. Rochat, Phil. Mag., 41, 583. *434.*

see O. Rochat.

Menzel, D. H.

1948: ——— and W. W. Salisbury, Nucleonics, 2, no. 4, 67. *509.*

Merlin, M.

1950: ——— and O. Pierucci, Nuovo Cim., 8, 528. *353.*

Messerschmidt, W.

1933: ———, Z. Phys., 85, 332. *492.*

1932: ——— and W. S. Pforte, Z. Phys., 73, 677. *456.*

Meyer, H. A.

1949: ———, G. Schwachheim, A. Wataghin, G. Wataghin, Phys. Rev., 76, 598. *355.*

Michel, L.

1949: ———, Nature, Lond., 163, 959. *161.*

1950: ———, Proc. Phys. Soc., A63, 514, 1371. *139, 162, 176.*
1950: ———, Nature, Lond., 166, 654. *130.*
1951: ———, to be published. *133, 159.*
MIESOWICZ, M.
1950: ———, K. Jurkiewicz, J. M. Massalski, Phys. Rev., 77, 380. *331, 400, 401.*
MILLER, R. D.
1951: ———, Phys. Rev., 82, 260. *411, 428.*
MILLIKAN, R. A.
1925: ———, Nature, Lond., 116, 823. *395.*
1926: ——— and G. H. Cameron, Phys. Rev., 28, 851. *395.*
1928: ———————————, Phys. Rev., 31, 163, 921. *395.*
1931: ———————————, Phys. Rev., 37, 235. *395.*
1935: ——— and H. V. Neher, Phys. Rev., 47, 205. *251.*
1936: ———————————, Phys. Rev., 50, 15. *251, 257, 266.*
1942: ——————————— and W. H. Pickering, Phys. Rev., 61, 397. *237.*
1944: ——————————————————, Phys. Rev., 66, 295. *297, 304.*
——————— *296.*
see I. S. Bowen.
MILLMAN, S.
see J. H. Manley.
MIYAMOTO, Y.
see H. Fukuda.
MIYAZAKI, Y.
1949: ———, Phys. Rev., 76, 1733. *396.*
MIYAZIMA, T.
see H. Fukuda; S. Hanawa.
MOFFAT, R. J. D.
see L. M. Langer.
MØLLER, C.
see F. Bloch.
MONK, A. T.
1939: ——— and A. H. Compton, Rev. Mod. Phys., 11, 175. *498.*
MONTGOMERY, D. J. X.
1949: ———, Cosmic Ray Physics (Princeton University Press). *246, 284.*
MONTGOMERY, R. A.
1949: ———, Phys. Rev., 75, 1407. *271, 333, 334.*
see A. T. Biehl.
MORELLET, D.
see L. Leprince-Ringuet.
MORGAN, K. Z.
see W. M. Nielsen.
MORLEY, R. F.
see O. Chamberlain.

Morrish, A. H.
see J. S. Allen.
Morrison, P.
see W. F. Hornyak.
Mott, N. F.
1929: ———, Proc. Roy. Soc., A124, 425. *199.*
Moyer, B. J.
see R. Bjorklund.
Muether, H. R.
see R. Sherr.
Muirhead, H.
see R. Brown; J. H. Davies; U. Camerini.
Mura, A.
1947: ———, G. Salvini, G. Tagliaferri, Nuovo Cim., 4, 10. *326.*
see A. Lovati.
Myssowsky, L.
1928: ——— and L. Tuwim, Z. Phys., 50, 273. *456.*
Mylroi, M. G.
1951: ——— and J. G. Wilson, Proc. Phys. Soc., A64, 404. *359, 398.*

Nahmias, M. E.
1935: ———, Proc. Camb. Phil. Soc., 31, 99. *160.*
Nakamura, S.
1950: ———, H. Fukuda, K. Ono, M. Sasaki, M. Taketani, Progr. Theor. Phys., 5, 740. *177, 178.*
Nash, F.
1951: ———, Ph. D. Thesis, Manchester. *406, 411, 442, 448.*
Nassar, S.
see W. E. Hazen.
Neher, H. V.
1935: ———, Phys. Rev., 47, 417. *251.*
1938: ——— and W. H. Pickering, Phys. Rev., 53, 111. *306.*
1942: ————————————, Phys. Rev., 61, 407. *259, 260, 285, 296, 297.*
1950: ———, Phys. Rev., 78, 674. *318, 336.*
see A. T. Biehl; R. A. Millikan.
Nelson, E. C.
1941: ———, Phys. Rev., 60, 830. *144.*
Nereson, N.
1942: ———, Phys. Rev., 61, 111. *352.*
1948: ———, Phys. Rev., 73, 565. *172.*
——————— *345.*
Newth, J. A.
see P. Astbury.
Newton, H. W.
1942: ———, Observatory, 64, 260. *503.*

NEY, E. P.
1951: ——— and D. M. Thon, Phys. Rev., 81, 1068. *195, 218, 225.*
see L. Critchfield; P. Freier.
NICOLSON, P.
1948: ——— and V. Sarabhai, Proc. Phys. Soc., 60, 509. *483.*
NIELSEN, W. M.
1938: ——— and K. Z. Morgan, Phys. Rev., 54, 245. *398.*
NISHIJIMA, K.
1950: ———, Progr. Theor. Phys., 5, 187. *131.*
NORDHEIM, L. W.
see H. A. Bethe.

OCCHIALINI, G. P. S.
1949: ———, Nuovo Cim., 6, 413. *211, 410.*
see C. M. G. Lattes.
O'CEALLAIGH, C.
1950: ———, Phil. Mag., 41, 838. *160.*
——————— *65, 110, 116, 119.*
OGAWA, S.
1950: ——— and S. Kamefuchi, Progr. Theor. Phys., 5, 311. *136.*
1950: ——— and E. Yamada, Progr. Theor. Phys., 5, 503. *152.*
OLEKSA, S.
see L. Critchfield.
ONEDA, S.
1950: ———, S. Sasaki, S. Osaki, Progr. Theor. Phys., 5, 165. *133, 155, 158.*
see S. Sasaki.
ONO, K.
see S. Nakamura.
OPPENHEIMER, J. R.
see P. Freier; H. W. Lewis.
ORTNER, G.
1940: ———, S. B. Akad. Wiss. Wien, 149, 259. *40, 41.*
OSAKI, S.
1949: ———, S. Oneda, S. Sasaki, Progr. Theor. Phys., 4, 524. *133, 155, 158.*
1950: ———, Progr. Theor. Phys., 5, 373. *133, 155.*
see S. Oneda; S. Sasaki.
OSBORNE, L. S.
1951: ———, Phys. Rev., 81, 239. *27, 36, 365.*
OWEN, B. G.
1951: ——— and J. G. Wilson, Proc. Phys. Soc. Lond., A64, 417. *343.*

PAGE, N.
1950: ———, Proc. Phys. Soc., A63, 250. *42, 44, 48.*
PAIS, A.
1950: ——— and G. E. Uhlenbeck, Phys. Rev., 79, 145. *183.*

PANCINI, E.
see M. Conversi.
PANOFSKY, W. K. H.
1950: ———, L. Aamodt, H. F. York, Phys. Rev., 78, 825. *12*, *152*.
1950: ———, L. Aamodt, J. Hadley, R. Phillips, Phys. Rev., 80, 94. *12*, *152*.
1951: ———, L. Aamodt, J. Hadley, Phys. Rev., 81, 565. *368*.
see J. Steinberger; E. A. Martinelli; W. Blocker.
PARRY, J. K.
see D. E. Caro.
PAULI, W.
1941: ———, Rev. Mod. Phys., 13, 203. *129*, *137*.
1949: ——— and F. Villars, Rev. Mod. Phys., 21, 434. *145*. *159*.
PEASLEE, D. C.
1950: ———, Helv. Phys. Acta, 23, 845. *132*, *133*.
PEKERIS, C. L.
1937: ———, Proc. Roy. Soc., A158, 650. *482*.
1939: ———, Proc. Roy. Soc., A171, 634. *482*.
PERKINS, D. H.
1950: ———, Phil. Mag., 41, 138. *42*, *44*, *48*.
1950: ———, Proc. Roy. Soc., A203, 399. *4*, *51*, *52*, *53*, *196*, *197*.
PERLOW, G. J.
1951: ——— and L. R. Davis, private communication. *217*, *218*, *220*.
PETERS, B.
see H. L. Bradt; M. Kaplon.
PETERSON, J. M.
see E. M. McMillan; R. S. White.
PETERSON, V. Z.
1950: ———, Phys. Rev., 79, 407. *150*.
PEYROU, C.
1950: ——— and A. Lagarrigue, J. Phys. Radium, 11, 666. *129*.
see A. Lagarrigue.
PFORTE, W. S.
see W. Messerschmidt.
PHILLIPS, R.
see W. K. H. Panofsky.
PICCIONI, O.
1948: ———, Phys. Rev., 74, 1754. *173*.
1950: ———, Phys. Rev., 77, 1. *7*, *19*, *368*.
see M. Conversi; J. G. Walsh.
PIERUCCI, O.
see M. Merlin.
PICKERING, W. H.
1935: ———, Phys. Rev., 47, 423. *438*, *439*.
see A. T. Biehl; R. A. Millikan; H. V. Neher.

PLEASANTON, F.
see A. H. Snell.
POMERANTZ, M. A.
1949: ———, Phys. Rev., 75, 69. *336, 337.*
1949: ———, Phys. Rev., 75, 1721. *320, 333, 334, 336, 350.*
1949: ——— and F. L. Hereford, Phys. Rev., 76, 997. *195, 218, 220.*
1950: ———, Phys. Rev., 77, 830. *319, 320, 323.*
PONTECORVO, B.
1947: ———, Phys. Rev., 72, 247. *173.*
see E. P. Hincks.
POWELL, C. F.
1950: ———, Rept. on Progress in Physics, 13, 350. *128, 161, 368, 370.*
———— *147.*
see R. Brown; C. M. G. Lattes.
POWER, S.
1949: ———, Phys. Rev., 76, 865. *158.*
see W. Heitler.
PRENTKI, J.
1951: ———, C. R. Acad. Sci., Paris, 232, 940. *150.*
see P. Benoist-Gueutal; C. Marty.
PUPPI, G.
1948: ———, Nuovo Cim., 5, 587. *174.*
1949: ———, Nuovo Cim., 6, no. 3, *174.*

QUERCIA, I. F.
1950: ———, B. Rispoli, S. Sciuti, Nuovo Cim., 7, 715. *342, 347.*

RACAH, G.
1937: ———, Nuovo Cim., 14, 322. *139.*
RAINWATER, J.
see H. L. Friedman.
RAKEMURA, S.
see M. Taketani.
RANDALL, C. A.
1950: ———, N. Sherman, W. E. Hazen, Phys. Rev., 79, 905. *398.*
1951: ——— and W. E. Hazen, Phys. Rev., 81, 144. *398, 401.*
RATIER, J.
see P. Benoist-Gueutal.
RATHGEBER, H. D.
———— *414.*
see D. E. Caro.
RAU, R. R.
see J. Tiomno.
RAU, W.
1939: ———, Naturwiss. 27, 803. *418.*
1939: ———, Z. Phys., 114, 265, 465. *466, 482.*

1940: ———, Z. Phys., 116, 105. *482.*
————— *424.*

Regener, E.
1931: ———, Nature, Lond., 127, 233. *396.*

Retallack, S. G.
1949: ——— and R. B. Brode, Phys. Rev., 75, 1716. *129.*

Reynolds, J. H.
see M. G. Inghram.

Richtmeyer, R. D.
1949: ——— and E. Teller, Phys. Rev., 75, 1729. *497.*

Richardson, J. R.
1948: ———, Phys. Rev., 74, 1720. *161.*

Rispoli, B.
see I. F. Quercia.

Ritson, D. M.
see R. Brown.

Robson, J. M.
1950: ———, Phys. Rev., 78, 311. *163, 166.*
1951: ———, Phys. Rev., 81, 297. *129, 163.*

Rochat, O.
see M. G. K. Menon.

Rochester, G. D.
1947: ——— and C. C. Butler, Nature, Lond., 160, 855. *65, 67, 85, 101, 109, 118, 119, 153.*
see L. Janossy.

Roesch, W. C.
see A. T. Biehl.

Rose, D. C.
1950: ———, Phys. Rev., 78, 181. *422, 506.*

Rosenbluth, M. N.
1949: ———, Phys. Rev., 75, 532. *173.*
see T. D. Lee.

Rosenfeld, L.
1948: ———, Nuclear Forces (Amsterdam: North-Holland Publishing Co.). *135, 141, 153.*
1948: ———, Rept. Solvay Conf., *127, 146.*
1950: ———, Progr. Theor. Phys., 5, 519. *183.*
————— *159.*
see K. J. Le Couteur.

Rozental, S.
1941: ———, K. Danske Vidensk. Selsk. Mat.fys. Medd., 18, no. 7. *179.*
1941: ———, Phys. Rev., 60, 612. *180.*
1945: ———, K. Danske Vidensk. Selsk. Mat.-fys. Medd., 23, no. 11. *179.*

Rosser, W. G. V.
1951: ——— and M. J. Swift, private communication. *21.*
see C. C. Butler.

Rossi, B.
1939: ———, and L. Janossy, Rev. Mod. Phys., 11, 279. *352.*
1940: ———, N. Hilberry, J. B. Hoag, Phys. Rev., 57, 461. *336.*
1940: ———, Phys. Rev., 57, 660. *248.*
1948: ———, Rev. Mod. Phys., 20, 537. *333, 335, 350, 356, 358, 381.*
1949: ———, Rev. Mod. Phys., 21, 104. *352.*
1949: ——— and R. I. Hulsizer, Nature, Lond., 163, 246. *325.*
—————— *357.*
see H. Bridge, B. P. Gregory; A. J. McMahon.
Ruderman, M.
1949: ——— and R. Finkelstein, Phys. Rev., 76, 1458. *176, 178.*

Sahiar, A. B.
see P. Astbury.
Sakata, S.
1941: ———, Proc. Phys.-Mat. Soc., Japan, 23, 283. *180.*
1941: ————————————, 23, 291. *179.*
see H. Yukawa.
Salant, E. O.
1950: ———, J. Hornbostel, C. B. Fisk, J. E. Smith, Phys. Rev., 79, 184. *7, 11, 355, 358, 359, 376.*
Salisbury, W. W.
see D. H. Menzel.
Salvini, G.
see A. Lovati; A. Mura.
Samoilovich, E. M.
see A. I. Alikhaniyan.
Sands, M.
1950: ———, Phys. Rev., 77, 180. *335, 338, 339.*
Sarabhai, V.
see P. Nicolson.
Sard, R. D.
1948: ———, W. B. Ittner, A. M. Conforto, M. F. Crouch, Phys. Rev., 74, 97. *173, 435.*
1949: ———, A. M. Conforto, M. F. Crouch, Phys. Rev., 76, 1134. *173.*
1950: ———, W. B. Ittner, A. M. Conforto, M. F. Crouch, Phys. Rev., 79, 179. *435.*
see A. M. Conforto.
Sasaki, S.
1949: ———, S. Oneda, S. Osaki, Science Rept., Tohoku Univ., 33, 77. *176.*
1950: ———, S. Oneda, S. Osaki, Progr. Theor. Phys., 5, 25. *133, 155.*
see S. Nakamura; S. Oneda; M. Taketani.
Schein, M.
1941: ———, W. P. Jesse, E. O. Wollan, Phys. Rev., 59, 615. *193.*
1951: ———, private communication. *201.*

1948: ———, V. H. Yngve, H. L. Kraybill, Phys. Rev., 73, 928. *325.*
see S. E. Forbush; J. J. Lord; H. K. Ticho; M. Vidale.

SCHOENBERG, M.
1941: ———, Phys. Rev., 60, 468. *140.*

SCHONLAND, B. J. F.
1937: ———, B. Delatizky, J. Gaskell, Terr. Mag. Atmos. Elect., 42, 137. *466.*

SCHOPPER, E.
1947: ———, Naturwiss., 34, 118. *51.*

SCHULZ, A.
see M. Jacobson.

SCHWACHHEIM, G.
see H. A. Meyer.

SCHWINGER, J.
1948: ———, Phys. Rev., 73, 416. *145.*

SCIUTI, S.
see I. F. Quercia.

SCOTT, J. M. C.
1950: ——— and E. W. Titterton, Phil. Mag., 41, 318. *130.*

SEABORG, G. T.
see C. A. Levine.

SEKIDO, Y.
1950: ——— and S. Yoshida, Rept. on Ionospheric Research in Japan, 4, 37. *479.*

SERIFF, A. J.
1950: ———, R. D. Leighton, C. Hsiao, E. W. Cowan, C. D. Anderson, Phys. Rev., 78, 290. *65, 68, 69, 73, 78, 85, 101, 109, 114, 120, 156.*
see R. B. Leighton.

SHANLEY, J. B.
see E. O. Kane; J. R. Winckler.

SHERMAN, N.
see C. A. Randall.

SHERR, R.
1949: ———, H. R. Muether, M. G. White, Phys. Rev., 75, 282. *169.*

SIGURGEIRSSON, T.
1947: ——— and K. A. Yamakawa, Phys. Rev., 71, 319. *172.*
1949: ————————————, Rev. Mod. Phys., 21, 124. *172.*

SIMPSON, J. A.
1948: ———, Phys. Rev., 73, 1389. *351, 356.*
1949: ——— and R. B. Uretz, Phys. Rev., 76, 569. *259.*

SINGER, S. F.
1949: ———, Phys. Rev., 76, 701. *221, 325.*
1950: ———, Phys. Rev., 77, 47. *319.*
1950: ———, Phys. Rev., 80, 47. *195, 221, 319.*

SLOTNICK, M.
1949: ——— and W. Heitler, Phys. Rev., 75, 1645. *145.*

SMITH, F. M.
1950: ———, W. H. Barkas, A. S. Bishop, H. Bradner, E. Gardner, Phys. Rev., 78, 86. *129.*
SMITH, J. E.
see E. O. Salant.
SNEDDON, I. N.
1949: ——— and B. F. Touschek, Proc. Roy. Soc., A199, 352. *411.*
SNELL, A. H.
1950: ———, E. Pleasanton, R. V. McCord, Phys. Rev., 78, 310. *163, 166.*
SORENSEN, S. O. C.
1949: ———, Phil. Mag., 40, 947. *4, 51, 229.*
1951: ———, Phil. Mag., 42, 188. *4, 51, 55.*
STEARNS, J. C.
see A. H. Compton.
STAGG, J. M.
see C. Chree.
STAKER, W. P.
1950: ———, Phys. Rev., 80, 52. *355.*
STEINBERGER, J.
1948: ———, Phys. Rev., 74, 500. *160.*
1949: ———, Phys. Rev., 75, 1136. *160, 381.*
1949: ———, Phys. Rev., 75, 1180. *132, 148, 155, 176.*
1950: ———, W. K. H. Panofsky, J. Steller, Phys. Rev., 78, 802. *12, 151.*
see O. Chamberlain; M. Jacobson.
STEINMAURER, R.
1933: ——— and H. T. Graziadei, S. B. Akad. Wiss. Wien, 22, 672. *492.*
see H. Gheri.
STELLER, J. S.
1951: ——— and W. K. H. Panofsky, Phys. Rev., 81, 649. *151.*
see W. Steinberger.
STINCHCOMB, T. G.
1950: ———, Phys. Rev., 80, 479. *355.*
see S. E. Forbush.
STORMER, C.
1930: ———, Zeit. f. Astrophys., 1, 237. *246.*
————————— *193, 288.*
STROUD, W. G.
see J. R. Winckler.
SWANN, W. F. G.
1933: ———, Phys. Rev., 43, 217. *509.*
1933: ———, Phys. Rev., 44, 224. *247.*
1943: ———, J. Franklin Inst., 236, 1. *194.*
1950: ———, Phys. Rev., 78, 243. *322.*
SUCCI, C.
see A. Lovati.

SUN, K. H.
  1949: ———, Phys. Rev., 76, 1266. *130.*

TAGLIAFERRI, G.
  see A. Lovati, A. Mura.
TAKADA, G.
  see K. Aidzu.
TAKAYANAGI, K.
  see K. Aidzu.
TAKETANI, M.
  1949: ———, S. Rakamura and M. Sasaki, Phys. Rev., 76, 852. *174.*
  see S. Nakamura, H. Yukawa.
TAMOR, S.
  1950: ——— and R. E. Marshak, Phys. Rev., 80, 766. *150.*
  see R. E. Marshak.
TANIKAWA, Y.
  1947: ———, Progr. Theor. Phys., 2, 31. *148.*
TELLER, E.
  see G. Gamow, R. D. Richtmeyer.
THERREAUX, M.
  ——————— *17, 30, 33.*
THOMAS, J. E.
  see W. L. Kraushaar.
THOMPSON, J. L.
  1939: ———, Phys. Rev., 55, 11. *486, 487.*
THOMPSON, R. W.
  1951: ———, H. O. Cohn and R. S. Flum, Phys. Rev., 83, 175. *65, 68, 70, 73.*
THON, D. M.
  see E. P. Ney.
TICHO, H. K.
  1947: ———, Phys. Rev., 72, 255. *172.*
  1947: ——— and M. Schein, Phys. Rev., 72, 248. *172.*
  1948: ——— and M. Schein, Phys. Rev., 73, 81. *172.*
  1948: ——— and M. Schein, Phys. Rev., 74, 492. *172.*
  1948: ——— and M. Schein, Phys. Rev., 74, 1337. *172.*
TIFFANY, O. L.
  1950: ——— and W. E. Hazen, Phys. Rev., 77, 849. *331, 398, 399, 407.*
TIOMNO, J.
  1949: ———, Phys. Rev., 76, 856. *162.*
  1949: ———, J. A. Wheeler and R. R. Rau, Rev. Mod. Phys., 21, 144. *161.*
  1949: ——— and J. A. Wheeler, Rev. Mod. Phys., 21, 153. *173, 174, 435.*
  see C. N. Yang.
TINLOT, J. H.
  1948: ———, Phys. Rev., 73, 1476. *70.*

1948: ———, Phys. Rev., 74, 1197. *355.*
see G. Bernardini, B. P. Gregory.
Titterton, E. W.
see J. M. C. Scott.
Tobin, N.
see U. Camerini.
Tomonaga, S.
1940: ——— and G. Araki, Phys. Rev., 58, 90. *127.*
see H. Fukuda.
Touschek, B. F.
see I. N. Sneddon.
Townes, C. H.
see C. Longmire.
Trent, P. T.
1951: ———, Ph. D. Thesis, London. *406.*
1951: ——— and E. P. George, (in press). *446.*
Trigg, G. L.
1951: ———, Phys. Rev., 82, 325. *171.*
Trumpy, B.
1943: ———, K. Danske Vidensk. Selsk. Mat.-fys. Medd., 20, 6. *352.*
Turner, R. N.
see A. H. Compton.
Tuwim, L.
see L. Myssowsky.

Uhlenbeck, G. E.
see E. J. Konopinski, A. Pais.
Uretz, R. B.
see J. A. Simpson.

Vallarta, M. S.
1935: ———, Phys. Rev., 47, 647. *246, 252, 286.*
1939: ———, Rev. Mod. Phys., 11, 239. *327.*
1939: ——— and O. Godart, Rev. Mod. Phys., 11, 180. *462, 500.*
1939: ———, C. Graef and S. Kusaka, Phys. Rev., 55, 1. *485.*
1948: ———, Phys. Rev., 74, 1837. *288, 290, 291, 292, 293, 294, 318, 320.*
1950: ———, Phys. Rev., 77, 419. *329.*
see S. E. Forbush, G. Lemaitre.
Valley, G.
1947: ———, Phys. Rev., 72, 772. *172.*
1948: ——— and B. Rossi, Phys. Rev., 73, 177. *172.*
Van Allen, J. A.
1950: ——— and A. V. Gangnes, Phys. Rev., 78, 50. *217, 311, 319.*
1950: ——— and S. F. Singer, Phys. Rev., 78, 819. *302, 311, 319, 320.*
1950: ——— and A. V. Gangnes, Phys. Rev., 79, 51. *319, 320.*
——————— *258.*

see A. V. Gangnes.

VAN HOVE, L.
1949: ———, Phys. Rev., 75, 1519. *147.*

VAN WYCK, L. B.
1949: ———, Proc. Phys. Soc., A62, 697. *155.*
1950: ———, Proc. Phys. Soc., A63, 350. *158.*
1950: ———, Phys. Rev., 80, 487. *143.*

VIDALE, M.
1951: ——— and M. Schein, Phys. Rev., 81, 1065. *336.*
see J. J. Lord.

VILLARS, F.
see W. Pauli.

WAGNER, N.
1949: ——— and D. Cooper, Phys. Rev., 76, 449. *66, 156.*

WAFFLER, H.
1941: ———, Helv. Phys. Acta, 14, 248. *501.*

WALKER, S. P.
see K. Greisen.

WALKER, W. D.
1950: ———, Phys. Rev., 77, 686. *356.*
see K. Greisen.

WALSH, J. G.
1950: ——— and O. Piccioni, Phys. Rev., 80, 619. *355, 358.*

WAMBACHER, H.
see M. Blau.

WANLESS, S. D.
see R. B. Leighton.

WATAGHIN, G.
1938: ———, Accad. Lincei Atti., 27, 675. *5.*
1946: ———, Phys. Rev., 70, 787. *5.*
1947: ———, Phys. Rev., 71, 453. *355.*
see M. Cini; C. M. Garelli; H. A. Meyer.

WATSON, K. M.
1949: ——— and J. V. Lepore, Phys. Rev., 76, 1157. *147.*
see K. A. Brueckner.

WEEKES, K.
1947: ——— and M. V. Wilkes, Proc. Roy. Soc., A175, 143. *482.*

WEISSENBERG, A.
see A. I. Alikhaniyan.

WEISSKOPF, V.
1937: ———, Phys. Rev., 52, 295. *39.*

WENTZEL, G.
1949: ———, Phys. Rev., 75, 1810. *149.*

WHEELER, J. A.
1947: ———, Phys. Rev., 71, 320. *172.*
1949: ———, Rev. Mod. Phys., 21, 132. *172.*

see E. O. Kane; J. Tiomno.
WHITE, M. G.
see R. Sherr.
WHITE, R. S.
1950: ———, E. M. McMillan, J. M. Peterson, Phys. Rev., 78, 84. *368, 370.*
see E. M. McMillan.
WHYTE, G. N.
1950: ———, Phys. Rev., 78, 630. *356.*
WICK, G. C.
1934: ———, Atti. Accad. Naz. Lincei, 19, 319. *127.*
WIEGAND, C.
see O. Chamberlain.
WIGHTMAN, A. S.
1950: ———, Phys. Rev., 77, 521. *149.*
see R. E. Marshak.
WIGNER, E.
1927: ———, Göttingen Nachr., 375. *132.*
1939: ———, Phys. Rev., 56, 519. *167.*
see L. Critchfield.
WILKES, M. V.
see K. Weekes.
WILKINSON, D. H.
see E. Broda.
WILLIAMS, R. W.
1948: ———, Phys. Rev., 74, 1689. *383.*
WILSON, J. G.
see M. G. Mylroi, B. G. Owen.
WILSON, V. C.
1938: ———, Phys. Rev., 53, 337, 908. *396, 398, 399, 439, 440.*
1939: ———, Phys. Rev., 55, 6. *331.*
1943: ——— and D. J. Hughes, Phys. Rev., 63, 161. *331, 404.*
WINCKLER, J. R.
1949: ———, W. G. Stroud, T. J. B. Shanley, Phys. Rev., 76, 10. *320.*
1950: ———, T. Stix, K. Dwight, R. Sabin, Phys. Rev., 79, 656. *227, 302, 311, 319, 320, 322, 323, 329, 383.*
WOLFENDALE, A.
1951: ———, private communication. *411, 449.*
WOLLAN, E. O.
see A. H. Compton; M. Schein.
WU, C. S.
1950: ———, Rev. Mod. Phys., 22, 386. *169.*
see C. Longmire.
WOUTHUYSEN, S. A.
see H. W. Lewis.

Yagoda, H.
1949: ——— and N. Kaplan, Phys. Rev., 75, 339. *355.*
1949: ———, N. Kaplan and C. H. Conner, Phys. Rev., 76, 171. *356.*
Yamada, E.
see S. Ogawa.
Yamaguchi, Y.
see Y. Fujimoto; K. Aidzu.
Yamakawa, K. A.
see T. Sigurgeirsson.
Yang, C. N.
1950: ———, Phys. Rev., 77, 242. *132.*
1950: ———, Phys. Rev., 77, 722. *148.*
1950: ——— and J. Tiomno, Phys. Rev., 79, 495. *140, 175.*
Yekutiele, G.
see U. Camerini; W. O. Lock.
York, H. F.
see R. Bjorklund; W. K. H. Panofsky.
Yoshida, S.
see Y. Sekido.
Yngve, V. H.
see M. Schein.
Yuan, L. C. L.
1948: ———, Phys. Rev., 74, 504. *356.*
1951: ———, Phys. Rev., 81, 175. *358, 378.*
Yukawa, H.
1935: ———, Proc. Phys. Mat. Soc., Japan, 17, 48. *127.*
1938: ———, S. Sakata and M. Taketani, Proc. Phys. Mat. Soc., Japan, 20, 720. *180.*
1938: ———, S. Sakata, M. Kobayasi and M. Taketani, Proc. Phys. Mat. Soc., Japan, 20, 720. *179.*
1949: ———, Rev. Mod. Phys., 21, 474. *127.*

SUBJECT INDEX

Absolute cosmic ray flux at sea-level 333.
absorption measurements underground 398.
acceleration of charge in $\mu-e$ decay 161.
albedo, atmospheric (for charged particles) 217, 321, 322, 383.
α-particles, nucleons independent in 14, 49.
    primary flux of 218, 328.
    secondary, at high altitudes 220
altitude variation of soft component 350
analytical form of primary spectrum 300
angular correlation of high energy fragments 53, 57.
angular distribution of star fragments 47.
    of heavy nuclei in atmosphere 210.
    of shower particles 25.
annihilation of atoms (Millikan) 237.
annihilation of matter with antimatter 237.
antinucleons 130, 327.
assemblage of nucleons (interaction with) 4.
atmospheric albedo (charged particles) 217, 321, 322, 383.
atmospheric temperature effect 456, 458.
azimuth effect at given zenith angle 254, 266, 280, 326, 327.
barometer coefficient 457
β-radioactivity — direct coupling 166, 179, 182.
    — of neutron 163
    — selection rules 167, 168.
black tracks (emulsion) 6, 16, 38.
cascade component in atmosphere 348.
centre of mass (C) system 5, 22.
Cerenkov radiation 412.
charge determination of heavy nuclei 197.
    — comparison of grain and δ-ray counting 201
charged V-particles 109, 112, 121, 155.
    — competing modes of decay 157.
    — explanation of 110.
    — lifetime at rest 120, 156.
    — mass of 116.
    — nature of 158.
    — nature of secondaries 114.
    — statistical data 109.
charge independence of nuclear forces 13, 146.
chemical composition of cosmic ray primaries 228.
classification of particles 128.

collimation of grey tracks 36.
collision cross-section per nucleon 5.
collisions, elastic 3, 374.
    radiative 3, 5, 361.
collisions in interstellar space 233, 235.
collisions with interstellar magnetic fields 237.
collision mean free path — of fast π-mesons 18, 19.
    — of heavy nuclei 209.
    — of heavy nuclei in air 210, 329.
conservation laws — of charge 131.
    — of momentum and energy 131.
    — of angular momentum 132.
    — of parity 132.
correlation of azimuth effect and zenith angle effect 294.
    — of latitude effect and zenith angle effect 289.
    — of latitude, longitude and zenith angle effects 295.
    — of meson intensity 456.
Coulomb scattering 7.
coupling between fields 127, 133, 136, 139, 176.
Critchfield–Wigner interaction 165, 175, 176.
C-system, Lorentz transformation to (multiple theory) 22.
    — spectrum of π-mesons in 22.
decay protons in nuclear excitation 44.
degree of inelasticity 5.
degree of stripping of primaries 224.
depth-intensity relation (underground) 330, 397.
    — existence of "knee" 397.
Dirac equation 130.
direct coupling in β-radioactivity 179.
dynamics of $\pi-\mu$ decay 111.
early emulsions (characteristics) 38.
earth as magnetic analyzer 245.
east-west asymmetry 266, 276, 280, 311.
eccentricity of terrestrial dipole 247, 251.
elastic collisions (of nucleons) 374.
elastic scattering cross-section 5.
electron capture by heavy nuclei 197.
electrons in primary cosmic rays 194, 256, 324.
electron pair production 82.
electron sensitive emulsions 7.
emission probabilities in nuclear evaporation 48.
emulsion — black tracks 6, 16, 38.
    — composition of grey tracks 34.
    — electron sensitive 7.
    — experimental methods 6.
    — frequency of grey tracks 34.
    — grain density in 6.

- — grey tracks 6, 16, 34, 37, 203.
- — magnetic deflection in 7.
- — minimum grain density 6.
- — shower particles 6, 202.

emulsion stars — formation 6.
- — produced by π-mesons 20.

emulsion stars underground 424.
- — frequency as function of depth 425.
- — spectrum of initiating particles 428.
- — star types 426.

energy integration through atmosphere 299.

energy loss of π-mesons in nuclear collisions 20.

equilibrium of cosmic ray primaries in space 234.

equivalence theorem 144.

energy balance, of cosmic ray beam 380.
- — in meson showers 12.

energy spectrum of primary radiation 216, 223, 225, 300.

evaporation α-particles of heavy nuclei 213.

evaporation process (nuclear) 4, 38, 374.

evaporation protons 6, 40, 43.
- — of fast heavy nuclei 204.

excitation (nuclear) 39.
- — barrier height 41, 45.
- — decay protons 42.
- — surface waves 42, 45.
- — treatment of Bagge 40.
- — treatment of Le Couteur 42.
- — treatment of Weisskopf 39.

experimental methods, emulsion 6.

extensive showers in atmosphere 380.

extensive showers underground 443.

fermions, interaction between four, 138, 159, 174.

Fermi, theory of inelastic collision 10.
- — mechanism for primary acceleration 237.

Feynmann graph 134
- — order of phenomena 136.

fission of excited nucleus 54.

flux of α-particle primaries 218.

flux of heavy primaries 216.

Furry's theorem 142.

Geiger counters of light construction 263.

genetic relations in atmosphere 363.

geomagnetic and solar activity, effects of 492.

geomagnetic effects -- correlation 288, 296
- — definitions 253.

geomagnetic latitude, variation of star intensity with, 7.

geomagnetic poles, location of, 246.

geometrical nuclear cross-section, $(\hbar/m_{\pi}c)^2$ 6.
grain density in emulsion 6, 198.
  — minimum 6.
grey tracks (emulsion) 6, 16, 37, 203.
  — composition of, 35.
  — angular distribution of 36.
  — frequency of 34.
Gross transformation 376, 377.
heavy fragments from stars 51, 54, 55.
heavy nuclei in primary cosmic rays 194, 327.
  — angular distribution of 210.
  — flux and energy spectrum of 216, 328.
heavy nuclei — charge determination 197.
  — δ-ray density from 51, 196, 199.
  — determination of relativistic energies for 212.
  — electron capture by 196.
  — evaporation α-particles from 213.
  — geomagnetic cut-off 224.
  — ionization by 196, 198.
  — mean free path 209.
  — mean free path in air 210, 329.
  — nuclear interactions of 202.
  — survival probability in air 210.
  — thin-down length of 51, 197.
high energy fragments, angular correlation 53, 57.
inelasticity, degree of, 15, 374.
insensitive emulsions, application of 201.
intensity variations with altitude 255.
interaction between four fermions 138, 159, 174.
interstellar space, interactions in 235.
ionization bursts underground 444.
isotopic spin, isotopic variable 141.
knock-on nucleons 16, 21.
Lamb shift 145.
latitude effect 7, 254, 272, 303, 351, 354.
  — correlation with zenith angle effect 289.
  — with longitude and zenith angle effects 295.
  — at 30,000 feet 272.
level density in excited nuclei 39.
lifetime at rest, $\pi-\mu$ 161.
Liouville's theorem 247, 248, 289, 297, 299.
lithium group of nuclei, primary flux 221, 231, 236.
longitude effect 252, 254, 274.
Lorentz transformation to C-system (multiple theory) 22.
low energy cut-off of heavy primaries 224.
low pressure counters, application of 195, 218, 221.
magnetic deflection in emulsions 7.

magnetic field of the earth 246.
magnetic storms and cosmic ray intensity 492.
Majorana particle 130, 138.
Majorana representation 136.
many body (nucleon) interaction 17.
maximum detectable momentum (cloud chamber) 69.
meson (mu) — capture of 127, 172.
  — decay of 160, 161, 456.
  — direct creation of 3.
  — intensity-height distribution 336.
  — local production of, (low energy) 335, 337.
  — processes of loss of energy 353, 408.
  — range-energy relation 412.
  — sea-level spectrum 339, 414.
  — spectrum of decay electrons 162.
meson (pi) — capture in hydrogen 149, 152.
  — capture in deuterium 149, 150.
  — collision mean free path 18, 21.
  — differential spectrum of 26, 369.
  — diffusion equation 370, 371.
  — energy loss in nuclear collisions 20.
  — formation of, energy variation 8, 9, 369.
  — genetic relation with μ-mesons 367, 370.
  — nature of 149, 151.
  — nuclear scattering, of slow 20.
  — pluro-multiple production 30.
  — production 8, 149, 368.
  — ratio of charged to neutral 12, 151, 384, 386.
  — scattering in nucleus 22.
  — showers, energy balance in 12.
  — spectrum at formation 24.
  — spectrum in C-system 22, 23.
  — star production by 20, 29.
meson-nucleon cascade 4.
meson-nucleon interaction 18, 29.
minimum grain density in emulsion 6.
multiple and plural processes 5, 365.
multiple Coulomb scattering 7, 211.
multiple theory of meson production 5.
  — Lorentz transformation for 22.
multiplicity of charged particles 305, 306.
multiplicity-primary energy relation (mesons) 13.
nature of particles underground 403.
N-component 352.
  — absolute intensity 357.
  — absorption length 355.
  — absorption length as function of energy 386.

- — diffusion equation 366.
- — equilibrium between stars and neutrons 375.
- — latitude effect 354.
- — proton-neutron ratio 361, 363, 375.
- — spectrum of 359.
- — techniques 353.

negative proton 130, 327.
- — in V° decay 103.

neutral (pi) mesons 12, 147, 372.
- — decay of 148.
- — γ-ray spectrum from, at high altitude 373.

neutrino 159.

neutron, decay of 163.

neutrons, equilibrium with stars 375.

nomenclature in emulsion stars 6.

nuclear forces 145, 159.
- — charge independence 13, 146.
- — magic numbers 146.
- — pure neutral theory 146.
- — spin-orbit coupling 146.
- — symmetrical theory 146.

nuclear evaporation 4, 38, 378.

nuclear interactions of heavy nuclei 202.

nuclear matter 33.

nuclear temperature 39.

nucleon-antinucleon pairs 130.

nucleons, knock-on 16, 21.

nucleon-meson interaction 18.

nucleon-nucleon encounters 3.

nucleons, recoil 13.

pairs of penetrating particles underground 448.

penetrating showers 3.
- — in hydrogen 6, 58.
- — underground 441.

penumbra (of Störmer cone) 250, 288, 318, 327.

π—p particles 8, 23, 25.

photons, direct creation of 3.

plural theory of meson production 5.

positive excess — momentum variation 343, 346.
- — asymmetries of 327, 347.

positive (local) temperature effect 458.

pseudoscalar meson theory 145, 147.

primary electrons, existence of 194, 256.

primary collision process (nucleon-nucleon) 5.

primary cosmic rays — chemical composition 228, 302.
- — comparison with cosmic abundance 231.
- — contribution of heavy nuclei 194.

  - electrons, existence of 194, 256, 288, 324, 348.
  - energy spectrum 225, 301, 303, 317, 322.
  - energy spectrum of heavy nuclei 216, 225, 328.
  - equilibrium in space 234.
  - flux of α-particles 218, 328.
  - flux of heavy nuclei 216, 221, 328.
  - flux of lithium group 221, 231, 236, 328.
  - geomagnetic cut-off 224.
  - heavy nuclei in 194, 302, 327.
  - integral energy spectra 223.
  - nuclear interactions of 202, 204.
  - origin 237.
  - rocket measurements 319.
  - techniques of observation 195.
  - time variations 304, 330.
  - vertical data 320.

prong number (stars) and excitation 47, 49.
protons, evaporation 6, 40, 43, 46.
proton gas 235, 239.
proton-proton collisions 6.
pseudo-scalar meson theory, particular characteristics 151.
radiation damping 5.
radiative collisions 3.
  - cross-section for 5.

radiative corrections 144.
ratio, charged to neutral π-mesons 12.
recoil nucleons 3.
regularization and renormalization 144, 145, 155.
ring current of Chapman and Ferraro 494.
scintillation measurements on primaries 218, 220.
seasonal variations of cosmic ray intensity 461.
secondary (nucleon-nucleon) collisions 16.
semi-diurnal effect 481.
  - north-south difference of 483.

shadow cone of the earth 250.
showers (meson), energy balance in 12.
shower particles, angular distribution 23, 25.
shower particles, interaction with nucleus 29.
shower tracks (emulsion) 6, 202.
sidereal diurnal effect at sea-level 484.
  - Compton-Getting effect 484.
  - separation from solar effect 485.
  - experimental data 488.

sidereal diurnal effect, underground 419, 423.
"side showers", corrections for, 268.
single scattering in gas 85.
slow neutrons, intensity-altitude variation 378.

"soaking" of nucleus 29.
soft component, percentage of beam underground 398.
solar diurnal effect at great altitudes 480.
solar diurnal effect at sea-level 466.
— phase variations of 470.
— east-west difference effect 477.
— effect of geomagnetic activity 477.
— north-south difference effect 474.
— with directional counter arrays 472.
solar diurnal effect underground 419, 423.
solar flares and cosmic ray intensity 502.
— neutron intensity 505, 507.
— star production 508.
specific ionization in the atmosphere 256, 299.
specific ionization of particles underground 406.
spin-orbit coupling (in nuclei) 146.
stars (emulsion) 6.
— equilibrium with neutrons 375.
— produced by α-particles 32.
— produced by neutrons 83, 362.
— produced by π-mesons 20.
— produced by singly charged primaries 32, 362.
statistical distribution of energy (in nucleus) 3, 39.
Störmer cone 249.
Störmer cone, the penumbra 250.
surface waves on excited nucleus 42.
survival of heavy nuclei in atmosphere 210.
tapering of tracks of heavy nuclei 51.
tau (τ) mesons 65, 105, 155.
— decay of 81, 105.
— energy balance at decay 106.
— mass of 106, 108.
thin tracks (shower particles) 6.
time fluctuations of heavy primaries 225.
time of traversal of nucleus 3.
time variations underground 418.
27-day recurrence effects 497.
underground — absorption measurements 330, 398.
— associated particles 411, 441, 448.
— barometer effect 420.
— extensive showers 443.
— fraction soft component 398, 408.
— influence of magnetic storms 421.
— influence of π-meson interaction 416.
— ionization bursts 444.
— nature of particles 331, 398, 404.
— observations at great depths 407.

— radioactive effects 331, 400.
— scattering 406.
— slow mesons 432.
— slow neutrons 436.
— specific ionization 406.
— stars (emulsion) 331, 424.
— time variations 418.
— zenith angle distribution 401.

universal coupling between fermions 165, 175, 176.

varitrons 66, 128.

V-particles 65—, 153, 155, 373. see also "charged V-particles".

V°-particles — application of conservation laws to competing modes of decay 154.
— competing modes of decay 153.
— coplanarity of decay 86.
— decay to $\pi + \pi$ 87, 90, 91, 98.
— decay to $p + \pi$ 86, 89, 93.
— decay schemes 85, 86.
— dynamics of decay schemes 93, 98.
— experimental arrangements 68.
— lifetime at rest 101.
— mass determinations 89, 90, 92.
— momentum spectrum of, 88.
— momentum spectrum of secondaries 79.
— nature of 154.
— nature of secondary particles 73, 102.
— negative protons as secondaries 103.
— number of secondaries 85.
— penetrating properties of secondaries 78.
— source of 73.
— statistical data 70.
— unstable state of neutron? 153.

V-shaped tracks 65, 67.

Wave functions — of charged particles 130.
— of neutral quanta 130.
— of uncharged particles with magnetic moment 130.

Y-shaped event 84.

zenith angle effect at given azimuth 254, 272, 283, 286, 320.
— underground 401.